

The Design and Synthesis of Small Molecule Inhibitors of mTOR Kinase for the Treatment of Idiopathic Pulmonary Fibrosis

Hannah Rose Marie Davies

Thesis submitted to the University of Strathclyde as part of the
assessment towards a degree of Doctor of Philosophy

2020



**CONFIDENTIAL: Property of GSK.
Not to be copied or circulated**

CONFIDENTIAL – DO NOT COPY

This thesis is the result of the author's original research. It has been composed by the author and has not been previously submitted for examination which has led to the award of a degree.

The copyright of this thesis belongs to the author under the terms of the United Kingdom Copyright Acts as qualified by University of Strathclyde Regulation 3.50. Due acknowledgement must always be made of the use of any material contained in, or derived from, this thesis.

Signed:

Date:

The human biological samples were sourced ethically, and their research use was in accord with the terms of the informed consents under an IRB/EC (Institutional Review Board/Ethics Committee) approved protocol.

Abstract

Idiopathic pulmonary fibrosis (IPF) is a progressive and fatal disease of the lung, characterised by excessive collagen deposition. A median survival time of 2-3 years gives IPF a worse prognosis than many cancers. The two currently approved treatments only slow progression of the disease, while the best treatment – a lung transplant – has long waiting lists, risks associated with organ rejection and is not a viable option for all patients. Researchers at GlaxoSmithKline (GSK) have demonstrated that inhibition of mTOR kinase halts the deposition of collagen. Research is underway to develop an inhaled small molecule inhibitor of mTOR kinase for the treatment of IPF.

Chapter I describes the lead optimisation of a novel series of directly-linked sulfone mTOR kinase inhibitors (**A, Figure**). Compounds were designed and synthesised to explore structure activity relationships (SAR) by modifying the substituents at the 2-, 4-, and 6-positions (R^1 , R^2 and R^3). The aims of this research were to: a) identify optimal combinations of the three substituents; b) synthesise compounds that met the target property profile (suitable efficacy, affinity and selectivity with no mutagenic risks); and c) investigate a range of novel sulfone moieties. While these aims were achieved, an *in vivo* study demonstrated that compounds from within this directly-linked sulfone series did not have the required *in vivo* efficacy.



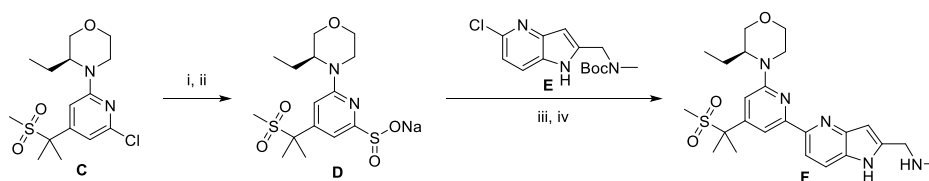
Figure: The two series of mTOR kinase inhibitors discussed in this Thesis. A – the directly-linked sulfone series and B – the carbon-linked sulfone series. Substituents in each of the three vectors coloured in red, green and blue.

In parallel to the research into the directly-linked sulfone compound, an alternative series of carbon-linked sulfone mTOR kinase inhibitors was explored (**B, Figure**). As compounds in this series were progressed, larger quantities were needed, requiring a

robust synthesis. Chapter II describes the work carried out to overcome the three key challenges in the synthesis:

- 1) To develop an improved synthesis of the 1-(5-chloro-1*H*-pyrrolo[3,2-*b*]pyridin-2-yl)-*N*-methylmethanamine moiety (**E**, **Scheme**, here referred to as the azaindole).
- 2) To improve the S_NAr reaction conditions to install the (*S*)-3-ethylmorpholine to give compound **C** (**Scheme**).
- 3) To identify a suitable cross-coupling methodology to couple the 2-chloropyridine core (**C**) and the azaindole (**E**) to give final compound **F**.

An improved synthesis of the azaindole (**E**) was designed, employing the Larock indole synthesis and a solvent and base screen gave improved conditions for the S_NAr reaction to give compound **C**. Originally only feasible using Stille chemistry and toxic organostannanes, the bipyridyl cross-coupling reaction was improved by employing a desulfinate cross-coupling reaction (coupling **D** and **E** to give **F**, **Scheme**).



Scheme: Forming the sulfinate and the successful desulfinate cross-coupling reaction. *Reagents and Conditions:* i) SMOPS (sodium 3-methoxy-3-oxopropane-1-sulfinate), Cu(I)I, DMSO, 110 °C. ii) NaOMe (0.5 M in MeOH), THF, 21 °C. iii) K_2CO_3 , Pd(OAc) $_2$, PCy $_3$, 1,4-dioxane, 150 °C. iv) HCl (4 M in 1,4-dioxane), 1,4-dioxane.

The scope of this desulfinate cross-coupling reaction was subsequently explored in Chapter III, with a particular focus on the synthesis of bipyridyl compounds. This demonstrated that a range of bipyridyl compounds could be made by this method. Finally, a high-throughput screening platform for the desulfinate cross-coupling reaction was designed and validated giving a rapid method to screen catalysts, bases and solvents and optimise the reaction. This proved particularly valuable to develop conditions for some of the more challenging cross-coupling substrates.

Acknowledgements

Firstly, I would like to thank my industrial supervisor, Dr Heather Hobbs. Thank you for your encouragement in my scientific and professional development and for sharing your expertise in medicinal and synthetic chemistry. Thank you for giving me the opportunity to pursue interesting projects and for your support. Additionally, thank you for reading and correcting several of my reports.

I would also like to thank my academic supervisor, Professor Glenn Burley. Thank you for providing guidance and for your support, especially during the last few months of my PhD. I would also like to thank Dr Craig Jamieson for your time, patience and thorough examination of my 12- and 30-month reports.

I would like to thank Dr Simon Peace. Thank you for your support and guidance throughout my PhD, for giving me the opportunity and for entrusting me with the route development. Thank you also to the mTOR project team, my fellow PhD students and all of my colleagues at GSK who have helped motivate me throughout this process.

Thank you to all of the scientists at GSK who have helped me with this work. Thank you Dr Sandeep Pal and Chris Luscombe for your computational support. Thank you to Esme Clarke, Steve Richards, Sean Lynn and Andy Hobbs for your help in the analysis and purification of compounds included in this Thesis. Additionally, thank you to Dr Simon Nicolle, Dr Blandine McKay, Dr David Battersby and to placement students Jo, Claire and Elizabeth for help with aspects of the chemistry.

Thank you to Professor Harry Kelly and Professor William Kerr for the opportunity to undertake this PhD, and for your assistance throughout.

Importantly, thank you to my family and friends. To my family, thank you for your advice, encouragement, motivation and understanding. Additionally, thank you for your support and care throughout my academic studies. To my friends, thank you for always being there for me. And to Martin, thanks for being my study buddy.

Finally, I would especially like to thank my husband James. Thank you for your understanding and encouragement, for putting up with me working all those weekends and for supporting me through the difficult patches.

Contents

Abstract	2
Acknowledgements	4
Contents	5
Abbreviations	9
Introduction to Idiopathic Pulmonary Fibrosis (IPF) and mTOR Kinase Inhibitors .	14
1. Introduction	15
1.1 Idiopathic pulmonary fibrosis	15
1.1.1 Diagnosis and disease progression	16
1.1.2 Current treatments for IPF	17
1.1.3 Normal wound healing and the pathway leading to IPF.....	18
1.2 Comparison of the properties of oral and inhaled drugs	20
1.3 mTOR kinase (FRAP) and IPF	24
1.4 Biological and physicochemical assays to determine affinity, efficacy, selectivity and physicochemical properties of mTOR kinase inhibitors	32
1.4.1 Assays to measure the affinity and efficacy of mTOR kinase inhibitors ..	32
1.4.2 Assays to monitor the off-target effects of mTOR kinase inhibitors.....	35
1.4.3 Physicochemical assays to determine the physicochemical properties of mTOR kinase inhibitors.....	37
1.5 Previous research from our laboratories to develop mTOR kinase inhibitors .	38
1.6 Comparison of the mTOR kinase inhibitors synthesised so far	54
1.7 Project aims	55
Chapter I: Results and discussion of the medicinal chemistry of a directly-linked sulfone series to develop the next generation of mTOR kinase inhibitors	56
2. Results and Discussion.....	57
2.1 Aims of Chapter I and the desired profile of compounds in the directly-linked sulfone series of mTOR kinase inhibitors	57
2.2 Methods for the preparation of directly-linked sulfone mTOR kinase inhibitors	58
2.3 Investigating SAR in the directly-linked sulfone series.....	61
2.3.1 Results and discussion of an initial investigation of directly-linked sulfone mTOR kinase inhibitors.....	62
2.3.2 Improving the synthesis of bipyridyl-containing compounds	81

2.4 Investigation of mTOR kinase inhibitors with novel 4-position sulfone moieties	86
2.4.1 Exploration novel 4-position sulfone moieties	86
2.4.2 Synthesis of mTOR kinase inhibitors with a variety of 4-position sulfone moieties	88
2.4.3 Results and discussion of mTOR kinase inhibitors containing novel 4-position sulfone moieties	94
2.5 Summary of Chapter I	103
Chapter II: Synthesis of the lead compound in an alternative series of mTOR kinase inhibitors	106
3. Synthesis of the lead compound in an alternative series of mTOR kinase inhibitors	107
3.1 Introduction	107
3.2 Aims of Chapter II	108
3.3 The original azaindole synthesis	110
3.3.1 Developing an improved synthetic route to the azaindole	111
3.3.2 Route change to enable use of a bromoazaindole	112
3.4 The original method to install (<i>S</i>)-3-ethylmorpholine	113
3.4.1 Palladium-catalysed cross-couplings to access the (<i>S</i>)-3-ethylmorpholine-substituted pyridine intermediate	114
3.4.2 Base, solvent and concentration screens to efficiently access the (<i>S</i>)-3-ethylmorpholine-substituted pyridine intermediate	115
3.4.3 Route change to enable use of a bromopyridine	119
3.5 Bipyridyl cross-coupling reactions to install the azaindole	121
3.6 Miyaura borylation and Suzuki cross-coupling reactions to access the pyridine azaindole	122
3.7 Negishi cross-coupling reactions	124
3.8 Nickel-catalysed reductive cross-coupling reactions	125
3.9 Desulfinate cross-coupling reactions	127
3.9.1 Sulfinate synthesis	132
3.9.2 Use of brominated starting materials to enable sulfinate synthesis	142
3.9.3 The desulfinate cross-coupling reaction	143
3.10 Further improvements to the desulfinate cross-coupling reaction	146
3.11 Summary of Chapter II	146

Chapter III: Investigating the scope of the desulfinate cross-coupling reaction...	148
4. Investigating the scope of the desulfinate cross-coupling reaction.....	149
4.1 Introduction	149
4.2 Aims of Chapter III	151
4.3 Sodium pyridine sulfinate synthesis	152
4.4 Optimisation of the desulfinate cross-coupling reaction.....	153
4.4.1 Solvent and temperature screens.....	153
4.4.2 Investigating the effects of varying the number of equivalents of the pyridyl sulfinate	159
4.5 The scope of the desulfinate cross-coupling	161
4.6 Further investigation of the reaction	171
4.7 Application of a high-throughput screening platform to optimise the desulfinate cross coupling reaction	173
4.8 Summary of Chapter III	177
Conclusions and Future Work.....	179
5. Conclusions and future work	180
Experimental Section	186
6. Experimental	187
6.1 General experimental details	187
6.2 General procedures	191
6.3 Experimental	192
6.4 General procedure used in array reactions (Section 4.5).....	276
6.5 General procedure used in HTS reactions (Section 4.7)	285
6.6 HPLC with a chiral stationary phase data for selected compounds	286
Appendix	293
7. Appendix	294
7.1 Appendix A: Full data on compounds discussed in Section 2.3	294
7.2 Appendix B: Selectivity data on compounds discussed in Section 2.4.....	299
7.3 Appendix C: Quantitative NMR example	300
7.4 Appendix D: Assay experimental procedures	301
7.4.1 PI3K-Isoform HTRF assay	301
7.4.2 mTOR Kinobead assay	302

7.4.3 pAkt Cellular assay	303
7.4.4 SIAJ	304
7.4.5 DNA-PK	305
7.4.6 MDCK	306
7.4.7 AMP.....	306
7.4.8 Kinetic solubility (CLND and CAD solubility).....	306
7.4.9 SLF.....	307
7.4.10 ChromLogD	307
8. References	310

Abbreviations

2-MeTHF:	2-Methyltetrahydrofuran
3D:	3-Dimensional
ACD:	Advanced Chemistry Development Labs Inc.
ADME:	Absorption, Distribution, Metabolism and Excretion
Akt:	Also known as Protein Kinase B (PKB)
AMP:	Artificial Membrane Permeability
APC:	Allophycocyanin – a fluorescent protein
API:	Active Pharmaceutical Ingredient
ATM:	Ataxia Telangiectasia Mutated
ATP:	Adenosine Triphosphate
ATR:	ATM and RAD3-Related
Boc:	<i>tert</i> -Butyloxycarbonyl
br.:	Broad
BSA:	Bovine Serum Albumin
CAD:	Charged Aerosol Detector
CataCXium A:	Di(1-adamantyl)- <i>n</i> -butylphosphine
CHAPS:	Cholamidopropyl)dimethylammonio]-1-propanesulfonate
CHI:	Chromatographic Hydrophobicity Index
ChromLogD _{7.4} :	Chromatographic Log D at pH 7.4 – measured lipophilicity in buffer at pH 7.4
ChromLogP:	Chromatographic Log P – measured lipophilicity in water
CLND:	Chemi-Luminescent Nitrogen Detection
cLogD:	Calculated LogD
cLogP:	Calculated LogP
CPME:	Cyclopentyl Methyl Ether
CPP:	Cyclopropylpyran (3-Oxabicyclo[4.1.0]heptane)
CV:	Column volumes
DAPC:	Discovery Automation and Platform Chemistry
dba:	Dibenzylideneacetone
DBU:	1,8-Diazabicyclo[5.4.0]undec-7-ene

CONFIDENTIAL – DO NOT COPY

DFT:	Density Functional Theory
DHP:	3,6-Dihydro-2 <i>H</i> -pyran
DIPEA:	<i>N,N</i> -Diisopropylethylamine
DMA:	Dimethylacetamide
DMAP:	4- <i>N,N</i> -Dimethylacetamide Dimethylaminopyridine
DMF:	<i>N,N</i> -Dimethylformamide
DMPU:	<i>N,N'</i> -Dimethylpropyleneurea
DMS:	Dimethyl Sulfide
DMSO:	Dimethyl Sulfoxide
DNA:	Deoxyribonucleic Acid
DNA-PK:	DNA-Dependant Protein Kinase
DoE:	Design of Experiment
dppf:	1,1'-Bis(diphenylphosphino)ferrocene
DPU:	Discovery Performance Unit
DTBPF:	1,1'-Bis(di- <i>tert</i> -butylphosphino)ferrocene
DTT:	Dithiothreitol
E1cB:	Elimination unimolecular conjugate base
ECM:	Extra Cellular Matrix
EDTA:	Ethylenediaminetetraacetic Acid
EMT:	Epithelial-Mesenchymal Transition
Equiv.:	Equivalents
FaSSIF:	Fasted-State Simulated Intestinal Fluid
FBS:	Foetal Bovine Serum
FRAP:	FK506 Binding Protein 12-Rapamycin Associated Protein or FKBP-12-Rapamycin Associated Protein
GPR-1:	General Receptor of Phosphoinositides 1
GSK:	GlaxoSmithKline
GST:	Glutathione S-Transferase, GST-tagged protein
h:	Hour
HATU:	<i>O</i> -(7-Azabenzotriazol-1-yl)- <i>N,N,N',N'</i> -tetramethyluronium Hexafluorophosphate
HCl:	Hydrochloric Acid

CONFIDENTIAL – DO NOT COPY

HEPES:	4-(2-Hydroxyethyl)-1-piperazineethanesulfonic Acid
hERG:	Human Ether a go-go Related Gene
HLF:	Human Lung Fibroblast
HPLC:	High Performance Liquid Chromatography
HRCT:	High-Resolution Computed Tomography
HRMS:	High-Resolution Mass Spectrometry
HTRF:	Homogeneous Time-Resolved Fluorescence
HTS:	High-Throughput Screen
HuT-78:	Human T Cell Lymphoma Cell Line
IPA:	2-Propanol
IPF:	Idiopathic Pulmonary Fibrosis
KB:	Kinobead, Kinobead Assay
LCMS:	Liquid Chromatography Mass Spectrometry
LDA:	Lithium Diisopropylamide
LE:	Ligand Efficiency
LHMDS:	Lithium Bis(Trimethylsilyl)amide
LLE:	Lipophilic Ligand Efficiency
Lysosome:	Cellular organelles which contain acid hydrolase enzymes
M.pt.:	Melting Point
MDAP:	Mass Directed Auto Preparative Chromatography
MDCK:	Madin-Darby Canine Kidney Cells
MDCKII-MDR1:	Madin-Darby Canine Kidney (MDCK) cells transfected with Human Multidrug Resistance Gene-1 (MDR1)
Min:	Minutes
MMPP:	Magnesium Bis(Monoperoxyphthalate) Hexahydrate
MPO:	Multi-Parameter Optimisation or Multi-Parameter Profile
MSD:	Mesoscale Discovery
mTOR Kinase:	The kinase domain of mTORC1 and mTORC2, also known as FRAP
mTOR:	Mechanistic Target of Rapamycin
mTORC1/2:	Mechanistic Target of Rapamycin Complex 1/2
mTOR KB pIC ₅₀ :	The pIC ₅₀ in the mTOR Kinobead affinity assay

CONFIDENTIAL – DO NOT COPY

NMM:	<i>N</i> -Methylmorpholine
NMP:	<i>N</i> -Methylpyrrolidone
NMR:	Nuclear Magnetic Resonance
OBB:	Odyssey Blocking Buffer
pAkt:	phosphoAkt (phosphorylated Akt)
pAkt pIC ₅₀ :	The pIC ₅₀ in the pAkt efficacy assay
PBS:	Phosphate Buffered Saline
PDB:	Protein Database
PDGF:	Platelet-Derived Growth Factor
PDGF-BB:	PDGF – a dimeric glycoprotein composed of two B subunits
PFI:	Property Forecast Index
PH Domain:	Pleckstrin Homology Domain
PI3K:	Phosphoinositide-3-Kinase (four isoforms: α , β , γ and δ)
pIC ₅₀ :	The log of the concentration of compound required to reduce the activity of the biological target in question by 50%
PIKKs:	Phosphoinositide Kinase Related Kinases
PIP ₂ :	Phosphatidylinositol 4,5-Bisphosphate
PIP ₃ :	Phosphatidylinositol 3,4,5-Trisphosphate
PKB:	Protein Kinase B
PKPD:	Pharmacokinetic/Pharmacodynamic
ppm:	Parts Per Million
Quant.:	Quantitative
SA:	Streptavidin-Allophycocyanin (APC)
SAR:	Structure Activity Relationship
SCX:	Strong Cation Exchange
SDS:	Sodium Dodecyl Sulfate
SIAJ:	Scar In a Jar
SLF:	Simulated Lung Fluid
SMOPS:	Sodium 3-Methoxy-3-oxopropane-1-sulfinate
S _N 2:	Nucleophilic Biomolecular Substitution
S _N Ar:	Nucleophilic Aromatic Substitution
SPhos:	2-Dicyclohexylphosphino-2',6'-dimethoxybiphenyl

CONFIDENTIAL – DO NOT COPY

STAB:	Sodium Triacetoxyborohydride
TAA:	<i>tert</i> -Amyl Alcohol, 2-Methylbutan-2-ol
TBAB:	Tetra- <i>n</i> -Butylammonium Bromide
TBACl:	Tetra- <i>n</i> -Butylammonium Chloride
TBME:	<i>tert</i> -Butylmethyl Ether
TBS:	Tris-Buffered Saline
TEA:	Triethylamine
TFA:	Trifluoroacetic Acid
TGFβ:	Transforming Growth Factor Beta
THF:	Tetrahydrofuran
THP:	Tetrahydropyran
TI:	Therapeutic Index – the ratio of the concentration of drug required to give a therapeutic effect to the concentration at which adverse effects are seen
TMEDA:	Tetramethylethylenediamine
TMP:	2,2,6,6-Tetramethylpiperidine
TMS:	Trimethylsilyl
TR-FRET:	Time-Resolved Fluorescence Resonance Energy Transfer
UIP:	Usual Interstitial Pneumonia
UPLC:	Ultra-Performance Liquid Chromatography
UV:	Ultraviolet
Val:	Valine
XPhos:	2-Dicyclohexylphosphino-2',4',6'-triisopropylbiphenyl

Introduction to Idiopathic Pulmonary Fibrosis (IPF) and mTOR Kinase Inhibitors

1. Introduction

This Thesis describes the development of a small molecule inhibitor of the mechanistic target of rapamycin (mTOR) kinase for the treatment of idiopathic pulmonary fibrosis (IPF).

1.1 Idiopathic pulmonary fibrosis

IPF is a progressive, fatal lung disease.¹ It is characterised by excessive collagen deposition in the lungs, leading to the formation of scar tissue and there is no definitively known cause.^{2,3} It is the most common form of the idiopathic interstitial pneumonias (diseases affecting the lung interstitium – the space between the alveolar epithelium and the capillary endothelium, part of the blood-gas barrier⁴).⁵ A median survival time from diagnosis of 2-3 years gives IPF a worse mortality rate than many cancers.⁶⁻⁹ IPF is more frequent in smokers, and both genetic and environmental factors have been implicated.^{3,10-12} Typical symptoms include non-productive coughing and exertional breathlessness, which can lead to patients becoming housebound.⁴ Clubbing (widening of the tips of fingers or toes) is also seen in approximately 50% of IPF patients.³ The deposition of collagen in the lung tissue causes many changes to the structure, including the characteristic honeycomb appearance of the lung tissue (**Figure 1**).⁴

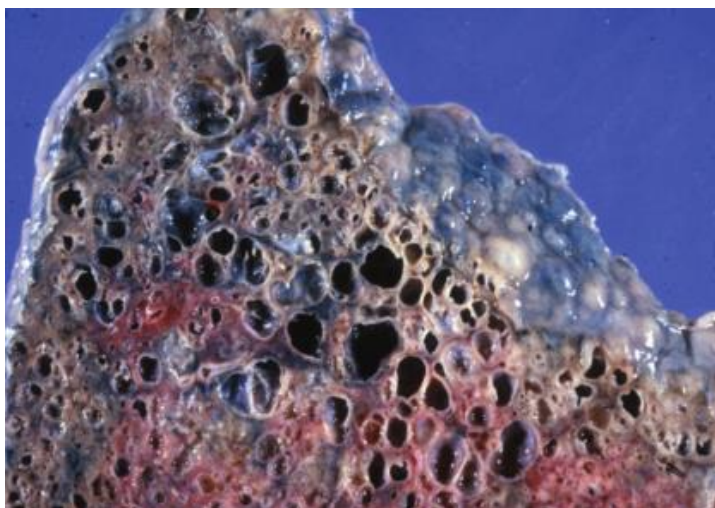


Figure 1: The lung of a patient with advanced IPF showing the honeycomb structure.⁴

1.1.1 Diagnosis and disease progression

Previously, in order to diagnose IPF unambiguously, a lung biopsy was required, showing the histopathologic pattern of usual interstitial pneumonia (UIP, usual to indicate that it is most commonly seen and pneumonia referring to inflammation, not infection⁴); this needed to be combined with the following criteria:¹¹

- Exclusion of any other cause of interstitial lung disease (e.g. environmental).
- Abnormal pulmonary function including evidence of restricted gas exchange.
- Abnormal high-resolution computed tomography (HRCT) scans.

More recently, the diagnostic criteria have changed due to the ability of HRCT scans to detect the histopathologic pattern of UIP, meaning a surgical biopsy is no longer essential to diagnose IPF.⁶ HRCT uses a normal CT scanner and X-ray images are taken at frequent intervals to build up a picture of the lung and show areas with different densities of lung tissue. In HRCT scans, more dense areas are white and less dense areas (such as air) are black. HRCT of the lungs of IPF patients show the characteristic honeycombing as the lung walls thicken (white areas) and the alveoli enlarge (black areas) allowing their use in the diagnosis of IPF (**Figure 2**).⁵

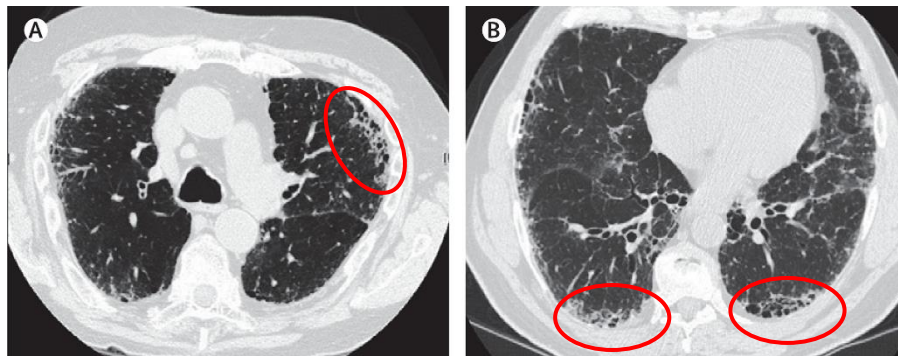


Figure 2 A and B: HRCT images of the lungs of patients with IPF, demonstrating the honeycombing of the lung structure (red). Adapted from a figure by King *et al.*⁵

IPF is most common in middle-aged and older people, with a median age of 66 years at diagnosis.⁵ This can make diagnosis difficult given that the initial symptom of breathlessness can be attributed to aging or emphysema.³ This in turn can lead to delays in diagnosis of 6-24 months after the symptoms first appear.^{3,13} Additionally, IPF can have several years of asymptomatic progression before patients develop

symptoms,⁵ and, once diagnosed, individual patients progress at different rates.¹⁴ With a stable or slowly progressive course, patients experience gradual decline in lung function and can survive for months to years from the onset of symptoms.⁵ With an accelerated variant, patients experience rapid decline and shortened survival.⁵ Around 10% of patients may also experience acute exacerbations, often recognised by worsening breathlessness, leading to poor outcomes with mortality of over 60% during admission to hospital and over 90% within 6 months of discharge (**Figure 3**).^{3,15,16}

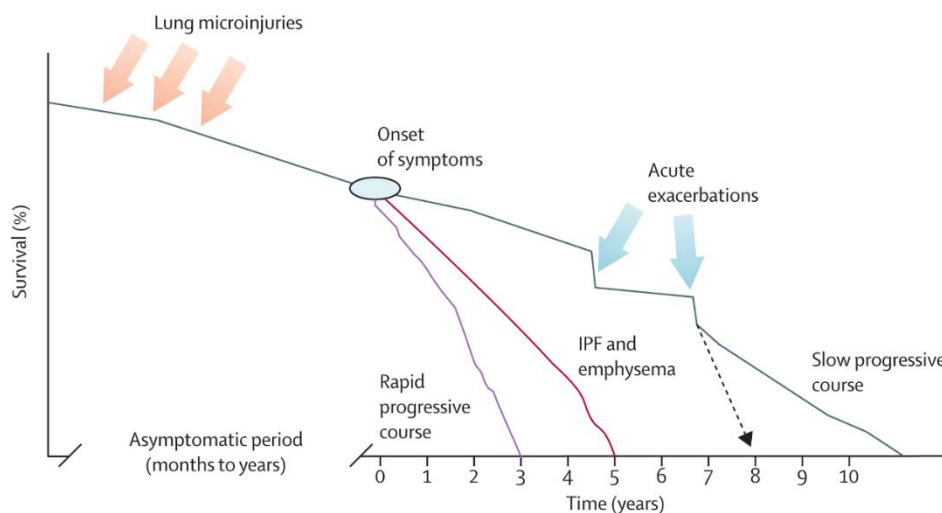


Figure 3: Schematic showing the different rates of progression of IPF, from King *et al.*⁵ The disease can start years before symptoms develop, possibly followed by slow decline (blue line). Some patients may show rapid decline (purple line), leading to shorter survival times. Patients with both emphysema and IPF may also have reduced survival compared to patients with IPF alone (red line).⁵

1.1.2 Current treatments for IPF

There are currently two approved treatments for IPF: nintedanib (**1**, Boehringer Ingelheim) and pirfenidone (**2**, Roche) (**Figure 4**).^{10,17} Both are orally administered compounds and have been shown to slow the progression of the disease, but neither halts or reverses the progression and both have gastrointestinal side effects.^{7,9,18,19}

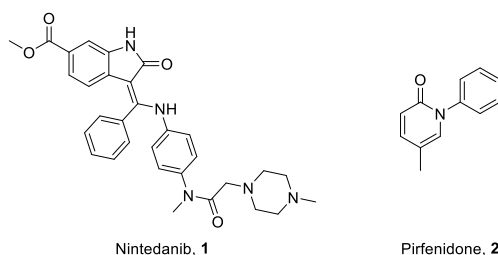


Figure 4: The chemical structures of two approved IPF therapies, nintedanib (**1**) and pirfenidone (**2**).

The exact mechanism of action of pirfenidone is not known but it has been shown to reduce disease progression compared to a placebo.¹ Nintedanib is a multiple tyrosine kinase inhibitor; the exact mechanism of action however was unclear when it was approved.²⁰ Rangarajan *et al.* have subsequently shown that nintedanib inhibits transforming growth factor β (TGF β) signalling (as well as having other effects) and this may lead to its ability to slow the progression of IPF.²⁰ The best existing treatment option for IPF patients is lung transplantation, but donor lungs are limited and the procedure is only possible for a small number of patients.⁷ Additionally, even with a transplanted lung, patients survive only an average of 3 years post-transplant.^{7,21}

1.1.3 Normal wound healing and the pathway leading to IPF

While the precise details of the process leading to the development of IPF remains unknown, the understanding of the mechanism has progressed in the last 20-30 years.^{17,22} It is believed that IPF is caused by unencumbered activation of multiple pathways involved in wound healing.²² Normal wounds bleed and this enables various cells (including platelets) and proteins (such as fibrin) to access the site of injury, enabling blood clotting.²³ Platelets contain various factors, including TGF β , which initiate the wound healing process by recruiting fibroblasts, endothelial cells and macrophages to the site of injury.²³ Once at the site of injury, fibroblasts proliferate and transform into myofibroblasts, the effector cell in fibrosis (and wound healing).^{22,24} In response to activation by TGF β , myofibroblasts synthesise extracellular matrix (ECM) and secrete collagen, one of the main fibrous ECM proteins.^{22,23,25} Once the wound is healed, fibroblasts undergo apoptosis and the ECM is broken down, leading to wound contraction.^{22,26}

Fibrosis can develop if any stage of the wound healing process is dysregulated, or if the lung continues to be damaged (for example by repeated microinjuries such as those caused by cigarette smoke¹⁰), leading to excess ECM deposition (including collagen secreted by fibroblasts in fibroblastic foci) and a permanent ‘fibrotic scar’.^{26,27} **Figure 5**, from a paper by Wynn, describes the process schematically.²⁶

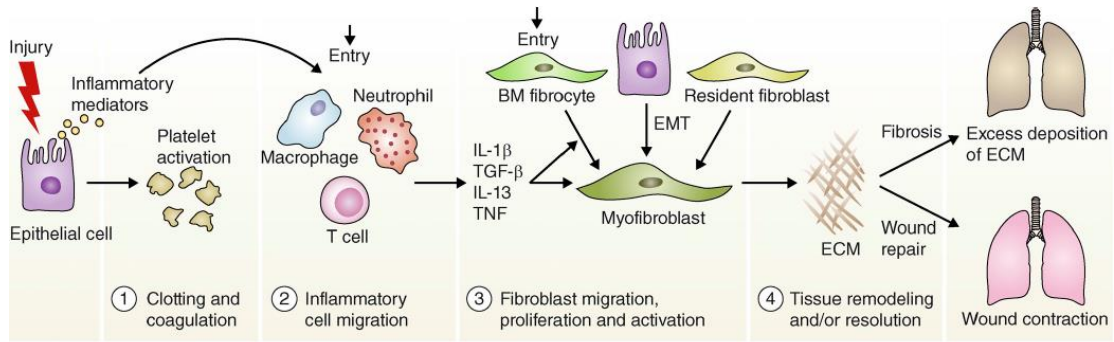


Figure 5: Schematic demonstrating disruption of normal wound healing and the possible development of IPF. The 4 main stages of wound healing: 1) clotting, 2) migration of inflammatory cells and secretion of profibrotic cytokines (IL-1 β , TNF, IL-13, and TGF β), 3) migration, proliferation and differentiation of fibroblasts into myofibroblasts and formation of ECM (note, fibroblasts and myofibroblasts may also be derived from epithelial cells undergoing epithelial-mesenchymal transition (EMT, when epithelial cells transform into fibroblast-like cells)) and 4) tissue remodeling.²⁶

Three mechanisms have been proposed as being responsible for accumulation of ECM and myofibroblasts in IPF (**Figure 6**):²⁴

- Inflammation and immune mechanisms (there is evidence that inflammation-related cytokines are implicated in profibrotic mechanisms; recently the inflammatory role in IPF has been disputed due to the lack of success of anti-inflammatory treatments).^{24,28,29}
- Oxidative stress (data suggest that there may be an oxidant/antioxidant imbalance in the lungs of IPF patients).
- Coagulation disruption (evidence suggests that there is an imbalance of procoagulant in the lungs of IPF patients).

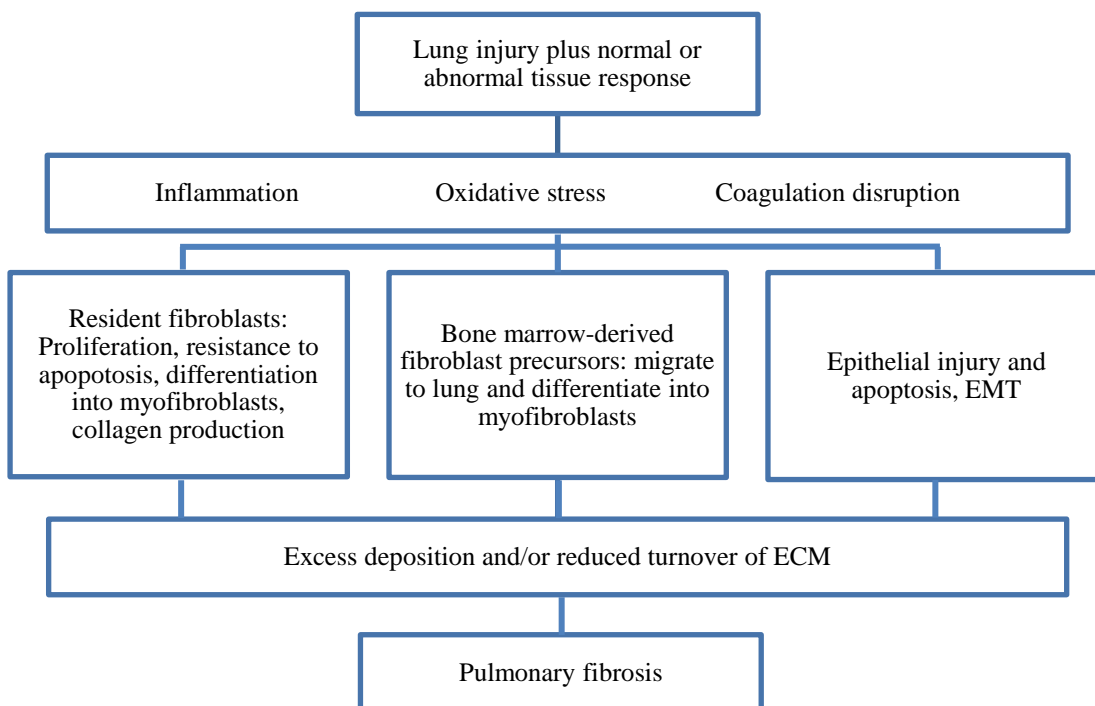


Figure 6: Schematic representing three broad mechanisms proposed to lead to IPF, based on a figure by Todd *et al.*²⁴

It is suspected that there is significant interplay of these three factors in patients with IPF. Despite efforts to develop treatments, the two approved therapies for IPF only slow disease progression. Combined with the recent suggestion that the prevalence of IPF has increased,³⁰ this demonstrates a clear need for a treatment that will halt the progression of IPF.

1.2 Comparison of the properties of oral and inhaled drugs

In the drug discovery process, lead optimisation involves making incremental changes to the structure of a lead compound or series to identify a molecule that has, or exceeds, the target profile for the drug candidate. To do this, a compound must be designed with the desired balance of affinity, efficacy, selectivity, ADME (absorption, distribution, metabolism and excretion) and physicochemical properties, and must have the lowest possible predicted clinical dose. This stage in the drug discovery process aims to generate a pre-candidate compound that, through further work including additional safety studies, will be developed into a clinical candidate that will progress through clinical trials to become a successful drug.

Broad rules or guidelines for drug discovery have been suggested – most famously in the Lipinski Rule of Five. Lipinski derived an empirical set of ‘rules’ of target properties optimal for oral absorption based on calculated property distributions of compounds taken into Phase II clinical trials.³¹ Key properties highlighted as leading to poor permeability and absorption were lipophilicity ($\text{LogP} > 5$), the number of hydrogen bond donors (> 5) and acceptors (> 10) and molecular weight (> 500).³¹

The original objective of the current study was to develop an orally administered treatment for IPF. However, this objective was subsequently changed, and an inhaled treatment was preferred. Topical delivery allows the therapeutic agent to be delivered directly to the site of action. However, a large portion of the dose (40-90%) is swallowed after inhalation and, if available for systemic absorption, can lead to off-target effects.³² It is therefore desirable for an inhaled compound to have low oral bioavailability. If this is the case, the inhaled delivery method may avoid systemic effects and reduce the problem of off-target activity.³³⁻³⁵ Another proposed advantage of inhaled delivery is that many of the usual physicochemical restraints on drug structure dictated by oral absorption (such as those outlined in the Lipinski Rule of Five) can be avoided, suggesting that the drug discovery process for an inhaled drug may be faster than for an oral drug.³⁴ However, the drug development process including formulation, obtaining a suitable crystalline form and developing a suitable device can be more challenging for an inhaled compound.³⁴

Analysis of the physicochemical properties of marketed inhaled drugs have been carried out and comparisons drawn to the Lipinski Rule of Five for oral drugs.^{34,35} One study found that inhaled or intranasal drugs may have higher numbers of hydrogen bonds/greater polarity and corresponding reduced lipophilicity compared to oral drugs.³⁴ However, many inhaled drugs do adhere to the Lipinski Rule of Five.³⁵ It is not fully understood if this is due to drugs initially developed as oral compounds being repurposed for inhaled delivery, or if compounds outside of the Lipinski Rules are not considered for inhaled drugs.^{34,35} There is a suggestion that the Lipinski Rules may be too restrictive for inhaled delivery and intentional violation may offer a benefit if, when the inhaled drug is swallowed, the compound is less orally available, potentially limiting systemic exposure.^{34,35}

A common goal in the design of an inhaled compound is achieving duration of action. Ideally, duration of action should be due to pharmacodynamic effects (such as interactions with the receptor leading to slow off rates) but this can be hard to design into a compound.^{33,34,36} Duration of action can also be driven by the compound physically remaining in the lung for longer, for example by slowing its absorption from the lung.^{33,34} This can be achieved through modification of the physicochemical properties of a compound, for example by increasing the molecular weight or reducing lipophilicity.^{34,37} Retention can also be driven through slow dissolution but this can increase the risk of adverse effects such as macrophage toxicity.³³ Guidelines for inhaled compounds have been developed in our laboratories and classes of compounds identified, based on permeability (in the Madin-Darby canine kidney (MDCK) permeability assay) and solubility levels:³³

1. High solubility (> 250 µg/mL), high permeability (MDCK permeability > 100 nm/s).
2. High solubility, moderate permeability (MDCK permeability 10-100 nm/s).
3. Moderate solubility (10-250 µg/mL), high permeability.
4. Moderate solubility, moderate permeability – tolerated but can carry some risk of macrophage toxicity.

This can also be represented as a plot of solubility against permeability, leading to a 9-box model (**Figure 7**):³³

- Green boxes: compounds are in class 1 above; these compounds are least likely to exhibit macrophage toxicity. If a compound has high solubility, a range of permeabilities are tolerated.
- Yellow boxes: compounds are in classes 2-4 with combinations of moderate solubility and moderate or high permeability to ensure the compound can leave the cell, mitigating the risk of macrophage toxicity.
- Red box: poorly soluble and poorly permeable compounds, known to lead to macrophage toxicity.

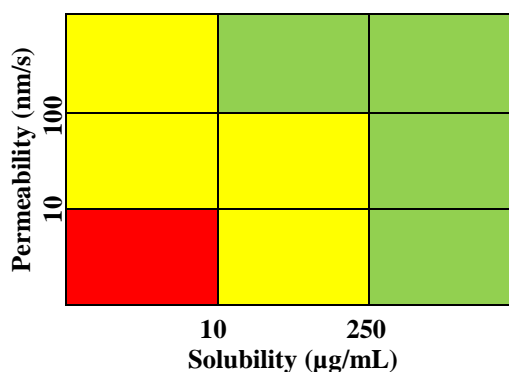


Figure 7: The 9-box model developed in our laboratories to demonstrate the desired property space (green) for inhaled drugs.³³

Inhalation of solid particles leads to a normal, reversible macrophage response but the point at which the physiological response becomes an irreversible problem is not clearly defined.³⁸ Macrophages are known to play a key role in removal of particulates from the lungs and can therefore be activated in response to the inhalation of medicines.³⁸ Responses include increased numbers and becoming ‘foamy’ – the macrophage is enlarged and has a granulated appearance when viewed under a light microscope.³⁸ Foamy macrophages, combined with additional effects such as inflammation, suggest the compound may exhibit macrophage toxicity.³⁸ One way to mitigate the risk of macrophage toxicity is by avoiding solid compound remaining undissolved in the lung, therefore low solubility and low permeability compounds would not be developable.

In this research, to achieve a candidate-quality inhaled compound, a wide range of solubilities and permeabilities were targeted in order to gain an understanding of what properties were required to drive lung retention. The only area of the 9-box plot that was not considered was the low solubility, low permeability space (red) to avoid macrophage toxicity.

Ion class has also been shown to influence lung retention and zwitterionic, neutral and acidic compounds have shorter half-lives than mono or dibasic compounds.³⁹ Bases have higher affinity for tissues and this leads to higher lung concentrations relative to plasma.³⁹ This has been noted for several basic compounds, suggesting that increasing basicity may be a strategy for increasing lung retention and duration of action.³⁹ Additionally, dibasic compounds have been shown to exhibit improved lung retention,

but the precise pK_a requirements of each of the basic centres has not been defined.^{39,40} Lysosomal trapping has been proposed as an explanation for the increased half-life of basic compounds, occurring as a result of the pH difference between lysosomes (pH 5) and cytosol (pH 7.2).³⁹ One study reported that dibasic compounds demonstrated ‘surprisingly long’ half-lives.⁴⁰ This was hypothesised to be due to trapping of the dication in lung lysosomes while the monocation was membrane permeable. The rate of the monocation leaving the lysosome, and subsequently the half-life, is therefore related to the pK_a of the second basic centre and to the lipophilicity of the compound.⁴⁰ The more lipophilic the compound, the higher the membrane permeability; therefore the longest lung retention is seen for polar dibasic compounds.⁴⁰ However, driving lung retention through basicity and lysosomal trapping is only attractive if the compound is still available at sufficient concentrations in the lung to be efficacious.³⁹ Additionally, highly basic compounds can lead to phospholipidosis risks, so in this project a range of moderately basic compounds were considered.⁴¹

1.3 mTOR kinase (FRAP) and IPF

mTOR, the mechanistic target of rapamycin, is so named because it was first found to be inhibited by rapamycin, a polyketide natural product (macrolide) produced by bacteria.⁴² mTOR belongs to a group of serine/threonine protein kinases: the Class IV phosphoinositide 3-kinases (PI3K) of the PI3K family, also known as the phosphoinositide kinase related kinases (PIKKs).^{27,43,44} The PI3Ks are a family of 15 lipid kinases, enzymes that catalyse the phosphorylation of phosphatidylinositol, as well as other processes, with varied roles in cell survival, proliferation and metabolism.⁴⁴⁻⁴⁷ There are four Class I isoforms of PI3K: PI3K α , PI3K β , PI3K γ and PI3K δ , each of which is a heterodimer made up of a catalytic (p110 α , p110 β , p110 γ and p110 δ) and a regulatory subunit.⁹ The Class IV isoforms, including mTOR, are lipid-like kinases related to the PI3Ks (lipid kinases) but their role is to phosphorylate protein substrates.^{42,48} Other Class IV PI3Ks include ATM (ataxia telangiectasia mutated), ATR (ATM and RAD3-related) and DNA-PK (DNA protein kinase, required for repairing DNA damage such as strand breaks).^{44,49}

Kinases catalyse the transfer of a phosphate group from ATP to a variety of substrates. Therefore all kinases have an ATP-binding site. mTOR is an atypical serine/threonine

protein kinase and interacts with several proteins to form two distinct complexes: mTOR complex 1 (mTORC1) and mTOR complex 2 (mTORC2).⁴² Both mTORC1 and mTORC2 are large complexes made up of six and seven known protein subunits respectively, four of which are the same, including scaffold proteins and the catalytic mTOR subunit.⁴² The catalytic subunit of the mTOR kinase domain is known as FKBP-12-rapamycin associated protein (FRAP), also called mTOR kinase and is conserved in both mTORC1 and mTORC2.^{42,50} Each of the two mTOR complexes occupy different places in the cell signalling pathway and have different up- and downstream effects (**Figure 8**).⁴² mTORC1 responds to a remarkable number of stimuli, including stress, oxygen and growth factors and is sensitive to rapamycin (an allosteric inhibitor) whereas mTORC2 is only known to be responsive to growth factors.^{27,42} mTORC1 has been shown to regulate a remarkable number of downstream functions including both protein production and synthesis of lipids required for cell membranes, thus regulating growth.⁴² Additionally mTORC1 regulates autophagy, a process required for recycling cell components, important in adaptation to reduced nutrient levels.⁴² Less is known about mTORC2 which is generally thought to be rapamycin insensitive, although recent evidence suggests that prolonged treatment with rapamycin may reduce mTORC2 signalling in some cell types.^{42,51,52} mTORC2 activates Akt (another serine/threonine protein kinase, also known as protein kinase B (PKB))⁴⁴ through phosphorylation (to form phosphoAkt (pAkt)) and Akt regulates several cellular processes such as growth, proliferation and apoptosis.^{42,53} The role of mTORC2 in proliferation and survival continues to be researched.⁵⁴ An ATP-competitive active site in mTOR has been reported and ATP-competitive mTOR kinase inhibitors that block both mTORC1 and mTORC2 are known.²⁷

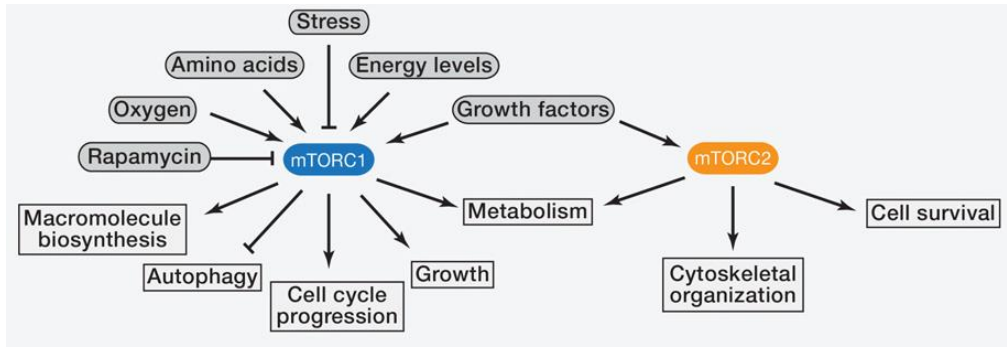


Figure 8: Demonstrating the different roles of the two mTOR complexes, how they interact and what stimuli they respond to.⁴²

Figure 9 (below) shows the signalling pathway of the Class I PI3K isoforms, mTORC1, mTORC2 and many other proteins that contribute to downstream functions including cell growth, proliferation and survival.⁵⁵

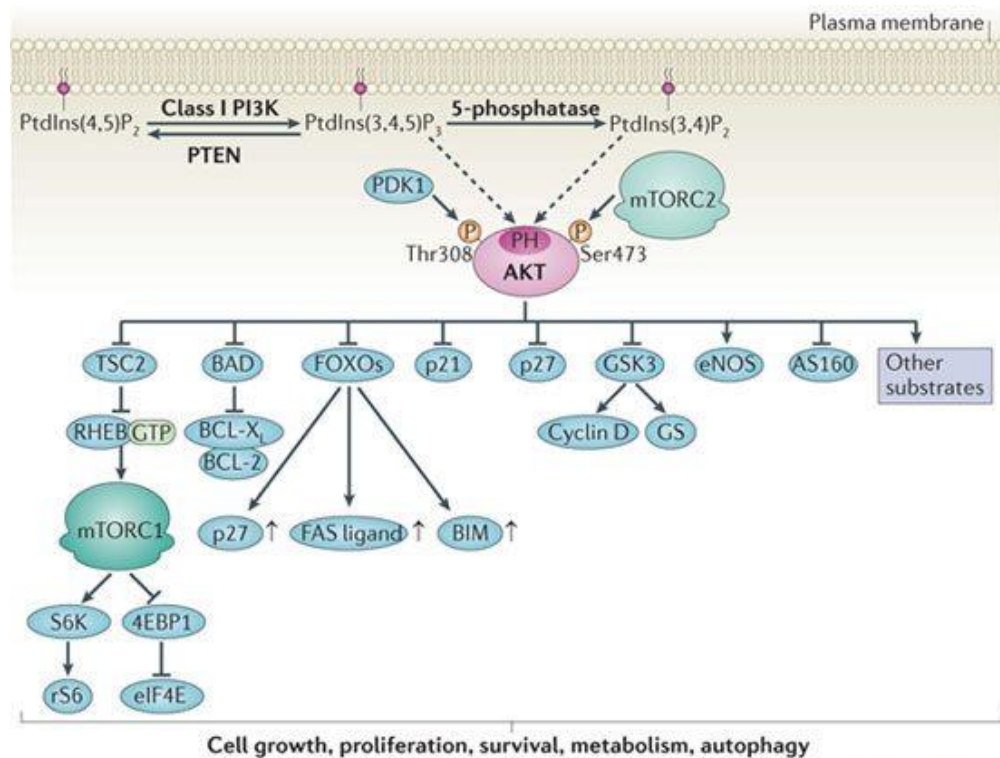


Figure 9: The interaction of several proteins including mTOR and the PI3Ks lead to a variety of downstream effects.⁵⁵

Due to the varied roles of both the Class I PI3Ks and mTOR, the PI3K/mTOR pathway is believed to be dysregulated in several diseases including cancer, type 2 diabetes, and IPF.^{9,28,38,44,45,53} Abnormal activation of the PI3K/mTOR signalling pathway is involved in the formation of human tumours and is one of the most frequently activated

pathways in cancer.^{56,57} Recently, parallels between IPF and cancer including similarities in genetic changes, activation of certain cell-signalling pathways and delayed apoptosis have been recognised.^{58,59} As in oncology patients, IPF patients have been reported to have increased uptake of glucose in their lungs (shown in PET studies using ¹⁸F-fluorodeoxyglucose).^{58,60}

The antifibrotic effect of a pan PI3K-mTOR inhibitor, originally developed for oncology, has been demonstrated, prompting the suggestion that compounds developed for cancer indications could be repositioned as IPF treatments.^{9,58} Indeed, nintedanib (**1**, **Figure 4**) was originally developed as an anticancer treatment.^{9,61} Activation of the Class I PI3Ks has been shown to lead to TGFβ-induced proliferation and differentiation of fibroblasts.⁶² Additionally, there is evidence to suggest that the Class I PI3K isoforms, particularly PI3Kγ, are upregulated in IPF tissue.⁶² Dual PI3K/mTOR inhibition has been shown to lead to attenuation of TGFβ-induced collagen production in IPF fibroblasts.⁵⁸ There is also limited evidence to suggest that selective mTOR inhibitors exhibit antifibrotic effects.²⁷ However, a selective mTORC1 inhibitor (a derivative of rapamycin) failed in an IPF clinical trial,⁶³ suggesting that inhibition of mTORC1 in isolation is not sufficient.²⁷ Selective inhibition of mTORC1 is proposed to activate mTORC2 and thus activate Akt.⁶⁴ This has led to the suggestion that mTORC2 has a critical role in fibrosis.²⁷ It has been proposed that dual mTORC1 and mTORC2 inhibitors may be appropriate as treatments for IPF as mTOR is believed to be involved in many stages of the disease progression.^{27,54} Several ATP-competitive mTOR kinase inhibitors have been demonstrated in the literature, often as anticancer treatments (**3-6**, **Figure 10**).²⁷ Due to the importance of mTOR kinase (FRAP) as a target for anticancer treatments, much research has been carried out to establish structure activity relationship (SAR) profiles as ATP-competitive mTOR kinase inhibitors share many common features such as the core, hinge group, back pocket group and ribose-binding region group (**Figure 10**, box).⁶⁵⁻⁷³ The core is often a substituted monocyclic or bicyclic heteroaromatic ring. One ring is often a pyrimidine, with either a 5- or 6- membered ring adjacent. The main role of the core is to control both the vectors of the substituents and the overall electronics of the compound.

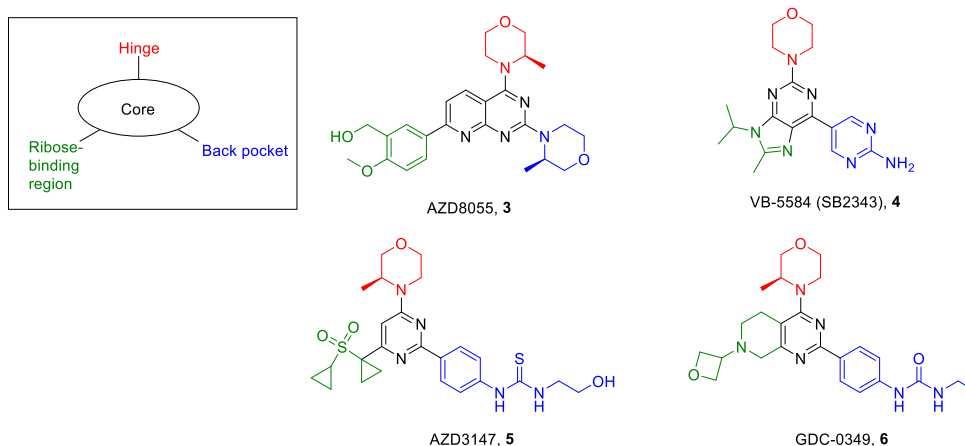


Figure 10: Demonstrating the common core (black), hinge group (red), back pocket group (blue) and ribose-binding region (green) of several published mTOR inhibitors. AZD8055 (**3**),^{66,67} VB-5584 (SB2343, **4**),^{65,69} AZD3147 (**5**)⁷⁰ and GDC-0349 (**6**).⁷¹

Kinases predominantly use ATP as the phosphoryl group donor and therefore have structurally similar active sites.⁷⁴ **Figure 11** exemplifies some of the key interactions of ATP in the PI3K γ active site.⁷⁵ The hinge region is a key recognition motif, forming a hydrogen bond between the adenine pyrimidine and valine 882 in PI3K γ .^{74,75} The polar phosphate residues interact with water molecules in a hydrophilic region not often exploited by ATP-competitive PI3K inhibitors.⁷⁵ Opposite the ribose-binding region, there is a hydrophobic region (near the adenine binding area) and many ATP-competitive PI3K inhibitors extend further into this region than ATP itself.^{74,75}

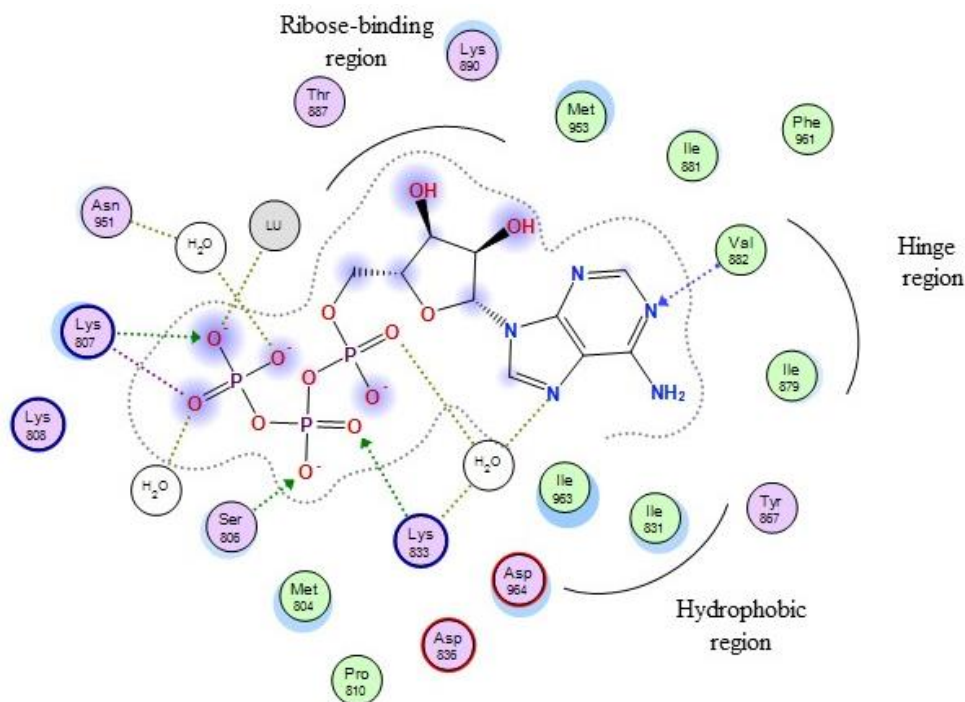


Figure 11: ATP in the active site of PI3K γ , adapted from crystal structure by Walker and co-workers (PDB code 1E8X).⁷⁵

The size of the mTOR complex (approximately 280 kDa) has hindered structural analysis but a truncated version of the complex has been crystallised in the presence of ATP inhibitors.⁷⁶ This low-resolution (3.2 Å) truncated crystal structure consisted of two of the mTOR complex subunits: mTOR kinase and mammalian lethal with SEC13 protein 8 (mLST8).⁷⁶ Additionally, binding models of small molecule ATP-competitive inhibitors in the mTOR kinase active site have been proposed (**Figure 12**).⁷⁷ Two key regions have been identified: a hinge region, so called because it typically sits between two protein domains and allows them to move relative to each other; and a hydrophobic pocket (or back pocket), so called because typically the binding site is viewed from the solvent-exposed region and the hydrophobic pocket is at the back. Docking studies suggest that small molecules (such as compounds **3-6**, **Figure 10**) form key hydrogen bonding interactions with the hinge region of the protein (and therefore the area in the compound forming this interaction is referred to as the hinge group), while forming additional hydrogen bonds with acid moieties in the back pocket region (formed with a lipophilic part of the molecule, here referred to as the back pocket group). The back pocket group is frequently a hydrophobic aromatic (or heteroaromatic) group, often elongated into a urea. Both the hinge and back pocket

groups are essential to achieve affinity and selectivity for mTOR over other related kinases.^{44,77} The ribose-binding pocket, so called because it accommodates the ribose of the natural substrate (ATP) and solvent exposed area in the active site are reported to be occupied by ‘other parts of the molecule’ (here referred to as the ribose-binding region group).⁷⁷ This suggests that the exact requirements of the substituent are not known, perhaps providing rationale for the variety in this region seen in the structures of known mTOR kinase inhibitors. This region may provide adequate space for a variety of groups that could be used to control physicochemical properties of compounds as well as add additional selectivity and affinity.⁷⁷

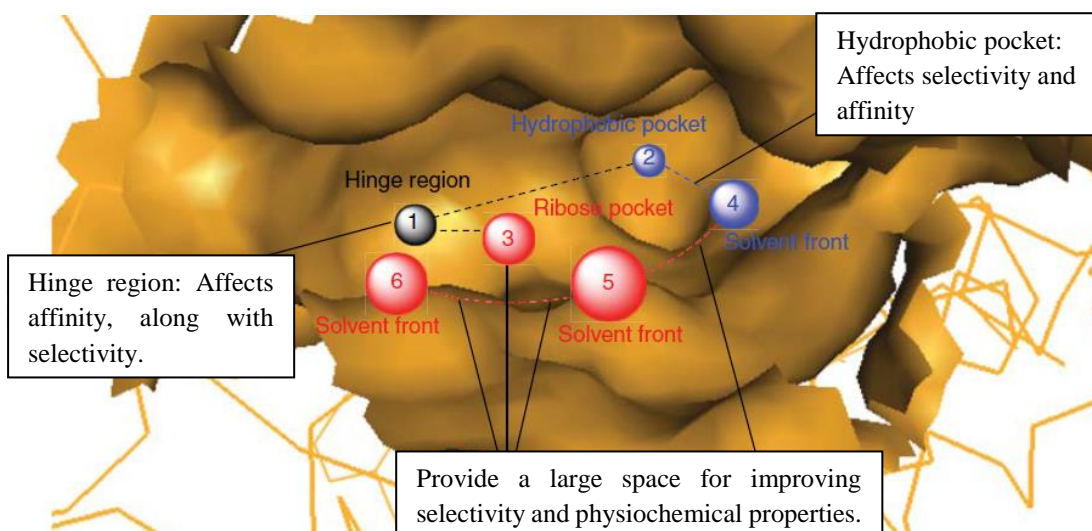


Figure 12: Hypothetical model of the mTOR kinase active site demonstrating the key regions. 1) The hinge region; 2) back pocket hydrophobic region; 3) ribose-binding region; 4-6) regions occupied by solvent.⁷⁷

GSK has demonstrated that GSK2126458 (**7**, **Figure 13**), a pan-PI3K/mTOR kinase inhibitor, attenuated TGF β -induced collagen production in IPF fibroblasts.⁵⁸ Pan-PI3K/mTOR kinase inhibitors are known to have mechanism-based off-target toxicities, particularly in inducing apoptosis.^{58,78} In this study, GSK2126458 was shown to decrease the cell count, although not until the concentration was higher than that required to see antifibrotic effects (**Figure 13**).⁵⁸

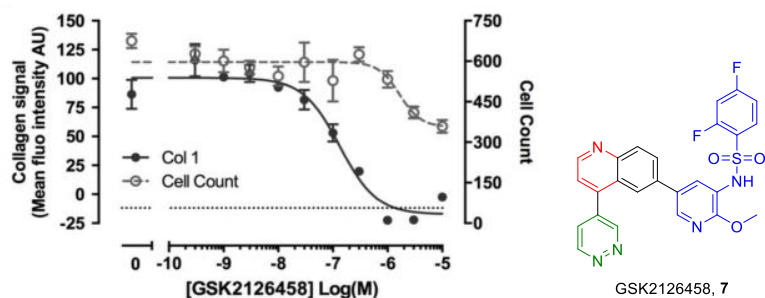


Figure 13: Demonstrating the dose-dependent antifibrotic effect of GSK2126458 (7), coloured by hinge group (red), ribose-binding region group (green) and back pocket group (blue).⁵⁸

Pan-PI3K-mTOR inhibitors such as GSK2126458 (7) inhibit the four class I PI3K isoforms as well as mTORC1 and mTORC2. It was proposed that a more selective inhibitor might improve the therapeutic index (TI – the ratio of the concentration of drug required to give a therapeutic effect to the concentration at which adverse effects are seen).^a Therefore, work was carried out as part of an unpublished study to identify which aspect of the pharmacology of this compound led to the antifibrotic effect.^{b,79}

The key outcomes of this study were as follows:

- Selective PI3K inhibitors (for each of the four different Class I PI3K isoforms: α , β , γ and δ) were found to have no effect on collagen deposition – this suggested that they are not of use as treatments for IPF.
- A pan-PI3K inhibitor without mTOR activity was found to have limited or no effect on collagen deposition, suggesting that combined inhibition of all the Class I PI3K isoforms was unlikely to interfere with the production of collagen.
- A selective mTOR kinase inhibitor was shown to exhibit antifibrotic effect, without causing apoptosis – the cell count remained the same at all concentrations of the inhibitor.

^a Inhaled FRAP1 (mTOR Kinase) Programme Executive Summary, S. Peace, 2015.

^b Investigations carried out in our laboratories by several scientists in the Fibrosis and Lung Injury (FLI) DPU and Computational Chemistry including; N. Anderson, G. Bravi, H. Hobbs, G. Inglis, P. Lukey, C. Luscombe, C. Nanthakumar, S. Pal, S. Peace, J. Redmond, J. Simpson, S. Swanson. The work referred to here was carried out by FLI DPU chemists including G. Inglis, S. Peace and J. Simpson, 2012.

The selective mTOR kinase inhibitor used (**8**, **Figure 14**) was originally developed as an anticancer treatment by Cellzome (a company acquired by GSK).^{68,72} This work provided evidence to suggest that a selective mTOR kinase inhibitor may be able to halt the progression (deposition of collagen) of IPF, without causing cell death.^c

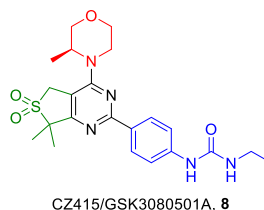


Figure 14: A selective mTOR kinase inhibitor CZ415/GSK3080501A (**8**), coloured by hinge group (red), ribose-binding region group (green) and back pocket group (blue).

With this knowledge in hand, chemistry was initiated in our laboratories to develop a novel, potent and selective small molecule inhibitor of mTOR kinase.

1.4 Biological and physicochemical assays to determine affinity, efficacy, selectivity and physicochemical properties of mTOR kinase inhibitors

This Section outlines the *in vitro* biological and physicochemical assays used to assess compounds made in this project and enable compound progression. In each of the biological assays, the pIC₅₀ – the log of the concentration at which half maximal inhibition is achieved – is reported. The assays were performed elsewhere in our laboratories.

1.4.1 Assays to measure the affinity and efficacy of mTOR kinase inhibitors

The primary assay used in this project was the mTOR kinobead (KB) assay. This was a disease-relevant biochemical affinity assay, used to assess the mTOR affinity of a compound. This chemoproteomic assay used full-length native mTOR protein to provide a more physiologically relevant assessment of compound binding than assays using recombinant proteins.⁸⁰ The mTOR KB assay was a competition binding assay, using endogenous mTOR from whole cell lysate (HuT-78 cells) that was competed for by immobilised kinase capturing beads (kinobeads) and the test compound.^{81,82}

^c Inhaled FRAP1 (mTOR Kinase) Programme Executive Summary, S. Peace, 2015; C. Nanthakumar, internal presentation, 2014; both unpublished GSK research.

Kinobeads are polymer beads, the surface of which contain broad-spectrum kinase inhibitors.⁸² The cell lysate was incubated in the presence of kinobeads and the test compound. After 2 hours the lysate was removed and the plates washed to remove any enzyme not bound to a kinobead. Any bound enzyme was then separated from the kinobead and transferred to a nitrocellulose membrane. After incubation with a primary anti-mTOR kinase antibody, a secondary anti-rabbit antibody coupled to an infra-red dye was added and the membrane scanned to quantify the amount of enzyme present. A potent mTOR kinase inhibitor would compete with the kinobead for the target enzyme in the cell lysate and little enzyme would remain bound to the kinobead after the initial incubation, leading to a reduced signal. **Figure 15** shows this process schematically.⁸¹

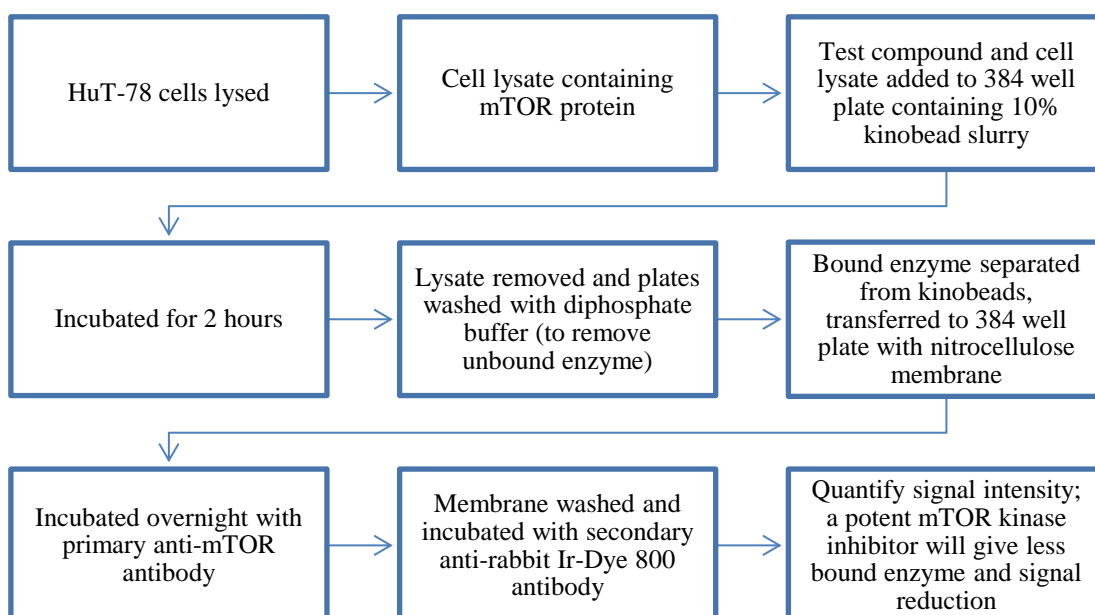


Figure 15: The mTOR KB assay protocol.⁸¹

The phosphoAkt (pAkt) assay, a cellular efficacy assay, was also used. The pAkt assay was not disease relevant as Akt inhibitors do not inhibit collagen deposition. However this assay provided information on the ability of a compound to cross the cellular phospholipid bilayer and interact with an intracellular target. Additionally, this assay was relevant to the signalling pathway. **Figure 9** showed the PI3K/mTOR/Akt cellular pathway: inhibition of mTORC2 (by the dual mTORC1/mTORC2 kinase inhibitors investigated here) will prevent phosphorylation of Akt. In this assay, the extent of

phosphorylation was measured, and the assay was used as a surrogate cellular assay for mTOR kinase inhibition. Human lung fibroblasts were used, as these cells were the intended site of action of the test compounds. The cells were dispensed onto a 384-well plate, treated with the test compound and incubated for 1 hour. Cell signalling lysis buffer was then added, to prevent any further phosphorylation of Akt. The cell lysate was transferred to a new plate for detection of both total Akt and phosphorylated Akt using antibodies. These antibodies were attached to electro-chemiluminescent labels (SULFO-TAG) that emit light when an electric current is applied, and this light emission was used to quantify the amount of phosphorylated Akt. A potent mTOR kinase inhibitor should prevent phosphorylation of Akt leading to reduced amount of pAkt and a weaker light emission. **Figure 16** shows the process schematically.^{83,84}

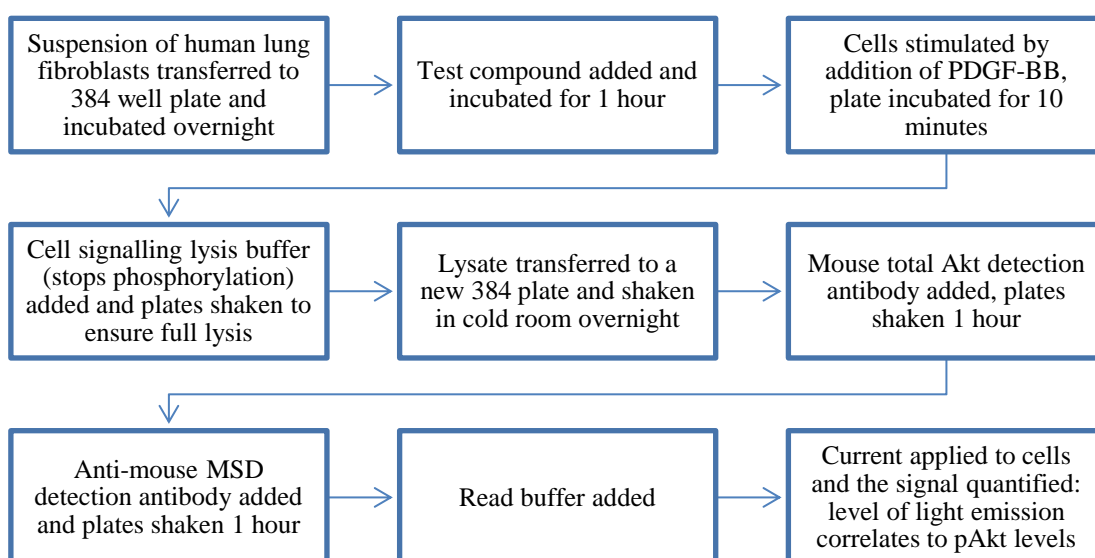


Figure 16: The pAkt assay protocol.⁸³

The third target-related assay was a cellular, disease-relevant efficacy assay with a fibrotic end point: the scar in a jar (SIAJ) assay. IPF is characterised by excessive collagen deposition and associated loss of lung function.^{85,86} The phenotypic SIAJ assay assessed the ability of a compound to reduce collagen production. The assay measured collagen deposits produced by cells in a macromolecular environment; FiColl (a hydrophilic polysaccharide) was added to mimic molecular crowding and accelerate deposition of mature collagen (mimicking the clinical disease).^{85,86} TGF β was used to stimulate the production of collagen in cultured fibroblasts (healthy or diseased), causing the fibroblasts to lay down mature collagen I. The amount of

collagen I produced was detected by immunocytochemistry and quantified with image algorithms using an INCell 2000.⁸⁶ The effect on collagen deposition upon dosing the lung cells with compounds at different concentrations was measured. This assay was not routinely in use throughout this project, so data were not always generated. **Figure 17** shows the process schematically.⁸⁶

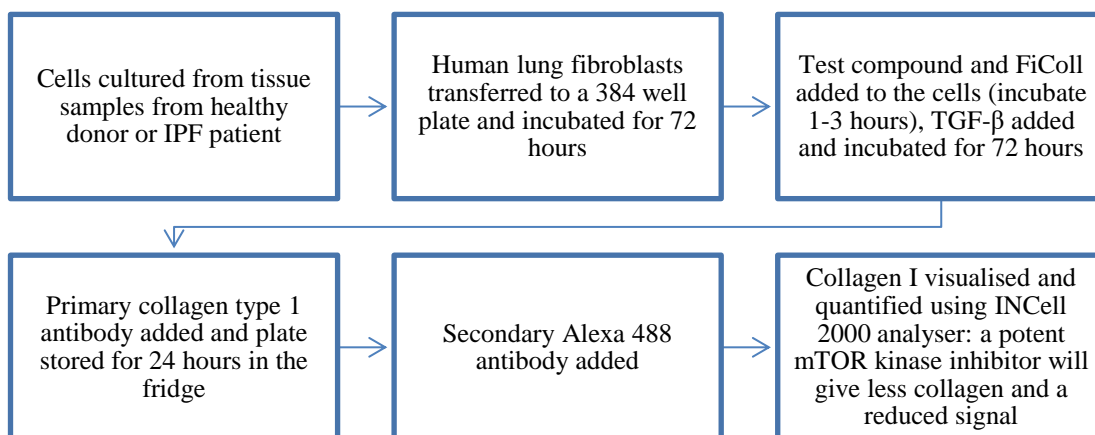


Figure 17: The SIAJ assay protocol.⁸⁶

1.4.2 Assays to monitor the off-target effects of mTOR kinase inhibitors

It was advantageous for compounds to be highly specific for mTOR kinase inhibition since off-target activity could lead to undesirable side effects. Therefore, the affinity of compounds for some closely related kinases was also routinely measured to give selectivity data.

To assess selectivity over the Class I PI3Ks (α , β , γ and δ), a time-resolved fluorescence resonance energy transfer (TR-FRET) assay was used. Class I PI3K enzymes use phosphatidylinositol 4,5-bisphosphate (PIP₂) to generate phosphatidylinositol 3,4,5-trisphosphate (PIP₃) in the presence of ATP (**Figure 9**). PIP₃ binds to the PH (pleckstrin homology) domain of GPR-1.⁸⁷ In this assay, the amount of PIP₃ produced was detected by displacement of a biotinylated-PIP₃ ligand from an energy transfer complex consisting of a Europium (Eu)-labelled anti-GST monoclonal antibody, a GST-tagged PH domain and Streptavidin-Allophycocyanin (APC, a fluorescent protein). In the absence of inhibitor, the PIP₃ formed by the action of the PI3K enzymes displaced the biotin-PIP₃ from the complex by binding to the Eu-labelled PH domain of GPR-1, and excitation of Eu with light of 330 nm led to

emission at 620 nm. If an inhibitor was present, the Eu-labelled anti-GST monoclonal antibody-GST-tagged PH domain-Streptavidin-APC complex was intact and Eu excitation at 330 nm caused an energy transfer to APC, which emitted light at 665 nm.⁸⁷ The assay was run with each of the PI3K α , β , γ and δ enzymes. **Figure 18** shows the process schematically.^{87,88}

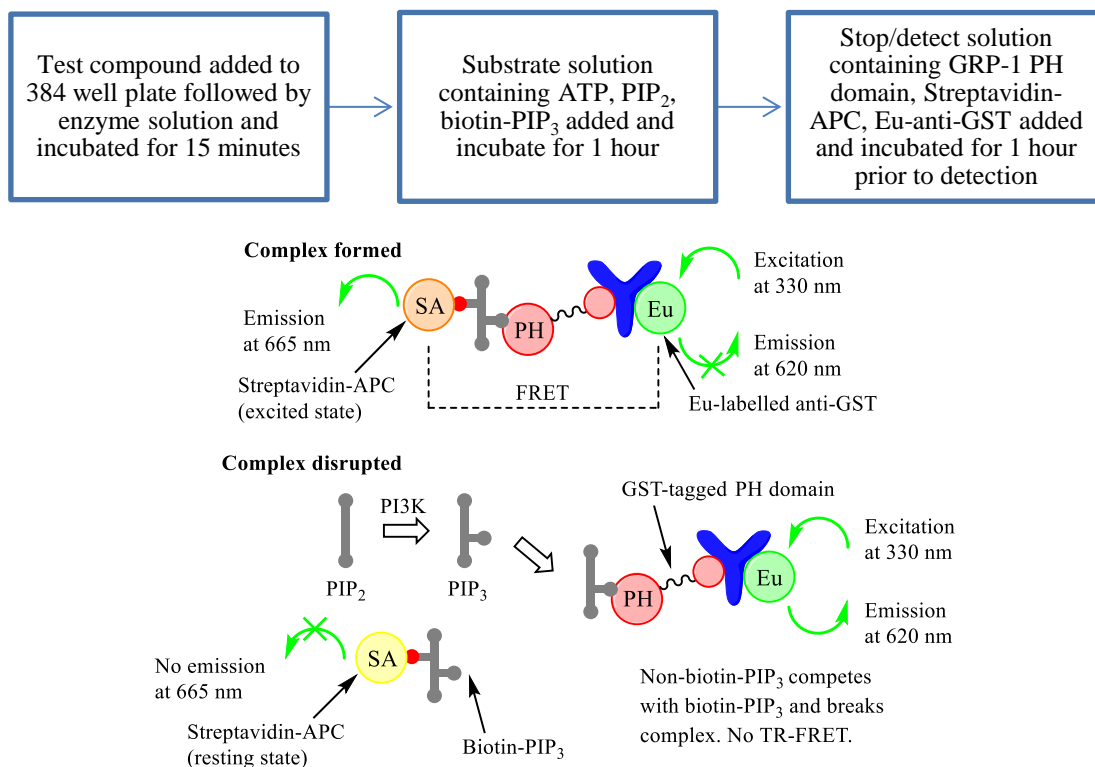


Figure 18: The PI3K assay protocol and schematic demonstrating the complex formed in the presence of a PI3K inhibitor (without PI3K activity). If no inhibitor is present, the naturally formed PIP₃ will compete with the biotin-PIP₃ for the PH binding site and give a reduction in signal.^{87,88}

Selectivity was also routinely assessed against DNA-dependant protein kinase (DNA-PK, a Class IV PI3K) which shares close homology with mTOR kinase, again using a TR-FRET assay. DNA-PK phosphorylates p53-peptide.⁸⁹ In the assay, in the presence of double stranded DNA, a synthetic fluorescein-conjugated p53-peptide was phosphorylated on serine-15 (to give phosphorylated-p53-peptide) which was detected by a terbium (Tb)-labelled anti-p53-peptide. Binding of fluorescein-conjugated phosphorylated p53-peptide to the Tb-antibody caused an energy transfer from terbium to fluorescein upon excitation with light at 337 nm. The ratio of fluorescein emission (530 nm) to terbium emission (492 nm) was proportional to the amount of

phosphorylated p53-peptide. Inhibition of DNA-PK enzyme activity by a test compound led to a reduction in the amount of phosphorylated-p53-peptide, leading to a reduction in the signal from the assay. **Figure 19** shows the process schematically.⁸⁹

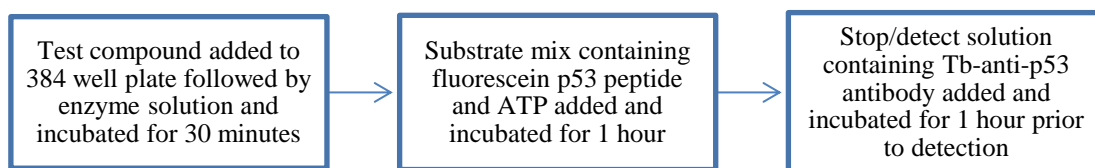


Figure 19: The DNA-PK assay protocol.⁸⁹

1.4.3 Physicochemical assays to determine the physicochemical properties of mTOR kinase inhibitors

In addition to achieving high affinity and efficacy and good selectivity, compounds must have the correct balance of physicochemical properties to ensure they reach the desired site of action. To assess these properties, compounds were evaluated in various physicochemical assays.

Solubility was evaluated in two assays measuring kinetic or thermodynamic solubility. Kinetic solubility was measured using either chemi-luminescent nitrogen detection (CLND) or charged aerosol detection (CAD) in high-throughput solubility assays.⁹⁰ The kinetic aqueous solubility of a compound from a DMSO solution into an aqueous buffer at pH 7.4 was determined by measuring the concentration of solute in solution after precipitation from a DMSO stock solution.⁹¹ This high-throughput measure of solubility was routinely measured for all compounds. Simulated lung fluid (SLF) solubility was measured in a lower throughput but more realistic assay to determine dissolution from a solid (ideally crystalline) sample into SLF, a buffer with an ionic composition similar to human lung fluid.^{92,93} SLF solubility values vary depending on the form of the compound. For example, if a compound was not crystalline, it was likely that a crystalline form of the compound would have lower SLF solubility. Additionally, different crystalline forms may have had different solubilities.

Permeability – a measure of the ability of a compound to cross the cellular phospholipid bilayer – was measured in two ways. A high-throughput artificial membrane permeability (AMP) assay used high performance liquid chromatography

(HPLC) to monitor the concentration of compound on either side of a membrane after three hours of incubation.⁹⁴ A lower-throughput but more realistic permeability assay, the Madin-Darby canine kidney assay (MDCK, a cell line derived from dog kidneys) was also used.⁹⁵

Lipophilicity affects a number of physicochemical properties including solubility and permeability. Furthermore, an increase in lipophilicity can favour the binding of drug compounds to an active site.⁹⁶ This leads to an increase in affinity and can lead to an increase in the promiscuity of compounds as their binding affinity for all proteins is increased. There are two measures of lipophilicity. LogP, reflects the molecular desolvation occurring when a compound transfers from aqueous solution to a cell membrane or a protein binding site, both of which are largely hydrophobic.⁹⁷ Specifically, P is the partition coefficient of the compound between 1-octanol and water and clogP is an *in silico* prediction of lipophilicity (**Equation 1**). If a compound can be ionised, logP will be reduced, leading to increased solubility and decreased permeability. Another measure of lipophilicity, logD, takes this ionisation into account. LogD is the ratio of the distribution of a solute between 1-octanol and a buffer solution of known pH, with D being the partition coefficient between 1-octanol and buffer (**Equation 2**).⁹⁸ In our laboratories, a chromatographic method (HPLC) was used to obtain measures of lipophilicity – ChromLogD.

$$\text{LogP} = \text{Log} \frac{\text{concentration of solute in 1-octanol}}{\text{concentration of solute in water}}$$

$$\text{LogD} = \text{Log} \frac{\text{concentration of solute in 1-octanol}}{\text{concentration of solute in buffer}}$$

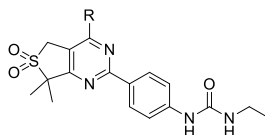
Equations 1 and 2: Different ways to quantify the lipophilicity of a compound.

1.5 Previous research from our laboratories to develop mTOR kinase inhibitors

Morpholine rings have been reported to be a hinge binder in both PI3K and mTOR inhibitors.^{45,99,100} An oxygen lone pair forms a key hydrogen bond to a Val2240 residue in the active site and removal of this oxygen by replacing morpholine with piperidine results in a reduction in affinity.^{99,101-103} Note, amino acid residues are numbered according to their positions in PI3K γ , Val882 in PI3K γ is Val2240 in mTOR.¹⁰³ In

addition to the requirement for a hydrogen bond acceptor in the hinge region, the orientation of the lone pair is important, requiring the correct conformation of the hinge group in order to achieve the desired interaction.

Modifications to the hinge group have been shown in the literature¹⁰³ and internally¹⁰⁴ to give increased affinity and selectivity for mTOR kinase over the Class I PI3K isoforms (**Table 1**). Exchanging the parent morpholine (**9**) for both of the 3-methylmorpholines (**8**, **10**) and either of the bridged morpholines (**11**, **12**), gave compounds of increased affinity (mTOR KB assay pIC₅₀ value). These morpholine modifications also gave more lipophilic compounds therefore lipophilic ligand efficiency (LLE, affinity corrected for lipophilicity (ChromLogD)) was used to enable comparison.¹⁰⁵ LLE is an estimate of how specifically a compound binds to the desired target relative to partitioning into 1-octanol (mTOR KB pIC₅₀ – ChromLogD).¹⁰⁵ Compounds **8** and **12** demonstrated the best balance of affinity and lipophilicity with improved LLE values compared to compound **9**. Conversely, compound **13** demonstrated no improvement in affinity and a higher lipophilicity (compared to compound **9**), resulting in a low LLE value. Compounds **8** and **9** demonstrated similar PI3K affinities. However, the increased affinity for mTOR kinase of compound **8** leads to the improved selectivity of this compound. The reduced PI3K affinities of compounds **12** and **13** suggested that the larger bridged morpholine or (*S*)-3-ethylmorpholine groups were not tolerated.



Compound Number	R	mTOR KB pIC ₅₀ (n) ^a	PI3K pIC ₅₀ (α,β,γ,δ)	Selectivity over PI3Ks	Chrom LogD ^b	LLE
9		7.1 (2)	5.2,4.7,5.2,4.5	>80	3.8	3.3
10		7.4 (2)	-	-	-	-
8		8.0 (21)	5.3,<4.8,5.1,5.0	>500	4.3	3.7
11		7.4 (2)	-	-	4.4	3.0
12		8.0 (2)	4.6,<4.5,4.5,<4.5	>2500	4.1	3.9
13		7.2 (2)	4.5,<4.5,<4.5,<4.5	>500	4.6	2.6

Table 1: Demonstrating the effect on affinity, selectivity, lipophilicity and LLE of changing the hinge group from morpholine to a substituted morpholine.¹⁰⁴ ^apIC₅₀ recorded as the mean of the data obtained on each of a number of test occasions (n). ^bChromLogD at pH7.4. < Affinity recorded was at the lower assay limit. - Data not generated. Affinity (mTOR KB pIC₅₀): < 7.0 = red; ≥ 7.0 = orange; ≥ 7.5 = green. Selectivity: < 100 = orange; ≥ 100 = green. Lipophilicity: ≥ 4 = orange; < 4 = green. LLE: ≤ 3.0 = red; < 3.5 = orange; ≥ 3.5 = green.

It was proposed that the increased selectivity over the Class I PI3K isoforms on modifying the hinge group was due to a difference of one amino acid between the mTOR kinase and PI3K active sites.¹⁰³ This amino acid difference (phenylalanine in the Class I PI3K isoforms, compared to leucine in mTOR kinase) makes the mTOR kinase active site slightly larger and able to accommodate ethyl (**13**), methyl (**8**, **10**) and bridged morpholine hinge groups (**12**, **13**).^{103,106} Additionally, the mTOR kinase active site is suggested to have a small hydrophobic pocket in the hinge region, formed by a tryptophan residue that is rigidly held in place (compared to a less rigidly held leucine residue in PI3Kγ).¹⁰⁷ This lipophilic pocket is proposed to be one of the reasons for the high affinity and selectivity seen for many 3-methylmorpholine hinge binders.¹⁰⁷

Due to the prevalence of morpholine-containing compounds in the mTOR kinase inhibitor literature,¹⁰⁸ investigations have been carried out to identify morpholine bioisosteres. Bioisosteres need to be able to make the same favourable hydrogen bonding interaction as morpholine and therefore require a hydrogen bond acceptor in the correct orientation. 3,6-Dihydro-2*H*-pyran (DHP) is a known morpholine bioisostere,¹⁰⁹ and gives compounds of similar affinity and selectivity (against the PI3Ks) to morpholine analogues.^{104,109} However, reduction of the DHP double bond to give the tetrahydropyran (THP) leads to a reduction in affinity at mTOR kinase.^{104,109} These findings were verified in our laboratories, demonstrated in simple monocyclic pyrimidines (**Table 2**). Exchanging morpholine (**14**) for DHP (**15**) was tolerated but THP (**16**) gave reduced affinity. Further research in our laboratories led to the discovery of a novel morpholine bioisostere: a cyclopropylpyran (CPP) ring (**17**) that can act as a hinge binder.^{104,110}

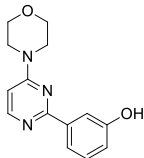
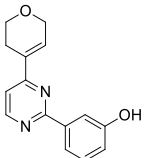
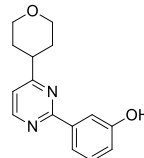
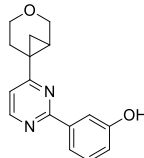
Structure				
Compound Number	14	15	16	17
mTOR KB pIC ₅₀ (n) ^a	5.9 (7)	5.7 (4)	4.5 (3)	4.8 (4)

Table 2: Comparison of affinities (mTOR KB pIC₅₀) in the mTOR KB assay for morpholine, DHP, THP and CPP (racemic) compounds.¹⁰⁴ ^apIC₅₀ recorded as the mean of the data obtained on each of a number of test occasions (n).

Both monocyclic (pyrimidine and triazine cores) and bicyclic mTOR kinase inhibitors are exemplified in the literature and have been developed in-house.^{66,68-70,111} In our laboratories mTOR kinase inhibitors with bicyclic, pyrimidine, pyridine and substituted pyridine cores were compared (**Table 3**).¹¹² Monocyclic pyrimidine compounds (**18**) were shown to have reduced affinity compared to bicyclic compounds (**8**) and this was proposed to be, at least in part, due to the decrease in size and lipophilicity. The reduction in affinity of pyridine compounds (**19**) compared to pyrimidines (**18**) was proposed to be due to the electronics of the core, and a subsequent investigation revealed that addition of either a directly-linked sulfone (**21**) or an amide (**22**) moiety to the pyridine ring restored the affinity.

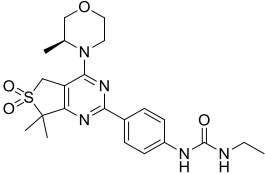
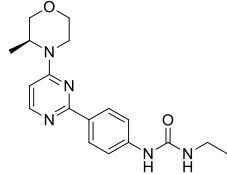
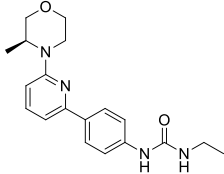
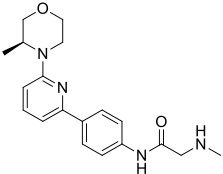
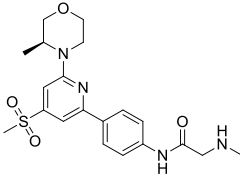
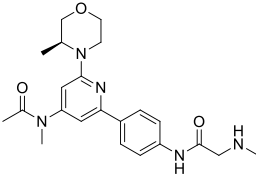
Structure			
Compound Number	8	18	19
mTOR KB pIC ₅₀ (n) ^a	8.0 (21)	6.1 (11)	< 5.0 (2)
Structure			
Compound Number	20	21	22
mTOR KB pIC ₅₀ (n) ^a	< 5.0 (2)	7.2 (4)	7.6 (2)

Table 3: Comparing the affinities (mTOR KB pIC₅₀) of bicyclic, pyrimidine and substituted pyridine cores. ^apIC₅₀ recorded as the mean of the data obtained on each of a number of test occasions (n). < Affinity recorded was at the lower assay limit.

The directly-linked sulfone and amide substituents have different electronics, suggesting that the increase in affinity may be due to an increased molar volume or 3D character in the ribose-binding region. This finding initiated further work in each of these series. Only the novel directly-linked sulfone series of mTOR kinase inhibitors (exemplified by compound **21**) will be discussed here.

Little was known about the SAR in the directly-linked pyridine sulfone series of compounds. Therefore, to explore the SAR and achieve compounds with increased affinity for mTOR kinase, an array of different sulfonyl pyridines was proposed. There are different ways to explore SAR:

- A standard array in which all possible combinations of compounds are made, ensuring all chemical space is explored. However, in an array exploring different vectors this requires a significant synthetic chemistry effort.
- A linear array in which one vector is explored at a time. For example, compounds are synthesised to explore region A, while the groups at positions B and C are fixed, followed by fixing positions A and C to explore position B, before exploring position C with the most active groups in positions A and B.

This approach may take longer to complete as data have to be generated on each set before the next set can be made. Additionally, not all of the chemical space will be explored and information may be missed.

- A sparse array: an innovative approach to explore chemical space, based on a similar concept to Design of Experiments (DoE).¹¹³

Here, a sparse array was considered to be an efficient way to explore the SAR of the ribose-binding region group and the different hinge and back pocket groups, without synthesising all possible combinations of compounds. DoE approaches are an established method of optimising multifactor reactions by exploring different combinations of variables, often used in development chemistry and manufacturing.¹¹³ For example, if a reaction yield could vary with temperature, number of equivalents of a reagent and concentration, a DoE approach could be used to simultaneously optimise for all of these factors. There are fewer examples of taking the same approach in lead optimisation in medicinal chemistry – using DoE-type approaches to ‘optimise’ for categorical (non-continuous) variables such as different substituents on a ring.¹¹³ The term ‘sparse array’ has been adopted within our laboratories for this type of experimental design. **Figure 20** provides a pictorial explanation of the three different approaches.

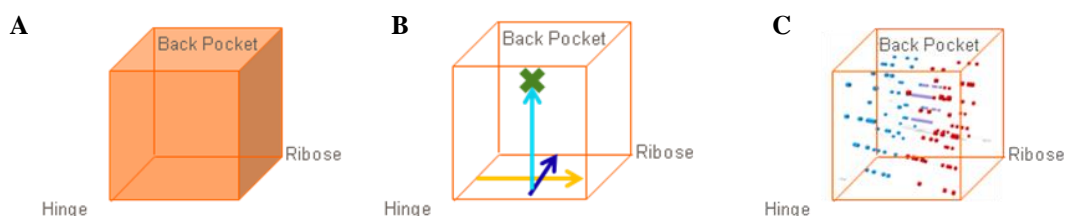


Figure 20: Pictorial representations of three approaches to exploring SAR. **A** and **B** are more traditional approaches in which all possible combinations of compounds are made by first intent (**A**) or just one vector is explored at a time (**B**). A sparse array can cover all of the ‘compound space’, without the need to synthesise every possible combination of compounds (**C**).

This is a non-traditional approach to medicinal chemistry, designed to make the process of drug discovery more efficient by minimising the number of compounds made and tested by better use of computer resources. In a sparse array, each possible substituent or monomer used in the array is treated as a categorical variable.¹¹³ From the set of possible combinations, a balanced fractional array design is generated.¹¹³

Once the compounds have been made and tested, the affinity values are analysed statistically to assess the additivity of the SAR, determine if the data are additive and the contribution each monomer has to the overall affinity or physicochemical properties (or other factor of interest) can be ascertained.¹¹³ Additivity in the data means that there is no interaction between the different substituents and that all contribute independently to the overall affinity of the compound.

The balanced fractional array design selected for use here considered making only a quarter of all possible compounds.¹¹⁴ In this compound set, there were four examples of each sulfone substituent and no matched pairs (two compounds differing in only one substituent). This led to sets of compounds that were ‘related’, not as matched pairs (‘siblings’), but as ‘cousins’. Setting out to make a quarter of the possible compounds meant that if some compounds could not be made, there would still be enough information gained from the array to develop SAR.

To develop a SAR profile for the sulfonyl pyridine series of mTOR kinase inhibitors, final compounds with a spread of affinities (not all clustered at high or low values) were required. This was controlled by the selection of both hinges and back pockets; of the four groups selected for each vector, three were known to give high affinity compounds and one was known to give compounds of lower affinity. Selection of the sulfone monomers was more involved. The proposed synthetic route used a sulfinic acid and 316 sulfinic acids or sulfinate salts were found to be commercially available. These sulfone monomers were enumerated with each of the four hinges and back pockets giving 6,320 compounds in total. The fully enumerated compounds were then analysed based on their predicted physicochemical properties. In particular, a lead-likeness multi-parameter optimisation (MPO) profile was used to score the compounds. The lead-likeness MPO score was developed specifically for this project to provide a summary of the quality of the compound with respect to the required properties.^d This was achieved by combining the key properties of interest and assigning the compounds a number between 0 and 1 based on the individual contributions. Properties considered included molecular weight, lipophilicity, number

^d Lead-likeness MPO developed by S. Swanson, 2015.

of hydrogen bond donors and acceptors, polar surface area, the number of rotatable bonds, hERG and PFI.^e A good property-space for these compounds was defined as a lead-likeness score of over 0.5. Structurally similar compounds may have a similar lead-likeness score. In order to target a wide range of sulfones, each sulfone monomer with a score of greater than 0.5 was considered by a team of medicinal chemists, who voted to determine which monomer should be included. While not necessarily the most scientific approach, it enabled the inclusion of a range of monomers and using a team of chemists avoided personal bias. This gave a set of 16 sulfone groups (**Figure 21**).

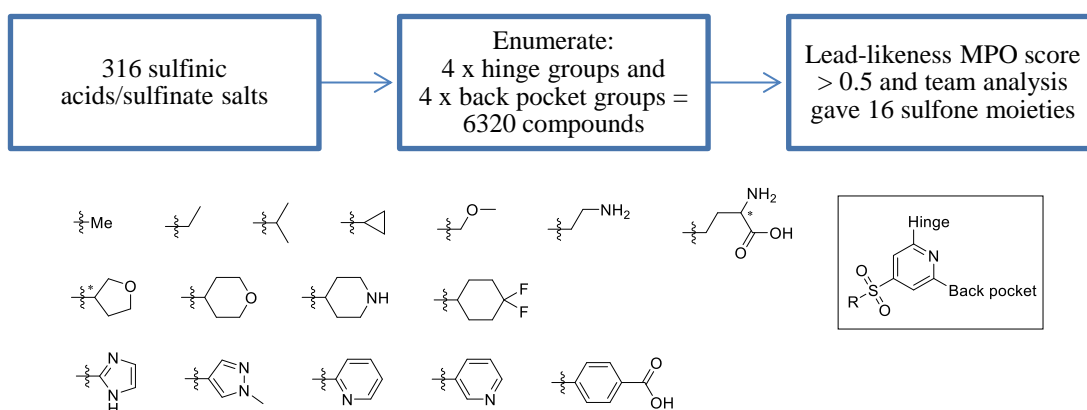


Figure 21: The selection process and 16 sulfone groups selected to be installed at the 4-position of the pyridine. *Racemic compounds.

Once the sulfone monomers had been selected, a quarter of the total 256 compounds were synthesised, the data generated and a Free-Wilson analysis – a mathematical way of describing SAR – was carried out.¹¹⁵ A Free-Wilson analysis gives a formula where y is the overall affinity, A is the average affinity and the coefficients a_1 , a_2 and a_3 are the contribution that monomer, x_1 , x_2 or x_3 , makes to the overall affinity of the compound (**Equation 3**).¹¹⁵ For example, when x_1 is a methyl group, the coefficient a_1 will be defined as whatever increase or decrease in affinity this substituent causes. Therefore, a mathematical relationship between the identity of a monomer at a specific position on the core and the affinity of the compound was developed.¹¹³ This analysis is based on the assumption that the individual contributions to the overall affinity made

^e Off target activity can lead to blocking the human Ether a go-go Related Gene (hERG) channel, causing cardiac problems so a hERG liability can make a compound unprogressable. Property forecast index (PFI = $\text{ChromlogD}_{\text{pH}7.4} + \text{number of aromatic rings}$) is related to solubility and permeability.

by substituents at different positions on a core are additive.¹¹³ In this project, a previous analysis had shown data generated in this directly-linked sulfone series to be additive.

$$y = A + a_1x_1 + a_2x_2 + a_3x_3$$

Equation 3: Formulae of the type generated in the Free-Wilson analysis.

A Free-Wilson analysis can be used in a predictive sense. Only a quarter of the total possible number of compounds were synthesised as part of the sparse array^f and the Free-Wilson analysis was used to determine what contribution each monomer (hinge, back pocket or sulfone R group) made to the affinity (the mTOR KB pIC₅₀) of the compound. This was then used to predict affinities of compounds that were not prepared. For example, if hinge A was predicted (on average) to add 0.5 of a log unit of affinity more than hinge B, and if a compound that originally had hinge B had an affinity pIC₅₀ of 7, then swapping to hinge A would, theoretically, give a compound with an affinity pIC₅₀ of 7.5.

A graphical visualisation of the output of the Free-Wilson analysis shows the average contribution to the affinity made by each of the hinge, back pocket and sulfone R groups, relative to the mean affinity value (**Figure 22**). Monomers can either have a negative or positive contribution to affinity, shown by their position above or below zero on the y axis. For example, of the back pocket groups, the glycinamide and methyleurea were both shown to have a positive contribution to affinity (relative to the average) and the indole back pocket had a negative contribution.

^f In reality, several compounds were made – not just the sparse set – but only the sparse set of compounds was considered in the Free-Wilson analysis.

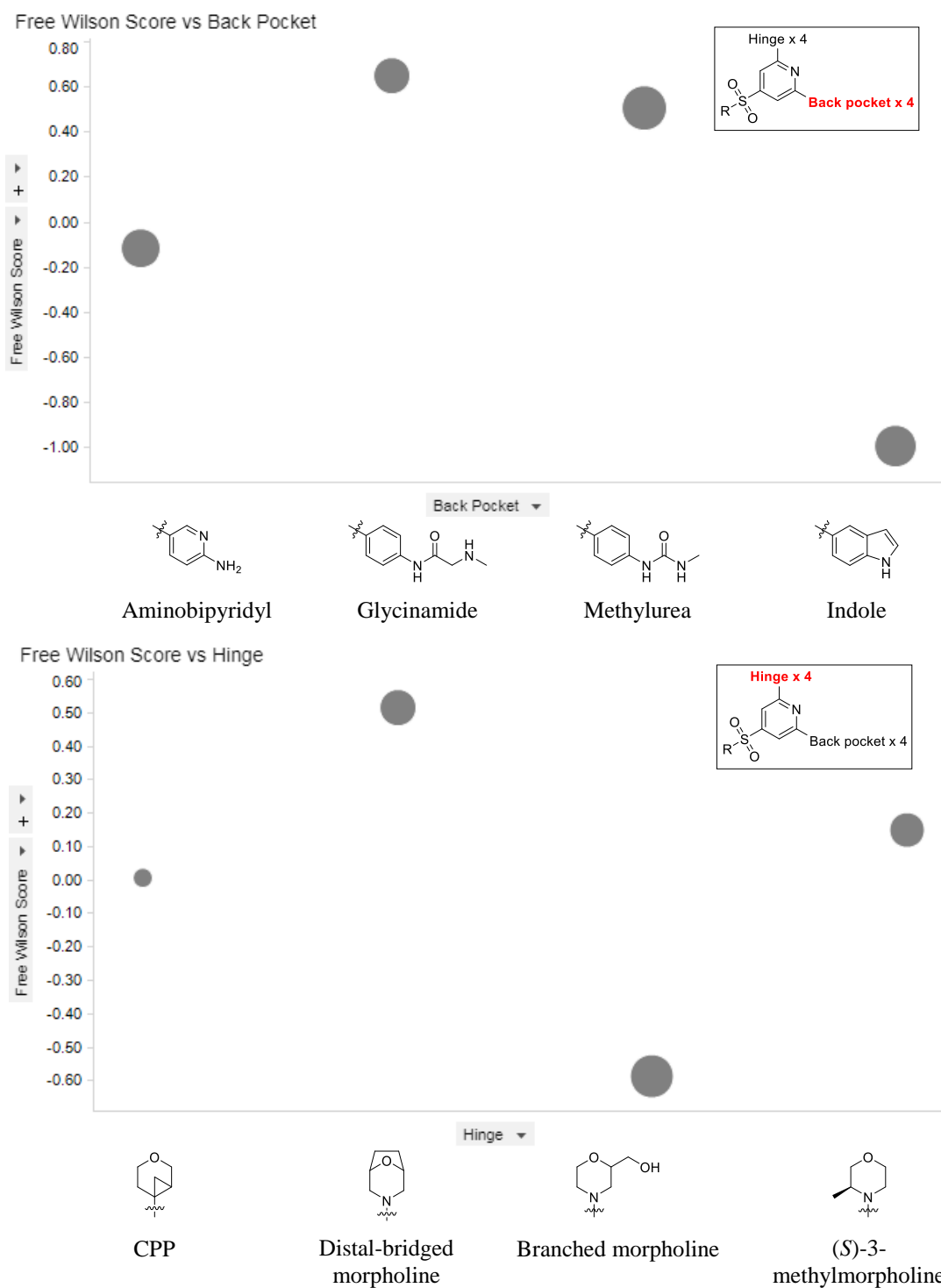


Figure 22: Graphical representation of the sulfone sparse array Free-Wilson analysis, showing the average contribution of the back pocket and the hinge groups to affinity. The size of the spot indicates how many compounds contained that group; the larger the spot, the more compounds it represents.

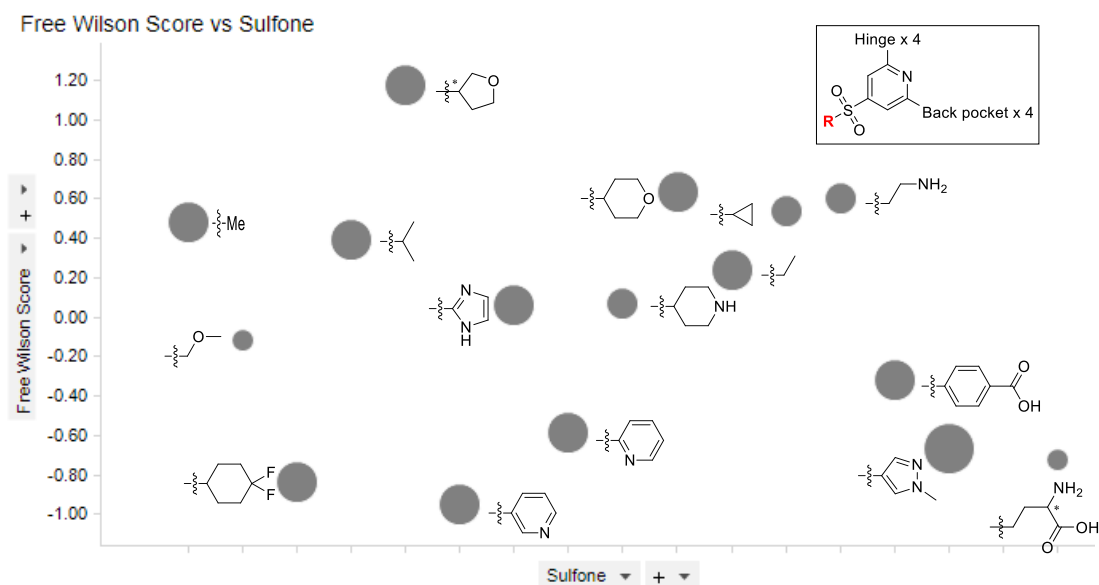


Figure 22 continued: Graphical representation of the sulfone sparse array Free-Wilson analysis, showing the average contribution of each of the sulfone monomers to affinity. The size of the spot indicates how many compounds contained that group; the larger the spot, the more compounds it represents. *Synthesised as a racemic mixture at this stereocentre.

The Free-Wilson analysis suggested that two of the hinge groups had a positive contribution to affinity (distal bridged morpholine and (*S*)-3-methylmorpholine), the CPP (all compounds with this substituent were racemic or diastereomeric mixtures) had a neutral effect and the branched morpholine had a deleterious effect, relative to average. Several sulfone moieties, including isopropyl, cyclopropyl, aminoethyl, ethyl, methyl, tetrahydrofuryl (THF) and tetrahydropyryl (THP), gave increased affinity. In general, aromatic sulfone moieties were found to give reduced affinity compared to the average.

In addition to synthesising the ‘sparse’ set, several compounds were made combining different sulfone moieties with each hinge and back pocket group (key compounds in **Table 4**).¹¹¹ Only two of these compounds were in the original ‘sparse’ set (**23** and **24**). However, many of these compounds were predicted to have high affinity by the Free-Wilson analysis. For example, compound **25** gave one of the highest affinity compounds synthesised in this series so far, demonstrating good agreement between the predicted and measured affinity. The urea variant, compound **26**, had comparable affinity, as predicted by the Free-Wilson analysis. Compound **27** demonstrated the potential to achieve high affinity compounds using a non-morpholine hinge group, the

CPP. One compound that was not predicted to have a high affinity was ethyl sulfone compound **28**, which demonstrated remarkable affinity compared to compound **29**.

Structure	Compound Number	mTOR KB pIC ₅₀ (n) ^a	Predicted mTOR KB pIC ₅₀	pAkt pIC ₅₀ (n) ^a	Chrom LogD ^b
	23	7.4 (4)	-	7.0 (2)	3.0
	24 Racemic	7.7 (4)	-	7.0 (2)	3.5
	25 Racemic	8.0 (2)	7.8	-	2.6
	26 Racemic	7.7 (4)	7.7	7.3 (3)	3.4
	27^c Diastereo- isomeric	7.5 (2)	7.3	-	2.8
	28	8.1 (4)	6.9	7.0 (4)	3.1
	29	7.3 (4)	6.7	6.3 (2)	3.8

Table 4: Key data on selected compounds. ^apIC₅₀ recorded as the mean of the data obtained on each of a number of test occasions (n). ^bChromLogD at pH 7.4. ^cThe formic salt. - Data not generated. *Chiral centre. Affinity (mTOR KB pIC₅₀) and efficacy (pAkt pIC₅₀): < 7.0 = red; ≥ 7.0 = orange; ≥ 7.5 = green. Lipophilicity: ≥ 4 = orange; < 4 = green. Predicted mTOR KB pIC₅₀: Measured value ±0.3 log units = green; ±0.6 log units = orange; > ±0.6 log units difference in measured/predicted values = red.

Overall, the sparse array and Free Wilson analysis provided insight into the SAR of the directly-linked pyridine sulfone series. To further explore the SAR of the back pocket group, a linear back pocket group array was completed (key compounds in **Table 5**).¹¹¹ These data demonstrate the profound effect of the back pocket group on affinity (mTOR KB assay pIC₅₀ values), efficacy (pAkt assay pIC₅₀ values) and lipophilicity. Compounds **21** (parent glycinamide) and **33** (fluorophenylthiourea) had the highest affinity. However, there was a concern that the embedded aniline in the parent glycinamide (**21**) may present a mutagenicity risk. To mitigate this, it was demonstrated that a fluorine-substituent and a ring nitrogen were tolerated in both the 2- and 3- positions (compounds **30-32** and **34-36**). In addition to the linear back pocket groups, indoles and azaindoles were made. Azaindoles demonstrated a remarkable improvement in affinity compared to the parent indoles, along with the expected decrease in lipophilicity (compounds **37-40**).

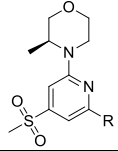
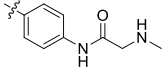
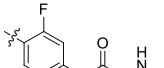
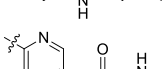
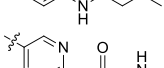
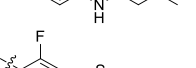
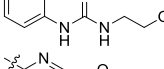
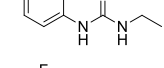
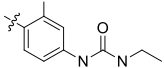
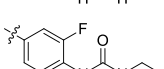
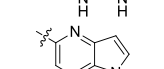
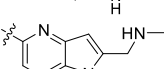
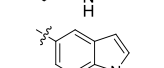
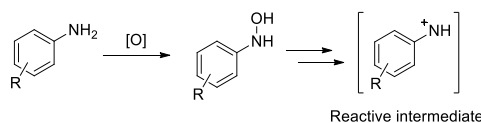
	Compound Number	mTOR KB pIC ₅₀ (n) ^a	pAkt pIC ₅₀ (n) ^a	ChromLogD ^b
	21	7.2 (4)	6.4 (2)	2.5
	30	6.8 (3)	6.0 (3)	2.9
	31	6.6 (2)	5.7 (2)	2.2
	32	6.6 (2)	-	2.4
	33	7.2 (4)	6.4 (2)	3.7
	34	6.4 (3)	5.8 (2)	3.5
	35	6.1 (2)	6.6 (2)	4.3
	36	5.7 (2)	6.2 (1)	4.5
	37	6.7 (6)	6.7 (2)	3.6
	38	6.7 (3)	6.8 (3)	2.1
	39	4.8 (6)	6.3 (2)	4.8
	40	5.9 (8)	6.7 (3)	2.7

Table 5: Key data of compounds made in the back pocket group array. ^apIC₅₀ recorded as the mean of the data obtained on each of a number of test occasions (n). ^bChromLogD at pH7.4. - Data not generated. Affinity (mTOR KB pIC₅₀): bottom third = red (4.8-5.5); middle third = orange (5.6-6.3); top third = green (6.4-7.2). Efficacy (pAkt pIC₅₀): bottom third = red (5.7-6.0); middle third = orange (6.1-6.4); top third = green (6.5-6.8). Lipophilicity: ≥ 4 = orange; < 4 = green.

Anilines, a potential metabolite of the urea and glycinamide back pocket groups, are a known mutagenic species.^{116,117} Evidence of mutagenic activity may indicate that the compound is a carcinogen.¹¹⁸ Anilines are known to be converted into reactive and mutagenic species through metabolic reactions such as oxidation.^{116,117,119} An aniline can be activated by oxidation giving a hydroxylamine, which is then converted into a cationic nitrenium ion, the reactive intermediate (**Scheme 1**).¹¹⁹ It is thought that the

mutagenicity of aromatic amines is related to the ease of formation (the ease of oxidation of the amine) or the stability of the nitrenium ion.^{119,120}



Scheme 1: The oxidative activation of an aniline to give an electrophilic reactive intermediate, capable of reacting with DNA.¹¹⁹

Not all aromatic amines are mutagenic but, as a known toxicophore, the mutagenic risk needs to be assessed. One way to assess mutagenicity *in vitro* is through an Ames test, developed in the 1970s by Bruce Ames, with a positive Ames test indicating that a compound is mutagenic and therefore likely to be carcinogenic.^{118,121,122} The Ames test is a bacterial mutation screening assay that detects the ability of a substance to cause mutations to engineered strains of *Salmonella Typhimurium* bacteria.¹¹⁶ These bacteria are unable to produce histidine and, without added histidine, are unable to grow. Therefore random mutations or mutations caused by an added compound are required in order for colonies to grow in histidine-deficient medium.¹¹⁶ Compounds might be converted into mutagens only after metabolism, so the assay is run both with and without pre-incubation of the compound with rat liver enzymes.¹¹⁶ If a compound enables the bacteria to grow in the absence of added histidine, the compound must have caused mutations to the bacteria DNA (the compound is mutagenic) and is therefore a possible carcinogen.¹¹⁶ The results of an Ames test can be reported as a standardised quantity of the number of bacterial colonies formed, but it is more common to simply report compounds as Ames positive or Ames negative.¹¹⁶

In silico tools can also be used to predict mutagenicity. Various pyridine sulfone-hinge-aniline combinations including compound **41** (**Table 6**) were predicted *in silico* to be mutagenic and this was confirmed by a positive result in a mini-Ames test. Compounds with potential mutagenic liabilities were not ideal for progressing through to pre-candidate stage, therefore alternative back pocket groups were investigated. In-house experience and literature evidence suggested that making the anilines more electron poor would mitigate the mutagenic liability.¹²³ Addition of a fluorine substituent or a ring nitrogen makes the ring more electron deficient, the lone pair on

the aniline nitrogen less available and the aniline more stable to oxidation. Additionally, the nitrenium ion that would be formed (**Scheme 1**) is less stable (and therefore less likely to form). This means that the parent aniline is more likely to be non-mutagenic. Addition of a fluorine substituent to mTOR inhibitors with urea back pockets had been demonstrated in the literature to mitigate mutagenicity risks and give Ames negative compounds.^{108,124} Here, the addition of a fluorine substituent or a ring nitrogen to the aniline of directly-linked pyridine sulfone compounds, was predicted *in silico* to give Ames negative compounds. For the fluorinated compounds this was confirmed in a mini-Ames test using one strain of bacteria (compounds **42** and **43**, **Table 6**). The bipyridyl aniline compounds (**44** and **45**) were predicted *in silico* to be non-mutagenic and were not tested in the Ames test.

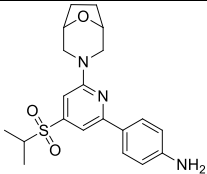
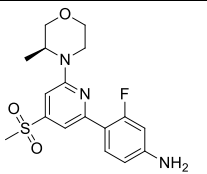
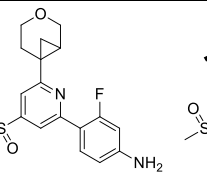
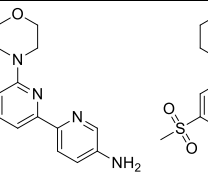
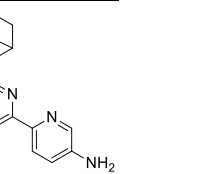
					
	41	42	43	44	45
<i>In silico</i>	Positive	Negative	Negative*	Negative	Negative*
Ames test	Positive	Negative	Negative*	-	-

Table 6: Comparison of the *in silico* predicted Ames liability of the pyridine sulfone anilines with the results found in the mini-Ames test. - Data not generated. *Both isomers.

It was found previously (**Table 5**) that a fluorine substituent or a ring nitrogen *meta* to the aniline gave compounds of comparable affinity to substitution *ortho* to the aniline. Moreover, compared to the parent phenyl compounds, introduction of a fluorine or ring nitrogen was suggested to give compounds of comparable affinity and so featured in the majority of compounds proposed subsequently. Of these two methods to mitigate the mutagenicity risk, the synthesis to introduce a fluorine substituent was initially simpler, therefore more fluorinated back pocket groups were considered for synthesis.

1.6 Comparison of the mTOR kinase inhibitors synthesised so far

Previously, improvements in the affinity for mTOR kinase had been demonstrated in this novel directly-linked sulfone series. The initial compound (**21**, **Table 3**) had an affinity of 7.2 (the mTOR KB pIC₅₀ value) and, while compounds made in the sparse array demonstrated improved affinities (**24**, **Table 4**), further improvements were necessary. A comparison of the best compounds from this initial work with the best compounds developed previously highlighted the areas requiring development (**Table 7**). Bicyclic sulfone (**8**), originally developed as an oral mTOR kinase inhibitor, was one of the first compounds to demonstrate an antifibrotic effect. This compound was found to have very low solubility – too low for either oral or inhaled administration and further development gave a more soluble compound (**46**). Gratifyingly, the novel sulfonyl pyridine compound (**25**) maintained similar affinity, efficacy and selectivity. Compounds **8** and **46** were known to contain an embedded mutagenic aniline. While the mutagenic risk of compound **25** was not known, it also contained a potential mutagenic liability. Furthermore, no optimisation of physicochemical properties had been considered, and it was expected that the limited capacity of the inhaled delivery device³⁹ would dictate the need for a low dose. None of the compounds synthesised up to this point were believed to be developable to achieve the required low-dose treatment. Therefore, further work was required to achieve a more active compound and explore physicochemical properties.

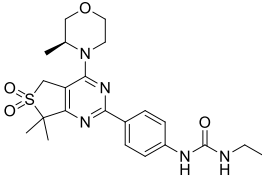
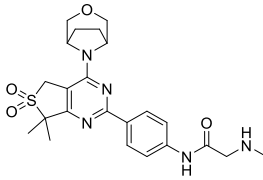
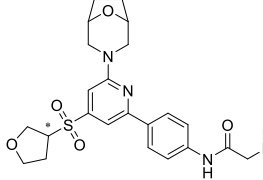
Structure			
Compound Number	8	46 ^c	25 ^d
mTOR KB pIC ₅₀ (n) ^a	8.0 (21)	8.1 (4)	8.0 (2)
pAkt pIC ₅₀ (n) ^a	7.7 (45)	8.0 (3)	-
PI3K selectivity	> 500	> 3500	> 1500
DNA-PK pIC ₅₀	5.5 (5)	5.0 (2)	-
ChromLogD ^b	4.3	3.0	2.6
CLND	69	136	104
FaSSIF (μg/mL) ^e	12 (3)	558 (2)	-
AMP	200	200	67
MDCK P _{exact} (nm/s)	363	124	-
Ames ^f	Positive	Proposed positive	Proposed positive

Table 7: Comparison of mTOR kinase inhibitors containing sulfone moieties, highlighting the areas for improvement. ^apIC₅₀ recorded as the mean of the data obtained on each of a number of test occasions (n). ^bChromLogD at pH7.4. ^cThe formic salt. ^dRacemic mixture. ^eMean of data obtained on each of a number of test occasions. ^fThe Ames mutagenic liability of the compound with the free aniline (not elongated to form a urea or glycinamide). - Data not generated.

1.7 Project aims

Poor prognosis and lack of appropriate medicines are evidence of an unmet need for a treatment for IPF that will halt disease progression. Research in our laboratories had demonstrated that mTOR kinase inhibitors had an anti-fibrotic effect and several series of compounds were under investigation. The primary aim was to develop a novel inhibitor of mTOR kinase appropriate for use as an inhaled treatment for IPF. To achieve this, compounds with high affinity and efficacy, selectivity over related kinases and the correct balance of physicochemical properties were required. It was hypothesised that such a compound could be achieved in the directly-linked sulfone series. To achieve a non-mutagenic compound, 6-position (back pocket) groups without an embedded mutagenic liability were explored. Additionally, an iteration of compounds was designed with the aim of discovering a novel sulfone 4-position substituent that would achieve the desired affinity, efficacy and selectivity.

Chapter I: Results and discussion of the medicinal chemistry of a directly-linked sulfone series to develop the next generation of mTOR kinase inhibitors

2. Results and Discussion

2.1 Aims of Chapter I and the desired profile of compounds in the directly-linked sulfone series of mTOR kinase inhibitors

In the lead optimisation stage of a medicinal chemistry project, a desired property profile is established. In order to become a pre-candidate, a compound must meet all or most of these required properties. An inhaled mTOR kinase inhibitor has been defined as requiring the following properties (**Table 8**):

Property	Desired value
mTOR KB pIC ₅₀ (affinity)	> 7.5
pAkt pIC ₅₀ (efficacy)	> 7.5
SIAJ pIC ₅₀	> 7.0
Lipophilicity (ChromLogD)	2-5
Selectivity over PI3K ($\alpha,\beta,\gamma,\delta$)	> 100-fold
Selectivity over DNA-PK	> 100-fold

Table 8: The desired property profile for an inhaled mTOR kinase inhibitor.

Additional criteria also needed to be met including:

- No mutagenic risk.
- No hERG risk.
- Duration of action or lung retention, believed to be achievable through targeting a range of solubility, permeability and basicity.

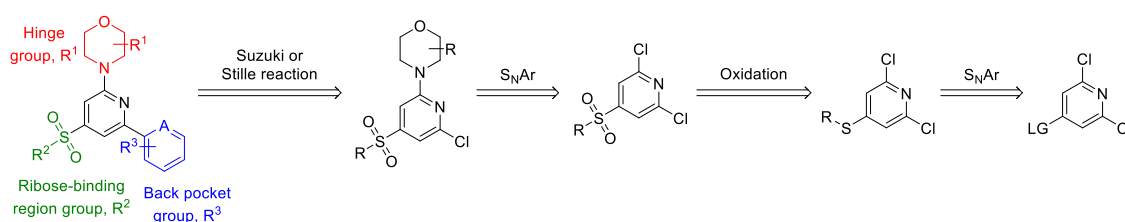
The compounds described so far did not meet these criteria, largely due to the risk of an embedded mutagenic liability and insufficient affinity and efficacy. To achieve duration of action, the compound should maintain a suitable concentration in the lung between each dose.³⁹ Lung retention is often targeted for inhaled compounds due to device-related dose restrictions and can be achieved through modifications to the physicochemical properties of the compound.³⁹

It was proposed that a compound with this target property profile could be achieved in the directly-linked sulfone series. First, 6-position (back pocket) groups without an embedded mutagenic liability were investigated (R³, **Scheme 2**). Subsequently, novel

sulfone substituents (R^2 , **Scheme 2**) were explored to achieve the desired affinity, efficacy and selectivity.

2.2 Methods for the preparation of directly-linked sulfone mTOR kinase inhibitors

The synthesis of many of the directly-linked sulfone compounds was achieved using a straightforward route (**Scheme 2**). The 4-position of the pyridine core was functionalised, followed by a S_NAr reaction to install the morpholine moiety and a carbon-carbon cross coupling to add the aromatic back pocket group.



Scheme 2: Demonstrating the points of variation in the directly-linked sulfone series of compounds, a retrosynthetic analysis and the typical reactions conducted to complete the synthesis. R^1 = alkyl, R^2 = aromatic, alkyl or heteroalkyl, R^3 = alkyl or heteroalkyl; LG = Leaving group; A = CH, CF or N.

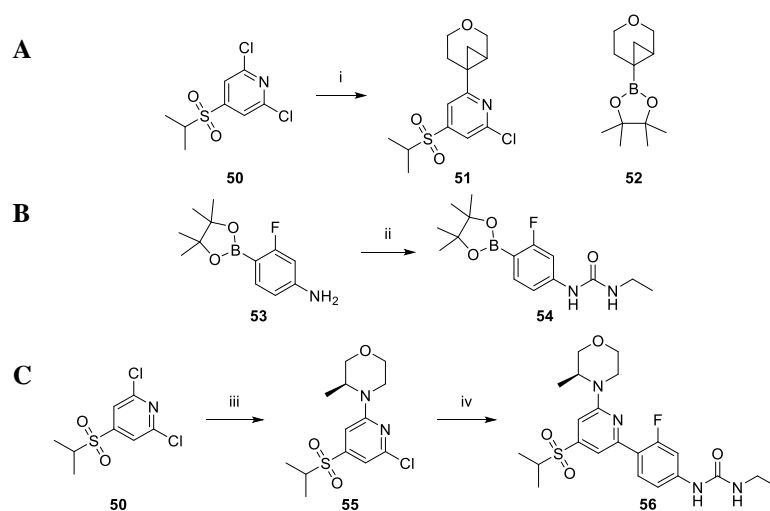
For some compounds, a slightly shorter route was possible. Starting from a 2,4,6-trisubstituted pyridine such as **47**, the methyl sulfone (**48**) could be obtained in one step using sodium methanesulfinate as a nucleophile to displace the leaving group at the 4-position (**Scheme 3A**). However, the same procedure gave little or no product when sulfinic acids or sulfinate salts other than sodium methanesulfinate were used. To synthesise all other compounds, a thiol was used to displace the nitro leaving group (**47**) in a S_NAr reaction followed by oxidation to give the functionalised sulfone (**49**, **Scheme 3B**).



Scheme 3A and B: The chemistry used to install the methyl sulfone and the thiol route used for many of the sulfones, reaction conditions shown for the synthesis of ethyl sulfone. *Reagents and Conditions:*

- i) Sodium methanesulfinate (1.2 equiv.), DMF, 21 °C, 1.0 h, 62%. Synthesis by H. Davies.
- ii) Ethanethiol (1.0 equiv.), NaOH (1.0 equiv.), 25 °C, 12.0 h, 45%. iii) MMPP (2.0 equiv.), MeOH (1.0 equiv.), dichloromethane, 25 °C, 12.0 h, 87%. Synthesis by GVK Biosciences.

Next, the 2-position was functionalised; the CPP was incorporated via a Suzuki cross-coupling with a bespoke boronic ester (**52**) to obtain a racemate (**51**, **Scheme 4A**), with the single enantiomers accessed after chromatographic separation using a chiral stationary phase. Various substituted morpholine groups were incorporated via an often high-yielding S_NAr reaction. A subsequent Suzuki reaction using either commercially available or bespoke boronic esters gave the final mTOR kinase inhibitor. Bespoke boronic esters, such as fluoroethylurea **54** (**Scheme 4B**), allowed installation of the 6-position back pocket group in one step (**Scheme 4C**). The majority of the starting dichlorosulfonyl pyridines were synthesised externally by GVK Biosciences¹²⁵ (as described in **Scheme 3**), with the hinge and back pocket groups installed subsequently in our laboratories.

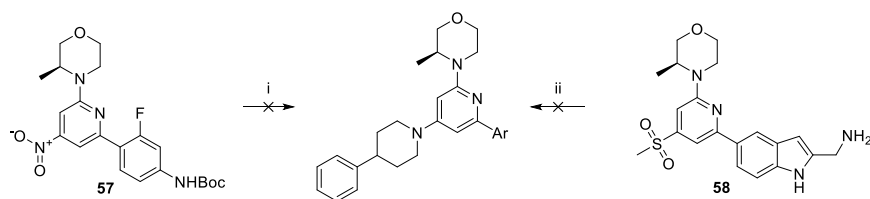


Scheme 4A: Installing the 2-position CPP in a Suzuki reaction with bespoke boronic ester **52**. **B:** The chemistry used to prepare the bespoke fluoroethylurea boronic ester **54**. **C:** Installing a substituted morpholine and fluorourea-containing back pocket group to make an mTOR kinase inhibitor.

Reagents and Conditions: i) **52** (1.1 equiv.), CsOH.H₂O (2.2 equiv.), PdCl₂(dppf).dichloromethane adduct (10 mol%), 2-MeTHF:H₂O (3:1), 100 °C, 40.0 h, 23% (60% purity). ii) Ethyl isocyanate (6.0 equiv., portion-wise), dichloromethane, 21-60 °C, 52.0 h, 90%. iii) (*S*)-3-Methylmorpholine (1.1 equiv.), DIPEA (4.0 equiv.), 81-100 °C, 20.0 h, 91%. iv) **54** (1.2 equiv.), K₂CO₃ (2.3 equiv.), PdCl₂(dppf) (10 mol%), IPA:H₂O (5:1), 120 °C, 3.0 h, 21%. Synthesis by H. Davies.

To enhance the modularity of the approach, an alternative route was proposed to functionalise the 4-position of the pyridine core at a late stage. The initial method investigated, displacing either a nitro-group (**57**) or a methyl sulfone (**58**) on a 2,6-disubstituted pyridine, was unsuccessful (**Scheme 5**). A cyclic secondary amine

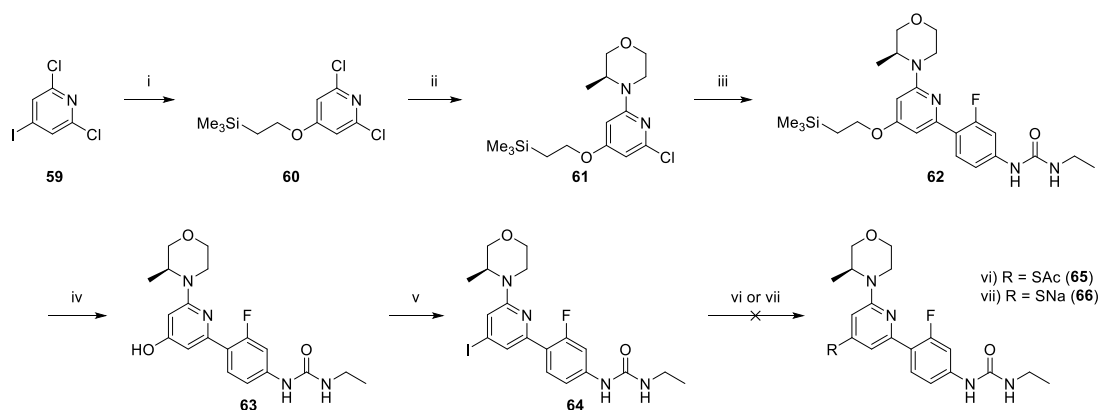
nucleophile was used as the piperidine was proposed to have reduced steric hindrance around the nucleophilic nitrogen and the phenyl group enabled UV visualisation by LCMS. The use of stronger nucleophiles, such as thiols, was not investigated due to their stench, making them unsuitable for use in a communal laboratory. Decomposition of starting material was seen in all reactions. With starting material **57**, a mass ion corresponding to the Boc-protected product was observed but could not be isolated. Electron donation from the morpholine ring into the pyridine was proposed to decrease the electrophilicity of the pyridine, making it more stable and less susceptible to attack by the amine nucleophile.



Scheme 5: Reactions to displace either the methyl sulfone or nitro group in the 4-position with a secondary amine nucleophile in a S_NAr reaction. *Reagents and Conditions:* i) 4-Phenylpiperidine (4.0 equiv.), K_2CO_3 (3.4 equiv.), DMF, 150 °C, 50.0 h. ii) 4-Phenylpiperidine (3.6 equiv.), K_2CO_3 (6.9 equiv.), DMF, 100-150 °C, 55.0 h. Reactions by H. Davies.

A second method was investigated: protection of the 4-position prior to installation of the morpholine and aromatic 6-position group, followed by deprotection and reaction to form the sulfone. Literature precedent suggested that trimethylsilyl ethanol could be used as an oxygen surrogate, installed on an iodopyridine and easily removed to give a pyridinol.¹²⁶ In a second precedent reaction, 4-iodopyridine was synthesised from pyridin-4-ol.¹²⁷ It was proposed that functionalisation of the 4-position as the final step may be possible from this 4-iodopyridine (**Scheme 6**). The first step to install trimethylsilyl ethanol onto the 2,6-dichloro-4-iodopyridine (**59**) gave a poor yield of impure material (**60**) due to the formation of various side products, leading to a difficult purification. Due to the electron-donating effect of the 4-position oxygen, the resultant pyridine ring was more electron rich than the iodopyridine starting material. This led to a slow S_NAr reaction, requiring forcing conditions (neat, high temperature and long reaction time) to obtain compound **61**. This reaction also gave unreacted starting material (**60**), which could be isolated and re-reacted. The subsequent Suzuki reaction gave a quantitative yield of compound **62** which was deprotected to obtain

alcohol **63** and subjected to iodination conditions to give 4-iodopyridine **64**. The overall yield for this 5-step linear synthesis was 5.5%, resulting in only a small amount of iodopyridine **64**. Disappointingly, reactions to displace the iodine in compound **64** with a sulfur-containing group (to give compounds **65** or **66**) gave no desired product, and degradation of the starting material gave several unidentified species.



Scheme 6: The route to iodo-pyridine **64** and the reactions investigated to replace the 4-position iodide with a sulfur moiety. *Reagents and Conditions:* i) 2-(Trimethylsilyl)ethanol (3.0 equiv.), Cu(I) (10 mol%), 1,10-phenanthroline (20 mol%), Cs₂CO₃ (2.0 equiv.), toluene, 110 °C, 17.5 h, 32%. ii) (*S*)-3-Methylmorpholine (2.2 equiv., portion-wise), DIPEA (3.0 equiv.), 170 °C, 84.0 h, 68%. iii) **54** (1.1 equiv.), Pd(dppf)Cl₂ (10 mol%), K₂CO₃ (2.0 equiv.), IPA:H₂O (5:1), 1.5 h, 120 °C, quant. iv) CsF (2.9 equiv.), DMF, 60 °C, 2.0 h, 55%. v) Tf₂O, pyridine, MeCN, 5-21 °C, 1.3 h, then NaI (9.0 equiv., portion-wise), HCl (3.0 equiv., portion-wise), 21-90 °C, 19.0 h, 54%. vi) Potassium ethanethiolate (3.5 equiv.), Cu(I) (0.3 equiv.), 1,10-phenanthroline (0.8 equiv.), toluene, 110 °C, 25.0 h. Or vii) Na₂S (4.2 equiv., portion-wise), Cu(I) (2.0 equiv., portion-wise), DMF, 80-120 °C, 56.0 h. Synthesis by H. Davies.

2.3 Investigating SAR in the directly-linked sulfone series

It was proposed that the target property profile could be met by combining a sulfone moiety described in the Introduction with a non-mutagenic variant of the 6-position aniline, achieved through electronic modifications. Additionally, investigating alternative 2-position morpholine moieties was hypothesised to give increased affinity and efficacy, as well as variety in physicochemical properties. The aims of this work were to:

- Synthesise compounds with acceptable affinity and efficacy (mTOR KB pIC₅₀ > 7.5 and pAkt pIC₅₀ > 7.5, the SIAJ efficacy assay was not routinely in use at this time) and a non-mutagenic aniline.
- Identify optimal combinations of the three pyridine substituents.

2.3.1 Results and discussion of an initial investigation of directly-linked sulfone mTOR kinase inhibitors

A total of 36 compounds were designed to test the hypotheses outlined above (**Figure 23A**). No new sulfone groups were considered, apart from single enantiomers of the THF sulfones. To achieve a non-mutagenic compound, both fluorine-substituted and nitrogen-containing variants of the urea and glycinamide back pocket groups were proposed. These were combined with the four most active sulfone groups and both the distal bridged and CPP hinge groups (**Figure 23B**, Set A). The back pocket group array described in the Introduction highlighted a high affinity, non-mutagenic fluorothiourea-containing compound (**33**, **Table 5**). Combining this substituent with single enantiomers of the THF sulfone and the four substituted morpholines was predicted to give active compounds with low lipophilicity (**Figure 23B**, Set B). Furthermore, preceded mTOR hinge groups had been shown to modulate both physicochemical properties and selectivity.¹⁰⁸ 12 compounds were made as part of a hinge group array, investigating four substituted morpholines, three non-mutagenic back pocket groups (pyridyl, fluoroethylurea and fluoroglycinamide) and the isopropyl sulfone – selected as it was predicted to achieve a suitable balance of lipophilicity (**Figure 23B**, Set C).

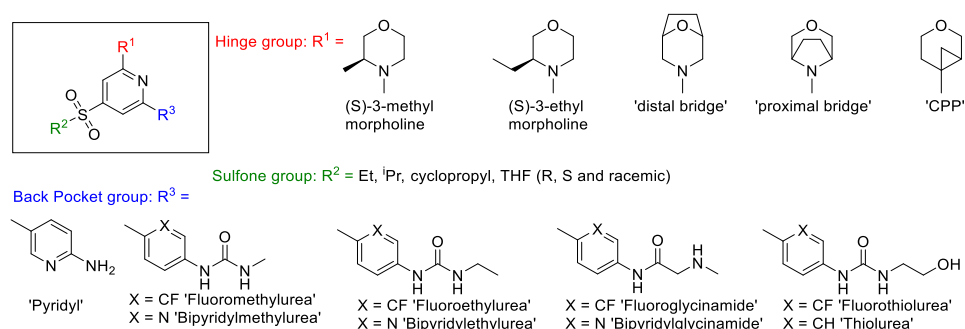


Figure 23A: The three main areas of SAR investigated; the hinge (R¹), the sulfone group (R²) and the back pocket (R³). Not every combination was synthesised. Full data in **Appendix A**, Section 7.1.

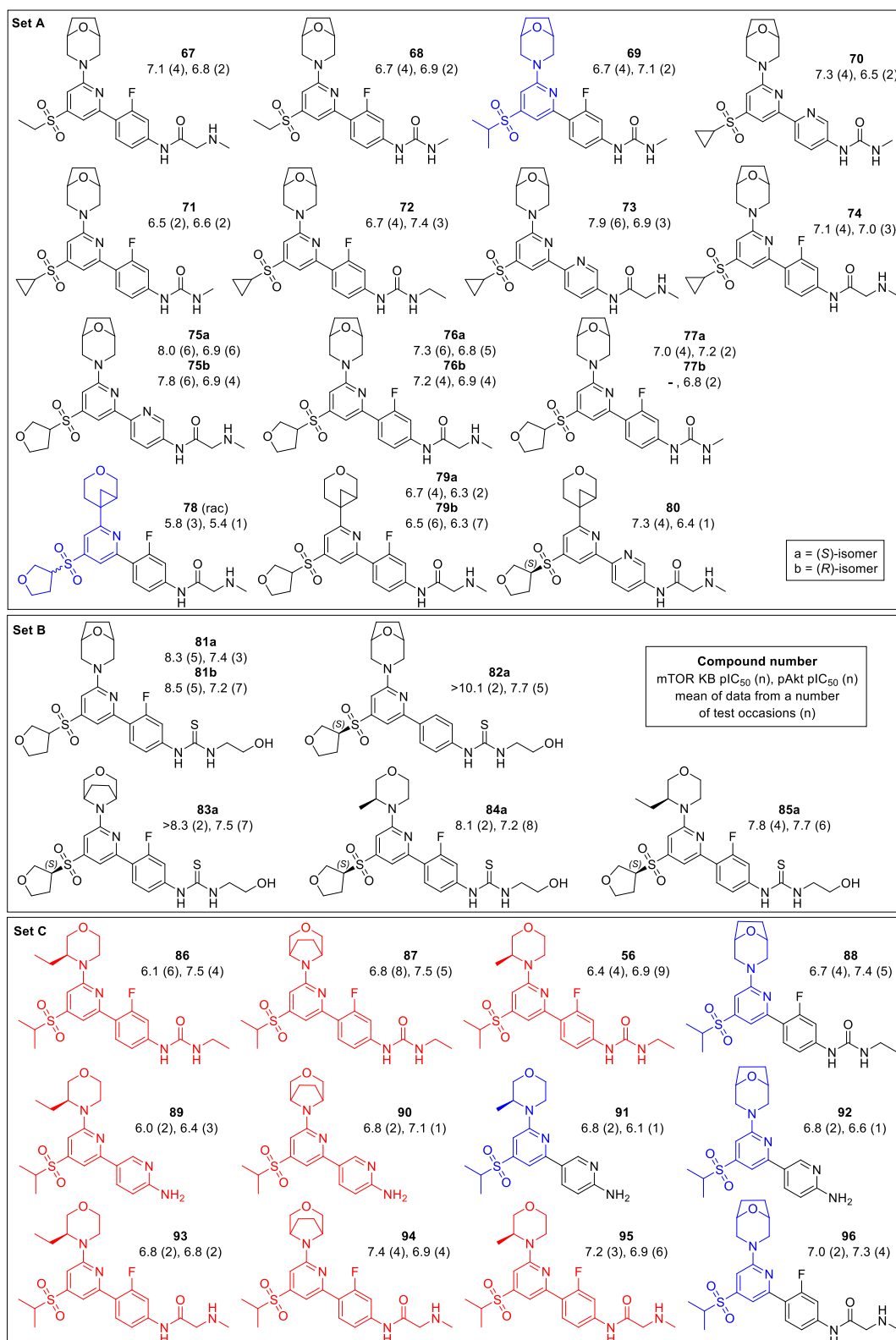
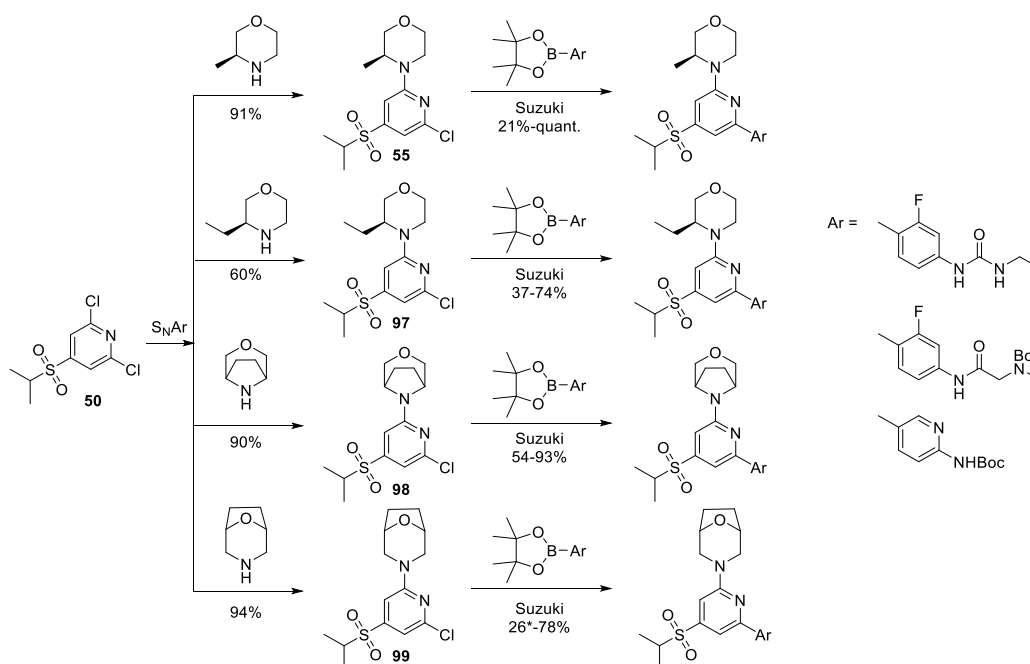


Figure 23B: The 36 compounds synthesised and key data; mTOR KB pIC₅₀ (n), pAkt pIC₅₀ (n), both as the mean of the data obtained on each of a number of test occasions (n) (full data in **Appendix A**). Red = Final compound made by H. Davies; Blue = Chloropyridine intermediate made by H. Davies; Black = Made by V. Clayton, A. Hancock, H. Hobbs, E. Hounslea, E. Mogaji, S. Nicolle.

Synthesis of these compounds followed a similar method, exemplified here for compounds **56** and **86-96** (Set C, **Figure 23B**). Starting from a 2,6-dichloropyridine with a sulfone in the 4-position (synthesised at GVK Biosciences as described previously, **Scheme 3**), the morpholine ring was installed first in a S_NAr reaction by heating the chloropyridine, amine and DIPEA in DMSO. The aromatic 6-position groups were then installed in either a Suzuki or Stille (for bipyridyl compounds **70**, **73**, **75** and **80**) reaction using the appropriate boronic ester, K_2CO_3 and $PdCl_2(dppf)$. This was followed by a Boc-deprotection, if required, using HCl and isolation of the final compound as the free base (**Scheme 7**).



Scheme 7: Exemplifying the synthesis of compounds **56** and **86-96** (Set C, **Figure 24B**). *Reagents and Conditions:* S_NAr : Amine, DIPEA, DMSO, heat. Suzuki: Boronic ester, K_2CO_3 , $PdCl_2(dppf)$, IPA:H₂O, heat. Boc-deprotection (if required): HCl, dioxane, heat, or TFA, DCM, rt. Compounds isolated as the free base. Yield ranges quoted for the S_NAr and Suzuki reaction steps only, not the deprotection reaction. *Yield quoted for telescoped Suzuki and deprotection reactions. 8 out of 12 final compounds synthesised by H Davies.

In silico predictions of physicochemical properties were used to aid compound selection. In general, the calculated ChromLogD (at pH 7.4) correlated well with the measured values and both AMP and CLND solubility demonstrated some correlation (**Figure 24A**). Only high or low solubility was calculated *in silico*. However, compounds predicted to have high solubility were more likely to have a measured

value of over 100 $\mu\text{g/mL}$ than those predicted to have low solubility. As desired, a range of solubility and permeability values were achieved, as shown in the 9-box model plot of MDCK permeability (P_{exact}) against SLF solubility (**Figure 24B**). Not all compounds had measured values in these low throughput assays, but it was notable that compounds containing a thiourea back pocket group (red) were in a distinct low solubility, low-mid permeability space, and compounds with a pyridine back pocket group (green) were in a distinct high permeability, low solubility space.

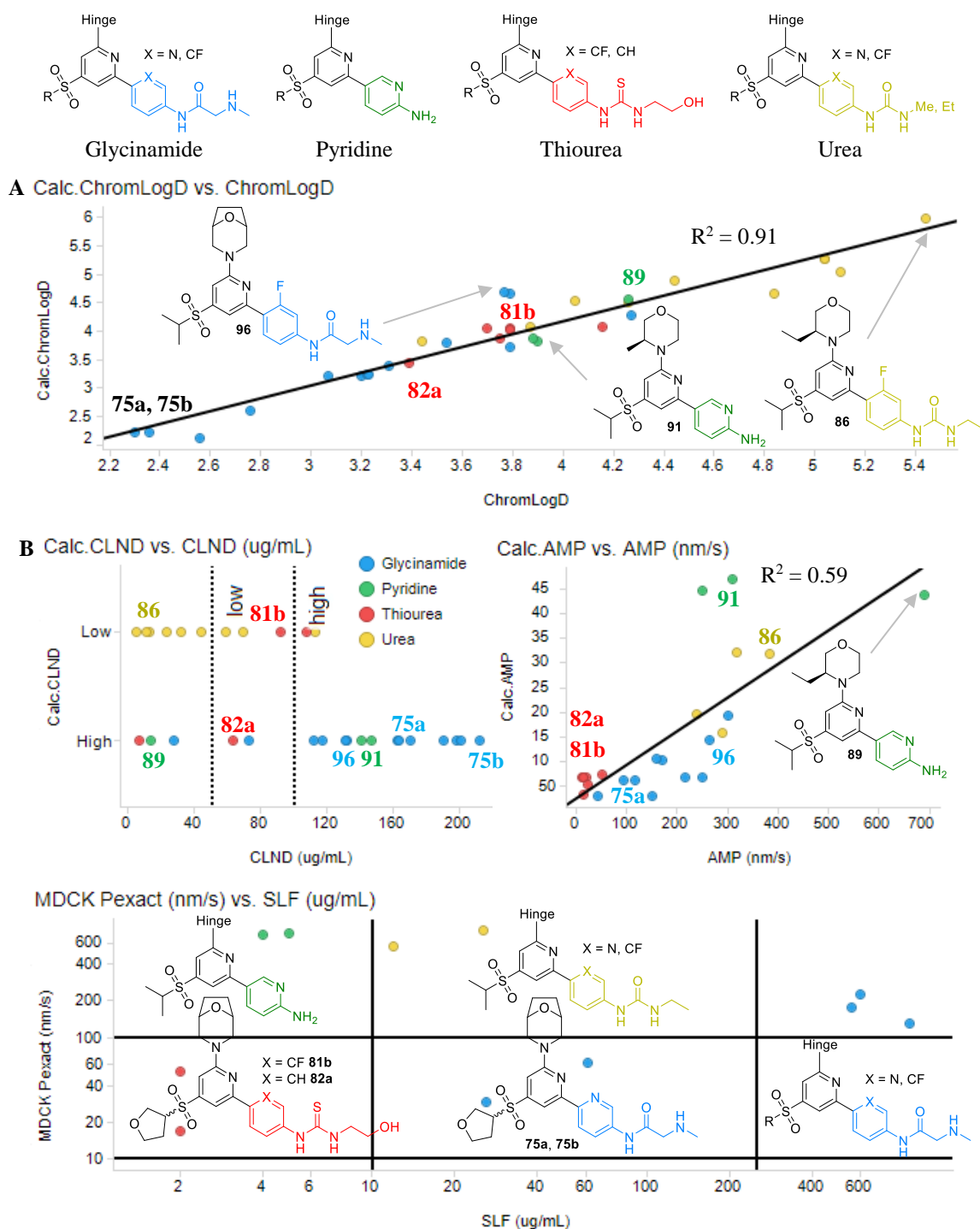


Figure 24A: The correlation between predicted and measured physicochemical properties with representative compounds highlighted. **B:** A plot of MDCK permeability vs. SLF solubility shows the different areas of the allowed property space occupied by the exemplified compounds. All graphs coloured according to the 6-position (back pocket) group. a = (*S*)-isomer, b = (*R*)-isomer of the THF-sulfone group. Calc. = calculated, AMP = artificial membrane permeability, MDCK Pexact = Madin-Derby canine kidney permeability, SLF = simulated lung fluid solubility.

Affinity and efficacy data were obtained for the compounds in this first iteration using the mTOR KB and pAkt assays respectively (key data on selected compounds in **Table 9** and full data in **Appendix A**, Section 7.1). The higher a compound's affinity or efficacy, the harder it was to obtain a true IC₅₀ value because at very low concentrations (nanomolar), the error in the concentration became larger than the concentration itself. Therefore, it was not possible to accurately distinguish between measured affinity or efficacy pIC₅₀ values greater than 8.5. Additionally, there was an error in the mTOR KB affinity assay of ± 0.3 log units and in the cellular pAkt efficacy assay of ± 0.4 log units (with n=4 data).

Key features of this first iteration of compounds are highlighted in **Table 9** and **Figure 25** and will be explored in further detail subsequently. In summary:

- Compound **67** (**Table 9**), a non-mutagenic variant of compound **28** (**Table 4**) showed that addition of a fluorine decreased affinity (the mTOR KB pIC₅₀). The comparable levels of cellular efficacy (the pAkt pIC₅₀) were proposed to be driven by lipophilicity (ChromLogD, **Table 9**).
- Compounds **73** and **74** (**Table 9**) suggest that bipyridyl glycinamide compounds (X = N) have higher affinity than fluoroglycinamides (X = CF). Again, the comparable levels of cellular efficacy were proposed to be driven by lipophilicity.
- Single enantiomers of the THF sulfone compound (**75a** and **75b**, **Table 9**) showed good affinity and reasonable efficacy.
- Compound **82a** was reported to have an affinity value (mTOR KB pIC₅₀) of greater than 10 (this value should strictly have been reported as greater than 8.5) but was subsequently shown to contain a mutagenic aniline in the back pocket and was therefore not progressed. Proposed non-mutagenic variants, compounds **81a** and **81b** (**Table 9**) showed good affinity and efficacy but poor selectivity over DNA-PK.
- Hinge group array compounds **94** and **96** (Set C, **Figure 23B**, **Table 9**) demonstrated that this feature could have subtle effects on the affinity and efficacy.

- Compounds containing the CPP did not have comparable affinity or efficacy to those containing the morpholine-based hinge groups (red circle, **Figure 25**). These compounds were all racemic and synthesis of single enantiomers required a chiral separation. For these reasons, no further CPP hinge compounds were considered for synthesis.

Structure	Compound Number	mTOR KB pIC ₅₀ (n) ^a	pAkt pIC ₅₀ (n) ^a	DNA-PK pIC ₅₀ (n) ^a	PI3K selectivity	Chrom Log D ^b	CLND, SLF (µg/mL) ^{c,d}	AMP, MDCK P _{exact} (nm/s) ^{c,e}
	X = CF: 67	7.1 (4)	6.8 (2)	5.1 (1)	>300	3.3	198,373	170,243
	X = CH: 28	8.1 (4)	7.0 (4)	-	-	3.1	-	-
	X = N: 73	7.9 (6)	6.9 (3)	5.8 (1)	>2500	2.8	201,903	-,129
	X = CF: 74	7.1 (4)	7.0 (3)	5.9 (1)	>300	3.5	73,-	160,-
	75a	8.0 (6)	6.9 (6)	5.5 (4)	>2500	2.3	162,26	42,29
	75b	7.8 (6)	6.9 (4)	5.2 (1)	>2000	2.4	212,61	-,61
	X = CF: 81a	8.3 (5)	7.4 (3)	7.2 (3)	>5000	3.7	108,2	12,35
	X = CF: 81b	8.5 (5)	7.2 (7)	7.9 (1)	>4500	3.8	92,2	21,52
	X = CH: 82a	>10.1 (2)	7.7 (5)	6.2 (3)	>500	3.4	63,2	14,17
	Hinge A: 94	7.4 (4)	6.9 (4)	4.9 (3)	>750	3.8	131,560	-,178
	Hinge B: 96	7.0 (2)	7.3 (4)	5.1 (1)	>300	3.8	-,-	265,-

Table 9: Key data on selected compounds synthesised in this iteration. a = (*S*)-isomer, b = (*R*)-isomer. ^apIC₅₀ recorded as the mean of the data obtained on each of a number of test occasions (n). ^bChromLogD at pH7.4. ^cIf more than one measurement, the mean was reported. ^dSolubility data. ^ePermeability data. -Data not generated.

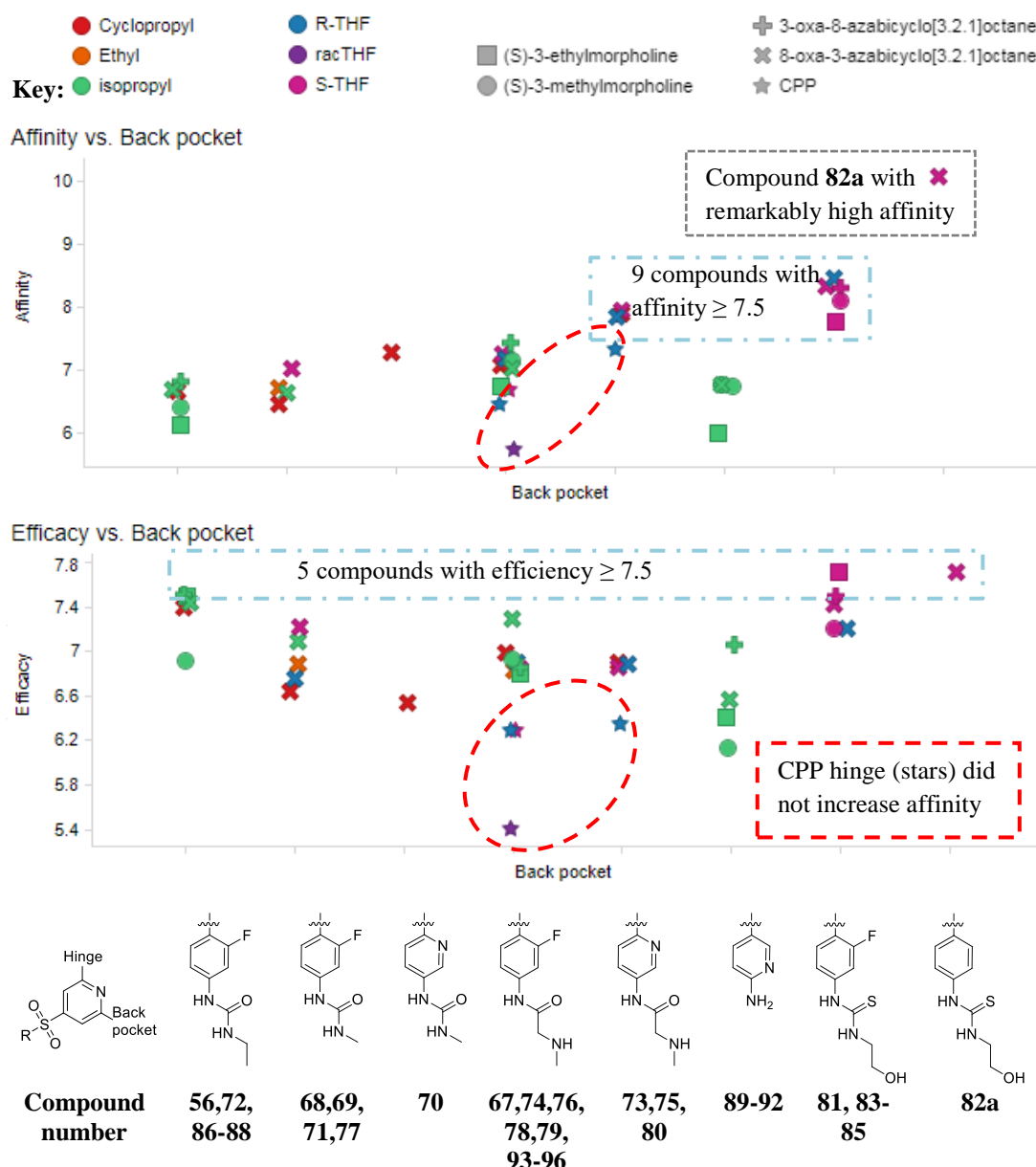


Figure 25: Demonstrating the affinity (mTOR KB pIC_{50}) and efficacy (pAkt pIC_{50}) of the compounds synthesised in this iteration. Coloured according to 4-position sulfone group and shaped according to 2-position hinge group. a = (*S*)-isomer, b = (*R*)-isomer. Compound numbers refer to compounds in **Figure 23B**.

Despite displaying disappointing affinity and efficacy, these compounds warrant further discussion. To mitigate the mutagenicity risk, 6-position anilines with modified electronic properties were investigated. While addition of a fluorine-substituent or ring-nitrogen did reduce the mutagenicity risk, comparison of non-mutagenic variants of the back pocket groups with the parent anilines demonstrated that these changes led to reduced activity (**Figure 26**). The average affinity of compounds with both bipyrindyl

and fluorinated back pocket groups was lower than the parent aniline versions. The more lipophilic parent aniline and fluorinated compounds were more efficacious than the polar bipyrindyl compounds.

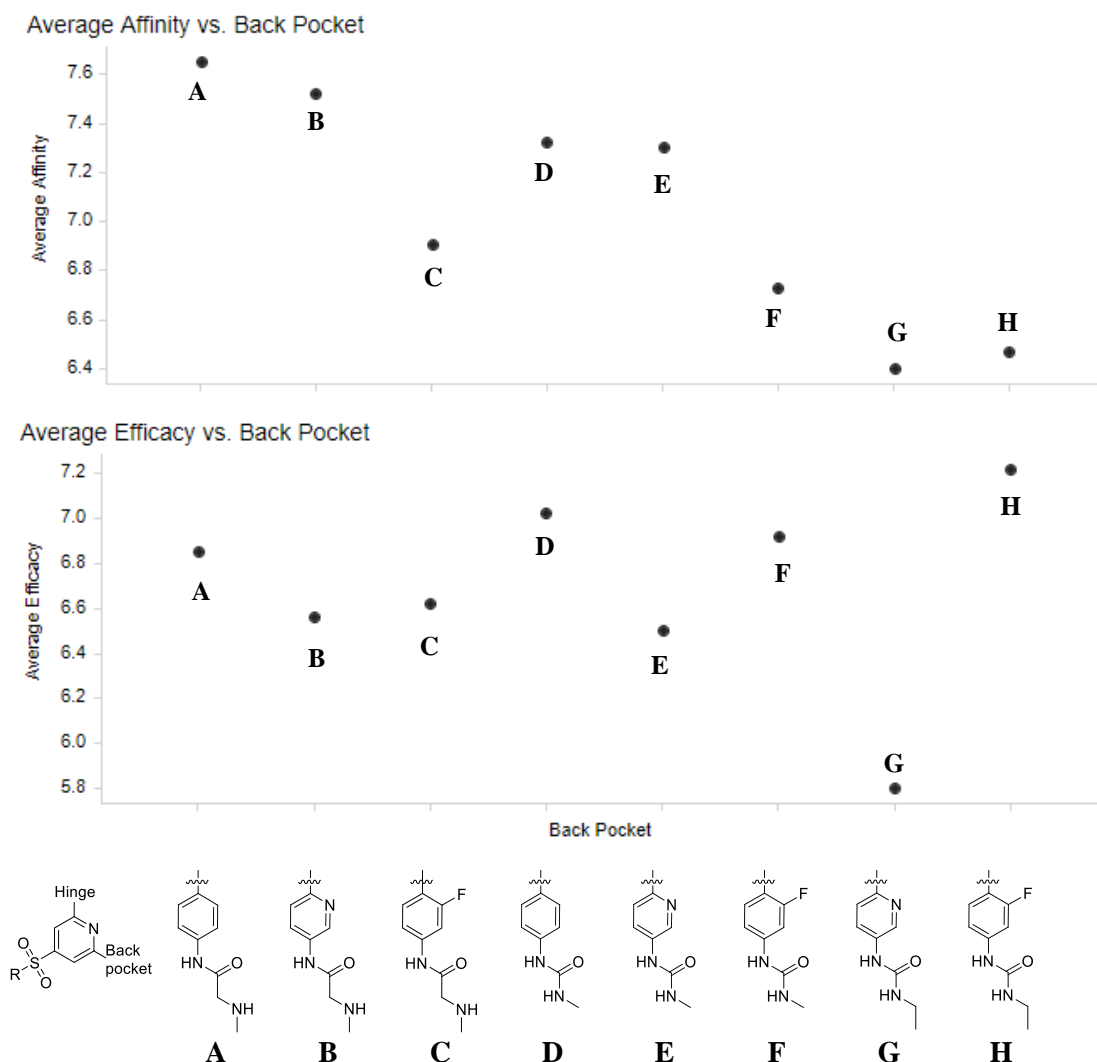


Figure 26: Demonstrating the change in average affinity (mTOR KB pIC₅₀) and efficacy (pAkt pIC₅₀) when non-mutagenic variants of the 6-position aniline group were used.

The hydrophobic region the back pocket group occupies in the mTOR kinase active site is relatively narrow and – in order to make favourable interactions – the core, hinge and back pocket groups need to be coplanar (**Figure 27A**). Energy barriers to rotation of approximately 12.5 kJ/mol and below can be overcome by most compounds at room temperature, with larger energy barriers requiring additional energy.¹²⁸

Energy minimised conformations of the core and back pocket aromatic rings in solution were calculated and, displayed graphically, these suggest the preferred

conformation in solution and the energy barriers between different conformations (**Figure 27B**).^{a,129} To calculate this, the dihedral angle between the core pyridine and the back pocket group (demonstrated by atoms 1-4, compound **B**, **Figure 27B**) was increased from 0-360° in increments of 10° and the minimum energy in each conformation calculated.¹²⁹ For simplicity, only the core and back pocket aromatic rings were considered in the calculation.

For all three compounds, the lowest energy conformation was calculated to be a dihedral angle of 180° (coplanar). In this conformation, electrons can delocalise over both rings, giving increased stability. Increasing the dihedral angle from 180° to 270° disrupted this conjugation, giving a higher energy, more unstable conformation. Further increasing the dihedral angle to 360° regained the electronic conjugation, leading to a lower energy, more stable conformation for pyridyl-phenyl compound **B** with a symmetrical phenyl ring in the back pocket group position. For bipyridyl **A** and pyridyl-fluorophenyl **C**, a dihedral angle of 360° was suggested to lead to unfavourable electronic and steric interactions between the two nitrogen lone pairs (conformation **A'**) or the nitrogen lone pair and fluorine (conformation **C''**) respectively, giving a higher energy, more unstable conformation. Both pyridyl-phenyl **B** and pyridyl-fluorophenyl **C** were calculated to have broader energy minima (150-200°) than bipyridyl **A**, suggesting these compounds can occupy slightly different conformations with little change in energy. This was proposed to be because twisting the back pocket slightly avoids unfavourable electronic and steric interactions between the C-H or C-F and either a C-H or a nitrogen lone pair on the core.

Bipyridyl compound **A** was calculated to have the greatest difference between the energy maximum and minimum and correspondingly the largest increase in stability in a conformation with dihedral angle of 180° (conformation **A''**). Therefore, this compound will spend almost all the time in this lowest energy (and most favourable for binding) conformation, perhaps explaining why bipyridyl compounds retained affinity. An additional factor not considered in these calculations is the ability of bipyridyl compounds to form favourable hydrogen bonding interactions in this

^a Dihedral angle scanning calculations performed using Density Functional Theory (DFT), 6-31G** (B3LYP) basis set in Jaguar by S. Pal.

conformation (A''), further increasing the stability of the conformation required for binding. While these energy minima calculations suggested a rationale for the affinity of bipyridyl compounds, they did not explain the reduction in affinity for compounds with fluorinated back pocket groups.

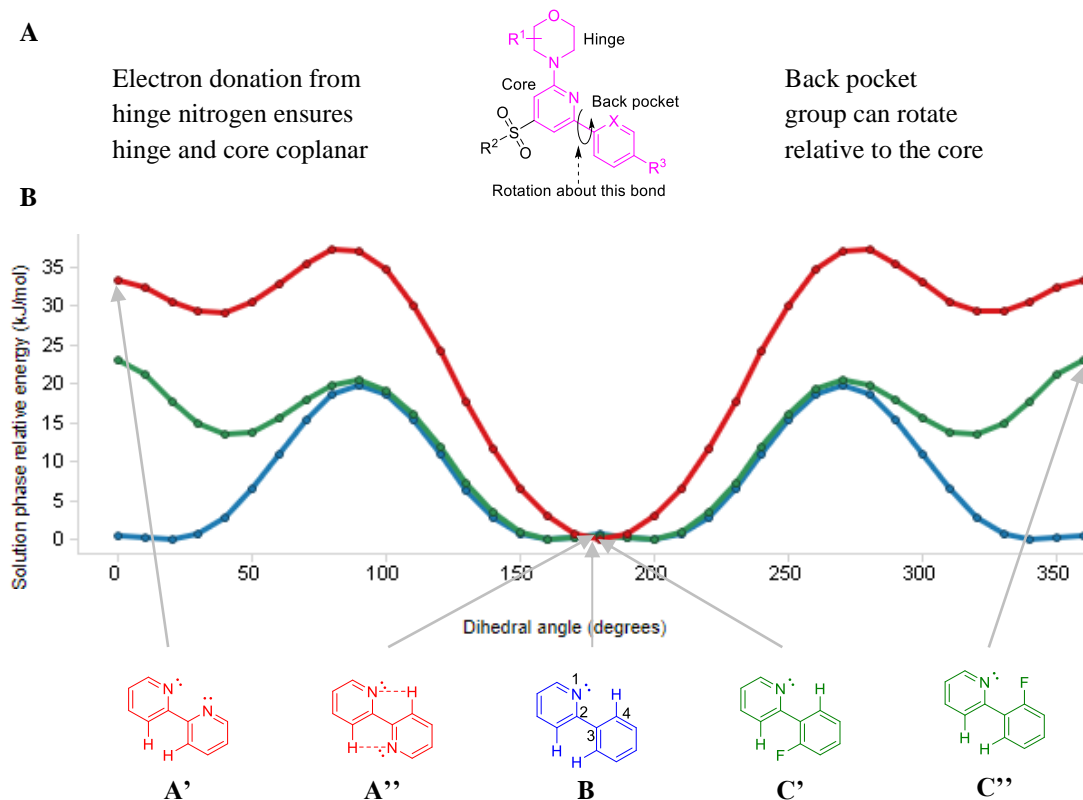


Figure 27A: Demonstrating the components of mTOR kinase inhibitors required to be coplanar to make favourable interactions with the mTOR kinase active site (in pink). Rotation about the highlighted bond (between the core and back pocket group) was investigated in cut-down compounds.

B: The calculated changes in energy (kJ/mol) of the compound in solution as the dihedral angle between the back pocket and the core is increased from 0 to 360°. Calculations by S. Pal.

Both high affinity (mTOR KB pIC₅₀) and efficacy (pAkt pIC₅₀) were important in mTOR kinase inhibitors. The mTOR KB affinity assay measured how well the compound binds to isolated mTOR kinase, while the pAkt efficacy assay monitored the downstream response to a compound binding to and inhibiting mTOR kinase. As described in the introduction, these two assays measured the effect of inhibition at different points in the pathway, therefore the same pIC₅₀ value may not be obtained from both. However, frequently in this study, good correlation between affinity and efficacy values was found. Any differences could be explained by considering the different assay formats as well as by consideration of physicochemical properties of

the mTOR kinase inhibitors. For example, the efficacy was lower than the affinity for most of the glycinamide and some urea-containing compounds. The mTOR affinity assay used cell lysate whereas the pAkt efficacy assay used whole cells, so compounds first had to pass through the cell membrane to interact with the intracellular mTOR kinase target. Therefore, differences in values obtained from each assay could be explained by the ability of a compound to cross a cell membrane – its permeability.

Permeability is related to lipophilicity and molecular size. Cell membranes consist of a phospholipid bilayer with hydrophilic head groups that point out towards the aqueous extra- and intra-cellular environment with hydrophobic tail groups in-between (**Figure 28A**). Diffusion across the hydrophobic interior of the lipid bilayer of a cell membrane is rate-limiting in passive diffusion.¹³⁰ This hydrophobic nature of a bilayer makes it intolerable to water or charged species, therefore molecules must be desolvated and neutral in order to pass passively through the cell membrane.¹³¹ Charged species can be actively transported into cells via specific proteins or ion channels (**Figure 28B**).¹³² It was hypothesised that the majority of compounds considered here would permeate passively. In addition to the effects of measuring at different points in the mTOR pathway, it was proposed that the reduced efficacy of less permeable compounds compared to their affinity could be due to lower intracellular concentrations at a given external concentration. A higher external concentration of these compounds would be required to increase the intracellular concentration to that at which half maximal inhibition was seen, translating into apparent lower efficacy.

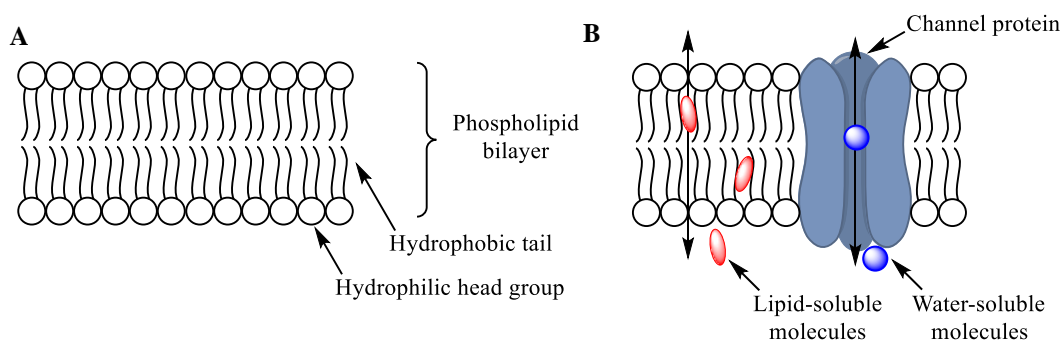


Figure 28A: Schematic of the hydrophilic head group and hydrophobic tail components of the phospholipid bilayer of cell membranes. **B:** Schematic showing active and passive permeability of both lipid- and water-soluble molecules, adapted from the Medical Gallery of Blausen Medical.¹³²

The difference between the affinity and efficacy of a compound, here called drop off (mTOR KB pIC₅₀ – pAkt pIC₅₀), demonstrated that there was a lower lipophilicity limit (ChromLogD ~3), below which the cellular efficacy of compounds may be permeability limited (**Figure 29**). More lipophilic, more permeable compounds, such as those containing the fluoroethylurea back pocket group (red), were less likely to have permeability-limited efficacy in the pAkt assay and demonstrated comparable efficacy and affinity. Indeed, in some cases these lipophilic compounds had higher efficacy than affinity, leading to a negative drop off. Conversely, compounds containing the polar bipyridylglycinamide group (light blue), had lower permeability leading to reduced efficacy, despite achieving higher affinity.

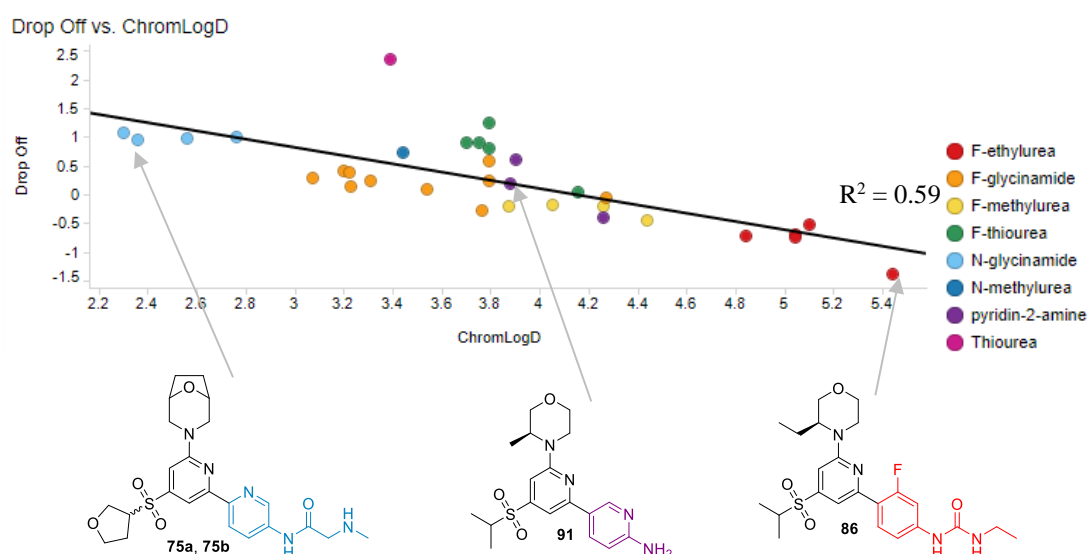


Figure 29: A plot of drop off (affinity (mTOR KB pIC₅₀) – efficacy (pAkt pIC₅₀)) against ChromLogD at pH 7.4 ($R^2 = 0.59$) with exemplar compounds shown and coloured according to the 6-position back pocket group. $R^2 = 0.56$. a = (*S*)-isomer, b = (*R*)-isomer.

Affinity and efficacy were not the only considerations – selectivity was also important. The four Class I PI3K isoforms (α , β , γ and δ) and DNA-PK were the most closely structurally related kinases routinely screened in this project, as high-throughput assays were available in our laboratories. Many of the compounds described here demonstrated reasonable (100-200-fold) selectivity over the PI3Ks and this will not be discussed further. Achieving selectivity over DNA-PK was more challenging. More lipophilic molecules tend to be more promiscuous and can bind to multiple targets, a potential source of off-target interactions.⁹⁷ However, there was no correlation

between lipophilicity and DNA-PK activity (**Figure 30A**). It was realised in subsequent work that selectivity over DNA-PK could be achieved in compounds with a basic centre (Section 2.4.3). Compounds containing the glycinamide back pocket group (calculated pK_a of the conjugate acid of 8.5 – the pK_{aH}) demonstrated improved selectivity compared to the slightly less basic aminopyridyl (calculated pK_a of the conjugate acid of 6) and non-basic urea-containing compounds (**Figure 30B**). The only compounds to achieve the desired 100-fold selectivity over DNA-PK were those containing a bipyridyl- or fluoroglycinamide back pocket (**Figure 30C**). Compound **82a** with anomalously high affinity (**Table 9**) achieved good selectivity over DNA-PK but a DNA-PK pIC_{50} of 6.2 was prohibitively high and this compound could not be progressed.

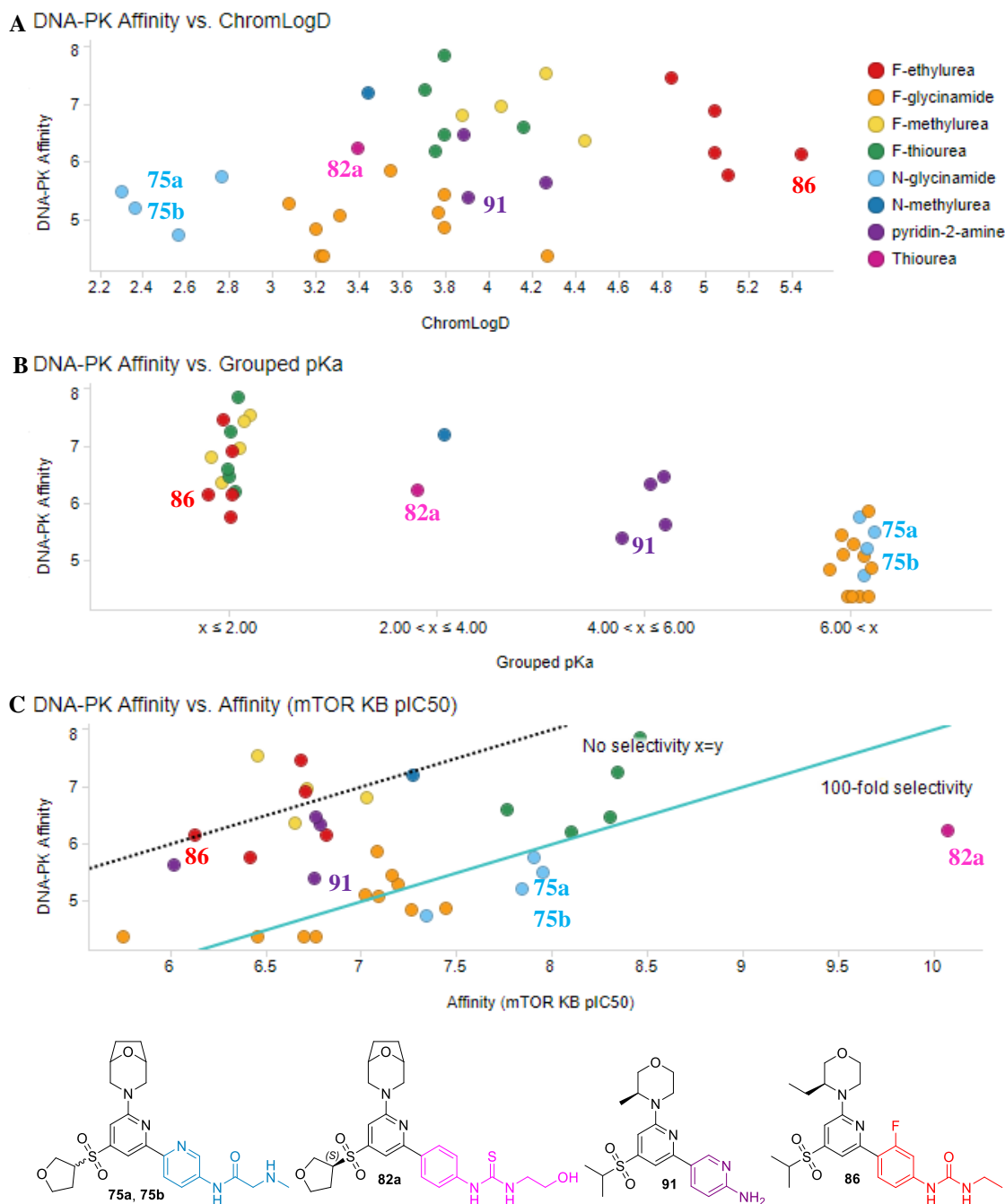


Figure 30A: DNA-PK affinity plotted against ChromLogD (at pH 7.4) demonstrating no correlation ($R^2 = 0.17$). **B:** The correlation between DNA-PK affinity and calculated pK_a of the conjugate acid (pK_{aH}). **C:** Demonstrating the acceptable 100-fold level of selectivity (blue line). Coloured according to back pocket group with exemplar compounds shown. a = (*S*)-isomer, b = (*R*)-isomer.

DNA-PK shares significant homology in its kinase domain with that of mTOR kinase as well as ATR and ATM.^{133,134} Therefore it was not surprising that achieving selectivity over DNA-PK, as well as other related kinases, was challenging. For example, wortmannin, an irreversible ATP-competitive non-selective inhibitor of the

PI3Ks also inhibits several of the PIKKs including mTOR and DNA-PK, as well as several other kinases, due to the similarity between the PI3K and PIKK catalytic domains.¹³⁵ Additionally, programmes to develop potent and specific DNA-PK inhibitors have encountered issues of selectivity against mTOR kinase.^{133,135,136} Many DNA-PK inhibitors feature a morpholine motif (compounds **100** and **101**, **Figure 31**), proposed to make the same key interaction in the active site as the morpholine in mTOR kinase inhibitors, potentially contributing to the lack of selectivity.^{75,136}

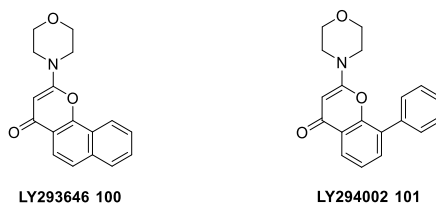


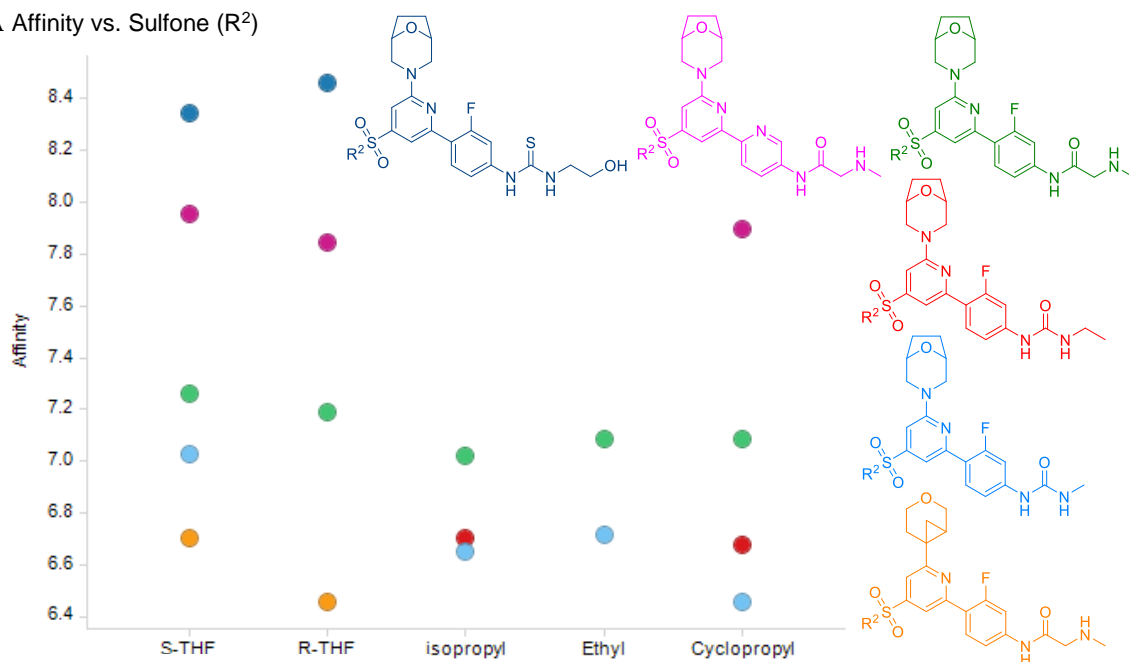
Figure 31: Two DNA-PK inhibitors known to exhibit micromolar activity, both with a morpholine hinge binder group. LY293646 (**100**) showed increased activity at DNA-PK and increased selectivity over both mTOR kinase and PI3K α compared to LY294002 (**101**).¹³⁶

Comparison of matched pairs – compounds with the same hinge and back pocket groups differing only in the 4-position sulfone moiety – demonstrated that the sulfone moiety did not have a profound effect on the affinity of these compounds; the small individual differences could have been within the error limits of the assay. However, considering the (*S*)- and (*R*)-isomers of the THF sulfone group shows that, in three of the four matched pairs, the (*S*)-isomer produced compounds of slightly higher affinity (**Figure 32A**). Overall, this matched pair data demonstrated that the back pocket had the greatest effect on affinity.

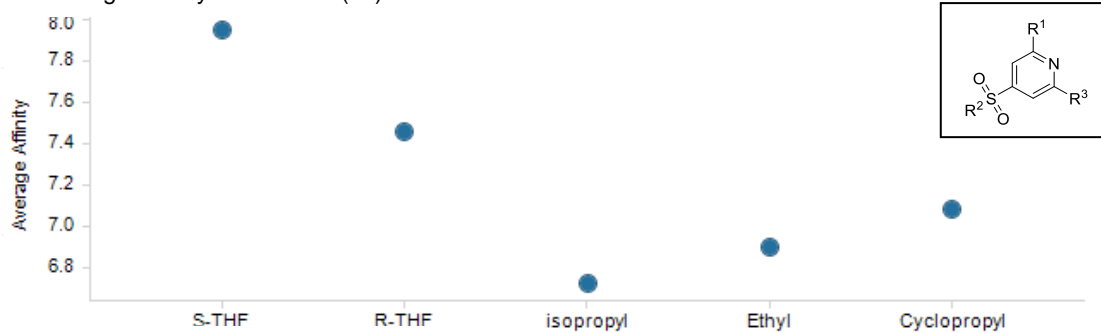
Comparison of the average affinity and efficacy across all compounds demonstrated overall trends (**Figure 32B**). Cyclopropyl, ethyl and isopropyl sulfone substituents all gave compounds of lower average affinity than the THF sulfone group. Particularly, the ethyl sulfones synthesised here showed compound **28** (**Table 4**) to be an outlier and introduction of a non-mutagenic variant of the 6-position aniline (glycinamide to fluoroglycinamide) reduced the affinity (mTOR KB pIC₅₀ of 8.1 to 7.1). Therefore no more ethyl sulfones were investigated. The contribution of lipophilicity to efficacy was demonstrated – the lipophilic isopropyl sulfone had a high average efficacy. Again,

these data suggested the (*S*)-isomer of the THF sulfone group to have higher affinity and efficacy than the (*R*)-isomer.

A Affinity vs. Sulfone (R^2)



B Average Affinity vs. Sulfone (R^2)



Average Efficacy vs. Sulfone (R^2)

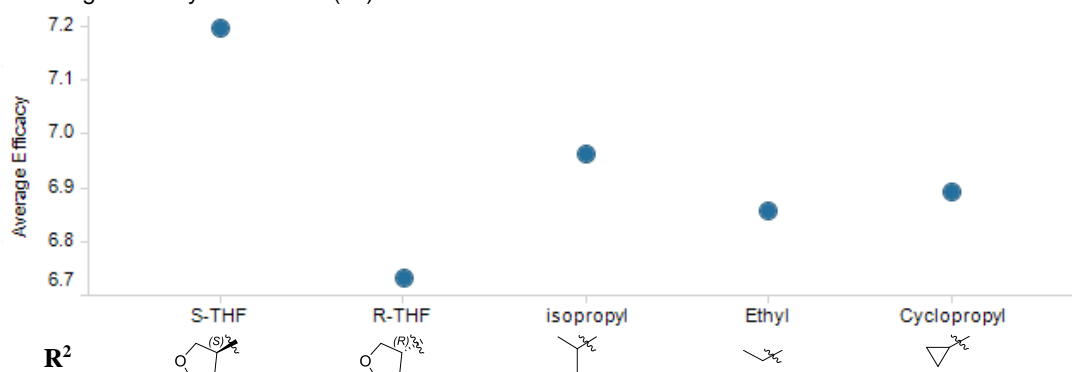


Figure 32A: Comparison of affinity (mTOR KB pIC_{50}) and efficacy (pAkt pIC_{50}) of matched pairs, differing only in the sulfone substituent (R^2). **B:** Average affinity (mTOR KB pIC_{50}) and efficacy (pAkt pIC_{50}) of all compounds with differing sulfone substituents (not only matched pairs).

The second hypothesis – that installing different morpholine rings in the 2-position would give increased affinity, efficacy and variety in physicochemical properties – was largely disproved. The morpholine moieties investigated were shown to have only a small effect on affinity and efficacy but a larger effect on lipophilicity, with the most lipophilic (*S*)-3-ethylmorpholine giving compounds of higher efficacy (**Figure 33**). Interestingly, despite their relative low lipophilicity, the fluorothiourea compounds with the (*S*)-THF sulfone (green) demonstrated high affinity and efficacy.

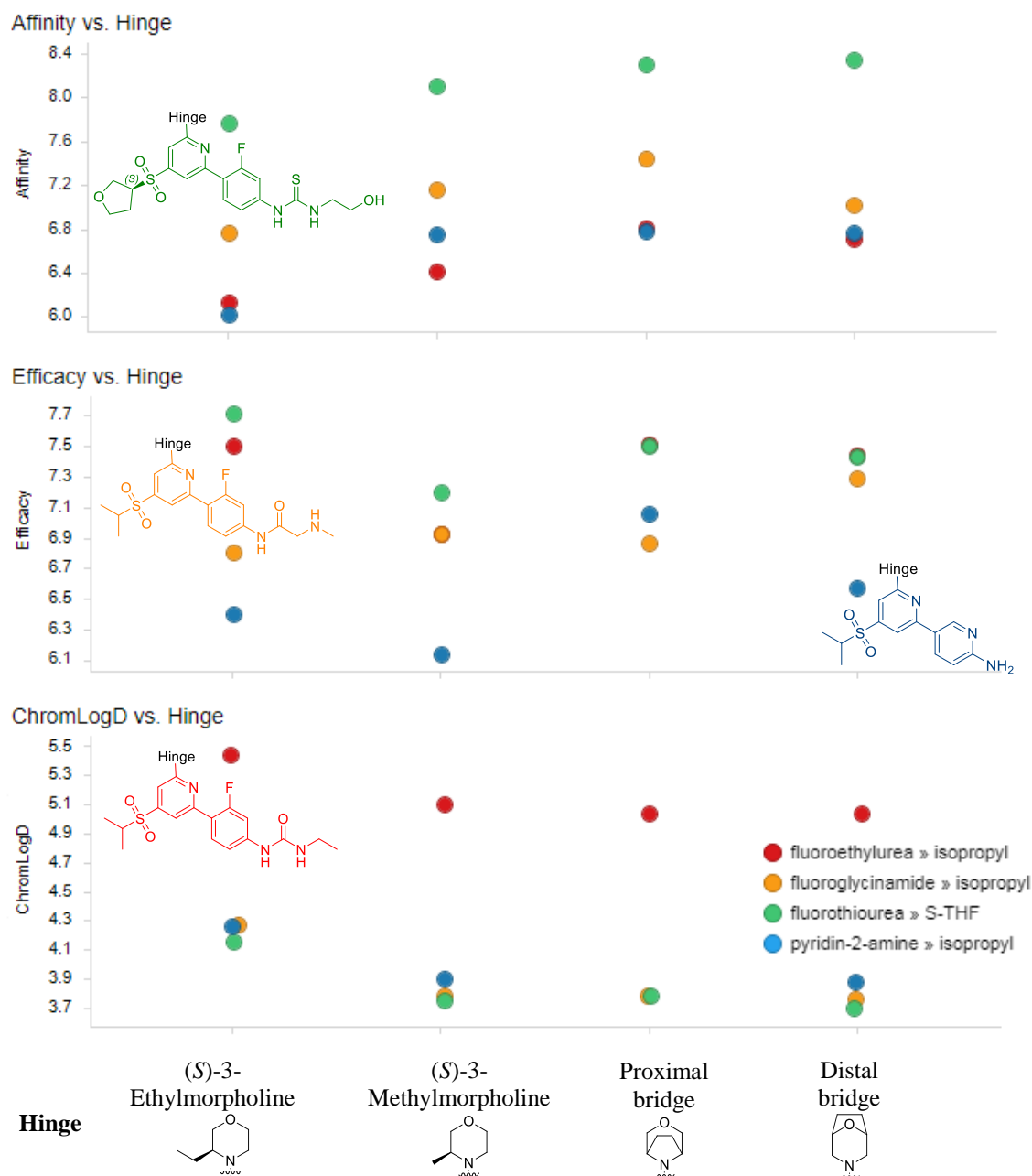


Figure 33: Demonstrating the effect of the hinge group on affinity (mTOR KB pIC₅₀), efficacy (pAkt pIC₅₀) and lipophilicity (ChromLogD).

This research expanded on the preliminary SAR established in this series of mTOR kinase inhibitors (as described in the Introduction, Section 1.5). The hinge group was shown to modulate lipophilicity and have a small effect on affinity and efficacy. This work highlighted the (*S*)-3-ethyl- and the proximal bridge morpholine hinges, both of which were preceded but had not been used in this series before. The 4-position sulfone group was demonstrated to have a modest effect on the affinity and efficacy, especially the THF sulfone. The unique activity of ethyl sulfone-containing compound (**28**, **Table 9**) was found not to be generally applicable to other compounds. Investigations of new sulfone groups was proposed to achieve increases in both affinity and efficacy and was subsequently explored (Section 2.4). The non-mutagenic 6-position anilines investigated gave compounds with moderate affinity and efficacy, with a range of physicochemical properties. Overall, the back pocket group was shown to have the largest contribution to affinity, efficacy and selectivity; the presence of a basic centre was suggested to achieve selectivity over DNA-PK. Thiourea back pocket groups gave active compounds that could not be progressed due to their poor selectivity over DNA-PK. The pyridylglycinamide was demonstrated to be the most promising 6-position substituent from this work as it gave compounds with high affinity and good selectivity over DNA-PK, and the low lipophilicity led to reduced permeability. However, the synthesis of these bipyridyl compounds was challenging, requiring Stille chemistry and toxic organostannanes, so an alternative route was required.

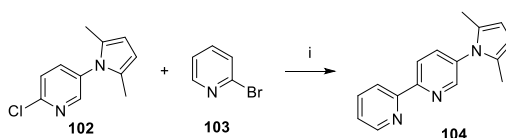
2.3.2 Improving the synthesis of bipyridyl-containing compounds

Stille and Negishi couplings are commonly used to synthesise bipyridyl compounds, with Suzuki conditions developed only relatively recently.¹³⁷ To synthesise bipyridyl compounds in our laboratories, initial investigations employing Suzuki reaction conditions achieved low conversions and poor isolated yields, so were abandoned in favour of the Stille reaction.^b Stille chemistry was successfully used to synthesise several mTOR kinase inhibitors, including compounds **70**, **73**, **75** and **80** (**Figure 23B**).

^b Trial reactions, including *in situ* formation of the boronic ester, by H. Hobbs and S. Nicolle, 2016.

However, due to the toxicity of organostannanes, Stille chemistry was not an acceptable method to make these compounds and an alternative route was required.

First developed in the 1970s, the Negishi cross-coupling follows the same reaction steps as the Suzuki reaction – oxidative addition, transmetalation and reductive elimination – but uses organozinc reagents as the transmetalation partner. Negishi reactions are preceded for biaryl couplings, and in 2002 Lutzen and Hapke reported the development of a general method for the synthesis of 5-monosubstituted 2,2-bipyridines in a modified palladium-catalysed Negishi reaction.^{138,139} Different catalysts and ligands were investigated to identify optimal conditions and the scope of coupling pyridyl zinc compounds with 5-substituted-2-chloropyridines explored. While the reaction generally gave the desired products in fair to excellent yields, there was a notable exception: a primary amino substituted pyridine gave no reaction. However, the authors found that a readily installed and removed pyrrole protecting group gave good conversion to the desired product (**Scheme 8**).¹³⁹



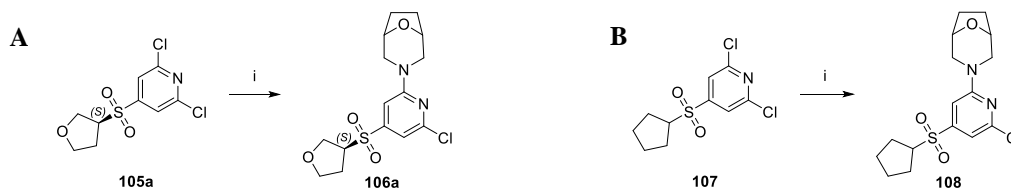
Scheme 8: A protecting group strategy enabled synthesis of bipyridyl compound **104**. Without the pyrrole group (using 6-chloropyridin-3-amine) no reaction occurred. *Reagents and Conditions:* i) ^tBuLi (1.7 M in pentane, 2.1 equiv.), **103** (1.1 equiv.), THF, -78 °C, 30-40 min, then ZnCl₂ (in THF, 2.7 equiv.), 21 °C, 2.0-3.0 h then, Pd₂dba₃CHCl₃ (3 mol%), P(^tBu)₃ (6 mol%), **102** (1.0 equiv.), THF, reflux, 21.0 h, 72%.¹³⁹

Subsequently, Lutzen *et al.* reported an extension of their Negishi cross-coupling reactions to couple a brominated variant of pyridine **102** with a chloropyridine,¹⁴⁰ and in 2007, the use of commercially available tetrakis(triphenylphosphine) palladium catalyst was reported.¹⁴¹ The modified conditions were initially shown to couple two bromopyridines, with the cross-coupling of chloro- and bromopyridines requiring more forcing conditions.¹⁴¹

Here, these bipyridyl Negishi cross-coupling conditions were investigated for the synthesis of bipyridylglycinamide-containing compounds.^{c,139-142} The low

^c Negishi reaction conditions suggested and trialled by T. Barrett.

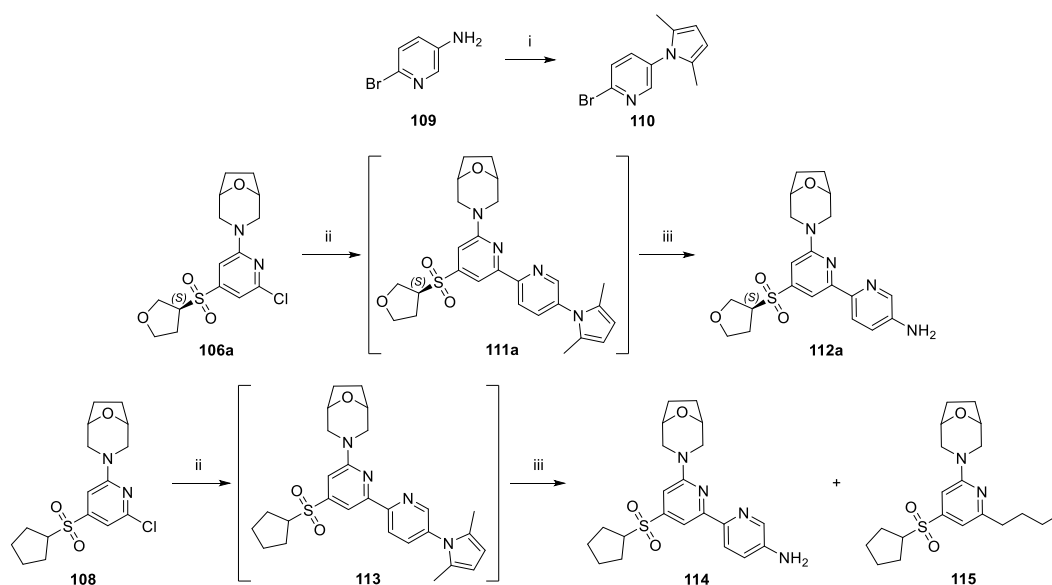
lipophilicity of this back pocket group had been shown to lead to reduced efficacy. Therefore a lipophilic cyclopentyl sulfone substituent was selected to achieve increased efficacy. Additionally, compound **75a** – a relatively polar compound employing the (*S*)-isomer of the THF sulfone – was remade using this methodology. As previously, the dichloropyridines were made at GVK Biosciences¹²⁵ and functionalised in high-yielding S_NAr reactions to give intermediates **106a** and **108** (Scheme 9A and 9B).



Scheme 9A and 9B: Preparation of 6-chloropyridine starting materials for the Negishi chemistry.

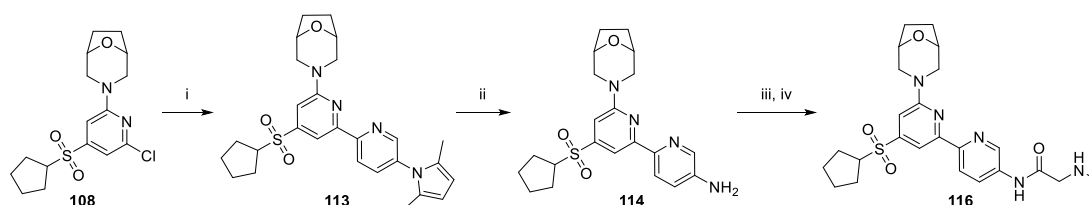
Reagents and Conditions: i) 8-Oxa-3-azabicyclo[3.2.1]octane.HCl (1.0 equiv.), DIPEA (2.0 equiv.), DMSO, 100 °C, 1.5-3.0 h, 97% (**106a**) and 94% (**108**). Synthesis by H. Davies.

The pyrrole-protected bromopyridine (**110**) was synthesised in a moderate yield in a Paal–Knorr reaction, following a variation of the procedure by Lutzen *et al.*, and the coupling reaction explored.¹⁴⁰ Initially the reactions were telescoped to achieve the deprotected bipyridyl product, without isolation of the protected intermediate. Both THF sulfone (**106a**) and cyclopentyl sulfone (**108**) compounds gave desired product in acceptable yields. Using the cyclopentyl sulfone, a by-product (**115**) was isolated and demonstrated to be the product of a S_NAr reaction of the nucleophilic *n*-butyllithium with the chloropyridine (**108**). However, using the (*S*)-THF sulfone, some unreacted starting material (**106a**) was isolated but no butylated by-product was observed, suggesting that this substrate may be less reactive (Scheme 10).



Scheme 10: The synthesis of pyrrole-protected bromopyridine coupling partner (**110**) and subsequent Negishi reactions to form two bipyridyl compounds (**112a** and **114**). *Reagents and Conditions:*
 i) Hexane-2,5-dione (1.0 equiv.), *p*-TsOH.H₂O (0.1 equiv.), toluene, 100 °C, 3.0 h, 65%.¹⁴¹ ii) **110** (1.0 equiv.), *n*-BuLi (1.2 M in hexane, 1.2 equiv.), THF, -78 °C, 30 min then ZnCl₂ (2 M in 2-MeTHF, 1.2 equiv.), -78-21 °C, 30-40 min then pyridylchloride (**106a** or **108**, 1.0 equiv.), Pd(PPh₃)₄ (0.1 equiv.), 100 °C, 1.5-1.7 h. iii) HCl (12 M in H₂O, 29.0-36.0 equiv.), EtOH, 100-120 °C, 20-30 min, 27% (**112a**) and 54% (**114**, 80% purity). Synthesis by H. Davies.

The reaction conditions employed here differed from those in the literature. Lutzen *et al.* used a longer reaction time for zincate formation, a lower reaction temperature in the cross-coupling and isolated the pyrrole-protected bipyridyl compound before deprotecting it using milder conditions (90 °C and 4 M HCl instead of 120 °C and 12 M HCl).^{140,141,142} A subsequent reaction with chloropyridine **108** used these refinements (**Scheme 11**). Combined with a titrated solution of *n*-butyllithium, this achieved improved conversion (90%) to the pyrrole-protected bipyridyl (**113**, 78% purity by LCMS). Pleasingly, no butylated by-product (**115**) was observed, thought to be due to the use of titrated base. The isolated intermediate was deprotected to give aniline **114** in quantitative yield with 85% purity.^{140,142} Bipyridylaniline **114** was then converted in two more steps to give bipyridylglycinamide (**116**). The product of the amide coupling with HATU was taken through to the deprotection without purification and this, combined with a poor return from the final purification, was proposed to explain the low yield.



Scheme 11: The synthesis of mTOR kinase inhibitor **116** with only one purification. *Reagents and Conditions:* i) *n*-BuLi (2.1 M in hexanes, 1.1 equiv.), **110** (1.5 equiv.), THF, -78 °C, 30 min then ZnCl₂ (1.9 M in 2-MeTHF, 1.2 equiv.), -78-21 °C, 2.5 h then **108** (1.0 equiv.), Pd(PPh₃)₄ (2 mol%), THF, 70 °C, 2.0 h, 90% crude.¹⁴¹ ii) Hydroxylamine.HCl (20.0 equiv.), TEA (5.0 equiv.), EtOH, H₂O, 100 °C, 24.0 h, quant..¹⁴² iii) HATU (3.0 equiv.), *N*-(*tert*-butoxycarbonyl)-*N*-methylglycine (3.0 equiv.), DIPEA (4.0 equiv.), DMF, 70 °C, 4.0 h, quant. crude. iv) HCl (4 M in 1,4-dioxane, 5.0 equiv.), 1,4-dioxane, 90 °C, 7.0 h, 11%. Synthesis by H. Davies.

This Negishi reaction gave a stannane-free method to make bipyridylglycinamide-containing compounds. Pleasingly, these compounds had good selectivity (greater than 100-fold) over DNA-PK, hypothesised to be due to the presence of the basic amine (**Table 10**). Compound **75a** (a re-make of a previous compound) demonstrated the target affinity (mTOR KB pIC₅₀), but decreased lipophilicity (ChromLogD) and permeability led to a log unit reduction in efficacy (pAkt pIC₅₀). The more lipophilic cyclopentyl sulfone **116** had lower affinity and comparable efficacy (to **75a**).

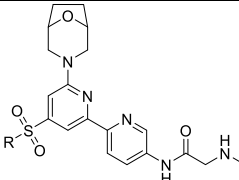
 R, Compound number	mTOR KB pIC₅₀ (n)^a	pAkt pIC₅₀ (n)^a	DNA-PK pIC₅₀ (n)^a	Chrom LogD^b	CLND, SLF (µg/mL)^{c,f}	AMP, MDCK P_{exact} (nm/s)^{c,g}
 75a^d	8.0 (6)	6.9 (6)	5.5 (4)	2.3	162,26	42,29
 116^e	7.5 (3)	7.0 (4)	5.5 (1)	3.6	-,	230,-

Table 10: Key data for two of the bipyridylglycinamide compounds synthesised. a = (*S*)-isomer.

^apIC₅₀ recorded as the mean of the data obtained on each of a number of test occasions (n).

^bChromLogD at pH 7.4. ^cIf more than one measurement taken, the mean was reported. ^dNegishi chemistry by H. Davies, deprotection by E. Mogaji. ^eSynthesis by H. Davies. ^fSolubility data.

^gPermeability data. -Data not generated.

Despite development of a viable route and achieving improved selectivity over DNA-PK, neither compound **75a** or **116** (or other bipyridylglycinamide compounds synthesised in our laboratories) were progressed further; the required efficacy was not

achieved. Therefore, very few other bipyridylglycinamide compounds were made and subsequent work focussed on discovering a new sulfone substituent.

2.4 Investigation of mTOR kinase inhibitors with novel 4-position sulfone moieties

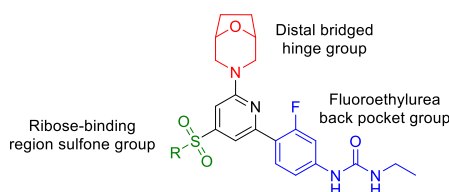
With some of the results from the previous work in hand, research was focussed on exploring the sulfone substituent. Compounds synthesised so far lacked sufficient affinity and efficacy. It was proposed that using a novel sulfone moiety could achieve increased affinity and efficacy, in a non-mutagenic compound. Additionally, achieving selectivity over DNA-PK had been challenging in this compound series. It was proposed that modifications to the sulfone moiety may mitigate this. The aims of the work in this Section were to:

- Synthesise compounds with increased affinity, efficacy and selectivity over DNA-PK, through modifications to the sulfone group.
- Investigate a range of sulfone moieties.

2.4.1 Exploration novel 4-position sulfone moieties

The sulfone moieties investigated previously (described in the Introduction and in Section 2.3), including 5- and 6-membered (hetero)cycles, heteroaromatic and aminoethyl compounds (**Figure 21**), were used as a starting point for modifications. This gave a large set of structurally diverse sulfones (**Table 11**). Modifications were suggested based on known effects. For example, addition of a methyl group is known to be capable of having a dramatic positive effect on affinity,¹⁴³ as well as more subtle effects on physicochemical properties through increases in steric bulk, conformation and pK_a.¹⁴⁴ Increased volume in the 4-position (the part of the compound proposed to reside in the ribose-binding region of the protein) was proposed early on in this series to give enhanced affinity (**Table 3**). This was further investigated by methylation adjacent to the sulfone and increasing the hydrophobic steric bulk by expanding the ring size from cyclopropyl up to cyclohexyl. These changes would also increase the lipophilicity and permeability of these compounds. The THF sulfone moiety gave the highest affinity compounds in the sparse array, therefore a pyrrolidine group was suggested in order to explore the importance of the hydrogen bond acceptor.

Pyrrolidine sulfone moieties placed a basic group in the ribose-binding region and the option to alkylate on the nitrogen gave scope to further vary the physicochemical properties. Another basic group, the aminoethyl sulfone, gave active compounds in the sparse array, but the low lipophilicity of these compounds led to poor permeability. Both methylation and fluorination were proposed to increase the permeability, as well as modulate the basicity. Fluorination or dimethylation of the aminoethyl nitrogen or monomethylation of the pyrrolidine nitrogen would decrease the basicity, while monomethylation of the aminoethyl nitrogen atoms would increase the basicity. Additionally, to further investigate tolerance of aromaticity in the ribose-binding region, a few 5-membered heteroaromatic sulfones were proposed. All of these sulfone moieties were combined with the distal bridged hinge and most synthetically accessible fluoroethylurea back pocket group. This combination was predicted to be lipophilic enough to give good efficacy and the anticipated high DNA-PK affinity meant that any increased selectivity due to the novel sulfone group would be detected.



Proposed modification	Original R group	Modified R group
Methylate, increased 3D volume		
Increased 3D volume		
Hydrogen bond acceptor/donor		
Methylate, alter pKa		
Explore aromaticity		

Table 11: The proposed modifications to the existing sulfone moieties, suggested to increase affinity, efficacy and modulate physicochemical properties. All compounds would be combined with the distal bridged morpholine hinge group (red) and the fluoroethylurea back pocket group (blue).

All 40 sulfones in **Table 11** were computationally enumerated with the distal bridged morpholine hinge and fluoroethylurea back pocket groups and the physicochemical properties calculated, as was an *in silico* prediction of macrophage toxicity (**Figure 34**).³³ Eight compounds predicted to have high risk of macrophage toxicity were discounted, as were two compounds made previously in Section 2.3 (compounds containing the cyclopropyl (**72**) and isopropyl (**88**) sulfone moieties). Calculated properties were compared for the remaining 30 compounds, with selections made from each of the classes of solubility and permeability and a lipophilicity range of 2-5 (**Figure 34**). Additionally, pK_a values were calculated (for the conjugate acid of the basic centre, pK_{aH}) and basicity defined as a pK_a of 7-10 (pK_{aH}) to ensure a mixture of both basic and non-basic sulfone groups were considered.

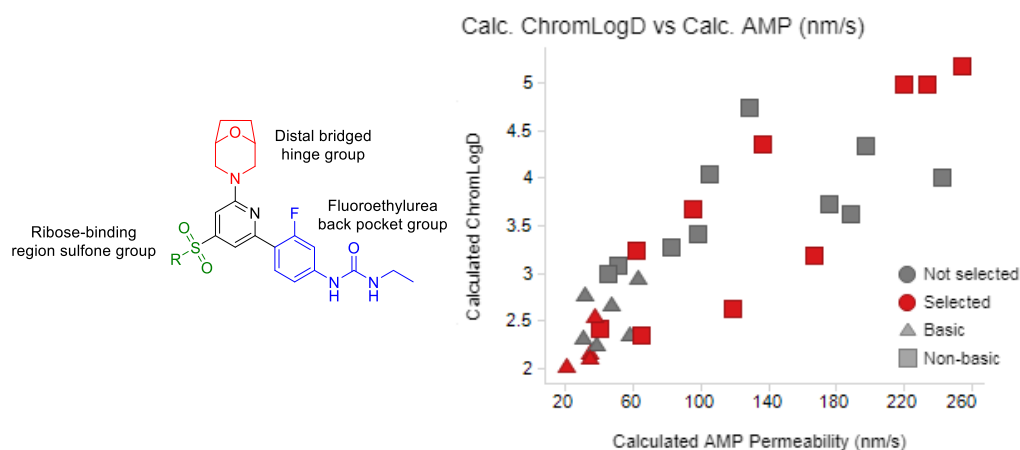
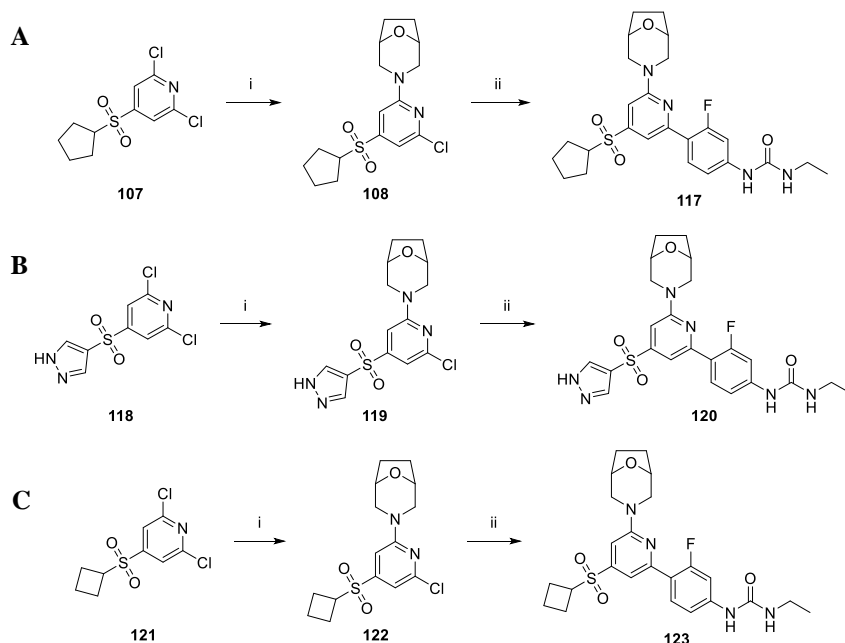


Figure 34: Plot of calculated AMP (artificial membrane permeability) against calculated ChromLogD used to aid selection of compounds for synthesis. The triangles show the compounds with a calculated pK_a of the conjugate acid (pK_{aH}) of 7-10 (basic) and the squares show non-basic compounds. The compounds highlighted in red were selected for synthesis.

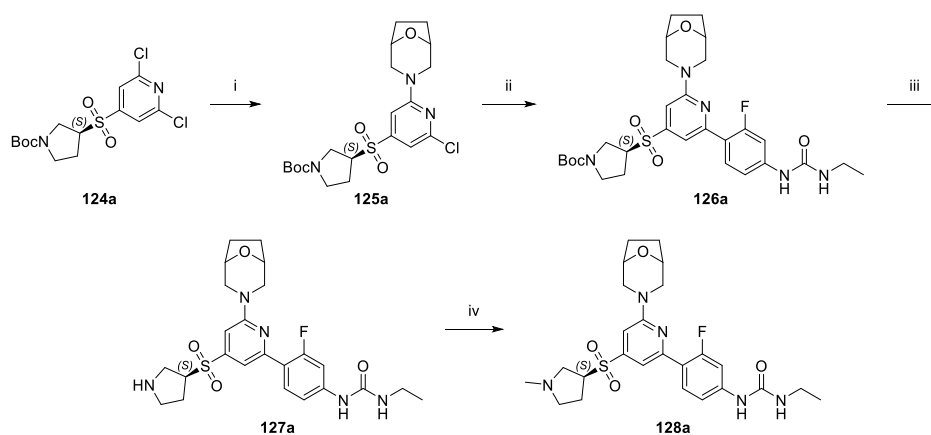
2.4.2 Synthesis of mTOR kinase inhibitors with a variety of 4-position sulfone moieties

Once selected, the compounds were synthesised. The 4-position of the pyridine was installed as previously discussed (at GVK Biosciences, exemplified in **Scheme 3**).¹²⁵ Some of these sulfones were used without modification, with the final compounds all synthesised using a similar route: a high-yielding S_NAr reaction, followed by a Suzuki reaction using the bespoke fluorourea-boronic ester (**54**). The synthesis is exemplified for compounds **117**, **120** and **123** (**Scheme 12A-C**).



Scheme 12A-C: Demonstrating the synthesis of compounds **117**, **120** and **123**. *Reagents and Conditions:* i) 8-Oxa-3-azabicyclo[3.2.1]octane.HCl (1.1 equiv.), DIPEA (2.0 equiv.), DMSO, 100 °C, 1.5-4.0 h, 94% (**108**), 86% (**119**) and quant. (**122**). ii) **54** (1.1 equiv.), K₂CO₃ (2.0-2.6 equiv.), PdCl₂(dppf) (10 mol%), IPA:water (5:1), 100-120 °C, 1.0-5.0 h, 57% (**117**), 8% (**120**) and 42% (**123**).
Synthesis by H. Davies.

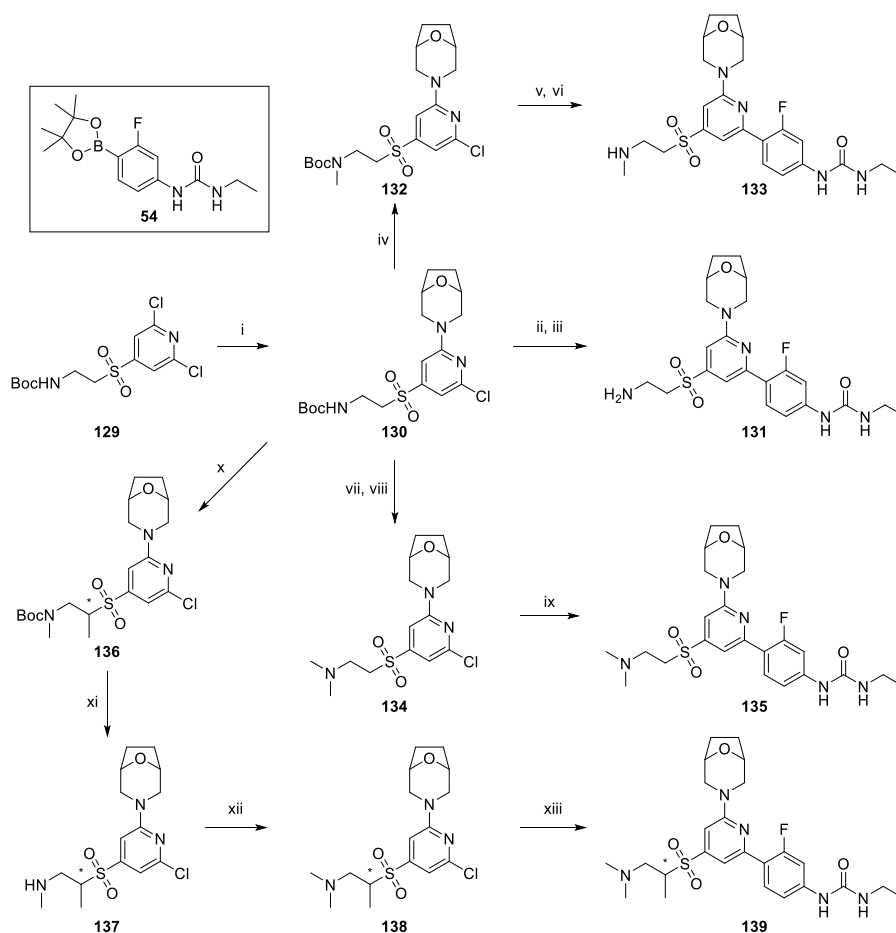
To make some of the desired compounds, the sulfone substituent was further modified in our laboratories, either before or after the hinge and back pocket groups were installed. For example, the synthesis of the (*S*)-isomer of pyrrolidine sulfone **128a** (**Scheme 13**). Single enantiomers of the pyrrolidine sulfone (**124a**, **124b**) were synthesised at GVK Biosciences,¹²⁵ the hinge installed in a high-yielding S_NAr reaction to give **145a**, followed by installing the back pocket group in quantitative yield, using the bespoke boronic ester (**54**) to give **126a**. The pyrrolidine was then deprotected to give **127a**, the reaction mixture was split, a portion purified to give the final product **127a** and the remainder subjected to reductive amination using Eschweiler-Clarke conditions to provide methylated pyrrolidine **128a**.¹⁴⁵



Scheme 13: The reaction scheme to produce two of the pyrrolidine final compounds, **127a** and **128a**.

Reagents and Conditions: i) 8-Oxa-3-azabicyclo[3.2.1]octane.HCl (1.1 equiv.), DIPEA (2.0 equiv.), DMSO, 100 °C, 1.5 h, 97%. ii) **54** (1.1 equiv.), Pd(dppf)Cl₂ (10 mol%), K₂CO₃ (2.0 equiv.), IPA:H₂O (5:1), 6.0 h, 120 °C, quant. (86% purity). iii) HCl (4 M in 1,4-dioxane, 3.0 equiv.), 1,4-dioxane, 80 °C, 5.0 h, 56%. iv) Formaldehyde (37% in H₂O, 1.2 equiv.), formic acid (38 equiv.), H₂O, 90 °C, 1.0 h, 22%.¹⁴⁵ Synthesis by H. Davies.

Similarly, compounds **131**, **133**, **135** and **139** were synthesised from a common intermediate (compound **130**), with methylation at the appropriate stage in the synthesis (**Scheme 14**). First, the substituted morpholine was installed in the 2-position in a high-yielding S_NAr reaction, giving common intermediate **130**. To form compound **131**, the 6-position was functionalised in a Suzuki reaction with bespoke boronic ester **54**, and the aminoethyl sulfone moiety deprotected. To form compound **133**, the aminoethyl sulfone moiety was first methylated using iodomethane and a base. A subsequent Suzuki reaction installed the 6-position aromatic group and finally a Boc-deprotection produced compound **133**. To form compound **135**, the Boc-group was removed first, giving a free amine in the sulfone moiety. This was methylated, using the Eschweiler-Clarke reaction to prevent formation of a quaternary ammonium salt, producing dimethylated compound **134**. A Suzuki reaction again gave the final compound (**135**). Finally, to form compound **139**, sodium hydride was used to deprotonate the two most basic sites in compound **130** and an excess of iodomethane was used to form dimethylated compound **136**. Boc-deprotection followed by another methylation gave compound **138**, before a Suzuki reaction with bespoke boronic ester **54** again gave the desired compound (**139**).



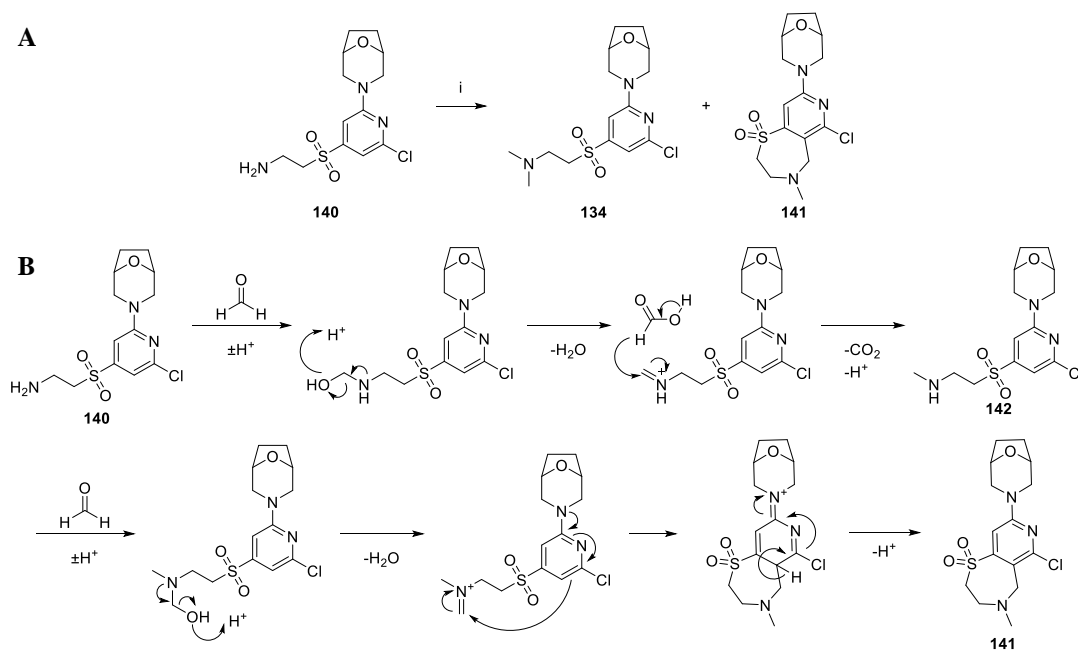
Scheme 14: Synthesis of the aminoethyl sulfone-containing compounds. *Reagents and Conditions:*

- i) 8-Oxa-3-azabicyclo[3.2.1]octane.HCl (1.1 equiv.), DIPEA (2.0 equiv.), DMSO, 100 °C, 2.0 h, 85%.
- ii) **54** (1.1 equiv.), K₂CO₃ (2.0 equiv.), PdCl₂(dppf) (0.1 equiv.), IPA:H₂O (5:1), 140 °C, 2.0 h, 97%.
- iii) HCl (4 M in 1,4-dioxane, 4.8 equiv., portion-wise), 1,4-dioxane, 26.0 h, 40 °C, 64.0 h standing, 21 °C, 32%.
- iv) NaH (60% dispersion in mineral oil, 1.0 equiv.), THF, 0-21 °C, 1.0 h then MeI (1.5 equiv.), 25.0 h, 21 °C, 42%.¹⁴⁵
- v) **54** (3.0 equiv., portion-wise), K₂CO₃ (4.0 equiv., portion-wise), PdCl₂(dppf) (0.2 equiv., portion-wise), IPA:H₂O (5:1), 120 °C, 12.0 h, 79%.
- vi) HCl (4 M in 1,4-dioxane, 5.0 equiv.), 1,4-dioxane, 4.0 h, 80 °C, 17%.
- vii) HCl (4 M in 1,4-dioxane, 3.3 equiv.), 1,4-dioxane, 6.0 h, 80 °C, quant..
- viii) Formaldehyde (37% in H₂O, 4.0 equiv.), formic acid (14.0 equiv.), 90 °C, 2.0 h, 31%.¹⁴⁵
- ix) **54** (1.1 equiv.), K₂CO₃ (2.0 equiv.), PdCl₂(dppf) (0.1 equiv.), IPA:H₂O (5:1), 120 °C, 2.0 h, 36%.
- x) NaH (60% dispersion in mineral oil, 2.2 equiv.), THF, 0-21 °C, 1.5 h then MeI (7.0 equiv.), 22.0 h, 21 °C, 91%.¹⁴⁶
- xi) HCl (4 M in 1,4-dioxane, 2.8 equiv.), 1,4-dioxane, 5.0 h, 90 °C, 98%.
- xii) NaH (60% in mineral oil, 1.3 equiv.), THF, 0-21 °C, 2.0 h then MeI (1.3 equiv.), 22.0 h, 21 °C, then NaH (60% in mineral oil, 0.2 equiv.), MeI (0.2 equiv.), 21 °C, 5.0 h, 35%.¹⁴⁶
- xiii) **54** (1.2 equiv.), K₂CO₃ (2.5 equiv.), PdCl₂(dppf) (0.1 equiv.), IPA:H₂O (5:1), 120 °C, 3.0 h, 30%.

*Stereoic centre, compounds synthesised as a racemic mixture. Synthesis by

H. Davies.

Many of these reactions proceeded smoothly with acceptable yields. Only the dimethylation of compound **140** to form compound **134** gave an unexpected by-product (**141**) that was isolated, and the structure confirmed by NMR spectroscopy (**Scheme 15A**).^d A mechanism to explain the formation of this by-product was proposed (**Scheme 15B**). Compound **140** underwent the first reductive amination with formaldehyde and formic acid. Monomethylated intermediate **142** reacted with formaldehyde to give a cationic species, some of which was not reduced by formic acid to give desired compound **134**, but instead underwent a cyclisation reaction to give compound **141**. An attempt to install a back pocket via a Suzuki reaction – so that this unprecedented bicyclic compound could be sent for biological testing – failed, giving no desired material and several by-products.



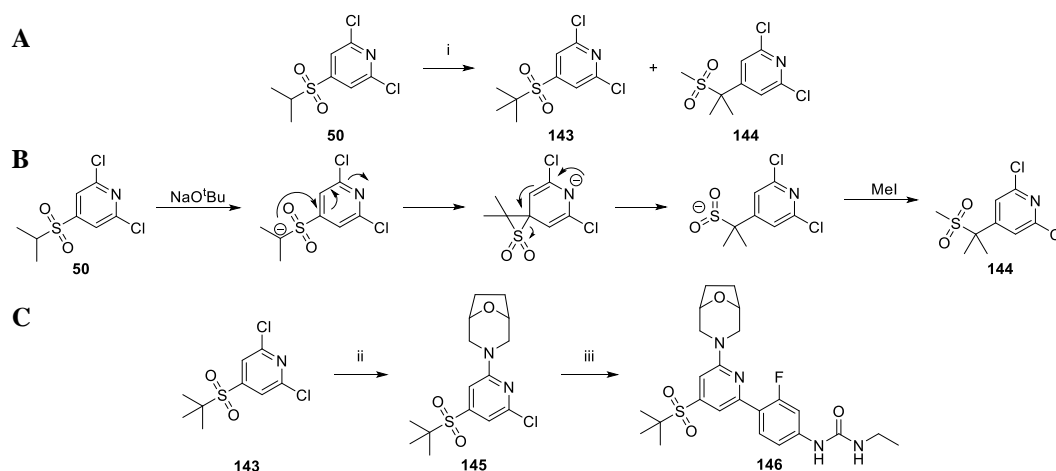
Scheme 15A: Reaction conditions and **B:** proposed mechanism of formation of unexpected by-product, **141**. *Reagents and Conditions:* i) Formaldehyde (4.0 equiv., 37% in water), formic acid (14.0 equiv.), 90 °C, 2.0 h, 31%.¹⁴⁵ Synthesis by H. Davies.

Attempts to fluorinate at the α -position of the aminoethyl sulfone failed on both the dichloro-intermediate **129** and 2-substituted pyridine **130** (compounds in **Scheme 14**). Selectfluor[®] and sodium hydride failed to enable electrophilic fluorination of the carbon alpha to the sulfone, giving largely remaining starting material.¹⁴⁷ A second

^d Structure confirmed by NMR spectroscopist, R. Upton.

precedented method that employed fluorinating agent *N*-fluorobenzene sulfonamide and LHMDS led to consumption of starting material and several unidentified by-products.¹⁴⁸

To form the bulky 4-(*tert*-butylsulfonyl)-2,6-dichloropyridine (**143**), base and methyl iodide were used to methylate isopropyl sulfone compound **50** (synthesised using propane-2-thiol at GVK Biosciences),¹²⁵ giving the desired product and a by-product proposed to result from a rearrangement reaction (**Scheme 16A**). A mechanism was suggested: deprotonation of the carbon alpha to the sulfone gave an anion that could either methylate directly to form the desired *tert*-butylsulfone (**143**), or displace the sulfone from the aromatic ring in an intramolecular S_NAr reaction and the resultant sulfur anion was methylated (**Scheme 16B**).^e Carbon-linked dimethylated sulfone **144** had a similar ribose-binding region substituent to a known mTOR kinase inhibitor (**Figure 10**, AZD3147),⁷⁰ suggesting a possible alternative synthesis for these compounds. Here, the desired *tert*-butyl product was isolated (**143**) and taken forward into the S_NAr and Suzuki reactions to give the final compound (**146**, **Scheme 16C**).



Scheme 16 A: The methylation of isopropyl sulfone **50** to give the desired product (**143**), and an unexpected by-product (**144**). **B:** The proposed rearrangement mechanism giving the unexpected by-product, **144**. **C:** The S_NAr and Suzuki reactions carried out to give final compound **146**. *Reagents and Conditions:* i) MeI (1.1 equiv.), NaO^tBu (2 M in THF, 1.1 equiv.), THF, 21 °C, 5.0 h, 24% (**143**), 12% (**144**). ii) 8-Oxa-3-azabicyclo[3.2.1]octane.HCl (2.4 equiv.), DIPEA (4.1 equiv.), DMSO, 100 °C, 30.0 h, 19%. iii) **54** (2.8 equiv.), Pd(dppf)Cl₂ (20 mol%), K₂CO₃ (2.0 equiv.), IPA:H₂O (5:1), 7.0 h, 120 °C, 54%. Synthesis by H. Davies.

^e Mechanism proposed by S. Nicolle and structure confirmed by NMR spectroscopist R. Upton.

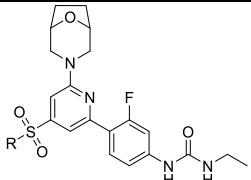
	R, Compound Number	mTOR KB pIC₅₀ (n)^a	pAkt pIC₅₀ (n)^a	DNA- PK pIC₅₀ (n)^a	Chrom LogD^b	LLE	CAD, SLF (µg/mL)^{c,f}	AMP, MDCK P_{exact} (nm/s)^{c,g}
	131	6.6 (4)	5.9 (4)	6.0 (3)	3.1	3.5	122*, -	<10,-
	133	6.1 (3)	6.2 (4)	-	3.1	3.0	148,-	<10,-
	135	6.2 (3)	6.7 (4)	5.7 (2)	4.1	2.1	142,-	100,-
	139	6.8 (4)	7.2 (4)	-	4.8	2.0	85,-	205,-
	148a	7.0 (9)	7.3 (3)	7.0 (1)	4.4	2.6	8*,1	105,226
	148b	6.6 (5)	7.3 (3)	7.6 (1)	4.4	2.2	9*,1	97,382
	127a	7.1 (4)	6.5 (4)	6.1 (2)	3.3	3.8	156*,250	<10,21
	127b	7.0 (5)	6.3 (4)	6.5 (2)	3.3	3.7	164*, 297	<7,21
	128a	7.2 (3)	7.1 (9)	5.9 (1)	4.3	2.9	110*,221	68,91
	128b	6.9 (4)	6.8 (6)	6.0 (3)	4.2	2.7	155,168	70,138
	149(1)^d	7.0 (4)	7.5 (5)	5.9 (2)	4.4	2.6	113,-	135,-
	149(2)^d	7.3 (5)	7.6 (5)	6.2 (2)	4.4	2.9	107,-	140,-
	149^e	7.1 (4)	7.6 (7)	6.1 (2)	4.5	2.6	113,-	130,-
	150^e	6.9 (6)	7.2 (4)	6.4 (1)	3.2	3.7	133,-	<3,-
	120	5.5 (2)	6.1 (1)	6.1 (1)	3.8	1.7	-, -	66,-
	72	6.7 (4)	7.4 (3)	7.5 (1)	4.8	1.9	-, -	240,-
	151	6.7 (4)	7.4 (4)	7.0 (1)	5.3	1.4	20,-	345,-
	123	6.0 (4)	7.3 (2)	7.2 (1)	5.2	0.8	19,-	280,-
	117	6.3 (4)	7.4 (4)	-	5.5	0.8	16,-	345,-
	88	6.7 (4)	7.4 (5)	6.9 (1)	5.0	1.7	5*,12	-,588
	146	6.8 (4)	7.5 (3)	6.8 (1)	5.3	1.5	47*,3	360,422

Table 12: Key data on compounds exploring different sulfone groups. a = (*S*)-isomer, b = (*R*)-isomer.

^apIC₅₀ recorded as the mean of the data obtained on a number of test occasions (n). < Value at the lower assay limit. ^bChromLogD at pH 7.4. ^cIf more than one measurement taken, the mean was reported. ^dSingle enantiomers from a chiral separation, 1 and 2 denote the order compound eluted from the column. ^eRacemic mixture. ^fSolubility data. ^gPermeability data. *CLND solubility.

LLE = affinity (mTOR KB pIC₅₀) – lipophilicity (ChromLogD). Efficacy = pAkt pIC₅₀. Final compounds made by H. Davies, E. Mogaji, D. Summers.

The aim was to achieve compounds with affinity and efficacy values of greater than 7.5. Disappointingly, no compound in this set achieved this. However, this iteration led to the discovery of a new sulfone substituent: the pyrrolidine moiety that gave compounds of comparable affinity to those containing THF sulfone moiety (**127**, **128**, **149** and **150**, compared to THF sulfone-containing compound **148**), suggesting that the hydrogen bond acceptor was not important (**Figure 35**). Indeed, the best overall compounds contained a pyrrolidine sulfone moiety (including monomethylated (*S*)-pyrrolidine **128a**, and all isomers of the dimethylated pyrrolidine **149**).

The (*S*)-isomer of the 5-membered heterocyclic sulfone-containing compounds consistently gave compounds of higher affinity than the (*R*)-isomer (**127a**, **128a** and **148a**, compared to **127b**, **128b** and **148b**) and, despite the difference in affinity being within the error limits of the assay, this was seen on each of a number of test occasions. Altering the ring size from cyclopropyl to cyclopentyl sulfone substituents gave decreased affinity and similar efficacy, proposed to be driven by the comparable lipophilicity of the three compounds (**72**, **117** and **123**). Pyrazole sulfone (**120**) had poor affinity and efficacy, demonstrating that aromaticity was not tolerated in the ribose-binding region, in agreement with the results of the sparse array (**Figure 22**). Methylation adjacent to the sulfone to increase the 3D volume was not favourable; any increase in efficacy was driven only by increased lipophilicity. Cyclopropyl (**72**) and isopropyl (**88**) sulfone compounds were methylated to give 1-methylcyclopropyl (**151**) *tert*-butyl (**146**) sulfone substituents, neither of which showed improved affinity or efficacy, despite the increased lipophilicity.

The low LLE (mTOR KB pIC₅₀ – ChromLogD) of the cyclopropyl, isopropyl, cyclobutyl, cyclopentyl and *tert*-butyl sulfone-containing compounds (**72**, **88**, **117**, **123**, **146** and **151**) demonstrated that the affinity of these compounds was due to high lipophilicity (**Figure 35**). Compounds with low LLE values may have off-target interactions and a higher risk of attrition.¹⁰⁵ In contrast, the higher LLE (≥ 3) of the aminoethyl and pyrrolidine sulfone-containing compounds (**127**, **131**, **133** and **150**) suggested that lipophilicity was not driving the affinity, giving better quality compounds. Unfortunately, some of these compounds had reduced efficacy, proposed to be due to their low permeability (**127**, **131** and **133** all had AMP < 10 nm/s).

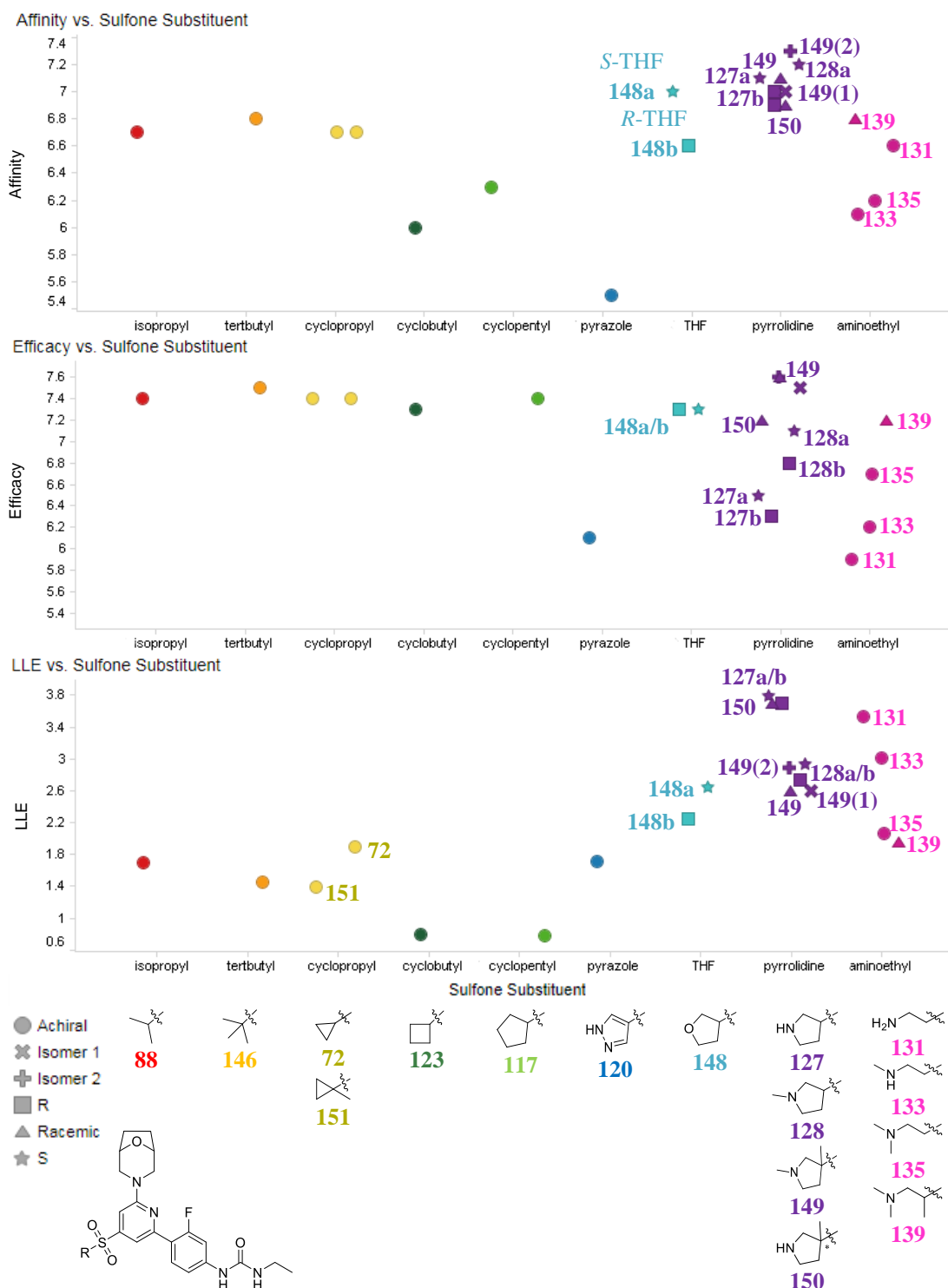


Figure 35: Demonstrating the affinity (mTOR KB pIC₅₀), efficacy (pAkt pIC₅₀) and LLE (mTOR KB pIC₅₀ – ChromLogD) of compounds synthesised in this iteration (**Table 12**). Coloured according to sulfone moiety and shaped according to enantiomer. a = (*S*)-isomer, b = (*R*)-isomer.

The pyrrolidine and aminoethyl sulfone-substituted compounds had a range of affinities and efficacies. Methylation of these compounds was used to explore the effect of increased 3D volume and alter the pK_a . No dramatic increase in affinity or ‘magic methyl’ effect was seen on addition of a methyl group.¹⁴³ The magic methyl effect is a well-known concept, but relatively rare occurrence in medicinal chemistry.¹⁴³ Methylation often results in increased affinity, due to desolvation effects.¹⁴³ Increasing the lipophilicity of a compound reduces the free energy of desolvation (energy required to remove water molecules) when it moves from an aqueous environment to a hydrophilic enzyme active site.¹⁴³ When addition of a methyl gives a greater increase in affinity than that expected due to desolvation effects, it is referred to as a magic methyl. While the likelihood of the addition of a methyl giving a dramatic boost in affinity was low, it was considered here because it a) would increase the volume of the ribose binding region substituent, b) was proposed to have other effects (including altered pK_a) and c) was experimentally relatively facile.

Each successive methylation of the aminoethyl-containing compounds (**131**, **133**, **135** and **139**) slightly increased the efficacy of the compound, proposed to be due to the increased lipophilicity. However, mono- (**133**) and di- (**135**) methylation decreased the affinity compared to the parent aminoethyl sulfone compound (**131**) and only the trimethylated sulfone compound (**139**) achieved comparable affinity. Each methylation of the pyrrolidine sulfone compounds (**127**, **128**, **149** and **150**) gave slightly increased efficacy (due to the increased lipophilicity) but little variation in affinity was achieved. These amines demonstrated a larger increase in lipophilicity when methylated compared to the aliphatic compounds (such as the isopropyl and cyclopropyl sulfone compounds), particularly when the methylation removed a hydrogen bond donor. An effect was also seen on the predicted pK_a of the conjugate acid (pK_{aH}). The monomethylated aminoethyl compound (**133**) had comparable predicted basicity to the parent compound (**131**), while dimethylation of the nitrogen (**135** and **139**) was predicted to give less basic compounds. Again, in the pyrrolidine sulfone compounds, methylation of the nitrogen (**128** and **149**) was predicted to give reduced basicity (**Figure 36**). The most notable feature of pyrrolidine compounds **127a**, **128a** and all isomers of compound **149** was the reduction in DNA-PK affinity

(Table 12). These were the only compounds to achieve ≥ 100 -fold selectivity over DNA-PK (Figure 40).

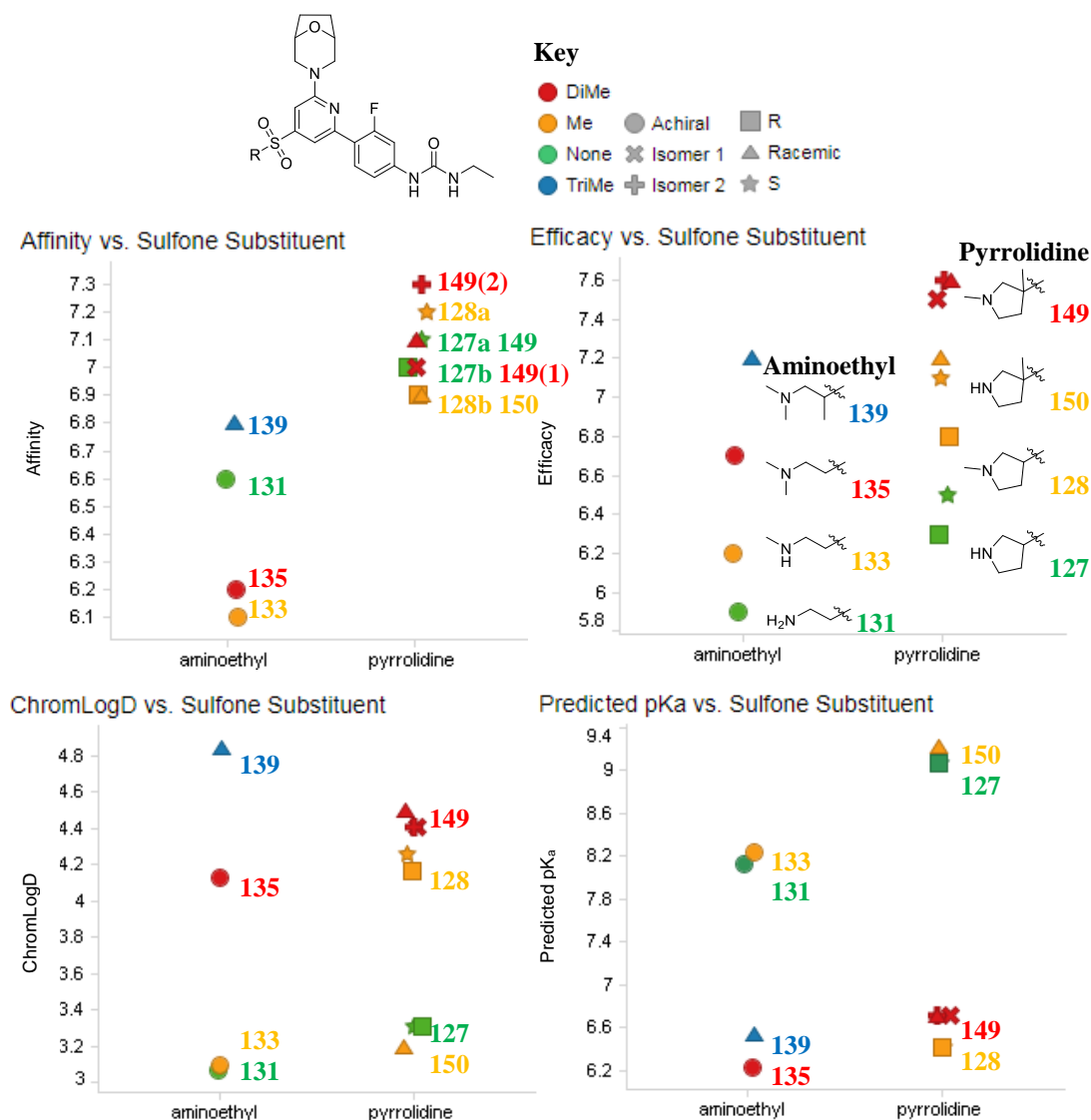


Figure 36: Demonstrating the effect of methylation of aminoethyl and pyrrolidine sulfones on affinity, efficacy, lipophilicity and calculated pK_a of the conjugate acid (pK_{aH}). Coloured according to methylation (NH₂, monomethylated (on *N* or *C*), dimethylated, trimethylated), shaped according to enantiomer. Compound numbers refer to compounds in Table 12. a = (*S*)-isomer, b = (*R*)-isomer.

An initial suggestion to account for the variation in affinity between compounds containing different sulfone moieties was to consider the molar volume of the compounds (Figure 37). With the compound set considered here, no correlation was shown; the R² value of 0.23 was not considered to be statistically significant, due to

the error in the affinity assay of ± 0.3 . Therefore, no conclusion of the effect of molar volume on affinity could be made.

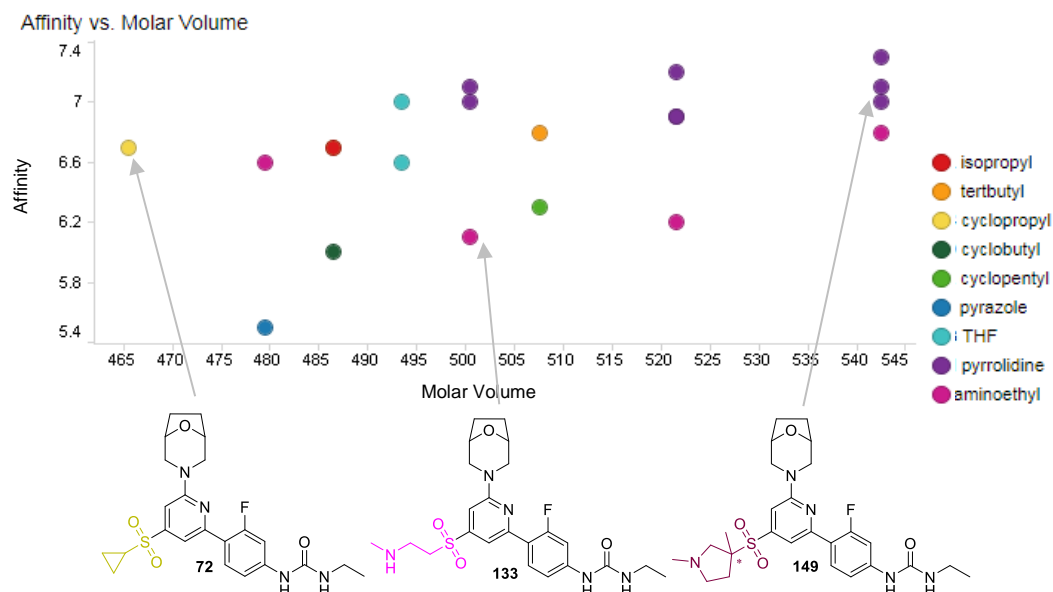


Figure 37: No correlation was observed between the affinity of a compound and the predicted molar volume, coloured by sulfone moiety ($R^2 = 0.23$ – no correlation).

Compounds from this iteration (compounds in **Table 12**) were docked into the mTOR kinase active site to ascertain whether any interactions between the sulfone group and the ribose-binding region of the protein were possible. The aliphatic (isopropyl, *tert*-butyl, cyclopropyl, cyclobutyl and cyclopentyl) and THF sulfones were not suggested to make any specific interactions with the protein in the ribose-binding region, although a hydrophobic interaction may be possible. It was proposed that compounds with a hydrogen bond donor (demonstrated by compounds **127a** and **131**) may interact with a serine residue in the mTOR kinase active site (**Figure 38A** and **B**). However, these interactions did not appear to lead to an increase in affinity (seen by comparing the affinity of compounds **127a** and **127b** with compounds **148a** and **148b**).

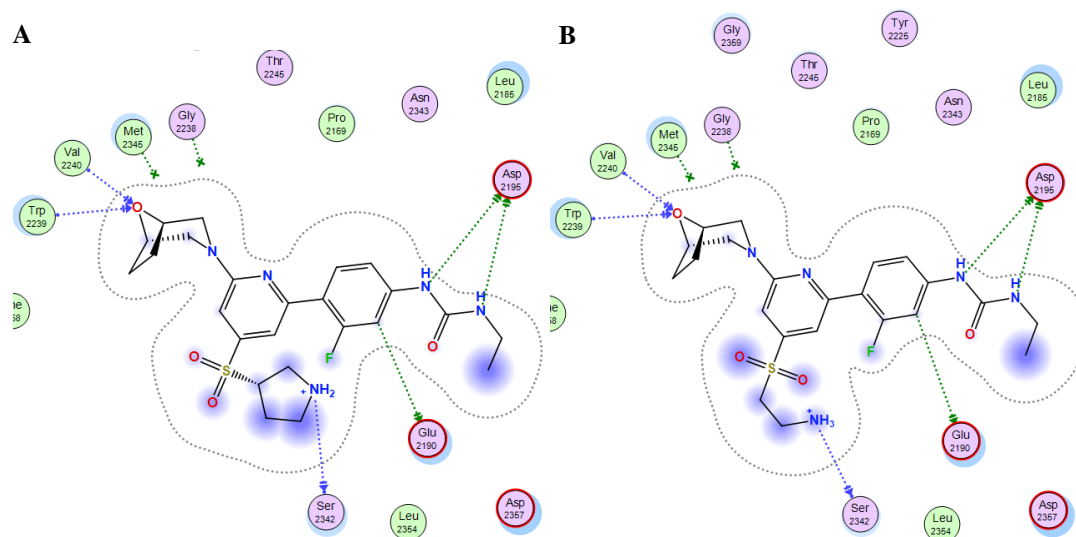


Figure 38A: Compound **127a** and **B:** Compound **131** docked into the published mTOR kinase crystal structure.⁷⁶ Docking model prepared by S. Pal.

The compounds in this iteration (compounds in **Table 12**) demonstrated a range of MDCK permeability and SLF solubility, as shown in the 9-box plot for inhaled compounds (**Figure 39**). These permeability and solubility assays were not high-throughput so not every compound was tested. Of those that were, the THF and *tert*-butyl sulfone-containing compounds (**148** and **146**) had low solubility and high permeability, while compounds containing the pyrrolidine sulfone moiety had high solubility and a range of permeabilities. Compounds containing the non-*N*-methylated pyrrolidine sulfone moieties (**127** and **150**) had lower permeability than the *N*-methylated (**128** and **149**), due to their lower lipophilicity. The compound containing the *tert*-butyl sulfone moiety (**146**) had high lipophilicity and, as a result, low solubility and high permeability. Similarly, the THF sulfone (**148**) had low solubility – the oxygen of the THF was not enough to solubilise this compound – and high permeability due to its lipophilicity.

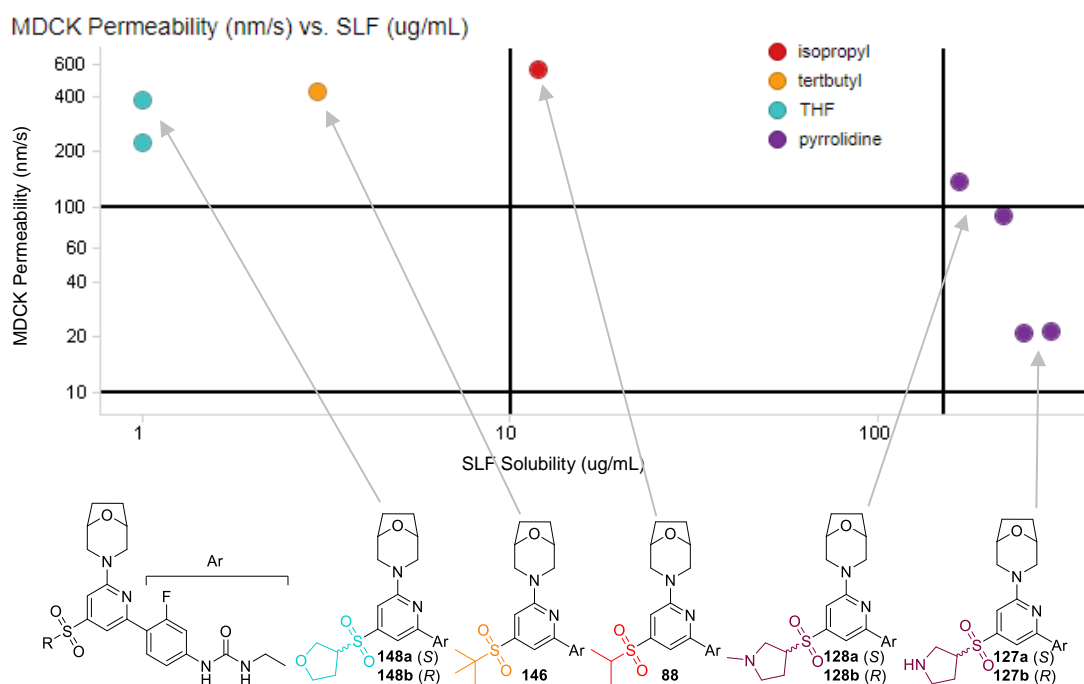


Figure 39: Showing different areas of allowed solubility (SLF Solubility) and permeability (MDCK Permeability) property space occupied by these compounds, coloured according to the sulfone moiety.

Considering selectivity, some selectivity was achieved for all compounds over the four class I PI3K isoforms (α , β , γ and δ), with at least 100-fold selectivity seen for most of the highest affinity compounds (those with an affinity greater than 7, full selectivity data in **Appendix B**, Section 7.2). Importantly, this compound data set enabled better understanding of DNA-PK SAR. More lipophilic compounds are, in general, more promiscuous; but this was not the dominant cause of increased DNA-PK affinity. Compounds containing the pyrrolidine sulfone moieties (**128a** and **128b**) and THF sulfone moieties (**148a** and **148b**) had comparable lipophilicity but different selectivity profiles (**128a** 40-fold, **148a** no selectivity over DNA-PK, **Table 12** and **Figure 40A**). This highlighted another role of basicity: the more basic pyrrolidine and aminoethyl sulfones (purple and pink) demonstrated reduced DNA-PK affinity (**Figure 40**). However, it was not understood why the more basic compounds were more selective.

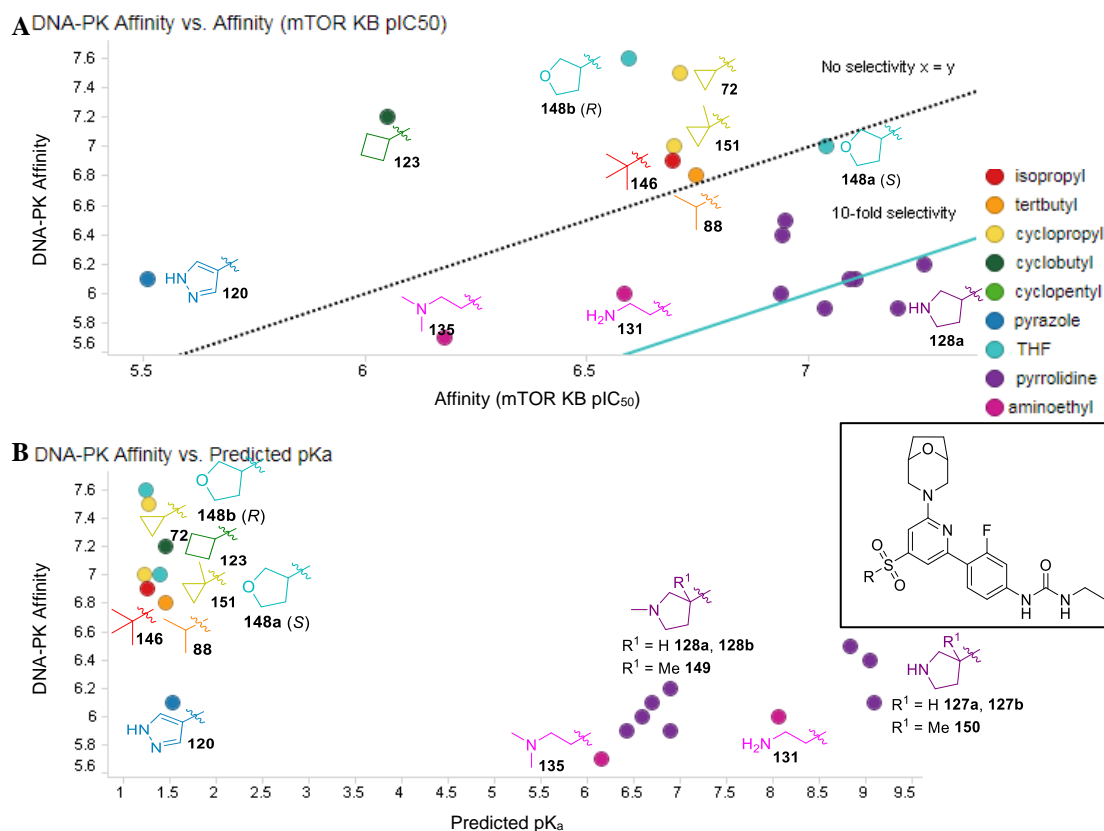


Figure 40A: The only compounds to achieve any selectivity over DNA-PK were those containing aminoethyl (pink) and pyrrolidine (purple) sulfone moieties. **B:** Demonstrating the effect of basicity on DNA-PK affinity. Both coloured according to the sulfone moiety. Full selectivity data in **Appendix B** (Section 7.2).

2.5 Summary of Chapter I

This Chapter described the investigation of a novel series of sulfones directly linked to a pyridine core as inhaled inhibitors of mTOR kinase. One of the aims – exploration of a variety of 4-position sulfone groups – was met. Modifications proposed to improve affinity and efficacy and manipulate physicochemical properties in a non-mutagenic compound were explored (**Table 13**). From an initial compound (**25**), introducing single enantiomers of the THF sulfone moiety into a compound with a non-mutagenic back pocket (**75a** and **148a**) were key improvements. This was further improved by using a pyrrolidine-substituted sulfone compound (**128a**). Pleasingly, this demonstrated that a basic group was tolerated in the ribose-binding region. This finding was important for two reasons: 1) basic compounds were proposed to be able

to achieve lung retention and 2) in this research, basic compounds were found to achieve increased selectivity over DNA-PK.

The second aim – to achieve compounds of improved affinity and efficacy and selectivity over DNA-PK – was partially met as more selective compounds were synthesised. However, few compounds with the target affinity and efficacy were achieved. Notably, the use of the more synthetically tractable fluorourea back pocket group to explore different 4-position sulfone moieties led to diminished absolute affinity values, but enabled comparison of the relative affinities of a range of sulfone moieties. Overall, while it was pleasing that the selectivity over DNA-PK was improved, the required affinity and efficacy were not achieved.

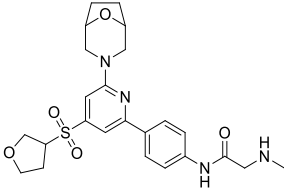
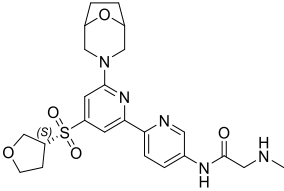
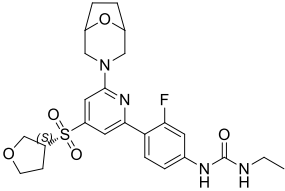
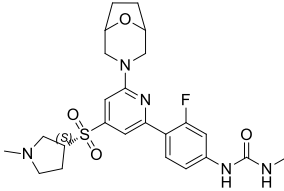
Structure				
Compound number	25	75a	148a	128a
KB pIC ₅₀ (n) ^a	8.0 (2)	8.1 (5)	7.0 (9)	7.5 (3)
pAkt pIC ₅₀ (n) ^a	-	6.9 (5)	7.3 (3)	7.2 (8)
PI3K selectivity	> 1000	> 1000	20	> 1000
DNA-PK pIC ₅₀ ^a	-	5.6 (3)	7.0 (1)	5.9 (1)
ChromLogD ^b	2.6	2.3	4.4	4.3
CLND Solubility (µg/mL) ^c	-	162	8*	110*
SLF Solubility (µg/mL) ^c	-	26	1	221
AMP Permeability (nm/s) ^c	-	42	105	68
MDCK P _{exact} Permeability (nm/s) ^c	-	29	226	91
Ames ^d	Positive	Negative	Negative	Negative

Table 13: Demonstrating the progress made in the directly-linked sulfone series. ^apIC₅₀ recorded as the mean of the data obtained on each of a number of test occasions (n). ^bChromLogD at pH 7.4. ^cIf more than one measurement taken, the mean was reported. ^dThe Ames mutagenic liability of the compound with the free aniline (not elongated to form a urea or glycinamide). Affinity = mTOR KB pIC₅₀; Efficacy = pAkt pIC₅₀. -Data not generated. *CLND solubility. a = (S)-isomer.

Chapter II: Synthesis of the lead compound in an alternative series of mTOR kinase inhibitors

3. Synthesis of the lead compound in an alternative series of mTOR kinase inhibitors

3.1 Introduction

The previous Chapter described the development of a series of compounds with a directly-linked sulfone moiety in the 4-position, often with a monocyclic urea or glycinamide-containing back pocket group in the 6-position. Compounds with higher affinity and efficacy were required to meet the programme objectives. Elsewhere in our laboratories, alternative compounds were investigated, leading to potent (high affinity and efficacy) and selective compounds: **152** and **153** (Table 14).¹¹¹ Compound **153** was the lead compound from an alternative series of mTOR kinase inhibitors, referred to here as a carbon-linked sulfone series. Both compounds were developed elsewhere in the team, so the discovery and medicinal chemistry of these compounds will not be discussed.

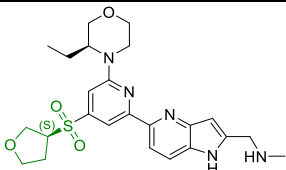
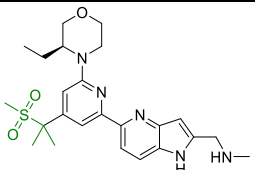
Structure		
Compound number	152	153
mTOR KB pIC ₅₀ (n) ^a	7.6 (7)	7.8 (18)
pAkt pIC ₅₀ (n) ^a	8.2 (9)	8.2 (11)
SIAJ pIC ₅₀ (n) ^a	6.8 (16)	7.0 (15)
PI3K selectivity	> 100	> 100
DNA-PK pIC ₅₀ (n) ^a	5.3 (2)	4.8 (1)
ChromLogD ^b	2.7	2.6
CAD Solubility (µg/mL) ^c	231	159
SLF Solubility (µg/mL) ^c	858	> 1000
AMP Permeability (nm/s) ^c	103	120
MDCK P _{exact} Permeability (nm/s) ^c	55	31

Table 14: Comparison of the best compounds from the directly-linked sulfone series (**152**) and one of the best compounds in a carbon-linked sulfone series (**153**). Affinity = mTOR KB pIC₅₀; Efficacy = pAkt pIC₅₀. ^apIC₅₀ recorded as the mean of the data obtained on each of a number of test occasions (n).

^bChromLogD at pH 7.4. ^cIf more than one measurement taken, the mean was reported.

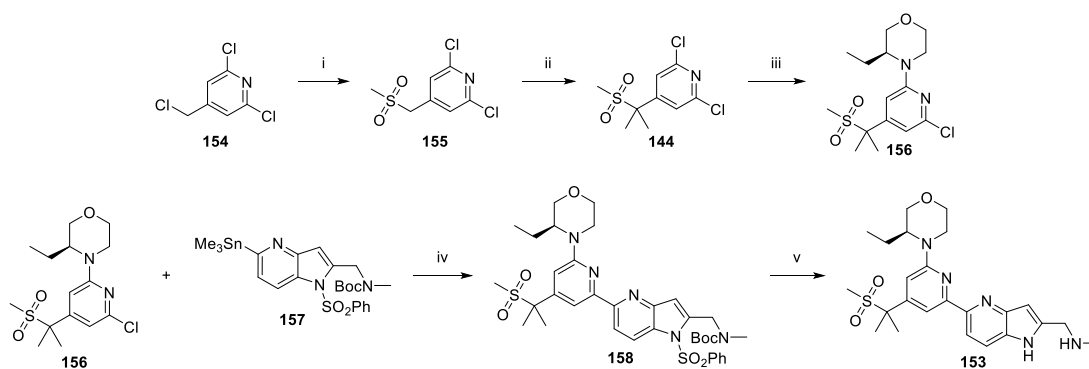
Structurally, compounds **152** and **153** differed only in the 4-position substituent. Both had similar cellular activities and **153** was more selective over DNA-PK. Additionally, both had similar properties including high solubility and moderate permeability. An intranasal *in vivo* PK study was carried out elsewhere in our laboratories.^a Compound **153** demonstrated improved lung retention compared to compound **152**. Therefore the decision was taken to terminate the directly-linked sulfone series.

Carbon-linked sulfone compound **153** demonstrated promising *in vitro* and *in vivo* data (**Table 14**). The decision to progress this compound into additional studies meant gram-quantities were required. However, the synthesis was challenging. The work discussed in this Chapter describes the improvements to the route to enable the large-scale synthesis of compound **153** and facilitate the synthesis of similar compounds.

3.2 Aims of Chapter II

The original route to synthesise pyridylzaindole compound **153** consisted of 5 linear steps and was acceptable for small-scale syntheses in lead optimisation (**Scheme 18**). The first two reactions: sodium methanesulfinate substitution of the benzylic chloride in a S_N2 reaction, followed by dimethylation adjacent to the sulfone, gave acceptable yields of compound **144**, with neither reaction requiring purification. The (*S*)-3-ethylmorpholine hinge was installed in a low-yielding S_NAr reaction that required elevated temperatures and more than one equivalent of the morpholine nucleophile. The second problematic step, a Stille cross-coupling reaction, required toxic stannanes, two protecting groups and subsequently two deprotection reactions to give compound **153**. This unoptimised route gave an overall yield of 5.7% across 5 linear steps, with some of the reactions affording reduced yields on larger scale.

^a PK study and analysis carried out by J. Morrell, J. Barrett, M. Hogg, G. Vitulli. All animal studies were ethically reviewed and carried out in accordance with U.K. Animals (Scientific Procedures) Act 1986 as amended 2012 and the GSK Policy on the Care, Welfare and Treatment of Laboratory Animals.



Scheme 18: The route to synthesise compound **153** on a small scale. *Reagents and Conditions:*

i) Sodium methanesulfinate (1.2 equiv.), KI (0.2 equiv.), MeCN, 90 °C, 2.5 h then sodium methanesulfinate (0.3 equiv.), 90 °C, 5.0 h, 57%. ii) NaO^tBu (2 M in THF, 2.5 equiv.), MeI (2.0 equiv.), THF, 0 °C, 2.0 h, 73%. iii) (*S*)-3-Ethylmorpholine.HCl (1.2 equiv.), DIPEA (3.0 equiv.) DMSO, 160 °C, 19.0 h, 47%. iv) LiCl (1.0 equiv.), PdCl₂(dppf) (0.1 equiv.), **157** (1.0 equiv.), toluene, 100 °C, 15.0 h then LiCl (1.0 equiv.), PdCl₂(dppf) (0.1 equiv.), 100 °C, 4.0 h, 56%. v) Methanamine (2 M in THF, 2.9 equiv.), NaOH (2 M in water, 5.0 equiv.), THF, MeOH, 21 °C, 2.0 h, followed by HCl (4 M in 1,4-dioxane, 14.9 equiv.), 1,4-dioxane, 21 °C, 1.0 h, 40%. Synthesis by H. Davies.

There were three main challenges to overcome in this synthesis (**Figure 41**): 1) the low-yielding S_NAr reaction; 2) the use of tin (possible on a small scale but undesirable in a large-scale synthesis and unacceptable in active pharmaceutical ingredient (API) campaigns), and; 3) the inefficient use of two protecting groups. Therefore, optimisation of the route was required.

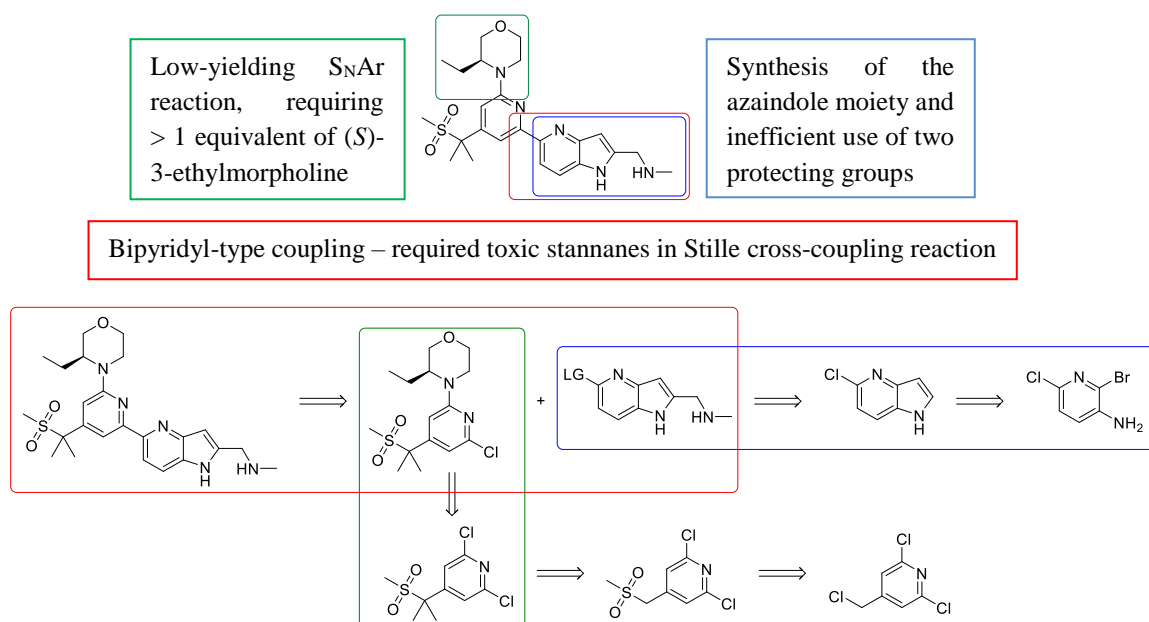


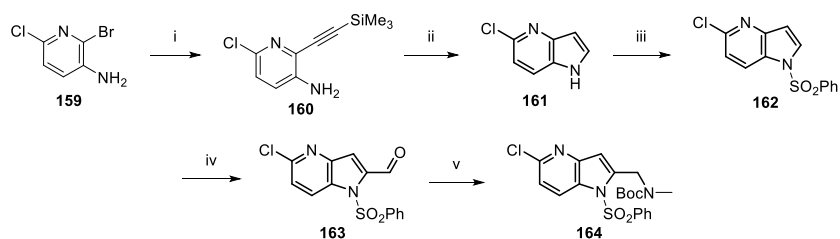
Figure 41: Highlighting the three main synthetic challenges associated with the synthesis of compound **153**, and a retrosynthetic analysis, showing some of the key intermediates.

It was hypothesised that these problems could be mitigated to achieve a higher yielding optimised synthesis. The key aims were to:

- Improve the synthesis of the 1-(5-chloro-1*H*-pyrrolo[3,2-*b*]pyridin-2-yl)-*N*-methylmethanamine moiety (here referred to as the azaindole) and optimise the protecting group strategy.
- Improve the S_NAr reaction conditions to enable a faster, more efficient and higher-yielding reaction requiring only one equivalent of the (*S*)-3-ethylmorpholine.
- Avoid Stille chemistry and the use of toxic stannanes by investigation and development of an alternative coupling strategy.

3.3 The original azaindole synthesis

The original unoptimised route to azaindole **164** was a five-step synthesis, carried out at GVK Biosciences.¹²⁵ A two-step modified Larock indole synthesis was followed by installation of a protecting group onto the indole nitrogen, deprotonation and formation of an aldehyde (**Scheme 19**). A final one-pot amide synthesis, reduction and protection reaction gave the bis-protected chloroazaindole in an overall yield of 4.3%.



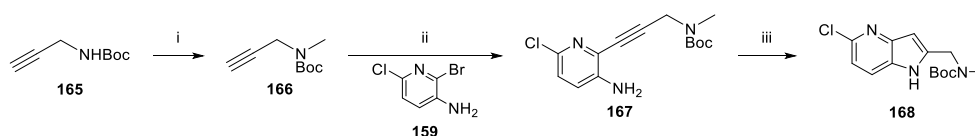
Scheme 19: The original route to the azaindole **164**, completed at GVK Biosciences.¹²⁵ *Reagents and Conditions:* i) Cu(I)I (4 mol%), TEA (8.3 equiv.), Pd(PPh₃)₂Cl₂ (2 mol%), ethynyltrimethylsilane (3.0 equiv.), DMF, 80 °C, 1.0 h, 53%. ii) KO^tBu (1.3 equiv.), NMM, 21 °C, 3.0 h, 58%. iii) DMAP (0.1 equiv.), benzenesulfonyl chloride (1.3 equiv.), triethylamine (1.6 equiv.), dichloromethane, 21 °C, 3.0 h, 45%. iv) LDA (2 M in THF, 1.6 equiv.), DMF (2.0 equiv.), THF, -78 °C, 2.0 h, 64%. v) Methanamine (2 M in THF, 4.0 equiv.), acetic acid (2.0 equiv.), THF, 21 °C, 5.0 h then STAB (2.0 equiv.), 21 °C, 15.0 h then NaOH (0.5 M in water, 2.5 equiv.), 21 °C, 7.0 h, then Boc-anhydride (2.4 equiv.), 21 °C, 2.0 h, 49%.¹²⁵

3.3.1 Developing an improved synthetic route to the azaindole

A more direct route employing an alternative alkyne in the Larock indole synthesis was proposed to achieve chloroazaindole **168** more efficiently.^b Additionally, it was suggested that the cross-coupling of the substituted azaindole may not require the indole nitrogen to be protected. Typically, the Larock indole synthesis consists of a Sonogashira-type palladium and copper-catalysed cross-coupling of an aryl halide with an alkyne, followed by a cyclisation, in one pot. Here, again, a modified two-step procedure was used. Methylation of the readily available Boc-protected propargylic amine (**165**) proceeded in good yield, followed by a Sonogashira reaction and subsequent cyclisation to give the substituted azaindole in 3 steps (**Scheme 20**). The use of *N*-methylmorpholine (NMM) as the solvent in the cyclisation step made the work-up challenging and THF was subsequently shown to be a suitable solvent.^c

^b Similar method was initially examined at GVK Biosciences without success. Successful method carried out in our laboratories by H. Davies.

^c THF method carried out by H. Hobbs.

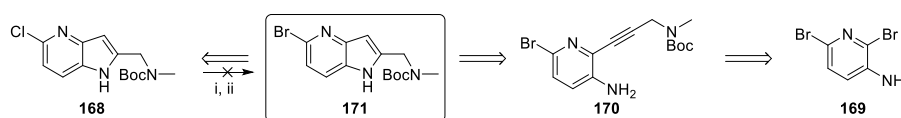


Scheme 20: The improved synthesis of mono-protected azaindole **168**. *Reagents and Conditions:*
 i) MeI (2.0 equiv.), NaH (60% in mineral oil, 1.5 equiv.), DMF, 0 °C 16.0 h, 85%. ii) **166** (1.5 equiv.), **159** (1.0 equiv.), PdCl₂dppf (8 mol%), Cu(I)I (11 mol%), TEA (1.5 equiv.), THF, 70 °C, 17.0 h, 98%
 iii) KO^tBu (1.3 equiv.), NMM (19 equiv.), 21 °C, 3.0 h, 71%. Synthesis by H. Davies.

This route gave the mono-protected chloroazaindole **168** in an overall yield of 59%, a significant improvement over the 4.3% previously achieved.

3.3.2 Route change to enable use of a bromoazaindole

The subsequent cross-coupling of chloropyridine **156** and azaindole **168** was thought to be more facile using a bromo- (or iodo-) azaindole, instead of the original chloroazaindole. A bromide was preferable and two strategies were proposed to synthesise the bromoazaindole (**171**): resynthesis from bromopyridine starting material **169** or bromination reactions on existing intermediate **168** (**Scheme 21**). It was anticipated that using bromopyridine starting material **169** may give poor regiochemistry in the Sonogashira reaction to form the indole ring. Therefore, bromination reactions were examined first. Unfortunately, reactions of azaindole **168** with both bromotrimethylsilane and tribromophosphane produced none of the desired product and no remaining starting material was seen by LCMS.

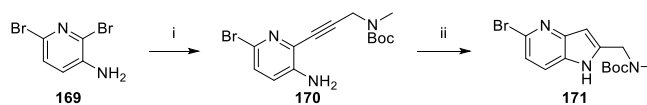


Scheme 21: The reactions tried to form the bromo variant of the azaindole back pocket directly from the chloride. *Reagents and Conditions:* i) Bromotrimethylsilane (2.0 equiv.), MeCN, 130 °C, 2.5 h then 100 °C, 1.5 h. ii) Tribromophosphane (1.9 equiv.), DMF (3.8 equiv.), 120 °C, 1.0 h.

Reactions by H. Davies.

Subsequently, elsewhere in our laboratories, the Larock indole synthesis was used to form the bromoazaindole (**Scheme 22**). As anticipated, the Sonogashira reaction with bromopyridine **169** produced the desired compound in a reduced yield, compared to that with the original chloropyridine starting material (46% vs a quantitative reaction),

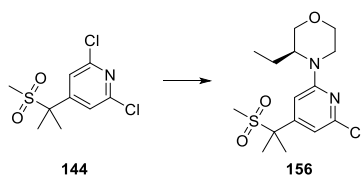
as double addition of the alkyne was seen in the reaction mixture. The use of THF as the solvent in the cyclisation again gave a good yield.



Scheme 22: The synthesis of bromoazaindole **171**. *Reagents and Conditions:* i) TEA (9.9 equiv.), *tert*-butyl methyl(prop-2-yn-1-yl)carbamate (**166**, 2.0 equiv.), Pd(PPh₃)₂Cl₂ (10 mol%), THF, 80 °C, 23.0 h, 46%. ii) NaO'Bu (2.0 equiv.), THF, 21 °C, 3.0 h, 96%. Synthesis by C. Mitchell.

3.4 The original method to install (*S*)-3-ethylmorpholine

(*S*)-3-Ethylmorpholine was installed onto dichloropyridine (**144**) in a S_NAr reaction. Typically, and as previously described in Section 2.3, these reactions worked well with a variety of morpholine moieties, often forming the desired product in good to excellent yields. It had been seen previously that S_NAr reactions employing (*S*)-3-ethylmorpholine gave reduced yields compared to both (*S*)-3-methylmorpholine and 8-oxa-3-azabicyclo[3.2.1]octane. This was proposed to be due to the increased steric bulk of the (*S*)-3-ethylmorpholine nucleophile. This reaction was also demonstrated to be scale-dependent, requiring longer reaction times, multiple additions of the (*S*)-3-ethylmorpholine nucleophile and/or DIPEA and/or increased temperatures (**Table 15**). Furthermore, the reaction did not go to completion, with unreacted starting material remaining. Both the product and pyridine starting material could be re-isolated using a normal phase purification, but as the scale increased, normal-phase chromatographic separation was not always effective, requiring additional reverse-phase chromatography. Improved conversion to product would avoid this difficult chromatographic separation. Several solutions were proposed, including a comprehensive solvent and base screen, carrying out the reaction neat and heating to increased temperatures, doing the reaction in flow and investigating palladium catalysed methods.



Entry	Scale (g)	(<i>S</i>)-3-Ethylmorpholine.HCl salt (equiv.)	Reaction time (h)	Yield (%)
1	1.2	1.2	19	47
2	5	1.9 (portion-wise)	89	38

Table 15: Demonstrating the effect of scale on the S_NAr reaction. *Reagents and Conditions:* **Entry 1:** (*S*)-3-Ethylmorpholine.HCl (1.2 equiv.), DIPEA (3.0 equiv.), DMSO (1.4 M), 160 °C, 19.0 h, 47%.

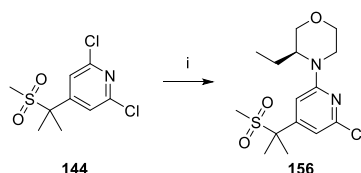
Entry 2: (*S*)-3-Ethylmorpholine.HCl (1.4 equiv.), DIPEA (1.4 equiv.), DMSO (0.87 M), 130 °C, 65 h, then (*S*)-3-ethylmorpholine.HCl (0.5 equiv.), DIPEA (1.0 equiv.), 150 °C, 24.0 h, 38%.

Reactions by H. Davies.

3.4.1 Palladium-catalysed cross-couplings to access the (*S*)-3-ethylmorpholine-substituted pyridine intermediate

Buchwald-Hartwig reaction conditions were proposed as one method to improve this reaction. Therefore, a palladium-catalysed carbon-nitrogen cross-coupling screen was run.^d Eleven catalysts, four bases and two solvents were screened using 2.5 equivalents of the base, 1.1 equivalents of the (*S*)-3-ethylmorpholine (as the HCl salt) and a concentration of 0.1 M at 100 °C for 16 hours. Little or no reaction was seen with every catalyst, except $P(tBu)_3Pd$ G3; this reaction was repeated in our laboratories. None of the exact catalyst was readily available, so a fourth-generation version was used instead. Using potassium phenoxide as the base gave the highest conversion in the screen. However, the phenoxide anion was found to act as the nucleophile and displace either one or both chlorides, leading to the formation of by-products. Therefore in the repeated reaction, sodium *tert*-butoxide (which gave the second highest conversion) was used. Pleasingly, in the first attempt at this reaction in our laboratories, 50% conversion to the desired product (**156**) was observed (**Scheme 23**).

^d Run with Discovery Automation Platform Chemistry (DAPC) in GSK by K. Arendt and B. McKay.



Scheme 23: The palladium catalysed reaction carried out in our laboratories. *Reagents and Conditions:* i) (*S*)-3-Ethylmorpholine.HCl (1.5 equiv.), NaO^tBu (4.0 equiv.), P(^tBu)₃Pd G4 (10 mol%), toluene, 100 °C, 16.0 h, 50% (LCMS conversion). Synthesis by J. Lee.

Despite the success of this palladium-catalysed reaction, no further work was carried out. The S_NAr approach was proposed to be better for use in a scale-up due to the use of cheaper reagents and more facile work-up.

3.4.2 Base, solvent and concentration screens to efficiently access the (*S*)-3-ethylmorpholine-substituted pyridine intermediate

An initial base and solvent screen investigated ten bases and five solvents (DMSO, sulfolane, NMP, DMPU and ethylene glycol)^e using microwave heating at 130 °C and the conversion (by LCMS) was recorded. Reactions in DMSO and sulfolane gave the highest conversion to product but disappointingly no reaction gave more than 18% conversion, with unreacted pyridine starting material the major component of the reaction mixture (**Figure 42**). A microwave malfunction while heating the reactions in NMP, DMPU and ethylene glycol led to a reduced reaction time. This was proposed to be responsible for the reduced conversion, confirmed by repeating the reactions in NMP, which gave up to 10% conversion after heating for 500 minutes.

^e Both NMP and DMPU absorb UV light meaning that the LCMS conversion of the reactions using these solvents were not directly comparable to those for the other three solvents. The use of an internal standard would have avoided this.

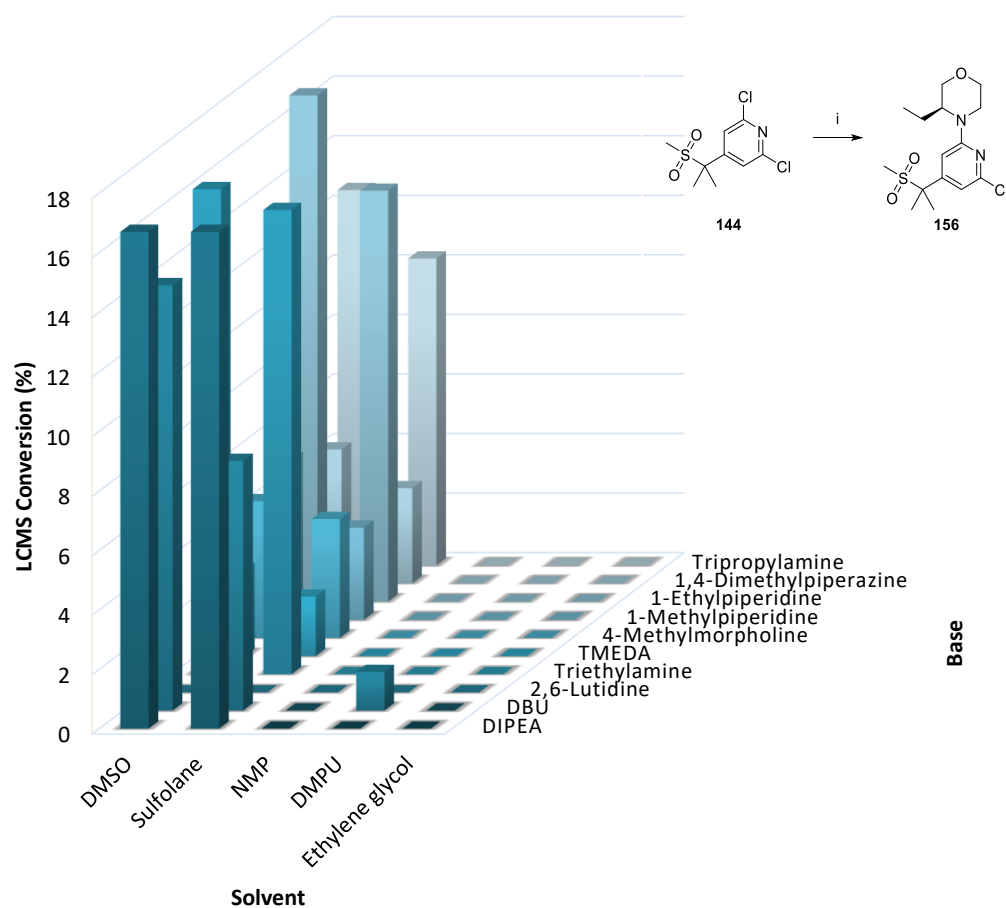


Figure 42: Demonstrating the conversion as measured by LCMS (%) to product **156** after heating the reactions for 500 minutes, the maximum run time of the microwave. *Reagents and Conditions:* i) Each reaction used (*S*)-3-ethylmorpholine.HCl (1.5 equiv.), base (3.0 equiv.), solvent (0.187 M), 130 °C.

Reactions by H. Davies.

The highest conversion was seen with DIPEA, DBU, triethylamine, 1-ethylpiperidine and tripropylamine. To confirm this result, the reactions with these five bases were repeated using both DMSO and sulfolane, selected because they were not visible in the LCMS and were more facile to use practically than viscous ethylene glycol. Comparable results were seen, suggesting the same order of base reactivity in both solvents; DIPEA and triethylamine gave the highest conversion. Additionally, the reaction mixtures with the highest conversion from the initial screen were reheated (those in DMSO and sulfolane) to ascertain whether the reaction stalled or continued when heated further. This confirmed that the reaction continued with all bases except DBU, giving significantly higher conversion to product after reheating (**Figure 43**).

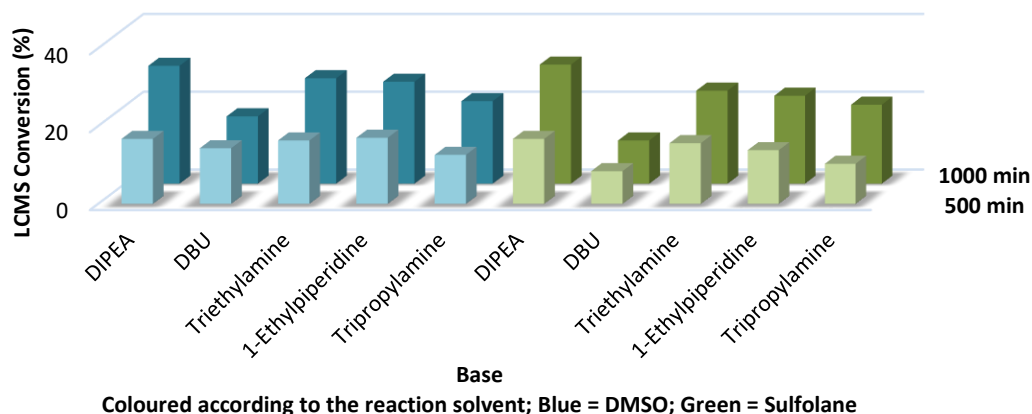


Figure 43: Demonstrating the conversion as measured by LCMS (%) to product (**156**) on continued heating at 130 °C of five of the initial reactions in two solvents DMSO (blue) and sulfolane (green).

Reactions by H. Davies.

Overall, no base-solvent combination showed great improvements over the original conditions, suggesting that reaction time was an important parameter: the longer the reaction time, the higher the conversion.

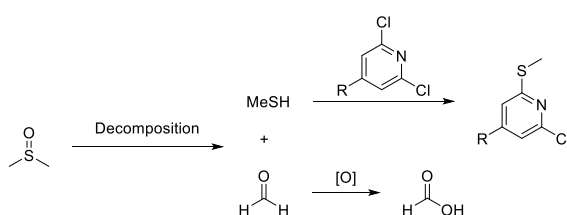
A more extensive solvent-base screen was carried out in collaboration with another team at GSK, employing 24 bases including amine bases, weak and strong inorganic bases and eight solvents, with the reactions heated at 100 °C for 16 hours.^f Disappointingly, none of the reactions gave greater than 10% conversion. A small study in-house into the use of strong bases produced one interesting result when sodium hydride was used with acetonitrile. Heating the reaction mixture at 100 °C for 15 hours gave no reaction but further heating at 130 °C for 22 hours gave a clean reaction to form 42% desired product (57% remaining starting material). Unfortunately, further heating and addition of sodium hydride led to formation of several unidentified impurities.^g

The lack of reactivity suggested that higher temperatures and/or longer reactions times were required to increase the formation of product. However, previous experience suggested that the reaction failed to progress on prolonged heating. Portion-wise

^f Run with DAPC by K. Arendt and B. McKay. Reaction conditions, base (2.5 equiv.), (*S*)-3-ethylmorpholine.HCl (1.1 equiv.), 0.1 M, 100 °C, 16.0 h and biphenyl used as internal standard.

^g Reaction by J. Lee.

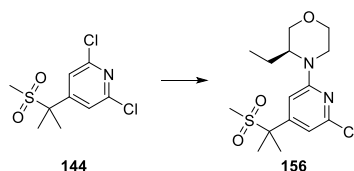
addition of (*S*)-3-ethylmorpholine and DIPEA pushed the reaction forward, but rarely to completion. It was therefore hypothesised that a component of the reaction mixture may decompose. Despite having a boiling point of 189 °C, DMSO is known to decompose under prolonged heating at temperatures above 150 °C, forming various products including methane thiol.¹⁴⁹ A by-product was observed by LCMS in some of the S_NAr reactions, proposed to be a thioether resulting from nucleophilic attack of the methane thiol on the dichloropyridine (**Scheme 24**). Furthermore, a separate series of experiments led to the conclusion that the DMSO decomposed to give an acidic impurity which quenched the DIPEA and formed a non-nucleophilic salt with the (*S*)-3-ethylmorpholine, causing the reaction to stall.^h



Scheme 24: Demonstrating the decomposition of DMSO on prolonged heating to form methanethiol and formate, which was proposed to oxidise to give formic acid – this may quench the DIPEA and cause the reaction to stall.¹⁴⁹ A by-product observed by LCMS was proposed to be a thioether; the result of nucleophilic attack of the pyridine starting material by methanethiol.

The base and solvent screens suggested that the reaction was slow and required a longer reaction time and higher temperature – something now proposed to be counter-productive in DMSO. Sulfolane, a higher boiling point and more heat-stable solvent gave similar conversion in the initial solvent and base screen and was therefore selected for use. Subsequent experiments investigated the effect of increasing the concentration on the reaction outcome, including running the reaction neat in DIPEA. Pleasingly, this led to the discovery of improved conditions (**Entry 2, Table 16**) with 1.1 equivalents of the (*S*)-3-ethylmorpholine giving complete conversion overnight.

^h Reactions by J Lee, H. Hobbs.



Entry	Scale (g)	(S)-3-Ethylmorpholine.HCl salt (equiv.)	Time (h)	Solvent	Conc. (M)	Temp. (°C)	Yield (%)
1	5.0	1.9 ^a	89	DMSO	0.87	130-150	38
2	4.8	1.1	16	Sulfolane	2.9	200	69

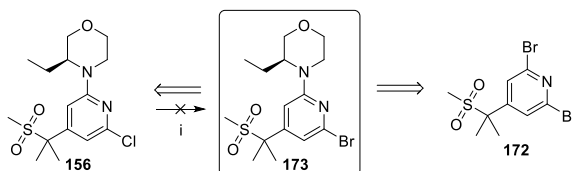
Table 16: Demonstrating the improved S_NAr conditions. ^aPortion-wise addition. **Entry 1** by H.

Davies, **Entry 2** by J. Lee.

Despite demonstrating improved yields, the forcing conditions required raised concerns about a possible build-up of pressure caused by heating DIPEA to temperatures above its boiling point. Additionally, this method still required two chromatographic purifications, one normal phase and one reverse phase. Incorporating these findings, further work was carried out elsewhere in our laboratories to address the remaining problems.

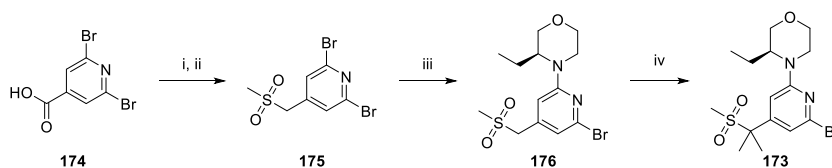
3.4.3 Route change to enable use of a bromopyridine

While chloropyridines are known to be more reactive in S_NAr reactions, the subsequent cross-coupling to install the azaindole was proposed to be more effective using a bromo- (or iodo-) pyridine. Again, two strategies were proposed to synthesise the bromopyridine core: resynthesis or bromination reactions on the existing intermediate (**Scheme 25**). Due to the anticipated issues with the S_NAr reaction, bromination of the existing chloropyridine intermediate was attempted first. Chloropyridine **156** gave 11% conversion to the desired bromide (**173**) using bromotrimethylsilane. With tribromophosphane, none of the desired product was observed and no starting material remained.



Scheme 25: The reaction trialed to form the bromopyridine core directly from the chloride. *Reagents and Conditions:* i) Bromotrimethylsilane (2.1 equiv.), MeCN, 130 °C, 3.0 h then 100 °C, 1.5 h, bromotrimethylsilane (5.3 equiv.), 60 °C, 15.0 h, bromotrimethylsilane (5.3 equiv.), 55 °C, 3.0 h, then concentrate, tribromophosphane (1.5 equiv.), DMF (9.0 equiv.), 120 °C, 1.0 h. Reaction by H. Davies.

Subsequently, elsewhere in our laboratories, methods were developed to synthesise bromopyridine intermediate **173** (**Scheme 26**).ⁱ The more readily available dibromoacid was used to form the dibromo sulfone (**175**) in acceptable yield over two steps. Literature precedent suggested that the reaction of bromopyridines with hindered amine nucleophiles was facilitated by the use of an auxiliary base, 2,2,6,6-tetramethylpiperidine (TMP).¹⁵⁰ Pleasingly, this gave a good yield for the previously problematic S_NAr reaction.



Scheme 26: The synthesis of the bromopyridine core and subsequent S_NAr reaction. *Reagents and Conditions:* i) BH₃.THF (1 M in THF, 1.5 equiv.), THF, 0-21 °C, 24.0 h then BH₃.DMS (2 M in THF, 2.0 equiv.), 0-21 °C, 18.0 h, 83%. ii) TEA (1.5 equiv.), MsCl (1.1 equiv.), MeCN, 0 °C, 1.0 h then 21 °C, 2.0 h, MsCl (0.2 equiv.), 5 min then sodium methanesulfinate (2.0 equiv.), KI (0.3 equiv.), concentrate then MeCN, reflux, 17.0 h, 70%. iii) (*S*)-3-Ethylmorpholine.HCl (1.3 equiv.), TMP (15.6 equiv.), 150 °C, 40.0 h, 79%.¹⁵⁰ iv) NaO^tBu (2 M in THF, 2.3 equiv.), MeI (2.1 equiv.), THF, 0-21 °C, 2.0 h, 95%. Synthesis by S. Nicolle.

This S_NAr reaction was subsequently carried out using these conditions (TMP, 150 °C) to form 180 g of a closely related pyridyl bromide (similar to **173**), in a 98% yield.^j

ⁱ Practical work carried out by H. Hobbs, J. Lee, C. Mitchell, S. Nicolle and M. Puente-Felipe. This method was suggested as a result of presenting the route at the GSK Chemistry Round Table Forum. Specifically, the use of TMP to enable the S_NAr with a bromopyridine was suggested by A. Richards.

^j Synthesis by L. Thorpe.

3.5 Bipyridyl cross-coupling reactions to install the azaindole

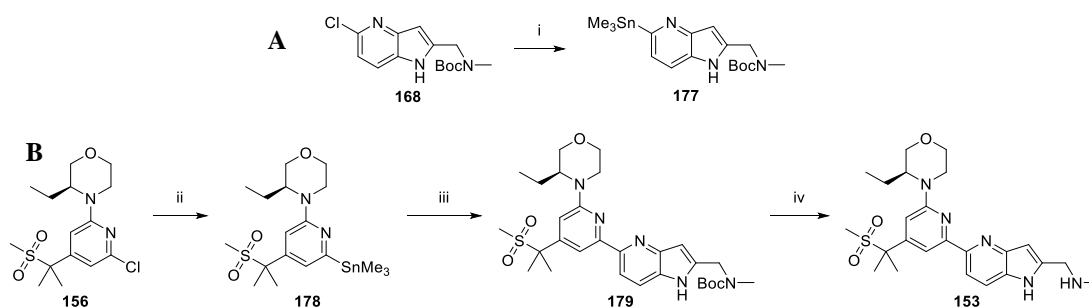
The third problem with the original synthesis of compound **153** was the bipyridyl cross-coupling. 2,2-Bipyridyl couplings are known to be challenging. Metal-catalysed reactions may fail due to the ability of bipyridyl compounds to chelate metals.^{137,139} Stille, Negishi and more recently Suzuki reactions have all been developed to synthesise bipyridyl compounds. However, Suzuki Miyaura reactions are often not possible due to the unavailability¹³⁷ or instability¹⁵¹ of heteroaryl boronic acids. While Stille chemistry has been reported to be the most reliable and robust approach for use on a large scale,^{152,153} it requires the use of toxic organostannanes. Therefore it is important to ensure no tin residues remain in the pharmaceutical product and strict limits are in place.¹⁵³ Additionally, working with organotin reagents requires special precautions in an industrial chemistry laboratory. For these reasons, the use of organostannane reagents is not acceptable in API campaigns carried out at GSK and an alternative was required.

Compounds containing various azaindole back pockets had been synthesised on a small scale in lead discovery. The use of both Negishi and Suzuki cross-coupling reactions had been explored in our laboratories, but no systematic screening of reaction conditions had been carried out and Stille chemistry was found to give the highest yields. In the original route to synthesise compound **153**, the stannane of azaindole **168** (compound **177**) was coupled with the chloropyridine core. Here, the stannane (**177**) of chloroazaindole **168** was made elsewhere in the group, in a 56% yield (**Scheme 27A**).^k However, further work demonstrated that the stannane of chloropyridine **156** could be made in a higher yield (73%) and coupled with chloroazaindole **168** in a 50% yield (**Scheme 27B**).^l A subsequent Boc-deprotection gave compound **153** in a 30% yield over the three steps. Furthermore, it was later demonstrated elsewhere in the group that the yields using organostannane **178** were improved on a larger scale (7.5 g compared to 0.5 g), giving an overall yield across the three steps of 51%.^m

^k Reaction by H. Hobbs.

^l Reaction by H. Davies.

^m Reaction by H. Hobbs.



Scheme 27A: The methods used to make the organostannane of both chloroazaindole **168** and **B**: Chloropyridine **156** and the subsequent Stille reaction. *Reagents and Conditions:* i) PdCl₂(dppf) (5 mol%), Sn₂Me₆ (1.8 equiv.), toluene, 110 °C, 3.0 h, 56%. Synthesis by H. Hobbs. ii) PdCl₂(dppf) (6 mol%), Sn₂Me₆ (1.8 equiv.), toluene, 110 °C, 4.0 h, 73%. Synthesis by H. Davies. iii) **168** (1.0 equiv.), **178** (1.1 equiv.), LiCl (1.1 equiv.), PdCl₂(dppf) (10 mol%), toluene, 100 °C, 3.0 h then PdCl₂(dppf) (10 mol%), LiCl (1.1 equiv.), 100 °C, 26.0 h, 50%. Synthesis by H. Davies. iv) HCl (4 M in 1,4-dioxane, 11.2 equiv.), 1,4-dioxane, 21 °C, 6.0 h, 81%. Synthesis by H. Davies.

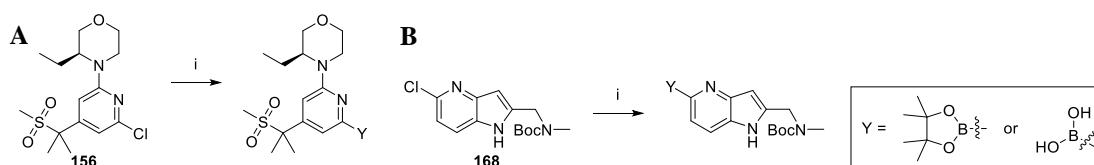
Despite improvements to the overall yield for the cross-coupling, the use of toxic stannanes was not an acceptable long-term strategy. Several other options were therefore considered.

3.6 Miyaura borylation and Suzuki cross-coupling reactions to access the pyridine azaindole

The reduced toxicity of organoboron reagents and ease of scalability made the Suzuki reaction one of the preferred options to replace the Stille chemistry. Suzuki reactions cross-couple heteroaryl halides with boronic acids or esters. Therefore, to evaluate this chemistry, one of the coupling partners, either the chloropyridine or the chloroazaindole, needed to be borylated to undergo transmetalation. At this stage, only the chlorinated intermediates (**156** and **168**) were available. Miyaura borylation reactions enable the synthesis of boronates via the palladium-catalysed borylation of aryl halides, and a systematic screen of a variety of borylation conditions was carried out.ⁿ Miyaura borylations are solvent dependent, with polar solvents often accelerating the rate of reaction, therefore, four different solvents were used (toluene, acetonitrile, 2-methylTHF and dimethylacetamide).^{154,155} Additionally, the choice of base is important to avoid the borylated product forming and undergoing cross-coupling with

ⁿ Work done in collaboration with DAPC, screens carried out by B. McKay, J. Lee and K. Mercer.

any remaining aryl halide, which leads to homocoupled by-products.¹⁵⁴ Weak bases, such as potassium acetate, accelerate the rate of the desired borylation but do not accelerate the rate of the competitive cross-coupling reaction and are therefore ideal for use in the borylation reaction.¹⁵⁴ Additionally, different boron sources and palladium ligands can be used. Here, tetrahydroxydiborane (BBA)¹⁵⁶ and bis(pinacolato)diborane (B₂pin₂) were investigated along with six palladium ligands (XPhos, SPhos, CataCXium A, DTBPF, PCy₃ and P(^tBu)₃) and one palladium source (a third generation palladium pre-catalyst (Pd G3)). A total of 96 reactions were carried out, using four 24-well reaction plates (each with six columns and four rows). For each substrate, one plate was used for each boron source. To every well in each of the six columns was added one of the six ligands and to each of the four rows was added a solution of the substrate and boron source in the appropriate solvent. The reactions used 10 mol% of the palladium pre-catalyst with a 0.1 M concentration of the substrate for both the substituted azaindole and the chloropyridine core (**Scheme 28A** and **B**).



Scheme 28A: The Miyaura borylation screen conditions used for chloropyridine core **156** and **B**:

azaindole **168**. *Reagents and Conditions:* i) Substrate (1.0 equiv.), boron source (3.0 equiv. x 2), KOAc (3.0 equiv.), Pd pre-catalyst (10 mol% x 6), ligand (10 mol% x 6), solvent (0.1 M x 4), 80 °C, 16.0 h. Reactions by B. McKay, J. Lee and K. Mercer.

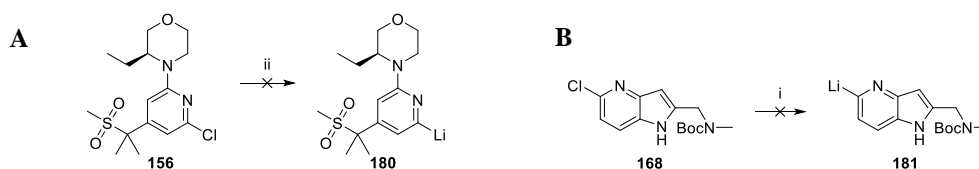
The results of these screens were disappointing: LCMS analysis suggested predominantly remaining starting material, with protodehalogenation products as the main impurities. Using the chloropyridine core as the starting material, traces of boronic ester and acid were observed in some of the reaction mixtures. 6-Membered 2-heteroaromatic boronic acids and esters, such as the 2-pyridyl species described here, are known to be unstable, decomposing both in air and more rapidly in the presence of a palladium catalyst, via protodeboronation.^{157,158} Therefore, it was considered likely that the boronic ester (or acid) was not stable, explaining why only small amounts were observed. Additionally, chloropyridines are more electron poor than the corresponding phenyl compounds, leading to slower reaction and often giving

higher conversion to the dechlorinated by-product.¹⁵⁹ In the reactions discussed here, it was not known if the boronic ester was forming and undergoing protodeboronation, or if the chloropyridine starting material was simply dehalogenated in a direct reaction with the palladium catalyst. Overall, the inability to form a borylated species meant the Suzuki reaction screen could not be run. It was suggested that the use of pyridyl bromides may lead to improved reactivity and the use of shorter reaction times was proposed to reduce the amount of the dehalogenated by-product, but this was not investigated. Additionally, it was suggested that a tandem Miyaura borylation-Suzuki reaction may have overcome any stability issues with the boronic esters. This type of one-pot borylation-cross-coupling reaction had been briefly investigated on similar substrates elsewhere in the team with little success, therefore this strategy was not investigated further.^o

3.7 Negishi cross-coupling reactions

Another palladium-catalysed cross-coupling reaction, involving the *in situ* formation of an organozinc species that undergoes transmetalation – the Negishi reaction – was an alternative for use on large scale. This *in situ* generation of the nucleophilic species was suggested as a method to overcome any potential instability. However, a previous investigation of Negishi chemistry using a similar azaindole was not successful; the organozinc species of the azaindole was suggested to have formed but did not react with the chloropyridine core. It was anticipated that synthesis of the organozinc species on the chloropyridine core and subsequent reaction may be possible. However, lithium-halogen exchange on both **156** and **168** was here shown to be unsuccessful (**Scheme 29 A and B**). In both cases, the use of 1.0 equivalent of *sec*-butyllithium was proposed to result in deprotonation (of the indole nitrogen in **168** and adjacent to the sulfone in **156**), not the desired lithium-halogen exchange. Addition of a further equivalent of *sec*-butyllithium again gave no lithium-halogen exchange.

^o R. Shah, H. Hobbs, S. Nicolle.



Scheme 29A: Investigating lithium-halogen exchange on chloropyridine **156** and **B:** Chloroazaindole **168**. *Reagents and Conditions:* i) **156** or **168** (1.0 equiv.), *s*-BuLi (1.12 M in cyclohexane, 1.0 equiv.), THF, -78 °C, 1.0 h then *s*-BuLi (1.12 M in cyclohexane, 1.0 equiv.), -78 °C 1.5 h then 21 °C, 19.0 h.

Reactions by H. Davies.

3.8 Nickel-catalysed reductive cross-coupling reactions

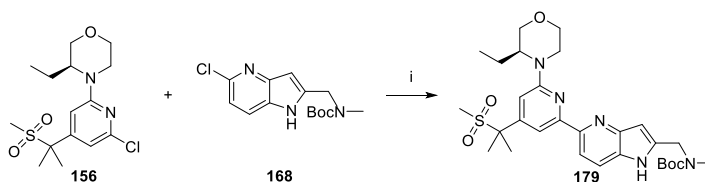
The cross-coupling methods explored so far aimed to couple an electrophilic component (aryl halide) with a nucleophilic component (organostannane, zinc or boron species).¹⁶⁰ Due to the difficulties in synthesising the nucleophilic component, an alternative approach was suggested – the use of nickel-catalysed reductive cross-coupling. This reaction had been demonstrated in our laboratories to successfully couple an unsubstituted azaindole (5-chloro-1*H*-pyrrolo[3,2-*b*]pyridine, **161**, **Scheme 19**) and optimal conditions were identified in a reaction screen.^p

This reductive cross-coupling method employed electrophilic coupling partners without forming a stoichiometric organometallic. Instead a stoichiometric reductant, often manganese or zinc, is used to regenerate the nickel catalyst.^{160,161} Previously this nickel-catalysed reductive coupling method for 2-halopyridines was most often employed to produce homocoupled by-products.¹⁶² When using this method to produce cross-coupled products, obtaining the desired cross-coupled product while suppressing homocoupling by-products can be challenging.^{160,162} However, there are a few methods to increase the amount of desired cross-coupled product.¹⁶³ For example, if both coupling partners are similarly reactive, using a large excess of one of the coupling partners can give high yields of the cross-coupled product, unfortunately at the expense of a large amount of one symmetrical by-product.^{160,163} Alternatively, electronic differences between the substrates to be coupled can be

^p Screen run in collaboration with DAPC, B. McKay, K. Arendt and A. Buitrago Santanilla. Further work in our laboratories by S. Nicolle, E. Hounslea.

exploited and the use of different catalyst and/or ligand systems can also limit the amount of homocoupled by-product.¹⁶³

Using the optimised conditions from the previous screen, some trial reactions were investigated (**Table 17**). Trifluoroacetic acid (TFA) was proposed to activate the manganese and increase its reactivity.¹⁶⁴ Therefore, reactions were tried both with (**Entry 1**) and without (**Entry 2**) TFA, heating to 120 °C for 30 minutes before reducing the temperature to 40 °C for 18 hours. Under these conditions, the addition of TFA appeared to lead to more dehalogenated products, while the absence of TFA gave increased conversion to product. A third reaction, again without TFA, and heated only at 40 °C, led to reduced conversion to product (**Entry 3**). It was proposed that the uncontrolled reactivity of the starting materials leading to various side-products and homocoupling might be reduced if fewer equivalents of manganese were used (**Entry 4**). However, this reduced the reactivity too far and no reaction occurred.



Entry	Temp. (°C)	Time (h)	Starting material (%)		Product (%)		Impurities (%)				
			156	168	179	182	183	184	185	186	
1 ^{a,b}	120	0.5	20	21	6	17	17	4	5	1	
	40	18	20	22	6	17	17	4	5	1	
2 ^c	120	0.5	No reaction								
	40	18	5	18	36	-	-	1	16	14	
3	40	5	No reaction								
	40	69	35	41	11	-	-	-	4	-	
4 ^d	40	5	No reaction								
	40	69	Majority starting material, no product.								

Proposed structures of impurities observed by LCMS:

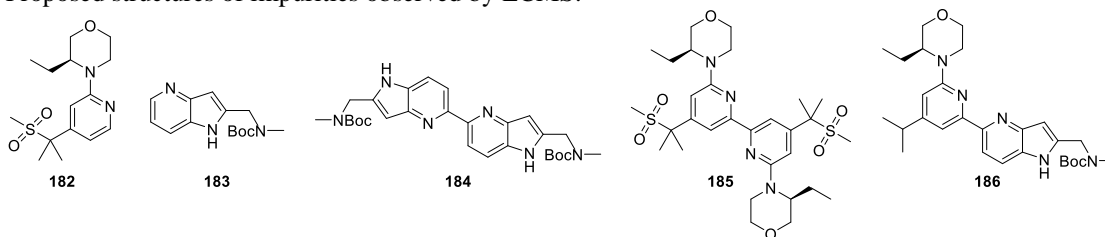


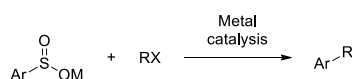
Table 17: The conditions investigated and the outcomes of the nickel reductive cross-coupling, including the proposed structures of impurities observed by LCMS. *Reagents and Conditions:* **156** (1.0 equiv.), **168** (1.0 equiv.), dichloro(dimethoxyethane)nickel (10 mol%), 1,10-phenanthroline (12 mol%), Mn (5.0 equiv.), DMA. ^aInitially heated at 120 °C for 0.5 h, on heating at 40 °C for 18.0 h no change in reaction profile was seen. ^bReaction run as above with TFA (2.0 equiv.). ^cInitially heated at 120 °C for 0.5 h, after which no reaction was seen, on heating at 40 °C for 18.0 h a reaction occurred. ^dReaction run as above with Mn (2.0 equiv.). Reactions by H. Davies.

This approach was the most promising so far as it produced up to 36% conversion to the desired product. It was hypothesised that using the bromide of one of the starting materials might reduce the amount of homocoupling by providing a difference in reactivity between the reactants. However, this was not attempted.

3.9 Desulfinate cross-coupling reactions

Recently, Willis and co-workers reported the use of pyridine sulfinates as the nucleophilic coupling partner in palladium-catalysed desulfinate cross-coupling

reactions.¹⁵¹ Desulfinate (or desulfinylative) carbon-carbon bond-forming cross-coupling reactions using sodium sulfinates were first reported in the 1970s and expanded on in the 1990s.¹⁶⁵⁻¹⁶⁹ In these reactions, an aryl sulfinate salt is reacted with an alkyl, aryl or heteroaryl halide (or pseudo-halide) under metal (including palladium) catalysis to form a carbon-carbon bond by breaking a carbon-sulfur bond (**Scheme 30**). Sulfur dioxide is the main by-product in these reactions and is also proposed to be the driving force of the reaction, making this method more atom efficient than many other cross-coupling reactions.^{167,170} Additionally, it has been suggested that, on a large scale, the sulfur dioxide by-product could be captured and recycled.¹⁶⁷

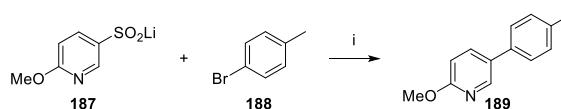


Scheme 30: Demonstrating the metal-catalysed cross-coupling reaction of a sulfinate salt with an alkyl, aryl or heteroaryl (pseudo-)halide. Ar = Aryl group; M = Alkali metal (Li, Na, K); R = Alkyl, aryl or heteroaryl; X = (Pseudo-)halide.

Many of the early examples of desulfinate coupling reactions were to form symmetrical biaryls using the sodium salt of an aryl sulfinate and stoichiometric palladium.¹⁶⁷⁻¹⁶⁹ Catalytic reactions were developed to couple Grignard reagents with sulfides, thiols, sulfones and sulfinate as the electrophilic coupling partner.^{167,171,172} However, examples of catalytic cross-coupling reactions using sulfinates as the nucleophilic coupling partner have only been explored relatively recently.¹⁶⁷ For example, Heck-type coupling reactions of aryl sulfinic acids with alkenes have been developed.^{166,173} Additionally, the use of sulfinates in palladium-catalysed cross-coupling has been demonstrated to synthesise biaryls^{165,167,174} and to couple phenyl derivatives to 5-membered heterocycles¹⁷⁵ or biarylheterocycles¹⁷⁶⁻¹⁷⁸ and the Willis group published the first reported example using pyridine sulfinates to form bipyridyl compounds.¹⁵¹

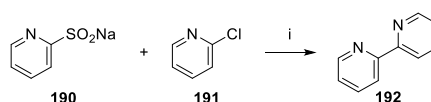
While carrying out other research,¹⁷⁹ Willis and co-workers observed a side-product resulting from the palladium-catalysed cross-coupling of a pyridyl sulfinate salt and an aryl halide to generate a biaryl compound.¹⁵¹ These biaryl species were more commonly formed when sulfinates of heterocyclic compounds were used.¹⁵¹ The

researchers went on to explore whether this side reaction could be usefully exploited to give a cross-coupling reaction using a stable and easy to prepare nucleophilic 2-pyridine species.¹⁵¹ A screen of different ligands, bases and reaction conditions using the reaction in **Scheme 31** gave a set of optimised conditions.¹⁵¹ Several ligands were investigated including both mono- and bidentate phosphine ligands, with tricyclohexylphosphine shown to give the best conversion. A base screen revealed that an inorganic base was required, with potassium or caesium carbonate giving the best conversion.¹⁵¹ Potassium, lithium and sodium sulfinate salts could all be used and a temperature of 150 °C was required to obtain complete conversion.¹⁵¹ Additionally, the reaction was carried out with both 1.5 and 2.0 equivalents of the sulfinate with 2.0 equivalents leading to a slightly increased conversion (99% with 2.0 equivalents compared to 88% with 1.5 equivalents).¹⁵¹



Scheme 31: The substrates used in the optimisation of the coupling reaction, and the optimised conditions. *Reagents and Conditions:* i) **187** (2.0 equiv.), **188** (1.0 equiv.), K₂CO₃ (1.5 equiv.), Pd(OAc)₂ (5 mol%), PCy₃ (10 mol%), 1,4-dioxane, 150 °C, 24.0 h, 99% conversion.¹⁵¹

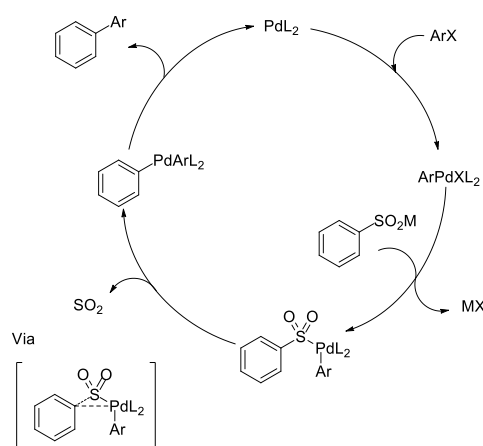
Various biaryl compounds were synthesised using this methodology, with the synthesis of four different 2,2-bipyridyl compounds demonstrated (**Scheme 32**).¹⁵¹



Scheme 32: One of the bipyridyl coupling reactions exemplified. *Reagents and Conditions:* i) **190** (2.0 equiv.), **191** (1.0 equiv.), Pd(OAc)₂ (5 mol%), PCy₃ (10 mol%), K₂CO₃ (1.5 equiv.), 1,4-dioxane, 150 °C, 69%.¹⁵¹

The outcome of this optimisation for the cross-coupling using a pyridine sulfinate differs from that carried out previously by Forgiione and co-workers to synthesise biaryl compounds using a phenylsulfinate (**Scheme 33**, conditions a).¹⁸⁰ One notable difference is the ligand. For biaryl synthesis, a bidentate ligand (dppf) was found to be optimal. The authors proposed that the bidentate ligand may suppress the formation of homocoupling by-products.¹⁸⁰ Additionally, 4.0 equivalents of the sulfinate were required in order to improve the conversion.¹⁸⁰ The scope of the reaction was

coupling reactions (**Scheme 35**).^{167,180} The key difference in the familiar oxidative addition, transmetalation/ligand exchange, reductive elimination cycle is the extrusion of sulfur dioxide.¹⁶⁷ The sulfinate anion formed after ligand exchange is tetrahedral.¹⁸⁰ This means that the attached aryl ring is not in the same plane as palladium and sulfur but is closer to the palladium.¹⁸⁰ This leads to extrusion of sulfur dioxide to give a bis-arylated palladium species.¹⁸⁰ While there appears to be no direct function of the base in this catalytic cycle, a base has been reported to be essential to the reaction.¹⁵¹ It is proposed that the base may prevent formation of the sulfinic acid, which may not be nucleophilic enough to undergo the reaction.



Scheme 35: Proposed catalytic cycle for the palladium-catalysed desulfinate cross-coupling reaction.⁹ Oxidative addition of the aryl halide gives a palladium(II) species which undergoes ligand exchange, swapping the halide for the sulfinate to give a sulfinate-complex. The sulfinate anion is tetrahedral with the aryl group close to palladium, leading to extrusion of sulfur dioxide to give a bis-arylated palladium species which can undergo reductive elimination to give the biaryl product and regenerate the palladium(0) catalyst.¹⁸⁰

Many examples of these cross-coupling reactions use an excess of the sulfinate. Optimisation processes have shown that this is key to achieving improved yields.^{151,180} When carrying out experiments to investigate the mechanism, Forgone and co-workers evaluated the use of sulfur dioxide scrubbers such as calcium oxide and calcium carbonate.¹⁸⁰ Addition of calcium oxide was shown to give decreased amounts of sulfinate-derived by-products. They found that, by adding six equivalents of calcium oxide and running the reaction in **Scheme 33** (above, where R = CF₃ (**195**))

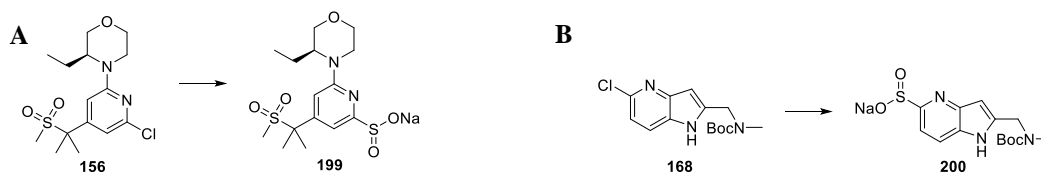
⁹ After the presentation of this Thesis, Willis *et al.* published a detailed mechanistic study of the desulfinate cross-coupling reaction. This is included in Appendix E.

using conditions a), the number of equivalents of the sulfinate could be decreased to 1.0 while only slightly reducing the yield (from 82% to 72%).¹⁸⁰

Willis and co-workers highlighted the potential utility of this desulfinative cross-coupling reaction to form bipyridyl compounds, stating that Suzuki reactions often fail due to difficulties in preparing boronic esters of 2-pyridyls or low reaction efficiency.¹⁵¹ This was one of the problems encountered in our work to synthesise compound **153**. Therefore this desulfinative cross-coupling method, which had been shown to couple bipyridyls with good to excellent yields, was investigated.

3.9.1 Sulfinate synthesis

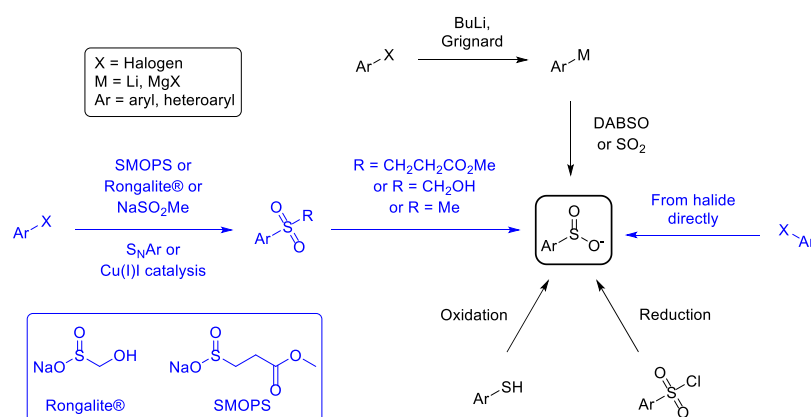
The first challenge encountered when attempting to employ this methodology in this research was the synthesis of the sulfinate. At this point only the chloro-intermediates were available, so a facile method to install the sulfinate directly onto either chloropyridine **156** or chloroazaindole **168** – without resynthesising either component with the sulfur installed from an earlier stage – was required (**Scheme 36A and B**).



Scheme 36A and B: Demonstrating the ideal transformations to give the required sulfinate (**199** and **200**) to trial the desulfinative cross-coupling chemistry.

There are many ways to make sulfinate from aryl halides using various sulfur dioxide surrogates, some of which are shown in **Scheme 37**. Metal-halogen exchange followed by trapping the anion with sulfur dioxide or a sulfur dioxide surrogate such as DABSO,¹⁸² oxidation of a thiol¹⁸³ or reduction of a sulfonyl chloride¹⁸⁴ are all viable methods.^{151,167} Not all of these options were believed to be suitable for use here. As seen previously, attempting metal-halogen exchange on either **156** or **168** resulted in deprotonation. Introduction of the sulfur at a lower oxidation state as the thiol and subsequent oxidation was not desirable as it was not known whether the rest of the compound would be stable to oxidising conditions. Furthermore, avoiding the reduction of sulfonyl chlorides was also preferable. This left two methods to examine.

One approach used potassium metabisulfite as a sulfur dioxide surrogate to give the sulfinate directly.¹⁸⁵ The other approach used sulfonates as sources of sulfur dioxide, including sodium 3-methoxy-3-oxopropane-1-sulfinate (SMOPS),¹⁸⁶ sodium hydroxymethyl sulfinate (Rongalite®)^{187,188} and sodium methanesulfinate,¹⁸⁹ all of which gave an isolated sulfone followed by a subsequent, relatively mild, reaction to give the desired aryl sulfinate salt. As demonstrated using Stille chemistry, either component could be the nucleophilic coupling partner and introduction of the sulfinate to both coupling partners was investigated.

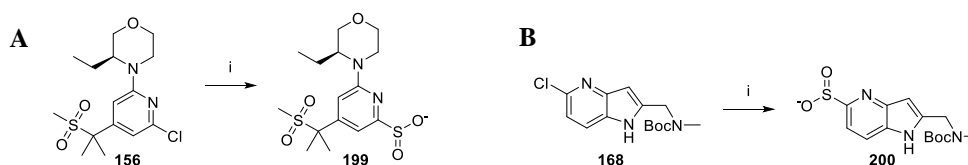


Scheme 37: Exploring some of the methods available to make sulfonates. The methods in blue were considered to be best to try initially, as it was proposed that the rest of the molecule would be stable to the required conditions.

The most efficient approach would install the sulfone in one step, directly from the chloropyridine. Potassium metabisulfite had been shown to be a sulfur dioxide surrogate.¹⁸⁵ Shavnya *et al.* reported the first example of a palladium-catalysed reaction of aryl and heteroaryl halides with potassium metabisulfite to directly form aryl (or heteroaryl) sulfonates.¹⁸⁵ These sulfonates were either isolated as a salt, or reacted without isolation to form sulfones and sulfonamides.¹⁸⁵ The majority of the examples employed aryl (or heteroaryl) bromides and iodides, with any chlorides exemplified giving lower yields.¹⁸⁵

In the current study, heteroaryl chlorides **156** and **168** were investigated (**Table 18**). Using chloropyridine **156**, this approach initially looked promising, appearing to give 28% conversion to the desired sulfinate after 17 hours (**Entry 1**). However, this was either an artefact in the LCMS or the product degraded, as on further heating, no

desired product was seen. A higher reaction temperature for a shorter time was investigated but gave no conversion to product and on further heating the starting material degraded (**Entry 2**). Interestingly, this reaction was more successful using chloroazaindole **168** as the starting material, giving 24% conversion to desired product after 17 hours (**Entry 3**). After further heating, the amount of desired product decreased, suggesting again that perhaps the sulfinate was unstable to the reaction conditions. Again, increased temperature gave no conversion and prolonged heating led to degradation of the starting material (**Entry 4**).



Entry	Scheme	Starting material	Temp. (°C)	Time (h) ^a	Product (%) ^b	Remaining starting material (%) ^b
1	A	156	70	17	28	45
				32	0	48
2	A	156	120	3	0	59
				18	0	0
3	B	168	70	17	24	47
				32	15	44
4	B	168	120	3	0	35
				18	0	0

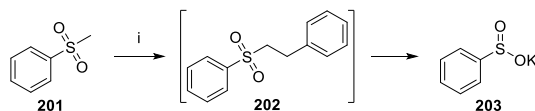
Table 18: The reactions trialled to directly synthesise the sulfinate salt, employing the reaction conditions demonstrated by Shavnya *et al.*¹⁸⁵ *Reagents and Conditions:* **156** or **168** (1.0 equiv.), TBAB (1.1 equiv.), K₂S₂O₅ (2.0 equiv.), 1,10-phenanthroline (15 mol%), Pd(OAc)₂ (5 mol%), PPh₃ (15 mol%), sodium formate (1.3 equiv.), DMSO. ^aTimes shown are cumulative. ^bLCMS conversion.

Reactions by H. Davies.

These reactions gave a complex mixture of unidentifiable by-products. Overall, this approach was not considered to be an effective way to make the sulfinate of chloropyridine **199**. However when chloroazaindole **168** was used, although the product was not isolated, a conversion to the desired sulfinate (**200**) of approximately 20% was seen. It was proposed that, had the bromide or iodide been available at the time, this method may have given better conversion.

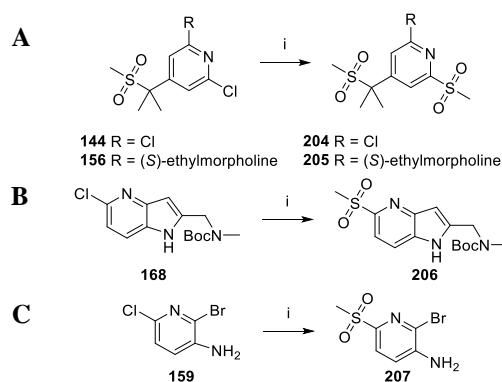
Next, three sources of sulfur dioxide were considered. First, methylsulfone was investigated. Literature precedent from Gauthier and Yoshikawa demonstrated that a

methyl sulfone could be converted into a sulfinic acid, exemplified using aryl methylsulfones (**Scheme 38**).¹⁸⁹ Reaction of an aryl methylsulfone with benzyl bromide and in an excess of potassium *tert*-butoxide gave the sulfinate salt as a precipitate in THF – a poor solvent for the sulfinate salt.¹⁸⁹



Scheme 38: The reaction of methyl phenyl sulfone and benzyl bromide with KO^tBu in THF to give potassium benzene sulfinate (as a precipitate that can be filtered off) via a transient dibenzylated species. *Reagents and Conditions:* i) Benzyl bromide (1.3 equiv.), KO^tBu (2.5 equiv.), THF, 23 °C, 98%.¹⁸⁹

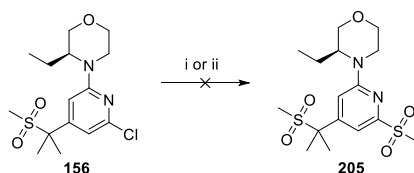
To investigate this, different starting materials were treated with sodium methanesulfinate in DMF (**Table 19**). Using chloropyridine **156** (**Entry 2**) and chloroazaindole **168** (**Entry 3**) there was no reaction, even with prolonged heating at 100 °C. The same was seen using 2-bromo-6-chloropyridin-3-amine (**159**), the starting material from which chloroazaindole **168** was made; no product formed and starting material remained (**Entry 4**). The only substrate that gave any reaction was dichloropyridine **144**, giving 12% conversion to desired (**Entry 1**). Unfortunately, double addition of the methylsulfone (40%) and unreacted starting material (45%) were also seen. This was not surprising since the methylsulfonyl-pyridine (formed from addition of the sulfinate, an electron withdrawing group) was activated to nucleophilic attack by a second molecule of the sulfinate to form the disubstituted product.



Entry	Scheme	Starting material	Temperature (°C)	Time (h)	Conversion (%) ^a
1	A	144	21-100	80	12
2	A	156	21-100	20	0
3	B	168	21-100	80	0
4	C	159	100	5	0

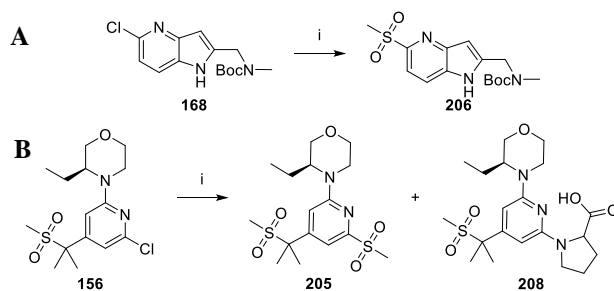
Table 19: Attempts to introduce the methylsulfone moiety using a S_NAr reaction. *Reagents and Conditions:* i) Chloropyridine (1.0 equiv.), sodium methanesulfinate (1.1-1.5 equiv.), DMF. ^aLCMS conversion. Reactions by H. Davies.

An alternative method of addition of sulfonates to chloropyridines employed a S_NAr reaction of chloropyridine and sodium sulfinate salt with tetrabutylammonium chloride (TBACl) as an additive.¹⁹⁰ TBACl was suggested to form a soluble complex with the sulfinate, leading to an increase in rate of reaction and increased conversion.¹⁹⁰ It was also found that addition of hydrochloric acid increased the yield when using electron-neutral chloropyridines, proposed to be due to protonation of the pyridine nitrogen.¹⁹⁰ This reaction was examined with chloropyridine **156**, both with and without hydrochloric acid (**Scheme 39**). Unfortunately, neither reaction gave any of the desired product, with both giving unreacted starting material as the major component of the reaction mixture.



Scheme 39: Reactions examined to form the methyl sulfone using TBACl. *Reagents and Conditions:* i) Sodium methanesulfinate (1.5 equiv.), TBACl (0.3 equiv.), DMA, 120 °C, 23.0 h. ii) As previously with addition of concentrated HCl (1.0 equiv.). Reactions by H. Davies.

Next, copper(I)-catalysed reactions were investigated. First, copper(I) iodide with a proline ligand and potassium carbonate in DMSO at 120 °C was trialled.¹⁹¹ With both starting materials (**156** and **168**), some conversion to the product was observed, with unreacted starting material as the major component of the reaction mixture (**Table 20, Entries 1 and 2**). Subsequent reactions were only attempted with chloropyridine **156** as it had been demonstrated to be more reactive in the borylation study. To achieve increased conversion, stoichiometric copper(I) iodide and proline (ligand 1) were investigated and, while slightly improved conversion was observed, more by-products were formed – including a proposed proline-adduct impurity (compound **208, Entry 3**). Stoichiometric copper(I) iodide without a ligand gave some conversion to product, but less than with proline (**Entry 4**). Increasing the stoichiometry of copper(I) iodide further and doubling the amount of sodium methanesulfinate gave a slight increase in conversion (**Entry 5**). This also resulted in 12% of a proposed methyl thioether impurity. This may have been formed by a reduction of the product sulfone (compound **205**) or as the result of decomposition of DMSO giving methanethiol, as discussed previously (**Scheme 24**). **Entries 6 and 7** suggested that catalytic copper(I) iodide reduced the formation of by-products (the conversion to product was not increased but more starting material remained). Comparison of **Entries 3 and 6** suggested that reduced equivalents of proline gave increased product formation, presumed to be due to reduced formation of the proline-adduct impurity. Investigation of an alternative ligand suggested that a diamine ligand (ligand 2) gave slightly improved conversion (44% compared to 35% with proline, **Entries 7 and 8**).¹⁹² Increased temperature and a shorter reaction time (**Entry 9**) did not improve the conversion. However, it was found that by using three separate additions of sodium methanesulfinate, potassium carbonate, copper(I) iodide and the diamine ligand, the amount of starting material could be greatly reduced (**Entry 10**). While a conversion to product of 28% was observed, an almost quantitative isolated yield suggested that many of the impurities seen by LCMS are not related to the starting material or product. This suggested that a reasonable isolated yield may have been achieved in other reactions where little unreacted starting material remained (**Entries 3 and 6**).



Entry (starting material)	Scheme	NaSO ₂ Me equiv.	Cu(I)I equiv.	Ligand identity (equiv.)	K ₂ CO ₃ equiv.	Time (h)	Product (%) ^a	Starting material (%) ^a	208 (%) ^a
1 (168)	A	1.5	0.9	1 (0.3)	0.3	3	20	40	n/a
2 (156)	B	1.5	0.3	1 (0.3)	0.3	3	21	58	8
3 (156)	B	1.5	1	1 (1)	1	18.5	27	3	38
4 (156)	B	1.5	1.6	-	1	22	10	47	-
5 ^b (156)	B	3	3	-	-	24	14	41	
6 (156)	B	1.5	1	1 (0.5)	1	21	35	5	25
7 (156)	B	1.5 x 2	0.2	1 (0.2)	0.2	92	35	52	6
8 (156)	B	1.5 x 2	0.2	2 (0.2)	0.2	92	44	40	n/a
9 ^c (156)	B	2.3	0.3	2 (0.3)	0.2	20	26	48	n/a
10 (156)	B	1.5 x 3	0.3 x 3	2 (0.3 x 3)	0.3 x 3	52	28 (98) ^d	8	n/a

Table 20: Using copper catalysis to install the methyl sulfone. **Entry 1** used starting material **168**

(**Scheme A**), **Entries 2-10** used starting material **156** (**Scheme B**). Ligand **1** = proline;

Ligand **2** = *N,N*-dimethylethane-1,2-diamine. *Reagents and Conditions*: Chloropyridine (1.0 equiv.), methanesulfonate, Cu(I)I, ligand, K₂CO₃, DMSO, 110 °C. ^aLCMS conversion. ^bLCMS suggested 12% thioether impurity (chloride of starting material replaced by SMe). ^cHeated at 173 °C. ^dIsolated yield.

Reactions by H. Davies.

With methylsulfone (**205**) in hand, the reaction to form the sulfinate was investigated and two precedented sets of conditions were trialed (**Table 21**).¹⁸⁹ Disappointingly, there was little success. The first method (**Entry 1**) employed benzyl bromide and potassium *tert*-butoxide in THF at 40 °C for 30 minutes.¹⁸⁹ This gave no conversion to product and little remaining starting material; desulfinated compound (**182**) was the main identifiable species. The second method (**Entry 2**) used 2,4-difluorobenzyl bromide at -78 °C for one hour.¹⁸⁹ A small amount of product was observed by LCMS. Again, little starting material remained and the same impurity (**182**) was the major identifiable species in the LCMS. After stirring at 0 °C for a further hour, none of the

product or starting material was observed by LCMS. Instead, mass ions corresponding to mono-, di-, tri-addition of the 2,4-difluorobenzyl bromide as well as several other impurities were seen.

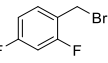
Entry	Bromide (equiv.)	KO ^t Bu equiv.	Temp. (°C)	Time (h)	199 (%) ^a	205 (%) ^a	182 (%) ^a	Mono Br addition (%) ^a
1	 (1.2)	4	40	0.5	0	5	25	-
2 ^b	 (2.3)	4.8	-78 0	1 2	4 -	3 -	21 9	4 12

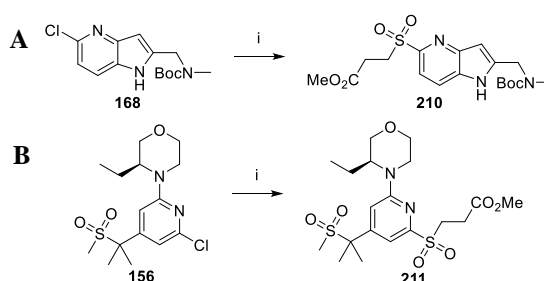
Table 21: Reactions trialed to form the sulfinate salt from the methyl sulfone. *Reagents and*

Conditions: i) KO^tBu (1 M in THF, 4.0 or 4.8 equiv.), benzyl bromide (1.2 equiv.) or 2,4-difluorobenzyl bromide (2.3 equiv.), THF. ^aLCMS conversion. ^bTimes are cumulative. Reactions by H. Davies.

A second sulfur dioxide source was investigated. Rongalite® (sodium hydroxymethanesulfinate dihydrate) was reported to be a cheap and stable source of sulfur dioxide that could be cleaved using mild conditions to give the sulfinate.¹⁸⁷ However, only reactions of Rongalite® with alkyl and benzylic halides have been demonstrated with no reported examples of reactions with aryl halides.^{187,188} Many examples using Rongalite® do not involve isolating the intermediate sulfinate; the Rongalite® adduct is treated with mild acid or base and subsequently reacted *in situ* to give a sulfone or sulfonamide.¹⁸⁷ However, if the Rongalite® sulfone adduct is treated with a base, the sulfinate salt can be isolated.¹⁸⁸

This reaction was attempted on chloropyridine **156** (Scheme 40). Initially, the chloropyridine and Rongalite® were stirred in DMSO at room temperature. After 4.5 hours, this gave no reaction, so the temperature was increased to 80 °C – again resulting in no reaction. In a second reaction, Rongalite® was pre-stirred in DMSO at room temperature for 30 minutes before adding the chloropyridine (**156**). These literature conditions had been shown to give improved reaction due to the poor

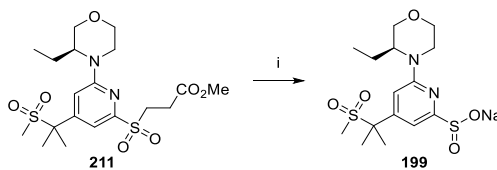
and copper(I) iodide (3.0 equivalents of each) were added after 22 hours at 110 °C when remaining starting material was observed by LCMS. The reaction mixture was reheated to 110 °C for 16 hours followed by 130 °C for 23 hours. This appeared to give increased conversion, but not an improved isolated yield (**Entry 4**). A similar isolated yield was maintained on a 1 g scale (**Entry 5**). Both the product (**211**) and starting material (**156**) could be isolated using column chromatography. A total recovered yield, taking the reisolated starting material in to account, was calculated (shown in parentheses). These total recovered yields were very good to excellent, highlighting the potential utility of this approach. However, re-isolation of the starting material was not optimal. Again, literature precedent suggested that the use of either a bromo- or iodopyridine starting material would improve the conversion.¹⁸⁶



Entry	Starting material	Scheme	SMOPs equiv.	CuI equiv.	Time (h)	Product conversion (%) ^a	Product yield (%) ^{b,c}	Starting material yield (%) ^c
1	168	A	3.2	3.0	16	13	-	-
2	168	A	3.2	3.2	21	13	-	-
3	156	B	3.0	3.0	22	20	39 (87)	47
4^d	156	B	3.0 x 2	3.0 x 2	61	19	41 (quant.)	44
5^e	156	B	3.0	3.0	25	17	31 (quant.)	68

Table 22: Demonstrating the reactions to install the SMOPs moiety onto both chloroazaindole **168** (**Scheme A**) and chloropyridine **156** (**Scheme B**), using literature conditions.^{151,186} *Reagents and Conditions:* i) **156** or **168** (1.0 equiv.), SMOPs, Cu(I)I, DMSO, 110 °C. ^aLCMS conversion. ^bYield in parentheses refers to the total recovered yield, taking recovered starting material into account. ^cIsolated yield. ^dReaction heated at 110-130 °C. ^eReaction on a 1 g scale. Reactions by H. Davies.

An E1cB elimination of the sulfone ester group gave the sulfinate salt (**199**) in excellent yield, using literature conditions (**Scheme 42**).¹⁵¹

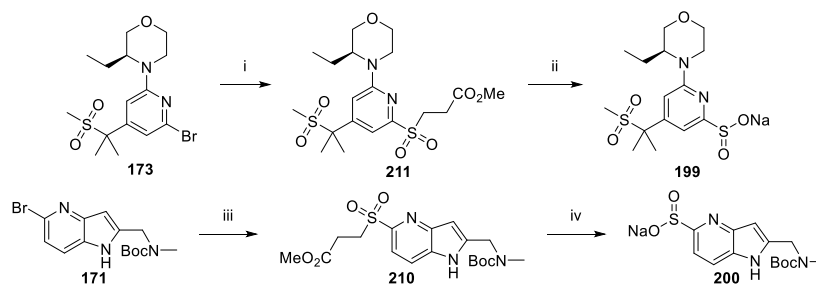


Scheme 42: Forming the sulfinate from the SMOPS adduct. *Reagents and Conditions:* i) NaOMe (0.5 M in MeOH, 1.0 equiv.), THF, 21 °C, 1.0 h, quant. Synthesis by H. Davies.

3.9.2 Use of brominated starting materials to enable sulfinate synthesis

It had been suggested that the best way to improve the yield would be to use a bromo- (or iodo-) pyridine as the starting material. Examples of the use of SMOPS in the literature employed aryl bromides or iodides and demonstrated improved yields. As discussed, the bromide starting materials were more atom economic and therefore preferable. Furthermore, using a bromopyridine (**173**) or bromoazaindole (**171**) would enable the subsequent desulfonative cross-coupling reaction. With the SMOPS conditions to form the sulfinate in hand, the reactions to form the sulfinate were repeated in our laboratories once the brominated intermediates (**171** and **173**) were available (**Scheme 43**).^r Pleasingly, using bromopyridine **173**, an improved yield of the SMOPS adduct was achieved (97% and 41% with bromo- and chloropyridine, respectively). Similarly, using bromoazaindole **171**, the reaction with SMOPS proceeded in a 96% yield – a significant improvement compared to the low reactivity of the corresponding chloroazaindole. Conversion to the sulfinate from both sulfone intermediates gave good yields.

^r Reactions by C. Mitchell and S. Nicolle.



Scheme 43: Forming the sulfinate from brominated intermediates. *Reagents and Conditions:*

- i) SMOPS (1.5 equiv.), Cu(I)I (1.5 equiv.), DMSO, 110 °C, 4.0 h, 97%. ii) NaOMe (0.5 M in MeOH, 1.0 equiv.), THF, 21 °C, 1.0 h, 72%. iii) SMOPS (2.0 equiv.), Cu(I)I (2.0 equiv.), DMSO, 110 °C, 2.0 h, 96%. iv) NaOMe (0.5 M in MeOH, 1.0 equiv.), THF, 21 °C, 1.5 h, 87%. Synthesis by C. Mitchell and S. Nicolle.

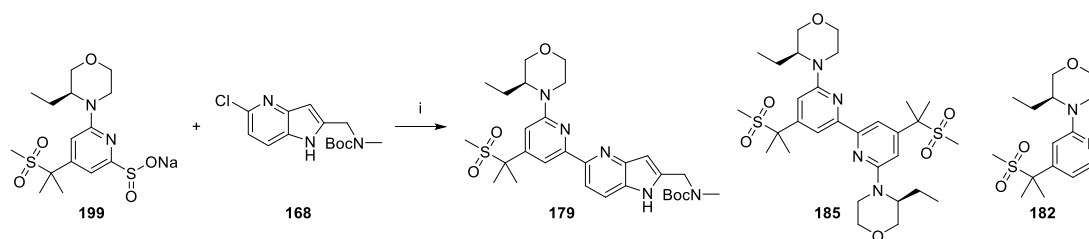
3.9.3 The desulfinate cross-coupling reaction

With sodium (*S*)-6-(3-ethylmorpholino)-4-(2-(methylsulfonyl)propan-2-yl)pyridine-2-sulfinate (**199**, referred to here as the pyridine sulfinate or sulfinate) in hand, the palladium-catalysed desulfinate cross-coupling was investigated. This was prior to the synthesis of bromo-variants, so the cross-coupling was trialed using chloroazaindole **168**. Pleasingly, the first coupling reaction attempted using the literature conditions and an excess of pyridine sulfinate **199** (1.9 equivalents) gave 56% conversion to the product and an isolated yield of 52% (**Entry 1, Table 23**). Small amounts of both starting materials were observed by LCMS, with the main impurity being homocoupling of the sulfinate (**185**). Additionally, a small amount of compound **182** (by-product formed from the loss of the sulfinate) was observed. The literature conditions used 2.0 equivalents of the pyridine sulfinate. As the sulfinate was not commercially available, reducing the number of equivalents was important. In a series of reactions (**Entries 1-5, Table 23**), the number of equivalents of sulfinate **199** was reduced from 1.9 to 1.1, demonstrating that comparable conversions were achievable, and 1.3 equivalents was suggested to give optimal conversion (**Entry 4**).

The next potential problem was the use of harsh conditions with a reaction temperature of 150 °C.^{151,194,195} While acceptable, the aim was to use this coupling reaction in a large-scale synthesis and milder conditions were preferable.^{194,195} In a follow up paper, the Willis group sought to address this.¹⁹⁴ After carrying out a second extensive screen of catalysts, bases, ligands and solvents, the group identified a more active ligand,

di-*tert*-butyl(methyl)phosphine (as the tetrafluoroboric acid salt, P(*t*Bu)₂Me.HBF₄).¹⁹⁴ Combining this ligand with the original base, catalyst and solvent enabled the use of a lower reaction temperature of 100 °C.^{194,196} Unfortunately, none of this ligand was available in our laboratories for immediate use, so a similar alternative was tried – tri-*tert*-butylphosphine (as the tetrafluoroboric acid salt, P(*t*Bu)₃.HBF₄) (**Table 23, Entry 6**). Interestingly, these two ligands (P(*t*Bu)₃.HBF₄ and P(*t*Bu)₂Me.HBF₄) had been compared in a previous optimisation of the desulfinate cross-coupling (between an aryl sulfinate and an aryl bromide) by Forgione and co-workers.¹⁸⁰ In this optimisation, little difference in yield was seen when using either ligand.¹⁸⁰

Here, a comparison of the desulfinate reactions with two ligands (P(*t*Bu)₃.HBF₄ and PCy₃) at 100 °C suggested similar conversion to desired product with both, but neither performed as well as using the original ligand at 150 °C (**Table 23, Entries 6 and 7**). For these reactions, 1.5 equivalents of the sulfinate was used as a compromise between achieving higher conversion and avoiding a large excess of the precious sulfinate. Interestingly, the P(*t*Bu)₃.HBF₄ ligand appeared to give less of the homocoupled by-product (**185**). However, since this ligand did not achieve increased conversion, no further investigations were carried out. Instead, alternative methods to reduce the amount of the homocoupled by-product (**185**) were investigated. Homocoupling can be caused by the presence of oxygen in a reaction mixture.^{197,198} Therefore, thorough degassing of the reaction mixture, especially the solvent, before use can reduce homocoupling.¹⁹⁷⁻¹⁹⁹ Pleasingly, degassing the solvent by sparging with nitrogen for 4.5-9 hours before use approximately halved the conversion to homocoupled by-product **185** (**Table 23, Entries 8 and 9**). This also allowed the number of equivalents of the sulfinate to be decreased further while maintaining the conversion.



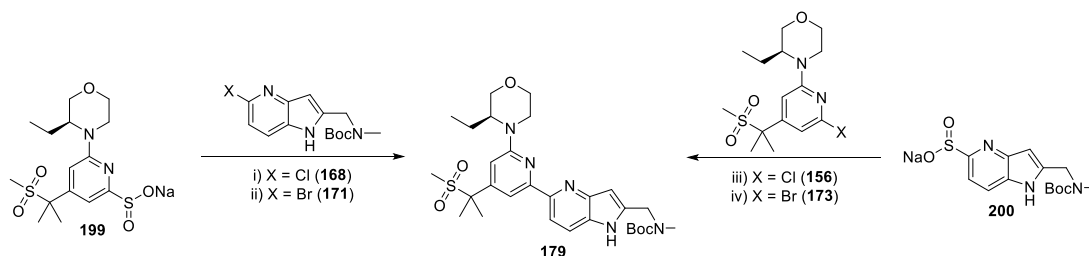
Entry	199 equiv.	Time (h)	179 (%) ^a	199 (%) ^a	168 (%) ^a	185 (%) ^a	182 (%) ^a	Yield 179 (%) ^b
1 ^c	1.9	18.5	56	5	4	21	4	52 ^d
2	1.7	18.0	53	-	9	24	1	-
3	1.5	18.0	53	-	17	23	1	-
4	1.3	18.0	58	-	13	18	1	-
5	1.1	18.0	52	-	22	17	1	-
6 ^{e,f}	1.5	24.5	19	26	39	8	7	-
7 ^f	1.5	24.5	14	16	40	28	1	-
8 ^g	1.3	16.5	74	-	-	9	4	73 ^h
9 ⁱ	1.1	14.0	74	-	-	10	3	61 ^h

Table 23: Demonstrating the optimisation carried out on the cross-coupling reaction using pyridine sulfinate **199**. *Reagents and Conditions:* i) **199** (1.9-1.1 equiv.), **168** (1.0 equiv.), K₂CO₃ (1.5 equiv.), Pd(OAc)₂ (10 mol%), PCy₃ (20 mol%), 1,4-dioxane, 150 °C, unless otherwise noted. Reactions by H. Davies. ^aLCMS conversion. ^bIsolated yield. ^cReaction used Pd(OAc)₂ (25 mol%), PCy₃ (80 mol%). ^dIsolated yield from MDAP purification. ^eReaction used P(^tBu)₃ (HBF₄ salt) (20 mol%) as the ligand. ^fReaction carried out at 100 °C. ^g1,4-Dioxane sparged with nitrogen for 4.5 h before use. ^hIsolated yield from normal phase followed by reverse phase column chromatography carried out by S. Nicolle due to absence of H. Davies. ⁱ1,4-Dioxane sparged with nitrogen for 9.0 h before use.

This short optimisation process achieved improvements of over 20% in isolated yield and a reduction from 1.9 to 1.3 equivalents of pyridine sulfinate **199**. This represented a substantial improvement to the coupling reaction and met the aims of this work. The use of a sulfinate as the nucleophilic coupling partner was the only approach investigated to give reasonable yields and avoided the use of toxic stannanes.

3.10 Further improvements to the desulfinate cross-coupling reaction

The synthesis of bromoazaindole **171** and bromopyridine **173** enabled the palladium-catalysed desulfinate cross-coupling to be carried out with either component as the sulfinate, with either the chloride or bromide coupling partner (**Scheme 44**).



Scheme 44: Synthesis of bromopyridine and bromoazaindole starting materials allowed the cross-coupling to be carried out with either component as the nucleophile. *Reagents and Conditions:*
 i) **199** (1.1 equiv.), **168** (X = Cl, 1.0 equiv.), K_2CO_3 (1.5 equiv.), $Pd(OAc)_2$ (10 mol%), PCy_3 (20 mol%), 1,4-dioxane, 150 °C, 14.0 h, 61%. ii) **199** (1.1 equiv.), **171** (X = Br, 1.0 equiv.), K_2CO_3 (1.5 equiv.), $Pd(OAc)_2$ (10 mol%), PCy_3 (20 mol%), 1,4-dioxane, 150 °C, 2.0 h, 84%. iii) **156** (X = Cl, 1.3 equiv.), **200** (1.0 equiv.), K_2CO_3 (1.5 equiv.), $Pd(OAc)_2$ (10 mol%), PCy_3 (20 mol%), 1,4-dioxane, 150 °C, 4.0 h, 29%. iv) **173** (X = Br, 1.2 equiv.), **200** (1.0 equiv.), K_2CO_3 (1.5 equiv.), $Pd(OAc)_2$ (10 mol%), PCy_3 (20 mol%), 1,4-dioxane, 150 °C, 4.0 h, 28%.^s

Overall, using pyridine sulfinate **199** and bromoazaindole **171** gave the highest yield in the coupling reaction. However, since the reactions to form bromoazaindole **171** were lower yielding, the chloroazaindole **168** was the preferred coupling partner. This desulfinate coupling was used on a 500 g scale to prepare a structurally similar compound, with a 70% yield for the coupling step.^t Furthermore, this method was also considered suitable for further scale-up in future API campaigns.

3.11 Summary of Chapter II

In this Chapter, the aim was to solve three problems in the synthesis of compound **153**. All aims were achieved (**Figure 44**):

- More efficient synthesis of the azaindole back pocket and reduced number of protecting groups.

^s Reactions by H. Davies, J. Lee and S. Nicolle.

^t Reactions by S. Sollis, L. Thorpe.

- Improved S_NAr reaction conditions, including a shorter reaction time and a reduced number of equivalents of the morpholine.^u
- A palladium-catalysed desulfinate cross-coupling to avoid Stille chemistry.

The highlight of this work was replacing the toxic stannanes and Stille chemistry with a pyridine sulfinate and a desulfinate cross-coupling reaction. Comparable yields could be achieved with approximately 50% yield achieved over both the two steps of stannane formation/Stille coupling and over the three steps of sulfinate formation/desulfinate coupling. The work described in this Chapter demonstrated that very good yields could be achieved for the desulfinate cross-coupling and this, combined with the use of a bromopyridine starting material to facilitate the synthesis of the pyridine sulfinate, gave a viable alternative to the Stille reaction. The additional safety benefits of avoiding the use of tin make this a significant achievement in the synthesis of compound **153**.

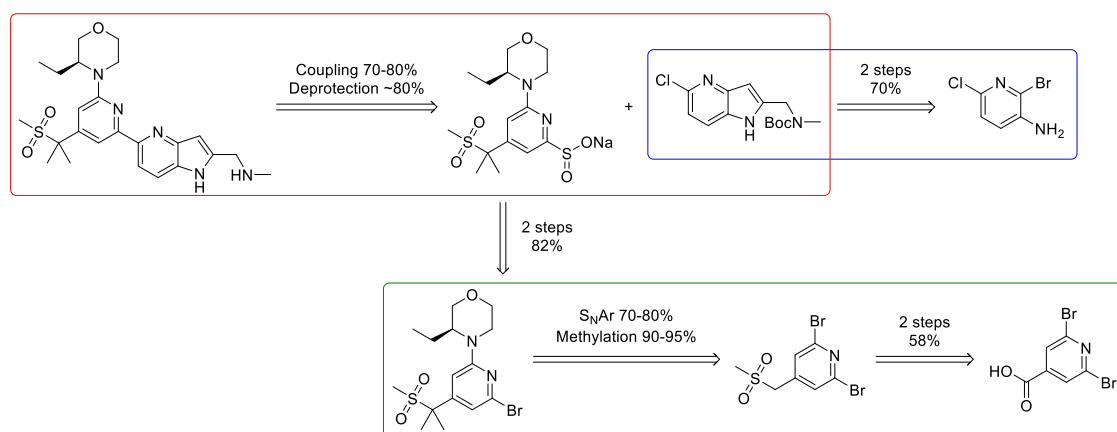


Figure 44: Highlighting the improvements to the route in each of the three areas; S_NAr (green), azaindole synthesis (blue) and cross-coupling (red). Approximate yields shown for each step.

The impact of the research described in this Chapter – demonstrating the utility of this palladium-catalysed desulfinate cross-coupling reaction – enabled significant advances in our research and has now been exemplified in:

- A scale-up campaign of a structurally related compound (500 g scale).
- The synthesis of over 150 analogues.

^u Initial work by H. Davies, subsequent work by A. Richards and mTOR project team.

Chapter III: Investigating the scope of the
desulfinate cross-coupling reaction

4. Investigating the scope of the desulfonative cross-coupling reaction

4.1 Introduction

Pyridine rings are prevalent scaffolds found in numerous pharmaceuticals.²⁰⁰ A 2014 study showed pyridines to be the second most commonly used nitrogen heterocycle in all FDA approved drugs.²⁰⁰ Furthermore, analysis of the substitution patterns of pyridine-containing drugs showed 2-substituted pyridines to be most common, appearing with a frequency of 66%.²⁰⁰ However, some of the precursors to 2-substituted pyridines, such as the boronic esters, are particularly challenging to synthesise.¹⁵¹ For example, one of the most commonly used sp^2 - sp^2 bond forming reactions, and a favourite reaction for use in industry – the Suzuki-Miyaura cross-coupling – often fails when using 2-pyridines as the nucleophilic coupling partner, proposed to be due to the instability of the corresponding boronic ester.^{151,201,202} Furthermore, metal-catalysed reactions to form bipyridyls are known to be problematic due to the ability of bipyridyl compounds to chelate metals.^{137,139}

Several drug molecules contain bipyridine or pyridine-heterocycle motifs, including Etoricoxib (Arcoxia, **212**), a treatment for arthritis, Imatinib (Gleevec, **213**) and Crizotinib (Xalkori, **214**), oncology drugs, and Perampanel (Fycompa, **215**), an antiepileptic drug (**Figure 45**).^{151,200,203-205} The challenging synthesis of these compounds is exemplified by Etoricoxib.²⁰³ The small-scale synthesis of this substituted pyridine and analogues could be completed using a Negishi or Suzuki reaction to install the 3-position phenyl, followed by a Stille reaction to install the 2-position pyridine.^{203,206,207} However, this was not considered feasible on a large scale due to the toxicity of the required stannane.²⁰³ The central pyridine ring was formed instead in a condensation reaction.^{203,207,208}

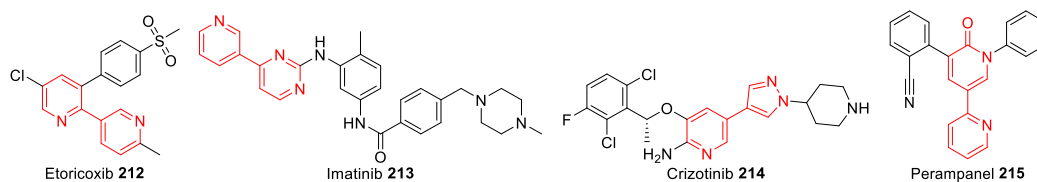
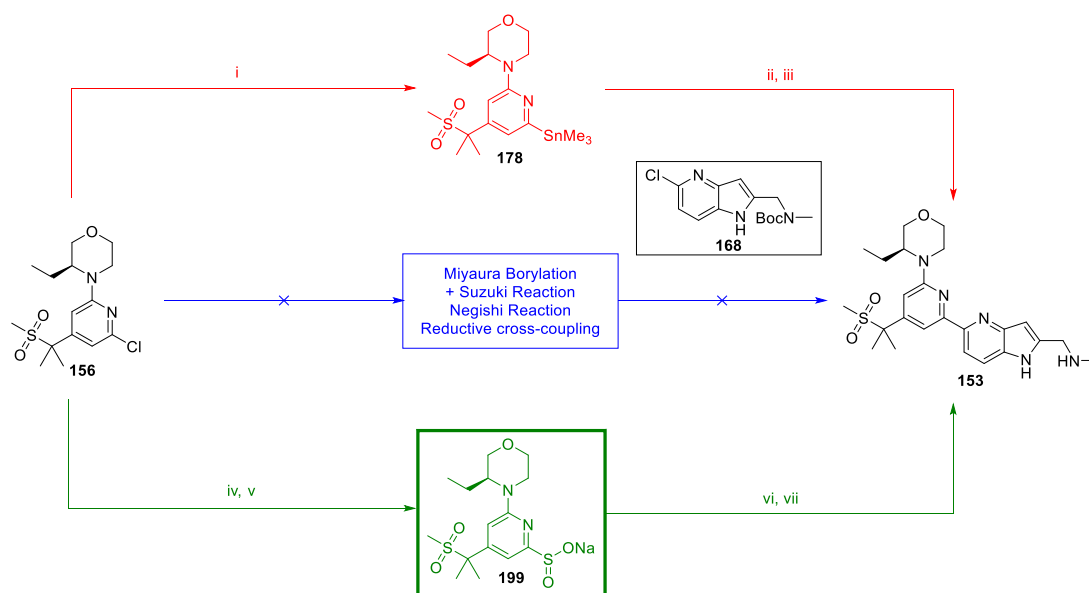


Figure 45: Examples of drugs containing bipyridine or pyridine-heterocycle motifs.

Furthermore, the challenging synthesis of 2,2-bipyridyl compounds, developed as mTOR kinase inhibitors for the treatment of IPF, has been demonstrated in this Thesis. A thorough exploration of traditional cross-coupling reactions (Suzuki-Miyaura, Negishi and nickel-catalysed reductive cross-coupling) was carried out and the desulfinate cross-coupling reaction was found to be the only suitable replacement for the Stille reaction (Section 3.9, **Scheme 45**).

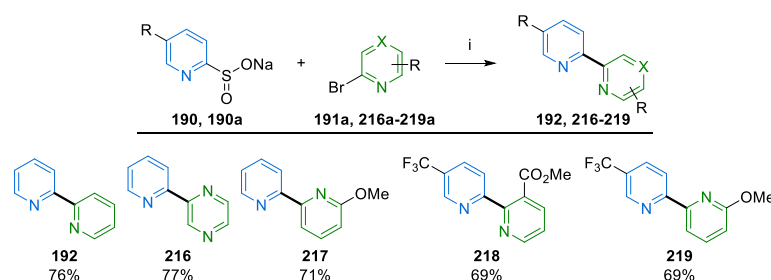


Scheme 45: Summary of the work previously described to couple chloropyridine **156** and azaindole **168**. *Reagents and Conditions:* i) PdCl₂(dppf) (6 mol%), Sn₂Me₆ (1.8 equiv.), toluene, 110 °C, 4.0 h, 73%. ii) **168** (1.0 equiv.), **178** (1.1 equiv.), LiCl (1.1 equiv.), PdCl₂(dppf) (10 mol%), toluene, 100 °C, 3.0 h then PdCl₂(dppf) (10 mol%), LiCl (1.1 equiv.), 100 °C, 23.0 h, 50%. iii) HCl (4 M in 1,4-dioxane, 11.2 equiv.), 1,4-dioxane, 21 °C, 5.5 h, 81%. iv) SMOPS (3.0 equiv.), Cu(I)I (3.0 equiv.), DMSO, 110 °C, 22.0 h, 39%. v) NaOMe (0.5 M in MeOH, 1.0 equiv.), THF, 21 °C, 1.0 h, quant. vi) **199** (1.1 equiv.), **168** (1.0 equiv.), K₂CO₃ (1.5 equiv.), Pd(OAc)₂ (10 mol%), PCy₃ (20 mol%), 1,4-dioxane, 150 °C, 14.0 h, 61%. vii) Boc-deprotection, as in step iii). Synthesis by H. Davies.

The desulfinate cross-coupling reaction was subsequently employed in our laboratories in the synthesis of several compounds containing the azaindole-pyridine motif.^a The importance and utility of this cross-coupling was recognised and further work to explore the scope of this reaction was initiated.

^a Analogue synthesis by chemists in our laboratories.

Desulfinate palladium-catalysed cross-coupling reactions involve the reaction of aryl sulfonates with alkyl, aryl or heteroaryl halides and, as discussed in Section 3.9, are preceded.^{151,167,180,181,194,196} Most recently published by the Willis group, desulfinate cross-coupling reactions have been demonstrated to couple a variety of pyridine-sulfonates with aryl or heteroaryl halides (**Scheme 46**).^{151,194,209} While the focus of the work in the Willis group was the synthesis of variously substituted 2-phenylpyridine compounds, several heteroaryl coupling partners were also explored. Additionally, a small number of 2,2-bipyridyl compounds were also exemplified (compounds **192** and **216-219**).¹⁵¹



Scheme 46: 2,2-Bipyridyl compounds and analogues previously exemplified using the desulfinate cross-coupling methodology, Willis *et al.*¹⁵¹ *Reagents and Conditions:* i) Pyridine sodium sulfinate (2.0 equiv.), (hetero)aryl halide (1.0 equiv.), Pd(OAc)₂ (5 mol%), PCy₃ (10 mol%), K₂CO₃ (1.5 equiv.), 1,4-dioxane, 150 °C, 3.0-18.0 h.

One of the key problems with this method was the use of two equivalents of the pyridine sodium sulfinate, which was undesirable in a large scale synthesis or an API campaign within GSK. Pleasingly, it was shown in our laboratories (described in Section 3.9.3) that the required amount of the pyridine sulfinate could be reduced to 1.1-1.3 equivalents, without effecting the conversion or isolated yield.

4.2 Aims of Chapter III

The aims in this Chapter were to:

- Investigate how the solvent and temperature influence the yield of the cross-coupling reaction.
- Explore the scope of the desulfinate cross-coupling, with particular emphasis on the synthesis of 2,2-bipyridyl compounds.

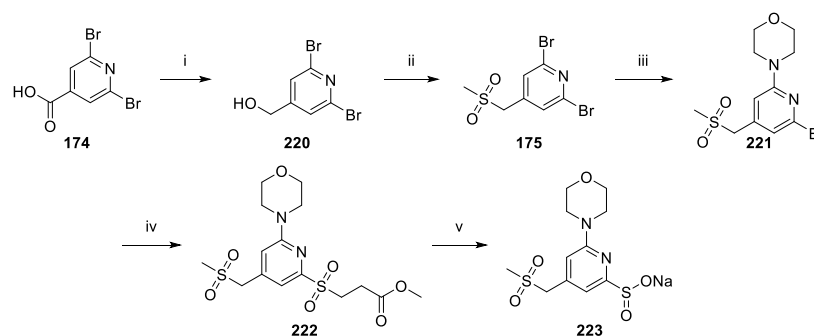
- Demonstrate that this cross-coupling reaction could be used in an array format to synthesise biologically relevant compounds related to the mTOR kinase inhibitors discussed in this Thesis.
- Develop and validate a high-throughput screening platform for the desulfinate cross-coupling reaction.

4.3 Sodium pyridine sulfinate synthesis

To explore the scope of the desulfinate cross-coupling reaction, a simplified version of compound **199** (precursor to mTOR kinase inhibitor **153**) was selected as a biologically relevant substrate (**223**). Pyridine sulfinate **223** had a morpholine in the 6-position and was chosen as morpholine was more readily available than the (*S*)-3-ethylmorpholine moiety used previously. Additionally, compounds made to demonstrate the scope of the desulfinate cross-coupling reaction would not be submitted for biological testing, therefore the use of the less selective (over the PI3Ks, **Table 1**, Section 1.5) morpholine hinge group was not an issue. Furthermore, a methylene linker in the ribose-binding region was chosen to simplify the synthesis.

Sulfinate **223** was synthesised starting from the commercially available 2,6-dibromoisonicotinic acid (**174**), a reduction using borane dimethyl sulfide complex gave (2,6-dibromopyridin-4-yl)methanol (**220**) in quantitative yield (**Scheme 47**). The sulfone group was installed in a one-pot mesylation- S_N2 reaction to form the carbon-linked sulfone compound **175**. The morpholine hinge was easily installed in 95% yield employing our standard DMSO and DIPEA conditions. Using morpholine as the nucleophile facilitated this S_NAr reaction, compared to the reaction with 3-(*S*)-ethylmorpholine (as described previously, Section 3.4). The reduced steric hinderance around the morpholine nitrogen was proposed to lead to its increased reactivity and improved conversion to desired product **221**. Finally, the sulfinate was installed in two steps: SMOPS (sodium 1-methyl 3-sulfinopropanoate) was used to form sulfone compound **222**, followed by base-promoted $ElcB$ elimination to give the desired sodium pyridine sulfinate (**223**) in quantitative yield. Pleasingly, using bromopyridine **221**, the number of equivalents of SMOPS could be reduced from 3.0 to

1.3 equivalents. Overall this gave a facile route to obtain gram-quantities of pyridine sodium sulfinate **223**.



Scheme 47: The synthesis of pyridine sodium sulfinate **223**. *Reagents and Conditions:* i) BH_3 .DMS (2 M in THF, 1.5 equiv.), THF, 0-21 °C, 20.0 h, quant.. ii) Triethylamine (1.1 equiv.), MsCl (1.1 equiv.), DMF, 0-5 °C, 1.0 h, then sodium methanesulfinate (2.0 equiv.), potassium iodide (0.3 equiv.), 60 °C, 2.5 h, 63%. iii) Morpholine (1.0 equiv.), DIPEA (2.0 equiv.), DMSO, 100 °C, 14.5 h, 95%. iv) Cu(I)I (1.3 equiv.), SMOPS (1.3 equiv.), 110 °C, 2.5 h, 79%. v) NaOMe (0.5 M in MeOH, 1.1 equiv., portion-wise), THF, 21 °C, 6.0 h, quant. Synthesis by H. Davies.

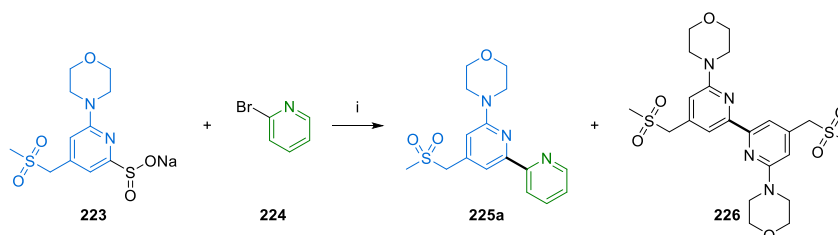
4.4 Optimisation of the desulfinative cross-coupling reaction

4.4.1 Solvent and temperature screens

Earlier screening of bases and ligands undertaken by Willis and co-workers revealed that potassium or caesium carbonate and a tricyclohexylphosphine ligand (PCy_3) were the optimal base/ligand combination at 150 °C.^{151,194,196} This was expanded on in subsequent work to show that a di-*tert*-butyl(methyl)phosphine ligand (used as its tetrafluoroboric acid salt, $\text{P}(\text{tBu})_2\text{Me.HBF}_4$) also gave good conversion and enabled the use of a lower temperature (120 °C).^{194,196} 1,4-Dioxane was found to be the optimal solvent in reactions with either of the ligands.^{151,194,196}

Here potassium carbonate and tricyclohexylphosphine were selected as the starting base/ligand combination.¹⁵¹ It had been demonstrated in our laboratories that alternative solvents could be used: primarily, that DMF could replace 1,4-dioxane, without affecting the yield of the reaction. Additionally, in some cases, this solvent was also found to enable the use of a lower temperature (130 °C instead of 150 °C), while keeping the other parameters (base, ligand and catalyst) the same. To further investigate this, a more detailed solvent and temperature screen was carried out. This

screen was conducted using pyridine sulfinate **223** and 2-bromopyridine (**224**) in a 1:1 ratio (**Scheme 48**).



Scheme 48: The reaction used in the solvent and temperature screen. *Reagents and Conditions:* i) **223** (1.0 equiv.), **224** (1.0 equiv.), K_2CO_3 (1.5 equiv.), $Pd(OAc)_2$ (10 mol%), PCy_3 (20 mol%), solvent, temperature. Reactions by H. Davies.

Five solvents were selected: 1,4-dioxane, *N,N*-dimethylformamide (DMF), *tert*-amyl alcohol (TAA), cyclopentyl methyl ether (CPME) and propionitrile (EtCN). TAA, DMF and propionitrile were explored by the Willis group¹⁹⁴ and CPME was selected as it had been reported to be a greener alternative to 1,4-dioxane.²¹⁰ All of these solvents have a boiling point of close to 100 °C and the reactions were carried out in a sealed vial. Three temperatures were used: 110, 130 and 150 °C and LCMS conversion to the desired product at 2, 4, 6 and 20 hours was recorded. The LCMS taken at 2, 4, 6 and 20 hours suggested that the reaction progressed slowly, with remaining pyridine sulfinate starting material still observed after 20 hours in some cases. It was subsequently proposed that sampling the reaction mixture may cause the reaction to stall, explaining why unreacted starting material was present. Homocoupling of the sulfinate to give by-product **226** (**Scheme 48**) was observed to various extents in all reactions. Previous evidence (**Table 23**, Section 3.9.3) suggested that homocoupling could be avoided by thorough degassing of the reaction solvent. Therefore, in all reactions, the solvent was degassed by sparging with nitrogen for a total of 2 hours before use. Additionally, the reaction mixtures were degassed by purging the vial under vacuum and filling with nitrogen (x 3) before addition of the solvent.

The optimal solvent and temperature combination was that which gave the lowest conversion to homocoupled by-product (**226**) and the highest conversion to the desired product (**225a**). The results of the screen displayed graphically (**Figure 46A-C**) suggested:

- Poor conversion to product **225a** (< 20%) was observed in all solvents at 110 °C.
- Improved conversion at both 130 and 150 °C was observed for reactions in all solvents, except those in DMF where no improved conversion to product **225a** was observed at higher temperatures.
- At 130 °C, 1,4-dioxane gave the highest conversion to desired product **225a**.
- At 150 °C, TAA gave the highest observed conversion to desired product, and the highest observed conversion to product **225a** of all reactions at 20 hours.
- Propionitrile and DMF gave low conversion to **225a** at 130 and 150 °C, despite the observation that DMF was the only solvent in which the reactants were fully in solution at room temperature.

Additionally, the LCMS conversion to compound **226**, resulting from the homocoupling of the pyridine sulfinate, was recorded. Displayed graphically (**Figure 47A-C**) this suggested:

- The reactions in propionitrile generally produced low levels of homocoupled by-product **226** at all temperatures.
- Comparable conversion to homocoupled by-product **226** was seen in CPME at all temperatures.
- The reactions in DMF and 1,4-dioxane generally gave high conversion to the homocoupled by-product **226** at all temperatures.
- TAA gave more homocoupled by-product at 110 than at 150 °C, with the amount of homocoupled by-product **226** appearing to decrease over time when the reactions were carried out at 130 °C – this was suggested to be an artefact in the LCMS.

Overall, TAA at 150 °C and 1,4-dioxane at 130 °C gave the highest conversion to desired product, 43% and 54%, respectively, after 20 hours. Least homocoupled by-product was seen in TAA at 150 °C (< 10%), therefore this solvent-temperature combination was suggested to be optimal.

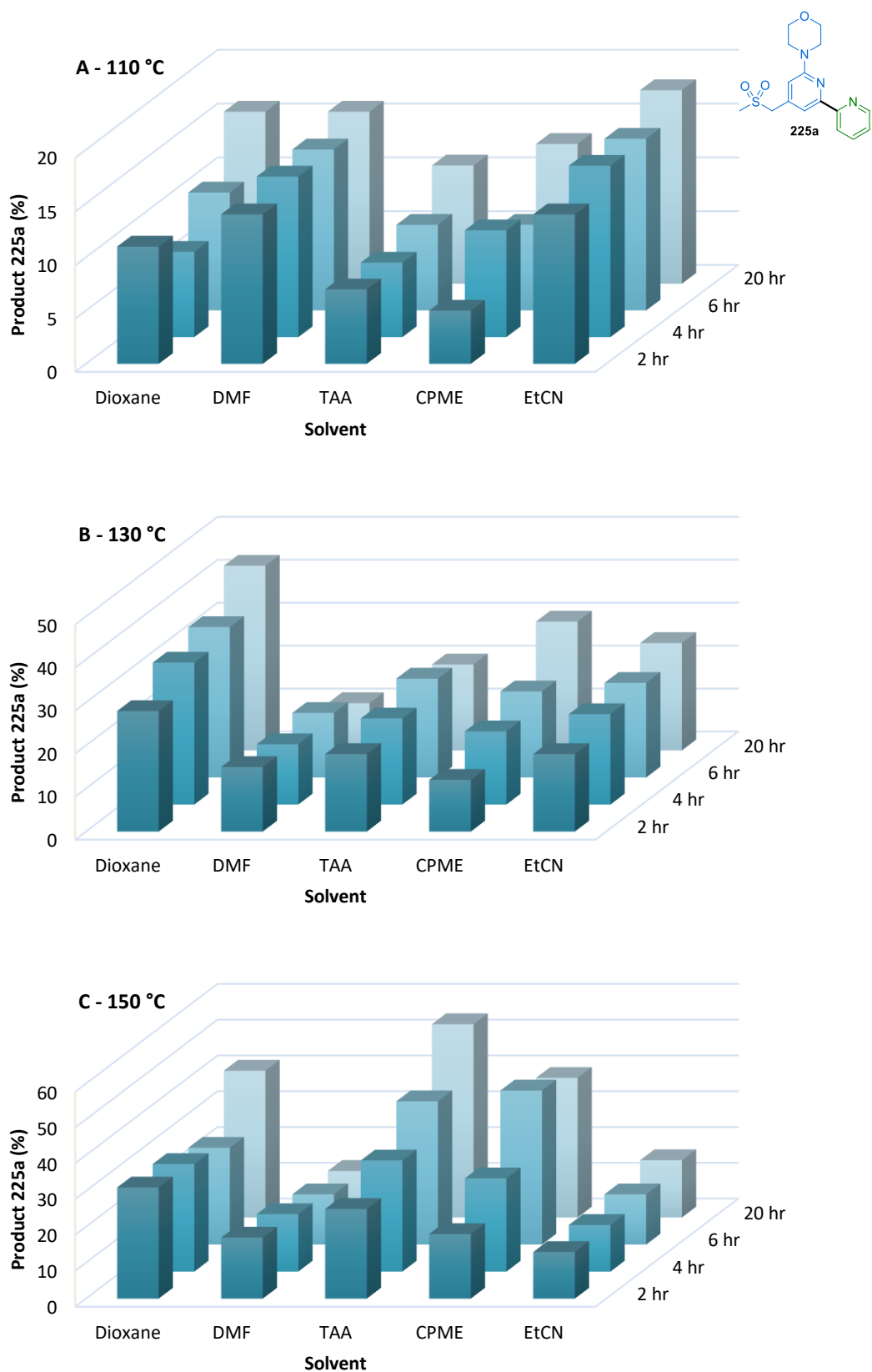


Figure 46A-C: The LCMS conversion to product **225a** (%) (**Scheme 48**) observed in the solvent-temperature screen. **46A:** 110 °C, **46B:** 130 °C and **46C:** 150 °C.

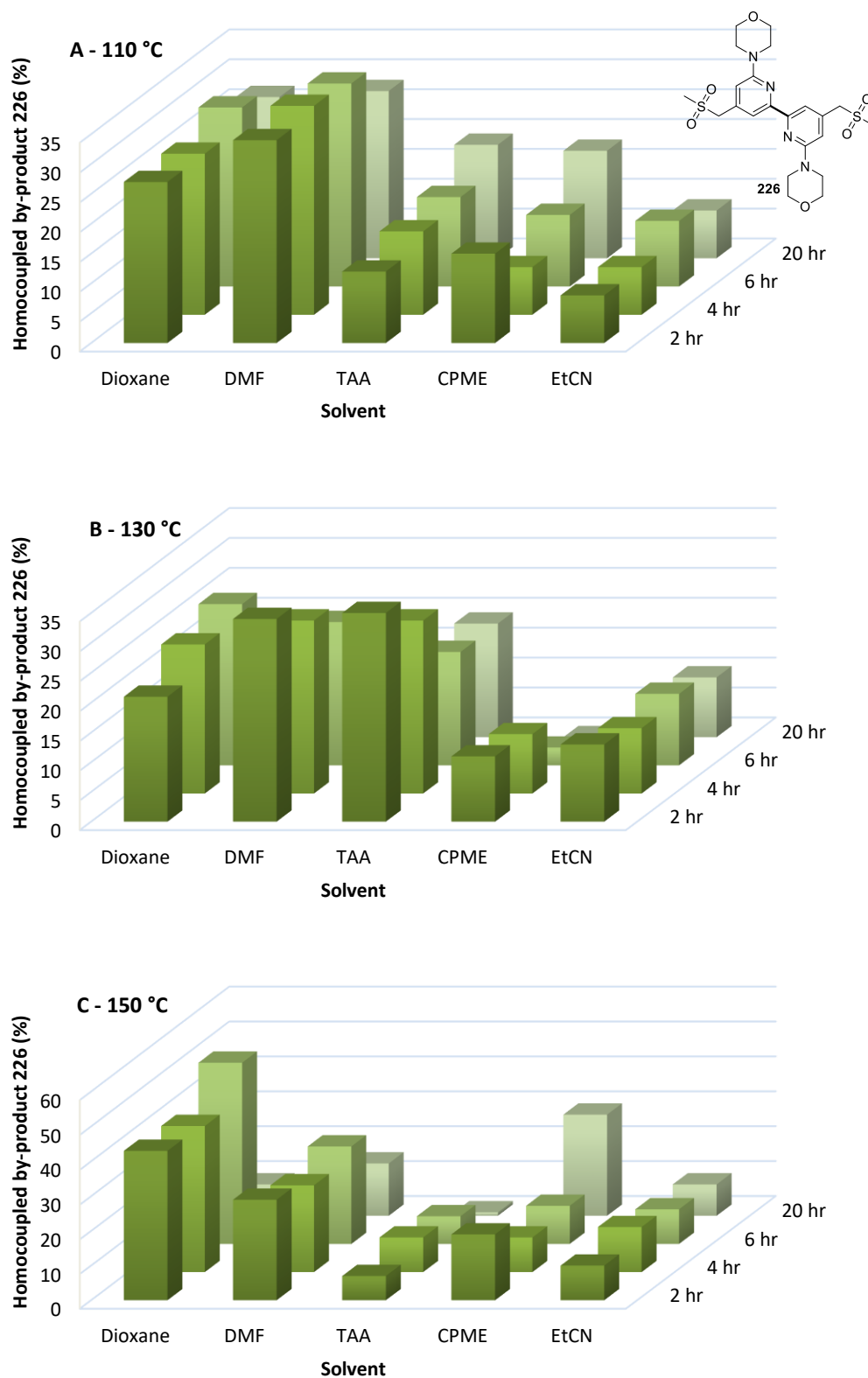
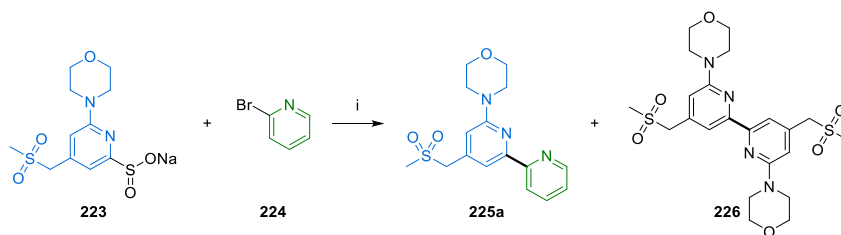


Figure 47A-C: The LCMS conversion to homocoupled by-product **226** (%) (**Scheme 48**), observed in the solvent-temperature screen. **47A:** 110 °C, **47B:** 130 °C and **47C:** 150 °C.

Three experiments were repeated to verify the results of the initial screen: those in 1,4-dioxane at 130 and 150 °C and TAA at 150 °C (**Table 24, Entries 1, 2 and 4**). Additionally, to investigate the effect of oxygen on the conversion to homocoupled by-product **226**, two experiments were carried out in which the reaction mixture was degassed by freezing under nitrogen and thawing under vacuum before heating at 150 °C (**Entries 3 and 5**). For comparison, the conversion to **225a** or **226** obtained after 20 hours in the original screen (**Figures 46A-C and 47A-C**) was included (values in parentheses in **Table 24**).

The repeated reaction in 1,4-dioxane at 130 °C (**Entry 1**), demonstrated comparable conversion to both **225a** and **226** to that observed in the previous screen. In this repeated reaction and in the screen (**Figure 47B**) the amount of homocoupled by-product appeared to decrease between 4 and 20 hours, proposed to be due to the formation of an unidentified by-product. The repeated reaction in 1,4-dioxane at 150 °C (**Entry 2**) gave a comparable conversion to product **225a** and increased conversion to the homocoupled by-product, compared to that observed in the screen (**Figures 46C and 47C**). The reaction using TAA as a solvent at 150 °C (**Entry 4**) gave comparable conversion to the desired product **225a** to that observed in the screen (**Figure 47C**), and increased conversion to the homocoupled by-product **226** was observed (**Figure 47C**). In both 1,4-dioxane and TAA, freeze-thawing the reaction mixture before heating (**Entries 3 and 5**) gave a comparable conversion to the desired product **225a** to that observed previously where the reaction mixture was degassed by purging the vial under vacuum and filling with nitrogen (x 3) (**Entries 2 and 4**).

These results suggested that the conversion to the desired product **225a** observed in the screen was reproducible. However, the results did not prove or disprove whether excluding oxygen from the reaction mixture by freeze/thawing resulted in reduced formation of the homocoupled by-product **226**. Overall, TAA was suggested to be the optimal solvent, giving good conversion to desired product and reduced homocoupled by-product **226** after 20 hours at 150 °C.



Entry	Solvent	Temperature (°C)	Time (h)	225a (%)	226 (%)
1	1,4-dioxane	130	2	15	30
			4	41	35
			20	51 (43)	3* (9)
2	1,4-dioxane	150	2	32	22
			4	32	41
			20	31 (41)	41 (9)
3	1,4-dioxane freeze/thaw degas	150	1	40	39
			2	40	28
			20	44	29
4	TAA	150	2	44	25
			4	46	25
			20	55 (54)	17 (1)
5	TAA, freeze/thaw degas	150	1	30	27
			2	42	21
			20	47	21

Table 24: Confirming the results of the solvent-temperature screen by repeating three of the reactions.

LCMS conversion (%) reported *The apparent decrease in homocoupled by-product **226** between 4 and 20 hours was suggested to be due to inefficient reaction sampling or the increased formation of an unidentified by-product. Values in parentheses refer to the conversion to **225a** or **226** obtained after 20 hours in the original screen (**Figures 48** and **49**). *Reagents and Conditions:* i) **223** (1.0 equiv.), **224** (1.0 equiv.), K₂CO₃ (1.5 equiv.), Pd(OAc)₂ (10 mol%), PCy₃ (20 mol%), solvent, temperature.

Reactions by H. Davies.

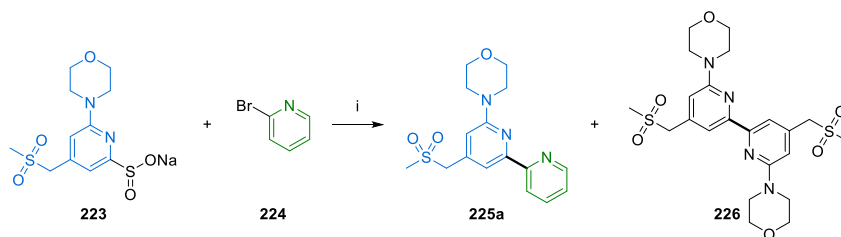
4.4.2 Investigating the effects of varying the stoichiometry of the pyridyl sulfinate

It had been previously demonstrated in our laboratories that the stoichiometry of the sulfinate could be reduced from 1.9 to 1.1 without affecting the conversion to the desired product (Section 3.9.3, **Table 23**). To confirm these results, a screen was carried out, again using 2-bromopyridine (**224**) and varying the stoichiometry of sulfinate **223**. These results (**Table 25**) suggest that higher equivalents of the sulfinate **223** gave increased conversion to product (> 30% conversion with 1.6 and 1.9

equivalents and 14% conversion with 1.3 equivalents). This was contradictory to the results found previously (**Table 23**).

The conversion to product **225a** observed in **Entry 4**, using 1.0 equivalent of **223** and only sampling at 19 hours, was much higher than the conversion seen in the more frequently monitored reactions in which large amounts of starting material remained, even after 20 hours (**Entries 1-3**). The reaction mixtures were sampled without cooling by venting the sealed tube and removing a small amount of the mixture. It was suggested that venting the reactions resulted in the loss of the inert atmosphere created by purging and filling with nitrogen. To verify this, reactions with differing equivalents of sulfinate **223** were repeated, only monitoring at 20 hours.

To repeat these experiments, a new batch of the pyridine sulfinate **223** was used. Unfortunately, this second batch was not of as high purity as the first batch used in **Entries 1-4** and the previous experiments. However, it was satisfying to note that even with this caveat, the repeated reactions (**Entries 5-8**), stirred at 150 °C for 20 hours without monitoring gave greatly improved conversion to bipyridyl product **225a**. **Entries 5-8** suggested that comparable conversion to product **225a** was achieved in all reactions, regardless of the number of equivalents of pyridine sulfinate **223** employed. Pleasingly in all reactions, only a small amount of homocoupled by-product **226** was observed. Overall it was decided that to use pyridine sulfinate **223** in the most economical way, 1.0 equivalent would be used to explore the reaction scope.



Entry	223 equiv.	Time (h)	225a (%)	226 (%)	224 (%)	223 (%)
1	1.9	2	8	4	18	65
		4	10	4	16	63
		20	33	8	9	44
2	1.6	2	13	3	49	17
		4	36	3	18	35
		20	32	3	10	50
3	1.3	1	12	4	21	55
		2	10	5	16	63
		20	14	7	16	56
4	1.0	19	87	3	8	0
5	1.7	20	68	4	5	7
6	1.5	20	78	5	0	0
7	1.2	20	65	4	14	0
8	1.1	20	60	7	8	8

Table 25: An equivalents screen to investigate the number of equivalents of pyridine sulfinate **223**. LCMS conversion (%) reported. *Reagents and Conditions:* i) **223** (1.9-1.0 equiv.), **224** (1.0 equiv.), K₂CO₃ (1.5 equiv.), Pd(OAc)₂ (10 mol%), PCy₃ (20 mol%), TAA, 150 °C. Reactions by H. Davies.

4.5 The scope of the desulfonative cross-coupling

Next, the scope of the reaction was examined. 24 Heteroaryl halides were selected as coupling partners, representing a variety of 5- and 6-membered heteroaromatic compounds: 2-, 3- and 4-pyridines, pyrimidines, 6,5- and 6,6-bicyclic heteroaromatic compounds and *para*-substituted 2- and 3-pyridines with both electron donating and electron withdrawing substituents (**Scheme 49**). To explore the scope efficiently, the syntheses were carried out as an array. Isolated yields from array chemistry are not always representative of the true yield that could be obtained from a bespoke synthesis.

For this reason, both the isolated yield and LCMS conversion were reported here.^b However, carrying out several reactions in parallel is an efficient way to explore chemical space and array chemistry is frequently used within medicinal chemistry teams in industry.²¹¹ It was therefore pleasing that the desulfonative cross-coupling was found to be amenable to parallel synthesis.

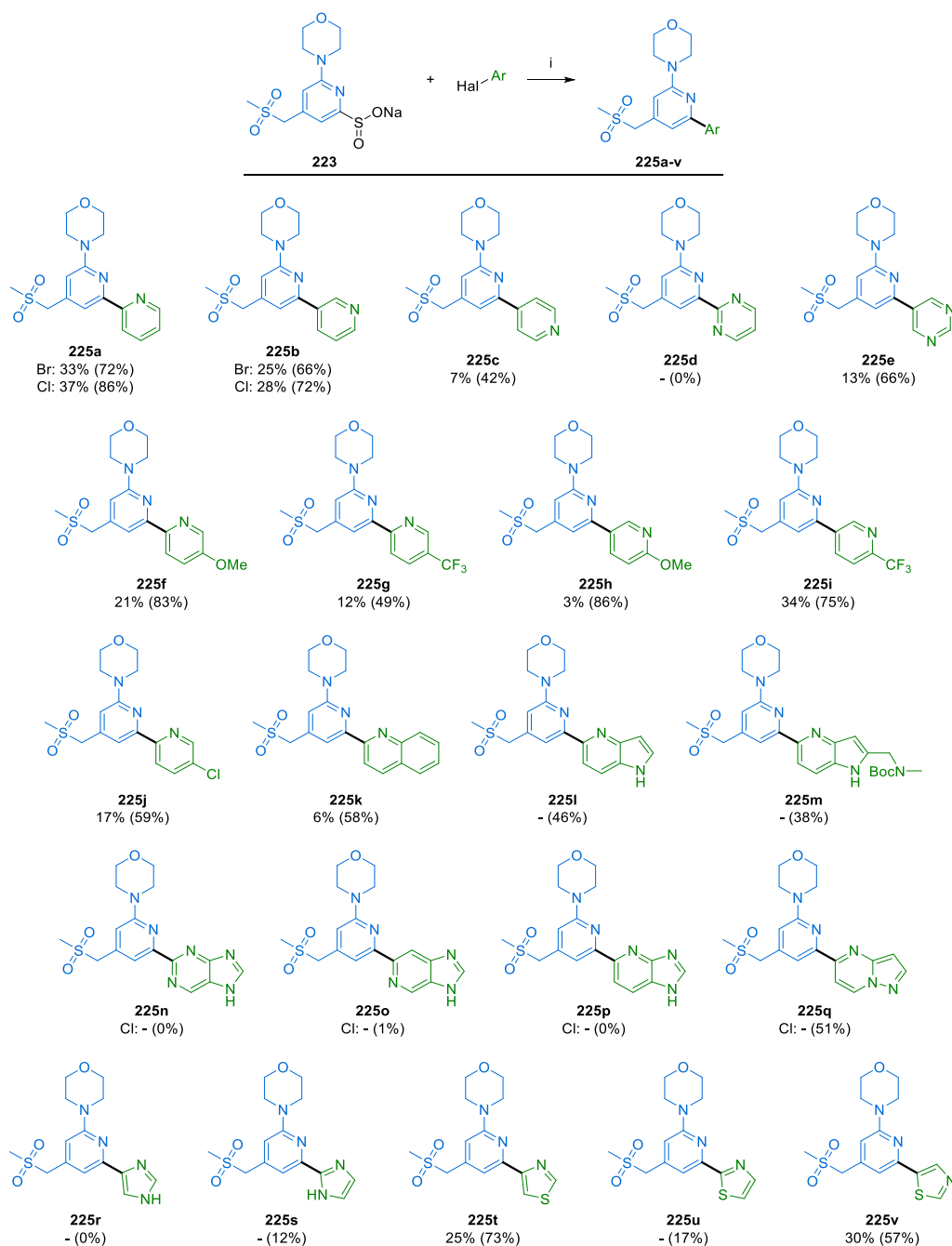
A wide variety of compounds were synthesised, in moderate to very good conversion (**Scheme 49**). It was satisfying that low conversion to homocoupled by-product **226** was obtained in all reactions. Where poor conversion to the desired product was observed, unreacted starting materials were often present in the reaction mixture.

A range of 6-membered heteroaryl halides was coupled to give bipyridyl and pyridinyl-pyrimidine compounds **225a-j**. Bromo- and chloro-pyridines gave comparable conversions and yields (**225a** and **225b**) and 2,2-, 2,3- and 2,4-bipyridyl compounds were synthesised (**225a-c**). One pyrimidine substrate was tolerated (5-bromopyridine), giving modest conversion but a poor isolated yield of product **225e**. The other pyrimidine isomer (2-bromopyrimidine) gave no conversion to the desired product (**225d**). Electron withdrawing and electron donating substituents were tolerated (**225f-i**), giving fair to very good conversion, but again poor isolated yields were obtained. In addition, 2-bromo-5-chloropyridine was also tolerated, giving compound **225j**, which provided a site for further functionalisation by, for example, Suzuki cross-coupling or Buchwald reactions.

Of the 5-membered monocyclic heteroaryl halides investigated, only three gave any conversion to the desired product, and only two were isolated, both in relatively low yield (**225t** and **225v**). Little or no conversion to the desired product was seen when heteroaryl halides with heteroatoms either side of the halide were used (**225d**, **225n**, **225s** and **225u**). Notably, no compounds like these with three heteroatoms around the newly formed bond were synthesised in the previous papers describing this desulfonative reaction.^{151,194,209}

^b Low isolated yields compared to the LCMS conversions were proposed to be as a result of a combination of factors including loss of material incurred during transfer between vessels, the standardised work-up procedure (filtration through a C₁₈ silica column) and the use of automated reverse phase purification.

While the 6-membered monocyclic heteroaryl halides were generally tolerated, bicyclic heteroaryl halides proved more challenging to couple. Quinoline-containing compound **225k** was formed in modest conversion, but isolated in poor yield. Three other bicyclic compounds were formed in fair conversion (**225l**, **225m** and **225q**); however, none of the desired compounds were successfully isolated. Compounds structurally similar to **225l** and **225m** had been synthesised in discrete reactions previously in our laboratories. For example, compound **179** was isolated in an improved yield under similar reaction conditions (Section 3.9.3). This suggested that the potential scope of this reaction was better exemplified by the conversion than the isolated yield.



Scheme 49: Demonstrating the scope of the desulfonative cross-coupling reaction, using a functionalised pyridine sulfinate starting material and carried out as an array. Isolated yield from reverse phase purification shown, with LCMS conversion in parentheses. Hal = Br unless specified.

Reagents and Conditions: i) **223** (1.0 equiv.), heteroaryl halide (1.0 equiv.), K_2CO_3 (1.5 equiv.), $Pd(OAc)_2$ (10 mol%), PCy_3 (20 mol%), TAA, 150 °C, 20.0 h. Synthesis by H. Davies.

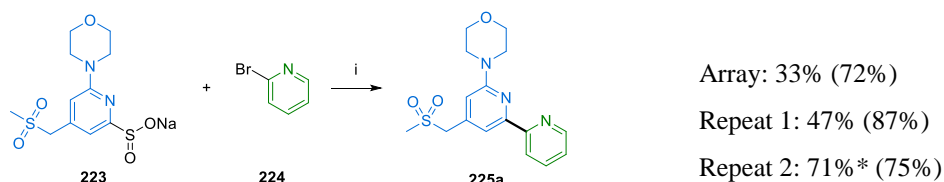
The array demonstrated the scope of the desulfonative cross-coupling reaction, with several compounds synthesised in modest to good conversion. Unfortunately, a good conversion did not lead to a good isolated yield. To mitigate some of the factors in the

array suggested to lead to the low isolated yield,^c several reactions were repeated individually, with the aim of confirming that a good conversion could give an acceptable isolated yield.

First, the reaction to form **225a** using 2-bromopyridine **224** was repeated (**Scheme 50**). Pleasingly, a conversion of 87% was observed after 19 hours. The reaction mixture was then filtered through a C₁₈ silica column (to remove the palladium), giving a residue suggested by LCMS to be 99% pure compound **225a**. This material was loaded directly onto a silica gel column and purified by normal phase flash chromatography, giving **225a** in a 47% isolated yield. While this was an improvement compared to the 33% obtained in the array, it did not demonstrate that the reaction mixture conversion could translate into an isolated yield. It was suggested that the low isolated yield may be due to the low solubility of the compound, hindering the purification.

To obtain a yield for the reaction, regardless of any purification issues, quantitative NMR was used, employing 1,3,5-trimethoxybenzene as an internal standard (**Appendix C**, Section 7.3). A third reaction to form **225a** was carried out. This reaction used the second batch of pyridine sulfinat **223** (75% w/w purity), and this was accounted for in the stoichiometry of the reaction. After 21 hours, a conversion of 75% was observed by LCMS. This reaction mixture was filtered and subjected to an aqueous work-up to give material suggested by LCMS to contain 93% desired product. Quantitative NMR was carried out to ascertain the purity more accurately. This suggested that the material was 71% pure, and enabled a yield, adjusted for the purity, of 71% to be obtained. While using quantitative NMR was not as good as obtaining an isolated yield, it was thought to be appropriate to confirm the conversion seen in the reaction mixture and give an approximate yield for the reactions.

^c Low isolated yields compared to the LCMS conversions were proposed to be as a result of a combination of factors including loss of material incurred during transfer between vessels, the standardised work-up procedure (filtration through a C₁₈ silica column) and the use of automated reverse phase purification.

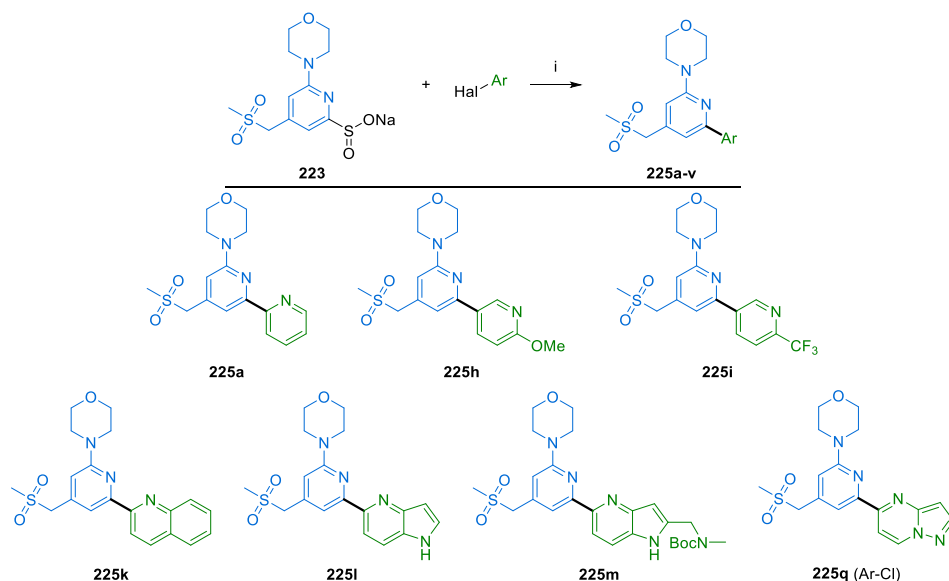


Scheme 50: Repeating the reaction with 2-bromopyridine (**244**) to compare the yields and conversions from three different methods. Isolated yield shown, with LCMS conversion in parentheses. *Yield calculated using the purity obtained from quantitative NMR. *Reagents and Conditions:* i) **223** (1.0 equiv.), heteroaryl halide (1.0 equiv.), K₂CO₃ (1.5 equiv.), Pd(OAc)₂ (10 mol%), PCy₃ (20 mol%), TAA, 150 °C, 20.0-22.0 h. Synthesis by H. Davies.

A selection of reactions was repeated. The calculated yields were representative of the conversion in the reaction mixture (**Table 26**). Additionally, comparable conversion was observed in the reaction mixtures in both the array and the repeated reactions. Where reduced conversion to the desired product was observed, the reaction profiles typically contained several unidentified impurities. In all reaction mixtures, conversion to homocoupled by-product (**226**) was less than 10%.

Substituted bromopyridines gave products **225a**, **225h** and **225i** in good conversion and comparable yield (**Entries 1-3, Table 26**). In these reactions, very little or none of the starting materials were observed in the reaction mixture. Employing 2-bromoquinoline, product **225k** was obtained in modest conversion and comparable yield, an improvement on the 6% isolated yield in the array experiment (**Entry 4**). Again, the 5,6-bicyclic heteroaryl halides gave reduced conversion and lower yields of products **225l**, **225m** and **225q** (**Entries 5-7**). In the reactions to form products **225l** and **225m** (**Entries 5** and **6**), unreacted starting materials were observed after 21 hours of reaction; further heating gave no increased conversion to the desired product and unreacted starting materials remained. These results differ significantly from previous reactions using these heteroaryl bromides (for example, similar experiments carried out in Section 3.9 and 3.10). This was proposed to be due to the change in solvent from 1,4-dioxane (used in Sections 3.9 and 3.10) to TAA. Again, poor conversion and yield of product **225q** was seen, alongside several unidentified by-products. Any remaining unreacted sulfinate starting material **223** in the mixtures after filtration was largely removed in the aqueous work-up. Therefore the impurities in the isolated material were

homocoupled by-product (**226**), unreacted heteroaryl halide or unidentified by-products.



Entry	Product	Array experiments		Repeated experiments			
		Conversion (%)	Yield (%)	Conversion (%)	LCMS purity (%) ^a	NMR purity (%) ^b	Yield (%) ^b
1	225a	72	33	75	93	71	71
2	225h	86	3	81	89	76	77
3	225i	75	34	82	93	72	68
4	225k	58	6	52	85	55	43
5 ^c	225l	46	0	27	40	33	23
6 ^c	225m	38	0	34	46	28	29
7	225q	51	0	39	75	20	11

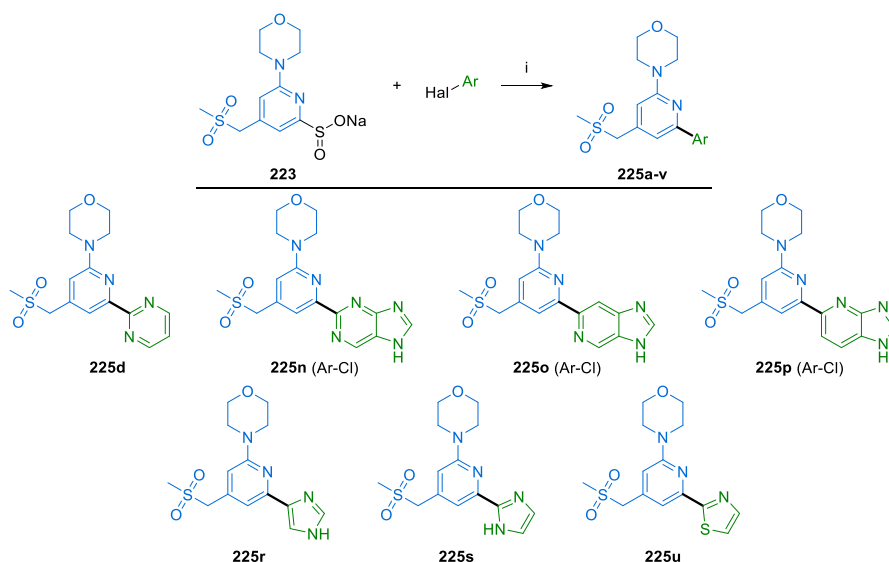
Table 26: Comparing the conversion and yield from the array experiments with the conversion and yield (corrected for purity) from individual repeated reactions. ^aLCMS purity after filtration and work-up. ^bQuantitative NMR using 1,3,5-trimethoxybenzene as an internal standard. ^cReaction mixture heated for 50 h. Hal = Br unless specified. *Reagents and Conditions:* i) **223** (75-95% purity, 1.0 equiv.), heteroaryl halide (1.0 equiv.), K₂CO₃ (1.5 equiv.), Pd(OAc)₂ (10 mol%), PCy₃ (20 mol%), TAA, 150 °C, 22.0 h. Synthesis by H. Davies.

2-bromopyrimidine gave poor conversion to product **225d**. In the array experiment to couple 2-bromopyrimidine and sulfinic acid **223**, unreacted sulfinic acid was the major component of the reaction mixture. Employing a P(^tBu)₂Me.HBF₄ ligand in TAA (**Entry 1, Table 27**), some conversion to the desired product was observed and repeating the reaction in 1,4-dioxane (**Entry 2**) did not improve the conversion. No

remaining starting materials were observed, only the homocoupled by-product **226** and an unidentified impurity.

Reaction with 2-chloro-7*H*-purine to form compound **225n** in TAA (**Entry 3**) gave no conversion to the desired product and both unreacted sulfinate starting material and heteroaryl halide were observed. However, in 1,4-dioxane (**Entry 4**) some conversion to desired product **225n** was seen in the reaction mixture (9% conversion by LCMS), in addition to increased conversion to homocoupled by-product **226**. After the work-up, **226** was the major identifiable component of the mixture. Reactions with 6-chloro-3*H*-imidazo[4,5-*c*]pyridine and 5-chloro-1*H*-imidazo[4,5-*b*]pyridine in TAA gave no conversion to products **225o** and **225p**, respectively, and large amounts of unreacted starting materials remained (**Entries 5** and **7**). Using 1,4-dioxane, some conversion to the desired products was obtained (**Entries 6** and **8**). However, increased conversion to homocoupled by-product **226** was also seen. While the yields of **225o** and **225p** were poor, these experiments suggested that changing the ligand may give increased conversion to product in some of the more challenging reactions.

With both bromoimidazoles and 2-bromothiazole none of the desired products **225r**, **225s** and **225u** were isolated from the array experiments (**Entries 9-11**). However, both 2-bromo-1*H*-imidazole and 2-bromothiazole gave some conversion to the desired products (**225s** and **225u**) when the reactions were repeated using the P(*t*Bu)₂Me.HBF₄ ligand in TAA and product **225u** was isolated with a quantitative NMR yield of 20%.



Entry	Product	Array experiments		Repeated experiments			
		Conversion (%)	Yield (%)	Conversion (%)	LCMS purity (%) ^a	NMR purity (%) ^b	Yield (%) ^b
1 ^c	225d	0	-	25	0	-	-
2 ^d	225d			9	12	-	-
3 ^c	225n	0	-	0	-	-	-
4 ^d	225n			9	-	-	-
5 ^c	225o	1	-	0	-	-	-
6 ^d	225o			16	34	20	6
7 ^c	225p	0	-	0	-	-	-
8 ^d	225p			54	37	28	8
9 ^c	225r	0	-	0	-	-	-
10 ^c	225s	12	-	8	40	6	1
11 ^c	225u	17	-	40	66	42	20

Table 27: Comparing the conversion and yield from the array experiments with the conversion and yield (corrected for purity) from individual repeated reactions. ^aLCMS purity after filtration and work-up. ^bQuantitative NMR using 1,3,5-trimethoxybenzene as an internal standard. Hal = Br unless specified. *Reagents and Conditions:* i) **223** (75-95% purity, 1.0 equiv.), heteroaryl halide (1.0 equiv.), K₂CO₃ (1.5 equiv.), Pd(OAc)₂ (10 mol%), P(^tBu)₂Me.HBF₄ (20 mol%), TAA or 1,4-dioxane, 150 °C, 22.0-23.0 h. ^cReaction carried out with P(^tBu)₂Me.HBF₄ and TAA. ^dReaction carried out with P(^tBu)₂Me.HBF₄ and 1,4-dioxane. Synthesis by H. Davies.

Unprotected, nitrogen-rich heteroaromatics are known to be challenging coupling partners in standard palladium-catalysed cross-coupling reactions.²¹² Indeed, Buchwald and co-workers investigated the reasons for the lack of reactivity of

substrates such as imidazoles, pyrazoles and azaindoles in Suzuki reactions.²¹² They found that the more acidic the heterocycle, the slower the rate of reaction.²¹² The authors proposed that if the heterocycles exist largely in their deprotonated forms under the basic Suzuki reaction conditions, the formation of *N*-azolyl palladium complexes may lead to the reduced reactivity of more acidic substrates.²¹²

A similar reactivity trend was observed here. Similarly it was suggested that under the basic desulfinative cross-coupling reaction conditions, the acidic heterocycles used here may also be deprotonated. Imidazoles, pyrazoles, azaindoles and purines all have an acidic N-H group. Plotting the calculated pK_a of the heteroaryl halide against the conversion observed in the array experiment demonstrated a trend: the more acidic heterocycles gave lower conversion to desired product (**Figure 48**). This was not proposed to be the only reason behind the poor reactivity of these compounds as it did not explain the low reactivity of 2-bromothiazole and 2-bromopyrimidine.

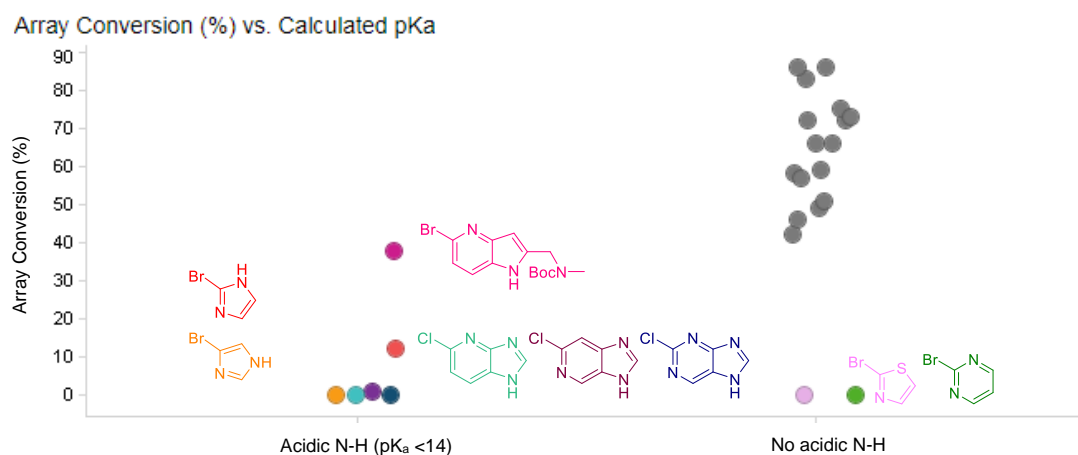
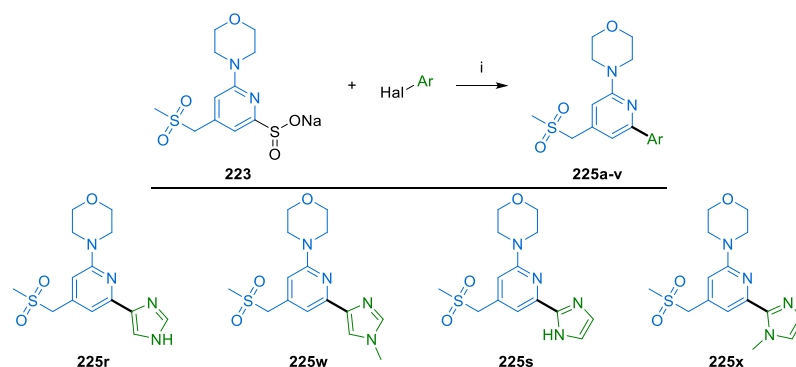


Figure 48: Demonstrating the correlation between calculated pK_a of the heteroaryl halide and conversion (%) observed in the array experiment. Coloured according to aryl halide, grey = all other aryl halides.

To probe the effect of the acidic N-H, further experiments were conducted (**Table 28**). First, methylated versions of both imidazoles were investigated. These reactions were carried out using the original conditions of the tricyclohexylphosphine ligand in TAA. The conversion achieved using the methylated imidazoles (2- and 4-bromo-1-methyl-1*H*-imidazole, **Entries 2** and **4**, to synthesise compounds **225w** and **225x**) was compared to that achieved with 2- and 4-bromo-1*H*-imidazole in the array experiment (**Entries 1** and **3**). This suggested that removing the free N-H did achieve increased

conversion. However, the quantitative NMR yield was again poor. With both 2- and 4-bromo-1-methyl-1*H*-imidazole, sulfinate starting material **223** was the major product observed by LCMS in the reaction mixture and after filtration. This was again removed in the aqueous work-up and homocoupled by-product **266** was the major impurity observed subsequently.



Entry	Product	Array experiments		Repeated experiments			
		Conversion (%)	Yield (%)	Conversion (%)	LCMS purity (%) ^a	NMR purity (%) ^b	Yield (%) ^b
1 ^c	225r	0	-				
2 ^d	225w	-	-	19	29	12	7
3 ^c	225s	0	-				
4 ^d	225x	-	-	57	69	22	11

Table 28: Comparing the conversion and yield from the array experiments with the conversion and yield (corrected for purity) from individual repeated reactions, using modified imidazole substrates, without any free-NH groups. ^aLCMS purity after filtration and work-up. ^bQuantitative NMR using 1,3,5-trimethoxybenzene as an internal standard. Hal = Br unless specified. *Reagents and Conditions:* i) **223** (75-95% purity, 1.0 equiv.), heteroaryl halide (1.0 equiv.), K₂CO₃ (1.5 equiv.), Pd(OAc)₂ (10 mol%), ligand (20 mol%), TAA, 150 °C, 20.0-23.0 h. ^cAs above with P(^tBu)₂Me.HBF₄. ^dAs above with PCy₃. Synthesis by H. Davies.

4.6 Further investigation of the reaction

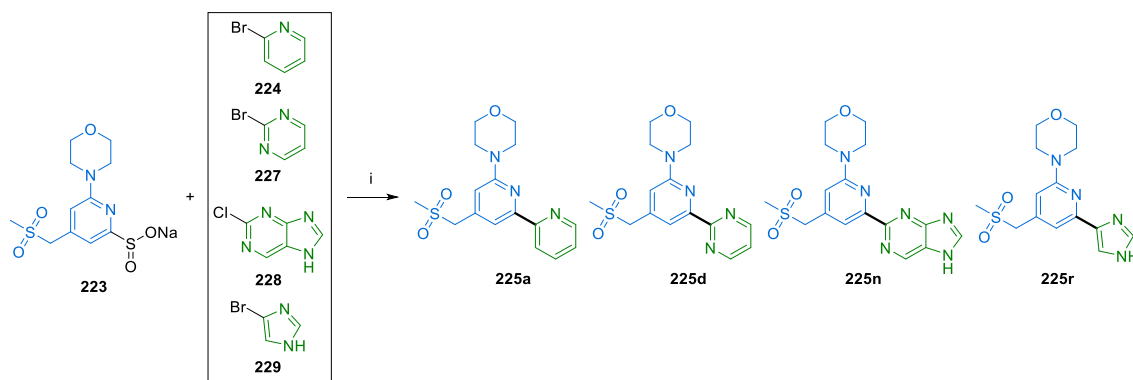
One of the reasons for the failure of palladium-catalysed reactions involving nitrogen-rich heterocycles is the ability of these substrates to form complexes with palladium.^{137,139} Indeed, substituted imidazoles, benzimidazoles and thiazoles can be used as ligands in palladium-catalysed reactions.²¹³⁻²¹⁶ Additionally, 2,2-bipyridyl compounds are known ligands for palladium, forming strong metal chelates.²¹³ This

was proposed to be one possible reason for the reduced conversion to desired product observed in reactions with similar heteroaryl halides.

To investigate whether the heteroaryl halides were forming complexes with the palladium catalyst and preventing the cross-coupling, reactions using stoichiometric palladium were conducted with three of the least reactive substrates – pyrimidine **227**, purine **228** and imidazole **229** (**Table 29**). The same experiment was also conducted with 2-bromopyridine **224** as a control. Furthermore, an experiment was conducted in which 4-bromo-1*H*-imidazole **229**, an unreactive substrate, was added to a reaction that was known to proceed well. If 4-bromo-1*H*-imidazole **229** was forming a non-catalytic complex with the palladium, addition of this imidazole to the reaction to form **225a**, should reduce the catalytic activity and therefore give reduced conversion to the desired product. The reaction of 2-bromopyridine with sulfinate **223** under standard conditions (Pd(OAc)₂ (10 mol%), PCy₃ (20 mol%)) was included for comparison (**Entry 6**).

Notably, in the control experiment with 2-bromopyridine, using stoichiometric palladium appeared to give a decreased conversion to **225a** compared to using catalytic palladium (**Entry 1** stoichiometric palladium compared to **Entry 6** catalytic palladium). No conversion to compounds **225d**, **225n** and **225r** was observed by LCMS in the array reactions. Using stoichiometric palladium gave some conversion to both **225d** and **225r** (**Entries 2** and **4**). Unfortunately, again no conversion to **225n** was observed (**Entry 3**). In all reactions with stoichiometric palladium, higher conversion to homocoupled by-product **226** than desired product was observed.

Interestingly, adding 0.2 equivalents of 4-bromo-1*H*-imidazole (**229**), led to reduced conversion to desired product **225a** and 2-bromopyridine (**224**) was the major component of the reaction mixture (**Entry 5** with the additive compared to **Entry 6** without additive). This suggested that addition of the 4-bromo-1*H*-imidazole (**229**) suppressed the formation of product. It was proposed that this could be due to the imidazole forming a non-catalytic species with the palladium, reducing the amount of active catalyst available to complete the desired reaction.



Entry	Product	Conversion (%)	Conversion to homocoupled 226 (%)	LCMS purity (%) ^a
1	225a	23	26	16
2	225d	18	30	21
3	225n	0	34	-
4	225r	7	26	-
5 ^b	225a	14	4	40
6 ^c	225a	75	9	93

Table 29: Examining the effect of using stoichiometric palladium on the outcome of the cross-coupling reaction with two of the most challenging substrates and using 2-bromopyridine (Entries 1-4). Entry 5 investigated the effect on the conversion on the addition of 0.2 equivalents of bromoimidazole 229. Entry 6 was included for comparison. ^aLCMS purity after filtration and work-up. Hal = Br unless specified. *Reagents and Conditions:* i) 223 (75% purity, 1.0 equiv.), heteroaryl halide (224, 227-229, 1.0 equiv.), K₂CO₃ (1.5 equiv.), Pd(OAc)₂ (1.0 equiv.), PCy₃ (1.0 equiv.), TAA, 150 °C, 22.0 h. ^bAs above with Pd(OAc)₂ (10 mol%), PCy₃ (20 mol%) and addition of 4-bromo-1H-imidazole (229, 0.2 equiv.). ^cAs above with Pd(OAc)₂ (10 mol%), PCy₃ (20 mol%), 21.0 h. Reactions by H. Davies.

4.7 Application of a high-throughput screening platform to optimise the desulfinate cross coupling reaction

It became apparent that the initial conditions used in this Chapter (K₂CO₃, Pd(OAc)₂ and PCy₃) were not suitable for use with every heteroaryl halide substrate of interest. To efficiently investigate different catalysts, bases and solvents, a high-throughput screen (HTS) was carried out. No HTS plate for screening the desulfinate cross-coupling existed, so a plate was developed. This plate was subsequently used to find desulfinate cross-coupling conditions for some of the more challenging heteroaryl halide substrates.

A desulfinate cross-coupling plate was designed.^d Six palladium pre-catalysts were chosen as they had shown promising results in the original screens done by the Willis group.^{151,194} Five G3 palladium catalysts (DTBPF, DPPF, DPPE, P(^tBu)₂Me and PCy₃) and one G4 (P(^tBu)₃ chosen because the G4 version is more stable) were used. Two bases (K₂CO₃ and Cs₂CO₃) and two solvents (TAA and 1,4-dioxane) were also used, giving a 24-well plate format (**Figure 49**).

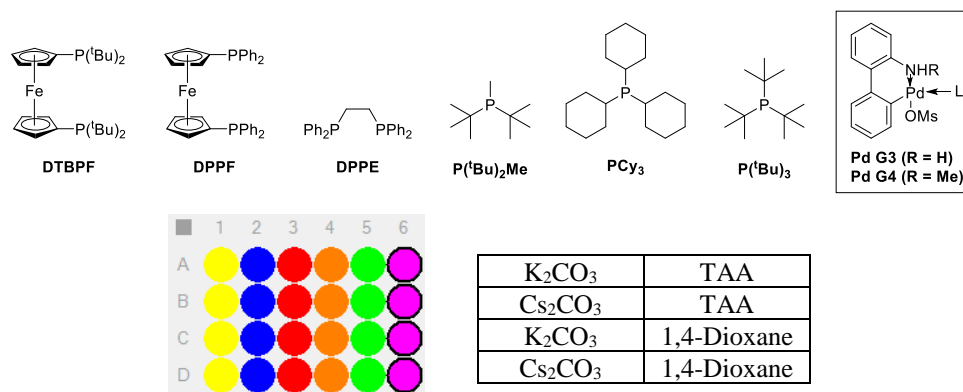


Figure 49: Demonstrating the plate format used in the HTS. Six palladium pre-catalysts were used in columns 1-6 (all were G3 (R = H) except P(^tBu)₃ which was G4 (R = Me), the same pre-catalyst was used in each of rows A-D in each column). TAA was used in rows A and B and 1,4-dioxane in rows C and D. K₂CO₃ was used in rows A and C and Cs₂CO₃ in rows B and D.

To validate the plate design, an initial screen using the standard reaction of pyridine sulfinate **223** and 2-bromoyridine **224**, in a 1:1 ratio was carried out. For this screen, a third batch of the sulfinate was used, which was 90% purity. The reaction mixtures were prepared in a glove box in a plate format and the plate sealed under the inert atmosphere before heating at 150 °C for 21 hours, after which the conversion to product **225a** by LCMS was recorded and the results analysed to give a conversion heat map (based on the absorbance of the product peak in the LCMS). The yellow areas demonstrated the reactions with the highest conversion (the maximum). The blue areas demonstrated the reactions with the lowest conversion (the minimum). The green areas were the average conversion (the maximum conversion observed minus the lowest conversion). In all reactions, some conversion to product **225a** was observed (**Figure 50**). Four reactions showed the highest conversion: reactions A6 (TAA, P(^tBu)₃ Pd G4, K₂CO₃), B2 (TAA, DPPF Pd G3, Cs₂CO₃), C2 (1,4-dioxane,

^d In collaboration with D. Battersby, DAPC, GSK.

DPPF Pd G3, K₂CO₃) and D4 (1,4-dioxane, P(^tBu)₂Me Pd G3, Cs₂CO₃). The spread of results highlighted the subtle solvent, base and catalyst dependence of this desulfinate cross-coupling reaction.

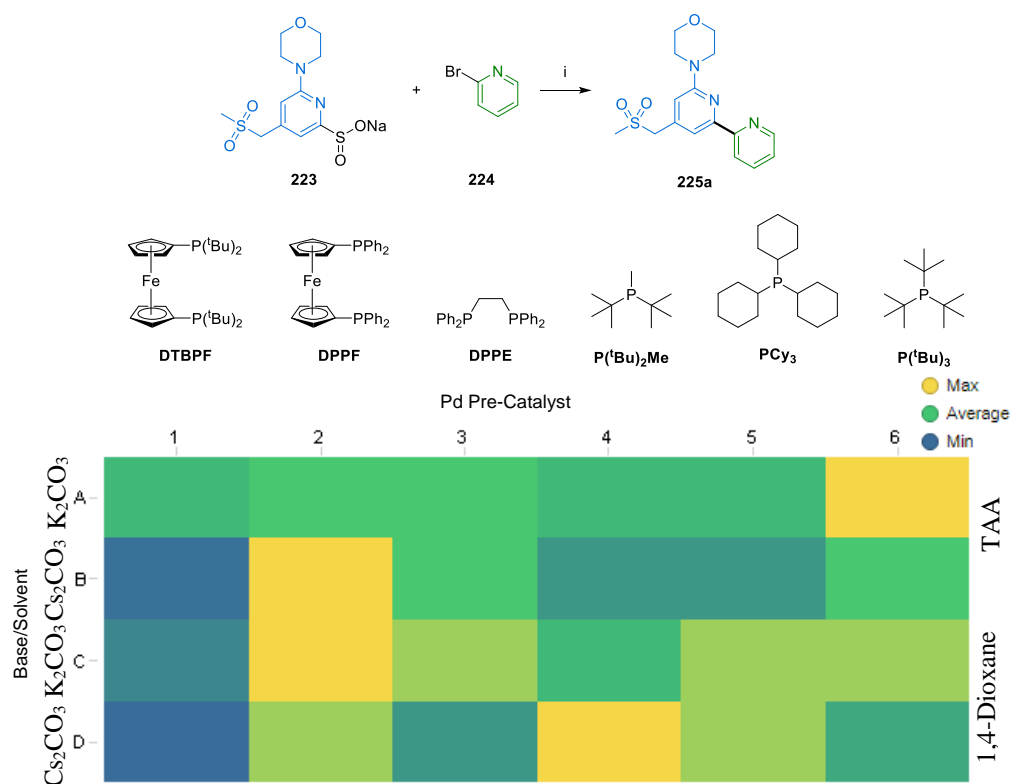


Figure 50: Heat map demonstrating the relative LCMS conversion to product **225a** in the HTS screen.

Yellow areas = highest conversion, blue areas = lowest conversion. *Reagents and Conditions:* i) **223** (90% purity, 1.0 equiv.), 2-bromopyridine **224** (1.0 equiv.), base (1.5 equiv.), Pd pre-catalyst (10 mol%), solvent, 150 °C, 21.0 h. HTS by H. Davies.

After these initial successful results, the same plate format was used to screen conditions for some of the more challenging heteroaryl halides, 2-bromopyrimidine (**227**) and 2-bromo-1*H*-imidazole (**230**). Previously, these heteroaryl halides had demonstrated poor conversion to products **225d** and **225s** (a maximum conversion observed of 25% (**Table 27**) and 12% (**Scheme 50**) respectively).

The HTS with 2-bromopyrimidine **227** to form product **225d** (**Figure 51**) gave one hit: reaction C1 (1,4-dioxane, DTBPF Pd G3, K₂CO₃). Two reactions did not demonstrate any conversion to product **225d**: D3 (1,4-dioxane, DPPE Pd G3, Cs₂CO₃) and D6 (1,4-dioxane, P(^tBu)₃ Pd G4, Cs₂CO₃).

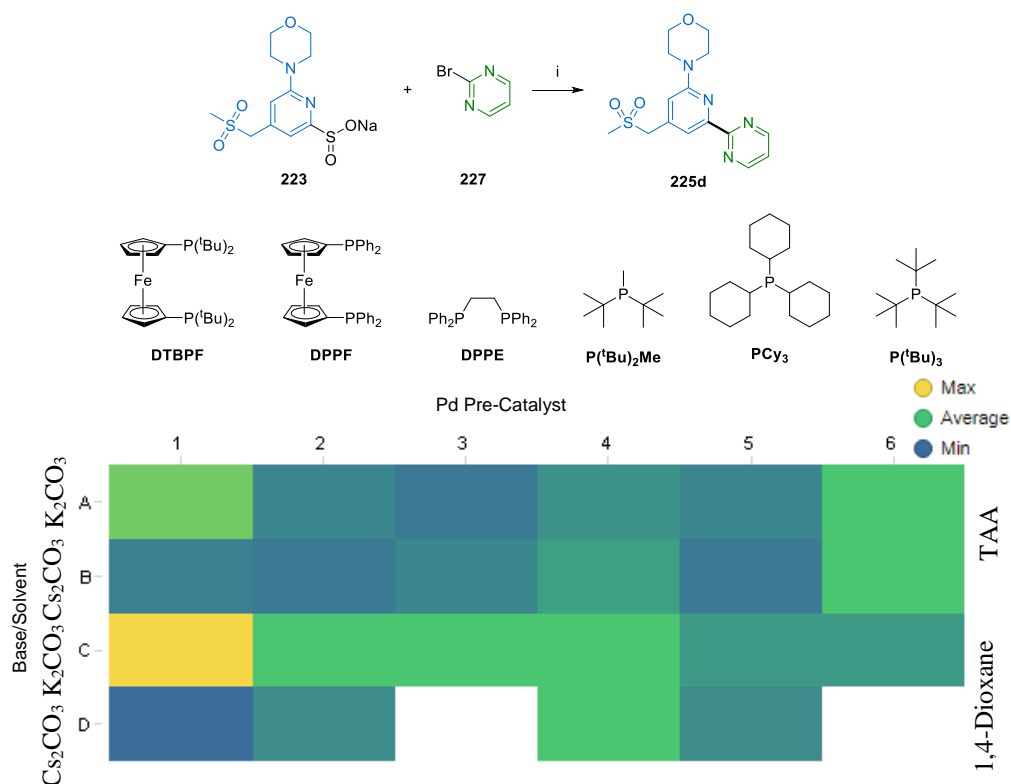


Figure 51: Heat map demonstrating the relative LCMS conversion to product **225d** in the HTS screen. Yellow areas = highest conversion, blue areas = lowest conversion. *Reagents and Conditions:* i) **223** (90% purity, 1.0 equiv.), 2-bromopyrimidine **227** (1.0 equiv.), base (1.5 equiv.), Pd pre-catalyst (10 mol%), solvent, 150 °C, 21.0 h. HTS by H. Davies.

Pleasingly, the HTS with 2-bromo-1*H*-imidazole **230** to form product **225s** (**Figure 52**) gave five hits: reactions D1-5 (1,4-dioxane, Cs₂CO₃, DTBPF, DPPF, DPPE, P(*t*Bu)₂Me and PCy₃, all Pd G3 pre-catalysts). Two reactions did not demonstrate any conversion to product **225s**: A1 (TAA, P(*t*Bu)₃ Pd G4, K₂CO₃) and C1 (DTBPF, 1,4-dioxane and K₂CO₃).

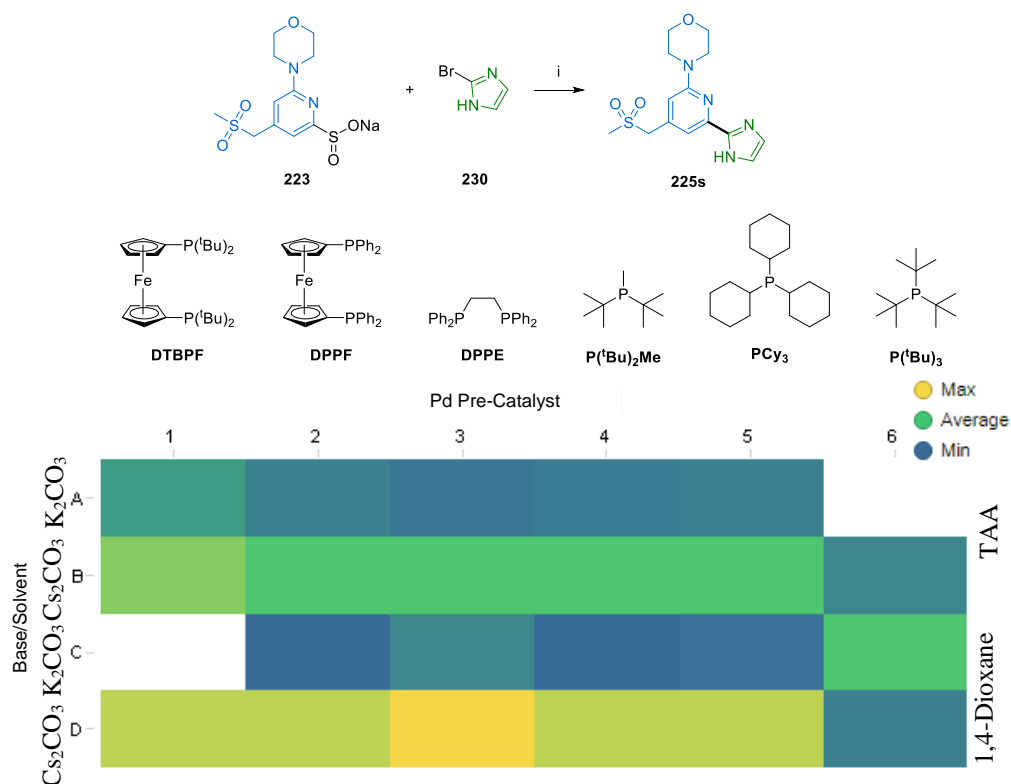


Figure 52: Heat map demonstrating the relative LCMS conversion to product **225s** in the HTS screen. Yellow areas = highest conversion, blue areas = lowest conversion. *Reagents and Conditions:* i) **223** (90% purity, 1.0 equiv.), 2-bromo-1H-imidazole **230** (1.0 equiv.), base (1.5 equiv.), Pd pre-catalyst (10 mol%), solvent, 150 °C, 21.0 h. HTS by H. Davies.

In all of the HTS, the main by-products observed were suggested to relate to the palladium pre-catalyst or the oxidised ligand and only low conversion to the homocoupled by-product **226** was observed.

These results suggested that this plate format was suitable for performing desulfinitive cross-coupling HTS reactions. Good results were found for both the standard 2-bromopyridine substrate (**224**), as well as more challenging heteroaryl halides that had previously given very low conversion to the desired products (2-bromopyrimidine (**227**) and 2-bromo-1H-imidazole (**230**)).

4.8 Summary of Chapter III

This Chapter demonstrated the scope of the desulfinitive cross-coupling reaction. Initial optimisation work considering temperatures and solvents suggested that TAA could be used as a solvent. Subsequently, a range of biologically relevant heteroaryl

halides were formed in acceptable conversion and isolated in moderate yields from an array experiment. Subsequent reactions were carried out using quantitative NMR to obtain a yield. Pleasingly, the calculated NMR yields were representative of the conversion in the reaction mixture.

Several of the heteroaryl halides chosen were more challenging to couple, giving no or low conversion to the desired products. A series of experiments suggested that this could be because the heteroaryl halides used may be good ligands for palladium. Furthermore, it was apparent that the standard conditions used – K_2CO_3 , $Pd(OAc)_2$ and PCy_3 – were not suitable for use with every heteroaryl halide substrate. To efficiently investigate different catalysts, bases and solvents, a high-throughput screening plate for the desulfonative cross-coupling was designed. This plate was used to find suitable conditions to couple two of the most challenging heteroaryl halides. It was proposed that this HTS plate could be used in future experiments to identify optimal coupling conditions for further challenging reactions.

Conclusions and Future Work

5. Conclusions and future work

IPF is a progressive and fatal lung disease, characterised by excessive deposition of collagen. The two approved treatments (nintedanib and pirfenidone) slow disease progression, with lung transplants currently providing the only potential cure for patients. Both nintedanib and pirfenidone have undesirable side effects and there is often a long wait to receive a lung transplant. Therefore there is an unmet need for a treatment that will halt the progression of the disease and, ideally, reverse the deposition of collagen and restore normal lung function. Inhibition of mTOR kinase has been demonstrated to reduce collagen deposition *in vivo*. An inhaled mTOR kinase inhibitor was proposed as a suitable treatment for patients with IPF, as topical delivery should reduce systemic side effects, resulting in a superior treatment for patients.

This Thesis describes the discovery and exploration of a novel series of mTOR kinase inhibitors: the pyridyl sulfone compounds. Several compounds were made with the aim of achieving the desired affinity, efficacy and physicochemical properties. A key *in vivo* study demonstrated that compounds in this series did not meet the target property profile. However, an alternative series of compounds was simultaneously identified: the carbon-linked pyridine sulfones. While compounds in this series met or exceeded the target property profile, the synthesis was more challenging. Three main problematic steps were identified and investigated. A more facile synthesis of the chloroazaindole moiety and a suitable protecting group strategy were established. Some of the problems in the S_NAr reaction between (*S*)-3-ethylmorpholine and a chloropyridine were solved. Initially, a solvent swap from DMSO to sulfolane enabled the reaction to be scaled-up. Further work demonstrated that, remarkably, a bromopyridine and alternative base could be used. Finally, the difficult bipyridyl cross-coupling reaction was enabled by employing a pyridine sulfinate as the nucleophile in a palladium-catalysed desulfinate cross-coupling reaction.

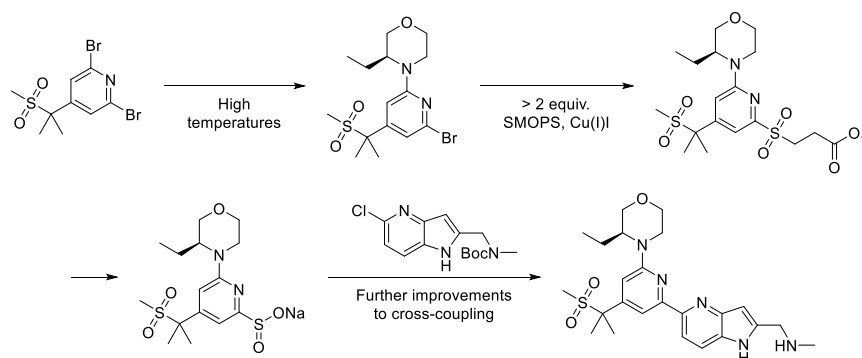
The scope of this desulfinate cross-coupling reaction was investigated, enabling the synthesis of a variety of biologically relevant bipyridyl compounds in an array format. Further work to facilitate the coupling of more challenging substrates led to the development of a HTS plate to screen a variety of bases, catalysts and solvents simultaneously. It is proposed that, due to the prevalence of bipyridyl compounds in

pharmaceuticals, this desulfinate reaction will find further applications in medicinal chemistry. With this screening plate, chemists will be able to rapidly assess a variety of conditions to achieve improved conversion. This represents a significant improvement in the capabilities to screen this reaction in our laboratories.

Research is ongoing in our laboratories to complete dose range finding and extended toxicity studies of a pre-candidate compound, structurally related to compound **153**, with the aim of declaring it a candidate compound and progressing it into clinical trials. If these studies are successful, the candidate compound will need to be synthesised on multi-gram scale in API campaigns. While the route developed in this Thesis is suggested to be appropriate for this, future work may be able to make further improvements (**Scheme 51**).

Both the S_NAr and cross-coupling reaction steps required high temperatures. One option considered here for the S_NAr , but not explored, was the use of flow chemistry. Carrying out this reaction in flow would enable high temperatures to be used more safely, as well as offering the advantages associated with continuous processing of material. For the desulfinate cross-coupling, the HTS plate format developed here may also enable the use of lower temperatures by identifying the optimal catalyst, base and solvent combination.

The method to form the sulfinate intermediate could also be improved. The number of equivalents of copper(I) iodide and SMOPS had been reduced from 3.0 to 1.3. However, a process employing catalytic copper(I) iodide in this Ullmann coupling would be preferable. This was not investigated here but should be considered in the future. Furthermore, the use of a more efficient sulfur dioxide source than SMOPS should be investigated. It was proposed that retrying some of the sulfur dioxide surrogates explored here with the bromopyridine would be a sensible place to start.



Scheme 51: Demonstrating areas for further improvements to the route.

While the scope of this Thesis was limited to the exploration of inhaled mTOR kinase inhibitors for the treatment of IPF, the PI3K-Akt-mTOR pathway (here referred to as the mTOR signalling pathway) is involved in numerous biological processes including cell growth proliferation and survival.⁵⁷ The understanding of the mTOR signalling pathway has increased rapidly in the last few years,⁵⁶ leading to the suggestion that there may be wide-ranging uses of small molecule mTOR kinase inhibitors. For example, mTOR inhibition has been demonstrated to extend life span and delay the onset of age-related diseases in mammals.⁵⁶ Additionally, mTOR kinase inhibitors are currently being investigated for the treatment of various cancers, often in combination with other chemotherapies.⁵⁷ This demonstrates the potential of mTOR kinase inhibitors to treat diseases other than IPF.

One of the main issues encountered when using mTOR kinase inhibitors in clinical trials is dose-limiting toxicity.⁵⁶ As discussed, the mTOR pathway has a critical function in many human tissues, therefore non-tissue selective inhibition can lead to off-target effects.⁵⁶ To our knowledge, the compounds contained in this Thesis represent the first example of inhaled inhibitors of mTOR kinase. These compounds demonstrated lung retention *in vivo*, suggesting that it is possible to selectively inhibit mTOR kinase in the lung. Inhibition of mTOR in the lung only has been demonstrated to avoid the systemic effects of mTOR inhibition. This could offer a substantial advantage over existing chemotherapies – known for their unpleasant side-effects – offering significant improvements to cancer patients' quality of life. It is therefore proposed that these mTOR kinase inhibitors could find application as treatments for lung cancer.

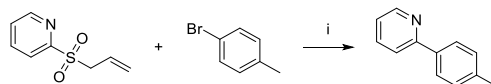
In our laboratories we have synthesised a variety of mTOR kinase inhibitors, with a wide variety of physicochemical properties. While an oral medicine was not targeted, within our series several compounds with the potential to be orally bioavailable were synthesised. These could be repurposed for other fibrotic diseases such as renal or liver fibrosis. Alternatively, these compounds may again offer potential anti-cancer treatments.

Another significant aspect of this work is that it highlights the importance of robust synthetic strategies in enabling drug discovery. Medicinal chemists can access a large amount of structural diversity relatively simply using well preceded methodology. However, one of the most commonly encountered features in pharmaceutical compounds – bipyridyl moieties – still remain challenging to synthesise. While these challenges can be overcome on a small scale, for example by using reliable but practically unpleasant Stille chemistry, on a large scale these challenges become more pronounced. This project was fortunate to benefit from recent publications that addressed the unmet need. This desulfinate cross-coupling enabled the multi-gram synthesis of a pre-candidate compound and was vital to facilitate the synthesis of a wide range of analogues. The use of this cross-coupling methodology has already been demonstrated in other medicinal chemistry projects within GSK.

While the Suzuki reaction is an industry favourite, forming boronic acids of heterocycles can be challenging and the cross-coupling does not always work well. Additionally, while previously thought to be non-toxic, and therefore ideal for use in the pharmaceutical industry, several boronic esters and acids have been shown to be mutagenic and pose a genotoxicity risk.^{217,218} This presents a problem when handling boronic esters and acids, as well as requiring strict regulation when using boronic esters and acids to form API.²¹⁷

Conversely, although forming the required sulfinates in the desulfinate cross-coupling reaction can be challenging, the sulfinates have no known toxicity. Additionally, the gaseous sulfur dioxide by-product is proposed to be recyclable.¹⁶⁷ To overcome difficulties in forming the sulfinates, the Willis group have recently reported an alternative strategy.²⁰⁹ Instead of forming the sulfinate using a sulfur dioxide surrogate and isolating it, this research enabled the use of an allylic sulfone directly in

the cross-coupling reaction (**Scheme 52**).²⁰⁹ This negates the need to form the sulfinate directly before the cross-coupling, as the allylic sulfone should be more stable to a variety of chemical transformations, meaning it can be installed earlier in the synthesis if desired.²⁰⁹ Additionally, this will also overcome any stability issues with the sulfonates. While the Willis group reported them to be stable,²⁰⁹ in our experience this was not always the case. This alternative strategy was not tried in our laboratories as part of this research but may be of interest in the future.



Scheme 52: Demonstrating the desulfinitive cross-coupling using allylic sulfones as the nucleophilic cross-coupling partner. i) Sulfone (1.5 equiv.), aryl halide (1.0 equiv.), Cs₂CO₃, Pd(OAc)₂ (5 mol%), P(^tBu)₂Me.HBF₄ (10 mol%), DMF, 130 °C, 18.0 h, 76%.²⁰⁹

The work described in Chapter II highlights the importance of beginning route development while still in the lead optimisation phase of drug discovery. Investing in synthetic strategy is far more efficient than ‘making do’ with a suboptimal route and pushing the problem down the line into process chemistry. The value of the mTOR kinase inhibitors described here was recognised and significant time and effort was invested in designing a more suitable and scalable route. Once this route was in place, it enabled the rapid synthesis of a variety of analogues, enabling exploration of SAR. While it was a risk to invest in route optimisation early, in this research this strategy resulted in significant time and cost savings. Having a scalable and well-planned route meant that the project team had access to enough material at all stages to enable key biological and safety studies to be carried out. Ultimately, this could mean that, if the pre-candidate compound described here does progress into clinical trials, IPF patients may get their life-changing medicines more quickly.

More generally, this work emphasises the importance of developing methodology to improve reactions that are not currently robust. This relies on publishing reactions that do not work, in addition to those that do. Partnerships between industry and academia offer an ideal solution. Industry can suggest transformations of interest that are currently problematic or unscalable and academic groups can apply their considerable knowledge and expertise to solve these synthetic challenges. Indeed, the desulfinitive

cross-coupling methodology was the result of such a partnership between the Willis group and Pfizer. This is just one example of the impact and importance of collaborations.

In conclusion, this Thesis demonstrates the potential of inhaled inhibitors of mTOR kinase as treatments for IPF and describes the development of a synthetic route to a pre-candidate compound. While this route is suitable for use in a large scale API campaign, future work should focus on further improvements, such as investigation of flow chemistry and investing in a catalytic synthesis of the key sulfinate intermediate. Excitingly, work is underway to progress a pre-candidate inhaled mTOR inhibitor through additional safety studies and potentially into clinical trials.

Experimental Section

6. Experimental

6.1 General experimental details

Unless otherwise stated:

Solvents and reagents. Magnetic stirrer bars were stirred vigorously using stirrer hot plates. The solvents used were anhydrous, except when water was added to the reaction as a solvent, in which case non-anhydrous solvents were used, unless otherwise stated. Solvents and reagents were purchased from commercial suppliers or obtained from GSK's internal compound storage or made by an external outsourcing company (GVK Biosciences) and used as received. Water used in reactions and work-ups was deionised Elga Purelab Chorus.

Reactions. Reactions were carried out in sealed vessels under a standard atmosphere of air at room temperature (assumed to be 21 °C) and glassware was not dried, unless otherwise stated. Reactions were monitored by thin layer chromatography (TLC) and/or liquid chromatography-mass spectroscopy (LCMS) and/or nuclear magnetic resonance (NMR) spectroscopy. Heating was conducted using hotplates with DrySyn adaptors, custom-made heating blocks, oil or sand baths. Microwave reactions were performed in a Biotage or an Anton Parr Multiwave Pro microwave reactor.

Chromatography. TLC was carried out using polyester-backed precoated silica plates (particle size 0.2 mm). Spots were visualised by ultraviolet (UV) light ($\lambda_{\text{max}} = 254$ nm or 365 nm). Flash column chromatography was carried out using the Teledyne ISCO CombiFlash® Rf+ apparatus with RediSep® silica cartridges or Biotage® SNAP KP-silica cartridges or Biotage® SNAP KP-NH-modified silica cartridges of various sizes. Fractions were collected by following UV trace ($\lambda_{\text{max}} = 254$ nm and 280 nm, or another appropriate wavelength).

Reverse-Phase Flash Column Chromatography. Reverse-Phase column chromatography was carried out using Teledyne ISCO CombiFlash® Rf+ apparatus and Biotage® SNAP KP-C₁₈ silica cartridges of various sizes.

Formic: Using a gradient elution with the mobile phases as (A) H₂O containing 0.1% volume/volume (v/v) formic acid and (B) acetonitrile containing 0.1% (v/v)

formic acid. Gradient conditions and flow-rate were variable depending on 2 min LCMS retention time of the desired product and the size of the column used.

High pH: Using a gradient elution with the mobile phases as (A) 10 mM aqueous ammonium hydrogen carbonate solution, adjusted to pH 10 with 0.88 M aqueous ammonia and (B) acetonitrile. Gradient conditions and flow were variable depending on 2 min LCMS retention time of the desired product and the size of the column used.

Reverse Phase Preparative High Performance Liquid Chromatography. Preparative (Prep.) HPLC was carried out on Grace Revalaris® Prep. apparatus.

High pH: Using Xbridge C₁₈ OBD™ (100 mm x 19 mm, 5 µm packing diameter, 32 mL/min flow rate), using a gradient elution at ambient temperature with the mobile phases as (A) H₂O containing 0.1% volume/volume (v/v) ammonium hydrogen carbonate and (B) acetonitrile.

Mass Directed Auto Preparation (MDAP). Mass-directed automatic purification was carried out using a Waters ZQ mass spectrometer using alternate-scan positive and negative electrospray ionisation and a summed UV wavelength of 210–350 nm. Three liquid phase methods were used:

Formic: Sunfire C₁₈ column (100 mm x 19 mm, 5 µm packing diameter, 20 mL/min flow rate) or Sunfire C₁₈ column (150 mm x 30 mm, 5 µm packing diameter, 40 mL/min flow rate), using a gradient elution at ambient temperature with the mobile phases as (A) H₂O containing 0.1% (v/v) formic acid and (B) acetonitrile containing 0.1% (v/v) formic acid.

High pH: Xbridge C₁₈ column (100 mm x 19 mm, 5 µm packing diameter, 20 mL/min flow rate) or Xbridge C₁₈ column (150 mm x 30 mm, 5 µm packing diameter, 40 mL/min flow rate), using a gradient elution at ambient temperature with the mobile phases as (A) 10 mM aqueous ammonium hydrogen carbonate solution, adjusted to pH 10 with 0.88 M aqueous ammonia and (B) acetonitrile.

Trifluoroacetic acid (TFA): Zorbax SB C₈ Column (30 x 150 mm, 3.5 µm packing diameter, 40 mL/min flow rate), using a gradient elution at ambient

temperature with the mobile phases as (A) 0.1% TFA in water and (B) 0.1% TFA in acetonitrile.

LCMS. Analysis was carried out on a Waters Acquity UPLC instrument equipped with a BEH column (ethylene bridged hybrid, 50 mm x 2.1 mm, 1.7 µm packing diameter) and Waters Micromass ZQ MS using alternate-scan positive and negative electrospray ionisation. Analytes were detected as a summed UV wavelength of 210-350 nm. Two liquid phase methods were used:

Formic: 40 °C, 1 mL/min flow rate, using a gradient elution with the mobile phases as (A) H₂O containing 0.1% volume/volume (v/v) formic acid and (B) acetonitrile containing 0.1% (v/v) formic acid. Gradient conditions were initially 1% B, increasing linearly to 97% B over 1.5 min, remaining at 97% B for 0.4 min then increasing to 100% B over 0.1 min.

High pH: 40 °C, 1 mL/min flow rate, using a gradient elution with the mobile phases as (A) 10 mM aqueous ammonium hydrogen carbonate solution, adjusted to pH 10 with 0.88 M aqueous ammonia and (B) acetonitrile. Gradient conditions were initially 1% B, increasing linearly to 97% B over 1.5 min, remaining at 97% B for 0.4 min then increasing to 100% B over 0.1 min.

High-Resolution Mass Spectrometry (HRMS). HRMS were recorded on one of two systems:

System A: Micromass Q-TOF Ultima hybrid quadrupole time-of-flight (Q-TOF) mass spectrometer, with analytes separated on an Agilent 1100 Liquid Chromatograph equipped with a Phenomenex Luna C₁₈ (2) reversed phase column (100 mm x 2.1 mm, 3 µm packing diameter). LC conditions were 0.5 mL/min flow rate, 35 °C, injection volume 2-5 µL, using a gradient elution with (A) H₂O containing 0.1% (v/v) formic acid and (B) acetonitrile containing 0.1% (v/v) formic acid. Gradient conditions were initially 5% B, increasing linearly to 100% B over 6.0 min, remaining at 100% B for 2.5 min then decreasing linearly to 5% B over 1.0 min followed by an equilibration period of 2.5 min prior to the next injection.

System B: Waters XEVO G2-XS Q-TOF mass spectrometer, with analytes separated on an Acquity UPLC CSH C₁₈ column (100 mm x 2.1 mm, 1.7 μm packing diameter). LC conditions were 0.8 mL/min flow rate, 50 °C, injection volume 0.2 μL, using a gradient elution with (A) H₂O containing 0.1% (v/v) formic acid and (B) acetonitrile containing 0.1% (v/v) formic acid. Gradient conditions were initially 3% B, increasing linearly to 100% B over 8.5 min, remaining at 100% B for 0.5 min then decreasing linearly to 3% B over 0.5 min followed by an equilibration period of 0.5 min prior to the next injection.

Mass to charge ratios (m/z) reported in Daltons.

NMR Spectroscopy. Proton (¹H), carbon (¹³C) and fluorine (¹⁹F) spectra were recorded in deuterated solvents at ambient temperature (unless otherwise stated) using standard pulse methods on any of the following spectrometers and signal frequencies: Bruker AV-400 (¹H = 400 MHz, ¹³C = 101 MHz, ¹⁹F = 376 MHz), Bruker AV-500 (¹H = 500 MHz, ¹³C = 126 MHz), Bruker AV-600 (¹H = 600 MHz, ¹³C = 150 MHz) or Bruker AV-700 (¹H = 700 MHz, ¹³C = 176 MHz). Chemical shifts (δ) are reported in ppm and are referenced to tetramethylsilane (TMS) or the following solvent peaks: Chloroform-*d* (¹H = 7.27 ppm, ¹³C = 77.0 ppm) or DMSO-*d*₆ (¹H = 2.50 ppm, ¹³C = 39.5 ppm). Peak assignments were made on the basis of chemical shifts, integrations, and coupling constants, using COSY, DEPT, HSQC and HMBC where appropriate. Coupling constants were quoted to the nearest 0.1 Hz and multiplicities described as singlet (s), doublet (d), triplet (t), quartet (q), quintet (quin), sextet (sxt), septet (sept), broad (br.) and multiplet (m). The number of carbon atoms represented by each peak in the ¹³C NMR was inferred by assigning the spectra.

Optical rotation. Optical rotation measurements were recorded on an Anton Parr MCP 150 Polarimeter using a sample cell with a 10 cm pathlength at the specified temperature and concentration. Specific rotations were calculated using **Equation 4**.

$$[\alpha]_{\lambda}^T = \frac{\alpha}{l \times c}$$

Equation 4: Calculating the specific rotation from the optical rotation. T = Temperature at which the measurement was taken (°C); λ = The wavelength (nm); α = The measured rotation in degrees (°); l = Pathlength (dm) and c = Concentration in g/100 mL.

Melting points. Melting points were recorded on either Stuart SMP10 or a Stuart SMP40 melting point apparatus.

Infrared (IR) Spectroscopy. Infrared spectra were recorded using a Perkin Elmer Spectrum 1 or Spectrum 2 machine. Absorption maxima (ν_{\max}) were reported in wavenumbers (cm^{-1}) and described as weak (w), medium (m), strong (s) and broad (br.). IR spectra were measured from solutions in the specified solvent, or as solids, as specified.

Hydrophobic frit. Hydrophobic frit cartridges by ISOLUTE® contain a frit which is selectively permeable to organic solutions. These were separated from aqueous phase under gravity. Various cartridge sizes were used.

Strong cation exchange (SCX) solid phase extraction (SPE). ISOLUTE® Si-propylsulfonic acid (SCX-2) SPE cartridges of various sizes were used for catch-and-release purification of amines. The acidic silica retained basic compounds or impurities, with all other components eluted off the cartridge. The basic compound was then released using a solution of ammonia in methanol.

Aminopropyl SPE. ISOLUTE® NH₂ (aminopropyl) SPE cartridges of various sizes were used for catch-and-release purification of acidic compounds. The basic silica retained acidic compounds or impurities, with all other components eluted off the cartridge.

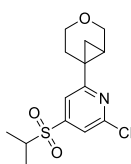
6.2 General procedures

General procedure A: To the combined reagents was added degassed IPA and degassed water (both degassed separately by sparging with nitrogen) in a 5:1 ratio. The mixture was degassed by sparging with a flow of nitrogen, the vial sealed and further degassed by purging the vial under vacuum and filling with nitrogen (x 3). The reaction mixture was heated for an appropriate time. The mixture was filtered through Celite® and an appropriate work-up carried out. The residue was purified by an appropriate method to give the desired product.

General procedure B: To an ice-cooled suspension of the substrate in THF was added sodium hydride (60% dispersion in mineral oil). The mixture allowed to warm to 21 °C and stirred under nitrogen at 21 °C for the appropriate time before iodomethane was added and the mixture stirred at the required temperature for the required time. An appropriate work-up was carried out, the organics dried through a hydrophobic frit, concentrated and the residue purified by an appropriate method to give the desired product.

6.3 Experimental

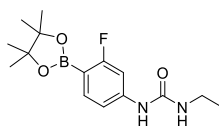
2-(3-Oxabicyclo[4.1.0]heptan-6-yl)-6-chloro-4-(isopropylsulfonyl)pyridine (51)



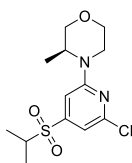
2,6-Dichloro-4-(isopropylsulfonyl)pyridine (401 mg, 1.58 mmol), 2-(3-oxabicyclo[4.1.0]heptan-6-yl)-4,4,5,5-tetramethyl-1,3,2-dioxaborolane (390 mg, 1.74 mmol), CsOH.H₂O (579 mg, 3.45 mmol) and PdCl₂(dppf)-dichloromethane adduct (131 mg, 0.16 mmol) were suspended in water (2 mL) and 2-MeTHF (6 mL).^a The vial was sealed and the mixture degassed by sparging with nitrogen for 5 min before heating at 100 °C for 40 h. The reaction mixture was concentrated under a flow of nitrogen, diluted with ethyl acetate (40 mL) and filtered through Celite® (10 g), eluting with ethyl acetate (30 mL) and the filtrate concentrated *in vacuo*. The residue was dissolved in minimal dichloromethane and purified by flash chromatography (silica, 120 g), eluting with 0-100% TBME in cyclohexane over 12 CV. Appropriate fractions were combined and concentrated *in vacuo* to give crude 2-(3-oxabicyclo[4.1.0]heptan-6-yl)-6-chloro-4-(isopropylsulfonyl)pyridine (189 mg, 0.36 mmol, 23% yield) as an orange oil that slowly solidified to an orange solid. LCMS (Formic, UV, ESI): R_t = 1.11 min, [M+H⁺] 315.97, 317.93 (Cl isotopes), 63% purity. Used without purification in subsequent reaction.

^a Experiment started by E. Hogarth and finished by H. Davies.

1-Ethyl-3-(3-fluoro-4-(4,4,5,5-tetramethyl-1,3,2-dioxaborolan-2-yl)phenyl)urea
(54)

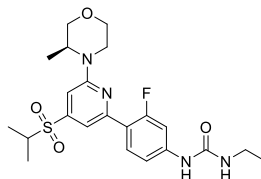


To a solution of 3-fluoro-4-(4,4,5,5-tetramethyl-1,3,2-dioxaborolan-2-yl)aniline (1.0 g, 4.22 mmol) in dichloromethane (10 mL) was added ethyl isocyanate (1 mL, 12.63 mmol) and the mixture was stirred at 21 °C for 29.5 h. Further ethyl isocyanate (1 mL, 12.63 mmol) was added and the mixture heated at 35 °C for 16.0 h, followed by 50 °C for 4.0 h and 60 °C for 2.5 h. The reaction mixture was allowed to cool and diluted with water (10 mL). The aqueous phase was extracted with dichloromethane (2 x 5 mL) and the combined organics were washed with brine (15 mL), dried through a hydrophobic frit and concentrated *in vacuo* to give 1-ethyl-3-(3-fluoro-4-(4,4,5,5-tetramethyl-1,3,2-dioxaborolan-2-yl)phenyl)urea (1.3 g, 3.81 mmol, 90% yield) as a brown solid. M.pt.: 175-178 °C. ν_{\max} (cm⁻¹) (Chloroform-*d*): 3340 (w, br., N-H), 2979 (w), 1660 (m, C=O), 1594 (m, C-N), 1542 (m), 1354 (s, B-C), 1133 (m, C-F). ¹H NMR (400 MHz, Chloroform-*d*) δ ppm 7.64 (dd, *J* = 7.9, 7.0 Hz, 1 H), 7.21 (dd, *J* = 11.2, 2.0 Hz, 1 H), 7.00 (dd, *J* = 8.1, 2.0 Hz, 1 H), 6.47 (br. s, 1 H), 3.31 (q, *J* = 7.3 Hz, 2 H), 1.35 (s, 12 H), 1.18 (t, *J* = 7.3 Hz, 3 H). [1 N-H not observed]. ¹³C NMR (101 MHz, DMSO-*d*₆): δ ppm 167.2 (d, *J* = 247.2 Hz, 1 C), 154.6 (s, 1 C), 145.8 (d, *J* = 12.5 Hz, 1 C), 136.8 (d, *J* = 10.3 Hz, 1 C), 112.6 (d, *J* = 2.2 Hz, 1 C), 103.4 (d, *J* = 29.3 Hz, 1 C), 83.2 (s, 2 C), 33.9 (s, 1 C), 24.6 (s, 4 C), 15.2 (s, 1 C). [1 C not observed]. ¹⁹F NMR (376 MHz, DMSO-*d*₆) δ ppm -105.4 (s, 1 F). LCMS (Formic, UV, ESI): *R*_t = 1.05 min, [M+H⁺] 309.04, 87% purity. HRMS: (C₁₅H₂₃BFN₂O₃) [M+H⁺] requires 309.1786, found [M+H⁺] 309.1786 (0 ppm). Only LCMS data given in literature.¹²⁴

(S)-4-(6-Chloro-4-(isopropylsulfonyl)pyridin-2-yl)-3-methylmorpholine (55)

2,6-Dichloro-4-(isopropylsulfonyl)pyridine (300 mg, 1.18 mmol), DIPEA (825 μ l, 4.72 mmol) and (S)-3-methylmorpholine (147 μ l, 1.30 mmol) were heated at 81 °C for 1.5 h followed by 100 °C for 18.0 h. The reaction mixture was diluted with ethyl acetate (10 mL) and water (10 mL). The aqueous phase was extracted with ethyl acetate (2 x 10 mL) and the combined organics were washed with brine (30 mL), dried through a hydrophobic frit, concentrated *in vacuo* and then under a flow of nitrogen to give (S)-4-(6-chloro-4-(isopropylsulfonyl)pyridin-2-yl)-3-methylmorpholine (363 mg, 1.07 mmol, 91% yield) as a light brown solid. M.pt.: 107-110 °C. ν_{max} (cm^{-1}) (Chloroform-*d*): 3094 (w, br.), 2974 (w), 2858 (w), 1582 (s, C=N), 1537 (m, C=C), 1441 (s), 1313 (s, S=O), 1162 (s), 1134 (s, S=O). ^1H NMR (400 MHz, Chloroform-*d*) δ ppm 6.51 (d, $J = 1.0$ Hz, 1 H), 6.40 (d, $J = 1.0$ Hz, 1 H), 3.86 (app. qd, $J = 6.7, 3.1$ Hz, 1 H), 3.59 (dd, $J = 11.5, 3.2$ Hz, 1 H), 3.52 (dd, $J = 13.0, 2.9$ Hz, 1 H), 3.37 (d, $J = 13.0$ Hz, 1 H), 3.29 (dd, $J = 11.5, 3.2$ Hz, 1 H), 3.15 (td, $J = 12.2, 3.2$ Hz, 1 H), 2.81 - 2.89 (m, 1 H), 2.79 (spt, $J = 6.8$ Hz, 1 H), 0.91 (app. dd, $J = 6.8, 2.3$ Hz, 6 H)^b, 0.86 (d, $J = 6.7$ Hz, 3 H). ^{13}C NMR (101 MHz, Chloroform-*d*) δ ppm 158.3 (s, 1 C), 151.1 (s, 1 C), 149.1 (s, 1 C), 109.4 (s, 1 C), 103.3 (s, 1 C), 70.9 (s, 1 C), 66.6 (s, 1 C), 55.3 (s, 1 C), 47.9 (s, 1 C), 39.9 (s, 1 C), 15.5 (s, 1 C), 15.4 (s, 1 C), 13.2 (s, 1 C). LCMS (Formic, UV, ESI): $R_t = 1.12$ min, $[\text{M}+\text{H}^+]$ 319.06, 321.05 (Cl isotopes), 97% purity. HRMS: ($\text{C}_{13}\text{H}_{20}\text{ClN}_2\text{O}_3\text{S}$) $[\text{M}+\text{H}^+]$ requires 319.0883, found $[\text{M}+\text{H}^+]$ 319.0879 (-1.3 ppm).

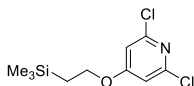
^b Suggest this is actually two overlapping doublets, $J = 6.8$ Hz.

(S)-1-Ethyl-3-(3-fluoro-4-(4-(isopropylsulfonyl)-6-(3-methylmorpholino)pyridin-2-yl)phenyl)urea (56)

Prepared according to general procedure A with: (*S*)-4-(6-chloro-4-(isopropylsulfonyl)pyridin-2-yl)-3-methylmorpholine (100 mg, 0.31 mmol), 1-ethyl-3-(3-fluoro-4-(4,4,5,5-tetramethyl-1,3,2-dioxaborolan-2-yl)phenyl)urea (116 mg, 0.38 mmol), K₂CO₃ (103 mg, 0.75 mmol), PdCl₂(dppf) (23 mg, 0.03 mmol), IPA (2.5 mL) and water (0.5 mL), heated at 120 °C for 3.0 h. The reaction mixture was diluted with ethyl acetate (10 mL) and water (5 mL) and filtered through Celite® (2.5 g). The filtrate was concentrated *in vacuo* and partitioned between ethyl acetate (10 mL) and water (10 mL). The aqueous phase was extracted with ethyl acetate (2 x 10 mL) and the combined organics were washed with brine (20 mL), dried through a hydrophobic frit and concentrated *in vacuo* and then under a flow of nitrogen. The residue was dissolved in 1:1 methanol:DMSO (2 x 1 mL) and purified by MDAP (formic acid modifier). Appropriate fractions were combined, concentrated *in vacuo* and then under a flow of nitrogen followed by drying in a vacuum oven. The residue was dissolved in DMSO (1 mL) and purified by MDAP (formic acid modifier). Appropriate fractions were combined, concentrated *in vacuo* and the residue loaded in methanol onto an aminopropyl SPE (10 g, primed with 2 CV methanol), eluting with methanol (6 CV). The eluent was concentrated *in vacuo* and then under a flow of nitrogen to give (*S*)-1-ethyl-3-(3-fluoro-4-(4-(isopropylsulfonyl)-6-(3-methylmorpholino)pyridin-2-yl)phenyl)urea (30 mg, 0.07 mmol, 21% yield) as an off-white solid. M.pt.: 122-125 °C. ν_{\max} (cm⁻¹) (Chloroform-*d*): 3362 (w, br., N-H), 2974 (w), 2928 (w), 1665 (m, N-O), 1578 (m, C=N), 1539, 1424, 1311 (s, S=O), 1231 (s), 1142 (s, S=O). ¹H NMR (600 MHz, Chloroform-*d*) δ ppm 7.91 (app. br. t, *J* = 8.6 Hz, 1 H), 7.28 - 7.51 (m, 3 H), 7.02 - 7.15 (m, 2 H), 6.90 (s, 1 H), 4.36 - 4.44 (m, 1 H), 4.00 - 4.08 (m, 2 H), 3.83 (d, *J* = 11.0 Hz, 1 H), 3.78 (dd, *J* = 11.6, 2.9 Hz, 1 H), 3.64 (td, *J* = 11.6, 3.1 Hz, 1 H), 3.24 - 3.36 (m, 4 H), 1.36 (app. dd, *J* = 7.0, 3.7,

6 H)^c, 1.30 (d, $J = 6.6$ Hz, 3 H), 1.16 - 1.21 (m, 3 H). ¹³C NMR (151 MHz, Chloroform-*d*) δ ppm 161.3 (d, $J = 249.9$ Hz, 1 C), 158.0 (s, 1 C), 154.9 (s, 1 C), 152.8 (d, $J = 3.3$ Hz, 1 C), 147.3 (s, 1 C), 142.0 (d, $J = 11.6$ Hz, 1 C), 131.0 (d, $J = 3.9$ Hz, 1 C), 114.7 (d, $J = 2.8$ Hz, 1 C), 110.3 (d, $J = 12.7$ Hz, 1 C), 110.0 (s, 1 C), 106.7 (d, $J = 28.8$ Hz, 1 C), 103.4 (s, 1 C), 71.2 (s, 1 C), 66.8 (s, 1 C), 55.2 (s, 1 C), 47.8 (s, 1 C), 39.9 (s, 1 C), 35.2 (s, 1 C), 15.6 (s, 1 C), 15.5 (s, 1 C), 15.3 (s, 2 C). ¹⁹F NMR (376 MHz, Chloroform-*d*) δ ppm -112.9 (s, 1 F). LCMS (Formic, UV, ESI): $R_t = 1.08$ min, $[M+H^+]$ 465.28, 100% purity. HRMS: (C₂₂H₃₀FN₄O₄S) $[M+H^+]$ requires 465.1972, found $[M+H^+]$ 465.1970 (-0.4 ppm).

2,6-Dichloro-4-(2-(trimethylsilyl)ethoxy)pyridine (60)

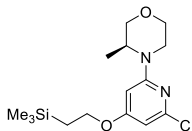


A mixture of 2,6-dichloro-4-iodopyridine (1.00 g, 3.65 mmol), Cs₂CO₃ (2.42 g, 7.44 mmol), 1,10-phenanthroline (0.13 g, 0.73 mmol), copper(I) iodide (0.07 g, 0.37 mmol) and 2-(trimethylsilyl)-ethanol (1.6 mL, 11.16 mmol) was degassed by purging under vacuum and filling with nitrogen (x 3). Toluene (8 mL) was added and the mixture was heated at 110 °C for 18 h. The reaction mixture was allowed to cool and filtered through silica (10 g), eluting with ethyl acetate (30 mL) and the filtrate was concentrated *in vacuo*. The residue was purified by flash chromatography (silica, 120 g), eluting with cyclohexane over 6 CV followed by 0-20% TBME in cyclohexane over 8 CV. Appropriate fractions were combined and concentrated *in vacuo*. The residue was dissolved in minimal dichloromethane and purified by flash chromatography (silica, 40 g), eluting with cyclohexane over 6 CV followed by 0-10% ethyl acetate in cyclohexane over 12 CV. Appropriate fractions were combined and concentrated *in vacuo* to give crude 2,6-dichloro-4-(2-(trimethylsilyl)ethoxy)pyridine (0.49 g, 1.17 mmol, 32% yield) as a colourless oil which solidified to a wet solid on standing. LCMS (Formic, UV, ESI): $R_t = 1.55$ min, $[M+H^+]$ 264.00, 265.97, 267.96

^c Suggest this is actually two overlapping doublets.

(Cl isotopes), 63% purity. ^1H NMR (400 MHz, DMSO- d_6) δ ppm 7.46 (s, 2 H), 4.78 (t, $J = 8.3$ Hz, 2 H), 1.64 (t, $J = 8.3$ Hz, 2 H), 0.55 (s, 9 H).

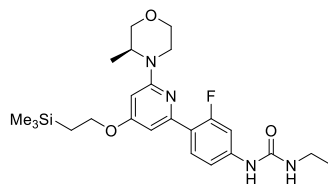
(S)-4-(6-Chloro-4-(2-(trimethylsilyl)ethoxy)pyridin-2-yl)-3-methylmorpholine (61)



2,6-Dichloro-4-(2-(trimethylsilyl)ethoxy)pyridine (490 mg, 1.11 mmol), (*S*)-3-methylmorpholine (0.14 mL, 1.22 mmol), DIPEA (0.58 mL, 3.34 mmol) and acetonitrile (1 mL) were heated at 70 °C for 17.5 h followed by 90 °C for 1 h. Further (*S*)-3-methylmorpholine (0.2 mL, 1.76 mmol) and DIPEA (0.5 mL, 2.86 mmol) were added and the reaction mixture was heated at 90 °C for 5 h before concentrating under a flow of nitrogen. To the residue was added (*S*)-3-methylmorpholine (0.2 mL, 1.76 mmol) and the reaction mixture was heated at 100 °C for 44 h followed by 150 °C for 115 h. Further (*S*)-3-methylmorpholine (0.2 mL, 1.76 mmol) and DIPEA (0.2 mL, 1.15 mmol) were added and the reaction mixture was heated at 150 °C for 46 h. The reaction mixture was partitioned between ethyl acetate (10 mL) and water (10 mL). The aqueous phase was extracted with ethyl acetate (2 x 10 mL) and the combined organics were washed with brine (20 mL), dried through a hydrophobic frit and concentrated *in vacuo*. The residue was dissolved in minimal dichloromethane and purified by flash chromatography (silica, 120 g), eluting with 0-15% ethyl acetate in cyclohexane over 12 CV. Appropriate fractions were combined, concentrated *in vacuo* and then under a flow of nitrogen to give (*S*)-4-(6-chloro-4-(2-(trimethylsilyl)ethoxy)pyridin-2-yl)-3-methylmorpholine (261 mg, 0.75 mmol, 68% yield) as a colourless oil. ν_{max} (cm^{-1}) (dichloromethane): 2956 (w), 2855 (w), 1589 (s, C=N), 1550 (s), 1437 (s), 1216 (s, Si-C), 1141 (s, C-O), 836 (s). ^1H NMR (400 MHz, DMSO- d_6) δ ppm 6.32 (d, $J = 1.5$ Hz, 1 H), 6.11 (d, $J = 1.5$ Hz, 1 H), 4.24 (m, $J = 6.8, 2.4$ Hz, 1 H), 4.12 (t, $J = 7.8$ Hz, 2 H), 3.89 (dd, $J = 11.5, 3.4$ Hz, 1 H), 3.77 (dd, $J = 13.2, 2.4$ Hz, 1 H), 3.68 (d, $J = 11.5$ Hz, 1 H), 3.57 (dd, $J = 11.5, 3.2$ Hz, 1 H), 3.43 (td, $J = 11.7, 3.4$ Hz, 1 H), 3.02 (td, $J = 13.2, 3.7$ Hz, 1 H), 1.10 (d, $J = 6.4$ Hz, 3 H), 1.05 (t, $J = 7.8$ Hz, 2 H), 0.06 (s, 9 H). ^{13}C NMR (101 MHz, DMSO- d_6) δ ppm

167.8 (s, 1 C), 159.1 (s, 1 C), 149.3 (s, 1 C), 99.8 (s, 1 C), 90.3 (s, 1 C), 70.3 (s, 1 C), 66.0 (s, 1 C), 65.9 (s, 1 C), 46.7 (s, 1 C), 16.9 (s, 1 C), 12.3 (s, 1 C), -1.4 (s, 1 C). LCMS (Formic, UV, ESI): $R_t = 1.58$ min, $[M+H]^+$ 329.04, 331.02 (Cl isotopes), 96% purity. HRMS: (C₁₅H₂₆ClN₂O₂Si) $[M+H]^+$ requires 329.1452, found $[M+H]^+$: 329.1450 (-0.6 ppm).

(S)-1-Ethyl-3-(3-fluoro-4-(6-(3-methylmorpholino)-4-(2-(trimethylsilyl)ethoxy)pyridin-2-yl)phenyl)urea (62)

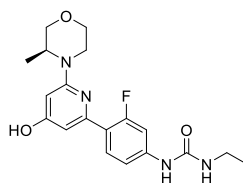


Prepared according to general procedure A with (S)-4-(6-chloro-4-(2-(trimethylsilyl)ethoxy)pyridin-2-yl)-3-methylmorpholine (888 mg, 2.38 mmol), 1-ethyl-3-(3-fluoro-4-(4,4,5,5-tetramethyl-1,3,2-dioxaborolan-2-yl)phenyl)urea (915 mg, 2.61 mmol), K₂CO₃ (657 mg, 4.75 mmol), PdCl₂(dppf) (174 mg, 0.24 mmol) IPA (16 mL) and water (3.2 mL)^d, heated at 120 °C for 1.5 h. The reaction mixture was filtered through Celite® (10 g), eluting with ethyl acetate (40 mL) and water (20 mL). The filtrate was concentrated *in vacuo* and diluted with ethyl acetate (30 mL) and water (20 mL). The organic phase was washed with water (2 x 20 mL) and brine (40 mL), dried through a hydrophobic frit and concentrated *in vacuo*. The residue was dissolved in minimal dichloromethane and purified by flash chromatography (silica, 120 g), eluting with 0-100% ethyl acetate in cyclohexane over 40 min. Appropriate fractions were combined and concentrated *in vacuo* and under nitrogen to give (S)-1-ethyl-3-(3-fluoro-4-(6-(3-methylmorpholino)-4-(2-(trimethylsilyl)ethoxy)-pyridin-2-yl)phenyl)urea (1250 mg, 2.53 mmol, quant.), as a brown oil. ν_{\max} (cm⁻¹) (dichloromethane): 3335 (w, br., N-H), 2968 (w), 1669 (w, N=O), 1592 (s, C=N), 1538 (s), 1432 (s), 1224 (s, Si-C), 1176 (s, C-O), 835 (s). ¹H NMR (400 MHz, Chloroform-*d*) δ ppm 7.93 (t, $J = 8.8$ Hz, 1 H), 7.60 (br. s, 1 H), 7.35 (dd, $J = 13.7, 2.1$ Hz, 1 H), 7.03 (dd, $J = 8.8, 2.1$ Hz, 1 H), 6.75 - 6.78 (m, 1 H), 5.97 (d, $J = 2.0$ Hz, 1 H), 5.55 (br.

^d 5:1 mixture of IPA and water was combined, degassed by sparging with nitrogen and added to the reagents.

t, $J = 5.4$ Hz, 1 H), 4.33 (m, $J = 6.7, 6.7, 6.7$ Hz, 1 H), 4.13 (t, $J = 8.3$ Hz, 2 H), 3.99 (dd, $J = 11.5, 3.0$ Hz, 1 H), 3.87 (dd, $J = 12.7, 2.0$ Hz, 1 H), 3.78 (app. br. d, $J = 2.0$ Hz, 2 H), 3.62 (td, $J = 11.7, 3.0$ Hz, 1 H), 3.15 - 3.31 (m, 3 H), 1.24 (d, $J = 6.4$ Hz, 3 H), 1.08 - 1.16 (m, 5 H), 0.08 (s, 9 H). ^{13}C NMR (101 MHz, Chloroform-*d*) δ ppm 167.1 (s, 1 C), 161.0 (d, $J = 248.7$ Hz, 1 C), 155.7 (s, 1 C), 159.6 (s, 1 C), 152.0 (d, $J = 2.9$ Hz, 1 C), 140.9 (d, $J = 11.7$ Hz, 1 C), 131.1 (d, $J = 5.1$ Hz, 1 C), 121.9 (d, $J = 11.7$ Hz, 1 C), 114.6 (d, $J = 2.9$ Hz, 1 C), 106.8 (d, $J = 28.6$ Hz, 1 C), 101.6 (d, $J = 11.7$ Hz, 1 C), 91.0 (s, 1 C), 71.5 (s, 1 C), 67.1 (s, 1 C), 65.3 (s, 1 C), 47.7 (s, 1 C), 40.0 (s, 1 C), 35.0 (s, 1 C), 15.3 (s, 1 C), 12.3 (s, 1 C), -1.4 (s, 3 C). ^{19}F NMR (376 MHz, Chloroform-*d*) δ ppm -113.4 (s, 1 F). LCMS (Formic, UV, ESI): $R_t = 1.20$ min, $[\text{M}+\text{H}^+]$ 475.17, 96% purity. HRMS: ($\text{C}_{24}\text{H}_{36}\text{FN}_4\text{O}_3\text{Si}$) $[\text{M}+\text{H}^+]$ requires 475.2541, found $[\text{M}+\text{H}^+]$ 475.2546 (1.1 ppm).

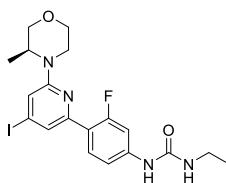
(*S*)-1-Ethyl-3-(3-fluoro-4-(4-hydroxy-6-(3-methylmorpholino)pyridin-2-yl)phenyl)urea (63)



(*S*)-1-Ethyl-3-(3-fluoro-4-(6-(3-methylmorpholino)-4-(2-(trimethylsilyl)ethoxy)pyridin-2-yl)phenyl)urea (1.20 g, 2.52 mmol), caesium fluoride (1.10 g, 7.24 mmol) and DMSO (16 mL) were heated at 60 °C for 1.8 h. The reaction mixture was diluted with ethyl acetate (40 mL) and water (40 mL). The organic phase was washed with water (2 x 40 mL) and brine (50 mL), dried through a hydrophobic frit and concentrated *in vacuo*. The residue was diluted with ethyl acetate (30 mL) and water (30 mL). The organic phase was washed with water (2 x 20 mL) and brine (30 mL), dried through a hydrophobic frit and concentrated *in vacuo*. The residue was diluted with ethyl acetate (20 mL) and water (100 mL). The organic phase was washed with water (100 mL) and brine (2 x 100 mL), dried through a hydrophobic frit and concentrated *in vacuo* to give (*S*)-1-ethyl-3-(3-fluoro-4-(4-hydroxy-6-(3-methylmorpholino)pyridin-2-yl)phenyl)urea (0.56 g, 1.38 mmol, 55% yield) as a brown solid. M.pt.: 168-170 °C. ν_{max} (cm^{-1}) (dichloromethane): 3373 (m, br., C-O),

1681 (m, N=O), 1596 (s, C=N), 1539 (s), 1231 (s, C-F), 1024 (s). ¹H NMR (400 MHz, DMSO-*d*₆) δ ppm 10.12 (s, 1 H), 8.75 (s, 1 H), 7.87 (t, *J* = 8.9 Hz, 1 H), 7.54 (dd, *J* = 15.0, 1.8 Hz, 1 H), 7.05 (dd, *J* = 8.6, 2.0 Hz, 1 H), 6.62 (app. br. t, *J* = 1.5 Hz), 6.20 (t, *J* = 5.4 Hz, 1 H), 6.01 (d, *J* = 1.5 Hz, 1 H), 4.21 - 4.33 (m, 1 H), 3.92 (dd, *J* = 11.1, 3.1 Hz, 1 H), 3.83 (dd, *J* = 13.0, 1.7 Hz, 1 H), 3.71 (d, *J* = 11.3 Hz, 1 H), 3.62 (dd, *J* = 11.7, 3.2 Hz, 1 H), 3.47 (td, *J* = 11.6, 2.9 Hz, 1 H), 3.08 - 3.16 (m, 2 H), 3.04 (dt, *J* = 12.5, 3.4 Hz, 1 H), 1.12 (d, *J* = 6.6 Hz, 3 H), 1.06 (t, *J* = 7.1 Hz, 3 H). ¹³C NMR (101 MHz, DMSO-*d*₆) δ ppm 165.6 (s, 1 C), 160.3 (d, *J* = 245.8 Hz, 1 C), 159.3 (s, 1 C), 154.7 (s, 1 C), 151.5 (d, *J* = 2.9 Hz, 1 C), 142.3 (d, *J* = 8.8 Hz, 1 C), 130.4 (d, *J* = 5.1 Hz, 119.5, 1 C), (d, *J* = 11.7 Hz, 1 C), 113.2 (d, *J* = 2.2 Hz, 1 C), 104.4 (d, *J* = 30.1 Hz, 1 C), 102.3 (d, *J* = 11.0 Hz, 1 C), 91.2 (s, 1 C), 70.6 (s, 1 C), 66.3 (s, 1 C), 59.7 (s, 1 C), 46.7 (s, 1 C), 33.9 (s, 1 C), 15.3 (s, 1 C), 12.0 (s, 1 C). ¹⁹F NMR (376 MHz, DMSO-*d*₆) δ ppm -114.3 (s, 1 F). LCMS (Formic, UV, ESI): Rt = 0.58 min, [M+H⁺] 375.15, 92% purity. HRMS: (C₁₉H₂₄FN₄O₃) [M+H⁺] requires 375.1832, found [M+H⁺] 375.1833 (0.3 ppm).

(S)-1-Ethyl-3-(3-fluoro-4-(4-iodo-6-(3-methylmorpholino)pyridin-2-yl)phenyl)urea (64)

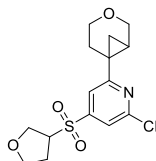


Based on literature procedure.¹²⁷ A solution of (S)-1-ethyl-3-(3-fluoro-4-(4-hydroxy-6-(3-methylmorpholino)pyridin-2-yl)phenyl)urea (50 mg, 0.12 mmol) in acetonitrile (1 mL) was cooled to 5 °C and pyridine (10 μl, 0.12 mmol) was added. Triflic anhydride (21 μl, 0.12 mmol) was added slowly and the resulting mixture was stirred at 21 °C for 1.3 h. Sodium iodide (55 mg, 0.37 mmol) was added followed by hydrochloric acid (37% in water) (10 μl, 0.12 mmol) and the mixture was stirred at 21 °C for 2.5 h, followed by heating at 35 °C for 0.5 h and 40 °C for 12.8 h. Further sodium iodide (110 mg, 0.73 mmol) and hydrochloric acid (37% in water) (20 μL, 0.24 mmol) were added and the reaction mixture was heated at 90 °C for 3.0 h. The reaction mixture was quenched with water (2 mL), diluted with acetonitrile (1 mL) and NaOH

(2 M in water) was added to achieve a pH of ~10. The resulting solution was diluted with ethyl acetate (10 mL), the aqueous phase was extracted with ethyl acetate (2 x 10 mL), the combined organics were washed with brine (20 mL), dried through a hydrophobic frit and concentrated *in vacuo*. The crude product was dissolved in 1:1 methanol:DMSO (1 mL) and purified by MDAP^e (formic acid modifier). Appropriate fractions were combined and concentrated under a flow of nitrogen to give (*S*)-1-ethyl-3-(3-fluoro-4-(4-iodo-6-(3-methylmorpholino)pyridin-2-yl)phenyl)urea (35 mg, 0.07 mmol, 54%) as a pale yellow solid. M.pt.: 221-224 °C. ν_{\max} (cm⁻¹) (dichloromethane): 3339 (w, br., N-H), 2969 (w), 2856 (w), 1656 (w, N-O), 1598 (m), 1560 (s, C=N), 1541 (s), 1420 (m), 1233 (m, C-F). ¹H NMR (400 MHz, DMSO-*d*₆) δ ppm 8.84 (br. s, 1 H), 7.86 (t, *J* = 8.9 Hz, 1 H), 7.57 (dd, *J* = 15.0, 2.1 Hz, 1 H), 7.36 (s, 1 H), 7.08 (d, *J* = 1.0 Hz, 1 H), 7.09 (d, *J* = 8.5 Hz, 2 H), 6.24 (t, *J* = 5.6 Hz, 1 H), 4.40 (br. dd, *J* = 6.5, 2.1 Hz, 1 H), 3.94 (dd, *J* = 11.9, 2.8 Hz, 2 H), 3.72 (d, *J* = 11.2 Hz, 1 H), 3.62 (dd, *J* = 11.4, 2.8 Hz, 1 H), 3.48 (td, *J* = 11.6, 2.7 Hz, 1 H), 3.05 - 3.20 (m, 3 H), 1.15 (d, *J* = 6.6 Hz, 3 H), 1.06 (t, *J* = 7.1 Hz, 2 H). ¹³C NMR (101 MHz, DMSO-*d*₆) δ ppm 160.4 (d, *J* = 245.8 Hz, 1 C), 157.8 (s, 1 C), 154.7 (s, 1 C), 151.0 (d, *J* = 3.7 Hz, 1 C), 143.1 (d, *J* = 12.5 Hz, 1 C), 130.4 (s, 1 C), 120.3 (d, *J* = 12.5 Hz, 1 C), 117.9 (d, *J* = 11.0 Hz, 1 C), 113.4 (s, 1 C), 113.3 (s, 1 C), 107.8 (s, 1 C), 104.4 (d, *J* = 29.3 Hz, 1 C), 70.5 (s, 1 C), 66.1 (s, 1 C), 54.8 (s, 1 C), 46.5 (s, 1 C), 34.0 (s, 1 C), 15.3 (s, 1 C), 12.4 (s, 1 C). ¹⁹F NMR (376 MHz, DMSO-*d*₆) δ ppm -114.0 (s, 1 F). LCMS (formic, UV, ESI): *R*_t = 1.29 min, [M+H⁺] 485.14, 100% purity. HRMS: (C₁₉H₂₃FIN₄O₂) [M+H⁺] requires 485.0850, found [M+H⁺] 485.0850 (0 ppm).

^e Due to absence, purification carried out by S. Nicolle.

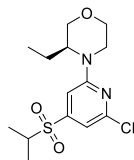
2-(3-Oxabicyclo[4.1.0]heptan-6-yl)-6-chloro-4-((tetrahydrofuran-3-yl)sulfonyl)pyridine (precursor to compound **78**)



To 2,6-dichloro-4-((tetrahydrofuran-3-yl)sulfonyl)pyridine (100 mg, 0.35 mmol) was added 2-(3-oxabicyclo[4.1.0]heptan-6-yl)-4,4,5,5-tetramethyl-1,3,2-dioxaborolane (79 mg, 0.35 mmol), PdCl₂(dppf)-dichloromethane adduct (29 mg, 0.04 mmol), CsOH.H₂O (124 mg, 0.74 mmol), anhydrous THF (2 mL) and degassed water (0.4 mL, degassed by sparging with nitrogen). The suspension was degassed by sparging with nitrogen followed by purging under vacuum and filling with nitrogen (x 3) and the reaction mixture heated at 100 °C for 23 h. The reaction mixture was filtered through Celite® (10 g), eluting with ethyl acetate (70 mL) and concentrated *in vacuo*. The residue was diluted with ethyl acetate (30 mL), the organic phase was washed with water (20 mL x 3) and brine (40 mL), dried through a hydrophobic frit and concentrated *in vacuo*. The residue was dissolved in minimal dichloromethane and purified by flash chromatography (silica, 40 g), eluting with 0-100% TBME in cyclohexane over 12 CV. Appropriate fractions were combined and concentrated *in vacuo* and then under a flow of nitrogen to give 2-(3-oxabicyclo[4.1.0]heptan-6-yl)-6-chloro-4-((tetrahydrofuran-3-yl)sulfonyl)pyridine (39 mg, 0.09 mmol, 27% yield) as a pale yellow gum. ν_{\max} (cm⁻¹) (dichloromethane): 2956 (w), 2857 (w), 1576 (m, C=N), 1547 (m), 1355 (m), 1323 (s, S=O), 1165 (s, S=O), 1077 (m). ¹H NMR (400 MHz, DMSO-*d*₆) δ ppm 7.76 (d, *J* = 1.0 Hz, 1 H), 7.70 (d, *J* = 1.0 Hz, 1 H), 4.39 - 4.49 (m, 1 H), 4.01 - 4.10 (m, 1 H), 3.93 (dd, *J* = 11.2, 4.4 Hz, 1 H), 3.78 - 3.88 (m, 3 H), 3.61 - 3.70 (m, 1 H), 3.50 - 3.58 (m, 1 H), 3.34 - 3.43 (m, 1 H), 2.52 - 2.57 (m, 1 H), 2.12 - 2.22 (m, 2 H), 2.04 (app. ddd, *J* = 13.9, 8.3, 5.6 Hz, 1 H), 1.74 - 1.83 (m, 1 H), 1.36 (dd, *J* = 9.3, 4.4 Hz, 1 H), 1.14 - 1.18 (m, 1 H). ¹³C NMR (101 MHz, DMSO-*d*₆) δ ppm 168.1 (s, 1 C), 149.8 (s, 1 C), 118.4 (s, 1 C), 116.0 (s, 1 C), 67.7 (s, 1 C), 66.3 (s, 1 C), 64.5 (s, 1 C), 62.8 (s, 1 C), 61.8 (s, 1 C), 26.9 (s, 1 C), 25.3 (s, 1 C), 22.6 (s, 1 C), 22.6 (s, 1 C), 22.3 (s, 1 C) [one Ar-C not observed]. LCMS (Formic, UV, ESI):

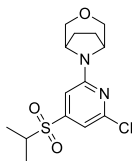
R_t = 1.02 min, [M+H⁺] 343.96, 345.95 (Cl isotopes), 83% purity. HRMS: (C₁₅H₁₉ClNO₄S) [M+H⁺] requires 344.0723, found [M+H⁺] 344.0724 (0.3 ppm).

(S)-4-(6-Chloro-4-(isopropylsulfonyl)pyridin-2-yl)-3-ethylmorpholine (97)



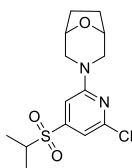
2,6-Dichloro-4-(isopropylsulfonyl)pyridine (300 mg, 1.18 mmol), (S)-3-ethylmorpholine hydrochloride (179 mg, 1.18 mmol), DIPEA (0.83 mL, 4.73 mmol) and DMSO (1 mL) were heated at 120 °C for 22 h. The reaction mixture was diluted with ethyl acetate (10 mL) and water (10 mL). The aqueous phase was extracted with ethyl acetate (2 x 10 mL) and the combined organics were washed with water (2 x 30 mL) and brine (30 mL), dried through a hydrophobic frit and concentrated *in vacuo*. The residue was dissolved in minimal dichloromethane and purified by flash chromatography (silica, 24 g), eluting with 0-100% ethyl acetate in cyclohexane over 10 CV. Appropriate fractions were combined and concentrated *in vacuo* to give (S)-4-(6-chloro-4-(isopropylsulfonyl)pyridin-2-yl)-3-ethylmorpholine (237 mg, 0.71 mmol, 60% yield) as a yellow oil. ν_{\max} (cm⁻¹) (Chloroform-*d*): 2967 (w), 2861 (w), 1581 (s, C=N), 1536 (m), 1311 (s, S=O), 1128 (s, S=O). ¹H NMR (400 MHz, Chloroform-*d*) δ ppm 6.91 (d, *J* = 1.0 Hz, 1 H), 6.82 (d, *J* = 1.0 Hz, 1 H), 3.97 - 4.10 (m, 3 H), 3.95 (d, *J* = 11.7 Hz, 1 H), 3.64 (dd, *J* = 11.7, 2.9 Hz, 1 H), 3.57 (td, *J* = 12.2, 2.9 Hz, 1 H), 3.24 - 3.32 (m, 1 H), 3.21 (spt, *J* = 6.8 Hz, 1 H), 1.84 - 1.96 (m, 1 H), 1.65 - 1.77 (m, 1 H), 1.34 (app. dd, *J* = 6.8, 3.9 Hz, 6 H), 0.94 (t, *J* = 7.6 Hz, 3 H). ¹³C NMR (101 MHz, Chloroform-*d*) δ ppm 158.5 (s, 1 C), 151.1 (s, 1 C), 149.0 (s, 1 C), 109.0 (s, 1 C), 103.3 (s, 1 C), 68.0 (s, 1 C), 66.6 (s, 1 C), 55.3 (s, 1 C), 53.8 (s, 1 C), 40.3 (s, 1 C), 20.9 (s, 1 C), 15.5 (s, 1 C), 15.4 (s, 1 C), 11.0 (s, 1 C). LCMS (Formic, UV, ESI): R_t = 1.20 min, [M+H⁺] 333.24, 335.21 (Cl isotopes), 99% purity. HRMS: (C₁₄H₂₂ClN₂O₃S) [M+H⁺] requires 333.1040, found [M+H⁺] 333.1038 (0.6 ppm).

**8-(6-Chloro-4-(isopropylsulfonyl)pyridin-2-yl)-3-oxa-8-azabicyclo[3.2.1]octane
(98)**

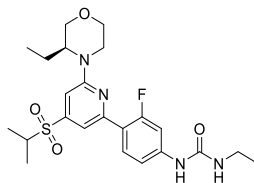


2,6-Dichloro-4-(isopropylsulfonyl)pyridine (505 mg, 1.99 mmol), 3-oxa-8-azabicyclo[3.2.1]octane hydrochloride (316 mg, 2.11 mmol), DIPEA (0.69 mL, 3.93 mmol) and DMSO (8 mL) were heated at 100 °C for 3.5 h. The reaction mixture was diluted with ethyl acetate (20 mL) and water (20 mL). The aqueous phase was extracted with ethyl acetate (20 mL) and the combined organics were washed with water (20 mL) and brine (30 mL), dried through a hydrophobic frit and concentrated *in vacuo* and then under a flow of nitrogen to give 8-(6-chloro-4-(isopropylsulfonyl)pyridin-2-yl)-3-oxa-8-azabicyclo[3.2.1]octane (634 mg, 1.78 mmol, 90% yield) as an orange solid. M.pt.: 138-144 °C. ν_{\max} (cm⁻¹) (Chloroform-*d*): 2955 (w), 2855 (w), 1580 (s, C=N), 1535 (m), 1464 (m), 1311 (s, S=O), 1173 (m), 1142 (s, S=O), 689 (s, C-Cl), 589 (s). ¹H NMR (400 MHz, Chloroform-*d*) δ ppm 6.91 (d, *J* = 1.2 Hz, 1 H), 6.78 (d, *J* = 1.2 Hz, 1 H), 4.48 (br. s, 2 H), 3.77 (d, *J* = 11.0 Hz, 2 H), 3.64 (dd, *J* = 11.0, 1.5 Hz, 2 H), 3.18 - 3.26 (m, 1 H), 2.11 - 2.18 (m, 2 H), 1.98 - 2.06 (m, 2 H), 1.35 (d, *J* = 6.8 Hz, 7 H). ¹³C NMR (101 MHz, Chloroform-*d*) δ ppm 156.7 (s, 1 C), 151.7 (s, 1 C), 149.1 (s, 1 C), 109.2 (s, 1 C), 104.9 (s, 1 C), 70.9 (s, 2 C), 56.2 (s, 2 C), 55.3 (s, 1 C), 26.9 (s, 2 C), 15.4 (s, 2 C). LCMS (Formic, UV, ESI): *R*_t = 1.10 min, [M+H⁺] 331.09, 333.06 (Cl isotopes), 93% purity. HRMS: (C₁₄H₁₉ClN₂O₃S) [M+H⁺] requires 331.0883, found [M+H⁺] 331.0885 (0.6 ppm).

**3-(6-Chloro-4-(isopropylsulfonyl)pyridin-2-yl)-8-oxa-3-azabicyclo[3.2.1]octane
(99)**



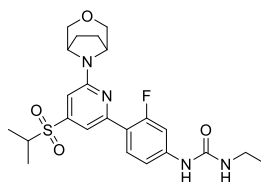
2,6-Dichloro-4-(isopropylsulfonyl)pyridine (500 mg, 1.97 mmol), 8-oxa-3-azabicyclo[3.2.1]octane hydrochloride (309 mg, 2.07 mmol), DIPEA (0.69 mL, 3.94 mmol) and DMSO (8 mL) were heated at 100 °C for 3 h. The reaction mixture was diluted with ethyl acetate (20 mL) and water (20 mL). The aqueous phase was extracted with ethyl acetate (20 mL) and the combined organics were washed with water (20 mL) and brine (30 mL), dried through a hydrophobic frit and concentrated *in vacuo* and then under a flow of nitrogen to give 3-(6-chloro-4-(isopropylsulfonyl)pyridin-2-yl)-8-oxa-3-azabicyclo[3.2.1]octane (643 mg, 1.85 mmol, 94% yield) as an orange solid. M.pt.: 173-176 °C. ν_{\max} (cm⁻¹) (Chloroform-*d*): 2978 (w), 2854 (w), 1579 (s, C=N), 1538 (m), 1440 (m), 1312 (s, S=O), 1134 (s, S=O). ¹H NMR (400 MHz, Chloroform-*d*) δ ppm 6.97 (d, *J* = 1.0 Hz, 1 H), 6.80 (d, *J* = 1.2 Hz, 1 H), 4.47 - 4.56 (m, 2 H), 3.85 (br. d, *J* = 12.5 Hz, 2 H), 3.17 - 3.26 (m, 3 H), 1.96 - 2.03 (m, 2 H), 1.79 - 1.85 (m, 2 H), 1.34 (d, *J* = 6.8 Hz, 6 H). ¹³C NMR (101 MHz, Chloroform-*d*) δ ppm 159.9 (s, 1 C), 151.0 (s, 1 C), 149.0 (s, 1 C), 109.8 (s, 1 C), 103.0 (s, 1 C), 73.4 (s, 2 C), 55.3 (s, 1 C), 50.8 (s, 2 C), 27.9 (s, 2 C), 15.4 (s, 2 C). LCMS (Formic, UV, ESI): *R*_t = 1.09 min, [M+H⁺] 331.10, 333.06 (Cl isotopes), 96% purity. HRMS: (C₁₄H₁₉ClN₂O₃S) [M+H⁺] requires 331.0883, found [M+H⁺] 331.0882 (-0.3 ppm).

(S)-1-Ethyl-3-(4-(6-(3-ethylmorpholino)-4-(isopropylsulfonyl)pyridin-2-yl)-3-fluorophenyl)urea (86)

A solution of (S)-4-(6-chloro-4-(isopropylsulfonyl)pyridin-2-yl)-3-ethylmorpholine (75 mg, 0.23 mmol) in IPA (2 mL) was added to 1-ethyl-3-(3-fluoro-4-(4,4,5,5-tetramethyl-1,3,2-dioxaborolan-2-yl)phenyl)urea (76 mg, 0.25 mmol), K₂CO₃ (62 mg, 0.45 mmol) and PdCl₂(dppf) (16 mg, 0.02 mmol). Water (0.4 mL) was added and the mixture degassed by purging under vacuum and filling with nitrogen (x 3) and heated at 120 °C for 2 h. The reaction mixture was diluted with ethyl acetate (10 mL) and water (5 mL) and filtered through Celite® (2.5 g). The filtrate was concentrated *in vacuo* and partitioned between ethyl acetate (10 mL) and water (10 mL). The aqueous phase was extracted with ethyl acetate (2 x 10 mL) and the combined organics were washed with water (20 mL) and brine (20 mL), dried through a hydrophobic frit and concentrated *in vacuo* and then under a flow of nitrogen. The residue was dissolved in 1:1 methanol:DMSO (2 x 1 mL) and purified by MDAP (formic acid modifier). Appropriate fractions were combined, concentrated *in vacuo* and then under a flow of nitrogen to give (S)-1-ethyl-3-(4-(6-(3-ethylmorpholino)-4-(isopropylsulfonyl)pyridin-2-yl)-3-fluorophenyl)urea (68 mg, 0.14 mmol, 62% yield) as an orange amorphous solid. ν_{\max} (cm⁻¹) (Chloroform-*d*): 3358 (w, br., N-H), 2968 (w), 2863 (w), 1662 (m, C=O), 1578 (m, C=N), 1537 (s), 1423 (s), 1306 (s, S=O), 1229 (s, C-F), 1140 (s, S=O). ¹H NMR (400 MHz, Chloroform-*d*) δ ppm 7.93 (t, *J* = 8.8 Hz, 1 H), 7.44 (s, 1 H), 7.37 (dd, *J* = 13.7, 2.0 Hz, 1 H), 7.11 (dd, *J* = 8.8, 2.0 Hz, 1 H), 6.90 (s, 1 H), 6.68 (br. s, 1 H), 4.84 (br. t, *J* = 5.4 Hz, 1 H), 4.14 - 4.27 (m, 1 H), 4.08 (br. d, *J* = 11.7 Hz, 1 H), 3.96 - 4.05 (m, 2 H), 3.59 - 3.71 (m, 2 H), 3.24 - 3.38 (m, 4 H), 1.86 - 2.00 (m, 1 H), 1.65 - 1.76 (m, 1 H), 1.37 (app. dd, *J* = 6.8, 3.4 Hz, 6 H), 1.20 (t, *J* = 7.1 Hz, 3 H), 0.96 (t, *J* = 7.3 Hz, 3 H). ¹³C NMR (101 MHz, Chloroform-*d*) δ ppm 161.3 (d, *J* = 250.2 Hz, 1 C), 158.3 (s, 1 C), 155.0 (s, 1 C), 152.9 (d, *J* = 2.9 Hz, 1 C), 147.0 (s, 1 C), 142.0 (d, *J* = 11.7 Hz, 1 C), 130.9 (d,

$J = 4.4$ Hz, 1 C), 120.1 (d, $J = 11.0$ Hz, 1 C), 114.5 (s, 1 C), 109.8 (d, $J = 12.5$ Hz, 1 C), 106.5 (d, $J = 28.6$ Hz, 1 C), 103.1 (s, 1 C), 68.0 (s, 1 C), 66.8 (s, 1 C), 55.3 (s, 1 C), 53.7 (s, 1 C), 40.2 (s, 1 C), 35.2 (s, 1 C), 20.5 (s, 1 C), 15.6 (s, 1 C), 15.5 (s, 1 C), 15.3 (s, 1 C), 11.2 (s, 1 C). ^{19}F NMR (376 MHz, Chloroform-*d*) δ ppm -112.8 (s, 1 F). LCMS (Formic, UV, ESI): $R_t = 1.14$ min, $[\text{M}+\text{H}^+]$ 479.37, 99% purity. HRMS: ($\text{C}_{23}\text{H}_{32}\text{FN}_4\text{O}_4\text{S}$) $[\text{M}+\text{H}^+]$ requires 479.2128, found $[\text{M}+\text{H}^+]$ 479.2128 (0 ppm).

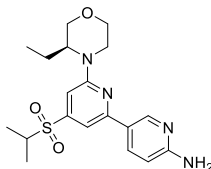
1-(4-(6-(3-Oxa-8-azabicyclo[3.2.1]octan-8-yl)-4-(isopropylsulfonyl)pyridin-2-yl)-3-fluorophenyl)-3-ethylurea (87)



Prepared according to general procedure A with 8-(6-chloro-4-(isopropylsulfonyl)pyridin-2-yl)-3-oxa-8-azabicyclo[3.2.1]octane (150 mg, 0.45 mmol), 1-ethyl-3-(3-fluoro-4-(4,4,5,5-tetramethyl-1,3,2-dioxaborolan-2-yl)phenyl)urea (190 mg, 0.51 mmol), K_2CO_3 (125 mg, 0.91 mmol), $\text{PdCl}_2(\text{dppf})$ (33 mg, 0.05 mmol), IPA (4 mL) and water (0.8 mL), heated at 120 °C for 5.5 h. The reaction mixture was diluted with ethyl acetate (10 mL) and water (5 mL) and filtered through Celite® (2.5 g). The filtrate was concentrated *in vacuo* and partitioned between ethyl acetate (10 mL) and water (10 mL). The aqueous phase was extracted with ethyl acetate (2 x 10 mL) and the combined organics were washed with brine (20 mL), dried through a hydrophobic frit and concentrated *in vacuo* and then under a flow of nitrogen. The residue was dissolved in minimal dichloromethane and purified by flash chromatography (silica, 40 g), eluting with 0-100% ethyl acetate in cyclohexane over 16 CV. Appropriate fractions were combined, concentrated *in vacuo* and under nitrogen to give crude material. The residue was dissolved in 1:1 methanol:DMSO (2 x 1 mL) and purified by MDAP (ammonium hydrogen carbonate modifier). Appropriate fractions were combined, concentrated *in vacuo* and then under a flow of nitrogen to give 1-(4-(6-(3-oxa-8-azabicyclo[3.2.1]octan-8-yl)-4-(isopropylsulfonyl)pyridin-2-yl)-3-fluorophenyl)-3-ethylurea (116 mg, 0.24 mmol, 54% yield) as a pale yellow-orange solid. M.pt.: 157-159 °C. ν_{max} (cm^{-1}) (Chloroform-

yl)carbamate (62 mg, 0.08 mmol, 37% yield) as a yellow oily solid. LCMS (Formic, UV, ESI): $R_t = 1.35$ min, $[M+H^+]$ 491.38, 65% purity. Used without purification in subsequent reaction.

(S)-6-(3-Ethylmorpholino)-4-(isopropylsulfonyl)-[2,3'-bipyridin]-6'-amine (89)

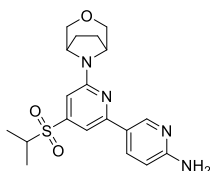


To *tert*-butyl (*S*)-(6-(3-ethylmorpholino)-4-(isopropylsulfonyl)-[2,3'-bipyridin]-6'-yl)carbamate (55 mg, 0.07 mmol) was added 1,4-dioxane (0.6 mL) and HCl (4 M in 1,4-dioxane, 0.1 mL, 0.40 mmol). The reaction mixture was heated at 30 °C for 2.5 h followed by 50 °C for 19.0 h. The reaction mixture was concentrated *in vacuo* and loaded in methanol onto an aminopropyl column (10 g, primed with 1 CV methanol), eluting with methanol (3 CV). The eluent was concentrated *in vacuo*. The residue was dissolved in 1:1 methanol:DMSO (1 mL) and purified by MDAP (ammonium hydrogen carbonate modifier). Appropriate fractions were combined and concentrated *in vacuo* and then under a flow of nitrogen. The residue was dissolved in DMSO (3.5 mL) and purified by MDAP (formic acid modifier).^f Appropriate fractions were combined and concentrated under a flow of nitrogen to give (*S*)-6-(3-ethylmorpholino)-4-(isopropylsulfonyl)-[2,3'-bipyridin]-6'-amine (6 mg, 0.02 mmol, 21% yield) as an off-white solid. M.pt.: 209-213 °C. ν_{\max} (cm⁻¹) (dichloromethane): 3464 (w), 3368 (w, N-H), 3210 (w, br.), 2966 (w), 1621 (m), 1579 (s, C=N), 1556 (s, N-H), 1422 (s), 1308 (s, S=O), 1142 (s, S=O). ¹H NMR (400 MHz, Chloroform-*d*) δ ppm 8.75 (d, $J = 2.4$ Hz, 1 H), 8.09 (dd, $J = 8.8, 2.4$ Hz, 1 H), 7.26 (d, $J = 1.0$ Hz, 1 H), 6.85 (d, $J = 1.0$ Hz, 1 H), 6.58 (d, $J = 8.8$ Hz, 1 H), 4.89 (br. s, 2 H), 4.17 - 4.25 (m, 1 H), 4.10 (br. d, $J = 12.2$ Hz, 1 H), 3.96 - 4.06 (m, 2 H), 3.59 - 3.71 (m, 2 H), 3.32

^f MDAP purification (formic modifier) by A. Hobbs (Discovery Analytical Purification Team). MDAP purification was carried out using a Waters ZQ mass spectrometer using positive electrospray ionisation and a summed UV wavelength of 210–350 nm. Formic: Acquity UPLC CSH C₁₈ column (150 mm x 30 mm, 5 μ m packing diameter, 40 mL/min flow rate), using a gradient elution at ambient temperature with the mobile phases as (A) H₂O containing 0.1% (v/v) formic acid and (B) acetonitrile containing 0.1% (v/v) formic acid.

(td, $J = 12.8, 4.2$ Hz, 1 H), 3.24 (spt, $J = 6.8$ Hz, 1 H), 1.88 - 1.99 (m, 1 H), 1.65 - 1.77 (m, 1 H), 1.36 (app. dd, $J = 6.8, 3.4$ Hz, 6 H), 0.97 (t, $J = 7.3$ Hz, 3 H). ^{13}C NMR (101 MHz, Chloroform-*d*) δ ppm 159.0 (s, 1 C), 158.5 (s, 1 C), 155.2 (s, 1 C), 147.6 (s, 1 C), 147.2 (s, 1 C), 136.4 (s, 1 C), 124.7 (s, 1 C), 108.2 (s, 1 C), 104.8 (s, 1 C), 102.8 (s, 1 C), 68.0 (s, 1 C), 66.8 (s, 1 C), 55.2 (s, 1 C), 53.7 (s, 1 C), 40.3 (s, 1 C), 20.5 (s, 1 C), 15.6 (s, 1 C), 15.5 (s, 1 C), 11.2 (s, 1 C). LCMS (Formic, UV, ESD): $R_t = 0.66$ min, $[\text{M}+\text{H}^+]$ 391.26, 100% purity. HRMS: ($\text{C}_{19}\text{H}_{26}\text{N}_4\text{O}_3\text{S}$) $[\text{M}+\text{H}^+]$ 391.1804, found $[\text{M}+\text{H}^+]$ 391.1804 (0 ppm).

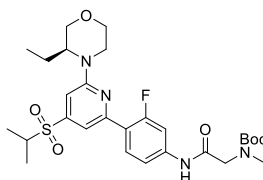
6-(3-Oxa-8-azabicyclo[3.2.1]octan-8-yl)-4-(isopropylsulfonyl)-[2,3'-bipyridin]-6'-amine (90)



Prepared according to general procedure A with 8-(6-chloro-4-(isopropylsulfonyl)pyridin-2-yl)-3-oxa-8-azabicyclo[3.2.1]octane (100 mg, 0.30 mmol), 5-(4,4,5,5-tetramethyl-1,3,2-dioxaborolan-2-yl)pyridin-2-amine (73 mg, 0.33 mmol), K_2CO_3 (84 mg, 0.61 mmol), $\text{PdCl}_2(\text{dppf})$ (24 mg, 0.03 mmol), IPA (2 mL) and water (0.4 mL), heated at 120 °C for 3 h. The reaction mixture was diluted with ethyl acetate (10 mL) and water (5 mL), filtered through Celite® (2.5 g) and the filtrate was concentrated *in vacuo*. The residue was dissolved in minimal dichloromethane and purified by flash chromatography (silica, 40 g), eluting with 0-100% ethyl acetate in cyclohexane over 14 CV, followed by 0-100% 3:1 ethyl acetate:ethanol in ethyl acetate over 8 CV. Appropriate fractions were combined and concentrated *in vacuo* and then under a flow of nitrogen to give 6-(3-oxa-8-azabicyclo[3.2.1]octan-8-yl)-4-(isopropylsulfonyl)-[2,3'-bipyridin]-6'-amine (87 mg, 0.22 mmol, 74% yield) as an off-white solid. M.pt.: 192-194 °C. ν_{max} (cm^{-1}) (dichloromethane): 3463 (w, br.), 3367 (w, br., N-H), 3210 (w), 2954 (w), 2856 (w), 1621 (m), 1577 (s, C=N), 1533 (s, N-H), 1455 (s), 1418 (s), 1308 (s, S=O), 1139 (s, S=O), 692 (s). ^1H NMR (400 MHz, Chloroform-*d*) δ ppm 8.77 (d, $J = 2.4$ Hz, 1 H), 8.08 (dd, $J = 8.8, 2.4$ Hz, 1 H), 7.29 (d, $J = 1.0$ Hz, 1 H), 6.84 (d, $J = 1.0$ Hz, 1 H),

6.58 (d, $J = 8.8$ Hz, 1 H), 4.72 (br. s, 2 H), 4.59 (br. s, 2 H), 3.86 (d, $J = 10.8$ Hz, 2 H), 3.66 (d, $J = 10.8$ Hz, 2 H), 3.27 (spt, $J = 6.8$ Hz, 1 H), 2.13 - 2.21 (m, 2 H), 2.00 - 2.09 (m, 2 H), 1.38 (d, $J = 6.8$ Hz, 6 H). ^{13}C NMR (101 MHz, Chloroform- d) δ ppm 159.1 (s, 1 C), 157.3 (s, 1 C), 155.9 (s, 1 C), 147.7 (s, 1 C), 147.6 (s, 1 C), 136.2 (s, 1 C), 124.6 (s, 1 C), 108.0 (s, 1 C), 105.1 (s, 1 C), 104.6 (s, 1 C), 70.7 (s, 2 C), 56.1 (s, 2 C), 55.2 (s, 1 C), 27.0 (s, 2 C), 15.5 (s, 2 C). LCMS (Formic, UV, ESI): $R_t = 0.58$ min, $[\text{M}+\text{H}^+]$ 389.35, 100% purity. HRMS: ($\text{C}_{19}\text{H}_{29}\text{N}_4\text{O}_3\text{S}$) $[\text{M}+\text{H}^+]$ requires 389.1647, found $[\text{M}+\text{H}^+]$ 389.1647 (0 ppm).

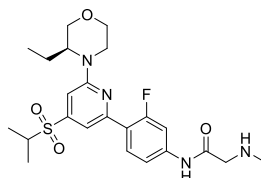
***tert*-Butyl (*S*)-(2-((4-(6-(3-ethylmorpholino)-4-(isopropylsulfonyl)pyridin-2-yl)-3-fluorophenyl)amino)-2-oxoethyl)(methyl)carbamate** (precursor to compound **93**)



(*S*)-4-(6-Chloro-4-(isopropylsulfonyl)pyridin-2-yl)-3-ethylmorpholine (87 mg, 0.26 mmol) in IPA (2 mL) and water (0.4 mL) was added to *tert*-butyl (2-((3-fluoro-4-(4,4,5,5-tetramethyl-1,3,2-dioxaborolan-2-yl)phenyl)amino)-2-oxoethyl)(methyl)carbamate (117 mg, 0.29 mmol), K_2CO_3 (72 mg, 0.52 mmol) and $\text{PdCl}_2(\text{dppf})$ (19 mg, 0.03 mmol). The mixture was degassed by purging under vacuum and filling with nitrogen (x 3) and heated at 120 °C for 5.5 h. The mixture was allowed to cool and further $\text{PdCl}_2(\text{dppf})$ (19 mg, 0.03 mmol) and *tert*-butyl (2-((3-fluoro-4-(4,4,5,5-tetramethyl-1,3,2-dioxaborolan-2-yl)phenyl)amino)-2-oxoethyl)(methyl)carbamate (50 mg, 0.12 mmol) added. The mixture was degassed by sparging with nitrogen and heated at 120 °C for 6.0 h. The reaction mixture was diluted with ethyl acetate (10 mL) and water (5 mL), filtered through Celite® (2.5 g) and the filtrate was concentrated *in vacuo*. The residue was diluted with ethyl acetate (20 mL) and water (10 mL). The aqueous phase was extracted with ethyl acetate (2 x 20 mL, brine (5 mL) added) and the combined organics were washed with water (20 mL, brine (5 mL) added) and brine (40 mL), dried through a hydrophobic frit and concentrated *in vacuo* and then under a flow of nitrogen to give crude *tert*-butyl (*S*)-(2-((4-(6-(3-ethylmorpholino)-4-(isopropylsulfonyl)pyridin-2-yl)-3-fluorophenyl)amino)-2-

oxoethyl)(methyl)carbamate (210 mg, 0.19 mmol, 74% yield) as a brown residue. LCMS (Formic, UV, ESI): $R_t = 1.30$ min, $[M+H]^+$ 579.39, 53% purity. Used without purification in subsequent reaction.

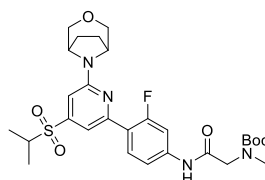
(S)-N-(4-(6-(3-Ethylmorpholino)-4-(isopropylsulfonyl)pyridin-2-yl)-3-fluorophenyl)-2-(methylamino)acetamide (93)



To *tert*-butyl (S)-2-((4-(6-(3-ethylmorpholino)-4-(isopropylsulfonyl)pyridin-2-yl)-3-fluorophenyl)amino)-2-oxoethyl)(methyl)carbamate (210 mg, 0.20 mmol) was added 1,4-dioxane (3 mL) and HCl (4 M in 1,4-dioxane) (0.3 mL, 1.2 mmol), and the reaction mixture was heated at 60 °C for 15 h. The reaction mixture was concentrated *in vacuo* and loaded in methanol onto an aminopropyl SPE (1 g, primed with 2 CV methanol), eluting with methanol (4 CV). The eluent was concentrated *in vacuo*, loaded in methanol onto an aminopropyl SPE (5 g, primed with 2 CV methanol), eluting with methanol (4 CV). The eluent was concentrated *in vacuo*, loaded in methanol onto an aminopropyl SPE (10 g, primed with 2 CV methanol), eluting with methanol (4 CV). The eluent was concentrated *in vacuo* and then under a flow of nitrogen, dissolved in 1:1 methanol:DMSO (2 x 1 mL) and purified by MDAP (ammonium hydrogen carbonate modifier). Appropriate fractions were combined and concentrated *in vacuo* and then under a flow of nitrogen to give (S)-N-(4-(6-(3-ethylmorpholino)-4-(isopropylsulfonyl)pyridin-2-yl)-3-fluorophenyl)-2-(methylamino)acetamide (41 mg, 0.08 mmol, 38% yield) as a brown amorphous solid. ν_{\max} (cm^{-1}) (Chloroform-*d*): 3280 (w, br., N-H), 2966 (w), 2856 (w), 1692 (m, C=O), 1583 (s, C=N), 1523 (s), 1427 (s), 1310 (s, S=O), 1143 (s, S=O). ^1H NMR (400 MHz, Chloroform-*d*) δ ppm 9.47 (br. s, 1 H), 8.01 (br. t, $J = 8.3$ Hz, 1 H), 7.69 (br. d, $J = 13.2$ Hz, 1 H), 7.49 (s, 1 H), 7.35 (br. d, $J = 8.3$ Hz, 1 H), 6.93 (s, 1 H), 4.20 (br. s, 1 H), 3.95 - 4.13 (m, 3 H), 3.59 - 3.74 (m, 2 H), 3.23 - 3.43 (m, 4 H), 2.54 (s, 3 H), 1.82 - 2.04 (m, 1 H), 1.66 - 1.77 (m, 1 H), 1.37 (dd, $J = 6.8, 2.4$ Hz, 6 H), 0.97 (br. t, $J = 7.3$ Hz, 3 H). [1 N-H not observed]. ^{13}C NMR (101 MHz, Chloroform-*d*) δ ppm 169.9 (s, 1 C), 159.8 (d, $J = 235.5$ Hz,

1 C), 158.3 (s, 1 C), 152.6 (d, $J = 3.7$ Hz, 1 C), 147.3 (s, 1 C), 140.1 (d, $J = 11.0$ Hz, 1 C), 130.9 (d, $J = 3.7$ Hz, 1 C), 121.9 (d, $J = 11.7$ Hz, 1 C), 114.8 (d, $J = 2.9$ Hz, 1 C), 110.2 (d, $J = 11.7$ Hz, 1 C), 107.2 (d, $J = 28.6$ Hz, 1 C), 103.6 (s, 1 C), 68.0 (s, 1 C), 66.8 (s, 1 C), 55.2 (s, 1 C), 55.0 (s, 1 C), 53.7 (s, 1 C), 40.3 (s, 1 C), 36.9 (s, 1 C), 20.5 (s, 1 C), 15.6 (s, 1 C), 15.5 (s, 1 C), 11.2 (s, 1 C). ^{19}F NMR (376 MHz, Chloroform-*d*) δ ppm -112.7 (s, 1 F). LCMS (Formic, UV, ESI): $R_t = 0.73$ min, $[\text{M}+\text{H}^+]$ 479.31, 97% purity. HRMS: ($\text{C}_{23}\text{H}_{32}\text{FN}_4\text{O}_4\text{S}$) $[\text{M}+\text{H}^+]$ requires 479.2128, found $[\text{M}+\text{H}^+]$ 479.2124 (-0.8 ppm).

***tert*-Butyl (2-((4-(6-(3-oxa-8-azabicyclo[3.2.1]octan-8-yl)-4-(isopropylsulfonyl)pyridin-2-yl)-3-fluorophenyl)amino)-2-oxoethyl)(methyl)carbamate** (precursor to compound **94**)

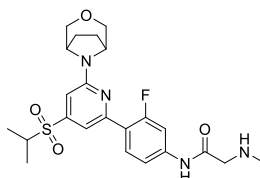


Prepared according to general procedure A with 8-(6-chloro-4-(isopropylsulfonyl)pyridin-2-yl)-3-oxa-8-azabicyclo[3.2.1]octane (150 mg, 0.45 mmol), *tert*-butyl (2-((3-fluoro-4-(4,4,5,5-tetramethyl-1,3,2-dioxaborolan-2-yl)phenyl)amino)-2-oxoethyl)(methyl)carbamate (204 mg, 0.50 mmol), K_2CO_3 (125 mg, 0.91 mmol), $\text{PdCl}_2(\text{dppf})$ (33 mg, 0.05 mmol), IPA (4 mL) and water (0.8 mL)[§], heated at 120 °C for 5.5 h. The reaction mixture was diluted with ethyl acetate (10 mL) and water (5 mL) and filtered through Celite® (2.5 g). The filtrate was concentrated *in vacuo* and partitioned between ethyl acetate (10 mL) and water (10 mL). The aqueous phase was extracted with ethyl acetate (2 x 10 mL) and the combined organic phases were washed with brine (20 mL), dried through a hydrophobic frit and concentrated *in vacuo* to give crude *tert*-butyl (2-((4-(6-(3-oxa-8-azabicyclo[3.2.1]octan-8-yl)-4-(isopropylsulfonyl)pyridin-2-yl)-3-fluorophenyl)amino)-2-oxoethyl)(methyl)carbamate (321 mg, 0.42 mmol, 93% yield)

[§] IPA and water not degassed before use.

as a brown oil. LCMS (Formic, UV, ESI): $R_t = 1.25$ min, $[M+H^+]$ 577.36, 76% purity. Used without purification in subsequent reaction.

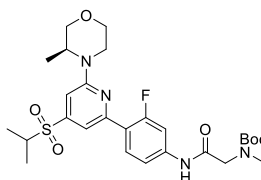
***N*-(4-(6-(3-Oxa-8-azabicyclo[3.2.1]octan-8-yl)-4-(isopropylsulfonyl)pyridin-2-yl)-3-fluorophenyl)-2-(methylamino)acetamide (94)**



To *tert*-butyl (2-((4-(6-(3-oxa-8-azabicyclo[3.2.1]octan-8-yl)-4-(isopropylsulfonyl)pyridin-2-yl)-3-fluorophenyl)amino)-2-oxoethyl)(methyl)carbamate (278 mg, 0.37 mmol) was added 1,4-dioxane (3 mL) and HCl (4 M in 1,4-dioxane) (1 mL, 4.00 mmol) and the reaction mixture heated at 70 °C for 4 h. The reaction mixture was diluted in methanol, concentrated *in vacuo* and loaded in methanol onto an aminopropyl SPE (5 g, primed with 2 CV methanol), eluting with methanol (4 CV). The eluent was concentrated *in vacuo* and then under a flow of nitrogen. The residue was dissolved in 1:1 methanol:DMSO (2 x 1 mL) and purified by MDAP (ammonium hydrogen carbonate modifier). Appropriate fractions were combined and concentrated under a flow of nitrogen to give two batches of product. Batch 1: *N*-(4-(6-(3-oxa-8-azabicyclo[3.2.1]octan-8-yl)-4-(isopropylsulfonyl)pyridin-2-yl)-3-fluorophenyl)-2-(methylamino)acetamide (55 mg, 0.11 mmol, 30% yield) and Batch 2: *N*-(4-(6-(3-oxa-8-azabicyclo[3.2.1]octan-8-yl)-4-(isopropylsulfonyl)pyridin-2-yl)-3-fluorophenyl)-2-(methylamino)acetamide (68 mg, 0.14 mmol, 39% yield) as brown amorphous solids. [Characterisation is for Batch 2.] ν_{\max} (cm⁻¹) (Chloroform-*d*): 3279 (w, br., N-H), 2952 (w), 2855 (w), 1690 (m, C=O), 1621 (m), 1580 (s, C=N), 1556 (m), 1520 (s), 1423 (s), 1308 (s, S=O), 1139 (s, S=O). ¹H NMR (400 MHz, Chloroform-*d*) δ ppm 9.46 (br. s, 1 H), 7.99 (t, $J = 8.6$ Hz, 1 H), 7.70 (dd, $J = 13.7, 2.0$ Hz, 1 H), 7.49 (t, $J = 1.0$ Hz, 1 H), 7.33 (dd, $J = 8.6, 2.0$ Hz, 1 H), 6.92 (d, $J = 1.0$ Hz, 1 H), 4.58 (br. s, 2 H), 3.86 (d, $J = 10.8$ Hz, 2 H), 3.66 (dd, $J = 10.8, 1.0$ Hz, 2 H), 3.50 (s, 1 H), 3.39 (s, 2 H), 3.27 (spt, $J = 6.8$ Hz, 1 H), 2.54 (s, 3 H), 2.13 - 2.20 (m, 2 H), 2.01 - 2.08 (m, 2 H), 1.38 (d, $J = 6.8$ Hz, 6 H). ¹³C NMR (101 MHz, Chloroform-*d*) δ ppm 169.8 (s, 1 C), 161.1 (d,

$J = 250.2$ Hz, 1 C), 157.2 (s, 1 C), 153.3 (d, $J = 2.9$ Hz, 1 C), 147.4 (s, 1 C), 140.1 (d, $J = 11.7$ Hz, 1 C), 131.0 (d, $J = 3.7$ Hz, 1 C), 114.8 (d, $J = 2.9$ Hz, 1 C), 110.6 (d, $J = 12.5$ Hz, 1 C), 107.2 (d, $J = 27.9$ Hz, 1 C), 105.6 (s, 1 C), 70.8 (s, 2 C), 56.1 (s, 2 C), 55.2 (s, 1 C), 55.0 (s, 1 C), 36.9 (s, 1 C), 27.0 (s, 2 C), 15.6 (s, 2 C). [1 C not observed]. ^{19}F NMR (376 MHz, Chloroform-*d*) δ ppm -112.7 (s, 1 F). LCMS (Formic, UV, ESI): $R_t = 0.68$ min, $[\text{M}+\text{H}^+]$ 477.31, 100% purity. HRMS: ($\text{C}_{23}\text{H}_{29}\text{FN}_4\text{O}_4\text{S}$) $[\text{M}+\text{H}^+]$ requires 477.1972, found $[\text{M}+\text{H}^+]$ 477.1970 (-0.4 ppm).

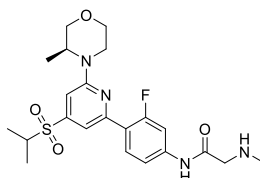
***tert*-Butyl (*S*)-(2-((3-fluoro-4-(4-(isopropylsulfonyl)-6-(3-methylmorpholino)pyridin-2-yl)phenyl)amino)-2-oxoethyl)(methyl)carbamate** (Precursor to compound **95**)



Prepared according to general procedure A with (*S*)-4-(6-chloro-4-(isopropylsulfonyl)pyridin-2-yl)-3-methylmorpholine (140 mg, 0.44 mmol), *tert*-butyl (2-((3-fluoro-4-(4,4,5,5-tetramethyl-1,3,2-dioxaborolan-2-yl)phenyl)amino)-2-oxoethyl)(methyl)carbamate (215 mg, 0.53 mmol), K_2CO_3 (121 mg, 0.88 mmol), $\text{PdCl}_2(\text{dppf})$ (32 mg, 0.044 mmol), IPA (3 mL) and water (0.6 mL), heated at 120 °C for 3 h. The reaction mixture was diluted with ethyl acetate (10 mL) and water (5 mL) and filtered through Celite® (2.5 g). The filtrate was concentrated *in vacuo* and partitioned between ethyl acetate (15 mL) and water (15 mL). The aqueous phase was extracted with ethyl acetate (2 x 15 mL) and the combined organics were washed with brine (30 mL), dried through a hydrophobic frit, concentrated *in vacuo* and then under a flow of nitrogen to give crude *tert*-butyl (*S*)-(2-((3-fluoro-4-(4-(isopropylsulfonyl)-6-(3-methylmorpholino)pyridin-2-yl)phenyl)amino)-2-oxoethyl)(methyl)carbamate (344 mg, 0.51 mmol, quant.) as a brown solid. LCMS (Formic, UV, ESI): $R_t = 1.25$ min, $[\text{M}+\text{H}]^+$ 565.29, 84% purity. ^1H NMR (400 MHz, Chloroform-*d*) δ ppm 8.01 (t, $J = 8.7$ Hz, 1 H), 7.65 (br. dd, $J = 13.9, 2.0$ Hz, 1 H), 7.52 (t, $J = 1.0$ Hz, 1 H), 7.21 (dd, $J = 8.7, 2.0$ Hz, 1 H), 6.95 (d, $J = 1.0$ Hz, 1 H), 4.35 - 4.50 (m, 1 H), 4.02 - 4.10 (m, 2 H), 3.99 (s, 2 H), 3.77 - 3.88 (m, 2 H), 3.65 (td, $J = 11.8, 3.1$ Hz, 1 H), 3.20

- 3.37 (m, 2 H), 3.04 (s, 3 H), 1.52 (s, 9 H), 1.37 (app. dd, $J = 6.8, 2.2$ Hz, 6 H), 1.32 (d, $J = 6.6$ Hz, 3 H).

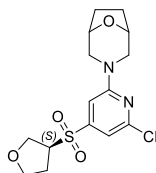
(S)-N-(3-Fluoro-4-(4-(isopropylsulfonyl)-6-(3-methylmorpholino)pyridin-2-yl)phenyl)-2-(methylamino)acetamide (95)



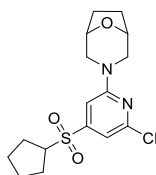
To *tert*-butyl (S)-2-((3-fluoro-4-(4-(isopropylsulfonyl)-6-(3-methylmorpholino)pyridin-2-yl)phenyl)amino)-2-oxoethyl(methyl) carbamate (340 mg, 0.51 mmol) was added 1,4-dioxane (4 mL) and HCl (4 M 1,4-dioxane) (0.4 mL, 1.60 mmol) and the reaction mixture heated at 80 °C for 4 h. The reaction mixture was diluted with methanol, concentrated *in vacuo* and loaded in methanol onto an aminopropyl SPE (10 g, primed with 2 CV methanol), eluting with methanol (5 CV). The filtrate was concentrated *in vacuo* and then under a flow of nitrogen. The residue was dissolved in 1:1 methanol:DMSO (3 x 1 mL) and purified by MDAP (ammonium hydrogen carbonate modifier). Appropriate fractions were combined and concentrated *in vacuo* and then under a flow of nitrogen to give (S)-N-(3-fluoro-4-(4-(isopropylsulfonyl)-6-(3-methylmorpholino)pyridin-2-yl)phenyl)-2-(methylamino)acetamide (146 mg, 0.30 mmol, 60% yield) as a pale yellow-orange solid. M.pt.: 148-153 °C. ν_{\max} (cm⁻¹) (dichloromethane): 2972 (w, N-H), 2936 (w), 2857 (w), 1703 (w), 1615 (m, C=O), 1579 (s, C=N), 1547 (s), 1423 (s), 1310 (m, S=O), 1143 (m, S=O). ¹H NMR (400 MHz, DMSO-*d*₆) δ ppm 8.27 (s, 1 H), 8.02 (t, $J = 8.9$ Hz, 1 H), 7.81 (dd, $J = 14.4, 2.0$ Hz, 1 H), 7.50 (dd, $J = 8.9, 2.0$ Hz, 1 H), 7.36 (br. s, 1 H), 7.03 (d, $J = 1.0$ Hz, 1 H), 4.41 - 4.52 (m, 1 H), 4.08 (br. d, $J = 11.7$ Hz, 1 H), 3.98 (br. dd, $J = 11.4, 3.5$ Hz, 1 H), 3.73 - 3.79 (m, 1 H), 3.64 - 3.70 (m, 1 H), 3.48 - 3.63 (m, 2 H), 3.31 (s, 2 H), 3.15 - 3.23 (m, 1 H), 2.34 (s, 3 H), 1.15 - 1.26 (m, 9 H). [1 N-H not observed]. ¹³C NMR (101 MHz, DMSO-*d*₆) δ ppm 170.1 (s, 1 C), 160.2 (d, $J = 258.2$ Hz, 1 C), 158.0 (s, 1 C), 151.6 (d, $J = 3.7$ Hz, 1 C), 147.6 (s, 1 C), 141.3 (d, $J = 11.7$ Hz, 1 C), 130.7 (d, $J = 4.4$ Hz, 1 C), 120.3 (d, $J = 11.0$ Hz, 1 C), 115.2 (d, $J = 2.2$ Hz, 1 C), 109.1 (d, $J = 12.5$ Hz, 1 C), 106.4 (d, $J = 28.6$ Hz, 1 C),

103.5 (s, 1 C), 70.3 (s, 1 C), 66.1 (s, 1 C), 54.1 (s, 1 C), 53.6 (s, 2 C), 46.8 (s, 1 C), 35.4 (s, 1 C), 14.9 (s, 1 C), 14.9 (s, 1 C), 12.6 (s, 1 C). ^{19}F (376 MHz, Chloroform-*d*) δ ppm -113.9. LCMS (Formic, UV, ESI): $R_t = 0.66$ min, $[\text{M}+\text{H}^+]$ 465.30, 96% purity. HRMS: ($\text{C}_{22}\text{H}_{30}\text{FN}_4\text{O}_4\text{S}$) $[\text{M}+\text{H}^+]$ requires 465.1972, found $[\text{M}+\text{H}^+]$ 465.1967 (-1.1 ppm).

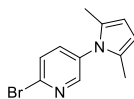
3-(6-Chloro-4-(((*S*)-tetrahydrofuran-3-yl)sulfonyl)pyridin-2-yl)-8-oxa-3-azabicyclo[3.2.1]octane (106a)



(*S*)-2,6-Dichloro-4-((tetrahydrofuran-3-yl)sulfonyl)pyridine (300 mg, 1.06 mmol), 8-oxa-3-azabicyclo[3.2.1]octane hydrochloride (167 mg, 1.12 mmol), DIPEA (0.37 mL, 2.13 mmol) and DMSO (5 mL) were heated at 100 °C for 3 h. The reaction mixture was diluted with ethyl acetate (20 mL) and washed with water (15 mL). The aqueous phase was extracted with ethyl acetate (20 mL) and the combined organics were washed with water (15 mL) and brine (20 mL), dried through a hydrophobic frit and concentrated *in vacuo* and then under a flow of nitrogen to give 3-(6-chloro-4-(((*S*)-tetrahydrofuran-3-yl)sulfonyl)pyridin-2-yl)-8-oxa-3-azabicyclo[3.2.1]octane (388 mg, 1.03 mmol, 97% yield) as an orange solid. M.pt.: 152-156 °C. ν_{max} (cm^{-1}) (Chloroform-*d*): 3096 (w), 2957 (w), 2870 (w, br.), 1579 (s, C=N), 1537 (m), 1447 (s), 1317 (s, S=O), 1136 (s, S=O), 982 (s), 912 (s), 727 (s, C-Cl), 568 (s). ^1H NMR (400 MHz, Chloroform-*d*) δ ppm 6.98 (d, $J = 1.0$ Hz, 1 H), 6.82 (d, $J = 1.0$ Hz, 1 H), 4.47 - 4.57 (m, 2 H), 4.17 (dd, $J = 10.1, 5.5$ Hz, 1 H), 3.92 - 4.02 (m, 2 H), 3.75 - 3.89 (m, 4 H), 3.23 (dd, $J = 12.5, 2.7$ Hz, 2 H), 2.34 - 2.47 (m, 1 H), 2.16 - 2.28 (m, 1 H), 1.99 - 2.04 (m, 2 H), 1.77 - 1.86 (m, 2 H). ^{13}C NMR (101 MHz, Chloroform-*d*) δ ppm 160.0 (s, 1 C), 151.4 (s, 1 C), 150.0 (s, 1 C), 109.0 (s, 1 C), 102.3 (s, 1 C), 73.3 (s, 2 C), 68.4 (s, 1 C), 67.3 (s, 1 C), 63.3 (s, 1 C), 50.7 (s, 2 C), 27.9 (s, 1 C), 27.5 (s, 2 C). LCMS (Formic, UV, ESI): $R_t = 0.99$ min, $[\text{M}+\text{H}^+]$ 359.15, 361.11 (Cl isotopes), 97% purity. HRMS: ($\text{C}_{15}\text{H}_{19}\text{ClN}_2\text{O}_4\text{S}$) $[\text{M}+\text{H}^+]$ requires 359.0832, found $[\text{M}+\text{H}^+]$ 359.0827 (-1.4 ppm).

3-(6-Chloro-4-(cyclopentylsulfonyl)pyridin-2-yl)-8-oxa-3-azabicyclo[3.2.1]octane (108)

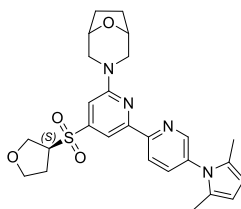
2,6-Dichloro-4-(cyclopentylsulfonyl)pyridine (400 mg, 1.43 mmol), 8-oxa-3-azabicyclo[3.2.1]octane hydrochloride (224 mg, 1.50 mmol), DIPEA (0.50 mL, 2.86 mmol) and DMSO (6 mL) were heated at 100 °C for 1.5 h. The reaction mixture was diluted with ethyl acetate (20 mL) and washed with water (20 mL). The aqueous phase was extracted with ethyl acetate (20 mL) and the combined organics were washed with water (20 mL) and brine (30 mL), dried through a hydrophobic frit and concentrated *in vacuo* and then under a flow of nitrogen to give 3-(6-chloro-4-(cyclopentylsulfonyl)pyridin-2-yl)-8-oxa-3-azabicyclo[3.2.1] octane (511 mg, 1.35 mmol, 94% yield) as an orange solid. M.pt.: 184-186 °C. ν_{\max} (cm⁻¹) (Chloroform-*d*): 3095 (w), 2957 (w, br.), 1582 (s, C=N), 1538 (m), 1447 (s), 1309 (s, S=O), 1157 (s), 1138 (s, S=O), 983 (m). ¹H NMR (400 MHz, Chloroform-*d*) δ ppm 6.98 (d, *J* = 1.0 Hz, 1 H), 6.83 (d, *J* = 1.0 Hz, 1 H), 4.47 - 4.56 (m, 2 H), 3.85 (br. d, *J* = 12.5 Hz, 2 H), 3.44 - 3.53 (m, 1 H), 3.22 (dd, *J* = 12.5, 2.7 Hz, 2 H), 1.98 - 2.11 (m, 4 H), 1.90 - 1.97 (m, 2 H), 1.79 - 1.88 (m, 4 H), 1.61 - 1.71 (m, 2 H). ¹³C NMR (101 MHz, Chloroform-*d*) δ ppm 159.9 (s, 1 C), 151.0 (s, 1 C), 150.8 (s, 1 C), 109.3 (s, 1 C), 102.4 (s, 1 C), 73.4 (s, 2 C), 63.6 (s, 1 C), 50.7 (s, 2 C), 27.9 (s, 2 C), 27.1 (s, 2 C), 25.9 (s, 2 C). LCMS (Formic, UV, ESI): *R*_t = 1.20 min, [M+H⁺] 357.15, 359.13 (Cl isotopes), 96% purity. HRMS: (C₁₆H₂₁ClN₂O₃S) [M+H⁺] requires 357.1040, found [M+H⁺] 357.1038 (-0.6 ppm).

2-Bromo-5-(2,5-dimethyl-1H-pyrrol-1-yl)pyridine (110)

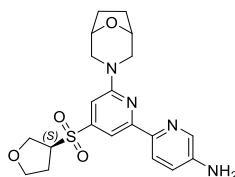
Based on literature procedure.¹⁴¹ A solution of hexane-2,5-dione (0.34 mL, 2.89 mmol), 6-bromopyridin-3-amine (500 mg, 2.89 mmol) and *para*-toluenesulfonic

acid (55 mg, 0.29 mmol) in toluene (15 mL) was heated at 110 °C for 3 h. The reaction mixture was partitioned between ethyl acetate (40 mL) and aqueous saturated sodium bicarbonate solution (40 mL). The organic phase was dried through a hydrophobic frit and concentrated *in vacuo*. The residue was dissolved in minimal dichloromethane and purified by flash chromatography (silica), eluting with 0-100% ethyl acetate in cyclohexane. Appropriate fractions were combined, concentrated *in vacuo* and then under a flow of nitrogen. The residue was dissolved in minimal dichloromethane and purified by flash chromatography (silica, 80 g), eluting with 0-100% ethyl acetate in cyclohexane over 16 CV. Appropriate fractions were combined, concentrated *in vacuo* and then under a flow of nitrogen. The residue was dissolved in minimal dichloromethane and purified by flash chromatography (silica, 40 g), eluting with 0-35% ethyl acetate in cyclohexane over 14 CV (compound eluted after 2 CV and gradient was stopped). Appropriate fractions were combined, concentrated *in vacuo* and then under a flow of nitrogen. The residue was preabsorbed onto Florisil® and purified by flash chromatography (silica, 40 g), eluting with 0-40% ethyl acetate in cyclohexane over 16 CV. Appropriate fractions were combined, concentrated *in vacuo* and then under a flow of nitrogen to give 2-bromo-5-(2,5-dimethyl-1*H*-pyrrol-1-yl)pyridine (470 mg, 1.87 mmol, 65% yield) as a yellow solid. ¹H NMR (400 MHz, Chloroform-*d*) δ ppm 8.30 (dd, *J* = 2.7, 0.7 Hz, 1 H), 7.62 (dd, *J* = 8.3, 0.7 Hz, 1 H), 7.44 (dd, *J* = 8.3, 2.7 Hz, 1 H), 5.95 (s, 2 H), 2.05 (s, 6 H). ¹³C NMR (101 MHz, Chloroform-*d*) δ ppm 149.4 (s, 1 C), 140.7 (s, 1 C), 137.9 (s, 1 C), 135.1 (s, 1 C), 128.8 (s, 2 C), 128.4 (s, 1 C), 107.1 (s, 2 C), 13.0 (s, 2 C), LCMS (Formic, UV, ESD): R_t = 1.17 min, [M+H⁺] 251.04, 253.01 (Br isotopes), 100%. Data in agreement with literature values.¹⁴¹

3-(5'-(2,5-Dimethyl-1*H*-pyrrol-1-yl)-4-(((*S*)-tetrahydrofuran-3-yl)sulfonyl)-[2,2'-bipyridin]-6-yl)-8-oxa-3-azabicyclo[3.2.1]octane (111)



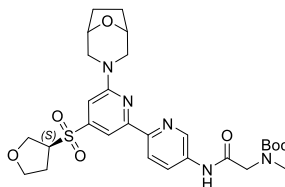
Based on literature procedure.¹⁴¹ To a vial (degassed by purging under vacuum and filling with nitrogen (x 3)) was added THF (4 mL). This was cooled to -78 °C and *n*-butyllithium (2.1 M in hexanes) (0.19 mL, 0.41 mmol) was added to give solution A. To a separate vial was added 2-bromo-5-(2,5-dimethyl-1*H*-pyrrol-1-yl)pyridine (142 mg, 0.56 mmol), the vial was degassed by purging under vacuum and filling with nitrogen (x 3) and THF (1 mL) was added to give solution B. Solution B was added to solution A at -78 °C. The resulting solution was stirred at -78 °C for 30 min, zinc chloride (1.9 M in 2-MeTHF) (0.24 mL, 0.45 mmol) was added, the mixture was allowed to warm to 21 °C and stirred for 2.5 h under nitrogen to give solution C. To a separate vial was added 3-(6-chloro-4-(((*S*)-tetrahydrofuran-3-yl)sulfonyl)pyridin-2-yl)-8-oxa-3-azabicyclo[3.2.1]octane (135 mg, 0.38 mmol) and tetrakis(triphenylphosphine)palladium(0) (9 mg, 7.52 μmol), the vial was degassed by purging under vacuum and filling with nitrogen (x 3) and THF (2 mL) was added to form solution D. Solution D was slowly added to solution C at 21 °C and the mixture was heated at 70 °C for 5.0 h. EDTA (0.5 M in water) (6 mL) was added, the mixture was stirred at 21 °C for 1.0 h and extracted with dichloromethane (3 x 5 mL). The combined organics were dried through a hydrophobic frit and concentrated *in vacuo* and then under a flow of nitrogen. The residue was dissolved in minimal dichloromethane and purified by flash chromatography (silica, 80 g), eluting with 0-100% ethyl acetate in cyclohexane over 16 CV. Appropriate fractions were combined and concentrated *in vacuo* and then under a flow of nitrogen to give crude 3-(5'-(2,5-dimethyl-1*H*-pyrrol-1-yl)-4-(((*S*)-tetrahydrofuran-3-yl)sulfonyl)-[2,2'-bipyridin]-6-yl)-8-oxa-3-azabicyclo[3.2.1]octane (98 mg, 0.12 mmol, 31% yield) as a yellow residue. LCMS (Formic, UV, ESI): $R_t = 1.30$ min, $[M+H]^+$ 495.31, 58% purity. Used without purification in subsequent reaction.

6'-(8-Oxa-3-azabicyclo[3.2.1]octan-3-yl)-4'-(((S)-tetrahydrofuran-3-yl)sulfonyl)-[2,2'-bipyridin]-5-amine (112)

To a solution of 2-bromo-5-(2,5-dimethyl-1*H*-pyrrol-1-yl)pyridine (245 mg, 0.98 mmol) in THF (4 mL) at -78 °C under nitrogen was added *n*-butyllithium (1.17 M in hexanes) (1.00 mL, 1.17 mmol) and the mixture was stirred for 30 min. Zinc chloride (1.9 M in 2-MeTHF) (0.62 mL, 1.17 mmol) was added and the reaction mixture allowed to warm to 21 °C and stirred for 40 min. 3-(6-Chloro-4-(((*S*)-tetrahydrofuran-3-yl)sulfonyl)pyridin-2-yl)-8-oxa-3-azabicyclo[3.2.1]octane (350 mg, 0.98 mmol) and tetrakis(triphenylphosphine)palladium(0) (113 mg, 0.01 mmol) were added and the reaction mixture was heated at 100 °C for 100 min. To the solution was added ethanol (2 mL) and HCl (12 M in water) (1 mL, 12.00 mmol) and the mixture was heated at 100 °C for 30 min. The reaction mixture was preabsorbed onto Florisil® and purified by flash chromatography (silica, 80 g), eluting with 0-75% ethyl acetate in cyclohexane over 8 CV, followed by 75-100% ethyl acetate in cyclohexane over 8 CV, followed by 100% ethyl acetate over 3 CV, followed by 0-100% 3:1 ethyl acetate:ethanol in ethyl acetate over 13 CV, followed by 0-100% ethanol in ethyl acetate. Appropriate fractions were combined and concentrated *in vacuo* and then under a flow of nitrogen. The residue was partitioned between dichloromethane (30 mL) and EDTA solution (0.5 M, in water) (30 mL). The organic phase was washed with EDTA solution (0.5 M in water) (20 mL), dried through a hydrophobic frit and concentrated *in vacuo* to give 6'-(8-oxa-3-azabicyclo[3.2.1]octan-3-yl)-4'-(((*S*)-tetrahydrofuran-3-yl)sulfonyl)-[2,2'-bipyridin]-5-amine (111 mg, 0.26 mmol, 27% yield) as a brown solid. M.pt.: 239-242 °C. ν_{\max} (cm⁻¹) (Chloroform-*d*): 3360 (w, N-H), 2955 (w, N-H), 2853 (w), 1586 (m, C=N), 1556 (s), 1416 (s), 1314 (m, S=O), 1145 (s, S=O), 912 (m), 728 (s), 570 (m). ¹H NMR (400 MHz, Chloroform-*d*) δ ppm 8.11 - 8.17 (m, 2 H), 8.04 (d, *J* = 1.2 Hz, 1 H), 7.00 - 7.08 (m, 1 H), 6.91 (d, *J* = 1.2 Hz, 1 H), 4.51 - 4.60 (m, 2 H), 4.21 (app. dd, *J* = 9.9,

5.5 Hz, 1 H), 3.79 - 4.02 (m, 8 H), 3.26 (dd, $J = 12.5, 2.7$ Hz, 2 H), 2.47 (ddt, $J = 13.2, 7.5, 5.7, 5.7$ Hz, 1 H), 2.10 - 2.30 (m, 1 H), 1.97 - 2.07 (m, 2 H), 1.84 - 1.93 (m, 2 H). ^{13}C NMR (101 MHz, Chloroform- d) δ ppm 159.8 (s, 1 C), 156.9 (s, 1 C), 148.9 (s, 1 C), 145.7 (s, 1 C), 143.3 (s, 1 C), 136.6 (s, 1 C), 121.9 (s, 1 C), 121.5 (s, 1 C), 106.0 (s, 1 C), 102.3 (s, 1 C), 73.7 (s, 2 C), 68.4 (s, 1 C), 67.4 (s, 1 C), 62.8 (s, 1 C), 50.8 (s, 2 C), 28.1 (s, 2 C), 27.6 (s, 1 C). LCMS (Formic, UV, ESI): $R_t = 0.56$ min, $[\text{M}+\text{H}^+]$ 417.31, 97% purity. HRMS: ($\text{C}_{20}\text{H}_{25}\text{N}_4\text{O}_4\text{S}$) $[\text{M}+\text{H}^+]$ 417.1597, found $[\text{M}+\text{H}^+]$ 417.1597 (0.0 ppm).

***tert*-Butyl (2-((6'-(8-oxa-3-azabicyclo[3.2.1]octan-3-yl)-4'-(((*S*)-tetrahydrofuran-3-yl)sulfonyl)-[2,2'-bipyridin]-5-yl)amino)-2-oxoethyl)(methyl)carbamate**
(precursor to compound **75a**)



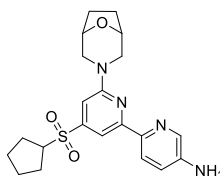
To a solution of HATU (128 mg, 0.34 mmol) and *N*-(*tert*-butoxycarbonyl)-*N*-methylglycine (63 mg, 0.34 mmol) in DMF (0.8 mL) was added DIPEA (0.08 mL, 0.45 mmol) and the resulting mixture was stirred at 21 °C for 10 min. A solution of 6'-(8-oxa-3-azabicyclo[3.2.1]octan-3-yl)-4'-(((*S*)-tetrahydrofuran-3-yl)sulfonyl)-[2,2'-bipyridin]-5-amine (96 mg, 0.22 mmol) in DMF (2 mL) was added and the resulting mixture was stirred at 70 °C for 2 h.

Additionally, to a solution of HATU (27 mg, 0.07 mmol) and *N*-(*tert*-butoxycarbonyl)-*N*-methylglycine (13 mg, 0.07 mmol) in DMF (0.3 mL) was added DIPEA (0.02 mL, 0.09 mmol) and the resulting mixture was stirred at 21 °C for 10 min. A solution of 6'-(8-oxa-3-azabicyclo[3.2.1]octan-3-yl)-4'-(((*S*)-tetrahydrofuran-3-yl)sulfonyl)-[2,2'-bipyridin]-5-amine (20 mg, 0.05 mmol) in DMF (0.8 mL) was added and the resulting mixture was stirred at 70 °C for 3 h.

The two reaction mixtures were allowed to cool, combined and ethyl acetate (40 mL) and water (40 mL) were added. The aqueous phase was extracted with ethyl acetate (30 mL, brine (5 mL) added) and the combined organics were washed with water

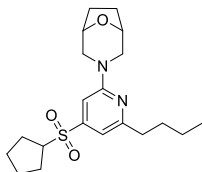
(40 mL) (brine (5 mL) added) and brine (40 mL), dried through a hydrophobic frit and concentrated *in vacuo* and then under a flow of nitrogen to give crude *tert*-butyl (2-((6'-(8-oxa-3-azabicyclo[3.2.1]octan-3-yl)-4'-(((*S*)-tetrahydrofuran-3-yl)sulfonyl)-[2,2'-bipyridin]-5-yl)amino)-2-oxoethyl)(methyl)carbamate (145 mg, 0.22 mmol, 77% combined yield) as a brown residue. LCMS (Formic, UV, ESI): $R_t = 1.06$ min, $[M+H]^+$ 588.39, 87% purity. Used without purification in subsequent reaction.

6'-(8-Oxa-3-azabicyclo[3.2.1]octan-3-yl)-4'-(cyclopentylsulfonyl)-[2,2'-bipyridin]-5-amine (114)



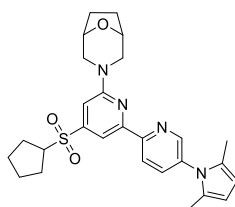
To a solution of 2-bromo-5-(2,5-dimethyl-1*H*-pyrrol-1-yl)pyridine (42 mg, 0.17 mmol) in THF (2 mL) at -78 °C under nitrogen was added *n*-butyllithium (1.17 M in hexanes) (0.17 mL, 0.20 mmol), and the mixture was stirred for 30 min. Zinc chloride (1.9 M in 2-MeTHF) (0.11 mL, 0.20 mmol) was added and the reaction mixture was allowed to warm to 21 °C and stirred for 30 min. 3-(6-Chloro-4-(cyclopentylsulfonyl)pyridin-2-yl)-8-oxa-3-azabicyclo[3.2.1]octane (60 mg, 0.17 mmol) and tetrakis(triphenylphosphine)palladium(0) (19 mg, 0.02 mmol) were added and the reaction mixture was heated at 100 °C for 1.5 h. To the solution was added ethanol (1 mL) and HCl (12 M in water) (0.5 mL, 6.00 mmol) and the mixture was heated at 120 °C for 20 min. The reaction mixture was concentrated under a flow of nitrogen. The residue was preabsorbed onto Florisil® and purified by flash column chromatography (silica, 40 g), eluting with 0-100% ethyl acetate in cyclohexane over 14 CV. Appropriate fractions were combined and concentrated *in vacuo* and then under a flow of nitrogen to give crude 6'-(8-oxa-3-azabicyclo[3.2.1]octan-3-yl)-4'-(cyclopentylsulfonyl)-[2,2'-bipyridin]-5-amine (47 mg, 0.09 mmol, 54% yield) as a green residue. LCMS (Formic, UV, ESI): $R_t = 0.74$ min, $[M+H]^+$ 415.26, 80% purity. Used without purification in subsequent reaction.

3-(6-Butyl-4-(cyclopentylsulfonyl)pyridin-2-yl)-8-oxa-3-azabicyclo[3.2.1]octane (115)



Additionally, appropriate fractions were combined and concentrated *in vacuo* and then under a flow of nitrogen to give crude 3-(6-butyl-4-(cyclopentylsulfonyl)pyridin-2-yl)-8-oxa-3-azabicyclo[3.2.1]octane (29 mg, 0.08 mmol, 46% yield) as an orange residue. LCMS (Formic, UV, ESI): $R_t = 1.39$ min, $[M+H]^+$ 379.30, 88% purity. 1H NMR (400 MHz, Chloroform-*d*) δ ppm 6.87 (d, $J = 1.0$ Hz, 1 H), 6.78 (d, $J = 1.0$ Hz, 1 H), 4.50 - 4.55 (m, 2 H), 3.93 (d, $J = 12.2$ Hz, 2 H), 3.46 - 3.54 (m, 1 H), 3.18 (dd, $J = 12.2, 2.4$ Hz, 2 H), 2.73 (t, $J = 7.4$ Hz, 2 H), 2.05 - 2.15 (m, 2 H), 1.97 - 2.02 (m, 2 H), 1.81 - 1.97 (m, 6 H), 1.61 - 1.76 (m, 4 H), 1.40 (dq, $J = 14.9, 7.4$ Hz, 2 H), 0.96 (t, $J = 7.4$ Hz, 3 H).

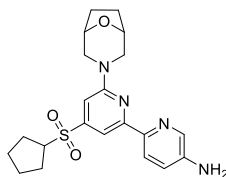
3-(4-(Cyclopentylsulfonyl)-5'-(2,5-dimethyl-1H-pyrrol-1-yl)-[2,2'-bipyridin]-6-yl)-8-oxa-3-azabicyclo[3.2.1]octane (113)



Based on literature procedure.¹⁴¹ To a vial (degassed by purging under vacuum and filling with nitrogen (x 3)) was added THF (2.3 mL). This was cooled to -78 °C and *n*-butyllithium (2.1 M in hexanes) (0.13 mL, 0.27 mmol) was added to give solution A. To a separate vial was added 2-bromo-5-(2,5-dimethyl-1H-pyrrol-1-yl)pyridine (95 mg, 0.38 mmol), the vial was degassed by purging under vacuum and filling with nitrogen (x 3) and THF (0.3 mL) was added to give solution B. Solution B was added to solution A at -78 °C. The resulting solution was stirred at -78 °C for 30 min, zinc chloride (1.9 M in 2-MeTHF) (0.16 mL, 0.30 mmol) was added, the mixture was allowed to warm to 21 °C and stirred for 2.5 h under nitrogen to give solution C. To a

separate vial was added 3-(6-chloro-4-(cyclopentylsulfonyl)pyridin-2-yl)-8-oxa-3-azabicyclo[3.2.1]octane (90 mg, 0.25 mmol) and tetrakis(triphenylphosphine)palladium(0) (6 mg, 5.04 μ mol), the vial was degassed by purging under vacuum and filling with nitrogen (x 3) and THF (1.5 mL) was added to form solution D. Solution D was slowly added to solution C at 21 °C and the mixture was heated at 70 °C for 4.0 h. EDTA (0.5 M in water) (3 mL) was added, the mixture was stirred at 21 °C for 35 min and extracted with dichloromethane (3 x 5 mL). The combined organics were dried through a hydrophobic frit, concentrated *in vacuo* and then under a flow of nitrogen to give crude 3-(4-(cyclopentylsulfonyl)-5'-(2,5-dimethyl-1*H*-pyrrol-1-yl)-[2,2'-bipyridin]-6-yl)-8-oxa-3-azabicyclo[3.2.1]octane (144 mg, 0.23 mmol, 90% yield) as a yellow oil. LCMS (Formic, UV, ESI): $R_t = 1.46$ min, $[M+H^+]$ 493.33, 78% purity. Used without purification in subsequent reaction.

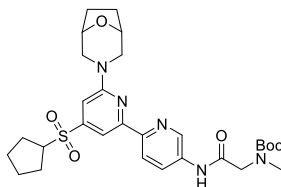
6'-(8-Oxa-3-azabicyclo[3.2.1]octan-3-yl)-4'-(cyclopentylsulfonyl)-[2,2'-bipyridin]-5-amine (114) Alternative procedure.



Based on literature procedure.¹⁴² To 3-(4-(cyclopentylsulfonyl)-5'-(2,5-dimethyl-1*H*-pyrrol-1-yl)-[2,2'-bipyridin]-6-yl)-8-oxa-3-azabicyclo[3.2.1]octane (144 mg, 0.23 mmol) was added hydroxylamine hydrochloride (79 mg, 1.14 mmol), triethylamine (0.15 mL, 1.08 mmol), ethanol (3 mL) and water (0.75 mL) and the resulting mixture was heated at 100 °C for 24 h. The reaction mixture was allowed to cool, quenched by pouring into ice-cold hydrochloric acid (1 M in water) (3.1 mL) and the resulting solution was extracted with TBME (5 mL). Sodium hydroxide (1 M in water) was added to the aqueous phase to achieve pH 6. The resulting mixture was extracted with dichloromethane (3 x 10 mL), the combined organics were dried through a hydrophobic frit and concentrated *in vacuo* to give crude 6'-(8-oxa-3-azabicyclo[3.2.1]octan-3-yl)-4'-(cyclopentylsulfonyl)-[2,2'-bipyridin]-5-amine (118 mg, 0.23 mmol, quant.) as a yellow amorphous solid. LCMS (Formic, UV, ESI):

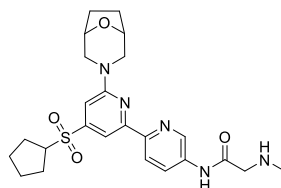
$R_t = 0.68$ min, $[M+H^+]$ 415.33, 85% purity. Used without purification in subsequent reaction.

***tert*-Butyl (2-((6'-(8-oxa-3-azabicyclo[3.2.1]octan-3-yl)-4'-(cyclopentylsulfonyl)-[2,2'-bipyridin]-5-yl)amino)-2-oxoethyl)(methyl)carbamate** (precursor to compound **116**)



To a solution of HATU (106 mg, 0.28 mmol) and *N*-(*tert*-butoxycarbonyl)-*N*-methylglycine (53 mg, 0.28 mmol) in DMF (0.8 mL) was added DIPEA (0.07 mL, 0.37 mmol) and the mixture was stirred at 21 °C for 10 min. A solution of 6'-(8-oxa-3-azabicyclo[3.2.1]octan-3-yl)-4'-(cyclopentylsulfonyl)-[2,2'-bipyridin]-5-amine (96 mg, 0.19 mmol) in DMF (2 mL) was added and the resulting mixture was stirred at 70 °C for 2.8 h. HATU (106 mg, 0.28 mmol), *N*-(*tert*-butoxycarbonyl)-*N*-methylglycine (53 mg, 0.28 mmol), DIPEA (0.07 mL, 0.37 mmol) and DMF (0.8 mL) were combined, stirred for 10 min and added to the reaction mixture. The resulting mixture was heated at 70 °C for 1.0 h. The reaction mixture was diluted with ethyl acetate (40 mL) and water (40 mL). The aqueous phase was extracted with ethyl acetate (30 mL, brine (5 mL) added) and the combined organics were washed with water (40 mL, brine (5 mL) added) and brine (40 mL), dried through a hydrophobic frit and concentrated *in vacuo* and then under a flow of nitrogen to give crude *tert*-butyl (2-((6'-(8-oxa-3-azabicyclo[3.2.1]octan-3-yl)-4'-(cyclopentylsulfonyl)-[2,2'-bipyridin]-5-yl)amino)-2-oxoethyl)(methyl)carbamate (231 mg, 0.25 mmol, quant.) as an orange residue. LCMS (Formic, UV, ESI): $R_t = 1.20$ min, $[M+H^+]$ 586.39, 64% purity. Used without purification in subsequent reaction.

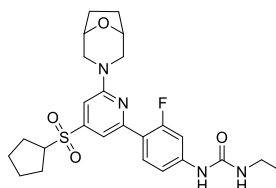
***N*-(6'-8-Oxa-3-azabicyclo[3.2.1]octan-3-yl)-4'-(cyclopentylsulfonyl)-[2,2'-bipyridin]-5-yl)-2-(methylamino)acetamide (116)**



To *tert*-butyl (2-((6'-(8-oxa-3-azabicyclo[3.2.1]octan-3-yl)-4'-(cyclopentylsulfonyl)-[2,2'-bipyridin]-5-yl)amino)-2-oxoethyl)(methyl)carbamate (224 mg, 0.29 mmol) was added 1,4-dioxane (2.2 mL) and HCl (4 M in 1,4-dioxane) (0.36 mL, 1.44 mmol) and the reaction mixture was heated at 90 °C for 7 h. The reaction mixture was diluted with methanol, concentrated *in vacuo*, the residue loaded in methanol onto an aminopropyl SPE (5 g, primed with 2 CV methanol), eluting with methanol (8 CV). The eluent was concentrated *in vacuo* and then under a flow of nitrogen. The residue was dissolved in 1:1 methanol:DMSO (4 x 1 mL) and purified by MDAP (formic acid modifier). Appropriate fractions were combined, concentrated *in vacuo* and the residue loaded in methanol onto an aminopropyl column (5 g, primed with 2 CV methanol), eluting with methanol (6 CV). The eluent was concentrated *in vacuo* and then under a flow of nitrogen. The residue was dissolved in 1:1 methanol:DMSO (1 mL) and purified by MDAP (ammonium hydrogen carbonate modifier). Appropriate fractions were combined and concentrated under a flow of nitrogen, then concentrated *in vacuo* and further dried in the vacuum oven to give *N*-(6'-8-oxa-3-azabicyclo[3.2.1]octan-3-yl)-4'-(cyclopentylsulfonyl)-[2,2'-bipyridin]-5-yl)-2-(methylamino)acetamide (15 mg, 0.03 mmol, 11% yield) as a colourless solid. M.pt.: 144-148 °C. ν_{\max} (cm⁻¹) (Chloroform-*d*): 3270 (w, br., N-H), 2956 (w, N-H), 2871 (w), 1687 (m, C=O), 1587 (m, C=N), 1569 (m), 1513 (s), 1443 (s), 1415 (s), 1304 (m, S=O), 1144 (s, S=O), 729 (s). ¹H NMR (400 MHz, Chloroform-*d*) δ ppm 9.51 (s, 1 H), 8.66 (dd, *J* = 2.6, 0.6 Hz, 1 H), 8.38 (dd, *J* = 8.6, 2.6 Hz, 1 H), 8.31 (dd, *J* = 8.6, 0.6 Hz, 1 H), 8.12 (d, *J* = 1.2 Hz, 1 H), 6.98 (d, *J* = 1.2 Hz, 1 H), 4.52 - 4.60 (m, 2 H), 4.00 (d, *J* = 12.4 Hz, 2 H), 3.57 - 3.69 (m, 1 H), 3.42 (s, 2 H), 3.27 (dd, *J* = 12.4, 2.6 Hz, 2 H), 2.56 (s, 3 H), 2.08 - 2.18 (m, 2 H), 1.99 - 2.06 (m, 2 H), 1.86 - 1.99 (m, 4 H), 1.78 - 1.86 (m, 2 H), 1.59 - 1.66 (m, 2 H) [1 NH not observed]. ¹³C NMR (101 MHz, Chloroform-*d*) δ ppm

170.3 (s, 1 C), 159.8 (s, 1 C), 155.8 (s, 1 C), 150.7 (s, 1 C), 149.7 (s, 1 C), 140.1 (s, 1 C), 135.0 (s, 1 C), 126.7 (s, 1 C), 121.4 (s, 1 C), 107.0 (s, 1 C), 103.6 (s, 1 C), 73.7 (s, 2 C), 63.2 (s, 1 C), 55.0 (s, 2 C), 50.8 (s, 1 C), 36.9 (s, 1 C), 28.1 (s, 2 C), 27.1 (s, 2 C), 25.9 (s, 2 C). LCMS (Formic, UV, ESI): $R_t = 0.63$ min, $[M+H^+]$ 486.32, 97% purity. HRMS: ($C_{24}H_{32}N_5O_4S$) $[M+H^+]$ requires 486.2175, found $[M+H^+]$ 486.2177 (0.4 ppm).

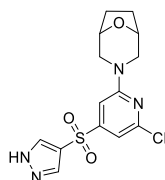
1-(4-(6-(8-Oxa-3-azabicyclo[3.2.1]octan-3-yl)-4-(cyclopentylsulfonyl)pyridin-2-yl)-3-fluorophenyl)-3-ethylurea (117)



Prepared according to general procedure A with 3-(6-chloro-4-(cyclopentylsulfonyl)pyridin-2-yl)-8-oxa-3-azabicyclo[3.2.1]octane (200 mg, 0.55 mmol), 1-ethyl-3-(3-fluoro-4-(4,4,5,5-tetramethyl-1,3,2-dioxaborolan-2-yl)phenyl)urea (186 mg, 0.60 mmol), K_2CO_3 (152 mg, 1.10 mmol), $PdCl_2(dppf)$ (40 mg, 0.06 mmol), IPA (3 mL) and water (0.6 mL), heated at 120 °C for 1 h. The reaction mixture was diluted with ethyl acetate (15 mL) and water (5 mL), filtered through Celite® (2.5 g) and the filtrate was concentrated *in vacuo*. The residue was partitioned between ethyl acetate (15 mL) and water (15 mL). The aqueous phase was extracted with ethyl acetate (2 x 15 mL) and the combined organics were washed with brine (20 mL), dried through a hydrophobic frit and concentrated *in vacuo* and then under a flow of nitrogen. The residue was dissolved in 1:1 methanol:DMSO (4 x 1 mL) and purified by MDAP (ammonium hydrogen carbonate modifier). Appropriate fractions were combined and concentrated *in vacuo* to give 1-(4-(6-(8-oxa-3-azabicyclo[3.2.1]octan-3-yl)-4-(cyclopentylsulfonyl)pyridin-2-yl)-3-fluorophenyl)-3-ethylurea (165 mg, 0.31 mmol, 57% yield) as a pale yellow solid. M.pt.: 157-160 °C. ν_{max} (cm^{-1}) (dichloromethane): 3353 (w, br., N-H), 2966 (w), 1665 (m, C=O), 1579 (m, C=N), 1539 (s), 1304 (m, S=O), 1425 (s), 1226 (s, C-F), 1145 (m, S=O). 1H NMR (400 MHz, $DMSO-d_6$) δ ppm 8.89 (s, 1 H), 7.95 (app. t, $J = 8.6$ Hz, 1 H), 7.62 (dd, $J = 15.0, 1.1$ Hz, 1 H), 7.37 (s, 1 H), 7.12 (br. d, $J = 8.6$ Hz, 1 H), 6.98 (s, 1 H), 6.25

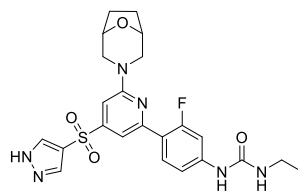
(br. t, $J = 5.0$ Hz, 1 H), 4.47 (br. s, 2 H), 3.99 (br. d, $J = 12.2$ Hz, 2 H), 3.86 - 3.96 (m, 1 H), 3.04 - 3.18 (m, 4 H), 1.82 - 1.95 (m, 6 H), 1.74 - 1.82 (m, 2 H), 1.62 - 1.71 (m, 2 H), 1.54 - 1.62 (m, 2 H), 1.06 (br. t, $J = 7.2$ Hz, 3 H). ^{13}C NMR (101 MHz, $\text{DMSO-}d_6$) δ ppm 160.6 (d, $J = 247.2$ Hz, 1 C), 159.6 (s, 1 C), 154.6 (s, 1 C), 151.7 (d, $J = 2.9$ Hz, 1 C), 149.0 (s, 1 C), 143.5 (d, $J = 12.5$ Hz, 1 C), 130.6 (d, $J = 4.4$ Hz, 1 C), 117.8 (d, $J = 11.0$ Hz, 1 C), 113.5 (s, 1 C), 108.5 (d, $J = 13.2$ Hz, 1 C), 104.4 (d, $J = 28.6$ Hz, 1 C), 102.2 (s, 1 C), 72.7 (s, 2 C), 61.8 (s, 1 C), 50.2 (s, 2 C), 33.9 (s, 1 C), 27.6 (s, 2 C), 26.5 (s, 2 C), 25.5 (s, 2 C), 15.2 (s, 1 C). ^{19}F NMR (376 MHz, $\text{DMSO-}d_6$) δ ppm -114.0 (s, 1 F). LCMS (Formic, UV, ESI): $R_t = 1.14$ min [$\text{M}+\text{H}^+$] 503.27 100% purity. HRMS: ($\text{C}_{25}\text{H}_{32}\text{FN}_4\text{O}_4\text{S}$) [$\text{M}+\text{H}^+$] requires 503.2128, found [$\text{M}+\text{H}^+$] 503.2129 (0.2 ppm).

3-(4-((1*H*-Pyrazol-4-yl)sulfonyl)-6-chloropyridin-2-yl)-8-oxa-3-azabicyclo[3.2.1]octane (119)



4-((1*H*-Pyrazol-4-yl)sulfonyl)-2,6-dichloropyridine (200 mg, 0.719 mmol), 8-oxa-3-azabicyclo[3.2.1]octane hydrochloride (113 mg, 0.76 mmol), DIPEA (0.25 mL, 1.44 mmol) and DMSO (3 mL) were heated at 100 °C for 3.5 h. The reaction mixture was diluted with ethyl acetate (20 mL) and washed with water (20 mL). The aqueous phase was extracted with ethyl acetate (20 mL) and the combined organics were washed with water (20 mL) and brine (30 mL), dried through a hydrophobic frit and concentrated *in vacuo* and then under a flow of nitrogen to give crude 3-(4-((1*H*-pyrazol-4-yl)sulfonyl)-6-chloropyridin-2-yl)-8-oxa-3-azabicyclo[3.2.1]octane (264 mg, 0.62 mmol, 86% yield) as a yellow/orange solid. LCMS (Formic, UV, ESI): $R_t = 0.93$ min, [$\text{M}+\text{H}^+$] 355.08, 357.09 (Cl isotopes), 83% purity. ^1H NMR (400 MHz, $\text{Chloroform-}d$) δ ppm 8.03 (s, 2 H), 6.95 (d, $J = 1.0$ Hz, 1 H), 6.91 (d, $J = 1.0$ Hz, 1 H), 4.48 - 4.53 (m, 2 H), 3.84 (br. d, $J = 12.4$ Hz, 2 H), 3.21 (dd, $J = 12.4, 2.4$ Hz, 2 H), 1.97 - 2.02 (m, 2 H), 1.79 - 1.85 (m, 2 H). [1 N-H not observed].

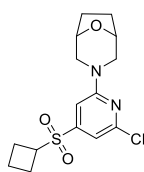
1-(4-(4-((1*H*-Pyrazol-4-yl)sulfonyl)-6-(8-oxa-3-azabicyclo[3.2.1]octan-3-yl)pyridin-2-yl)-3-fluorophenyl)-3-ethylurea (120)



Prepared according to general procedure A with 3-(4-((1*H*-pyrazol-4-yl)sulfonyl)-6-chloropyridin-2-yl)-8-oxa-3-azabicyclo[3.2.1]octane (100 mg, 0.23 mmol), 1-ethyl-3-(3-fluoro-4-(4,4,5,5-tetramethyl-1,3,2-dioxaborolan-2-yl)phenyl)urea (79 mg, 0.26 mmol), K_2CO_3 (65 mg, 0.47 mmol), $PdCl_2(dppf)$ (17 mg, 0.023 mmol), IPA (1.5 mL) and water (0.3 mL), heated at 100 °C for 5 h. The reaction mixture was diluted with ethyl acetate (15 mL) and water (5 mL), filtered through Celite® (2.5 g) and the filtrate concentrated *in vacuo*. The residue was partitioned between ethyl acetate (15 mL) and water (15 mL). The aqueous phase was extracted with ethyl acetate (2 x 15 mL) and the combined organics were washed with brine (20 mL), dried through a hydrophobic frit and concentrated *in vacuo* and then under a flow of nitrogen. The residue was dissolved in 1:1 methanol:DMSO (2 x 1 mL) and purified by MDAP (ammonium hydrogen carbonate modifier). Appropriate fractions were combined and concentrated *in vacuo* and then under a flow of nitrogen. The residue was preabsorbed onto Florisil® and purified by flash chromatography (silica, 24 g), eluting with 0-100% ethyl acetate in cyclohexane over 16 CV. Appropriate fractions were combined and concentrated *in vacuo* and then under a flow of nitrogen to give 1-(4-(4-((1*H*-pyrazol-4-yl)sulfonyl)-6-(8-oxa-3-azabicyclo[3.2.1]octan-3-yl)pyridin-2-yl)-3-fluorophenyl)-3-ethylurea (10 mg, 0.02 mmol, 8% yield) as a colourless solid. M.pt.: 160-164 °C. ν_{max} (cm^{-1}) (Chloroform-*d*): 3124 (w, br., N-H), 2970 (w), 2851 (w), 1665 (w, C=O), 1579 (m, C=N), 1539 (s), 1425 (m), 1316 (m, S=O), 1237 (m, C-F), 1144 (m, S=O). 1H NMR (400 MHz, DMSO-*d*₆) δ ppm 8.96 (s, 1 H), 8.33 (s, 2 H), 7.89 (app. t, $J = 8.6$ Hz, 1 H), 7.61 (dd, $J = 15.0, 1.6$ Hz, 1 H), 7.38 (s, 1 H), 7.11 (dd, $J = 8.6, 1.6$ Hz, 1 H), 7.03 (s, 1 H), 6.27 - 6.36 (m, 1 H), 4.46 (br. s, 2 H), 3.97 (br. d, $J = 12.7$ Hz, 2 H), 3.04 - 3.14 (m, 4 H), 1.72 - 1.87 (m, 4 H), 1.06 (t, $J = 7.2$ Hz, 3 H). ^{13}C NMR (101 MHz, DMSO-*d*₆) δ ppm 160.5 (d, $J = 246.5$ Hz, 1 C), 159.6 (s,

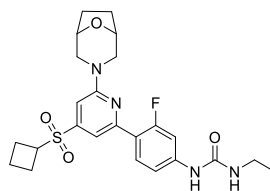
1 C), 154.6 (s, 1 C), 152.9 (s, 1 C), 151.9 (d, $J = 2.9$ Hz, 1 C), 143.6 (d, $J = 12.5$ Hz, 1 C), 135.7 (s, 2 C), 130.5 (d, $J = 4.4$ Hz, 1 C), 121.4 (s, 1 C), 117.8 (d, $J = 11.0$ Hz, 1 C), 113.4 (s, 1 C), 107.2 (d, $J = 12.5$ Hz, 1 C), 104.3 (d, $J = 29.3$ Hz, 1 C), 100.5 (s, 1 C), 72.7 (s, 2 C), 50.2 (s, 2 C), 33.9 (s, 1 C), 27.6 (s, 2 C), 15.3 (s, 1 C). ^{19}F NMR (376 MHz, $\text{DMSO-}d_6$) δ ppm -114.0 (s, 1 F). LCMS (Formic, UV, ESI): $R_t = 0.93$ min, $[\text{M}+\text{H}^+]$ 501.35, 99% purity. HRMS: ($\text{C}_{23}\text{H}_{26}\text{FN}_6\text{O}_4\text{S}$) $[\text{M}+\text{H}^+]$ requires 501.1720, found $[\text{M}+\text{H}^+]$ 501.1722 (0.4 ppm).

3-(6-Chloro-4-(cyclobutylsulfonyl)pyridin-2-yl)-8-oxa-3-azabicyclo[3.2.1]octane (122)



2,6-Dichloro-4-(cyclobutylsulfonyl)pyridine (200 mg, 0.75 mmol), 8-oxa-3-azabicyclo[3.2.1]octane hydrochloride (118 mg, 0.79 mmol), DIPEA (0.26 mL, 1.50 mmol) and DMSO (3 mL) were heated at 100 °C for 4 h. The reaction mixture was diluted with ethyl acetate (20 mL) and washed with water (20 mL). The aqueous phase was extracted with ethyl acetate (20 mL) and the combined organics were washed with water (20 mL) and brine (30 mL), dried through a hydrophobic frit and concentrated *in vacuo* and then under a flow of nitrogen to give 3-(6-chloro-4-(cyclobutylsulfonyl)pyridin-2-yl)-8-oxa-3-azabicyclo[3.2.1]octane (259 mg, 0.75 mmol, quant.) as a brown solid. M.pt.: 125-127 °C. ν_{max} (cm^{-1}) (Chloroform-*d*): 3095 (w), 2952 (w), 2854 (w), 1579 (s, C=N), 1446 (s), 1314 (s, S=O), 1155 (s), 1134 (s, S=O), 982 (s), 578 (s). ^1H NMR (400 MHz, Chloroform-*d*) δ ppm 6.93 (d, $J = 1.0$ Hz, 1 H), 6.79 (d, $J = 1.0$ Hz, 1 H), 4.47 - 4.54 (m, 2 H), 3.78 - 3.88 (m, 3 H), 3.21 (dd, $J = 12.5, 2.7$ Hz, 2 H), 2.52 - 2.64 (m, 2 H), 2.19 - 2.29 (m, 2 H), 1.97 - 2.10 (m, 4 H), 1.78 - 1.84 (m, 2 H). ^{13}C NMR (101 MHz, Chloroform-*d*) δ ppm 159.9 (s, 1 C), 151.0 (s, 1 C), 149.9 (s, 1 C), 109.0 (s, 1 C), 102.2 (s, 1 C), 73.4 (s, 2 C), 56.4 (s, 1 C), 50.6 (s, 2 C), 27.9 (s, 2 C), 22.7 (s, 2 C), 17.0 (s, 1 C). LCMS (Formic, UV, ESI): $R_t = 1.13$ min, $[\text{M}+\text{H}^+]$ 343.14, 345.13 (Cl isotopes), 99% purity. HRMS: ($\text{C}_{15}\text{H}_{20}\text{ClN}_2\text{O}_3\text{S}$) $[\text{M}+\text{H}^+]$ requires 343.0883, found $[\text{M}+\text{H}^+]$ 343.0884 (0.3 ppm).

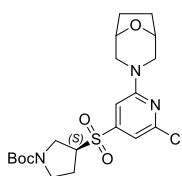
1-(4-(6-(8-Oxa-3-azabicyclo[3.2.1]octan-3-yl)-4-(cyclobutylsulfonyl)pyridin-2-yl)-3-fluorophenyl)-3-ethylurea (123)



Prepared according to general procedure A with 3-(6-chloro-4-(cyclobutylsulfonyl)pyridin-2-yl)-8-oxa-3-azabicyclo[3.2.1]octane (100 mg, 0.29 mmol), 1-ethyl-3-(3-fluoro-4-(4,4,5,5-tetramethyl-1,3,2-dioxaborolan-2-yl)phenyl)urea (99 mg, 0.32 mmol), K_2CO_3 (105 mg, 0.76 mmol), $PdCl_2(dppf)$ (21 mg, 0.029 mmol), IPA (1.5 mL) and water (0.3 mL), heated at 100 °C for 1.5 h. The reaction mixture was diluted with ethyl acetate (15 mL) and water (5 mL) and filtered through Celite® (2.5 g). The filtrate was washed with water (15 mL) and the combined aqueous phases were extracted with ethyl acetate (15 mL). The combined organics were washed with brine (20 mL), dried through a hydrophobic frit and concentrated *in vacuo* and then under a flow of nitrogen. The residue was dissolved in 1:1 methanol:DMSO (2 x 1 mL) and purified by MDAP (ammonium hydrogen carbonate modifier). Appropriate fractions were combined and concentrated *in vacuo* and then under a flow of nitrogen. The residue was dissolved in 1:1 methanol:DMSO (1 mL) and purified by MDAP (ammonium hydrogen carbonate modifier). Appropriate fractions were combined, concentrated under a flow of nitrogen and then *in vacuo* to give 1-(4-(6-(8-oxa-3-azabicyclo[3.2.1]octan-3-yl)-4-(cyclobutylsulfonyl)pyridin-2-yl)-3-fluorophenyl)-3-ethylurea (60 mg, 0.12 mmol, 42% yield) as an off-white solid. M.pt.: 152-154 °C. ν_{max} (cm^{-1}) (Chloroform-*d*): 3358 (w, br., N-H), 2953 (w), 1664 (w, C=O), 1578 (m, C=N), 1535 (s), 1425 (s), 1313 (m, S=O), 1224 (s, C-F), 1144 (s, S=O), 729 (s). 1H NMR (400 MHz, Chloroform-*d*) δ ppm 7.91 (app. br. t, $J = 8.1$ Hz, 1 H), 7.44 (s, 1 H), 7.36 (br. d, $J = 13.7$ Hz, 1 H), 7.01 - 7.19 (m, 2 H), 6.85 (s, 1 H), 5.12 (br. s, 1 H), 4.53 (app. br. s, 2 H), 3.84 - 3.99 (m, 3 H), 3.27 - 3.36 (m, 2 H), 3.22 (br. d, $J = 11.2$ Hz, 2 H), 2.55 - 2.69 (m, 2 H), 2.20 - 2.32 (m, 2 H), 1.92 - 2.09 (m, 4 H), 1.86 (br. d, $J = 6.6$ Hz, 2 H), 1.18 (br. t, $J = 7.0$ Hz, 3 H). ^{13}C NMR (101 MHz, Chloroform-*d*) δ ppm 161.3 (d, $J = 245.8$, 1 C),

159.7 (s, 1 C), 154.9 (s, 1 C), 152.8 (s, 1 C), 148.0 (s, 1 C), 142.1 (d, $J = 12.5$ Hz, 1 C), 131.0 (d, $J = 2.9$ Hz, 1 C), 119.6 (d, $J = 13.2$ Hz, 1 C), 114.5 (s, 1 C), 109.8 (d, $J = 2.2$ Hz, 1 C), 106.6 (d, $J = 29.3$ Hz, 1 C), 102.0 (s, 1 C), 73.6 (s, 2 C), 56.4 (s, 2 C), 50.7 (s, 1 C), 35.2 (s, 1 C), 28.0 (s, 2 C), 22.8 (s, 2 C), 17.0 (s, 1 C), 15.3 (s, 1 C). ^{19}F (376 MHz, Chloroform-*d*) δ ppm -113.0 (s, 1 F). LCMS (Formic, UV, ESI) $R_t = 1.08$ min, $[\text{M}+\text{H}^+]$ 489.29, 100% purity. HRMS: ($\text{C}_{24}\text{H}_{30}\text{FN}_4\text{O}_4\text{S}$) $[\text{M}+\text{H}^+]$ requires 489.1972, found $[\text{M}+\text{H}^+]$ 489.1972 (0 ppm).

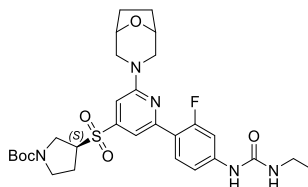
***tert*-Butyl (3*S*)-3-((2-(8-oxa-3-azabicyclo[3.2.1]octan-3-yl)-6-chloropyridin-4-yl)sulfonyl)pyrrolidine-1-carboxylate (125a)**



tert-Butyl (3*S*)-3-((2,6-dichloropyridin-4-yl)sulfonyl)pyrrolidine-1-carboxylate (837 mg, 2.20 mmol), 8-oxa-3-azabicyclo[3.2.1]octane hydrochloride (347 mg, 2.32 mmol), DIPEA (0.77 mL, 4.43 mmol) and DMSO (7 mL) were heated at 100 °C for 1.5 h. The reaction mixture was diluted with ethyl acetate (20 mL) and washed with water (20 mL). The aqueous phase was extracted with ethyl acetate (2 x 15 mL) and the combined organics were washed with water (2 x 30 mL) and brine (50 mL), dried through a hydrophobic frit and concentrated *in vacuo* and then under a flow of nitrogen to give *tert*-butyl (3*S*)-3-((2-(8-oxa-3-azabicyclo[3.2.1]octan-3-yl)-6-chloropyridin-4-yl)sulfonyl)pyrrolidine-1-carboxylate (987 mg, 2.13 mmol, 97% yield) as a brown solid. ν_{max} (cm^{-1}) (Chloroform-*d*): 2976 (w), 1694 (s, C=O), 1582 (w, C=N), 1538 (s), 1449 (m), 1407 (s), 1329 (s, S=O), 1163 (s), 1138 (m, S=O). ^1H NMR (400 MHz, Chloroform-*d*) δ ppm 6.96 (app. br. s, 1 H), 6.80 (d, $J = 1.2$ Hz, 1 H), 4.47 - 4.55 (m, 2 H), 3.84 (br. d, $J = 12.5$ Hz, 2 H), 3.65 - 3.77 (m, 2 H), 3.61 (br. s, 2 H), 3.36 - 3.44 (m, 1 H), 3.23 (dd, $J = 12.5, 2.6$ Hz, 2 H), 2.10 - 2.57 (m, 2 H), 1.95 - 2.04 (m, 2 H), 1.78 - 1.86 (m, 2 H), 1.45 (s, 9 H). ^{13}C NMR (101 MHz, Chloroform-*d*) δ ppm 180.9 (s, 1 C), 159.9 (s, 1 C), 151.4 (s, 1 C), 149.5 (s, 1 C), 121.3 (s, 1 C), 102.4 (s, 1 C), 80.2 (s, 1 C), 73.3 (s, 2 C), 61.8 (s, 1 C), 50.6 (s, 2 C), 45.9 (s, 1 C), 45.0 (s, 1 C), 28.4 (s, 3 C), 27.9 (s, 2 C), 25.8 (s, 1 C). LCMS (Formic, UV, ESI):

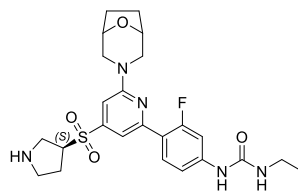
$R_t = 1.25$ min, $[M+H^+]$ 458.23, 460.25 (Cl isotopes), 99% purity. HRMS: ($C_{16}H_{21}ClN_3O_5S$) $[M+H^+]$ requires 402.0890, found $[M+H^+]$ 402.0887 (-0.7 ppm).

***tert*-Butyl (3*S*)-3-((2-(8-oxa-3-azabicyclo[3.2.1]octan-3-yl)-6-(4-(3-ethylureido)-2-fluorophenyl)pyridin-4-yl)sulfonyl)pyrrolidine-1-carboxylate (126a)**



Prepared according to general procedure A with *tert*-butyl (3*S*)-3-((2-(8-oxa-3-azabicyclo[3.2.1]octan-3-yl)-6-chloropyridin-4-yl)sulfonyl)pyrrolidine-1-carboxylate (712 mg, 1.56 mmol), 1-ethyl-3-(3-fluoro-4-(4,4,5,5-tetramethyl-1,3,2-dioxaborolan-2-yl)phenyl)urea (527 mg, 1.71 mmol), K_2CO_3 (430 mg, 3.11 mmol), $PdCl_2(dppf)$ (114 mg, 0.16 mmol), IPA (8 mL) and water (1.6 mL), heated at 120 °C for 6 h. The reaction mixture was diluted with ethyl acetate (20 mL) and water (15 mL), filtered through Celite® (2.5 g) and the filtrate concentrated *in vacuo*. The residue was partitioned between ethyl acetate (20 mL) and water (20 mL). The aqueous phase was extracted with ethyl acetate (2 x 20 mL) and the combined organics were washed with brine (30 mL), dried through a hydrophobic frit and concentrated *in vacuo* and then under a flow of nitrogen to give crude *tert*-butyl (3*S*)-3-((2-(8-oxa-3-azabicyclo[3.2.1]octan-3-yl)-6-(4-(3-ethylureido)-2-fluorophenyl)pyridin-4-yl)sulfonyl)pyrrolidine-1-carboxylate (1270 mg, 1.81 mmol, quant.) as a brown solid. LCMS (Formic, UV, ESI): $R_t = 1.19$ min, $[M+H^+]$ 604.37, 86% purity. Used without purification in subsequent reaction.

1-(4-(6-(8-Oxa-3-azabicyclo[3.2.1]octan-3-yl)-4-(((S)-pyrrolidin-3-yl)sulfonyl)pyridin-2-yl)-3-fluorophenyl)-3-ethylurea (127a)

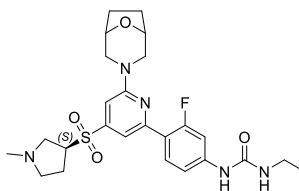


To *tert*-butyl (3*S*)-3-((2-(8-oxa-3-azabicyclo[3.2.1]octan-3-yl)-6-(4-(3-ethylureido)-2-fluorophenyl)pyridin-4-yl)sulfonyl)pyrrolidine-1-carboxylate (814 mg, 1.16 mmol) was added 1,4-dioxane (7 mL) and HCl (4 M in 1,4-dioxane) (0.87 mL, 3.48 mmol) and the reaction mixture was heated at 80 °C for 5 h. The reaction mixture was diluted with methanol, concentrated *in vacuo* and the residue loaded in methanol onto an aminopropyl SPE (5 g, primed with 2 CV methanol), eluting with 6 CV methanol. The eluent was concentrated *in vacuo* and then under a flow of nitrogen. 95 mg of crude material was dissolved in 1:1 methanol:DMSO (1 mL) and purified by MDAP (ammonium hydrogen carbonate modifier). Appropriate fractions were combined and concentrated *in vacuo* and then under a flow of nitrogen. The residue was dissolved in DMSO (2 x 1 mL) and purified by MDAP (formic acid modifier). Appropriate fractions were combined and concentrated *in vacuo* and then under a flow of nitrogen. The residue was diluted with water (15 mL) and ethyl acetate (15 mL) and saturated aqueous sodium hydrogen carbonate solution added to achieve pH 8. The aqueous phase was extracted with ethyl acetate (15 mL x 2), the combined organics were dried through a hydrophobic frit and concentrated *in vacuo* and then under a flow of nitrogen. The residue was loaded in methanol onto a SCX SPE (1 g, primed with 2 CV methanol), eluting with methanol (5 CV), followed by ammonia solution (2 M in methanol) (5 CV). Appropriate fractions were combined and concentrated *in vacuo* and then under a flow of nitrogen. The residue was loaded in methanol onto a SCX SPE (10 g, primed with 2 CV methanol), eluting with methanol (14 CV), followed by ammonia solution (2 M in methanol) (6 CV). Appropriate fractions were combined and concentrated *in vacuo*. The residue was dissolved in 1:1 methanol:DMSO (1 mL) and purified by MDAP (formic acid modifier). Appropriate fractions were combined, dichloromethane (20 mL) added and the organics were removed *in vacuo*. To the

resulting aqueous phase was added saturated aqueous sodium bicarbonate solution to achieve pH 7. The aqueous phase was extracted with dichloromethane (5 x 20 mL), the combined organics were dried through a hydrophobic frit and concentrated *in vacuo* and then under a flow of nitrogen to give 1-(4-(6-(8-oxa-3-azabicyclo[3.2.1]octan-3-yl)-4-(((S)-pyrrolidin-3-yl)sulfonyl)pyridin-2-yl)-3-fluorophenyl)-3-ethylurea (49 mg, 0.09 mmol, 8% yield) as an off-white solid. M.pt.: 191-193 °C. $[\alpha_D]^{20}$ °C (1 g/100 mL, methanol): -63.9°. ν_{\max} (cm⁻¹) (Chloroform-*d*): 3341 (w, br., N-H), 2925 (w), 2851 (w), 1671 (w, N=O), 1579 (m, C=N), 1541 (s), 1426 (m), 1311 (m, S=O), 1242 (m, C-F), 1145 (m, S=O). ¹H NMR (600 MHz, DMSO-*d*₆) δ ppm 8.95 (br. s, 1 H), 7.96 (app. t, *J* = 8.9 Hz, 1 H), 7.64 (dd, *J* = 15.2, 2.0 Hz, 1 H), 7.39 (s, 1 H), 7.12 (dd, *J* = 8.9, 2.0 Hz, 1 H), 7.02 (s, 1 H), 6.29 (br. s, 1 H), 4.45 - 4.51 (m, 2 H), 4.22 (br. s, 1 H), 4.01 (br. d, *J* = 12.5 Hz, 2 H), 3.26 - 3.28 (m, 2 H), 3.06 - 3.15 (m, 5 H), 3.01 (br. d, *J* = 7.3 Hz, 1 H), 2.07 - 2.18 (m, 2 H), 1.83 - 1.89 (m, 2 H), 1.74 - 1.80 (m, 2 H), 1.06 (t, *J* = 7.2 Hz, 3 H) [one N-H not observed]. ¹³C NMR (151 MHz, DMSO-*d*₆) δ ppm 159.6 (s, 1 C), 154.6 (s, 1 C), 135.0 (s, 1 C), 130.6 (s, 1 C), 122.1 (s, 1 C), 111.8 (s, 1 C), 109.5 (s, 1 C), 72.7 (s, 2 C), 61.0 (s, 1 C), 50.3 (s, 2 C), 46.3 (s, 2 C), 33.9 (s, 1 C), 27.6 (s, 1 C), 26.6 (s, 2 C), 15.3 (s, 1 C) [weak spectrum and no *J* coupling, 5 C not observed]. ¹⁹F (376 MHz, Chloroform-*d*) δ ppm -112.8 (s, 1 F). LCMS (Formic, UV, ESI): *R*_t = 0.66 min, [M+H⁺] 504.28, 97% purity. LCMS (Formic, UV, ESI): *R*_t = 0.66 min, [M+H⁺] 504.28, 97% purity. HRMS: C₂₄H₃₁FN₅O₄S [M+H⁺] requires 504.2081, found [M+H⁺] 504.2080 (-0.2 ppm).

The remaining crude material (approx. 475 mg) was dissolved in minimal dichloromethane and purified by flash chromatography (silica, 40 g), eluting with 50-100% ethyl acetate in cyclohexane, followed by 0-30% 3:1 ethyl acetate:ethanol in ethyl acetate followed by 0-100% 3:1 ethyl acetate:ethanol in ethyl acetate over 7 CV, followed by 100% 3:1 ethyl acetate:ethanol over 26 CV. Appropriate fractions were combined and concentrated *in vacuo* to give crude 1-(4-(6-(8-oxa-3-azabicyclo[3.2.1]octan-3-yl)-4-(((S)-pyrrolidin-3-yl)sulfonyl)pyridin-2-yl)-3-fluorophenyl)-3-ethylurea (355 mg, 0.56 mmol, 48% yield) as a brown foam. LCMS (Formic, UV, ESI): *R*_t = 0.66 min, [M+H⁺] 504.28, 79% purity. Used without purification in subsequent reaction.

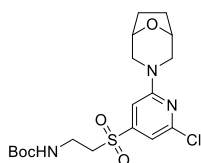
1-(4-(6-(8-Oxa-3-azabicyclo[3.2.1]octan-3-yl)-4-(((S)-1-methylpyrrolidin-3-yl)sulfonyl)pyridin-2-yl)-3-fluorophenyl)-3-ethylurea (128a)



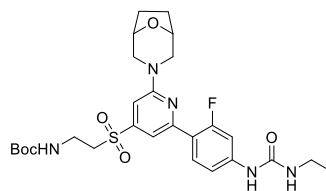
Based on literature procedure.¹⁴⁵ Formaldehyde (37% in water) (49 μ l, 0.66 mmol) was added dropwise to a solution of 1-(4-(6-(8-oxa-3-azabicyclo[3.2.1]octan-3-yl)-4-(((S)-pyrrolidin-3-yl)sulfonyl)pyridin-2-yl)-3-fluorophenyl)-3-ethylurea (351 mg, 0.55 mmol) and formic acid (800 μ l, 20.9 mmol) in water (0.8 mL) and the mixture heated at 90 °C for 1 h. The reaction mixture was partitioned between water (20 mL) and ethyl acetate (20 mL). Sodium hydroxide (1 M in water) was added to the aqueous phase to achieve pH 7, followed by extracting with ethyl acetate (2 x 20 mL). The combined organics were dried through a hydrophobic frit and concentrated *in vacuo* and then under a flow of nitrogen. The residue was dissolved in 1:1 methanol:DMSO (2 x 1 mL) and purified by MDAP (formic acid modifier). Appropriate fractions were combined and concentrated *in vacuo*, dissolved in methanol and loaded onto an aminopropyl SPE (10 g, primed with 3 CV methanol), eluting with methanol (6 CV). The eluent was concentrated *in vacuo* and then under a flow of nitrogen to give 1-(4-(6-(8-oxa-3-azabicyclo[3.2.1]octan-3-yl)-4-(((S)-1-methylpyrrolidin-3-yl)sulfonyl)pyridin-2-yl)-3-fluorophenyl)-3-ethylurea (64 mg, 0.12 mmol, 22% yield) as a pale yellow solid. M.pt.: 177-180 °C. ν_{\max} (cm^{-1}) (Chloroform-*d*): 3356 (w, br., N-H), 2968 (w), 2851 (w), 1599 (m), 1579 (m, C=N), 1541 (s), 1426 (m), 1317 (m, S=O), 1226 (m, C-F), 1147 (m, S=O). ^1H NMR (400 MHz, Chloroform-*d*) δ ppm 7.93 (app. t, $J = 8.6$ Hz, 1 H), 7.48 (s, 1 H), 7.36 (dd, $J = 13.8, 2.1$ Hz, 1 H), 7.13 (dd, $J = 8.6, 2.1$ Hz, 1 H), 7.02 (s, 1 H), 6.87 (d, $J = 1.2$ Hz, 1 H), 5.08 (br. t, $J = 5.5$ Hz, 1 H), 4.50 - 4.56 (m, 2 H), 3.94 (br. d, $J = 12.2$ Hz, 2 H), 3.76 - 3.89 (m, 1 H), 3.32 (qd, $J = 7.2, 5.5$ Hz, 2 H), 3.23 (br. d, $J = 12.2$ Hz, 2 H), 2.97 (br. d, $J = 7.3$ Hz, 2 H), 2.71 - 2.82 (m, 1 H), 2.64 - 2.71 (m, 1 H), 2.42 (s, 3 H), 2.33 - 2.41 (m, 1 H), 2.13 - 2.24 (m, 1 H), 1.97 - 2.03 (m, 2 H), 1.82 - 1.89 (m, 2 H), 1.19 (t, $J = 7.2$ Hz, 3 H). ^{13}C NMR (101 MHz, Chloroform-*d*) δ ppm 162.6 (d, $J = 249.4$ Hz, 1 C), 159.8 (s,

1 C), 154.8 (s, 1 C), 153.2 (s, 1 C), 131.0 (d, $J = 4.4$ Hz, 1 C), 114.6 (d, $J = 3.7$ Hz, 1 C), 109.8 (s, 1 C), 106.6 (d, $J = 28.6$ Hz, 1 C), 102.1 (s, 1 C), 73.6 (s, 2 C), 62.2 (s, 1 C), 55.6 (s, 1 C), 55.6 (s, 1 C), 50.7 (s, 2 C), 41.5 (s, 1 C), 35.2 (s, 1 C), 28.1 (s, 2 C), 26.2 (s, 1 C), 15.3 (s, 1 C). ^{19}F NMR (376 MHz, Chloroform-*d*) δ ppm -113.0 (s, 1 F). LCMS (Formic, UV, ESI): $R_t = 0.67$ min, $[\text{M}+\text{H}^+]$ 518.29, 100% purity. HRMS: ($\text{C}_{25}\text{H}_{33}\text{FN}_5\text{O}_4\text{S}$) $[\text{M}+\text{H}^+]$ requires 518.2237, found $[\text{M}+\text{H}^+]$ 518.2238 (0.1 ppm).

***tert*-Butyl (2-((2-(8-oxa-3-azabicyclo[3.2.1]octan-3-yl)-6-chloropyridin-4-yl)sulfonyl)ethyl)carbamate (130)**

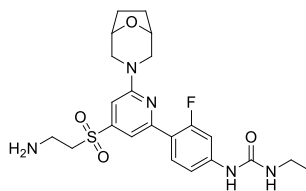


tert-Butyl (2-((2,6-dichloropyridin-4-yl)sulfonyl)ethyl)carbamate (1.00 g, 2.82 mmol), 8-oxa-3-azabicyclo[3.2.1]octane hydrochloride (0.46 g, 3.07 mmol), DIPEA (1.0 mL, 5.73 mmol) and DMSO (2 mL) were heated at 100 °C for 2 h. The reaction mixture was partitioned between ethyl acetate (10 mL) and water (10 mL). The aqueous phase was extracted with ethyl acetate (10 mL) and the combined organics were washed with water (10 mL) and brine (10 mL), dried through a hydrophobic frit and concentrated *in vacuo* to give *tert*-butyl (2-((2-(8-oxa-3-azabicyclo[3.2.1]octan-3-yl)-6-chloropyridin-4-yl)sulfonyl)ethyl)-carbamate (1.05 g, 2.38 mmol, 85% yield) as a yellow solid. M.pt.: 195-198 °C. ν_{max} (cm^{-1}) (Chloroform-*d*): 3389 (w, br., N-H), 2978 (w), 1709 (m, C=O), 1583 (s, C=N), 1449 (m), 1327 (m, S=O), 1252 (m, C-F), 1162 (s, S=O). ^1H NMR (400 MHz, Chloroform-*d*) δ ppm 6.97 (d, $J = 1.0$ Hz, 1 H), 6.82 (d, $J = 1.0$ Hz, 1 H), 5.08 (br. s, 1 H), 4.48 - 4.54 (m, 2 H), 3.85 (br. d, $J = 12.7$ Hz, 2 H), 3.59 (app. q, $J = 5.9$ Hz, 2 H), 3.34 (t, $J = 5.9$ Hz, 2 H), 3.23 (dd, $J = 12.7, 2.7$ Hz, 2 H), 1.98 - 2.04 (m, 2 H), 1.80 - 1.85 (m, 2 H), 1.42 (s, 9 H). ^{13}C NMR (101 MHz, Chloroform-*d*) δ ppm 160.0 (s, 1 C), 155.5 (s, 1 C), 151.3 (s, 1 C), 150.8 (s, 1 C), 108.5 (s, 1 C), 101.8 (s, 1 C), 80.2 (s, 1 C), 73.3 (s, 2 C), 55.4 (s, 1 C), 50.6 (s, 2 C), 34.6 (s, 1 C), 28.3 (s, 3 C), 27.9 (s, 2 C). LCMS (Formic, UV, ESI): $R_t = 1.16$ min, $[\text{M}+\text{H}^+]$ 432.23, 434.24 (Cl isotopes), 99% purity. HRMS: ($\text{C}_{18}\text{H}_{27}\text{ClN}_3\text{O}_5\text{S}$) $[\text{M}+\text{H}^+]$ requires 432.1360, found $[\text{M}+\text{H}^+]$ 432.1355 (-1.2 ppm).

***tert*-Butyl (2-((2-(8-oxa-3-azabicyclo[3.2.1]octan-3-yl)-6-(4-(3-ethylureido)-2-fluorophenyl)pyridin-4-yl)sulfonyl)ethyl)carbamate (precursor to compound 131)**

Prepared according to general procedure A with *tert*-butyl (2-((2-(8-oxa-3-azabicyclo[3.2.1]octan-3-yl)-6-chloropyridin-4-yl)sulfonyl)ethyl)carbamate (150 mg, 0.35 mmol), 1-ethyl-3-(3-fluoro-4-(4,4,5,5-tetramethyl-1,3,2-dioxaborolan-2-yl)phenyl)urea (118 mg, 0.38 mmol), K₂CO₃ (96 mg, 0.70 mmol), PdCl₂(dppf) (25 mg, 0.04 mmol), IPA (2 mL) and water (0.4 mL), heated at 140 °C for 2 h. The reaction mixture was diluted with ethyl acetate (10 mL) and water (5 mL), filtered through Celite® (2.5 g) and the filtrate was concentrated *in vacuo*. The residue was partitioned between ethyl acetate (10 mL) and water (10 mL). The aqueous phase was extracted with ethyl acetate (2 x 10 mL) and the combined organics were washed with brine (20 mL), dried through a hydrophobic frit and concentrated *in vacuo* and then under a flow of nitrogen to give crude *tert*-butyl (2-((2-(8-oxa-3-azabicyclo[3.2.1]octan-3-yl)-6-(4-(3-ethylureido)-2-fluorophenyl)pyridin-4-yl)sulfonyl)ethyl)carbamate (221 mg, 0.34 mmol, 97% yield) as a brown solid. LCMS (Formic, UV, ESI): R_t = 1.11 min, [M+H⁺] 578.12, 88% purity. ¹H NMR (400 MHz, Chloroform-*d*) δ ppm 7.96 (app. t, *J* = 8.6 Hz, 1 H), 7.51 (s, 1 H), 7.41 (dd, *J* = 13.7, 2.0 Hz, 1 H), 7.09 (dd, *J* = 8.6, 2.0 Hz, 1 H), 6.88 (d, *J* = 1.0 Hz, 1 H), 6.67 (br. s, 1 H), 5.16 (br. s, 1 H), 4.83 (br. s, 1 H), 4.50 - 4.57 (m, 2 H), 3.96 (d, *J* = 12.2 Hz, 2 H), 3.61 (br. d, *J* = 5.4 Hz, 2 H), 3.32 - 3.39 (m, 4 H), 3.25 (dd, *J* = 12.2, 2.4 Hz, 2 H), 1.97 - 2.04 (m, 2 H), 1.84 - 1.90 (m, 2 H), 1.41 (s, 9 H), 1.20 (t, *J* = 7.3 Hz, 3 H).

1-(4-(4-((2-Aminoethyl)sulfonyl)-6-(8-oxa-3-azabicyclo[3.2.1]octan-3-yl)pyridin-2-yl)-3-fluorophenyl)-3-ethylurea (131)

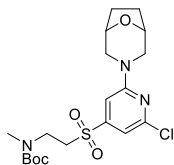


To *tert*-butyl (2-((2-(8-oxa-3-azabicyclo[3.2.1]octan-3-yl)-6-(4-(3-ethylureido)-2-fluorophenyl)pyridin-4-yl)sulfonyl)ethyl) carbamate (218 mg, 0.33 mmol) was added 1,4-dioxane (3 mL) and HCl (4 M in 1,4-dioxane) (0.1 mL, 0.40 mmol) and the reaction mixture was heated at 40 °C for 4 h. HCl (4 M in 1,4-dioxane) (0.1 mL, 0.40 mmol) was added and the mixture heated at 40 °C for 16 h. HCl (4 M in 1,4-dioxane) (0.1 mL, 0.40 mmol) was added and the mixture heated at 40 °C for 5.5 h before further HCl (4 M in 1,4-dioxane) (0.1 mL, 0.40 mmol) was added and the mixture stood at 21 °C for 64 h. The reaction mixture was diluted with methanol and concentrated *in vacuo*. The residue was loaded in methanol onto an aminopropyl SPE (5 g, primed with 2 CV methanol), eluting with methanol (4 CV). The eluent was concentrated *in vacuo* and then under a flow of nitrogen. The residue was dissolved in 1:1 methanol:DMSO (2 x 1 mL) and purified by MDAP (ammonium hydrogen carbonate modifier). Appropriate fractions were combined and concentrated *in vacuo* and then under a flow of nitrogen. The residue was dissolved in DMSO (5.1 mL) and purified by MDAP (TFA modifier).^h Appropriate fractions were combined, concentrated aqueous ammonium hydroxide solution was added to achieve pH 9 and the resulting mixture was concentrated *in vacuo* and then under a flow of nitrogen. The residue was dissolved in ethyl acetate (10 mL), the organic phase was washed with water (2 x 10 mL), brine (10 mL) and water (2 x 10 mL), dried through a hydrophobic frit and concentrated *in vacuo*. The combined aqueous phases were extracted with ethyl acetate (30 mL), saturated aqueous sodium hydrogen carbonate solution was added to the

^h Final MDAP purification (TFA modifier) by A. Hobbs (Discovery Analytical Purification Team). MDAP purification was carried out using a Waters ZQ mass spectrometer using positive electrospray ionisation and a summed UV wavelength of 210–350 nm. TFA: Zorbax SB C₈ column (150 mm x 30 mm, 5 µm packing diameter, 40 mL/min flow rate), using a gradient elution at ambient temperature with the mobile phases as (A) H₂O containing 0.1% (v/v) TFA and (B) acetonitrile containing 0.1% (v/v) TFA.

aqueous to achieve pH 10 and the aqueous was extracted with ethyl acetate (30 mL). The combined organics were dried through a hydrophobic frit, concentrated *in vacuo* and then under a flow of nitrogen and further dried in a vacuum oven to give 1-(4-(4-((2-aminoethyl)sulfonyl)-6-(8-oxa-3-azabicyclo[3.2.1]octan-3-yl)pyridin-2-yl)-3-fluorophenyl)-3-ethylurea (51 mg, 0.11 mmol, 32% yield) as a pale yellow solid. M.pt.: 217-218 °C. ν_{\max} (cm^{-1}) (dichloromethane): 3364 (w, br., N-H), 2924 (w, N-H), 2851 (w), 1673 (w, C=O), 1584 (m, C=N), 1541 (s), 1425 (m), 1226 (m, C-F), 1147 (m, S=O). ^1H NMR (400 MHz, DMSO- d_6) δ ppm 8.97 (s, 1 H), 7.96 (app. t, $J = 8.9$ Hz, 1 H), 7.64 (dd, $J = 15.2, 2.0$ Hz, 1 H), 7.39 (app. s, 1 H), 7.13 (dd, $J = 8.9, 2.0$ Hz, 1 H), 7.02 (d, $J = 1.0$ Hz, 1 H), 6.34 (t, $J = 5.5$ Hz, 1 H), 4.42 - 4.55 (m, 2 H), 4.01 (d, $J = 12.5$ Hz, 2 H), 3.56 (t, $J = 6.8$ Hz, 2 H), 3.06 - 3.17 (m, 4 H), 2.99 (t, $J = 6.8$ Hz, 2 H), 1.81 - 1.90 (m, 2 H), 1.72 - 1.81 (m, 2 H), 1.06 (t, $J = 7.2$ Hz, 3 H) [2 N-H not observed]. ^{13}C NMR (101 MHz, DMSO- d_6) δ ppm 159.6 (s, 1 C), 158.6 (d, $J = 151.9$, 1 C), 154.6 (s, 1 C), 151.9 (s, 1 C), 148.8 (s, 1 C), 143.6 (s, 1 C), 130.6 (d, $J = 3.7$ Hz, 1 C), 117.7 (d, $J = 11.0$ Hz, 1 C), 113.5 (s, 1 C), 108.0 (d, $J = 12.5$ Hz, 1 C), 104.3 (d, $J = 29.3$ Hz, 1 C), 102.0 (s, 1 C), 72.7 (s, 2 C), 54.4 (s, 1 C), 50.3 (s, 2 C), 34.5 (s, 1 C), 33.9 (s, 1 C), 27.6 (s, 2 C), 15.3 (s, 1 C). ^{19}F (376 MHz, Chloroform- d) δ ppm -113.8 (s, 1 F). LCMS (Formic, UV, ESI): $R_t = 0.64$ min, $[\text{M}+\text{H}^+]$ 478.29, 98% purity. HRMS: ($\text{C}_{22}\text{H}_{29}\text{FN}_5\text{O}_4\text{S}$) $[\text{M}+\text{H}^+]$ requires 478.1924, found $[\text{M}+\text{H}^+]$ 478.1924 (0 ppm).

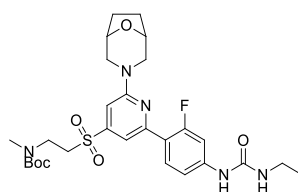
***tert*-Butyl (2-((2-(8-oxa-3-azabicyclo[3.2.1]octan-3-yl)-6-chloropyridin-4-yl)sulfonyl)ethyl)(methyl)carbamate (132)**



Based on literature procedure.¹⁴⁶ Prepared according to general procedure B with *tert*-butyl (2-((2-(8-oxa-3-azabicyclo[3.2.1]octan-3-yl)-6-chloropyridin-4-yl)sulfonyl)ethyl)carbamate (300 mg, 0.70 mmol), THF (3 mL) and sodium hydride (60% dispersion in mineral oil) (28 mg, 0.70 mmol), stirred for 1.3 h before iodomethane (65 μL , 1.04 mmol) was added and the mixture stirred at 21 °C for 25 h.

The reaction mixture was diluted with water (10 mL) and ethyl acetate (10 mL). The aqueous phase was extracted with ethyl acetate (2 x 15 mL) and the combined organics were washed with brine (30 mL), dried through a hydrophobic frit and concentrated *in vacuo* and then under a flow of nitrogen. The residue was dissolved in minimal dichloromethane and purified by flash chromatography (silica, 40 g), eluting with 0-100% ethyl acetate in cyclohexane over 16 CV. Appropriate fractions were combined and concentrated *in vacuo* and then under a flow of nitrogen to give crude *tert*-butyl (2-((2-(8-oxa-3-azabicyclo[3.2.1]octan-3-yl)-6-chloropyridin-4-yl)sulfonyl)ethyl)(methyl)carbamate (207 mg, 0.29 mmol, 42%) as a colourless solid. LCMS (Formic, UV, ESI): $R_t = 1.24$ min, $[M+H]^+$ 446.23, 448.21 (Cl isotopes), 63% purity. Used without purification in subsequent reaction.

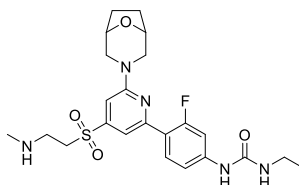
***tert*-Butyl (2-((2-(8-oxa-3-azabicyclo[3.2.1]octan-3-yl)-6-(4-(3-ethylureido)-2-fluorophenyl)pyridin-4-yl)sulfonyl)ethyl)(methyl)carbamate** (precursor to compound **133**)



Prepared according to general procedure A with *tert*-butyl (2-((2-(8-oxa-3-azabicyclo[3.2.1]octan-3-yl)-6-chloropyridin-4-yl)sulfonyl)ethyl)(methyl)carbamate (200 mg, 0.28 mmol), 1-ethyl-3-(3-fluoro-4-(4,4,5,5-tetramethyl-1,3,2-dioxaborolan-2-yl)phenyl)urea (131 mg, 0.42 mmol), K_2CO_3 (78 mg, 0.57 mmol), $PdCl_2(dppf)$ (21 mg, 0.03 mmol), IPA (2 mL) and water (0.4 mL), heated at 120 °C for 4.5 h. The mixture was allowed to cool, further 1-ethyl-3-(3-fluoro-4-(4,4,5,5-tetramethyl-1,3,2-dioxaborolan-2-yl)phenyl)urea (131 mg, 0.42 mmol) and $PdCl_2(dppf)$ (21 mg, 0.03 mmol) added, the mixture was degassed by purging under vacuum and filling with nitrogen (x 3) and heated at 120 °C for 7.0 h. The reaction mixture was diluted with ethyl acetate (10 mL) and water (5 mL), filtered through Celite® (2.5 g) and the filtrate was concentrated *in vacuo*. The residue was partitioned between ethyl acetate (10 mL) and water (10 mL). The aqueous phase was extracted with ethyl acetate (2 x 10 mL) and the combined organics were washed with brine (20 mL), dried through a

hydrophobic frit and concentrated *in vacuo* and then under a flow of nitrogen. The residue was dissolved in minimal dichloromethane and purified by flash chromatography (silica, 80 g), eluting with 20-100% ethyl acetate in cyclohexane over 16 CV. Appropriate fractions were combined and concentrated *in vacuo* and then under a flow of nitrogen to give crude *tert*-butyl (2-((2-(8-oxa-3-azabicyclo[3.2.1]octan-3-yl)-6-(4-(3-ethylureido)-2-fluorophenyl)pyridin-4-yl)sulfonyl)ethyl)(methyl)carbamate (245 mg, 0.22 mmol, 79% yield) as an orange amorphous solid. LCMS (Formic, UV, ESI) $R_t = 1.17$ min, $[M+H]^+$ 592.34, 54% purity. Used without purification in subsequent reaction.

1-(4-(6-(8-Oxa-3-azabicyclo[3.2.1]octan-3-yl)-4-((2-(methylamino)ethyl)sulfonyl)pyridin-2-yl)-3-fluorophenyl)-3-ethylurea (133)

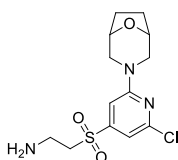


To *tert*-butyl (2-((2-(8-oxa-3-azabicyclo[3.2.1]octan-3-yl)-6-(4-(3-ethylureido)-2-fluorophenyl)pyridin-4-yl)sulfonyl)ethyl) (methyl)carbamate (280 mg, 0.26 mmol) was added 1,4-dioxane (3 mL) and HCl (4 M in 1,4-dioxane) (0.33 mL, 1.30 mmol) and the reaction mixture was heated at 80 °C for 4 h. The reaction mixture was diluted with methanol and concentrated *in vacuo*. The residue was loaded in methanol onto an aminopropyl SPE (10 g, primed with 2 CV methanol), eluting with methanol (5 CV). The eluent was concentrated *in vacuo* and then under a flow of nitrogen. The residue was dissolved in DMSO (10.9 mL) and purified by MDAP (TFA modifier). Appropriate fractions were combined, concentrated aqueous ammonium hydroxide solution was added to achieve pH 9 and the resulting mixture was concentrated *in vacuo* (using a Biotage V-10 evaporator). The residue was dissolved in DMSO (8.3 mL) and purified by MDAP (TFA modifier).ⁱ Appropriate fractions were

ⁱ MDAP purifications (TFA modifier) by A. Hobbs (Discovery Analytical Purification Team). MDAP purification was carried out using a Waters ZQ mass spectrometer using positive electrospray ionisation and a summed UV wavelength of 210–350 nm. TFA: Zorbax SB C₈ column (150 mm x 30 mm, 5 μm packing diameter, 40 mL/min flow rate), using a gradient elution at ambient temperature with the mobile phases as (A) H₂O containing 0.1% (v/v) TFA and (B) acetonitrile containing 0.1% (v/v) TFA.

combined, concentrated aqueous ammonium hydroxide solution was added to achieve pH 9 and the organic solvent was removed *in vacuo*. The resulting aqueous phase was extracted with dichloromethane (3 x 20 mL), the combined organics were dried through a hydrophobic frit and concentrated *in vacuo* and then under a flow of nitrogen. The residue was triturated with cyclohexane (3 x 2 mL) and the residue was dried under a flow of nitrogen to give 1-(4-(6-(8-oxa-3-azabicyclo[3.2.1]octan-3-yl)-4-((2-(methylamino)ethyl)sulfonyl)pyridin-2-yl)-3-fluorophenyl)-3-ethylurea (22 mg, 0.04 mmol, 17% yield) as an off-white solid. M.pt.: 167-169 °C. ν_{\max} (cm⁻¹) (Chloroform-*d*): 3338 (w, br., N-H), 2966 (w), 2853 (w), 1668 (m, C=O), 1580 (s, C=N), 1541 (s), 1425 (s), 1315 (m, S=O), 1226 (s, C-F), 1145 (s, S=O). ¹H NMR (600 MHz, Chloroform-*d*) δ ppm 7.96 (app. t, *J* = 8.6 Hz, 1 H), 7.52 (s, 1 H), 7.39 (dd, *J* = 13.6, 1.8 Hz, 1 H), 7.10 (dd, *J* = 8.6, 1.8 Hz, 1 H), 6.90 (s, 1 H), 6.57 (br. s, 1 H), 4.77 (br. s, 1 H), 4.52 - 4.55 (m, 2 H), 3.95 (br. d, *J* = 12.5 Hz, 2 H), 3.30 - 3.39 (m, 4 H), 3.24 (dd, *J* = 12.5, 2.2 Hz, 2 H), 3.08 (t, *J* = 6.4 Hz, 2 H), 2.45 (s, 3 H), 1.98 - 2.03 (m, 2 H), 1.83 - 1.89 (m, 2 H), 1.21 (t, *J* = 7.2 Hz, 3 H). [1 N-H not observed]. ¹³C NMR (151 MHz, Chloroform-*d*) δ ppm 159.8 (s, 1 C), 131.1 (s, 1 C), 114.7 (s, 1 C), 109.4 (s, 1 C), 106.9 (d, *J* = 27.6 Hz, 1 C), 101.8 (s, 1 C), 73.6 (s, 2 C), 50.7 (s, 1 C), 44.8 (s, 2 C), 36.0 (s, 1 C), 35.4 (s, 1 C), 29.7 (s, 1 C), 28.0 (s, 2 C), 15.3 (s, 1 C) [weak sample, not all *J* couplings observed and 6 C not observed]. ¹⁹F (376 MHz, Chloroform-*d*) δ ppm -112.7 (s, 1 F). LCMS (Formic, UV, ESI): *R*_t = 0.63 min, [M+H⁺] 492.29, 97% purity. HRMS: (C₂₃H₃₁FN₅O₄S) [M+H⁺] requires 492.2081, found [M+H⁺] 492.2081 (0 ppm).

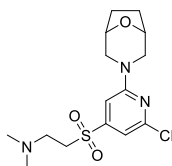
2-((2-(8-Oxa-3-azabicyclo[3.2.1]octan-3-yl)-6-chloropyridin-4-yl)sulfonyl)ethan-1-amine (precursor to compound **134**)



To *tert*-butyl (2-((2-(8-oxa-3-azabicyclo[3.2.1]octan-3-yl)-6-chloropyridin-4-yl)sulfonyl)ethyl)carbamate (52 mg, 0.12 mmol) was added 1,4-dioxane (1 mL) and HCl (4 M in 1,4-dioxane) (0.1 mL, 0.40 mmol) and the reaction mixture was heated at

80 °C for 5.5 h. The reaction mixture was diluted with methanol, concentrated *in vacuo* and loaded in methanol onto an aminopropyl SPE (5 g, primed with 3 CV methanol), eluting with methanol (5 CV). The eluent was concentrated *in vacuo* and then under a flow of nitrogen to give 2-((2-(8-oxa-3-azabicyclo[3.2.1]octan-3-yl)-6-chloropyridin-4-yl)sulfonyl)ethan-1-amine (40 mg, 0.12 mmol, quant.) as an orange amorphous solid. ν_{\max} (cm⁻¹) (Chloroform-*d*): 3373 (w, N-H), 3096 (w), 2959 (w), 2854 (w), 1582 (s, C=N), 1537 (m), 1447 (s), 1311 (s, S=O), 1156 (s), 1136 (s, S=O), 982 (s). ¹H NMR (400 MHz, Chloroform-*d*) δ ppm 6.98 (d, *J* = 1.0 Hz, 1 H), 6.83 (d, *J* = 1.0 Hz, 1 H), 4.46 - 4.54 (m, 2 H), 3.84 (br. d, *J* = 12.2 Hz, 2 H), 3.13 - 3.27 (m, 6 H), 1.96 - 2.02 (m, 2 H), 1.78 - 1.83 (m, 2 H) [2 N-H not observed]. ¹³C NMR (101 MHz, Chloroform-*d*) δ ppm 159.9 (s, 1 C), 151.2 (s, 1 C), 150.9 (s, 1 C), 108.6 (s, 1 C), 101.8 (s, 1 C), 73.3 (s, 2 C), 58.7 (s, 1 C), 50.6 (s, 2 C), 36.0 (s, 1 C), 27.9 (s, 2 C). LCMS (Formic, UV, ESI): *R*_t = 0.55 min, [M+H⁺] 332.10, 334.07 (Cl isotopes), 100% purity. HRMS: (C₁₃H₁₉ClN₃O₃S) [M+H⁺] 332.0836, found [M+H⁺] 332.0833 (-0.9 ppm).

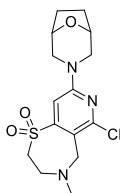
2-((2-(8-Oxa-3-azabicyclo[3.2.1]octan-3-yl)-6-chloropyridin-4-yl)sulfonyl)-*N,N*-dimethylethan-1-amine (134)



Based on literature procedure.¹⁴⁵ Formaldehyde (226 μ l, 3.04 mmol) (37% in water) was added dropwise to a stirred solution of 2-((2-(8-oxa-3-azabicyclo[3.2.1]octan-3-yl)-6-chloropyridin-4-yl)sulfonyl)ethan-1-amine (252 mg, 0.76 mmol) and formic acid (408 μ l, 10.63 mmol) and the reaction mixture heated at 90 °C for 2 h. The reaction mixture was concentrated *in vacuo* and partitioned between water (20 mL) and ethyl acetate (20 mL). Sodium hydroxide (1 M in water) was added to the aqueous phase to achieve approx. pH 7 and the aqueous phase was extracted with ethyl acetate (2 x 20 mL). The combined organics were dried through a hydrophobic frit and concentrated *in vacuo* and then under a flow of nitrogen. The residue was dissolved in 1:1 methanol:DMSO (2 x 1 mL) and purified by MDAP (ammonium hydrogen carbonate modifier). Appropriate fractions were combined, concentrated *in vacuo* and

then under a flow of nitrogen to give 2-((2-(8-oxa-3-azabicyclo[3.2.1]octan-3-yl)-6-chloropyridin-4-yl)sulfonyl)-*N,N*-dimethylethan-1-amine (70 mg, 0.19 mmol, 31% yield) as an off-white solid. M.pt.: 124-126 °C. ν_{\max} (cm⁻¹) (Chloroform-*d*): 2952 (w), 2856 (w), 2772 (w), 1584 (s, C=N), 1539 (m), 1449 (m), 1320 (m, S=O), 1160 (m), 1141 (m, S=O). ¹H NMR (400 MHz, Chloroform-*d*) δ ppm 7.00 (d, *J* = 1.0 Hz, 1 H), 6.85 (d, *J* = 1.0 Hz, 1 H), 4.47 - 4.56 (m, 2 H), 3.85 (br. d, *J* = 12.5 Hz, 2 H), 3.29 (t, *J* = 7.3 Hz, 2 H), 3.23 (dd, *J* = 12.5, 2.7 Hz, 2 H), 2.78 (t, *J* = 7.3 Hz, 2 H), 2.24 (s, 6 H), 1.97 - 2.03 (m, 2 H), 1.78 - 1.85 (m, 2 H). ¹³C NMR (101 MHz, Chloroform-*d*) δ ppm 159.9 (s, 1 C), 151.1 (s, 2 C), 108.8 (s, 1 C), 102.0 (s, 1 C), 73.4 (s, 2 C), 53.4 (s, 1 C), 51.9 (s, 1 C), 50.7 (s, 2 C), 44.9 (s, 2 C), 27.9 (s, 2 C). LCMS (Formic, UV, ESI): *R*_t = 0.58 min [M+H⁺] 360.15, 362.14 (Cl isotopes), 96% purity. HRMS: (C₁₅H₂₃ClN₃O₃S) [M+H⁺] requires 360.1149, found [M+H⁺] 360.1144 (-1.4 ppm).

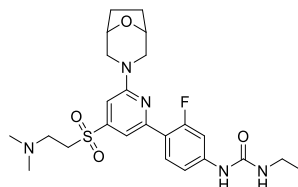
8-(8-Oxa-3-azabicyclo[3.2.1]octan-3-yl)-6-chloro-4-methyl-2,3,4,5-tetrahydropyrido[3,4-*f*][1,4]thiazepine 1,1-dioxide (141)



Additionally, appropriate fractions were concentrated under nitrogen to give 8-(8-oxa-3-azabicyclo[3.2.1]octan-3-yl)-6-chloro-4-methyl-2,3,4,5-tetrahydropyrido[3,4-*f*][1,4]thiazepine 1,1-dioxide (mass not determined) as a colourless solid. M.pt.: 193-195 °C. ν_{\max} (cm⁻¹) (dichloromethane): 2952 (w., br.), 2852 (w), 1587 (s, C=N), 1449 (m), 1311 (s, S=O), 1140 (s, S=O), 1004 (m), 733 (m, C-Cl), 530 (m). ¹H NMR (600 MHz, Chloroform-*d*) δ ppm 7.08 (s, 1 H), 4.49 - 4.53 (m, 2 H), 4.39 (s, 2 H), 3.85 (br. d, *J* = 12.5 Hz, 2 H), 3.44 (br. s, 2 H), 3.34 (br. s, 2 H), 3.22 (dd, *J* = 12.5, 2.6 Hz, 2 H), 2.36 (s, 3 H), 1.98 - 2.02 (m, 2 H), 1.80 - 1.83 (m, 2 H). ¹³C NMR (151 MHz, Chloroform-*d*) δ ppm 158.1 (s, 1 C), 152.1 (s, 1 C), 151.8 (s, 1 C), 110.0 (s, 1 C), 102.9 (s, 1 C), 73.4 (s, 2 C), 53.8 (s, 1 C), 52.9 (s, 1 C), 52.6 (s, 1 C), 50.5 (s, 2 C), 39.7 (s, 1 C), 27.9 (s, 2 C). LCMS (Formic, UV, ESI): *R*_t = 0.52 min [M+H⁺] 358.16, 360.11

(Cl isotopes), 100% purity. HRMS: (C₁₅H₂₁ClN₃O₃S) [M+H⁺] requires 358.0992, found [M+H⁺] 358.0993 (0.3 ppm).^j

1-(4-(6-(8-Oxa-3-azabicyclo[3.2.1]octan-3-yl)-4-((2-(dimethylamino)ethyl)sulfonyl)pyridin-2-yl)-3-fluorophenyl)-3-ethylurea (135)

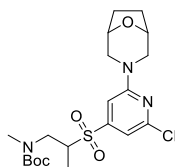


Prepared according to general procedure A with 2-((2-(8-oxa-3-azabicyclo[3.2.1]octan-3-yl)-6-chloropyridin-4-yl)sulfonyl)-*N,N*-dimethylethan-1-amine (65 mg, 0.17 mmol), 1-ethyl-3-(3-fluoro-4-(4,4,5,5-tetramethyl-1,3,2-dioxaborolan-2-yl)phenyl)urea (59 mg, 0.19 mmol), K₂CO₃ (48 mg, 0.35 mmol), PdCl₂(dppf) (13 mg, 0.017 mmol), IPA (1 mL) and water (0.2 mL), heated at 120 °C for 2 h. The reaction mixture was diluted with ethyl acetate (15 mL) and water (5 mL), filtered through Celite® (2.5 g) and the filtrate was concentrated *in vacuo*. The residue was partitioned between ethyl acetate (15 mL) and water (15 mL). The aqueous phase was extracted with ethyl acetate (2 x 15 mL) and the combined organics were washed with brine (20 mL), dried through a hydrophobic frit and concentrated *in vacuo* and then under a flow of nitrogen. The residue was dissolved in 1:1 methanol:DMSO (2 x 1 mL) and purified by MDAP (ammonium hydrogen carbonate modifier). Appropriate fractions were combined and concentrated *in vacuo* and then under a flow of nitrogen to give 1-(4-(6-(8-oxa-3-azabicyclo[3.2.1]octan-3-yl)-4-((2-(dimethylamino)ethyl)sulfonyl)pyridin-2-yl)-3-fluorophenyl)-3-ethylurea (34 mg, 0.06 mmol, 36% yield) as a brown solid. M.pt.: 132-135 °C. ν_{\max} (cm⁻¹) (Chloroform-*d*): 3357 (w, br., N-H), 2975 (w), 1671 (w, C=O), 1579 (m, C=N), 1537 (s), 1425 (m), 1317 (m, S=O), 1225 (s, C-F), 1148 (s, S=O). ¹H NMR (400 MHz, Chloroform-*d*) δ ppm 7.94 (app. t, *J* = 8.7 Hz, 1 H), 7.51 (br. s, 1 H), 7.37 (dd, *J* = 13.9, 2.0 Hz, 1 H), 7.12 (dd, *J* = 8.7, 2.0 Hz, 1 H), 6.96 (br. s, 1 H), 6.90 (d, *J* = 1.2 Hz, 1 H), 5.02 (br. s, 1 H), 4.49 - 4.57 (m, 2 H), 3.95 (d, *J* = 12.5 Hz, 2 H), 3.27 - 3.38 (m, 4 H), 3.24 (dd,

^j Structure confirmed by NMR spectroscopist, R. Upton.

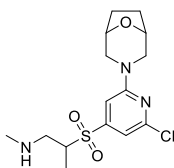
$J = 12.5, 2.4$ Hz, 2 H), 2.81 - 2.87 (m, 2 H), 2.26 (s, 6 H), 1.96 - 2.04 (m, 2 H), 1.80 - 1.90 (m, 2 H), 1.19 (t, $J = 7.2$ Hz, 3 H). ^{13}C NMR (101 MHz, Chloroform-*d*) δ ppm 161.3 (d, $J = 150.2$ Hz, 1 C), 159.8 (s, 1 C), 154.8 (s, 1 C), 152.3 (d, $J = 2.9$ Hz, 1 C), 149.2 (s, 1 C), 142.0 (d, $J = 11.7$ Hz, 1 C), 131.0 (s, 1 C), 120.2 (s, 1 C), 114.6 (d, $J = 2.2$ Hz, 1 C), 109.4 (s, 1 C), 106.7 (d, $J = 28.6$ Hz, 1 C), 101.8 (s, 1 C), 73.6 (s, 2 C), 53.1 (s, 1 C), 51.8 (s, 1 C), 50.7 (s, 2 C), 44.8 (s, 2 C), 35.3 (s, 1 C), 28.0 (s, 2 C), 15.3 (s, 1 C). ^{19}F NMR (376 MHz, Chloroform-*d*) δ ppm -112.9 (s, 1 F). LCMS (Formic, UV, ESI): $R_t = 0.64$ min, $[\text{M}+\text{H}^+]$ 506.29, 97% purity. HRMS: ($\text{C}_{24}\text{H}_{33}\text{FN}_5\text{O}_4\text{S}$) $[\text{M}+\text{H}^+]$ requires 506.2237, found $[\text{M}+\text{H}^+]$ 506.2236 (-0.2 ppm).

***tert*-Butyl (2-((2-(8-oxa-3-azabicyclo[3.2.1]octan-3-yl)-6-chloropyridin-4-yl)sulfonyl)propyl)(methyl)carbamate (136)**



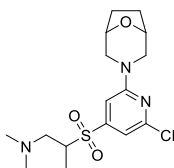
Based on literature procedure.¹⁴⁶ Prepared according to general procedure B with *tert*-butyl (2-((2-(8-oxa-3-azabicyclo[3.2.1]octan-3-yl)-6-chloropyridin-4-yl)sulfonyl)ethyl)carbamate (140 mg, 0.32 mmol), THF (2 mL) and sodium hydride (60% dispersion in mineral oil) (29 mg, 0.71 mmol), stirred for 1.5 h before iodomethane (0.14 mL, 2.27 mmol) was added and the mixture stirred at 21 °C for 22.0 h. The reaction mixture was diluted with water (10 mL) and ethyl acetate (10 mL). The aqueous phase was extracted with ethyl acetate (2 x 10 mL) and the combined organics were washed with brine (20 mL), dried through a hydrophobic frit and concentrated *in vacuo* and then under a flow of nitrogen to give crude *tert*-butyl (2-((2-(8-oxa-3-azabicyclo[3.2.1]octan-3-yl)-6-chloropyridin-4-yl)sulfonyl)propyl)(methyl)carbamate (168 mg, 0.30 mmol, 91% yield) as a yellow solid. LCMS (Formic, UV, ESI): $R_t = 1.30$ min $[\text{M}+\text{H}^+]$ 460.27, 462.22 (Cl isotopes), 81% purity. ^1H NMR (400 MHz, Chloroform-*d*) δ ppm 6.96 (s, 1 H), 6.81 (br. s, 1 H), 4.47 - 4.54 (m, 2 H), 3.86 (br. d, $J = 12.5$ Hz, 2 H), 3.60 - 3.74 (m, 1 H), 3.45 - 3.60 (m, 1 H), 3.31 - 3.45 (m, 1 H), 3.22 (dd, $J = 12.5, 2.2$ Hz, 2 H), 2.89 (s, 3 H), 1.98 - 2.04 (m, 2 H), 1.78 - 1.86 (m, 2 H), 1.42 (s, 9 H), 1.32 (br. s, 3 H).

2-((2-(8-Oxa-3-azabicyclo[3.2.1]octan-3-yl)-6-chloropyridin-4-yl)sulfonyl)-*N*-methylpropan-1-amine (137)



To *tert*-butyl (2-((2-(8-oxa-3-azabicyclo[3.2.1]octan-3-yl)-6-chloropyridin-4-yl)sulfonyl)propyl)(methyl)carbamate (163 mg, 0.29 mmol) was added 1,4-dioxane (2 mL) and HCl (4 M in 1,4-dioxane) (0.2 mL, 0.80 mmol) and the reaction mixture was heated at 90 °C for 5 h. The reaction mixture was diluted with methanol, concentrated *in vacuo* and loaded in methanol onto an aminopropyl SPE (5 g, primed with 2 CV methanol), eluting with methanol (6 CV). The eluent was concentrated *in vacuo* and then under a flow of nitrogen to give crude 2-((2-(8-oxa-3-azabicyclo[3.2.1]octan-3-yl)-6-chloropyridin-4-yl)sulfonyl)-*N*-methylpropan-1-amine (122 mg, 0.28 mmol, 98% yield) as an orange residue. LCMS (Formic, UV, ESI): $R_t = 0.58$ min, $[M+H^+]$ 360.15, 362.12 (Cl isotopes), 83% purity. ^1H NMR (400 MHz, Chloroform-*d*) δ ppm 6.97 (d, $J = 1.0$ Hz, 1 H), 6.80 (d, $J = 1.0$ Hz, 1 H), 4.48 - 4.55 (m, 2 H), 3.85 (br. d, $J = 12.5$ Hz, 2 H), 3.26 - 3.34 (m, 1 H), 3.22 (dd, $J = 12.5, 2.0$ Hz, 2 H), 3.09 - 3.17 (m, 1 H), 2.73 - 2.82 (m, 1 H), 2.44 (s, 3 H), 1.98 - 2.03 (m, 2 H), 1.80 - 1.84 (m, 2 H), 1.32 (d, $J = 7.1$ Hz, 3 H).

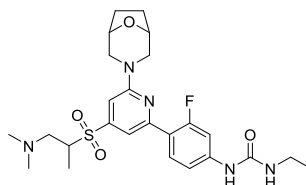
2-((2-(8-Oxa-3-azabicyclo[3.2.1]octan-3-yl)-6-chloropyridin-4-yl)sulfonyl)-*N,N*-dimethylpropan-1-amine (138)



Based on literature procedure.¹⁴⁶ Prepared according to general procedure B with 2-((2-(8-oxa-3-azabicyclo[3.2.1]octan-3-yl)-6-chloropyridin-4-yl)sulfonyl)-*N*-methylpropan-1-amine (118 mg, 0.27 mmol), THF (1.5 mL) and sodium hydride (60% dispersion in mineral oil) (12 mg, 0.30 mmol), stirred for 1.8 h before iodomethane (19 μL , 0.30 mmol) was added and the resulting mixture stirred at 21 °C for 22.0 h.

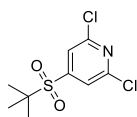
Further sodium hydride (60% dispersion in mineral oil) (2 mg, 0.05 mmol) and iodomethane (3 μ L, 0.05 mmol) were added and the mixture was stirred at 21 °C for 4.5 h. The reaction mixture was diluted with water (10 mL) and ethyl acetate (10 mL). The aqueous phase was extracted with ethyl acetate (2 x 10 mL) and the combined organics were washed with brine (20 mL), dried through a hydrophobic frit and concentrated *in vacuo* and then under a flow of nitrogen. The residue was dissolved in minimal dichloromethane and purified by flash chromatography (silica, 40 g), eluting with 0-100% ethyl acetate in cyclohexane over 8 CV, followed by 100% ethyl acetate for 3 CV, followed by 0-100% 3:1 ethyl acetate:ethanol in ethyl acetate over 10 CV. Appropriate fractions were combined and concentrated *in vacuo* and then under a flow of nitrogen to give 2-((2-(8-oxa-3-azabicyclo[3.2.1]octan-3-yl)-6-chloropyridin-4-yl)sulfonyl)-*N,N*-dimethylpropan-1-amine (36 mg, 0.09 mmol, 35% yield) as an off-white gum. ν_{\max} (cm^{-1}) (dichloromethane): 2951 (w), 2861 (w), 2277 (w), 1583 (s, C=N), 1538 (w), 1448 (m), 1314 (m, S=O), 1137 (m, S=O), 982 (m). ^1H NMR (400 MHz, Chloroform-*d*) δ ppm 6.98 (d, $J = 1.2$ Hz, 1 H), 6.82 (d, $J = 1.2$ Hz, 1 H), 4.48 - 4.55 (m, 2 H), 3.85 (br. d, $J = 12.5$ Hz, 2 H), 3.25 - 3.30 (m, 1 H), 3.22 (dd, $J = 12.5, 2.6$ Hz, 2 H), 2.77 (br. dd, $J = 12.3, 3.9$ Hz, 1 H), 2.46 (br. dd, $J = 12.3, 8.7$ Hz, 1 H), 2.21 (s, 6 H), 1.98 - 2.03 (m, 2 H), 1.79 - 1.86 (m, 2 H), 1.37 (d, $J = 6.8$ Hz, 3 H). ^{13}C NMR (101 MHz, Chloroform-*d*) δ ppm 159.8 (s, 1 C), 150.9 (s, 1 C), 149.9 (s, 1 C), 109.6 (s, 1 C), 102.9 (s, 1 C), 73.4 (s, 2 C), 58.5 (s, 1 C), 58.3 (s, 1 C), 50.7 (s, 2 C), 45.4 (s, 2 C), 27.9 (s, 2 C), 12.5 (s, 1 C). LCMS (Formic, UV, ESI): $R_t = 0.57$ min, $[\text{M}+\text{H}^+]$ 347.21, 376.19 (Cl isotopes), 98% purity. HRMS: ($\text{C}_{16}\text{H}_{25}\text{ClN}_3\text{O}_3\text{S}$) $[\text{M}+\text{H}^+]$ requires 374.1305, found $[\text{M}+\text{H}^+]$ 374.1305 (0.0 ppm).

1-(4-(6-(8-Oxa-3-azabicyclo[3.2.1]octan-3-yl)-4-((1-(dimethylamino)propan-2-yl)sulfonyl)pyridin-2-yl)-3-fluorophenyl)-3-ethylurea (139)

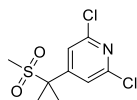


Prepared according to general procedure A with 2-((2-(8-oxa-3-azabicyclo[3.2.1]octan-3-yl)-6-chloropyridin-4-yl)sulfonyl)-*N,N*-dimethylpropan-1-

amine (33 mg, 0.09 mmol), 1-ethyl-3-(3-fluoro-4-(4,4,5,5-tetramethyl-1,3,2-dioxaborolan-2-yl)phenyl)urea (33 mg, 0.11 mmol), K₂CO₃ (30 mg, 0.22 mmol), PdCl₂(dppf) (7 mg, 9.57 μmol), IPA (0.75 mL) and water (0.15 mL), heated at 120 °C for 2.5 h. The reaction mixture was diluted with ethyl acetate (15 mL) and water (5 mL), filtered through Celite® (2.5 g) and the filtrate was concentrated *in vacuo*. The residue was partitioned between ethyl acetate (15 mL) and water (15 mL). The aqueous phase was extracted with ethyl acetate (2 x 15 mL) and the combined organics were washed with brine (20 mL), dried through a hydrophobic frit and concentrated *in vacuo* and then under a flow of nitrogen. The residue was dissolved in 1:1 methanol:DMSO (1 mL) and purified by MDAP (ammonium hydrogen carbonate modifier). Appropriate fractions were combined, concentrated *in vacuo* and then under a flow of nitrogen to give 1-(4-(6-(8-oxa-3-azabicyclo[3.2.1]octan-3-yl)-4-((1-(dimethylamino)propan-2-yl)sulfonyl)pyridin-2-yl)-3-fluorophenyl)-3-ethylurea (14 mg, 0.03 mmol, 30% yield) as an off-white solid. M.pt.: 112-114 °C. ν_{\max} (cm⁻¹) (Chloroform-*d*): 3347 (w, br., N-H), 2975 (w), 2851 (w), 1668 (w, C=O), 1579 (m, C=N), 1537 (s), 1424 (s), 1309 (m, S=O), 1224 (s, C-F), 1141 (m, S=O), 729 (s). ¹H NMR (600 MHz, Chloroform-*d*) δ ppm 7.95 (app. t, *J* = 8.4 Hz, 1 H), 7.49 (s, 1 H), 7.39 (dd, *J* = 13.9, 1.5 Hz, 1 H), 7.14 (dd, *J* = 8.4, 1.5 Hz, 1 H), 6.91 (br. s, 1 H), 6.89 (d, *J* = 1.1 Hz, 1 H), 5.00 (br. s, 1 H), 4.53 - 4.57 (m, 2 H), 3.97 (br. d, *J* = 12.5 Hz, 2 H), 3.31 - 3.40 (m, 3 H), 3.25 (br. d, *J* = 12.5 Hz, 2 H), 2.84 - 2.93 (m, 1 H), 2.53 - 2.61 (m, 1 H), 2.29 (s, 6 H), 2.00 - 2.04 (m, 2 H), 1.86 - 1.91 (m, 2 H), 1.43 (d, *J* = 7.0 Hz, 3 H), 1.21 (t, *J* = 7.2 Hz, 3 H). ¹³C NMR (151 MHz, Chloroform-*d*) δ ppm 161.3 (d, *J* = 250.4 Hz, 1 C), 159.7 (s, 1 C), 154.7 (s, 1 C), 152.7 (d, *J* = 3.3 Hz, 1 C), 147.6 (s, 1 C), 142.0 (d, *J* = 12.2 Hz, 1 C), 131.0 (d, *J* = 3.9 Hz, 1 C), 120.3 (d, *J* = 10.5 Hz, 1 C), 114.6 (d, *J* = 2.8 Hz, 1 C), 110.3 (d, *J* = 12.2 Hz, 1 C), 106.7 (d, *J* = 28.2 Hz, 1 C), 102.7 (s, 1 C), 73.7 (s, 2 C), 58.5 (s, 1 C), 57.9 (s, 1 C), 50.7 (s, 2 C), 45.4 (s, 1 C), 35.3 (s, 1 C), 28.0 (s, 2 C), 15.3 (s, 1 C), 12.7 (s, 1 C). ¹⁹F (376 MHz, Chloroform-*d*) δ ppm -113.0 (s, 1 F). LCMS (Formic, UV, ESI): R_t = 0.65 min, [M+H⁺] 520.30, 96% purity. HRMS: (C₂₅H₃₅FN₅O₄S) [M+H⁺] requires 520.2494 found, [M+H⁺] 520.2394 (0 ppm).

4-(*tert*-Butylsulfonyl)-2,6-dichloropyridine (143)

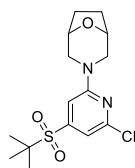
To a solution of 2,6-dichloro-4-(isopropylsulfonyl)pyridine (500 mg, 1.97 mmol) in THF (1.5 mL) under an atmosphere of nitrogen was added sodium *tert*-butoxide (525 μ L, 1.05 mmol) followed by dropwise addition of iodomethane (66 μ L, 1.05 mmol). The resulting mixture was stirred at 21 °C under nitrogen. After 4 h, further sodium *tert*-butoxide (508 μ L, 1.02 mmol) was added, followed by iodomethane (64 μ L, 1.02 mmol) and the resulting mixture was stirred at 21 °C under nitrogen for 30 min. Saturated aqueous ammonium chloride was added (2 mL) and the reaction mixture was stirred at 21 °C for 2 min. The reaction mixture was diluted with water (2 mL) and extracted with ethyl acetate (2 x 10 mL). The combined organics were washed with water (10 mL) and brine (10 mL), dried through a hydrophobic frit and concentrated *in vacuo*. The residue was dissolved in minimal dichloromethane and purified by flash chromatography (silica, 40 g), eluting with 0-100% TBME in cyclohexane over 12 CV followed by 100% TBME for 15 CV. Appropriate fractions were combined and concentrated *in vacuo* and then under a flow of nitrogen to give crude 4-(*tert*-butylsulfonyl)-2,6-dichloropyridine (197 mg, 0.46 mmol, 24% yield) as a colourless oil that solidified slowly. LCMS (Formic, UV, ESI): R_t = 1.30 min, $[M+H^+]$ no clear mass ion, 63% purity. 1H NMR (400 MHz, Chloroform-*d*) δ ppm 6.83 (s, 2 H), 1.51 (s, 9 H).

2,6-Dichloro-4-(2-(methylsulfonyl)propan-2-yl)pyridine (144)

Additionally, appropriate fractions were combined, concentrated *in vacuo* and then under a flow of nitrogen to give 2,6-dichloro-4-(2-(methylsulfonyl)propan-2-yl)pyridine (69 mg, 0.24 mmol, 12% yield) as a colourless solid. M.pt.: 191-195 °C. ν_{max} (cm^{-1}) (Chloroform-*d*): 2980 (w), 2933 (w), 1564 (m), 1545 (m), 1349 (s, S=O), 1176 (s), 1155 (s, S=O), 812 (s). 1H NMR (600 MHz, Chloroform-*d*) δ ppm 7.52 (s,

2 H), 2.69 (s, 3 H), 1.83 (s, 6 H). ^{13}C NMR (151 MHz, Chloroform-*d*) δ ppm 152.4 (s, 1 C), 151.4 (s, 2 C), 122.2 (s, 2 C), 64.0 (s, 1 C), 35.2 (s, 1 C), 22.2 (s, 2 C). LCMS (Formic, UV, ESI): $R_t = 0.89$ min, $[\text{M}+\text{H}^+]$ 268.02, 270.01, 271.97 (Cl isotopes), 95% purity. HRMS: ($\text{C}_9\text{H}_{12}\text{Cl}_2\text{NO}_2\text{S}$) $[\text{M}+\text{H}^+]$ requires 267.9966, found $[\text{M}+\text{H}^+]$ 267.9961 (-1.9 ppm).^k

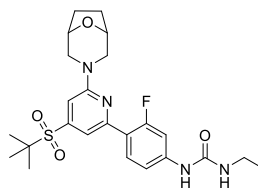
3-(4-(*tert*-Butylsulfonyl)-6-chloropyridin-2-yl)-8-oxa-3-azabicyclo[3.2.1]octane (145)



4-(*tert*-Butylsulfonyl)-2,6-dichloropyridine (150 mg, 0.39 mmol), 8-oxa-3-azabicyclo[3.2.1]octane hydrochloride (70 mg, 0.47 mmol), DIPEA (0.14 mL, 0.80 mmol) and DMSO (1.5 mL) were heated at 100 °C for 23 h. Further 8-oxa-3-azabicyclo[3.2.1]octane hydrochloride (70 mg, 0.47 mmol) and DIPEA (0.14 mL, 0.80 mmol) were added and the reaction mixture heated at 100 °C for 7 h. The reaction mixture was allowed to cool and diluted with water (10 mL) and ethyl acetate (10 mL). The aqueous phase was extracted with ethyl acetate (2 x 10 mL) and the combined organics were washed with brine (20 mL), dried through a hydrophobic frit and concentrated *in vacuo*. The residue was dissolved in minimal dichloromethane and purified by flash chromatography (silica, 40 g), eluting with 0-100% ethyl acetate in cyclohexane over 14 CV. Appropriate fractions were combined and concentrated *in vacuo* to give crude 3-(4-(*tert*-butylsulfonyl)-6-chloropyridin-2-yl)-8-oxa-3-azabicyclo[3.2.1]octane (32 mg, 0.07 mmol, 19% yield) as an off-white solid. LCMS (Formic, UV, ESI) $R_t = 1.17$ min, $[\text{M}+\text{H}^+]$ 344.98, 346.87 (Cl isotopes), 81% purity. ^1H NMR (400 MHz, Chloroform-*d*) δ ppm 6.98 (d, $J = 1.0$ Hz, 1 H), 6.79 (d, $J = 1.0$ Hz, 1 H), 4.47 - 4.54 (m, 2 H), 3.84 (d, $J = 12.5$ Hz, 2 H), 3.22 (dd, $J = 12.5, 2.7$ Hz, 2 H), 1.98 - 2.03 (m, 2 H), 1.79 - 1.85 (m, 2 H), 1.38 (s, 9 H).

^k Structure confirmed by NMR spectroscopist, R. Upton.

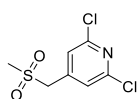
1-(4-(6-(8-Oxa-3-azabicyclo[3.2.1]octan-3-yl)-4-(*tert*-butylsulfonyl)pyridin-2-yl)-3-fluorophenyl)-3-ethylurea (146)



Prepared according to general procedure A with 3-(4-(*tert*-butylsulfonyl)-6-chloropyridin-2-yl)-8-oxa-3-azabicyclo[3.2.1]octane (32 mg, 0.07 mmol), 1-ethyl-3-(3-fluoro-4-(4,4,5,5-tetramethyl-1,3,2-dioxaborolan-2-yl)phenyl)urea (32 mg, 0.10 mmol), K₂CO₃ (21 mg, 0.15 mmol), PdCl₂(dppf) (5 mg, 7.42 μmol), IPA (0.5 mL) and water (0.1 mL), heated at 120 °C for 3 h. The reaction mixture was allowed to cool and further 1-ethyl-3-(3-fluoro-4-(4,4,5,5-tetramethyl-1,3,2-dioxaborolan-2-yl)phenyl)urea (32 mg, 0.10 mmol) and PdCl₂(dppf) (5 mg, 7.42 μmol) were added. The mixture was degassed by purging under vacuum and filling with nitrogen (x 3) and heated at 120 °C for 4 h. The reaction mixture was diluted with ethyl acetate (5 mL) and water (5 mL), filtered through Celite® (2.5 g) and the filtrate was concentrated *in vacuo*. The residue was partitioned between ethyl acetate (10 mL) and water (10 mL). The aqueous phase was extracted with ethyl acetate (2 x 10 mL) and the combined organics were washed with brine (20 mL), dried through a hydrophobic frit and concentrated *in vacuo* and then under a flow of nitrogen. The residue was dissolved in 1:1 methanol:DMSO (1 mL) and purified by MDAP (formic acid modifier). Appropriate fractions were combined and concentrated *in vacuo* and then under a flow of nitrogen to give 1-(4-(6-(8-oxa-3-azabicyclo[3.2.1]octan-3-yl)-4-(*tert*-butylsulfonyl)pyridin-2-yl)-3-fluorophenyl)-3-ethylurea (20 mg, 0.04 mmol, 54% yield) as an off-white amorphous solid. ν_{\max} (cm⁻¹) (Chloroform-*d*): 3369 (w, br., N-H), 2976 (w), 1666 (w, C=O), 1579 (m, C=N), 1541 (s), 1426 (m), 1301 (m, S=O), 1225 (m, C-F), 1135 (m, S=O). ¹H NMR (400 MHz, Chloroform-*d*) δ ppm 7.90 (app. t, *J* = 8.6 Hz, 1 H), 7.48 (s, 1 H), 7.34 (dd, *J* = 13.7, 2.0 Hz, 1 H), 7.13 (dd, *J* = 8.6, 2.0 Hz, 1 H), 7.10 (s, 1 H), 6.84 (s, 1 H), 5.12 (br. s, 1 H), 4.47 - 4.56 (m, 2 H), 3.93 (d, *J* = 12.2 Hz, 2 H), 3.31 (q, *J* = 7.0 Hz, 2 H), 3.23 (dd, *J* = 12.2, 2.4 Hz, 2 H), 1.96 - 2.04 (m, 2 H), 1.84 - 1.90 (m, 2 H), 1.41 (s,

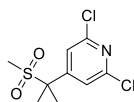
9 H), 1.17 (t, $J = 7.0$ Hz, 3 H). ^{13}C NMR (101 MHz, Chloroform- d) δ ppm 161.3 (d, $J = 250.2$ Hz, 1 C), 159.6 (s, 1 C), 154.9 (s, 1 C), 152.3 (d, $J = 3.7$ Hz, 1 C), 145.3 (s, 1 C), 142.1 (d, $J = 11.7$ Hz, 1 C), 131.0 (d, $J = 3.7$ Hz, 1 C), 120.2 (d, $J = 11.0$ Hz, 1 C), 114.6 (d, $J = 2.2$ Hz, 1 C), 112.4 (d, $J = 12.5$ Hz, 1 C), 106.6 (d, $J = 28.6$ Hz, 1 C), 104.4 (s, 1 C), 73.7 (s, 2 C), 60.4 (s, 1 C), 50.7 (s, 2 C), 35.2 (s, 1 C), 28.1 (s, 2 C), 23.6 (s, 3 C), 15.3 (s, 1 C). ^{19}F (376 MHz, Chloroform- d) δ ppm -113.4 (s, 1 F). LCMS (Formic, UV, ESI): $R_t = 1.13$ min, $[\text{M}+\text{H}^+]$ 491.29, 100% purity. HRMS: ($\text{C}_{24}\text{H}_{32}\text{FN}_4\text{O}_4\text{S}$) $[\text{M}+\text{H}^+]$ requires 491.2128, found $[\text{M}+\text{H}^+]$ 491.2130 (0.4 ppm).

2,6-Dichloro-4-((methylsulfonyl)methyl)pyridine (155)



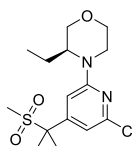
2,6-Dichloro-4-(chloromethyl)pyridine (3.00 g, 15.27 mmol), sodium methanesulfinate (1.88 g, 18.37 mmol) and potassium iodide (0.51 g, 3.08 mmol) were heated to reflux in acetonitrile (69 ml) at 90 °C for 2.5 h. Sodium methanesulfinate (0.47 g, 4.58 mmol) was added and the mixture was heated at 90 °C for 5.0 h. The mixture was diluted with ethyl acetate (90 mL) and washed with water (90 mL). The aqueous phase was extracted with ethyl acetate (50 mL) and the combined organics were washed with brine, dried through a hydrophobic frit and concentrated *in vacuo*. The residue was triturated with ethyl acetate and methanol (x 2), followed by TBME (x 2). The supernatant solution was concentrated *in vacuo* and triturated again with TBME. The solids were combined in dichloromethane and concentrated *in vacuo* to give 2,6-dichloro-4-((methylsulfonyl)methyl)pyridine (2.31 g, 8.67 mmol, 57% yield) as an off-white solid. M.pt.: 155-158 °C. ν_{max} (cm^{-1}) (dichloromethane): 3076 (w), 2988 (w), 1587 (m, C=N), 1547 (s), 1380 (s), 1311 (s, S=O), 1265 (m), 1168 (s), 1120 (s, S=O), 895 (m), 537 (m, C-Cl). ^1H NMR (400 MHz, DMSO- d_6) δ ppm 7.60 (s, 2 H), 4.65 (s, 2 H), 3.02 (s, 3 H). ^{13}C NMR (101 MHz, DMSO- d_6) δ ppm 149.2 (s, 2 C), 144.9 (s, 1 C), 125.3 (s, 2 C), 57.3 (s, 1 C), 40.1 (s, 1 C). LCMS (Formic, UV, ESI): $R_t = 0.72$ min, $[\text{M}+\text{H}^+]$ 240.00, 242.01, 243.99 (Cl isotopes), 99% purity. HRMS: ($\text{C}_7\text{H}_8\text{Cl}_2\text{NO}_2\text{S}$) $[\text{M}+\text{H}^+]$ requires 239.9653, found $[\text{M}+\text{H}^+]$ 239.9651 (-0.8 ppm).

2,6-Dichloro-4-(2-(methylsulfonyl)propan-2-yl)pyridine (144) Alternative preparation.



A stirring solution of 2,6-dichloro-4-((methylsulfonyl)methyl)pyridine (1.20 g, 5.00 mmol) in THF (10 mL) under nitrogen was cooled to 0 °C. Sodium *tert*-butoxide (2 M in THF) (6.25 mL, 12.49 mmol) was added dropwise and the resulting solution was stirred at 0 °C for 2 min. Iodomethane (0.63 mL, 10.00 mmol) was added dropwise over 5 min and the mixture stirred at 0 °C for 2 h. The reaction mixture was quenched by slow addition of saturated aqueous ammonium chloride solution (7 mL) and extracted with ethyl acetate (2 x 40 mL). The combined organics were washed with brine (40 mL), dried through a hydrophobic frit and concentrated *in vacuo* to give 2,6-dichloro-4-(2-(methylsulfonyl)propan-2-yl)pyridine (1.30 g, 3.65 mmol, 73% yield) as a yellow solid. M.pt.: 152-154 °C. ν_{\max} (cm⁻¹) (Chloroform-*d*): 2924 (w), 1580 (m, C=N), 1533 (m), 1377 (m, S=O), 1299 (s), 1164 (m), 1106 (m, S=O), 907 (s), 813 (s), 727 (s, C-Cl). ¹H NMR (400 MHz, Chloroform-*d*) δ ppm 7.51 (s, 2 H), 1.82 (s, 6 H), 2.68 (s, 3 H). ¹³C NMR (101 MHz, Chloroform-*d*) δ ppm 152.4 (s, 1 C), 151.2 (s, 2 C), 122.2 (s, 2 C), 64.0 (s, 1 C), 35.2 (s, 1 C), 22.2 (s, 2 C). LCMS (Formic, UV, ESI): R_t = 0.86 min, [M+H⁺] 268.03, 270.03, 272.00 (Cl isotopes), 61% purity (NMR suggested greater purity). HRMS: (C₉H₁₂Cl₂NO₂S) [M+H⁺] requires 267.9966, found [M+H⁺] 267.9965 (-0.4 ppm).

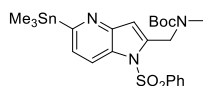
(S)-4-(6-Chloro-4-(2-(methylsulfonyl)propan-2-yl)pyridin-2-yl)-3-ethylmorpholine (156)



2,6-Dichloro-4-(2-(methylsulfonyl)propan-2-yl)pyridine (1.23 g, 4.27 mmol), (*S*)-3-ethylmorpholine hydrochloride (0.78 g, 5.12 mmol), DIPEA (2.2 mL, 12.60 mmol) and DMSO (3 mL) were heated at 160 °C for 19 h. The reaction mixture was diluted with

ethyl acetate (150 mL), washed with water (2 x 50 mL) and brine (50 mL) and the organic phase was dried through a hydrophobic frit and concentrated *in vacuo*. The residue was preabsorbed onto Florisil® and purified by flash chromatography (silica, 120 g), eluting with 0-70% ethyl acetate in cyclohexane over 16 CV. Appropriate fractions were combined and concentrated *in vacuo* to give (*S*)-4-(6-chloro-4-(2-(methylsulfonyl)propan-2-yl)pyridin-2-yl)-3-ethylmorpholine (780 mg, 2.02 mmol, 47% yield) as an orange oil. ν_{\max} (cm⁻¹) (Chloroform-*d*): 2965 (w), 2860 (w), 1591 (s, C=N), 1533 (s), 1453 (m), 1424 (m), 1294 (s, C-N), 1108 (s, S=O), 991 (m), 918 (m), 728 (s, C-Cl), 548 (m). ¹H NMR (400 MHz, Chloroform-*d*) δ ppm 6.74 (s, 1 H), 6.73 (s, 1 H), 3.90 - 4.03 (m, 4 H), 3.64 (dd, *J* = 11.5, 2.7 Hz, 1 H), 3.58 (td, *J* = 12.5, 2.7 Hz, 1 H), 3.22 (td, *J* = 12.5, 3.7 Hz, 1 H), 2.62 (s, 3 H), 1.84 - 1.94 (m, 1 H), 1.78 (s, 6 H), 1.60 - 1.73 (m, 1 H), 0.93 (t, *J* = 7.5 Hz, 3 H). ¹³C NMR (101 MHz, Chloroform-*d*) δ ppm 158.7 (s, 1 C), 150.8 (s, 1 C), 150.4 (s, 1 C), 109.9 (s, 1 C), 103.9 (s, 1 C), 68.0 (s, 1 C), 66.8 (s, 1 C), 64.3 (s, 1 C), 53.8 (s, 1 C), 40.2 (s, 1 C), 35.1 (s, 1 C), 22.2 (s, 1 C), 22.1 (s, 1 C), 20.5 (s, 1 C), 11.1 (s, 1 C). LCMS (Formic, UV, ESI): *R*_t = 1.08 min, [M+H⁺] 347.14, 349.13 (Cl isotopes), 90% purity. HRMS: (C₁₅H₂₄ClN₂O₃S) [M+H⁺] requires 347.1196, found [M+H⁺] 347.1196 (0.0 ppm).

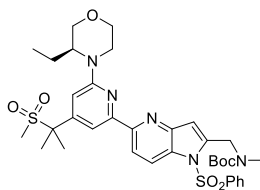
***tert*-Butyl methyl((1-(phenylsulfonyl)-5-(trimethylstannyl)-1*H*-pyrrolo[3,2-*b*]pyridin-2-yl)methyl)carbamate (157)**



A mixture of *tert*-butyl ((5-chloro-1-(phenylsulfonyl)-1*H*-pyrrolo[3,2-*b*]pyridin-2-yl)methyl)(methyl)carbamate (1.00 g, 2.29 mmol), PdCl₂(dppf) (0.08 g, 0.12 mmol) and 1,1,1,2,2,2-hexamethyldistannane (0.85 mL, 4.10 mmol) in toluene (8 mL) was degassed by sparging with nitrogen and heated at 110 °C for 2 h. The reaction mixture was allowed to cool and purified by flash chromatography (SNAP KP-NH-modified silica, 110 g), eluting with cyclohexane (200 mL), 1:1 TBME:cyclohexane (500 mL) and 2:1 TBME:cyclohexane (200 mL). Appropriate fractions were combined and concentrated *in vacuo* and then under a flow of nitrogen to give *tert*-butyl methyl((1-(phenylsulfonyl)-5-(trimethylstannyl)-1*H*-pyrrolo[3,2-*b*]pyridin-2-yl)methyl)carbamate (1.19 g, 1.83 mmol, 80% yield) as an off-white solid. LCMS

(Formic, UV, ESI): $R_t = 1.00$ min, $[M+H^+]$ 566.15, 87% purity. 1H NMR (400 MHz, Chloroform-*d*) δ ppm 8.24 (br. d, $J = 6.6$ Hz, 1 H), 7.80 (br. d, $J = 13.2$ Hz, 2 H), 7.53 - 7.63 (m, 1 H), 7.43 - 7.49 (m, 2 H), 7.35 (d, $J = 6.6$ Hz, 1 H), 6.69 (s, 1 H), 4.82 - 4.97 (m, 2 H), 2.95 (s, 3 H), 1.40 (s, 9 H), 0.35 (t, $J = 26.9$ Hz, 9 H).

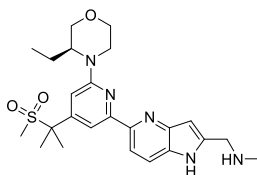
***tert*-Butyl (S)-((5-(6-(3-ethylmorpholino)-4-(2-(methylsulfonyl)propan-2-yl)pyridin-2-yl)-1-(phenylsulfonyl)-1*H*-pyrrolo[3,2-*b*]pyridin-2-yl)methyl)(methyl)carbamate (158)**



(*S*)-4-(6-Chloro-4-(2-(methylsulfonyl)propan-2-yl)pyridin-2-yl)-3-ethylmorpholine (630 mg, 1.64 mmol), lithium chloride (71 mg, 1.68 mmol) and $PdCl_2(dppf)$ (123 mg, 0.17 mmol) were combined in toluene (15 mL). *tert*-Butyl methyl((1-(phenylsulfonyl)-5-(trimethylstannyl)-1*H*-pyrrolo[3,2-*b*]pyridin-2-yl)methyl)carbamate (1110 mg, 1.71 mmol) was added, the mixture degassed by sparging with nitrogen and heated at 100 °C for 15 h. Further $PdCl_2(dppf)$ (123 mg, 0.17 mmol) and lithium chloride (71 mg, 1.68 mmol) were added, the mixture was degassed by sparging with nitrogen and heated at 100 °C for 4 h. The residue was filtered through Celite® (10 g), eluting with ethyl acetate (2 x 30 mL). The filtrate was washed with potassium fluoride solution (1 M in water) (2 x 60 mL) and brine (60 mL), dried through a hydrophobic frit and concentrated under a flow of nitrogen. The residue was preabsorbed onto Florisil® and purified by normal phase chromatography (silica, 120 g), eluting with 0-70% ethyl acetate in cyclohexane over 16 CV, followed by 70% ethyl acetate in cyclohexane for 1 CV, followed by 70-100% ethyl acetate in cyclohexane over 3 CV and 100% ethyl acetate for 3 CV. Appropriate fractions were combined and concentrated *in vacuo* to give *tert*-butyl (*S*)-((5-(6-(3-ethylmorpholino)-4-(2-(methylsulfonyl)propan-2-yl)pyridin-2-yl)-1-(phenylsulfonyl)-1*H*-pyrrolo[3,2-*b*]pyridin-2-yl)methyl)(methyl)carbamate (790 mg, 0.91 mmol, 56% yield) as a brown solid. LCMS (Formic, UV, ESI): $R_t = 1.45$ min, $[M+H^+]$ 712.49, 82% purity. 1H NMR (400 MHz, Chloroform-*d*) δ ppm 8.50 (br. s, 1 H), 8.36 (br. d, $J = 8.6$ Hz, 1 H), 8.02

(br. s, 1 H), 7.83 (br. s, 2 H), 7.56 - 7.66 (m, 1 H), 7.48 (br. s, 2 H), 7.00 (s, 1 H), 6.76 (br. s, 1 H), 4.95 (br. s, 1 H), 4.88 (br. s, 1 H), 3.97 - 4.15 (m, 4 H), 3.61 - 3.84 (m, 2 H), 3.33 (td, $J = 12.6, 3.7$ Hz, 1 H), 3.00 (s, 3 H), 2.65 (s, 3 H), 1.93 - 2.01 (m, 1 H), 1.91 (app. d, $J = 4.2$ Hz, 6 H), 1.65 - 1.75 (m, 1 H), 1.53 - 1.61 (m, 9 H), 1.00 (t, $J = 7.5$ Hz, 3 H).

(S)-1-(5-(6-(3-Ethylmorpholino)-4-(2-(methylsulfonyl)propan-2-yl)pyridin-2-yl)-1H-pyrrolo[3,2-b]pyridin-2-yl)-N-methylmethanamine (153) Scheme 18



tert-Butyl (S)-((5-(6-(3-ethylmorpholino)-4-(2-(methylsulfonyl)propan-2-yl)pyridin-2-yl)-1-(phenylsulfonyl)-1H-pyrrolo[3,2-b]pyridin-2-yl)methyl)(methyl)carbamate (770 mg, 0.89 mmol), methanamine (2 M in THF) (1.3 mL, 2.60 mmol) and NaOH (2 M in water) (2.2 mL, 4.40 mmol) were combined in THF (4 mL) and methanol (2 mL) and stirred at 21 °C under nitrogen for 2 h. Saturated aqueous ammonium chloride (20 mL) was added, the mixture was extracted with dichloromethane (2 x 20 mL) and the combined organics were concentrated *in vacuo*. The residue was dissolved in 1,4-dioxane (3 mL), HCl (4 M in 1,4-dioxane) (3.3 mL, 13.20 mmol) was added and the reaction mixture was stirred at 21 °C for 1 h. The mixture was concentrated *in vacuo* and then under a flow of nitrogen. The residue was dissolved in methanol (10 mL) and loaded onto an aminopropyl SPE (50 g, primed with methanol (1 CV)), eluting with methanol (3 CV). The eluent was concentrated *in vacuo*. The residue was dissolved in minimal dichloromethane and purified by flash chromatography (silica, 120 g), eluting with 0-100% 3:1 ethyl acetate:ethanol with 1% TEA in cyclohexane with 1% TEA. Appropriate fractions were combined and concentrated *in vacuo* to give 334 mg of crude material. 50 mg of this was dissolved in minimal methanol and purified by reverse phase preparative HPLC (Xbridge prep. C₁₈ column, ammonium hydrogen carbonate modifier). Appropriate fractions were combined and concentrated *in vacuo* to give 15 mg of product. The remaining material was dissolved in minimal 1:1 methanol:DMSO and purified by reverse phase

preparative HPLC (Xbridge prep. C₁₈ column, ammonium hydrogen carbonate modifier). Appropriate fractions were combined and concentrated *in vacuo* to give 308 mg of a yellow residue. This was triturated with TBME (x 5) and the solid was dried *in vacuo* to give 45 mg of a yellow solid.

The supernatant solution was concentrated under a flow of nitrogen to give an off-white solid, which was dissolved in dichloromethane and concentrated under nitrogen, almost to dryness before a few drops of TBME were added to form a colourless solid. All remaining solvent was removed under a flow of nitrogen, followed by further drying under vacuum overnight. The sample was further dried under vacuum while heating at 30 °C for 8 h, followed by drying under vacuum while heating at 35 °C for 17 h. 70 mg of this material was dissolved in DMSO (10.5 mL) and purified by MDAP (TFA modifier).¹ Appropriate fractions were combined and concentrated aqueous ammonia solution was added to achieve pH 10. The organics were removed *in vacuo* and concentrated aqueous ammonia solution was added to the remaining aqueous solution to achieve pH 10. Brine (200 mL) was added and the aqueous solution was extracted with dichloromethane (500 mL x 3). The combined organics were dried over sodium sulfate, filtered and concentrated under a flow of nitrogen. The resultant solid was dissolved in minimal water and freeze dried followed by further drying under vacuum to give 63 mg of the desired product.

The remaining 120 mg was dried under vacuum at 40 °C for 3 days, dissolved in minimal ethanol, concentrated *in vacuo* (repeated x 3) and dried under vacuum at 40 °C for 20 h to give (*S*)-1-(5-(6-(3-ethylmorpholino)-4-(2-(methylsulfonyl)propan-2-yl)pyridin-2-yl)-1*H*-pyrrolo[3,2-*b*]pyridin-2-yl)-*N*-methylmethanamine (111 mg, 0.23 mmol, 26% yield) as an off-white solid. M.pt.: 146-148 °C. ν_{\max} (cm⁻¹) (Chloroform-*d*): 2964 (w), 2857 (w), 1592 (m, C=N), 1552 (m), 1412 (s), 1289 (s, S=O), 1108 (m, S=O), 912 (m), 730 (s). ¹H NMR (400 MHz, DMSO-*d*₆) δ ppm 11.25

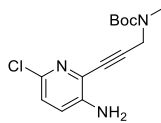
¹ MDAP purification (TFA modifier) and subsequent work-up completed by A. Hobbs (Discovery Analytical Purification Team). MDAP purification was carried out using a Waters ZQ mass spectrometer using positive electrospray ionisation and a summed UV wavelength of 210–350 nm. TFA: Sunfire Prep C₁₈ OBD column (150 mm x 30 mm, 5 μ m packing diameter, 40 mL/min flow rate), using a gradient elution at ambient temperature with the mobile phases as (A) H₂O containing 0.1% (v/v) TFA and (B) acetonitrile containing 0.1% (v/v) TFA.

(br. s, 1 H), 8.12 (d, $J = 8.6$ Hz, 1 H), 7.94 (d, $J = 1.0$ Hz, 1 H), 7.75 (d, $J = 8.6$ Hz, 1 H), 6.86 (d, $J = 1.0$ Hz, 1 H), 6.49 (s, 1 H), 4.18 - 4.34 (m, 1 H), 4.12 (br. d, $J = 12.0$ Hz, 1 H), 3.89 - 4.01 (m, 2 H), 3.85 (s, 2 H), 3.62 (dd, $J = 11.4, 2.8$ Hz, 1 H), 3.55 (td, $J = 11.7, 3.2$ Hz, 1 H), 3.16 (td, $J = 12.7, 3.2$ Hz, 1 H), 2.79 (s, 3 H), 2.33 (s, 3 H), 1.74 - 1.86 (m, 7 H), 1.49 - 1.68 (m, 1 H), 0.92 (t, $J = 7.5$ Hz, 3 H) [1 N-H not observed]. ^{13}C NMR (101 MHz, DMSO- d_6) δ ppm 157.9 (s, 1 C), 155.0 (s, 1 C), 148.5 (s, 2 C), 146.1 (s, 1 C), 143.7 (s, 1 C), 129.0 (s, 1 C), 118.0 (s, 1 C), 113.5 (s, 1 C), 107.9 (s, 1 C), 105.1 (s, 1 C), 100.1 (s, 1 C), 67.3 (s, 1 C), 66.2 (s, 1 C), 63.9 (s, 1 C), 52.8 (s, 1 C), 48.4 (s, 1 C), 40.5 (s, 1 C), 35.5 (s, 1 C), 34.9 (s, 1 C), 21.8 (s, 1 C), 21.8 (s, 1 C), 19.6 (s, 1 C), 11.1 (s, 1 C). LCMS (Formic, UV, ESI): $R_t = 0.44$ min, $[\text{M}+\text{H}^+]$ 471.34, 100% purity. HRMS: ($\text{C}_{24}\text{H}_{34}\text{N}_5\text{O}_3\text{S}$) $[\text{M}+\text{H}^+]$ requires 472.2382, found $[\text{M}+\text{H}^+]$ 472.2382 (-2.5 ppm).

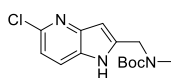
***tert*-Butyl methyl(prop-2-yn-1-yl)carbamate (166)**



Based on literature procedure.²¹⁹ To *tert*-butyl prop-2-yn-1-ylcarbamate (1.00 g, 6.44 mmol) in DMF (15 mL) was added NaH (60% dispersion in mineral oil) (0.39 g, 9.67 mmol) and the mixture stirred at 0 °C for 15 min. Iodomethane (0.81 mL, 12.89 mmol) was added and the resulting mixture was stirred at 0 °C for 16 h. The reaction mixture was diluted with water (40 mL) and ethyl acetate (40 mL). The aqueous phase was extracted with ethyl acetate (40 mL) and the combined organics were washed with saturated aqueous sodium hydrogen carbonate solution (40 mL), dried through a hydrophobic frit and concentrated *in vacuo* to give *tert*-butyl methyl(prop-2-yn-1-yl)carbamate (1.03 g, 5.49 mmol, 85% yield) as a yellow oil. ν_{max} (cm^{-1}) (Chloroform- d): 2982 (w), 2928 (w), 1692 (s, C=O), 1389 (s), 1367 (m), 1247 (m), 1145 (s), 869 (m), 733 (w, C-H alkyne bend). ^1H NMR (400 MHz, Chloroform- d) δ ppm 4.01 (br. s, 2 H), 2.89 (br. s, 3 H), 2.16 - 2.22 (app. m, 1 H), 1.44 (s, 9 H). ^{13}C NMR (101 MHz, Chloroform- d) δ ppm 162.5 (s, 1 C), 80.1 (s, 1 C), 79.1 (s, 1 C), 71.5 (s, 1 C), 33.4 (s, 2 C), 28.3 (s, 3 C).

***tert*-Butyl (3-(3-amino-6-chloropyridin-2-yl)prop-2-yn-1-yl)(methyl)carbamate (167)**

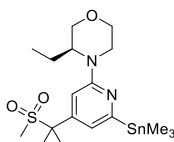
A mixture of *tert*-butyl methyl(prop-2-yn-1-yl)carbamate (612 mg, 3.62 mmol), 2-bromo-6-chloropyridin-3-amine (500 mg, 2.41 mmol), copper(I) iodide (51 mg, 0.27 mmol), PdCl₂(dppf) (148 mg, 0.20 mmol) and TEA (0.50 mL, 3.62 mmol) in a vial was degassed by purging under vacuum and filling with nitrogen (x 3) before adding THF (10 mL). The resulting suspension was degassed under a flow of nitrogen for 2 min and heated at 70 °C for 17 h. The reaction mixture was filtered through Celite® (2.5 g), eluting with ethyl acetate (30 mL) and water (10 mL). The filtrate was diluted with water (20 mL), the aqueous phase was extracted with ethyl acetate (3 x 30 mL) and the combined organics were washed with brine (20 mL), dried through a hydrophobic frit and concentrated *in vacuo* and then under a flow of nitrogen to give crude *tert*-butyl (3-(3-amino-6-chloropyridin-2-yl)prop-2-yn-1-yl)(methyl)carbamate (1074 mg, 2.36 mmol, 98% yield) as a brown oil. LCMS (Formic, UV, ESI) R_t = 1.08 min, [M+H⁺] 240.12, 242.11 (Cl isotopes), 81% purity. ¹H NMR (400 MHz, Chloroform-*d*) δ ppm 7.07 (d, *J* = 8.6 Hz, 1 H), 6.99 (d, *J* = 8.6 Hz, 1 H), 4.32 (s, 2 H), 2.99 (s, 3 H), 1.27 (s, 9 H) [2 N-H not observed].

***tert*-Butyl ((5-chloro-1*H*-pyrrolo[3,2-*b*]pyridin-2-yl)methyl)(methyl)carbamate (168)**

Potassium *tert*-butoxide (0.344 g, 3.07 mmol) was added to *tert*-butyl (3-(3-amino-6-chloropyridin-2-yl)prop-2-yn-1-yl)(methyl)carbamate (1.07 g, 2.36 mmol) and the mixture degassed by purging under vacuum and filling with nitrogen (x 3) followed by the addition of 4-methylmorpholine (5 mL, 45.50 mmol). The mixture was sonicated and stirred at 21 °C for 3 h. The reaction mixture was partitioned between ethyl acetate (30 mL) and water (30 mL). The aqueous phase was extracted with ethyl

acetate (20 mL x 3) and the combined organics were washed with brine (40 mL), dried through a hydrophobic frit and concentrated *in vacuo* and then under a flow of nitrogen. The residue was preabsorbed onto Florisil® and purified by flash chromatography (silica, 80 g), eluting with 0-100% ethyl acetate in cyclohexane. Appropriate fractions were combined and concentrated *in vacuo* to give *tert*-butyl ((5-chloro-1*H*-pyrrolo[3,2-*b*]pyridin-2-yl)methyl)(methyl)carbamate (0.53 g, 1.67 mmol, 71% yield) as a brown solid. M.pt.: 159-162 °C. ν_{\max} (cm⁻¹) (Chloroform-*d*): 3243 (w, br., N-H), 2977 (w), 1671 (s, C=O), 1563 (m, C=N), 1453 (m), 1392 (s), 1249 (m, C-N) 1148 (s), 1099 (s), 730 (s, C-Cl). ¹H NMR (400 MHz, Chloroform-*d*) δ ppm 9.31 (br. s, 1 H), 7.58 (dd, *J* = 8.3, 1.0 Hz, 1 H), 7.10 (d, *J* = 8.3 Hz, 1 H), 6.53 (d, *J* = 1.0 Hz, 1 H), 4.47 (br. s, 2 H), 2.92 (s, 3 H), 1.52 (s, 9 H). ¹³C NMR (101 MHz, Chloroform-*d*) δ ppm 165.8 (s, 1 C), 145.8 (s, 1 C), 144.0 (s, 1 C), 140.6 (s, 1 C), 127.9 (s, 1 C), 120.6 (s, 1 C), 116.8 (s, 1 C), 102.0 (s, 1 C), 80.7 (s, 1 C), 46.3 (s, 1 C), 34.9 (s, 1 C), 28.4 (s, 3 C). LCMS (Formic, UV, ESI): *R*_t = 1.03 min, [M+H⁺] 296.14, 298.12 (Cl isotopes), 94% purity. HRMS: (C₁₄H₁₉ClN₃O₂) [M+H⁺] requires 296.1166, found [M+H⁺] 296.1168 (0.7 ppm).

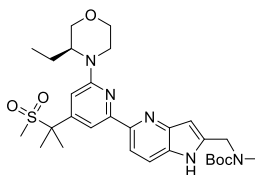
(*S*)-3-Ethyl-4-(4-(2-(methylsulfonyl)propan-2-yl)-6-(trimethylstannyl)pyridin-2-yl)morpholine (178)



A mixture of (*S*)-4-(6-chloro-4-(2-(methylsulfonyl)propan-2-yl)pyridin-2-yl)-3-ethylmorpholine (500 mg, 1.36 mmol), PdCl₂(dppf) (59 mg, 0.08 mmol) and 1,1,1,2,2,2-hexamethyldistannane (0.51 mL, 2.44 mmol) in toluene (8 mL) was degassed under a flow of nitrogen and heated at 110 °C for 4 h. The reaction mixture was allowed to cool and was purified by flash chromatography (SNAP KP-NH-modified silica, 55 g), eluting with cyclohexane (200 mL), 1:1 TBME:cyclohexane (500 mL) and TBME (300 mL). Appropriate fractions were combined, concentrated *in vacuo* and under nitrogen to give (*S*)-3-ethyl-4-(4-(2-(methylsulfonyl)propan-2-yl)-6-(trimethylstannyl)pyridin-2-yl)morpholine (0.50 g, 0.99 mmol, 73% yield) as an off-

white solid. LCMS (Formic, UV, ESI): $R_t = 0.67$ min, $[M+H^+]$ 477.21, 94% purity. 1H NMR (400 MHz, Chloroform-*d*) δ ppm 6.90 (d, $J = 1.5$ Hz, 1 H), 6.70 (d, $J = 1.5$ Hz, 1 H), 4.07 - 4.17 (m, 1 H), 3.91 - 4.04 (m, 3 H), 3.57 - 3.74 (m, 2 H), 3.20 (td, $J = 12.7, 3.8$ Hz, 1 H), 2.58 (s, 3 H), 1.86 - 1.93 (m, 1 H), 1.79 (s, 6 H), 1.54 - 1.65 (m, 1 H), 0.94 (t, $J = 7.5$ Hz, 3 H), 0.30 (t, $J = 26.9$ Hz, 9 H).

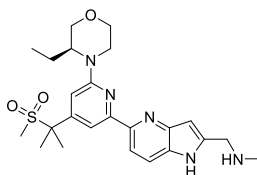
***tert*-Butyl (S)-((5-(6-(3-ethylmorpholino)-4-(2-(methylsulfonyl)propan-2-yl)pyridin-2-yl)-1*H*-pyrrolo[3,2-*b*]pyridin-2-yl)methyl)(methyl)carbamate (179)**



To *tert*-butyl ((5-chloro-1*H*-pyrrolo[3,2-*b*]pyridin-2-yl)methyl)(methyl)carbamate (100 mg, 0.32 mmol), lithium chloride (14 mg, 0.33 mmol) and $PdCl_2(dppf)$ (23 mg, 0.03 mmol) in toluene (3 mL) was added (*S*)-3-ethyl-4-(4-(2-(methylsulfonyl)propan-2-yl)-6-(trimethylstannyl)pyridin-2-yl)morpholine (169 mg, 0.33 mmol). The mixture was degassed by sparging with nitrogen and heated at 100 °C for 3 h. Further $PdCl_2(dppf)$ (23 mg, 0.032 mmol) and lithium chloride (14 mg, 0.33 mmol) were added, the reaction mixture was degassed by sparging with nitrogen and heated at 100 °C for 23 h. The reaction mixture was filtered through Celite® (2.5 g), eluting with ethyl acetate (30 mL). The filtrate was washed with potassium fluoride solution (1 M in water) (2 x 40 mL) and brine (40 mL), dried through a hydrophobic frit and concentrated under a flow of nitrogen. The residue was preabsorbed onto Florisil® and purified by flash chromatography (silica, 24 g), eluting with 0-100% ethyl acetate in cyclohexane over 14 CV. Appropriate fractions were combined and concentrated *in vacuo*, dissolved in dichloromethane and purified by flash chromatography (silica, 24 g), eluting with 70-100% ethyl acetate in cyclohexane over 6 CV. Appropriate fractions were combined and concentrated *in vacuo* to give crude *tert*-butyl (*S*)-((5-(6-(3-ethylmorpholino)-4-(2-(methylsulfonyl)propan-2-yl)pyridin-2-yl)-1*H*-pyrrolo[3,2-*b*]pyridin-2-yl)methyl)(methyl)carbamate (114 mg, 0.16 mmol, 50% yield) as an orange oil. LCMS (Formic, UV, ESI): $R_t = 0.84$ min, $[M+H^+]$ 572.23, 79% purity. 1H NMR (400 MHz, Chloroform-*d*) δ ppm 8.26 (d, $J = 8.6$ Hz, 1 H), 8.03 (br. s, 1 H),

7.91 (d, $J = 1.5$ Hz, 1 H), 7.70 (br. d, $J = 8.6$ Hz, 1 H), 6.98 (s, 1 H), 6.93 (d, $J = 1.5$ Hz, 1 H), 4.51 (br. s, 2 H), 4.17 - 4.23 (m, 1 H), 3.99 - 4.08 (m, 3 H), 3.67 - 3.78 (m, 2 H), 3.26 - 3.36 (m, 1 H), 2.93 (s, 3 H), 2.60 - 2.66 (m, 3 H), 1.88 - 2.02 (m, 7 H), 1.62 - 1.73 (m, 1 H), 1.49 - 1.55 (m, 9 H), 0.98 (t, $J = 7.1$ Hz, 3 H).

(S)-1-(5-(6-(3-Ethylmorpholino)-4-(2-(methylsulfonyl)propan-2-yl)pyridin-2-yl)-1H-pyrrolo[3,2-*b*]pyridin-2-yl)-*N*-methylmethanamine (153) Alternative preparation, **Scheme 27**.



To *tert*-butyl (S)-((5-(6-(3-ethylmorpholino)-4-(2-(methylsulfonyl)propan-2-yl)pyridin-2-yl)-1H-pyrrolo[3,2-*b*]pyridin-2-yl)methyl)(methyl)carbamate (103 mg, 0.14 mmol) in 1,4-dioxane (1 mL) was added 4 M HCl in 1,4-dioxane (0.4 mL, 1.60 mmol) and the reaction mixture was stirred at 21 °C for 5.5 h. The mixture was concentrated *in vacuo*, dissolved in minimal methanol and loaded onto an aminopropyl SPE (5 g, primed with methanol (1 CV)), eluting with methanol (3 CV). The eluent was concentrated *in vacuo*, dissolved in 1:1 methanol:DMSO (1 mL) and purified by MDAP (ammonium bicarbonate modifier). Appropriate fractions were combined and concentrated *in vacuo* to give (S)-1-(5-(6-(3-ethylmorpholino)-4-(2-(methylsulfonyl)propan-2-yl)pyridin-2-yl)-1H-pyrrolo[3,2-*b*]pyridin-2-yl)-*N*-methylmethanamine (54.7 mg, 0.12 mmol, 81 % yield) as a yellow solid. LCMS (Formic, UV, ESI): $R_t = 0.44$ min, $[M+H^+]$ 472.35, 100% purity. Data in agreement with that previously obtained.

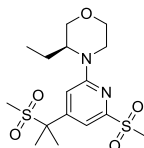
(S)-3-Ethyl-4-(6-(methylsulfonyl)-4-(2-(methylsulfonyl)propan-2-yl)pyridin-2-yl)morpholine (205)

Table 20, Entry 7: A mixture of (*S*)-4-(6-chloro-4-(2-(methylsulfonyl)propan-2-yl)pyridin-2-yl)-3-ethylmorpholine (50 mg, 0.14 mmol), sodium methanesulfinate (22 mg, 0.22 mmol), copper(I) iodide (6 mg, 0.03 mmol), *L*-proline (3 mg, 0.03 mmol) and K₂CO₃ (4 mg, 0.03 mmol) in a vial was degassed by purging under vacuum and filling with nitrogen (x 3) and DMSO (0.5 mL) was added. The resulting suspension was degassed by sparging with nitrogen and stirred at 120 °C for 92 h.

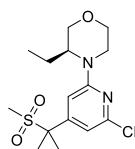
Table 20, Entry 8: A mixture of (*S*)-4-(6-chloro-4-(2-(methylsulfonyl)propan-2-yl)pyridin-2-yl)-3-ethylmorpholine (50 mg, 0.14 mmol), sodium methanesulfinate (22 mg, 0.22 mmol), copper(I) iodide (6 mg, 0.03 mmol), *N,N'*-Dimethylethane-1,2-diamine (3 μl, 0.03 mmol) and K₂CO₃ (4 mg, 0.03 mmol) in a vial was degassed by purging under vacuum and filling with nitrogen (x 3) and DMSO (0.5 mL) was added. The resulting suspension was degassed by sparging with nitrogen and stirred at 120 °C for 92 h.

Table 20, Entry 9: A mixture of (*S*)-4-(6-chloro-4-(2-(methylsulfonyl)propan-2-yl)pyridin-2-yl)-3-ethylmorpholine (50 mg, 0.14 mmol), sodium methanesulfinate (34 mg, 0.33 mmol), copper(I) iodide (8 mg, 0.04 mmol), *N,N'*-Dimethylethane-1,2-diamine (4 μl, 0.04 mmol) and K₂CO₃ (4 mg, 0.03 mmol) in a vial was degassed by purging under vacuum and filling with nitrogen (x 3) and sulfolane (0.5 mL) was added. The resulting suspension was degassed by sparging with nitrogen and stirred at 173 °C for 21 h.

The reaction mixtures were allowed to cool, combined and suspended in ethyl acetate (30 mL). Water was added (30 mL) and the aqueous phase was extracted with ethyl acetate (2 x 30 mL). The combined organics were washed with water (30 mL) and brine (30 mL), dried through a hydrophobic frit and concentrated *in vacuo*. The residue

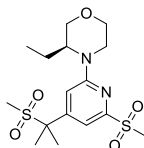
was dissolved in minimal dichloromethane and purified by flash chromatography (silica, 80 g), eluting with 0-100% ethyl acetate in cyclohexane over 12 CV. Appropriate fractions were combined, concentrated *in vacuo*, dissolved in dichloromethane and concentrated under a flow of nitrogen to give (*S*)-3-ethyl-4-(6-(methylsulfonyl)-4-(2-(methylsulfonyl)propan-2-yl)pyridin-2-yl)morpholine (48 mg, 0.12 mmol, 28% combined yield) as an off-white amorphous solid. ν_{\max} (cm^{-1}) (dichloromethane): 2859 (w), 1600 (m), 1530 (w, C=N), 1470 (w), 1296 (s, C-N), 1135 (m, S=O), 959 (w) 758 (w), 535 (m). ^1H NMR (400 MHz, $\text{DMSO-}d_6$) δ ppm 7.31 (d, $J = 1.2$ Hz, 1 H), 7.09 (d, $J = 1.2$ Hz, 1 H), 4.14 - 4.26 (m, 1 H), 4.09 (s, 1 H), 3.93 (dd, $J = 11.2, 3.7$ Hz, 1 H), 3.88 (d, $J = 11.5$ Hz, 1 H), 3.56 (dd, $J = 11.3, 2.9$ Hz, 1 H), 3.48 (td, $J = 12.0, 3.2$ Hz, 1 H), 3.21 (s, 3 H), 3.14 (td, $J = 13.0, 3.2$ Hz, 1 H), 2.83 (s, 3 H), 1.71 - 1.83 (m, 7 H), 1.52 - 1.68 (m, 1 H), 0.85 (t, $J = 7.5$ Hz, 3 H). ^{13}C NMR (101 MHz, $\text{DMSO-}d_6$) δ ppm 158.0 (s, 1 C), 155.8 (s, 1 C), 149.8 (s, 1 C), 110.3 (s, 1 C), 107.1 (s, 1 C), 67.4 (s, 1 C), 65.9 (s, 1 C), 63.9 (s, 1 C), 52.6 (s, 1 C), 35.1 (s, 1 C), 21.6 (s, 1 C), 21.5 (s, 1 C), 20.2 (s, 1 C), 10.8 (s, 1 C) [2 C not observed]. LCMS (Formic, UV, ESI): $R_t = 0.82$ min, $[\text{M}+\text{H}^+]$ 391.20, 99% purity. HRMS: ($\text{C}_{16}\text{H}_{27}\text{N}_2\text{O}_5\text{S}_2$) $[\text{M}+\text{H}^+]$ requires 391.1361, found $[\text{M}+\text{H}^+]$ 391.1360 (-0.3 ppm).

(*S*)-4-(6-Chloro-4-(2-(methylsulfonyl)propan-2-yl)pyridin-2-yl)-3-ethylmorpholine (156)



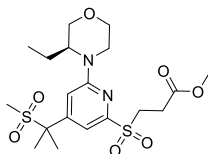
Appropriate fractions were also combined, concentrated *in vacuo*, dissolved in dichloromethane and concentrated under a flow of nitrogen to give (*S*)-4-(6-chloro-4-(2-(methylsulfonyl)propan-2-yl)pyridin-2-yl)-3-ethylmorpholine (105 mg, 0.30 mmol, 69% combined yield). LCMS (Formic, UV, ESI): $R_t = 1.07$ min, $[\text{M}+\text{H}^+]$ 347.16, 349.14, 99% purity. Data in agreement with that previously obtained.

(S)-3-Ethyl-4-(6-(methylsulfonyl)-4-(2-(methylsulfonyl)propan-2-yl)pyridin-2-yl)morpholine (205) Alternative preparation, **Table 20, Entry 10**.



Based on literature procedure.¹⁹¹ A mixture of (*S*)-4-(6-chloro-4-(2-(methylsulfonyl)propan-2-yl)pyridin-2-yl)-3-ethylmorpholine (100 mg, 0.25 mmol), sodium methanesulfinate (39 mg, 0.38 mmol), copper(I) iodide (15 mg, 0.08 mmol), *N,N'*-dimethylethane-1,2-diamine (8 μ l, 0.07 mmol) and K_2CO_3 (11 mg, 0.08 mmol) in a vial was degassed by purging under vacuum and filling with nitrogen (x 3). DMSO (1 mL) was added, the resulting suspension was degassed by sparging with nitrogen and stirred at 120 °C for 28 h. Further sodium methanesulfinate (39 mg, 0.38 mmol), K_2CO_3 (11 mg, 0.08 mmol), copper(I) iodide (15 mg, 0.08 mmol) and *N,N'*-dimethylethane-1,2-diamine (8 μ l, 0.07 mmol) were added. The suspension was degassed by sparging with nitrogen and the resulting mixture was stirred at 120 °C for 17 h. The reaction mixture was allowed to cool, further sodium methanesulfinate (39 mg, 0.38 mmol), K_2CO_3 (18 mg, 0.13 mmol), copper(I) iodide (15 mg, 0.08 mmol) and *N,N'*-Dimethylethane-1,2-diamine (8 μ l, 0.07 mmol) were added. The suspension was degassed by sparging with nitrogen and the resulting mixture was stirred at 120 °C for 7 h. The reaction mixture was allowed to cool and diluted with ethyl acetate (20 mL) and water (15 mL). The aqueous phase was extracted with ethyl acetate (20 mL) and the combined organics were washed with water (10 mL) and brine (10 mL), dried through a hydrophobic frit and concentrated *in vacuo* to give crude (*S*)-3-ethyl-4-(6-(methylsulfonyl)-4-(2-(methylsulfonyl)propan-2-yl)pyridin-2-yl)morpholine (113 mg, 0.25 mmol, 98% yield) as a yellow residue. LCMS (Formic, UV, ESI): R_t = 0.86 min, $[M+H^+]$ 391.11, 86% purity. Data in agreement with that previously obtained.

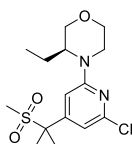
Methyl (S)-3-((6-(3-ethylmorpholino)-4-(2-(methylsulfonyl)propan-2-yl)pyridin-2-yl)sulfonyl)propanoate (211)



Based on literature procedure.¹⁵¹ To (S)-4-(6-chloro-4-(2-(methylsulfonyl)propan-2-yl)pyridin-2-yl)-3-ethylmorpholine (500 mg, 1.41 mmol) and sodium 3-methoxy-3-oxopropane-1-sulfinate (738 mg, 4.24 mmol) in DMSO (5 mL) was added copper(I) iodide (807 mg, 4.24 mmol). The mixture was degassed by purging under vacuum and filling with nitrogen (x 3) and stirred at 21 °C for 1.5 h followed by heating at 110 °C for 22.0 h. The reaction mixture was diluted with ethyl acetate and filtered through Celite®. The solid remaining on the Celite® was combined with the filtrate and concentrated *in vacuo*. The residue was diluted with ethyl acetate (30 mL) and washed with water (30 mL, brine (2 mL) added). The aqueous phase was extracted with ethyl acetate (20 mL, brine (2 mL) added) and the combined organics were washed with brine (20 mL). The combined aqueous phases were extracted with ethyl acetate (3 x 20 mL) and the combined organics were washed with brine (20 mL), dried through a hydrophobic frit, combined with the previous organic phase and concentrated *in vacuo*. The residue was dissolved in minimal dichloromethane and purified by flash chromatography (silica, 120 g), eluting with 0-100% ethyl acetate in cyclohexane. Appropriate fractions were combined and concentrated under a flow of nitrogen to give methyl (S)-3-((6-(3-ethylmorpholino)-4-(2-(methylsulfonyl)propan-2-yl)pyridin-2-yl)sulfonyl)propanoate (257 mg, 0.56 mmol, 39% yield) as an orange oil/foam. ν_{\max} (cm⁻¹) (Chloroform-*d*): 2966 (w, br.), 2853 (w, br.), 1739 (m, C=O), 1599 (s, C=N), 1532 (m, C=C), 1478 (m), 1425 (m), 1297 (s, S=O), 1120 (s, S=O), 992 (m), 921 (m), 729 (m), 536 (m), 501 (m). ¹H NMR (400 MHz, Chloroform-*d*) δ ppm 7.40 (d, *J* = 1.2 Hz, 1 H), 7.13 (d, *J* = 1.2 Hz, 1 H), 3.95 - 4.05 (m, 4 H), 3.70 (s, 3 H), 3.57 - 3.70 (m, 4 H), 3.28 (td, *J* = 12.7, 3.7 Hz, 1 H), 2.81 - 2.88 (m, 2 H), 2.65 (s, 3 H), 1.88 - 1.97 (m, 1 H), 1.84 (app. d, *J* = 1.0 Hz, 6 H), 1.59 - 1.71 (m, 1 H), 0.95 (t, *J* = 7.5 Hz, 3 H). ¹³C NMR (101 MHz, Chloroform-*d*) δ ppm 170.6 (s, 1 C), 158.6 (s, 1 C), 155.6 (s, 1 C), 150.2 (s, 1 C), 110.7 (s, 1 C), 107.8 (s, 1 C), 67.9 (s, 1 C), 66.6 (s,

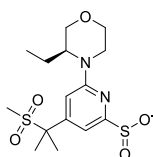
1 C), 64.4 (s, 1 C), 53.9 (s, 1 C), 52.3 (s, 1 C), 47.0 (s, 1 C), 40.3 (s, 1 C), 35.2 (s, 1 C), 27.3 (s, 1 C), 22.3 (s, 1 C), 22.3 (s, 1 C), 20.7 (s, 1 C), 11.1 (s, 1 C). LCMS (Formic, UV, ESI): $R_t = 0.88$ min, $[M+H^+]$ 463.24, 100% purity. HRMS: ($C_{19}H_{31}N_2O_7S_2$) $[M+H^+]$ requires 463.1573, found $[M+H^+]$ 463.1569 (-0.9 ppm).

(S)-4-(6-Chloro-4-(2-(methylsulfonyl)propan-2-yl)pyridin-2-yl)-3-ethylmorpholine (156)



Appropriate fractions were also combined, concentrated *in vacuo* and under nitrogen to give crude (S)-4-(6-chloro-4-(2-(methylsulfonyl)propan-2-yl)pyridin-2-yl)-3-ethylmorpholine (278 mg, 0.67 mmol, 47% yield as an orange oil. LCMS (Formic, UV, ESI): $R_t = 1.09$ min, $[M+H^+]$ 347.07, 349.02 (Cl isotopes), 83% purity. Data in agreement with that previously obtained.

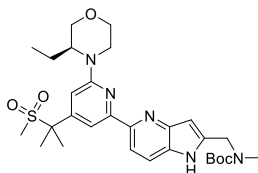
(S)-6-(3-Ethylmorpholino)-4-(2-(methylsulfonyl)propan-2-yl)pyridine-2-sulfinate, sodium salt (199)



Based on literature procedure.¹⁵¹ Sodium methoxide (0.5 M in methanol) (1.1 mL, 0.55 mmol) was added dropwise to a stirred solution of methyl (S)-3-((6-(3-ethylmorpholino)-4-(2-(methylsulfonyl)propan-2-yl)pyridin-2-yl)sulfonyl)propanoate (249 mg, 0.54 mmol) in THF (5 mL) at 21 °C. The reaction mixture was stirred at 21 °C for 1 h. The reaction mixture was concentrated *in vacuo*, diluted with methanol and concentrated *in vacuo* to give (S)-6-(3-ethylmorpholino)-4-(2-(methylsulfonyl)propan-2-yl)pyridine-2-sulfinate, sodium salt (232 mg, 0.55 mmol, quant.) as an orange residue/foam. ν_{max} (cm^{-1}) (Chloroform-*d*): 3505 (w, broad), 2865 (w), 1592 (s, C=N), 1532 (m), 1449 (m, S=O), 1286 (s, C-N), 1106 (s, S=O), 1042 (m, SO_2^-), 980 (s, SO_2^-), 958 (m), 862 (m), 767 (m), 547 (s), 517 (m), 485

(s). ^1H NMR (400 MHz, $\text{DMSO-}d_6$) δ ppm 7.17 (d, $J = 1.2$ Hz, 1 H), 6.69 (d, $J = 1.2$ Hz, 1 H), 4.03 (br. s, 2 H), 3.81 - 3.93 (m, 2 H), 3.50 - 3.56 (m, 1 H), 3.39 - 3.50 (m, 1 H), 2.97 - 3.08 (m, 1 H), 2.72 (s, 3 H), 1.66 - 1.79 (m, 7 H), 1.44 - 1.57 (m, 1 H), 0.84 (t, $J = 7.5$ Hz, 3 H) [O-H not observed]. ^{13}C NMR (101 MHz, $\text{DMSO-}d_6$) δ ppm 175.9 (s, 1 C), 157.6 (s, 1 C), 148.1 (s, 1 C), 104.7 (s, 1 C), 103.8 (s, 1 C), 67.3 (s, 1 C), 66.3 (s, 1 C), 64.0 (s, 1 C), 52.7 (s, 1 C), 39.6 (s, 1 C), 34.9 (s, 1 C), 21.8 (s, 1 C), 21.7 (s, 1 C), 19.5 (s, 1 C), 10.9 (s, 1 C). LCMS (Formic, UV, ESI): $R_t = 0.80$ min, $[\text{M}+\text{H}^+]$ 377.21, 100% purity. HRMS: ($\text{C}_{15}\text{H}_{25}\text{N}_2\text{O}_5\text{S}_2$) $[\text{M}+\text{H}^+]$ requires 393.1154, found $[\text{M}+\text{H}^+]$ 393.1145 (-2.3 ppm).

Desulfinate cross-coupling example: **Table 25 Entry 8: *tert*-Butyl (*S*)-((5-(6-(3-ethylmorpholino)-4-(2-(methylsulfonyl)propan-2-yl)pyridin-2-yl)-1*H*-pyrrolo[3,2-*b*]pyridin-2-yl)methyl)(methyl)carbamate (179)**

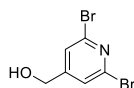


Based on literature procedure.¹⁵¹ A mixture of sodium (*S*)-6-(3-ethylmorpholino)-4-(2-(methylsulfonyl)propan-2-yl)pyridine-2-sulfinate (203 mg, 0.48 mmol), *tert*-butyl ((5-chloro-1*H*-pyrrolo[3,2-*b*]pyridin-2-yl)methyl)(methyl)carbamate (110 mg, 0.37 mmol), K_2CO_3 (77 mg, 0.56 mmol), palladium(II) acetate (8 mg, 0.04 mmol) and tricyclohexylphosphine (21 mg, 0.07 mmol) in a vial was degassed by purging under vacuum and filling with nitrogen (x 3) and degassed 1,4-dioxane (3 mL)^m was added. The resulting mixture was degassed by purging under vacuum and filling with nitrogen (x 3), further degassed by sparging with nitrogen and heated at 150 °C for 16.5 h. The reaction mixture was filtered through Celite® (2.5 g), eluting with ethyl acetate (3 x 10 mL) and the filtrate was concentrated *in vacuo*. The residue was preabsorbed onto Florisil® and purified by flash chromatography (silica, 40 g), eluting with 50-100% ethyl acetate in cyclohexane over 13 min and held at 100 % ethyl acetate for 4 min. Appropriate fractions were combined and concentrated *in vacuo*. The residue was

^m 1,4-Dioxane degassed under a flow of nitrogen for 4.5 h.

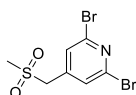
purified by reverse phase chromatography (Sunfire prep. C₁₈ column), eluting with 15-50% acetonitrile with 0.1% formic acid in water with 0.1% formic acid over 16 min. Appropriate fractions were concentrated *in vacuo*, the residue was dissolved in acetonitrile and filtered through an aminopropyl SPE (1 g), eluting with acetonitrile (3 x 10 mL). The eluent was concentrated *in vacuo* to give *tert*-butyl (*S*)-((5-(6-(3-ethylmorpholino)-4-(2-(methylsulfonyl)propan-2-yl)pyridin-2-yl)-1*H*-pyrrolo[3,2-*b*]pyridin-2-yl)methyl)(methyl)carbamate (155 mg, 0.27 mmol, 73% yield) as an off-white glassy solid. LCMS (Formic, UV, ESI): R_t = 0.80 min, [M+H⁺] 572.36, 100% purity. Data in agreement with that previously obtained.ⁿ

(2,6-Dibromopyridin-4-yl)methanol (220)

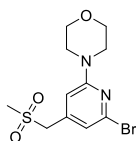


To a solution of 2,6-dibromoisonicotinic acid (9.0 g, 32.0 mmol) in THF (80 mL) at 0 °C under nitrogen was added BH₃.DMS (2 M in THF) (24.0 mL, 48.0 mmol) and the mixture stirred at 21 °C for 20 h. The reaction mixture was cooled to 0 °C, quenched by dropwise addition of methanol (100 mL) and stirred for 30 min under ice cooling prior to the addition of HCl (2 M in water, 2 mL). The reaction mixture was concentrated *in vacuo* and the residue was partitioned between ethyl acetate (100 mL) and saturated aqueous ammonium chloride solution (100 mL). The aqueous phase was extracted with ethyl acetate (100 mL x 2) and the combined organics were dried through a hydrophobic frit and concentrated *in vacuo* to give (2,6-dibromopyridin-4-yl)methanol (8.6 g, 32.2 mmol, quant.) as an off-white solid. M.pt.: 89-91 °C. ν_{\max} (cm⁻¹) (Dichloromethane): 3371 (w, br., O-H), 3220 (w, br.), 1583 (m, C=N), 1530 (s), 1454 (m), 1369 (s, S=O), 1158 (s, S=O), 1075 (m), 846 (m), 765 (s, C-Br). ¹H NMR (400 MHz, Chloroform-*d*) δ ppm 7.47 (s, 2 H), 4.86 - 4.99 (m, 1 H), 4.73 (s, 2 H), 2.02 - 2.15 (m, 1 H). ¹³C NMR (101 MHz, Chloroform-*d*) δ ppm 155.2 (s, 1 C), 140.9 (s, 2 C), 124.3 (s, 2 C), 62.2 (s, 1 C). LCMS (Formic, UV, ESI): R_t = 0.80 min, [M+H⁺] 265.83, 267.83, 269.80 (Br isotopes), 90% purity. HRMS: (C₆H₆Br₂NO) [M+H⁺] requires 265.8816, found [M+H⁺] 265.8816 (0 ppm).

ⁿ Work-up and analysis by S. Nicolle due to absence.

2,6-Dibromo-4-((methylsulfonyl)methyl)pyridine (175)

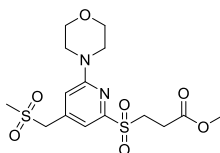
Methanesulfonyl chloride (1.3 ml, 16.7 mmol) was added dropwise over 1 min to a cooled (in an ice bath) solution of (2,6-dibromopyridin-4-yl)methanol (4.00 g, 15.0 mmol) and triethylamine (2.3 ml, 16.5 mmol) in DMF (30 ml) under nitrogen. The reaction mixture was stirred at 0-5 °C for 1.0 h, before sodium methanesulfinate (3.06 g, 30.0 mmol) and potassium iodide (0.75 g, 4.5 mmol) were added and the mixture stirred under nitrogen at 60 °C for 2.5 h. The reaction mixture was allowed to cool, poured into water (300 ml) and stirred for 15 min. The solid was collected by vacuum filtration, washed with water and dried under vacuum to give 2,6-dibromo-4-((methylsulfonyl)methyl)pyridine (3.26 g, 9.4 mmol, 63 % yield) as a colourless solid. M.pt.: 163-164 °C. ν_{\max} (cm⁻¹) (Dichloromethane): 3076 (w, br.), 3008 (w, br.), 2927 (w), 1578 (s, C=N), 1533 (s), 1370 (s), 1308 (s, S=O), 1163 (s), 1142 (m), 1118 (m, S=O), 903 (m), 763 (m), 531 (m, C-Br). ¹H NMR (400 MHz, DMSO-*d*₆) δ ppm 7.76 (s, 2 H), 4.61 (s, 2 H), 3.01 (s, 3 H). ¹³C NMR (101 MHz, DMSO-*d*₆) δ ppm 144.2 (s, 1 C), 139.9 (s, 2 C), 129.2 (s, 2 C), 57.0 (s, 1 C), 40.1 (s, 1 C). LCMS (Formic, UV, ESI): R_t = 0.81 min, [M+H⁺] 327.73, 329.73, 331.65 (Br isotopes), 93% purity. HRMS: (C₇H₈Br₂NO₂S) [M+H⁺] requires 327.8637, found [M+H⁺] 327.8640 (-0.9 ppm).

4-(6-Bromo-4-((methylsulfonyl)methyl)pyridin-2-yl)morpholine (221)

To 2,6-dibromo-4-((methylsulfonyl)methyl)pyridine (3.45 g, 10.5 mmol), DIPEA (3.66 mL, 21.0 mmol) and morpholine (0.96 mL, 11.0 mmol) was added DMSO (35 mL) and the mixture was heated to 100 °C under nitrogen for 14.5 h. The reaction mixture was allowed to cool and saturated aqueous ammonium chloride solution (50 mL) and water (20 mL) were added. The aqueous phase was extracted with ethyl acetate (3 x 70 mL) and the combined organics were washed with brine (50 mL), dried

through a hydrophobic frit and concentrated *in vacuo* to give 4-(6-bromo-4-((methylsulfonyl)methyl)pyridin-2-yl)morpholine (3.72 g, 10.0 mmol, 95% yield) as a brown solid. M.pt.: 160-164 °C. ν_{\max} (cm⁻¹) (Dichloromethane): 2969 (w, br.), 2925 (w), 2855 (w), 1597 (s, C=N), 1538 (s), 1446 (m), 1428 (m), 1307 (s, S=O), 1259 (s), 1117 (s, S=O), 1001 (m), 895 (m, C-Br). ¹H NMR (400 MHz, DMSO-*d*₆) δ ppm 6.88 (d, *J* = 0.7 Hz, 1 H), 6.84 (d, *J* = 0.7 Hz, 1 H), 4.42 (s, 2 H), 3.65 - 3.74 (m, 4 H), 3.39 - 3.49 (m, 4 H), 2.97 (s, 3 H). ¹³C NMR (101 MHz, DMSO-*d*₆) δ ppm 158.9 (s, 1 C), 142.2 (s, 1 C), 139.1 (s, 1 C), 117.3 (s, 1 C), 107.6 (s, 1 C), 65.6 (s, 2 C), 58.2 (s, 1 C), 44.7 (s, 2 C), 40.4 (s, 1 C). LCMS (Formic, UV, ESI): *R*_t = 0.85 min, [M+H⁺] 334.86, 336.85 (Br isotopes), 95% purity. HRMS: (C₁₁H₁₆BrN₂O₃S) [M+H⁺] requires 335.0065, found [M+H⁺] 335.0065 (0 ppm).

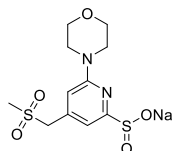
Methyl 3-((4-((methylsulfonyl)methyl)-6-morpholinopyridin-2-yl)sulfonyl)propanoate (222)



To 4-(6-bromo-4-((methylsulfonyl)methyl)pyridin-2-yl)morpholine (1.75 g, 4.70 mmol), copper(I) iodide (1.16 g, 6.11 mmol) and 3-methoxy-3-oxopropane-1-sulfinate, sodium salt (1.06 g, 6.11 mmol) was added DMSO (30 mL) and the mixture was degassed by purging under vacuum and filling with nitrogen (x 3) before heating at 110 °C for 2.5 h. The reaction mixture was allowed to cool and ethyl acetate (25 mL) and 2:2:1 water:saturated aqueous sodium bicarbonate solution:saturated aqueous ammonium chloride solution (20 mL) were added. The aqueous phase was extracted with ethyl acetate (50 mL) and the combined organics were washed with 2:2:1 water:saturated aqueous sodium bicarbonate solution:saturated aqueous ammonium chloride solution (5 x 15 mL), dried through a hydrophobic frit and concentrated *in vacuo*. The residue was preabsorbed onto Florisil® and purified by flash chromatography (silica, 80 g), eluting with 0-100% ethyl acetate in cyclohexane over 14 CV and held at 100% ethyl acetate for 11 CV. Appropriate fractions were combined and concentrated *in vacuo* and on the high vacuum line to give methyl 3-

((4-((methylsulfonyl)methyl)-6-morpholinopyridin-2-yl)sulfonyl)propanoate (1.50 g, 3.69 mmol, 79% yield) as a colourless solid. M.pt.: 172-173 °C. ν_{\max} (cm⁻¹) (solid): 2930 (w), 2856 (w), 1736 (m), 1606 (s, C=N), 1539 (m), 1433 (m), 1307 (s, S=O), 1263 (s), 1141 (m), 1116 (s, S=O), 1003 (m). ¹H NMR (400 MHz, Chloroform-*d*) δ ppm 7.32 (d, *J* = 1.2 Hz, 1 H), 6.93 (d, *J* = 1.2 Hz, 1 H), 4.23 (s, 2 H), 3.79 - 3.85 (m, 4 H), 3.69 (s, 3 H), 3.63 - 3.69 (m, 2 H), 3.60 - 3.63 (m, 4 H), 2.81 - 2.91 (m, 5 H). ¹³C NMR (101 MHz, Chloroform-*d*) δ ppm 170.5 (s, 1 C), 159.2 (s, 1 C), 155.6 (s, 1 C), 140.3 (s, 1 C), 112.3 (s, 1 C), 111.9 (s, 1 C), 66.3 (s, 2 C), 60.1 (s, 1 C), 52.3 (s, 1 C), 47.1 (s, 1 C), 45.0 (s, 2 C), 40.2 (s, 1 C), 27.3 (s, 1 C). LCMS (Formic, UV, ESI): *R*_t = 0.70 min, [M+H⁺] 407.12, 100% purity. HRMS: (C₁₅H₂₃N₂O₇S₂) [M+H⁺] requires 407.0947, found [M+H⁺] 407.0944 (-0.7 ppm).

Sodium 4-((methylsulfonyl)methyl)-6-morpholinopyridine-2-sulfinate (223)



To a solution of methyl 3-((4-((methylsulfonyl)methyl)-6-morpholinopyridin-2-yl)sulfonyl)propanoate (750 mg, 1.8 mmol) in THF (10 mL) was added sodium methoxide (0.5 M in methanol) (3.6 mL, 1.8 mmol). The mixture was degassed by purging under vacuum and filling with nitrogen (x 3) and stirred at 21 °C for 6 h. The reaction mixture was diluted with methanol, concentrated *in vacuo* and dried under high vacuum for 4 days to give sodium 4-((methylsulfonyl)methyl)-6-morpholinopyridine-2-sulfinate (716 mg, 1.8 mmol, quant., 90% purity) as a colourless hygroscopic solid. M.pt.: 175-180 °C (hygroscopic). ν_{\max} (cm⁻¹) (solid): 3374 (w, br.), 2980 (w), 1594 (s, C=N), 1542 (m), 1443 (m), 1300 (s, S=O), 1252 (s), 1113 (s, S=O), 1028 (s), 965 (s). ¹H NMR (400 MHz, DMSO-*d*₆) δ ppm 7.10 (d, *J* = 1.2 Hz, 1 H), 6.67 (d, *J* = 1.2 Hz, 1 H), 4.42 (s, 2 H), 3.64 - 3.72 (m, 4 H), 3.40 - 3.45 (m, 4 H), 2.93 (s, 3 H) [OH not observed]. ¹³C NMR (101 MHz, DMSO-*d*₆) δ ppm 175.9 (s, 1 C), 158.4 (s, 1 C), 139.5 (s, 1 C), 108.0 (s, 1 C), 107.6 (s, 1 C), 65.9 (s, 2 C), 59.4 (s, 1 C), 45.2 (s, 2 C), 34.2 (s, 1 C). LCMS (Formic, UV, ESI)

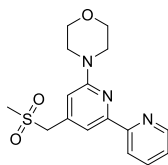
$R_t = 0.56$ min, $[M+H^+]$ 321.00, 100% purity. HRMS: $(C_{11}H_{17}N_2O_5S_2)$ $[M+H^+]$ requires 321.0579, found $[M+H^+]$ 321.0578 (-0.3 ppm).

6.4 General procedure used in array reactions (Section 4.5)

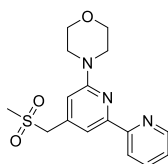
To sodium 4-((methylsulfonyl)methyl)-6-morpholinopyridine-2-sulfinate (50 mg, 0.15 mmol), K_2CO_3 (30 mg, 0.22 mmol), tricyclohexylphosphine (8.19 mg, 0.03 mmol) and $Pd(OAc)_2$ (3.28 mg, 0.02 mmol) in a vial was added the appropriate heteroaryl halide (0.15 mmol). The vial was sealed (crimp cap), the mixture degassed by purging the vial under vacuum and filling with nitrogen (x 3), tert-amyl alcohol (1.25 mL) was added and the mixture degassed again by purging the vial under vacuum and filling with nitrogen (x 3). The reaction mixture was heated at 150 °C for 20 h. The reaction mixture was allowed to cool, filtered through C_{18} silica (0.5 g), eluting with methanol (2 mL). The eluent was concentrated under a flow of nitrogen. The residue was dissolved in 1:1 methanol:DMSO (1 mL, filtered up to 3 times to get a homogeneous solution) and purified by MDAP (ammonium hydrogen carbonate modifier, method below). Appropriate fractions were concentrated under a flow of nitrogen, combined in methanol and dichloromethane and concentrated under a flow of nitrogen to give the desired products [225a, 225b, 225c, 225e, 225f, 225g, 225h, 225i, 225j, 225k, 225t and 225v].

Mass Directed Auto Preparation (MDAP) used in array experiments: MDAP carried out using Waters ZQ mass spectrometer using alternate-scan positive and negative electrospray ionisation and UV detection was at a selected wavelength generally 210 nm, 230 nm, or 280 nm. One liquid phase method was used:

High pH: Xselect CSH C_{18} column (100 mm x 19 mm, 5 μ m packing diameter, 20 mL/min flow rate) using a gradient elution at ambient temperature with the mobile phases (A) H_2O containing 10 mM ammonium hydrogen carbonate solution, adjusted to pH 10 with aqueous ammonia and (B) acetonitrile containing 0.1% aqueous ammonia.

4-(4-((Methylsulfonyl)methyl)-[2,2'-bipyridin]-6-yl)morpholine (225a)

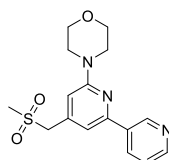
Prepared according to the general array procedure with 2-bromopyridine (23 mg, 0.15 mmol) to give 4-(4-((methylsulfonyl)methyl)-[2,2'-bipyridin]-6-yl)morpholine (16 mg, 0.05 mmol, 33%) as an off-white solid. M.pt.: 197-198 °C. ν_{\max} (cm⁻¹) (dichloromethane): 2973 (w), 2853 (w), 1603 (m), 1583 (m, C=N), 1561 (s), 1475 (m), 1431 (s), 1306 (s, S=O), 1264 (m), 1249 (m), 1116 (s, S=O), 1003 (m). ¹H NMR (700 MHz, DMSO-*d*₆) δ ppm 8.64 - 8.66 (m, 1 H), 8.34 (d, *J* = 7.7 Hz, 1 H), 7.92 (td, *J* = 7.7, 1.7 Hz, 1 H), 7.82 (s, 1 H), 7.42 (ddd, *J* = 7.4, 4.7, 1.1 Hz, 1 H), 6.93 (s, 1 H), 4.54 (s, 2 H), 3.76 (t, *J* = 4.7 Hz, 4 H), 3.57 (t, *J* = 4.7 Hz, 4 H), 2.98 (s, 3 H). ¹³C NMR (176 MHz, DMSO-*d*₆) δ ppm 158.8 (s, 1 C), 155.3 (s, 1 C), 153.3 (s, 1 C), 149.0 (s, 1 C), 140.4 (s, 1 C), 137.1 (s, 1 C), 124.0 (s, 1 C), 120.5 (s, 1 C), 112.2 (s, 1 C), 109.4 (s, 1 C), 65.9 (s, 2 C), 59.1 (s, 1 C), 45.0 (s, 2 C) [1 C not observed]. LCMS (Formic, UV, ESI): *R*_t = 0.55 min, [M+H⁺] 334.17, 100% purity. HRMS: (C₁₆H₂₀N₃O₃S) [M+H⁺] requires 334.1225, found [M+H⁺] 334.1225 (0 ppm).

4-(4-((Methylsulfonyl)methyl)-[2,2'-bipyridin]-6-yl)morpholine (225a)

Prepared according to the general array procedure with 2-chloropyridine (17 mg, 0.15 mmol) to give 4-(4-((methylsulfonyl)methyl)-[2,2'-bipyridin]-6-yl)morpholine (18 mg, 0.05 mmol, 37%) as an off-white solid. M.pt.: 195-196 °C. ν_{\max} (cm⁻¹) (dichloromethane): 2967 (w), 2854 (w), 1604 (m), 1584 (m, C=N), 1564 (s), 1475 (m), 1432 (s), 1307 (s, S=O), 1264 (m), 1250 (m), 1118 (s, S=O), 1004 (m). ¹H NMR (700 MHz, DMSO-*d*₆) δ ppm 8.64 - 8.66 (m, 1 H), 8.34 (d, *J* = 7.7 Hz, 1 H), 7.92 (td, *J* = 7.7, 1.7 Hz, 1 H), 7.82 (s, 1 H), 7.42 (ddd, *J* = 7.4, 4.8, 1.2 Hz, 1 H), 6.93 (s, 1 H), 4.54 (s, 2 H), 3.76 (t, *J* = 4.7 Hz, 4 H), 3.57 (t, *J* = 4.7 Hz, 4 H), 2.98 (s, 3 H). ¹³C NMR

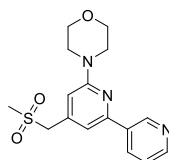
(176 MHz, DMSO-*d*₆) δ ppm 158.8 (s, 1 C), 155.3 (s, 1 C), 153.3 (s, 1 C), 149.0 (s, 1 C), 140.4 (s, 1 C), 137.1 (s, 1 C), 124.0 (s, 1 C), 120.5 (s, 1 C), 112.2 (s, 1 C), 109.4 (s, 1 C), 65.9 (s, 2 C), 59.1 (s, 1 C), 45.0 (s, 2 C), 40.0 (s, 1 C). LCMS (Formic, UV, ESI): R_t = 0.54 min, $[M+H^+]$ 334.16, 100% purity. HRMS: (C₁₆H₂₀N₃O₃S) $[M+H^+]$ requires 334.1225, found $[M+H^+]$ 334.1225 (0 ppm).

4-(4-((Methylsulfonyl)methyl)-[2,3'-bipyridin]-6-yl)morpholine (225b)



Prepared according to the general array procedure with 3-bromopyridine (23 mg, 0.15 mmol) to give 4-(4-((methylsulfonyl)methyl)-[2,3'-bipyridin]-6-yl)morpholine (12 mg, 0.04 mmol, 25%) as an off-white solid. M.pt.: 193-195 °C. ν_{max} (cm⁻¹) (dichloromethane): 2973 (w), 2927 (w), 2858 (w), 1606 (s), 1559 (m, C=N), 1437 (s), 1306 (s, S=O), 1245 (s), 1118 (s, S=O), 1004 (m). ¹H NMR (700 MHz, DMSO-*d*₆) δ ppm 9.21 (br. s, 1 H), 8.63 (d, J = 4.8 Hz, 1 H), 8.38 (br. d, J = 7.8 Hz, 1 H), 7.53 (dd, J = 7.8, 4.8 Hz, 1 H), 7.38 (s, 1 H), 6.91 (s, 1 H), 4.49 (s, 2 H), 3.75 (t, J = 4.8 Hz, 4 H), 3.57 (t, J = 4.8 Hz, 4 H), 3.00 (s, 3 H). ¹³C NMR (176 MHz, DMSO-*d*₆) δ ppm 159.1 (s, 1 C), 151.7 (s, 1 C), 149.4 (s, 1 C), 147.3 (s, 1 C), 140.6 (s, 1 C), 134.2 (s, 1 C), 134.1 (s, 1 C), 123.8 (s, 1 C), 111.9 (s, 1 C), 108.5 (s, 1 C), 65.9 (s, 2 C), 59.2 (s, 1 C), 44.9 (s, 2 C), 39.9 (s, 1 C). LCMS (Formic, UV, ESI): R_t = 0.50 min, $[M+H^+]$ 334.17, 100% purity. HRMS: (C₁₆H₂₀N₃O₃S) $[M+H^+]$ requires 334.1225, found $[M+H^+]$ 334.1227 (0.6 ppm).

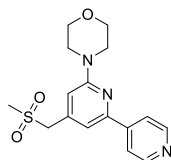
4-(4-((Methylsulfonyl)methyl)-[2,3'-bipyridin]-6-yl)morpholine (225b)



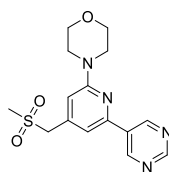
Prepared according to the general array procedure with 3-chloropyridine (17 mg, 0.15 mmol) to give 4-(4-((methylsulfonyl)methyl)-[2,3'-bipyridin]-6-yl)morpholine

(14 mg, 0.04 mmol, 28%) as an off-white solid. M.pt.: 196-197 °C. ν_{\max} (cm^{-1}) (dichloromethane): 2966 (w), 2924 (w), 2854 (w), 1604 (s), 1558 (m, C=N), 1436 (s), 1305 (s, S=O), 1244 (s), 1117 (s, S=O), 1004 (m). ^1H NMR (700 MHz, DMSO- d_6) δ ppm 9.20 (d, $J = 1.7$ Hz, 1 H), 8.61 (dd, $J = 4.7, 1.5$ Hz, 1 H), 8.35 (dt, $J = 8.2, 1.7$ Hz, 1 H), 7.50 (ddd, $J = 8.2, 4.7, 1.5$ Hz, 1 H), 7.37 (s, 1 H), 6.90 (s, 1 H), 4.49 (s, 2 H), 3.75 (t, $J = 4.7$ Hz, 4 H), 3.57 (t, $J = 4.7$ Hz, 4 H), 3.00 (s, 3 H). ^{13}C NMR (176 MHz, DMSO- d_6) δ ppm 159.1 (s, 1 C), 151.8 (s, 1 C), 149.7 (s, 1 C), 147.6 (s, 1 C), 140.5 (s, 1 C), 134.0 (s, 1 C), 133.7 (s, 1 C), 123.7 (s, 1 C), 111.8 (s, 1 C), 108.4 (s, 1 C), 65.9 (s, 2 C), 59.2 (s, 1 C), 44.9 (s, 2 C), 39.9 (s, 1 C). LCMS (Formic, UV, ESI): $R_t = 0.50$ min, $[\text{M}+\text{H}^+]$ 334.16, 100% purity. HRMS: ($\text{C}_{16}\text{H}_{20}\text{N}_3\text{O}_3\text{S}$) $[\text{M}+\text{H}^+]$ requires 334.1225, found $[\text{M}+\text{H}^+]$ 334.1224 (-0.3 ppm).

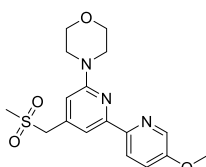
4-(4-((Methylsulfonyl)methyl)-[2,4'-bipyridin]-6-yl)morpholine (225c)



Prepared according to the general array procedure with 4-bromopyridine (23 mg, 0.15 mmol) to give 4-(4-((methylsulfonyl)methyl)-[2,4'-bipyridin]-6-yl)morpholine (4 mg, 0.01 mmol, 7%) as an off-white amorphous solid. ν_{\max} (cm^{-1}) (dichloromethane): 2967 (w), 2927 (w), 2855 (w), 1605 (s), 1568 (m, C=N), 1437 (s), 1307 (s, S=O), 1247 (s), 1118 (s, S=O), 1004 (m). ^1H NMR (700 MHz, DMSO- d_6) δ ppm 8.78 (d, $J = 5.9$ Hz, 2 H), 8.18 (d, $J = 5.9$ Hz, 2 H), 7.53 (s, 1 H), 7.03 (s, 1 H), 4.53 (s, 2 H), 3.76 (t, $J = 4.7$ Hz, 4 H), 3.59 (t, $J = 4.7$ Hz, 4 H), 3.01 (s, 3 H). ^{13}C NMR (176 MHz, DMSO- d_6) δ ppm 159.0 (s, 1 C), 150.4 (s, 1 C), 149.3 (s, 2 C), 147.7 (s, 1 C), 140.8 (s, 1 C), 124.9 (s, 1 C), 121.4 (s, 2 C), 110.4 (s, 1 C), 65.8 (s, 2 C), 59.0 (s, 1 C), 44.9 (s, 2 C), 40.0 (s, 1 C). LCMS (Formic, UV, ESI): $R_t = 0.46$ min, $[\text{M}+\text{H}^+]$ 334.16, 84% purity. HRMS: ($\text{C}_{16}\text{H}_{20}\text{N}_3\text{O}_3\text{S}$) $[\text{M}+\text{H}^+]$ requires 334.1225, found $[\text{M}+\text{H}^+]$ 334.1223 (-0.6 ppm).

4-(4-((Methylsulfonyl)methyl)-6-(pyrimidin-5-yl)pyridin-2-yl)morpholine (225e)

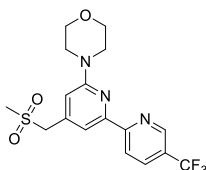
Prepared according to the general array procedure with 5-bromopyrimidine (23 mg, 0.15 mmol) to give 4-(4-((methylsulfonyl)methyl)-6-(pyrimidin-5-yl)pyridin-2-yl)morpholine (6 mg, 0.02 mmol, 13%) as a colourless solid. M.pt.: 243-246 °C. ν_{\max} (cm^{-1}) (dichloromethane): 2967 (w), 2924 (w), 2855 (w), 1606 (s), 1565 (m, C=N), 1444 (m), 1423 (m), 1303 (s, S=O), 1247 (s), 1116 (s, S=O), 1003 (m), 723 (m). ^1H NMR (700 MHz, $\text{DMSO}-d_6$) δ ppm 9.37 (s, 2 H), 9.23 (s, 1 H), 7.44 (s, 1 H), 6.96 (s, 1 H), 4.49 (s, 2 H), 3.74 (t, $J = 4.7$ Hz, 4 H), 3.58 (t, $J = 4.7$ Hz, 4 H), 3.01 (s, 3 H). ^{13}C NMR (176 MHz, $\text{DMSO}-d_6$) δ ppm 159.1 (s, 1 C), 158.3 (s, 1 C), 154.7 (s, 2 C), 149.3 (s, 1 C), 140.7 (s, 1 C), 131.7 (s, 1 C), 112.0 (s, 1 C), 109.2 (s, 1 C), 65.9 (s, 2 C), 59.2 (s, 1 C), 44.9 (s, 2 C), 40.0 (s, 1 C). LCMS (Formic, UV, ESI): $R_t = 0.68$ min, $[\text{M}+\text{H}^+]$ 335.17, 100% purity. HRMS: ($\text{C}_{15}\text{H}_{19}\text{N}_4\text{O}_3\text{S}$) $[\text{M}+\text{H}^+]$ requires 335.1178, found $[\text{M}+\text{H}^+]$ 335.1176 (-0.6 ppm).

4-(5'-Methoxy-4-((methylsulfonyl)methyl)-[2,2'-bipyridin]-6-yl)morpholine (225f)

Prepared according to the general array procedure with 2-bromo-5-methoxypyridine (28 mg, 0.15 mmol) to give 4-(5'-methoxy-4-((methylsulfonyl)methyl)-[2,2'-bipyridin]-6-yl)morpholine (11 mg, 0.03 mmol, 21%) as an off-white solid. M.pt.: 193-194 °C. ν_{\max} (cm^{-1}) (dichloromethane): 2973 (w), 2845 (w), 1604 (m), 1561 (s, C=N), 1483 (m), 1429 (s), 1305 (s, S=O), 1248 (s), 1223 (m), 1117 (s, S=O), 1003 (m). ^1H NMR (700 MHz, $\text{DMSO}-d_6$) δ ppm 8.35 (d, $J = 3.0$ Hz, 1 H), 8.28 (d, $J = 8.9$ Hz, 1 H), 7.72 (s, 1 H), 7.49 (dd, $J = 8.9, 3.0$ Hz, 1 H), 6.85 (s, 1 H), 4.51 (s, 2 H), 3.89 (s, 3 H), 3.76 (t, $J = 4.7$ Hz, 4 H), 3.55 (t, $J = 4.7$ Hz, 4 H), 2.97 (s, 3 H).

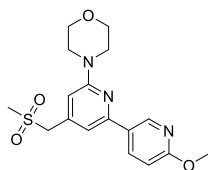
^{13}C NMR (176 MHz, $\text{DMSO-}d_6$) δ ppm 158.8 (s, 1 C), 155.8 (s, 1 C), 153.3 (s, 1 C), 148.0 (s, 1 C), 140.2 (s, 1 C), 136.7 (s, 1 C), 121.3 (s, 1 C), 121.0 (s, 1 C), 111.5 (s, 1 C), 108.4 (s, 1 C), 65.9 (s, 2 C), 59.2 (s, 1 C), 55.7 (s, 1 C), 45.1 (s, 2 C), 40.0 (s, 1 C). LCMS (Formic, UV, ESI): $R_t = 0.70$ min, $[\text{M}+\text{H}^+]$ 364.20, 100% purity. HRMS: ($\text{C}_{17}\text{H}_{22}\text{N}_3\text{O}_4\text{S}$) $[\text{M}+\text{H}^+]$ requires 364.1331, found $[\text{M}+\text{H}^+]$ 364.1331 (0 ppm).

4-(4-((Methylsulfonyl)methyl)-5'-(trifluoromethyl)-[2,2'-bipyridin]-6-yl)morpholine (225g)



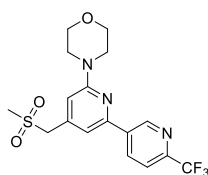
Prepared according to the general array procedure with 2-bromo-5-(trifluoromethyl)pyridine (33 mg, 0.15 mmol) to give 4-(4-((methylsulfonyl)methyl)-5'-(trifluoromethyl)-[2,2'-bipyridin]-6-yl)morpholine (7 mg, 0.02 mmol, 12%) as an off-white solid. M.pt.: 223-224 °C. ν_{max} (cm^{-1}) (dichloromethane): 2927 (w), 2855 (w), 1603 (m), 1562 (s, C=N), 1433 (m), 1327 (s, S=O), 1253 (m), 1161 (m), 1119 (s, S=O), 1079 (m), 1004 (m). ^1H NMR (700 MHz, $\text{DMSO-}d_6$) δ ppm 9.04 (br. app. d, $J = 1.7$ Hz, 1 H), 8.53 (d, $J = 8.5$ Hz, 1 H), 8.31 (dd, $J = 8.5, 2.1$ Hz, 1 H), 7.88 (s, 1 H), 7.02 (s, 1 H), 4.57 (s, 2 H), 3.77 (t, $J = 4.7$ Hz, 4 H), 3.59 (t, $J = 4.7$ Hz, 4 H), 2.99 (s, 3 H). ^{13}C NMR (176 MHz, $\text{DMSO-}d_6$) δ ppm 158.9 (s, 1 C), 158.9 (s, 1 C), 151.8 (s, 1 C), 145.9 (q, $J = 3.5$ Hz, 1 C), 140.7 (s, 1 C), 134.7 (br. q, $J = 3.5$ Hz, 1 C), 125.34 (q, $J = 272.4$ Hz, 1 C), 124.8 (q, $J = 32.4$ Hz, 1 C), 120.5 (s, 1 C), 113.0 (s, 1 C), 110.6 (s, 1 C), 65.9 (s, 2 C), 59.0 (s, 1 C), 45.0 (s, 2 C), 40.0 (s, 1 C). ^{19}F NMR (376 MHz, $\text{DMSO-}d_6$) δ ppm -60.7 (s, 3 F). LCMS (Formic, UV, ESI): $R_t = 1.09$ min, $[\text{M}+\text{H}^+]$ 402.22, 100% purity. HRMS: ($\text{C}_{17}\text{H}_{19}\text{F}_3\text{N}_3\text{O}_3\text{S}$) $[\text{M}+\text{H}^+]$ requires 402.1099, found $[\text{M}+\text{H}^+]$ 402.1099 (0 ppm).

4-(6'-Methoxy-4-((methylsulfonyl)methyl)-[2,3'-bipyridin]-6-yl)morpholine (225h)



Prepared according to the general array procedure with 5-bromo-2-methoxypyridine (28 mg, 0.15 mmol) to give 4-(6'-methoxy-4-((methylsulfonyl)methyl)-[2,3'-bipyridin]-6-yl)morpholine (2 mg, 4.13 μ mol, 3%) as a colourless amorphous solid. ν_{\max} (cm^{-1}) (dichloromethane): 2927 (w), 2858 (w), 1606 (s), 1558 (m, C=N), 1443 (m), 1304 (s, S=O), 1120 (s, S=O), 1034 (m), 1011 (m). ^1H NMR (700 MHz, DMSO- d_6) δ ppm 8.81 (d, $J = 2.5$ Hz, 1 H), 8.29 (dd, $J = 8.7, 2.5$ Hz, 1 H), 7.27 (s, 1 H), 6.92 (d, $J = 8.7$ Hz, 1 H), 6.82 (s, 1 H), 4.46 (s, 2 H), 3.91 (s, 3 H), 3.74 (t, $J = 4.7$ Hz, 4 H), 3.54 (t, $J = 4.7$ Hz, 4 H), 2.99 (s, 3 H). ^{13}C NMR (176 MHz, DMSO- d_6) δ ppm 165.3 (s, 1 C), 158.9 (s, 1 C), 151.9 (s, 1 C), 145.2 (s, 1 C), 140.4 (s, 1 C), 137.1 (s, 1 C), 128.0 (s, 1 C), 110.9 (s, 1 C), 110.3 (s, 1 C), 107.5 (s, 1 C), 65.9 (s, 2 C), 59.2 (s, 1 C), 53.3 (s, 1 C), 45.0 (s, 2 C), 40.0 (s, 1 C). LCMS (Formic, UV, ESI): $R_t = 0.90$ min, $[\text{M}+\text{H}^+]$ 364.18, 100% purity. HRMS: ($\text{C}_{17}\text{H}_{22}\text{N}_3\text{O}_4\text{S}$) $[\text{M}+\text{H}^+]$ requires 364.1331, found $[\text{M}+\text{H}^+]$ 364.1331 (0 ppm).

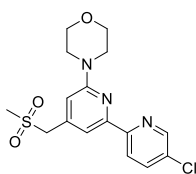
4-(4-((Methylsulfonyl)methyl)-6'-(trifluoromethyl)-[2,3'-bipyridin]-6-yl)morpholine (225i)



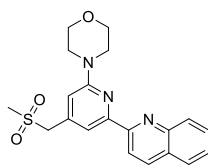
Prepared according to the general array procedure with 5-bromo-2-(trifluoromethyl)pyridine (33 mg, 0.15 mmol) to give 4-(4-((methylsulfonyl)methyl)-6'-(trifluoromethyl)-[2,3'-bipyridin]-6-yl)morpholine (20 mg, 0.05 mmol, 33%) as a colourless solid. M.pt.: 200-202 $^{\circ}\text{C}$. ν_{\max} (cm^{-1}) (dichloromethane): 2921 (w), 2852 (w), 1610 (m), 1560 (m, C=N), 1442 (m), 1339 (m, S=O), 1305 (m), 1247 (m), 1124 (s, S=O), 1005 (m). ^1H NMR (700 MHz, DMSO- d_6) δ ppm 9.50 (d, $J = 1.3$ Hz, 1 H),

9.02 (d, $J = 1.3$ Hz, 1 H), 8.64 (br. s, 1 H), 7.53 (s, 1 H), 6.98 (s, 1 H), 4.49 (s, 2 H), 3.75 (t, $J = 4.7$ Hz, 4 H), 3.58 (t, $J = 4.7$ Hz, 4 H), 3.01 (s, 3 H). ^{13}C NMR (176 MHz, DMSO- d_6) δ ppm 159.1 (s, 1 C), 151.4 (s, 1 C), 150.1 (s, 1 C), 146.1 (s, 1 C), 140.8 (s, 1 C), 134.3 (s, 1 C), 130.5 (q, $J = 3.4$ Hz, 1 C), 125.3 (q, $J = 32.1$ Hz, 1 C), 123.6 (q, $J = 272.8$ Hz, 1 C), 112.5 (s, 1 C), 109.3 (s, 1 C), 65.9 (s, 2 C), 59.2 (s, 1 C), 44.9 (s, 2 C), 40.0 (s, 1 C). ^{19}F NMR (376 MHz, DMSO- d_6) δ ppm -60.9 (s, 3 F). LCMS (Formic, UV, ESI): $R_t = 0.99$ min, $[\text{M}+\text{H}^+]$ 402.21, 100% purity. HRMS: ($\text{C}_{17}\text{H}_{19}\text{F}_3\text{N}_3\text{O}_3\text{S}$) $[\text{M}+\text{H}^+]$ requires 402.1099, found $[\text{M}+\text{H}^+]$ 402.1100 (0.2 ppm).

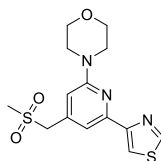
4-(5'-Chloro-4-((methylsulfonyl)methyl)-[2,2'-bipyridin]-6-yl)morpholine (225j)



Prepared according to the general array procedure with 2-bromo-5-chloropyridine (28 mg, 0.15 mmol) to give 4-(5'-chloro-4-((methylsulfonyl)methyl)-[2,2'-bipyridin]-6-yl)morpholine (9 mg, 0.03 mmol, 17%) as an off-white solid. M.pt.: 207-211 °C. ν_{max} (cm^{-1}) (dichloromethane): 2967 (w), 2924 (w), 2853 (w), 1605 (m), 1558 (s, C=N), 1471 (m), 1446 (m), 1429 (s), 1308 (s, S=O), 1265 (m), 1115 (s, S=O), 1004 (m). ^1H NMR (700 MHz, DMSO- d_6) δ ppm 8.69 (br. d, $J = 2.4$ Hz, 1 H), 8.35 (d, $J = 8.6$ Hz, 1 H), 8.03 (dd, $J = 8.6, 2.4$ Hz, 1 H), 7.78 (s, 1 H), 6.95 (s, 1 H), 4.54 (s, 2 H), 3.76 (t, $J = 4.7$ Hz, 4 H), 3.57 (t, $J = 4.7$ Hz, 4 H), 2.98 (s, 3 H). ^{13}C NMR (176 MHz, DMSO- d_6) δ ppm 158.8 (s, 1 C), 153.9 (s, 1 C), 152.2 (s, 1 C), 147.5 (s, 1 C), 140.5 (s, 1 C), 136.9 (s, 1 C), 131.2 (s, 1 C), 121.8 (s, 1 C), 112.2 (s, 1 C), 109.8 (s, 1 C), 65.9 (s, 2 C), 59.1 (s, 1 C), 45.0 (s, 2 C), 39.9 (s, 1 C). LCMS (Formic, UV, ESI): $R_t = 1.03$ min, $[\text{M}+\text{H}^+]$ 168.16, 370.16 [Cl isotopes], 100% purity. HRMS: ($\text{C}_{16}\text{H}_{19}\text{ClN}_3\text{O}_3\text{S}$) $[\text{M}+\text{H}^+]$ requires 368.0836, found $[\text{M}+\text{H}^+]$ 368.0832 (-1.1 ppm).

4-(4-((Methylsulfonyl)methyl)-6-(quinolin-2-yl)pyridin-2-yl)morpholine (225k)

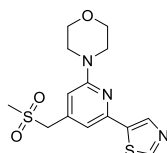
Prepared according to the general array procedure with 2-bromoquinoline (30 mg, 150 μmol) to give 4-(4-((methylsulfonyl)methyl)-6-(quinolin-2-yl)pyridin-2-yl)morpholine (4 mg, 9.39 μmol , 6%) as an off-white amorphous solid. ν_{max} (cm^{-1}) (dichloromethane): 2956 (w), 2927 (w), 2864 (w), 1601 (s), 1560 (s, C=N), 1428 (m), 1295 (m, S=O), 1262 (m), 1117 (s, S=O), 1006 (m), 835 (m), 765 (m). ^1H NMR (700 MHz, $\text{DMSO-}d_6$) δ ppm 8.54 (d, $J = 8.5$ Hz, 1 H), 8.48 (d, $J = 8.4$ Hz, 1 H), 8.09 (d, $J = 8.5$ Hz, 1 H), 7.97 - 8.07 (m, 2 H), 7.80 (ddd, $J = 8.4, 6.9, 1.3$ Hz, 1 H), 7.63 (ddd, $J = 8.4, 6.9, 1.3$ Hz, 1 H), 6.99 (s, 1 H), 4.61 (s, 2 H), 3.79 (t, $J = 4.7$ Hz, 4 H), 3.62 (t, $J = 4.7$ Hz, 4 H), 3.02 (s, 3 H). ^{13}C NMR (176 MHz, $\text{DMSO-}d_6$) δ ppm 158.9 (s, 1 C), 155.5 (s, 1 C), 153.3 (s, 1 C), 147.1 (s, 1 C), 140.4 (s, 1 C), 136.9 (s, 1 C), 129.9 (s, 1 C), 129.0 (s, 1 C), 127.9 (s, 1 C), 127.9 (s, 1 C), 126.8 (s, 1 C), 118.7 (s, 1 C), 112.8 (s, 1 C), 109.8 (s, 1 C), 65.9 (s, 2 C), 59.1 (s, 1 C), 45.1 (s, 2 C), 40.0 (s, 1 C). LCMS (Formic, UV, ESI): $R_t = 0.93$ min, $[\text{M}+\text{H}^+]$ 384.23, 100% purity. HRMS: ($\text{C}_{20}\text{H}_{22}\text{N}_3\text{O}_3\text{S}$) $[\text{M}+\text{H}^+]$ requires 384.1385, found $[\text{M}+\text{H}^+]$ 384.1385 (0.8 ppm).

4-(4-((Methylsulfonyl)methyl)-6-(thiazol-4-yl)pyridin-2-yl)morpholine (225t)

Prepared according to the general array procedure with 4-bromothiazole (24 mg, 0.15 mmol) to give 4-(4-((methylsulfonyl)methyl)-6-(thiazol-4-yl)pyridin-2-yl)morpholine (13 mg, 0.04 mmol, 25%) as an off-white solid. M.pt.: 191-192 $^{\circ}\text{C}$. ν_{max} (cm^{-1}) (dichloromethane): 2967 (w), 2927 (w), 2853 (w), 1603 (s), 1559 (s, C=N), 1435 (s), 1306 (s, S=O), 1263 (m), 1235 (m), 1142 (m), 1116 (s, S=O), 1003 (m), 882 (m). ^1H NMR (700 MHz, $\text{DMSO-}d_6$) δ ppm 9.18 (d, $J = 2.0$ Hz, 1 H), 8.27 (d, $J = 2.0$ Hz, 1 H), 7.53 (s, 1 H), 6.84 (s, 1 H), 4.51 (s, 2 H), 3.75 (t, $J = 4.7$ Hz, 4 H),

3.55 (t, $J = 4.7$ Hz, 4 H), 2.97 (s, 3 H). ^{13}C NMR (176 MHz, $\text{DMSO-}d_6$) δ ppm 158.9 (s, 1 C), 155.7 (s, 1 C), 154.6 (s, 1 C), 150.1 (s, 1 C), 140.4 (s, 1 C), 117.7 (s, 1 C), 112.3 (s, 1 C), 108.5 (s, 1 C), 65.9 (s, 2 C), 59.1 (s, 1 C), 44.9 (s, 2 C), 40.0 (s, 1 C). LCMS (Formic, UV, ESI): $R_t = 0.80$ min, $[\text{M}+\text{H}^+]$ 340.13, 100% purity. HRMS: ($\text{C}_{14}\text{H}_{18}\text{N}_3\text{O}_3\text{S}_2$) $[\text{M}+\text{H}^+]$ requires 340.0790, found $[\text{M}+\text{H}^+]$ 340.0788 (-0.6 ppm).

4-(4-((Methylsulfonyl)methyl)-6-(thiazol-5-yl)pyridin-2-yl)morpholine (225v)



Prepared according to the general array procedure with 5-bromothiazole (24 mg, 0.15 mmol) to give 4-(4-((methylsulfonyl)methyl)-6-(thiazol-5-yl)pyridin-2-yl)morpholine (15 mg, 0.04 mmol, 30%) as an off-white solid. M.pt.: 195-198°C. ν_{max} (cm^{-1}) (dichloromethane): 3085 (w), 2967 (w), 2924 (w), 2853 (w), 1599 (m), 1558 (m, C=N), 1440 (m), 1304 (s, S=O), 1243 (s), 1115 (s, S=O), 1003 (m), 890 (m). ^1H NMR (700 MHz, $\text{DMSO-}d_6$) δ ppm 9.10 (s, 1 H), 8.43 (s, 1 H), 7.28 (s, 1 H), 6.82 (s, 1 H), 4.46 (s, 2 H), 3.73 (t, $J = 4.7$ Hz, 4 H), 3.50 (t, $J = 4.7$ Hz, 4 H), 3.00 (s, 3 H). ^{13}C NMR (176 MHz, $\text{DMSO-}d_6$) δ ppm 158.8 (s, 1 C), 155.4 (s, 1 C), 147.8 (s, 1 C), 140.5 (s, 1 C), 140.4 (s, 1 C), 140.2 (s, 1 C), 111.1 (s, 1 C), 108.1 (s, 1 C), 65.8 (s, 2 C), 59.0 (s, 1 C), 44.8 (s, 2 C), 40.0 (s, 1 C). LCMS (Formic, UV, ESI): $R_t = 0.77$ min, $[\text{M}+\text{H}^+]$ 340.12, 91% purity. HRMS: ($\text{C}_{14}\text{H}_{18}\text{N}_3\text{O}_3\text{S}_2$) $[\text{M}+\text{H}^+]$ requires 340.0790, found $[\text{M}+\text{H}^+]$ 340.0786 (-1.2 ppm).

6.5 General procedure used in HTS reactions (Section 4.7)

To a vial labelled as solution A was added sodium 4-((methylsulfonyl)methyl)-6-morpholinopyridine-2-sulfinate (55 mg, 144 μmol , 90% purity), heteroaryl halide (144 μmol), and *tert*-amyl alcohol (1080 μL). To a vial labelled as solution B was added sodium 4-((methylsulfonyl)methyl)-6-morpholinopyridine-2-sulfinate (55 mg, 144 μmol), heteroaryl halide (144 μmol), and 1,4-dioxane (1080 μL). To a vial labelled as solution C was added K_2CO_3 (25 mg, 180 μmol) and *tert*-amyl alcohol (215 μL). To a vial labelled as solution D was added Cs_2CO_3 (59 mg, 180 μmol) and

tert-amyl alcohol (181 μ L). To a vial labelled as solution E was added K_2CO_3 (25 mg, 180 μ mol) and 1,4-dioxane (215 μ L). To a vial labelled as solution F was added Cs_2CO_3 (59 mg, 180 μ mol) and 1,4-dioxane (181 μ L). A reaction screening block was fitted with 24 vials in rows A-D and columns 1-6, with the palladium pre-catalyst pre-weighed into the appropriate vials (10 mol%, column 1: DTBPF Pd G3, column 2: DPPF Pd G3, column 3: DPPE Pd G3, column 4: $P(tBu)_2Me$ Pd G3, column 5: PCy_3 Pd G3 and column 6: $P(tBu)_3$ Pd G4). 80 μ L of solution A was added to vials A1, A2, A3, A4, A5, A6, B1, B2, B3, B4, B5, B6; 80 μ L of solution B was added to vials C1, C2, C3, C4, C5, C6, D1, D2, D3, D4, D5, D6; 20 μ L of solution C was added to vials A1, A2, A3, A4, A5, A6; 20 μ L of solution D was added to vials B1, B2, B3, B4, B5, B6; 20 μ L of solution E was added to vials C1, C2, C3, C4, C5, C6; and 20 μ L of solution F was added to vials D1, D2, D3, D4, D5, D6. The reaction block was sealed and heated and stirred using a tumble stirrer at 150 $^{\circ}C$ for 21 h. 125 μ L of quench solution (acetonitrile with 0.002 M of triphenylamine internal standard and 0.04 M of acetic acid (delivered 10 mol% of the internal standard compared to the starting materials)) was added to reaction plate and the plate shaken. 750 μ L of acetonitrile was dispensed into 24 wells of a LCMS plate and 20 μ L aliquots from the reaction plate added to the corresponding wells of the LCMS plate.

Screen 1 (Figure 52) as above with 2-bromopyridine (23 mg, 144 μ mol).

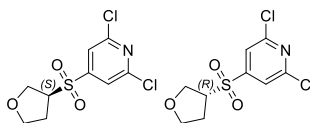
Screen 2 (Figure 53) as above with 2-bromopyrimidine (23 mg, 144 μ mol).

Screen 3 (Figure 54) as above with 2-bromo-1*H*-imidazole (21 mg, 144 μ mol).

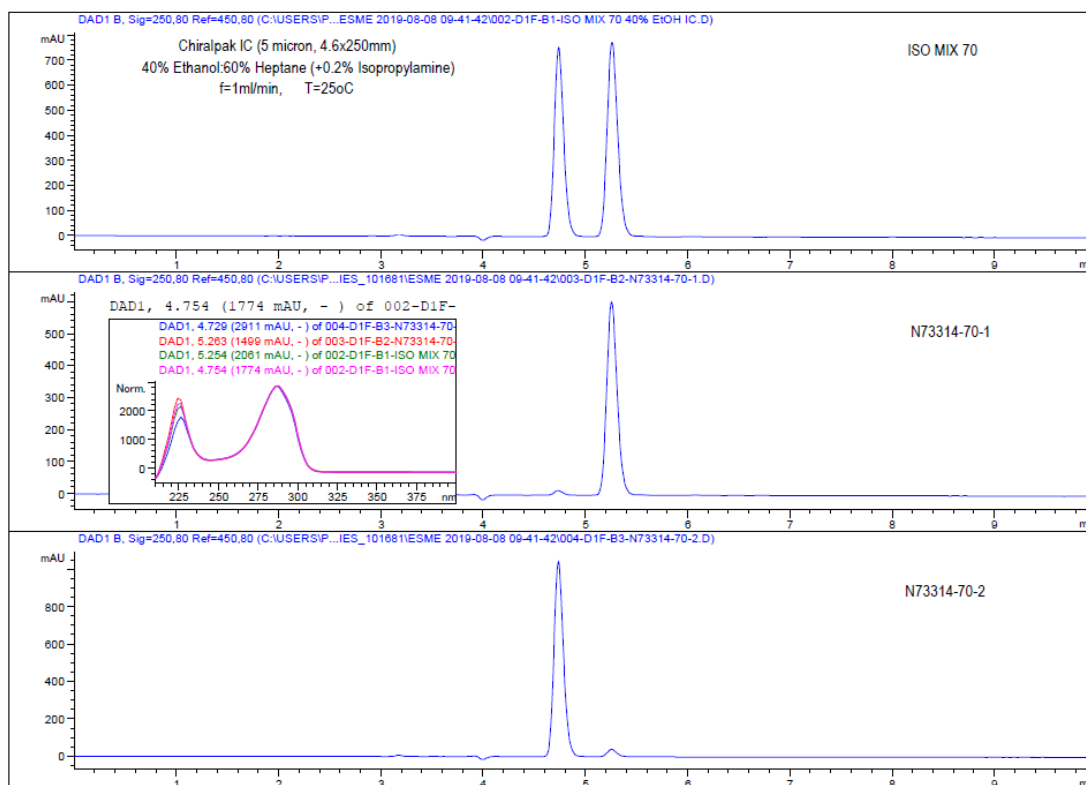
6.6 HPLC with a chiral stationary phase data for selected compounds

A racemic mixture (top chromatogram, made by combining equal amounts of the two enantiomers) and each enantiomer ((*S*)-isomer (-1) – middle chromatogram and (*R*)-isomer (-2) – lower chromatogram) was passed down a chiral stationary phase under the specified conditions, demonstrating different retention times. The two isomers continued to demonstrate different retention times throughout the steps taken to synthesise the final compounds and this was taken as evidence that the chirality was maintained throughout the synthesis, giving single isomers of the final compounds.

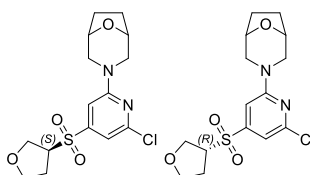
(S)-2,6-Dichloro-4-((tetrahydrofuran-3-yl)sulfonyl)pyridine and (R)-2,6-dichloro-4-((tetrahydrofuran-3-yl)sulfonyl)pyridine, chiral starting materials



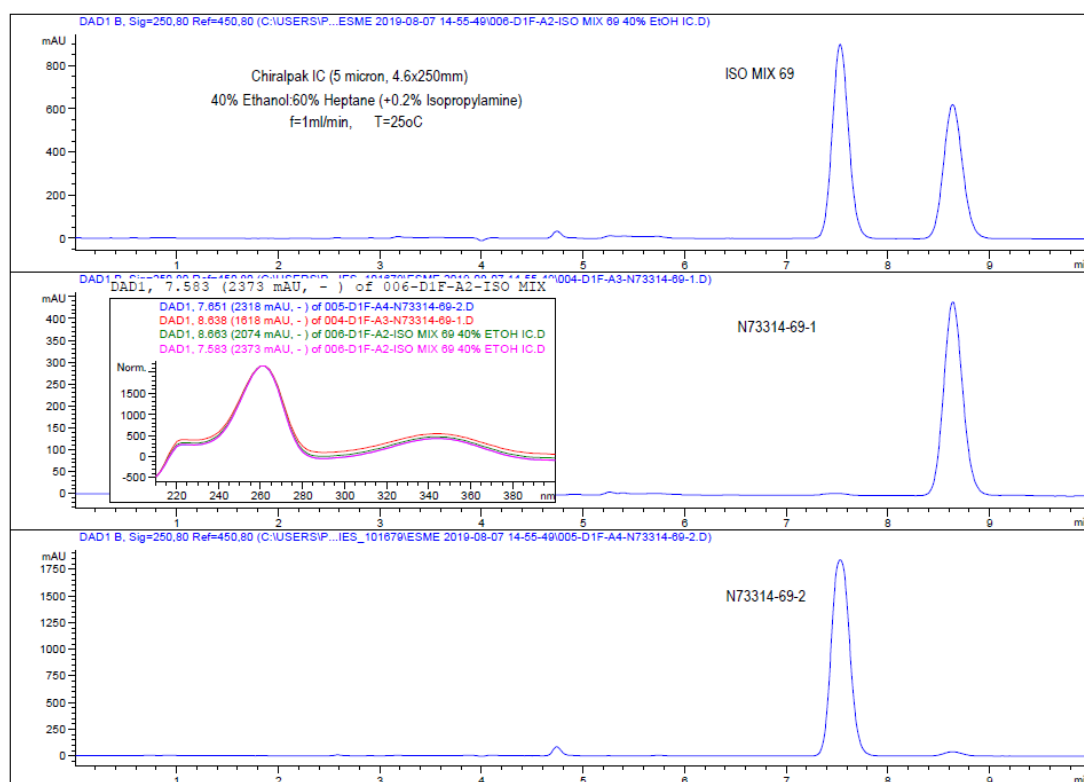
Using Chiralpak IC (4.6 mm x 250 mm, 5 μm packing diameter) column, eluting with 40% ethanol:60% heptane (+0.2% isopropyl amine), with parameters: flow = 1 mL/min, T = 25 °C the two compounds demonstrated different retention times.



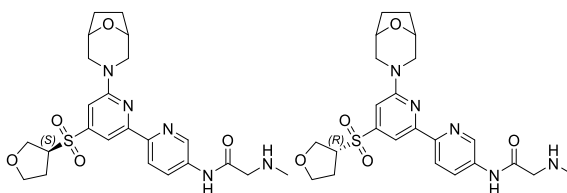
3-(6-Chloro-4-(((S)-tetrahydrofuran-3-yl)sulfonyl)pyridin-2-yl)-8-oxa-3-azabicyclo[3.2.1]octane (106a) and 3-(6-chloro-4-(((R)-tetrahydrofuran-3-yl)sulfonyl)pyridin-2-yl)-8-oxa-3-azabicyclo[3.2.1]octane (106b)



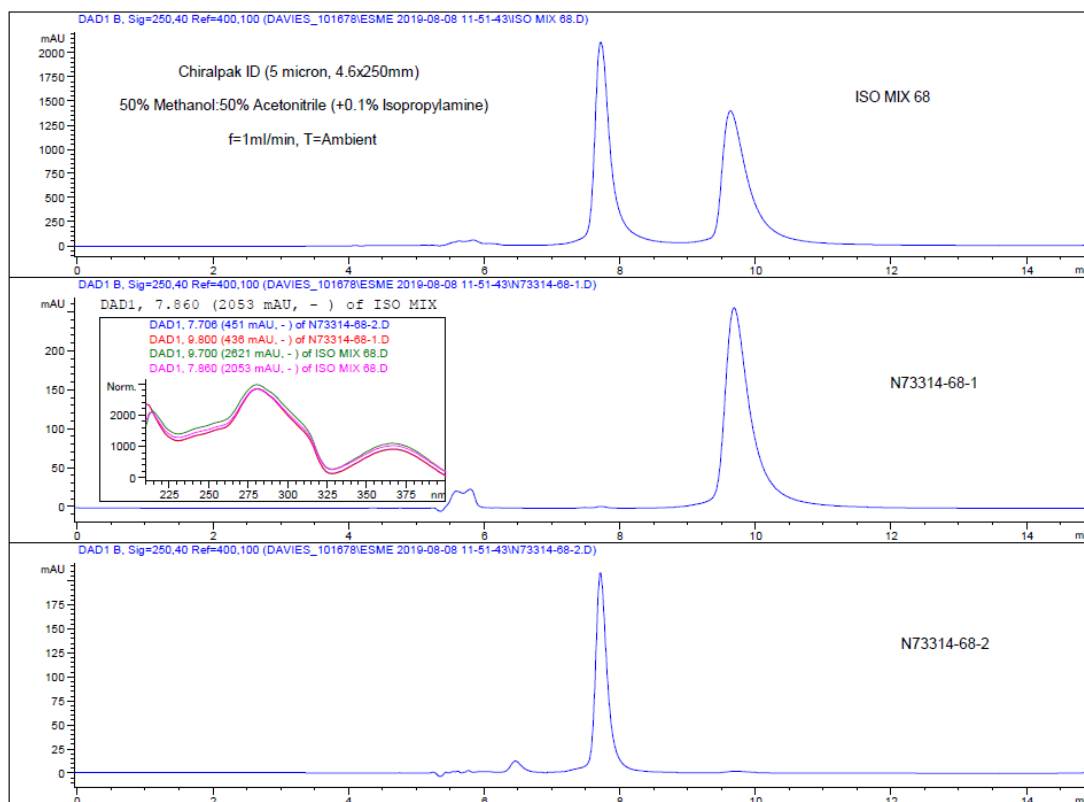
Using Chiralpak IC (4.6 mm x 250 mm, 5 μ m packing diameter) column, eluting with 40% ethanol:60% heptane (+0.2% isopropyl amine), with parameters: flow = 1 mL/min, T = 25 $^{\circ}$ C the two compounds demonstrated different retention times.



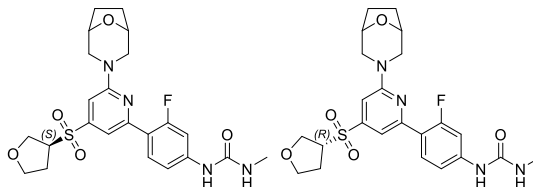
3-(6-Chloro-4-(((S)-tetrahydrofuran-3-yl)sulfonyl)pyridin-2-yl)-8-oxa-3-azabicyclo[3.2.1]octane (75a) and 3-(6-chloro-4-(((R)-tetrahydrofuran-3-yl)sulfonyl)pyridin-2-yl)-8-oxa-3-azabicyclo[3.2.1]octane (75b)



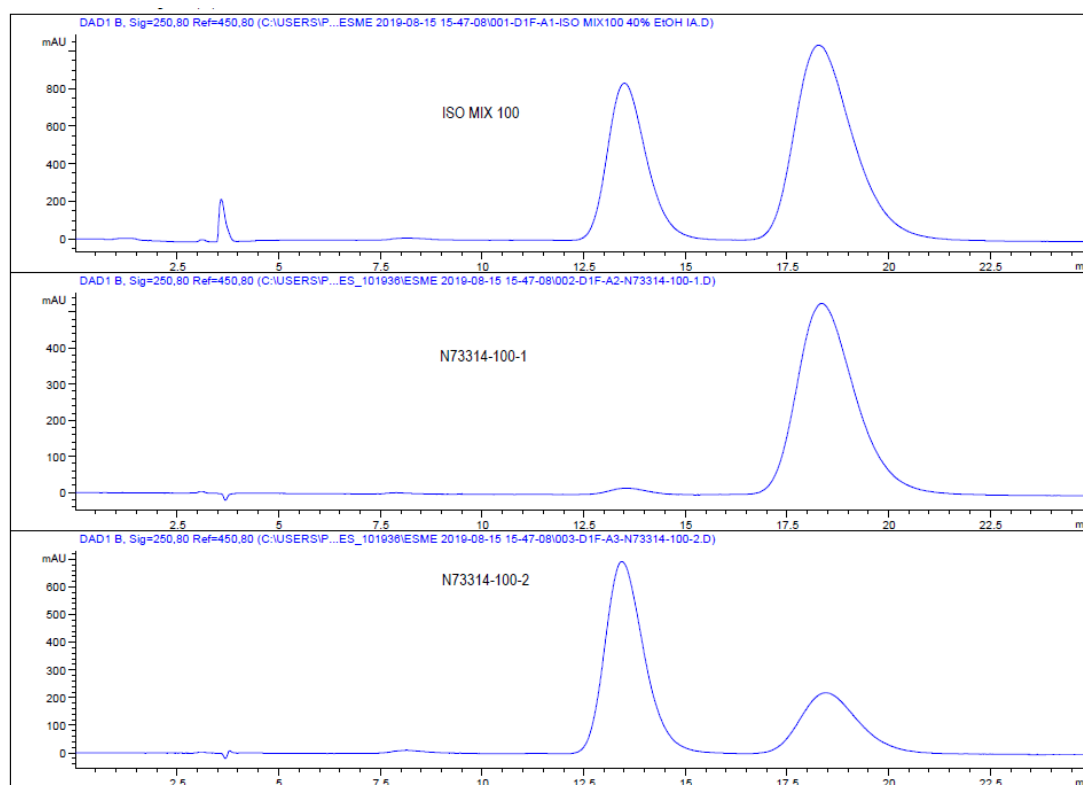
Using Chiralpak ID (4.6 mm x 250 mm, 5 µm packing diameter) column, eluting with 50% methanol:50% acetonitrile (+0.1% isopropyl amine), with parameters: flow = 1 mL/min, T = 25 °C, the two compounds demonstrated different retention times.



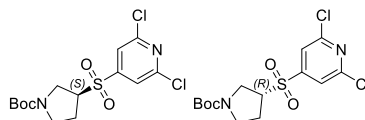
1-(4-(6-(8-Oxa-3-azabicyclo[3.2.1]octan-3-yl)-4-(((S)-tetrahydrofuran-3-yl)sulfonyl)pyridin-2-yl)-3-fluorophenyl)-3-methylurea (77a) and 1-(4-(6-(8-oxa-3-azabicyclo[3.2.1]octan-3-yl)-4-(((R)-tetrahydrofuran-3-yl)sulfonyl)pyridin-2-yl)-3-fluorophenyl)-3-methylurea (77b)



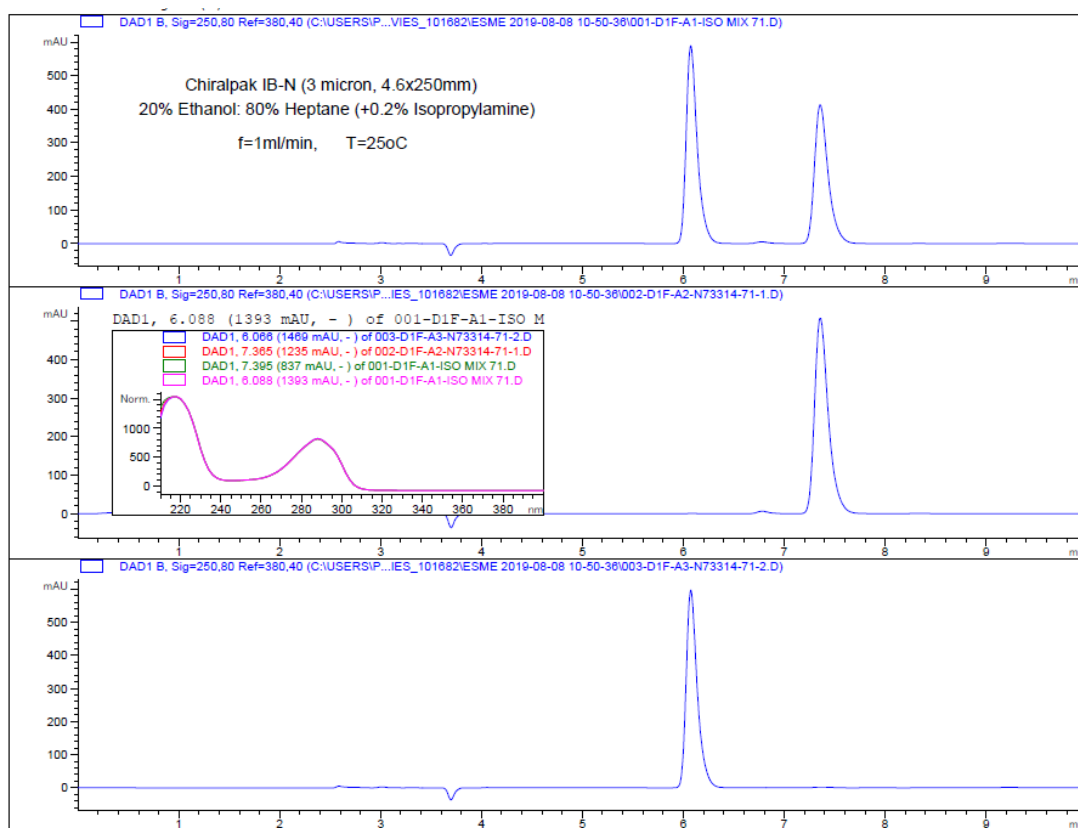
Using Chiralpak IA (4.6 mm x 250 mm, 5 μ m packing diameter) column, eluting with 40% ethanol:60% heptane (+0.2% isopropyl amine), with parameters: flow = 1 mL/min, T = 25 $^{\circ}$ C, the two compounds demonstrated different retention times.



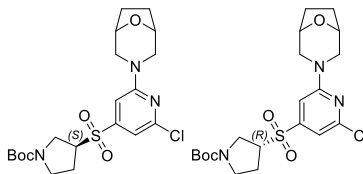
***tert*-Butyl (S)-3-((2,6-dichloropyridin-4-yl)sulfonyl)pyrrolidine-1-carboxylate
and *tert*-butyl (R)-3-((2,6-dichloropyridin-4-yl)sulfonyl)pyrrolidine-1-carboxylate, chiral starting materials**



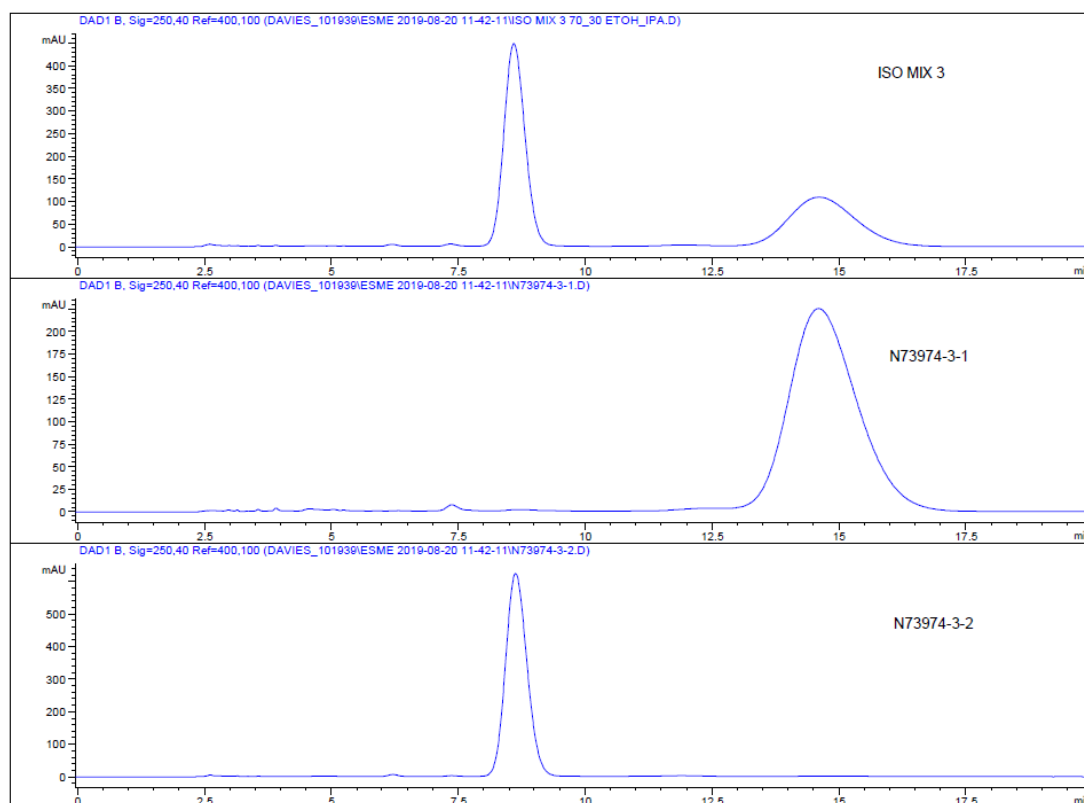
Using Chiralpak IB-N (4.6 mm x 250 mm, 3 μm packing diameter) column, eluting with 20% ethanol: 80% heptane (+0.2% isopropyl amine), with parameters: flow = 1 mL/min, T = 25 °C, the two compounds demonstrated different retention times.



tert-Butyl (3*S*)-3-((2-(8-oxa-3-azabicyclo[3.2.1]octan-3-yl)-6-chloropyridin-4-yl)sulfonyl)pyrrolidine-1-carboxylate (125a) and *tert*-butyl (3*S*)-3-((2-(8-oxa-3-azabicyclo[3.2.1]octan-3-yl)-6-chloropyridin-4-yl)sulfonyl)pyrrolidine-1-carboxylate (125b)



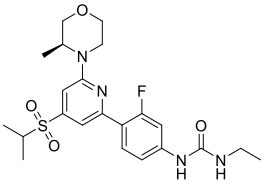
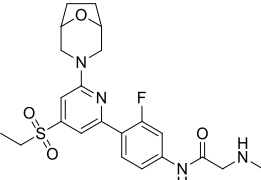
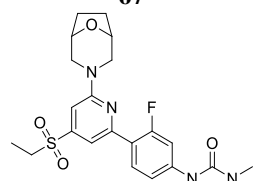
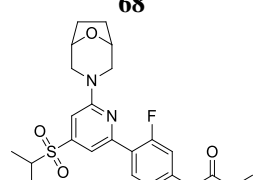
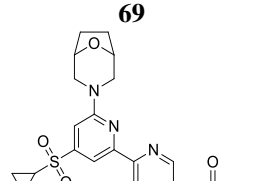
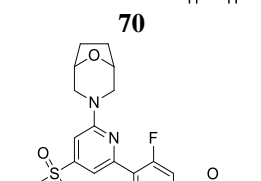
Using Chiralpak IG (4.6 mm x 250 mm, 5 μ m packing diameter) column, eluting with 70% ethanol:30% IPA (+0.1% isopropyl amine), with parameters: flow = 1 mL/min, T = 25 $^{\circ}$ C, the two compounds demonstrated different retention times.

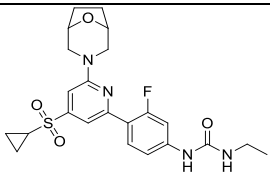
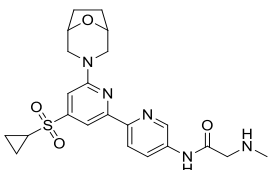
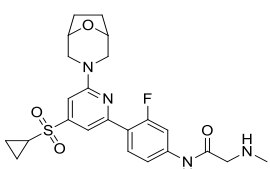
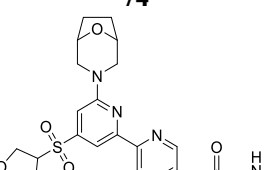
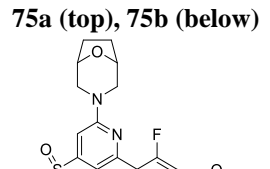
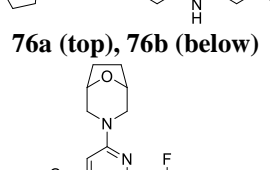
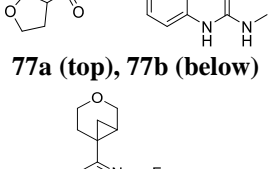
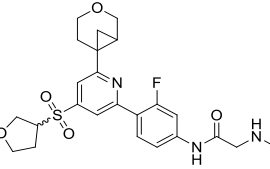


Appendix

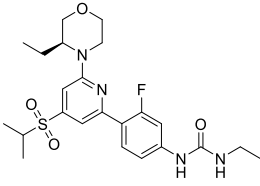
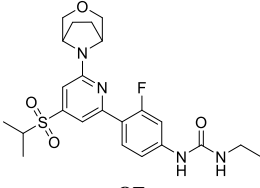
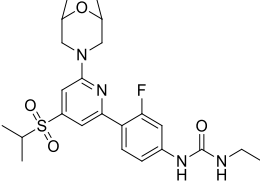
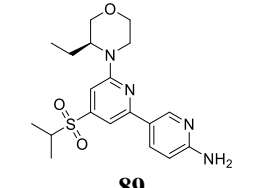
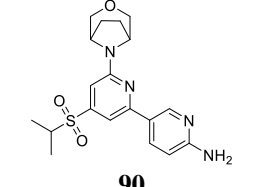
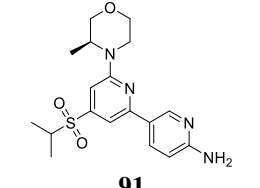
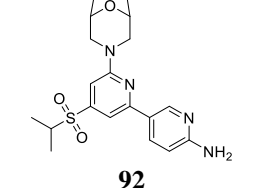
7. Appendix

7.1 Appendix A: Full data on compounds discussed in Section 2.3

Structure, Compound Number	mTOR KB pIC ₅₀ (n) ^a	pAkt pIC ₅₀ (n) ^a	DNA-PK pIC ₅₀ (n) ^a	PI3K Selectivity ^b	Chrom LogD ^c	CLND, SLF (µg/mL) ^d	AMP, MDCK P _{exact} (nm/s) ^d
 56	6.4 (4)	6.9 (9)	5.8 (2)	6	5.1	13,-	318,-
 67	7.1 (4)	6.8 (2)	5.1 (1)	>400	3.3	198, 373	170, 243
 68	6.7 (4)	6.9 (2)	7.0 (1)	>80	4.1	23,-	-,-
 69	6.7 (4)	7.1 (2)	6.4 (1)	~50	4.4	59,-	-,-
 70	7.3 (4)	6.5 (2)	7.2 (1)	>300	3.4	69,-	-,-
 71	6.5 (2)	6.6 (2)	7.5 (1)	20	4.3	44,27	-,-

Structure, Compound Number	mTOR KB pIC ₅₀ (n) ^a	pAkt pIC ₅₀ (n) ^a	DNA-PK pIC ₅₀ (n) ^a	PI3K Selectivity ^b	Chrom LogD ^c	CLND, SLF (µg/mL) ^d	AMP, MDCK P _{exact} (nm/s) ^d
 72	6.7 (4)	7.4 (3)	7.5 (1)	~40	4.8	-,-	240,-
 73	7.9 (6)	6.9 (3)	5.8 (1)	>2600	2.8	201, 903	-,129
 74	7.1 (4)	7.0 (3)	5.9 (1)	>400	3.5	73,-	160,-
 75a (top), 75b (below)	8.0 (6)	6.9 (6)	5.5 (4)	>2950	2.3	162, 26	42,29
 76a (top), 76b (below)	7.3 (6)	6.8 (5)	4.8 (1)	>600	3.2	190, 603	116, 226
 77a (top), 77b (below)	7.0 (4)	7.2 (2)	6.8 (1)	>250	3.9	113,5	-,-
 78 (racemic)	-	6.8 (2)	7.4 (1)	-	-	-,-	-,-
 78 (racemic)	5.8 (3)	5.4 (1)	<4.4 (3)	19	-	28,-	-,-

Structure, Compound Number	mTOR KB pIC ₅₀ (n) ^a	pAkt pIC ₅₀ (n) ^a	DNA-PK pIC ₅₀ (n) ^a	PI3K Selectivity ^b	Chrom LogD ^c	CLND, SLF (μg/mL) ^d	AMP, MDCK P _{exact} (nm/s) ^d
79a (top), 79b (below)	6.7 (4)	6.3 (2)	<4.4 (3)	>150	3.2	170, 957	250,-
80	7.3 (4)	6.4 (1)	4.7 (3)	>500	2.6	163, 596	150,-
81a (top), 81b (below)	8.3 (5)	7.4 (3)	7.2 (3)	>5650	3.7	108,2	12,35
82a	>10.1 (2)	7.7 (5)	6.2 (3)	*	3.4	63,2	14,17
83a	>8.3 (2) ^e	7.2 (8)	6.5 (3)	**	3.8	7,-	16,-
84a	8.1 (2)	7.2 (8)	6.2 (2)	>600	3.8	-,-	24,-
85a	7.8 (4)	7.7 (6)	6.6 (1)	>250	4.2	-,-	51,-

Structure, Compound Number	mTOR KB pIC ₅₀ (n) ^a	pAkt pIC ₅₀ (n) ^a	DNA-PK pIC ₅₀ (n) ^a	PI3K Selectivity ^b	Chrom LogD ^c	CLND, SLF (µg/mL) ^d	AMP, MDCK P _{exact} (nm/s) ^d
 86	6.1 (6)	7.5 (4)	6.1 (3)	7	5.4	11,-	385,-
 87	6.8 (8)	7.5 (5)	6.2 (2)	~100	5.0	32,26	290, 763
 88	6.7 (4)	7.4 (5)	6.9 (1)	18	5.0	5,12	-,558
 89	6.0 (2)	6.4 (3)	5.6 (2)	7	4.3	14,-	690,-
 90	6.8 (2)	7.1 (1)	6.3 (2)	-	-	-	-
 91	6.8 (2)	6.1 (1)	5.4 (1)	8	3.9	141,5	310, 727
 92	6.8 (2)	6.6 (1)	6.5 (1)	>40	3.9	147,4	250, 708

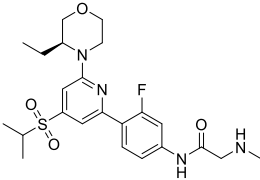
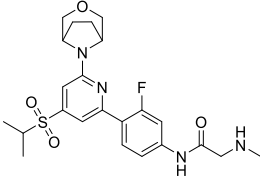
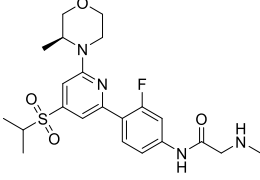
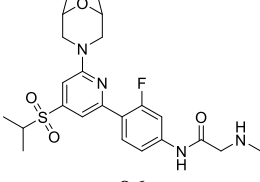
Structure, Compound Number	mTOR KB pIC ₅₀ (n) ^a	pAkt pIC ₅₀ (n) ^a	DNA-PK pIC ₅₀ (n) ^a	PI3K Selectivity ^b	Chrom LogD ^c	CLND, SLF (µg/mL) ^d	AMP, MDCK P _{exact} (nm/s) ^d
 93	6.8 (2)	6.8 (2)	<4.4 (3)	~40	4.3	117,-	-,-
 94	7.4 (4)	6.9 (4)	4.9 (3)	>900	3.8	131, 560	-,178
 95	7.2 (3)	6.9 (6)	5.4 (1)	~80	3.8	-,-	300,-
 96	7.0 (2)	7.3 (4)	5.1 (1)	>300	3.8	-,-	265,-

Table Appendix A: Key data on the compounds discussed in Section 2.4. a = (*S*)-isomer, b = (*R*)-isomer. The data for the (*S*)-isomer is reported first (top row), the (*R*)-isomer is second (bottom row). ^apIC₅₀ recorded as the mean of the data obtained on each of a number of test occasions (n). ^bSelectivity over PI3K (α , β , γ , δ) calculated by comparing the mTOR KB pIC₅₀ with the highest PI3K affinity obtained. Reported as follows: Selectivity values of under 20 are reported to the nearest whole number; selectivity values 20-100 are reported to the nearest 10; selectivity values over 100 are reported as > the nearest 50. ^cChromLogD at pH7.4. ^dIf more than one measurement taken, the mean was reported. ^eValue quoted as >8.3 as the individual data points recorded were 8.5, 8.1 and >10.1. - Data not generated. *No selectivity data reported for compound **82a** because it was not known what the mTOR KB affinity of the compound was (it was recorded at the upper limit of the assay). ** No selectivity data reported for compound **83a** because one of the mTOR KB test occasion data points was recorded at the upper limit of the assay. Compounds synthesised in the FLI DPU with final compounds made by H. Davies, E. Mogaji, S. Nicolle, H. Hobbs, A. Hancock, E. Hounslea and V. Clayton.

7.2 Appendix B: Selectivity data on compounds discussed in Section 2.4

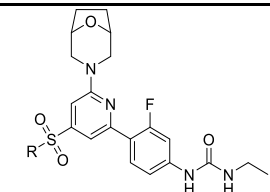
		mTOR KB pIC ₅₀ (n) ^a	pAkt pIC ₅₀ (n) ^a	DNA- PK pIC ₅₀ (n) ^a	DNA-PK Selectivity ^b	PI3K Selectivity ^c
R, Compound Number						
	131	6.6 (4)	5.9 (4)	6.0 (3)	4	~150
	133	6.1 (3)	6.2 (4)	-	-	>40
	135	6.2 (3)	6.7 (4)	5.7 (2)	3	50
	139	6.8 (4)	7.2 (4)	-	-	~200
	148a	7.0 (9)	7.3 (3)	7.0 (1)	-	21
	148b	6.6 (5)	7.3 (3)	7.6 (1)	-	>70
	127a	7.1 (4)	6.5 (4)	6.1 (2)	9	~400
	127b	7.0 (5)	6.3 (4)	6.5 (2)	3	>300
	128a	7.2 (3)	7.1 (9)	5.9 (1)	19	~550
	128b	6.9 (4)	6.8 (6)	6.0 (3)	9	>50
	149(1)^d	7.0 (4)	7.5 (5)	5.9 (2)	11	>100
	149(2)^d	7.3 (5)	7.6 (5)	6.2 (2)	12	>150
	149^d	7.1 (4)	7.6 (7)	6.1 (2)	9	>350
	150^e	6.9 (6)	7.2 (4)	6.4 (1)	3	>100
	120	5.5 (2)	6.1 (1)	6.1 (1)	-	4
	72	6.7 (4)	7.4 (3)	7.5 (1)	-	>40
	151	6.7 (4)	7.4 (4)	7.0 (1)	-	>40
	123	6.0 (4)	7.3 (2)	7.2 (1)	-	16
	117	6.3 (4)	7.4 (4)	-	-	13
	88	6.7 (4)	7.4 (5)	6.9 (1)	-	18
	146	6.8 (4)	7.5 (3)	6.8 (1)	-	>60

Table Appendix B: Selectivity data on compounds in **Table 12**. a = (*S*)-isomer, b = (*R*)-isomer.

^apIC₅₀ recorded as the mean of the data obtained on a number of test occasions (n). ^cSelectivity over DNA-PK recorded to the nearest whole number. ^eSelectivity over PI3K (α, β, γ, δ) calculated by comparing the mTOR KB pIC₅₀ with the highest PI3K affinity obtained. Reported as follows: Selectivity values of under 20 are reported to the nearest whole number; selectivity values 20-100 are reported to the nearest 10; selectivity values over 100 are reported as > the nearest 50. ^dSingle enantiomers from a chiral separation, 1 and 2 denote order compound eluted from the column.

^eRacemic mixture. Final compounds made by H. Davies, E. Mogaji, D. Summers.

7.3 Appendix C: Quantitative NMR example

NMR sample was prepared with 10 mg of reaction mixture containing compound **225a** (molar mass = 333) and 10 mg of internal standard (1,3,5-trimethoxybenzene, molar mass = 168). The ratio of integrals of the peaks corresponding to protons in both the internal standard and compound **225a** were used in **Equation 5** to calculate the purity of the sample.²²⁰

$$P_x = \frac{I_x}{I_{std}} \cdot \frac{N_{std}}{N_x} \cdot \frac{M_x}{M_{std}} \cdot \frac{W_{std}}{W_x} \cdot P_{std}$$

Equation 5: Calculation used in quantitative NMR to calculate the purity of a compound. I = Integral area in the NMR; N = Number of nuclei; M = Molar mass; W = Weight and P = Purity (of analyte (x) and standard (std) respectively).²²⁰

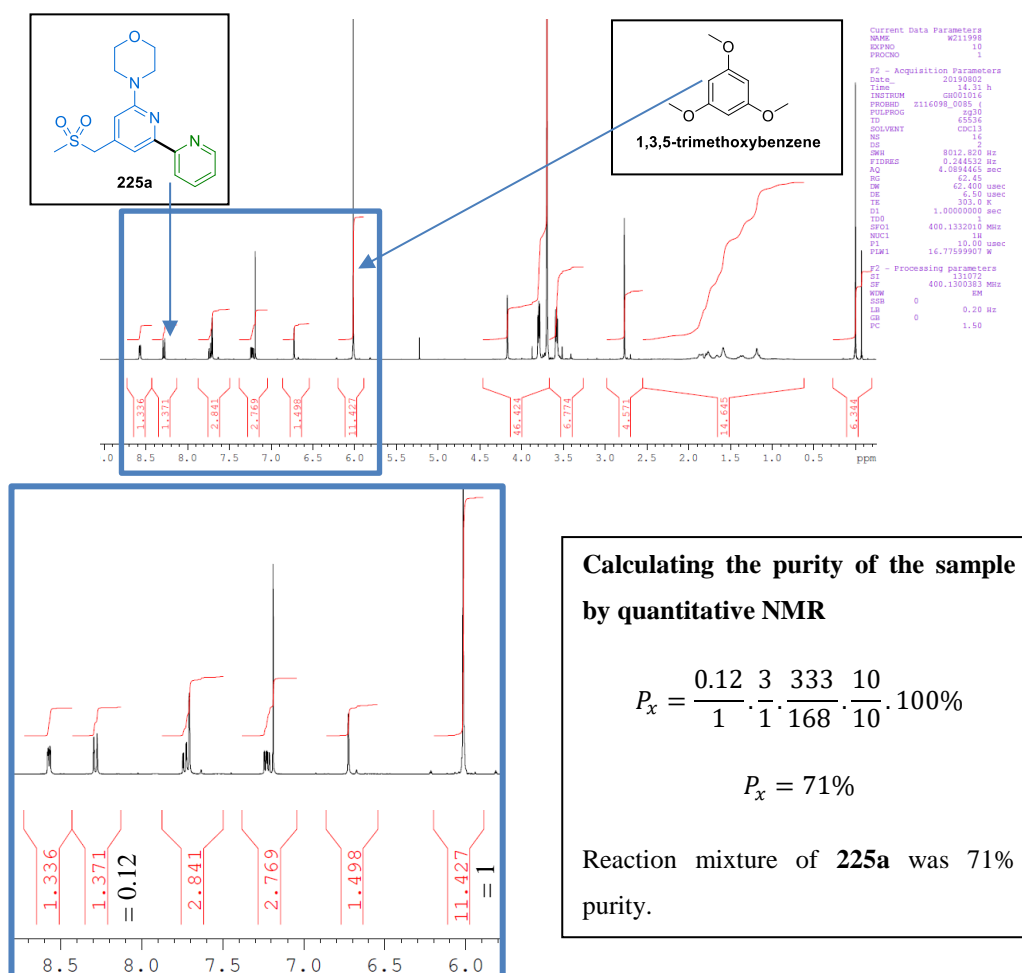


Figure Appendix C: Calculating the purity of the reaction mixture to form compound **225a** in the desulfonative cross-coupling reaction (Repeat 2 in **Scheme 50**) using quantitative NMR with 1,3,5-trimethoxybenzene as an internal standard.

7.4 Appendix D: Assay experimental procedures

7.4.1 PI3K-Isoform HTRF assay

Inhibition of each of the isoforms of PI3K was determined using a homogeneous time-resolved fluorescence (HTRF) kit assay format provided by Milipore and a method based on that described by Gray *et al.*²²¹ Reactions were performed in assay buffer containing 50 mM 4-(2-hydroxyethyl)-1-piperazineethanesulfonic acid (HEPES) pH 7.0, 150 mM NaCl, 10 mM MgCl₂, 2.3 mM sodium cholate, 10 μM 3-[(3-cholamidopropyl)dimethylammonio]-1-propanesulfonate (CHAPS), and 1 mM dithiothreitol (DTT). Enzymes were preincubated with the test compound (10 nM stock solution diluted 4-fold in DMSO) for 15 minutes at room temperature prior to reaction initiation by the addition of a substrate solution containing ATP at K_M for the specific isoform tested (α at 250 μM, β at 400 μM, δ at 80 μM, and γ at 15 μM), PIP₂ at either 5 μM (PI3K δ) or 8 μM (PI3K α , β , and γ) and 10 nM biotin-PIP₃.^a After 60 minutes of incubation at room temperature, the reactions were stopped by the addition of a stop/detect solution containing 50 mM HEPES pH 7.0, 150 mM NaCl, 2.3 mM sodium cholate, 10 μM CHAPS, 30 mM EDTA, 40 mM potassium fluoride and 1 mM DTT containing 16.5 nM GRP-1 PH domain, 8.3 nM streptavidin-APC and 2 nM europium-anti-GST. The assay plate was incubated in the dark for a further 60 minutes to equilibrate prior to reading using a Perkin Elmer EnVision plate reader. Ratio data were normalized to high (negative control, no compound present) and low (positive control, no enzyme or enzyme in the presence of 8.3 μM wortmannin (a PI3K inhibitor)) controls prior to fitting using a four-parameter logistic regression equation (**Equation 6**) to determine the IC₅₀. Taking the negative natural log (-log₁₀) of the IC₅₀ generated the pIC₅₀.

^a K_M – the Michaelis constant, defined as the substrate (here ATP) concentration at half the maximum reaction velocity (the speed of reaction of the enzyme – here PI3K α , β , λ and δ).

$$y = Bottom + \frac{Top - Bottom}{1 + \left(\frac{x}{IC_{50}}\right)^S}$$

Equation 6: A four-parameter logistic regression equation, frequently used for dose-response assays: y = Response; Bottom = The lowest plateau of the curve (positive control); Top = The highest plateau of the curve (negative control); x = The molar concentration of inhibitor and S = The Hill Slope.

7.4.2 mTOR Kinobead assay

A kinobead chemoproteomic assay was used to determine the affinity of test compounds for mTOR kinase. As previously described this competition binding assay, used endogenous mTOR from whole cell lysate (HuT-78 cells) that was competed for by immobilised kinase capturing beads (kinobeads) and the test compound.⁸⁰ The procedure was as previously described.^{80,110} As an overview, a 384 well Multiscreen filter plate was used with 25 μ L of 10% Kinobead slurry added per well, followed by 1.5 μ L of compound solution per well and 50 μ L HuT-78 total cell lysate solution^b per well. The plate was sealed and shaken at 4 °C for two hours. Unbound protein was removed from the beads by applying vacuum to remove the lysate followed by washing the plate with DP buffer (containing 50 mM Tris-HCl (pH 7.4), 0.4% (v/v) Igepal CA-630 (or Nonidet P-40 (NP-40)), 5% (v/v) glycerol, 150 mM NaCl, 1.5 mM MgCl₂, 25 mM NaF, 1 mM Na₃VO₄ and 1 mM DDT). Proteins retained on the kinobeads were then eluted by adding sample buffer (containing 100 mM tris (pH 7.4), 4% sodium dodecyl sulfate (SDS), 0.01% bromophenol blue, 20% glycerol and 50 mM DTT). The plate was incubated for 30 minutes and the eluent transferred to a 384-well collection plate. The eluent was then transferred to a nitrocellulose membrane. The nitrocellulose membrane was dried for one hour at room temperature before it was rehydrated in 20% (v/v) ethanol and rinsed with phosphate buffered saline (PBS, containing 137 mM NaCl, 2.7 mM KCl, 10 nM Na₂HPO₄ and 2 mM KH₂PO₄ at pH 7.4). The membranes were blocked by incubation with Odyssey blocking buffer (OBB) at room temperature for 60 minutes. The membranes were

^b HuT-78 cells were cultured according to vendor's instructions. Frozen cell pellets were homogenized in 3x pellet volumes lysis buffer (50 mM Tris-HCl (pH 7.5), 0.4% (v/v) Igepal-CA630, 5% (v/v) glycerol, 150 mM NaCl, 1.5 mM MgCl₂, 25 mM NaF, 1 mM Na₃VO₄ and 1 mM DTT). The mixture was centrifuged, the supernatant collected and centrifuged again before aliquots were frozen and stored at -80 °C. Prior to use the cell lysate was diluted with DP buffer to a final concentration of 5 mg/mL.

incubated overnight at 25 °C with primary anti-mTOR antibody in OBB containing 0.4% Tween-20. The membranes were washed in PBS containing 0.1% Tween-20 and incubated at room temperature for one hour with the detection antibody (a secondary anti-rabbit IrDye 800 antibody diluted in OBB containing 0.2% Tween-20). The membrane was washed with PBS to remove residual Tween-20. Finally, the membranes were scanned with Odyssey® Infrared Imaging System. Fluorescence signals were recorded and concentration response curves computed with Activity Base software. All data were normalised by comparison with negative and positive controls. IC₅₀ values were determined using a four-parameter logistic regression equation (**Equation 6**, above). Reduced binding of mTOR to the matrix in the presence of an inhibitor gave a lower or absent signal.

7.4.3 pAkt Cellular assay

The pAkt assay was used to measure the effect of test compounds on the phosphorylation of Akt at serine 473 (pAkt_{s473}) in primary human lung fibroblasts (HLF). The MesoScale Discovery (MSD) platform was used to quantify the levels of pAkt_{s473} and total Akt, in a previously described procedure.⁸⁴ 10 mM Stock solutions of compound were diluted 4-fold in DMSO. Frozen HLF (cells derived from primary tissue but sub-cultured with no original primary cells remaining) were used. HLF were cultured in fibroblast basal medium with fibroblast basal medium supplement pack containing foetal bovine serum (FBS), human fibroblast growth factor-basic (hFGF-B), insulin and gentamicin sulfate-amphotericin (GA-1000) at 37 °C for 5 days. Cells were plated into a 384 well black U-clear Greiner flat bottom plate. After plating, cells were incubated at 37 °C overnight followed by treatment with either vehicle or increasing concentrations of the test compound and incubation at 37 °C for 60 minutes. After incubation, 10 µL platelet-derived growth factor BB (PDGF-BB) was added and the plate was incubated at room temperature for 10 minutes. 10 µL Cell signalling lysis buffer was added and the plates were shaken for 30 minutes to ensure lysis. 30 µL of cell lysate was added to 384-well GAR plate^c containing 10µl rabbit pAkt antibody,

^c MSD GAR plates are MULTI-ARRAY plates coated with goat anti-rabbit antibody. The detection system used SULFO-TAG labels that emit light upon electrochemical stimulation initiated at the electrode surfaces of the plates.

diluted 1:1500 with block buffer (tris-buffered saline (TBS) (with 5% bovine serum albumin (BSA) and 0.1% Tween 20)). The GAR plates were then sealed and shaken overnight in a cold room. The GAR plates were washed with TBS wash buffer (3 x 50 μ L), 10 μ L mouse total AKT detection antibody diluted 1:1500 with block buffer was added and plates were shaken for 60 minutes at room temperature. The GAR plates were washed with TBS wash buffer before 10 μ L of the anti-mouse MSD detection antibody diluted 1:500 with block buffer was added and plates were shaken for 60 minutes at room temperature. The GAR plates were washed with TBS wash buffer before 30 μ L 2 x MSD read buffer was added and the plates were read (electrochemiluminescence detected) immediately on MSD Sector Imager 6000. Data analysis was performed by determining % inhibition values for test compounds relative to the minimum (with PDGF-BB stimulation) and maximum responses (without PDGF-BB stimulation) with non-linear regression analysis to determine IC₅₀ values for test compounds.

7.4.4 SIAJ

Collagen biosynthesis was measured in an assay based on a previously described protocol.⁸⁵ A macromolecule, FiCol (a hydrophilic polysaccharide), was used to induce collagen deposition in fibroblast cultures. Under these molecular crowding conditions, fibroblasts lay down mature collagen on plates which could be detected by immunocytochemistry. An overview of the assay procedure was as follows. Lung fibroblasts were cultured, plated onto either a 96- or 384-well plate and the plate was incubated at 37 °C for 72 hours. The fibroblasts were treated with either vehicle (0.1% DMSO) or increasing concentrations of test compounds and incubated at 37 °C for 1-3 hours. The fibroblasts were then stimulated by addition of TGF β 1 (1 ng/mL) and incubated at 37 °C for 72 hours. The media was removed from the plate, the cells fixed and the plate washed. PBS containing 1% bovine serum albumin (BSA) and 0.1% Triton X100 was added, followed by addition of a primary collagen I antibody. The plate was placed in the fridge for 24 hours, washed and a fluorescent secondary antibody (Alexa Fluo488) added. The plate was incubated for 60 minutes at room temperature followed by washing to remove any residual antibody solution. The

fluorescent signal and therefore the amount of collagen I present was quantified on an INCELL 2000 system.

7.4.5 DNA-PK

The ability of compounds to inhibit DNA-PK was ascertained in a TR-FRET assay. In this assay, in the presence of double stranded DNA, DNA-PK phosphorylated a synthetic fluorescein conjugated p53-peptide on Ser15. This was then recognised by a terbium(Tb)-labeled anti-p53 (pSer15) peptide. Binding of phosphorylated p53-peptide to Tb-antibody resulted in energy transfer from terbium to fluorescein upon excitation at 337 nm. The ratio of fluorescein emission (530 nm) to Tb emission (492 nm) was proportional to the amount of phosphorylated p53-(pSer15)-peptide. Inhibition of DNA-PK enzyme activity (by a DNA-PK inhibitor) would cause the assay signal to decrease. An overview of the assay procedure was as follows. A Greiner black hi base 384-well plate was prepared containing increasing concentrations of the test compounds. 3 μ L of reaction buffer (containing 1x kinase buffer A, 2.5 μ g/mL sheared calf thymus DNA and 1 mM DTT) was added to the positive control well and 3 μ L of enzyme mix (reaction buffer containing 0.75 μ g/mL DNA-PK) was added to all remaining wells. The plate was centrifuged for one minute followed by incubating for 30 minutes at room temperature. The reaction was initiated by addition of 3 μ L of substrate mix (reaction buffer containing 1 μ M fluorescein p53 peptide and 10 μ M ATP) to the plate. The plate was centrifuged for one minute followed by incubating for 60 minutes at room temperature. The reaction was stopped by addition of 6 μ L of a stop/read mixture (containing 5 nM LanthaScreen-Tb-anti-p53 antibody and 10 μ M EDTA in HPLC water) to the plate. The plate was centrifuged for one minute followed by incubating for 60 minutes at room temperature. Finally, the plate was read using Envision with 337 nm laser excitation, 492/8 nm (fluorescein signal) and 530/8 nm (terbium signal) emission filters with 400/630 nm dual bias dichroic mirror. Data analysis was performed by determining % inhibition values for test compounds relative to the minimum (positive control, no enzyme present) and maximum responses (negative control, no compound present) with non-linear regression analysis to determine IC₅₀ values for test compounds.

7.4.6 MDCK

The permeability of compounds across the cell membrane of MDCKII-MDR1 (Madin-Darby canine kidney (MDCK) cells transfected with human Multidrug Resistance gene-1 (MDR1)) cell monolayers was determined in the MDCK permeability assay following a similar procedure to that described by Lui *et al.*²²² MDCKII-MDR1 cell monolayers were cultured for four days (in cell culture medium containing Dulbecco's Modified Eagle's medium (DMEM), pH 7.4) to form a monolayer and washed with pre-warmed transport medium (vendor defined buffer without proteins (eg. DMEM without phenol red or Hank's Balanced Salt Solution (HBSS) with 25 mM HEPES and 4.45 mM glucose) before incubating for 20 minutes at 37 °C. The cell monolayer formed a barrier between donor and receiver wells. Therefore, to get from the donor well to the receiver well a compound must pass (either by passive permeability or active transport) through the cell monolayer. The assay was run in both the presence and absence of transporter protein inhibitors. Solutions of the test compound were dosed to the donor well and the cells incubated for 60-120 minutes at 37 °C under gentle agitation. The solutions from both donor and acceptor wells were sampled and the amount of test compound present quantified using LCMS to determine permeability across the cell monolayer.

7.4.7 AMP

The AMP assay was carried out according to the published protocol.²²³

7.4.8 Kinetic solubility (CLND and CAD solubility)

The kinetic aqueous solubility of test compounds at pH 7.4 was determined by measuring the concentration of solute in solution after precipitation from DMSO stock solution. The procedure was as follows. The DMSO stock solutions of the test compounds were diluted 20-fold with PBS (at pH 7.4) and the samples left to equilibrate for 60 minutes at room temperature. The plate was vacuum filtered for one minute to provide the aqueous analysis plate. Quantification of compound in solution was done by Charged Aerosol Detector (CAD). Calibration parameters generated for CAD response of two calibrants (Primidone and Ketoconazole) were

used to calculate the solubility of solutes taking into account the density of the compound and ion-pairing effects.⁹⁰

Kinetic solubility measurement using the HPLC-CLND technique was carried out according to the published procedure.²²³

7.4.9 SLF

Thermodynamic solubility of solid test compounds in stimulated lung fluid (SLF) was measured as follows. To the test compound (~1 mg) was added SLF (1 mL). SLF was prepared by adding 0.75 mM Lecithin Disperse (59 mg Lecithin) and 100 mg BSA to 100 mL of buffer solution (prepared by dissolving 3.9 g of NaH₂PO₄·2H₂O and 2.0 g of NaCl, in approximately 475 mL water, adjusted to pH 6.9 (±0.1) by addition of approximately 14 mL aqueous NaOH (1 M) and diluting to 500 mL with water). The sample was shaken for 4 hours before 175 µL was removed. The removed sample was filtered and analysed by HPLC (Waters Acquity UPLC System CSH C₁₈ column 50 mm x 2.1 mm, 1.7 µM packing diameter) to determine the solubility of the test compound in SLF compared to the solubility of the sample in DMSO.

7.4.10 ChromLogD

The chromatographic hydrophobicity index (ChromLogD) of a test compound was determined by fast-gradient HPLC, according to literature procedures.²²⁴⁻²²⁶ Measurements were made using a Waters Acquity UPLC System, Phenomenex Gemini NX 50 mm x 2 mm, 3 µM packing diameter HPLC column and a 0–100% appropriately buffered aqueous phase/acetonitrile gradient. The buffered aqueous systems used were as follows: pH 2.0 phosphoric acid solution and pH 7.4 or pH 10.5 ammonium acetate buffer. The retention time of the test compounds was compared to standards of known pH to ascertain the Chromatographic Hydrophobicity Index (CHI). Consecutive lipophilicity measurements were taken at three pH values (2.0, 7.4 and 10.5) and the CHI values converted to ChromLogD values at each of the three pH values ($\text{ChromLogD} = 0.0857\text{CHI} - 2$). In this Thesis, $\text{ChromLogD}_{7.4}$ (ChromLogD at pH 7.4) was used.

7.5 Appendix E: Current proposed mechanism of the desulfinate cross-coupling reaction

After the presentation of this Thesis, Willis *et al.* published a detailed mechanistic study of the desulfinate cross-coupling reaction between heteroaryl sulfinate salts and aryl bromides.²²⁷ This research led the authors to propose a modified catalytic cycle compared to that suggested previously (**Figure Appendix E** compared with **Figure 35**).¹⁸⁰ The first step was proposed to be the formation of the reactive Pd⁰ catalyst, with the formation of some of a homocoupled bipyridyl species. An oxidative addition, transmetalation, reductive elimination catalytic cycle was then proposed. First the aryl bromide (**E7**) underwent oxidative addition followed by loss of a ligand to give the intermediate species **E4**. This was then proposed to form a stable O-Pd-N cyclic intermediate (**E5**). The stability of this intermediate (**E5**) was suggested to be one of the reasons for the high reaction temperatures required. Loss of sulfur dioxide from this species gave a biaryl palladium complex (**E6**) that underwent reductive elimination to regenerate the Pd⁰ catalyst and give the desired biaryl product (**E8**).²²⁷

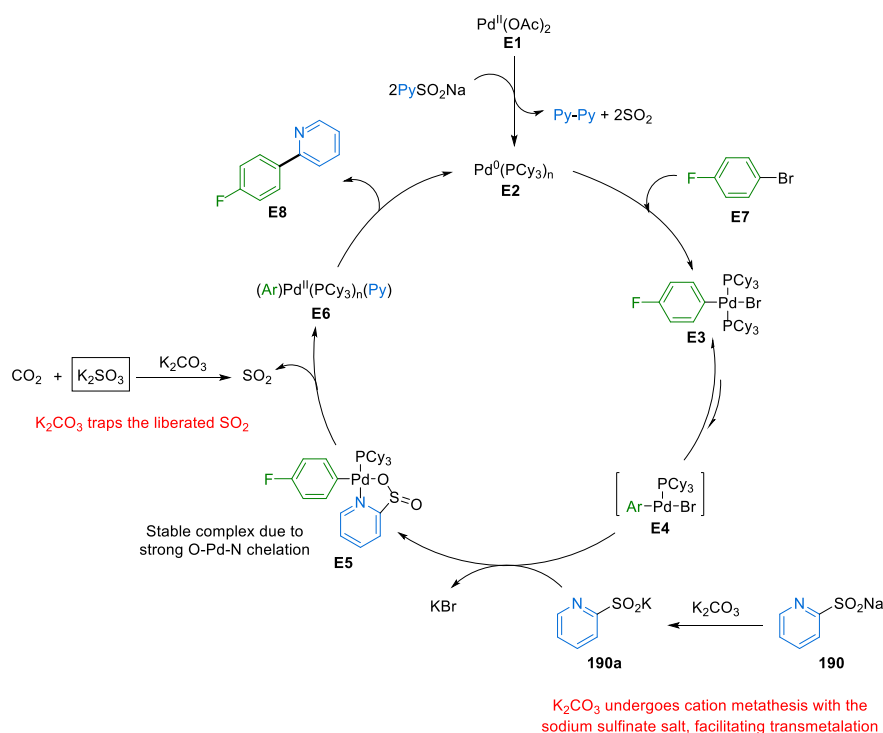


Figure Appendix E: A revised catalytic cycle for the desulfinate cross-coupling reaction, proposed in 2020 by Willis *et al.*²²⁷

Two roles were proposed for the potassium carbonate base: 1) cation metathesis with the sodium sulfinate salt (**190**) to give a potassium sulfinate salt (**190a**) which was demonstrated to facilitate transmetallation and 2) to trap the liberated sulfur dioxide.²²⁷ For every molecule of the desired product formed, one molecule of sulfur dioxide gas is released. If using 5 mol% of the palladium catalyst, at the end of the reaction a ratio of 20:1 between the gaseous byproduct and the catalyst will be reached. The sulfur dioxide gas was proposed to coordinate to the palladium and potentially disrupt catalysis. However, the potassium carbonate base was proposed to efficiently trap the formed sulfur dioxide, enabling a good turnover of the catalyst. Additionally, the cation of the carbonate base was also found to be important: the rate of transmetalation was significantly increased by using potassium carbonate and a sodium sulfinate salt compared to using the sodium sulfinate salt alone.²²⁷

8. References

1. Selvaggio, A. S.; Noble, P. W. *Annu. Rev. Med.* **2016**, *67*, 487-495.
2. Landi, C.; Bargagli, E.; Carleo, A.; Bianchi, L.; Gagliardi, A.; Prasse, A.; Perari, M. G.; Refini, R. M.; Bini, L.; Rottoli, P. *Proteomics Clin. Appl.* **2014**, *8*, 932-950.
3. Meltzer, E. B.; Noble, P. W. *Orphanet J. Rare Dis.* **2008**, *3*, 8-22.
4. Dempsey, O. J.; Kerr, K. M.; Gomersall, L.; Remmen, H.; Currie, G. P. *QJM* **2006**, *99*, 643-654.
5. King Jr., T. E.; Pardo, A.; Selman, M. *Lancet* **2011**, *378*, 1949-1961.
6. Raghu, G.; Collard, H. R.; Egan, J. J.; Martinez, F. J.; Behr, J.; Brown, K. K.; Colby, T. V.; Cordier, J. F.; Flaherty, K. R.; Lasky, J. A.; Lynch, D. A.; Ryu, J. H.; Swigris, J. J.; Wells, A. U.; Ancochea, J.; Bouros, D.; Carvalho, C.; Costabel, U.; Ebina, M.; Hansell, D. M.; Johkoh, T.; Kim, D. S.; King Jr., T. E.; Kondoh, Y.; Myers, J.; Muller, N. L.; Nicholson, A. G.; Richeldi, L.; Selman, M.; Dudden, R. F.; Griss, B. S.; Protzko, S. L.; Schunemann, H. J. *Am. J. Respir. Crit. Care Med.* **2011**, *183*, 788-824.
7. Nanthakumar, C. B.; Hatley, R. J.; Lemma, S.; Gauldie, J.; Marshall, R. P.; Macdonald, S. J. *Nat. Rev. Drug Discov.* **2015**, *14*, 693-720.
8. du Bois, R. M. *Eur. Respir. Rev.* **2012**, *21*, 141-146.
9. Staab-Weijnitz, C. A.; Eickelberg, O. *Thorax* **2016**, *71*, 675-676.
10. Liu, Y. M.; Nepali, K.; Liou, J. P. *J. Med. Chem.* **2017**, *60*, 527-553.
11. King Jr., T. E.; Costabel, U.; Cordier, J.-F.; DoPico, G. A.; du Bois, R. M.; Lynch, D.; Lynch, J. P. I.; Myers, J.; Panos, R.; Raghu, G.; Schwartz, D.; Smith, C. M. *Am. J. Respir. Crit. Care Med.* **2000**, *161*, 646-664.
12. Macneal, K.; Schwartz, D. A. *Proc Am Thorac Soc* **2012**, *9*, 120-125.
13. Nalysnyk, L.; Cid-Ruzafa, J.; Rotella, P.; Esser, D. *Eur. Respir. Rev.* **2012**, *21*, 355-361.
14. Kim, D. S.; Collard, H. R.; King Jr., T. E. *Proc. Am. Thorac. Soc.* **2006**, *3*, 285-292.
15. Collard, H. R.; Moore, B. B.; Flaherty, K. R.; Brown, K. K.; Kaner, R. J.; King Jr., T. E.; Lasky, J. A.; Loyd, J. E.; Noth, I.; Olman, M. A.; Raghu, G.; Roman, J.; Ryu, J. H.; Zisman, D. A.; Hunninghake, G. W.; Colby, T. V.; Egan, J. J.; Hansell, D. M.; Johkoh, T.; Kaminski, N.; Kim, D. S.; Kondoh, Y.; Lynch, D. A.; Muller-Quernheim,

- J.; Myers, J. L.; Nicholson, A. G.; Selman, M.; Toews, G. B.; Wells, A. U.; Martinez, F. J. *Am. J. Respir. Crit. Care Med.* **2007**, *176*, 636-643.
16. Song, J. W.; Hong, S. B.; Lim, C. M.; Koh, Y.; Kim, D. S. *Eur. Respir. J.* **2011**, *37*, 356-363.
17. Juillerat-Jeanneret, L.; Aubert, J. D.; Mikulic, J.; Golshayan, D. *J. Med. Chem.* **2018**, *61*, 9811-9840.
18. King Jr., T. E.; Bradford, W. Z.; Castro-Bernardini, S.; Fagan, E. A.; Glaspole, I.; Glassberg, M. K.; Gorina, E.; Hopkins, P. M.; Kardatzke, D.; Lancaster, L.; Lederer, D. J.; Nathan, S. D.; Pereira, C. A.; Sahn, S. A.; Sussman, R.; Swigris, J. J.; Noble, P. W. *N. Engl. J. Med.* **2014**, *370*, 2083-2092.
19. Richeldi, L.; du Bois, R. M.; Raghu, G.; Azuma, A.; Brown, K. K.; Costabel, U.; Cottin, V.; Flaherty, K. R.; Hansell, D. M.; Inoue, Y.; Kim, D. S.; Kolb, M.; Nicholson, A. G.; Noble, P. W.; Selman, M.; Taniguchi, H.; Brun, M.; Le Maulf, F.; Girard, M.; Stowasser, S.; Schlenker-Herceg, R.; Disse, B.; Collard, H. R. *N. Engl. J. Med.* **2014**, *370*, 2071-2082.
20. Rangarajan, S.; Kurundkar, A.; Kurundkar, D.; Bernard, K.; Sanders, Y. Y.; Ding, Q.; Antony, V. B.; Zhang, J.; Zmijewski, J.; Thannickal, V. J. *Am. J. Respir. Cell Mol. Biol.* **2016**, *54*, 51-59.
21. Hosenpud, J. D.; Bennett, L. E.; Keck, B. M.; Edwards, E. B.; Novick, R. J. *Lancet* **1998**, *351*, 24-27.
22. Maher, T. M. *Clin. Chest Med.* **2012**, *33*, 69-83.
23. Beanes, S. R.; Dang, C.; Soo, C.; Ting, K. *Exp. Rev. Mol. Med.* **2003**, *5*, 1-11.
24. Todd, N. W.; Luzina, I. G.; Atamas, S. P. *Fibrogenesis and Tissue Repair* **2012**, *5*, 11-34.
25. Frantz, C.; Stewart, K. M.; Weaver, V. M. *J. Cell Sci.* **2010**, *123*, 4195-4200.
26. Wynn, T. A. *J. Exp. Med.* **2011**, *208*, 1339-1350.
27. Chang, W.; Wei, K.; Ho, L.; Berry, G. J.; Jacobs, S. S.; Chang, C. H.; Rosen, G. D. *PLoS One* **2014**, *9*, e106155-e106166.
28. Richeldi, L.; Davies, H. R. H. R.; Ferrara, G.; Franco, F. *Cochrane Database Syst. Rev.* **2003**, 1-13.
29. Davies, H. R. H. R.; Richeldi, L.; Walters, E. H. *Cochrane Database Syst. Rev.* **2003**, 1-56.

30. Hutchinson, J.; Fogarty, A.; Hubbard, R.; McKeever, T. *Eur. Respir. J.* **2015**, *46*, 795-806.
31. Lipinski, C. A.; Lombardo, F.; Dominy, B. W.; Feeney, P. J. *Adv. Drug Deliv. Rev.* **1997**, *23*, 3-25.
32. Winkler, J.; Hochhaus, G.; Derendorf, H. *Proc. Am. Thorac. Soc.* **2004**, *1*, 356-363.
33. Harrell, A.; Hassall, D.; Eddershaw, P.; Edwards, C.; Sadler, R.; Allen, P.; Prodger, J.; Taylor, A. *GSK, Unpublished Work* **2015**.
34. Ritchie, T. J.; Luscombe, C. N.; Macdonald, S. J. F. *J. Chem. Inf. Model.* **2009**, *49*, 1025-1032.
35. Choy, Y. B.; Prausnitz, M. R. *Pharm. Res.* **2011**, *28*, 943-948.
36. Copeland, R. A.; Pompliano, D. L.; Meek, T. D. *Nat. Rev. Drug Discov.* **2006**, *5*, 730-740.
37. Patton, J. S. *Adv. Drug Deliv. Rev.* **1996**, *19*, 3-36.
38. Forbes, B.; O'Lone, R.; Pribul Allen, P.; Cahn, A.; Clarke, C.; Collinge, M.; Dailey, L. A.; Donnelly, L. E.; Dybowski, J.; Hassall, D.; Hildebrand, D.; Jones, R.; Kilgour, J.; Klapwijk, J.; Maier, C. C.; McGovern, T.; Nikula, K.; Parry, J. D.; Reed, M. D.; Robinson, I.; Tomlinson, L.; Wolfreys, A. *Adv. Drug Deliv. Rev.* **2014**, *71*, 15-33.
39. Cooper, A. E.; Ferguson, D.; Grime, K. *Curr. Drug Metab.* **2012**, *13*, 457-473.
40. Perry, M. W. D.; Bjorhall, K.; Bonn, B.; Carlsson, J.; Chen, Y.; Eriksson, A.; Fredlund, L.; Hao, H.; Holden, N. S.; Karabelas, K.; Lindmark, H.; Liu, F.; Pemberton, N.; Petersen, J.; Rodrigo Blomqvist, S.; Smith, R. W.; Svensson, T.; Terstiege, I.; Tyrchan, C.; Yang, W.; Zhao, S.; Oster, L. *J. Med. Chem.* **2017**, *60*, 5057-5071.
41. Hanumegowda, U. M.; Wenke, G.; Regueiro-Ren, A.; Yordanova, R.; Corradi, J. P.; Adams, S. P. *Chem. Res. Toxicol.* **2010**, *23*, 749-755.
42. Laplante, M.; Sabatini, D. M. *Cell* **2012**, *149*, 274-293.
43. Hentges, K. E.; Sirry, B.; Gingeras, A.; Sarbassov, D.; Sonenberg, N.; Sabatini, D.; Peterson, A. S. *PNAS* **2001**, *98*, 13796-13801.
44. Liu, P.; Cheng, H.; Roberts, T. M.; Zhao, J. J. *Nat. Rev. Drug Discov.* **2009**, *8*, 627-644.
45. Andrs, M.; Korabecny, J.; Jun, D.; Hodny, Z.; Bartek, J.; Kuca, K. *J. Med. Chem.* **2015**, *58*, 41-71.

46. Knight, S. D.; Adams, N. D.; Burgess, J. L.; Chaudhari, A. M.; Darcy, M. G.; Donatelli, C. A.; Luengo, J. I.; Newlander, K. A.; Parrish, C. A.; Ridgers, L. H.; Sarpong, M. A.; Schmidt, S. J.; Van Aller, G. S.; Carson, J. D.; Diamond, M. A.; Elkins, P. A.; Gardiner, C. M.; Garver, E.; Gilbert, S. A.; Gontarek, R. R.; Jackson, J. R.; Kershner, K. L.; Luo, L.; Raha, K.; Sherk, C. S.; Sung, C. M.; Sutton, D.; Tummino, P. J.; Wegrzyn, R. J.; Auger, K. R.; Dhanak, D. *ACS Med. Chem. Lett.* **2010**, *1*, 39-43.
47. Katso, R.; Okkenhaug, K.; Ahmadi, K.; White, S.; Timms, J.; Waterfield, M. D. *Annu. Rev. Cell. Dev. Biol.* **2001**, *17*, 615-675.
48. Liu, Q.; Thoreen, C.; Wang, J.; Sabatini, D.; Gray, N. S. *Drug Discov. Today Ther. Strateg.* **2009**, *6*, 47-55.
49. Moll, U.; Lau, R.; Sypes, M. A.; Gupta, M. M.; Anderson, C. W. *Oncogene* **1999**, *18*, 3114-3126.
50. Wullschleger, S.; Loewith, R.; Hall, M. N. *Cell* **2006**, *124*, 471-484.
51. Phung, T. L.; Ziv, K.; Dabydeen, D.; Eyiah-Mensah, G.; Riveros, M.; Perruzzi, C.; Sun, J.; Monahan-Earley, R. A.; Shiojima, I.; Nagy, J. A.; Lin, M. I.; Walsh, K.; Dvorak, A. M.; Briscoe, D. M.; Neeman, M.; Sessa, W. C.; Dvorak, H. F.; Benjamin, L. E. *Cancer Cell* **2006**, *10*, 159-170.
52. Sarbassov, D. D.; Ali, S. M.; Sengupta, S.; Sheen, J. H.; Hsu, P. P.; Bagley, A. F.; Markhard, A. L.; Sabatini, D. M. *Mol. Cell* **2006**, *22*, 159-168.
53. Sarbassov, D. D.; Guertin, D. A.; Ali, S. M.; Sabatini, D. M. *Science* **2005**, *307*, 1098-1102.
54. Lawrence, J.; Nho, R. *Int. J. Mol. Sci.* **2018**, *19*, 778-808.
55. Vanhaesebroeck, B.; Stephens, L.; Hawkins, P. *Nat. Rev. Mol. Cell Biol.* **2012**, *13*, 195-203.
56. Saxton, R. A.; Sabatini, D. M. *Cell* **2017**, *168*, 960-976.
57. Tian, T.; Li, X.; Zhang, J. *Int. J. Mol. Sci.* **2019**, *20*, 775-809.
58. Mercer, P. F.; Woodcock, H. V.; Eley, J. D.; Plate, M.; Sulikowski, M. G.; Durrenberger, P. F.; Franklin, L.; Nanthakumar, C. B.; Man, Y.; Genovese, F.; McAnulty, R. J.; Yang, S.; Maher, T. M.; Nicholson, A. G.; Blanchard, A. D.; Marshall, R. P.; Lukey, P. T.; Chambers, R. C. *Thorax* **2016**, *71*, 701-711.
59. Vancheri, C. *Eur. Respir. Rev.* **2013**, *22*, 265-272.

60. Groves, A. M.; Win, T.; Screatton, N. J.; Berovic, M.; Endozo, R.; Booth, H.; Kayani, I.; Menezes, L. J.; Dickson, J. C.; Ell, P. J. *J. Nucl. Med.* **2009**, *50*, 538-545.
61. Hilberg, F.; Roth, G. J.; Krssak, M.; Kautschitsch, S.; Sommergruber, W.; Tontsch-Grunt, U.; Garin-Chesa, P.; Bader, G.; Zoepfel, A.; Quant, J.; Heckel, A.; Rettig, W. *J. Cancer Res.* **2008**, *68*, 4774-4782.
62. Conte, E.; Fruciano, M.; Fagone, E.; Gili, E.; Caraci, F.; Iemmolo, M.; Crimi, N.; Vancheri, C. *PLoS One* **2011**, *6*, e24663-e24672.
63. Malouf, M. A.; Hopkins, P.; Snell, G.; Glanville, A. R. *Respirology* **2011**, *16*, 776-783.
64. Li, Y.; Wang, X.; Yue, P.; Tao, H.; Ramalingam, S. S.; Owonikoko, T. K.; Deng, X.; Wang, Y.; Fu, H.; Khuri, F. R.; Sun, S.-Y. *J. Biol. Chem.* **2013**, *288*, 13215-13224.
65. Poulsen, A.; Nagaraj, H.; Lee, A.; Blanchard, S.; Soh, C. K.; Chen, D.; Wang, H.; Hart, S.; Goh, K. C.; Dymock, B.; Williams, M. *J. Chem. Inf. Model.* **2014**, *54*, 3238-5320.
66. Duggan, H. M. E.; Leroux, F. G. M.; Malagu, K.; Martin, N. M. B.; Menear, K. A.; Smith, G. C. M. 2008; WO 2008/023161 A1.
67. Pike, K. G.; Malagu, K.; Hummersone, M. G.; Menear, K. A.; Duggan, H. M. E.; Gomez, S.; Martin, N. M. B.; Ruston, L.; Pass, S. L.; Pass, M. *Bioorg. Med. Chem. Lett.* **2013**, *23*, 1212-1216.
68. Lynch, R.; Cansfield, A. D.; Hardy, D. P.; Feutrill, J. T.; Adrego, R.; Ellard, K.; Ladduwahetty, T. 2013; WO 2013/050508 A1.
69. Chen, D.; Williams, M. 2010; WO 2010/114484 A1.
70. Pike, K. G.; Morris, J.; Ruston, L.; Pass, S. L.; Greenwood, R.; Williams, E. J.; Demeritt, J.; Culshaw, J. D.; Gill, K.; Pass, M.; Finlay, M. R. V.; Good, C. J.; Roberts, C. A.; Currie, G. S.; Blades, K.; Eden, J. M.; Pearson, S. E. *J. Med. Chem.* **2015**, *58*, 2326-2349.
71. Pei, Z.; Blackwood, E.; Liu, L.; Malek, S.; Belvin, M.; Koehler, M. F.; Ortwine, D. F.; Chen, H.; Cohen, F.; Kenny, J. R.; Bergeron, P.; Lau, K.; Ly, C.; Zhao, X.; Estrada, A. A.; Truong, T.; Epler, J. A.; Nonomiya, J.; Trinh, L.; Sideris, S.; Lesnick, J.; Bao, L.; Vijapurkar, U.; Mukadam, S.; Tay, S.; Deshmukh, G.; Chen, Y. H.; Ding, X.; Friedman, L. S.; Lyssikatos, J. P. *ACS Med. Chem. Lett.* **2013**, *4*, 103-107.

72. Cansfield, A. D.; Ladduwahetty, T.; Sunose, M.; Ellard, K.; Lynch, R.; Newton, A. L.; Lewis, A.; Bennett, G.; Zinn, N.; Thomson, D. W.; Ruger, A. J.; Feutrill, J. T.; Rausch, O.; Watt, A. P.; Bergamini, G. *ACS Med. Chem. Lett.* **2016**, *7*, 768-773.
73. Garcia-Echeverria, C. *Bioorg. Med. Chem. Lett.* **2010**, *20*, 4308-4312.
74. Urich, R.; Wishart, G.; Kiczun, M.; Richters, A.; Tidten-Luksch, N.; Rauh, D.; Sherborne, B.; Wyatt, P. G.; Brenk, R. *ACS Chem. Biol.* **2013**, *8*, 1044-1052.
75. Walker, E. H.; Pacold, M. E.; Perisic, O.; Stephens, L.; Hawkins, P. T.; Wymann, M. P.; Williams, R. L. *Mol. Cell* **2000**, *6*, 909-919.
76. Yang, H.; Rudge, D. G.; Koos, J. D.; Vaidialingam, B.; Yang, H. J.; Pavletich, N. *P. Nature* **2013**, *497*, 217-223.
77. Lv, X.; Ma, X.; Hu, Y. *Expert Opin. Drug Discov.* **2013**, *8*, 991-1012.
78. Fruman, D. A.; Rommel, C. *Nat. Rev. Drug Discov.* **2014**, *13*, 140-156.
79. Mercer, P. *Unpublished Work* **2012**.
80. Medard, G.; Pachel, F.; Ruprecht, B.; Klaeger, S.; Heinzlmeir, S.; Helm, D.; Qiao, H.; Ku, X.; Wilhelm, M.; Kuehne, T.; Wu, Z.; Dittmann, A.; Hopf, C.; Kramer, K.; Kuster, B. *J. Proteome Res.* **2015**, *14*, 1574-1586.
81. Rau, C.; Bauer, E. *GSK AESOP Protocol, Unpublished Work* **2013**.
82. Bantscheff, M.; Eberhard, D.; Abraham, Y.; Bastuck, S.; Boesche, M.; Hobson, S.; Mathieson, T.; Perrin, J.; Raida, M.; Rau, C.; Reader, V.; Sweetman, G.; Bauer, A.; Bouwmeester, T.; Hopf, C.; Kruse, U.; Neubauer, G.; Ramsden, N.; Rick, J.; Kuster, B.; Drewes, G. *Nat. Biotechnol.* **2007**, *25*, 1035-1044.
83. Ashby, C.; Brown, F.; Thomas, D. *GSK AESOP Protocol, Unpublished Work* **2016**.
84. Mesoscale <https://www.mesoscale.com/en/products/phospho-ser473-total-akt-whole-cell-lysate-kit-k15100d/>; Accessed 26.10.2019.
85. Chen, C. Z.; Peng, Y. X.; Wang, Z. B.; Fish, P. V.; Kaar, J. L.; Koepsel, R. R.; Russell, A. J.; Lareu, R. R.; Raghunath, M. *Br. J. Pharmacol.* **2009**, *158*, 1196-1209.
86. Ferens, D.; Pindoria, R.; Thomas, D. *GSK AESOP Protocol, Unpublished Work* **2018**.
87. Millipore https://www.emdmillipore.com/US/en/product/PI-3-Kinase-HTRF-Assay-385-wells,MM_NF-33-016#anchor_UG; Accessed 26.10.2019.

88. Hutchinson, S.; Rowedder, J.; Thomas, D. *GSK AESOP Protocol, Unpublished Work* **2016**.
89. Pell, T.; Heathcote, M. *GSK AESOP Protocol, Unpublished Work* **2011**.
90. Robinson, M. W.; Hill, A. P.; Readshaw, S. A.; Hollerton, J. C.; Upton, R. J.; Lynn, S. M.; Besley, S. C.; Boughtflower, B. J. *Anal. Chem.* **2017**, *89*, 1772-1777.
91. Johnson, T.; Reid, I. *GSK AESOP Protocol, Unpublished Work* **2017**.
92. Hill, A.; Reid, I.; Mann, K. *GSK AESOP Protocol, Unpublished Work* **2015**.
93. Marques, M. R. C.; Loebenberg, R.; Almukainzi, M. *Dissolution Technol.* **2011**, *18*, 15-28.
94. Wabuye, M.; Smith, K. *GSK AESOP Protocol, Unpublished Work* **2011**.
95. Irvine, J. D.; Takahashi, L.; Lockhart, K.; Cheong, J.; Tolan, J. W.; Selick, H. E.; Grove, J. R. *J. Pharm. Sci.* **1999**, *88*, 28-33.
96. Nadin, A.; Hattotuagama, C.; Churcher, I. *Angew. Chem. Int. Ed.* **2012**, *51*, 1114-1122.
97. Leeson, P. D.; Springthorpe, B. *Nat. Rev. Drug Discov.* **2007**, *6*, 881-890.
98. Johnson, T. W.; Dress, K. R.; Edwards, M. *Bioorg. Med. Chem. Lett.* **2009**, *19*, 5560-5564.
99. Malagu, K.; Duggan, H.; Menear, K.; Hummersone, M.; Gomez, S.; Bailey, C.; Edwards, P.; Drzewiecki, J.; Leroux, F.; Quesada Jimenez, M.; Hermann, G.; Maine, S.; Molyneaux, A.; Le Gall, A.; Pullen, J.; Hickson, I.; Smith, L.; Maguire, S.; Martin, N.; Smith, G.; Pass, M. *Bioorg. Med. Chem. Lett.* **2009**, *19*, 5950-5953.
100. Knight, Z. A.; Gonzalez, B.; Feldman, M. E.; Zunder, E. R.; Goldenberg, D. D.; Williams, O.; Loewith, R.; Stokoe, D.; Balla, A.; Toth, B.; Balla, T.; Weiss, W. A.; Williams, R. L.; Shokat, K. M. *Cell* **2006**, *125*, 733-747.
101. Nowak, P.; Cole, D. C.; Brooijmans, N.; Bursavich, M. G.; Curran, K. J.; Ellingboe, J. W.; Gibbons, J. J.; Hollander, I.; Hu, Y.; Kaplan, J.; Malwitz, D. J.; Toral-Barza, L.; Verheijen, J. C.; Zask, A.; Zhang, W.-G.; Yu, K. *J. Med. Chem.* **2009**, *52*, 7081-7089.
102. Verheijen, J. C.; Richard, D. J.; Curran, K.; Kaplan, J.; Lefever, M.; Nowak, P.; Malwitz, D. J.; Brooijmans, N.; Toral-Barza, L.; Zhang, W.-G.; Lucas, J.; Hollander, I.; Ayral-Kaloustian, S.; Mansour, T. S.; Yu, K.; Zask, A. *J. Med. Chem.* **2009**, *52*, 8010-8024.

103. Zask, A.; Kaplan, J.; Verheijen, J. C.; Richard, D. J.; Curran, K.; Brooijmans, N.; Bennett, E. M.; Toral-Barza, L.; Hollander, I.; Ayrál-Kaloustian, S.; Yu, K. *J. Med. Chem.* **2009**, *52*, 7942-7945.
104. Hobbs, H.; Inglis, G. A. I.; Peace, S.; Redmond, J. M. *GSK, Unpublished Work* **2013**.
105. Hopkins, A. L.; Keseru, G. M.; Leeson, P. D.; Rees, D. C.; Reynolds, C. H. *Nat. Rev. Drug Discov.* **2014**, *13*, 105-121.
106. Lee, W.; Ortwine, D. F.; Bergeron, P.; Lau, K.; Lin, L.; Malek, S.; Nonomiya, J.; Pei, Z.; Robarge, K. D.; Schmidt, S.; Sideris, S.; Lyssikatos, J. P. *Bioorg. Med. Chem. Lett.* **2013**, *23*, 5097-5104.
107. Cohen, F.; Bergeron, P.; Blackwood, E.; Bowman, K. K.; Chen, H.; DiPasquale, A. G.; Epler, J. A.; Koehler, M. F.; Lau, K.; Lewis, C.; Liu, L.; Ly, C. Q.; Malek, S.; Nonomiya, J.; Ortwine, D. F.; Pei, Z.; Robarge, K. D.; Sideris, S.; Trinh, L.; Truong, T.; Wu, J.; Zhao, X.; Lyssikatos, J. P. *J. Med. Chem.* **2011**, *54*, 3426-3435.
108. Zask, A.; Verheijen, J. C.; Richard, D. J. *Expert Opin. Ther. Pat.* **2011**, *21*, 1109-1127.
109. Kaplan, J.; Verheijen, J. C.; Brooijmans, N.; Toral-Barza, L.; Hollander, I.; Yu, K.; Zask, A. *Bioorg. Med. Chem. Lett.* **2010**, *20*, 640-643.
110. Hobbs, H.; Bravi, G.; Campbell, I.; Convery, M.; Davies, H.; Inglis, G.; Pal, S.; Peace, S.; Redmond, J.; Summers, D. *J. Med. Chem.* **2019**, *62*, 6972-6984.
111. *GSK Unpublished Work, Fibrosis and Lung Injury DPU.*
112. Hobbs, H.; Inglis, G. A. I.; Peace, S.; Davies, H. R. M. *GSK, Unpublished Work* **2015**.
113. Luscombe, C. N. In *5th Joint Sheffield Conference on Chemoinformatics* Sheffield, 2010.
114. Luscombe, C. N. *GSK, Unpublished Work* **2015**.
115. Free, S. M.; Wilson, J. W. *J. Med. Chem.* **1964**, *7*, 395-399.
116. McCarren, P.; Springer, C.; Whitehead, L. *J. Cheminformatics* **2011**, *3*, 51-71.
117. Kalgutkar, A. S.; Gardner, I.; Obach, R. S.; Shaffer, C. L.; Callegari, E.; Henne, K. R.; Mutlib, A. E.; Dalvie, D. K.; Lee, J. S.; Nakai, Y.; O'Donnell, J. P.; Boer, J.; Harriman, S. P. *Curr. Drug Metab.* **2005**, *6*, 161-225.

118. Hsu, K. H.; Su, B. H.; Tu, Y. S.; Lin, O. A.; Tseng, Y. J. *PLoS One* **2016**, *11*, e0148900-e0148916.
119. Cash, G. G.; Anderson, B.; Mayo, K.; Bogaczyk, S.; Tunkel, J. *Mutat. Res.* **2005**, *585*, 170-183.
120. Williams, R. V.; Patel, M.; Vessey, J. D.; Yeo, D. J.
<https://www.lhasalimited.org/Public/Library/2015/Examining%20the%20myths%20and%20realities%20of%20aromatic%20amine%20mutagenicity.pdf>; Accessed 05.08.2017.
121. Ames, B. N.; Lee, F. D.; Durston, W. E. *PNAS* **1973**, *70*, 765-768.
122. Ames, B. N.; McCann, J.; Yamasaki, E. *Mutat. Res.* **1975**, *31*, 347-363.
123. Birch, A. M.; Groombridge, S.; Law, R.; Leach, A. G.; Mee, C. D.; Schramm, C. *J. Med. Chem.* **2012**, *55*, 3923-3933.
124. Lynch, R.; Cansfield, A.; Niblock, H. S.; Hardy, D.; Scanlon, J. E.; Adrego, R.; Ramsden, N. 2010; WO 2010/103094 A1.
125. *GVK Biosciences, Unpublished Work.*
126. Dibakar, M.; Prakash, A.; Selvakumar, K.; Ruckmani, K.; Sivakumar, M. *Tetrahedron Lett.* **2011**, *52*, 5338-5341.
127. Maloney, K. M.; Nwakpuda, E.; Kuethe, J. T.; Yin, J. *J. Org. Chem.* **2009**, *74*, 5111-5114.
128. Roder, O.; Ludemann, H.-D.; Von Goldammer, E. *Eur. J. Biochem.* **1975**, *53*, 517-524.
129. Bochevarov, A. D.; Harder, E.; Hughes, T. F.; Greenwood, J. R.; Braden, D. A.; Philipp, D. M.; Rinaldo, D.; Halls, M. D.; Zhang, J.; Friesner, R. A. *Int. J. Quantum Chem.* **2013**, *113*, 2110-2142.
130. Lodish, H.; Berk, A.; Zipursky, S. L.; Matsudaira, P.; Baltimore, D.; Darnell, J. *Molecular Cell Biology*; 4 ed.; New York, 2000.
131. Sugano, K.; Kansy, M.; Artursson, P.; Avdeef, A.; Bendels, S.; Di, L.; Ecker, G. F.; Faller, B.; Fischer, H.; Gerebtzoff, G.; Lennernaes, H.; Senner, F. *Nat. Rev. Drug Discov.* **2010**, *9*, 597-614.
132. *Blausen.com Staff. Medical gallery of Blausen Medical (2014), Wikiversity Journal of Medicine*

https://en.wikiversity.org/wiki/WikiJournal_of_Medicine/Medical_gallery_of_Blausen_Medical_2014; Accessed 18.07.2017.

133. Hardcastle, I. R.; Cockcroft, X.; Curtin, N. J.; El-Murr, M. D.; Leahy, J. J. J.; Stockley, M.; Golding, B. T.; Rigoreau, L.; Richardson, C.; Smith, G. C. M.; Griffin, R. J. *J. Med. Chem.* **2005**, *48*, 7829-7846.
134. Shiloh, Y. *Nat. Rev. Cancer* **2003**, *3*, 155-168.
135. Ballou, L. M.; Lin, R. Z. *J. Chem. Biol.* **2008**, *1*, 27-36.
136. Griffin, R. J.; Fontana, G.; Golding, B. T.; Guiard, S.; Hardcastle, I. R.; Leahy, J. J.; Martin, N.; Richardson, C.; Rigoreau, L.; Stockley, M.; Smith, G. C. *J. Med. Chem.* **2005**, *48*, 569-585.
137. Jones, N. A.; Antoon, J. W.; Bowie Jr, A. L.; Borak, J. B.; Stevens, E. P. *J. Heterocycl. Chem.* **2007**, *44*, 363-367.
138. Newkome, G. R.; Patri, A. K.; Holder, E.; Schubert, U. S. *Eur. J. Org. Chem.* **2004**, 235-254.
139. Lützen, A.; Hapke, M. *Eur. J. Org. Chem.* **2002**, 2292-2297.
140. Lützen, A.; Hapke, M.; Staats, H.; Bunzen, J. *Eur. J. Org. Chem.* **2003**, 3948-3957.
141. Lützen, A.; Kiehne, U.; Bunzen, J.; Staats, H. *Synthesis* **2007**, 1061-1069.
142. Lützen, A.; Hapke, M.; Staats, H.; Wallmann, I. *Synthesis* **2007**, 2711-2719.
143. Schonherr, H.; Cernak, T. *Angew. Chem. Int. Ed.* **2013**, *52*, 12256-12267.
144. Barreiro, E. J.; Kummerle, A. E.; Fraga, C. A. *Chem. Rev.* **2011**, *111*, 5215-5246.
145. Rao, R.; Shewalkar, M. P.; Nandipati, R.; Yadav, J. S.; Khagga, M.; Shinde, D. B. *Synth. Commun.* **2012**, *42*, 589-598.
146. Imaeda, Y.; Miyawaki, T.; Sakamoto, H.; Itoh, F.; Konishi, N.; Hiroe, K.; Kawamura, M.; Tanaka, T.; Kubo, K. *Bioorg. Med. Chem.* **2008**, *16*, 2243-2260.
147. Alonso, D. A.; Fuensanta, M.; Gómez-Bengoa, E.; Nájera, C. *Adv. Synth. Catal.* **2008**, *350*, 1823-1829.
148. Shen, S.; Ni, X.; Zhang, Z.; Yang, Z.; He, X.; Wang, W.; Zhou, F. 2016; WO 2016/095833 A1.
149. GaylordChemicalCorporation http://chemistry-chemists.com/N3_2011/U/DMSO-technical_bulletin.pdf *Technical Bulletin Reaction Solvent Dimethylsulfoxide (DMSO)*; Accessed 16.11.2017.

150. Waldvogel, S.; Faust, A.; Wolff, O. *Synthesis* **2008**, 2009, 155-159.
151. Markovic, T.; Rocke, B. N.; Blakemore, D. C.; Mascitti, V.; Willis, M. C. *Chem. Sci.* **2017**, 8, 4437-4442.
152. Ragan, J. A.; Raggon, J. W.; Hill, P. D.; Jones, B. P.; McDermott, R. E.; Munchhof, M. J.; Marx, M. A.; Casavant, J. M.; Cooper, B. A.; Doty, J. L.; Lu, Y. *Org. Process Res. Dev.* **2003**, 7, 676-683.
153. Cordovilla, C.; Bartolomé, C.; Martínez-Ilarduya, J. M.; Espinet, P. *ACS Catal.* **2015**, 5, 3040-3053.
154. Ishiyama, T.; Murata, M.; Miyaura, N. *J. Org. Chem.* **1995**, 60, 7508-7510.
155. Chow, W. K.; Yuen, O. Y.; Choy, P. Y.; So, C. M.; Lau, C. P.; Wong, W. T.; Kwong, F. Y. *RSC Adv.* **2013**, 3, 12518-12539.
156. Molander, G. A.; Trice, S. L.; Kennedy, S. M.; Dreher, S. D.; Tudge, M. T. *J. Am. Chem. Soc.* **2012**, 134, 11667-11673.
157. Knapp, D. M.; Gillis, E. P.; Burke, M. D. *J. Am. Chem. Soc.* **2009**, 131, 6961-6963.
158. Billingsley, K.; Buchwald, S. L. *J. Am. Chem. Soc.* **2007**, 129, 3358-3366.
159. PraveenGanesh, N.; Demory, E.; Gamon, C.; Blandin, V.; Chavan, P. Y. *Synlett* **2010**, 16, 2403-2406.
160. Tasker, S. Z.; Standley, E. A.; Jamison, T. F. *Nature* **2014**, 509, 299-309.
161. Poremba, K. E.; Kadunce, N. T.; Suzuki, N.; Cherney, A. H.; Reisman, S. E. *J. Am. Chem. Soc.* **2017**, 139, 5684-5687.
162. Liao, L. Y.; Kong, X. R.; Duan, X. F. *J. Org. Chem.* **2014**, 79, 777-782.
163. Everson, D. A.; Weix, D. J. *J. Org. Chem.* **2014**, 79, 4793-4798.
164. Gosmini, C.; Bassene-Ernst, C.; Durandetti, M. *Tetrahedron* **2009**, 65, 6141-6146.
165. Sato, K.; Okoshi, T. US, 1992; US 005159082 A.
166. Zhou, X.; Luo, J.; Liu, J.; Peng, S.; Deng, G.-J. *Org. Lett.* **2011**, 13, 1432-1435.
167. Ortgies, D. H.; Hassanpour, A.; Chen, F.; Woo, S.; Forgione, P. *Eur. J. Org. Chem.* **2016**, 408-425.
168. Selke, V. R.; Thiele, W. *Journal fur Praktische Chemie* **1971**, 313, 875-881.
169. Garves, K. *J. Org. Chem.* **1970**, 35, 3273-3275.

170. O'Connor Sraj, L.; Khairallah, G. N.; da Silva, G.; O'Hair, R. A. J. *Organometallics* **2012**, *31*, 1801-1807.
171. Wenkert, E.; Ferreira, T. W.; Michelotti, E. L. *Chem. Comm.* **1979**, 637-638.
172. Luh, T.-Y.; Ni, Z.-J. *Synthesis* **1990**, 89-103.
173. Wang, G. W.; Miao, T. *Chem. Eur. J.* **2011**, *17*, 5787-5790.
174. Zhou, C.; Liu, Q.; Li, Y.; Zhang, R.; Fu, X.; Duan, C. *J. Org. Chem.* **2012**, *77*, 10468-10472.
175. Sevigny, S.; Forgione, P. *Chem. Eur. J.* **2013**, *19*, 2256-2260.
176. Liu, B.; Guo, Q.; Cheng, Y.; Lan, J.; You, J. *Chem. Eur. J.* **2011**, *17*, 13415-13419.
177. Wang, M.; Li, D.; Zhou, W.; Wang, L. *Tetrahedron* **2012**, *68*, 1926-1930.
178. Wu, M.; Luo, J.; Xiao, F.; Zhang, S.; Deng, G.-J.; Luo, H.-A. *Adv. Synth. Catal.* **2012**, *354*, 335-340.
179. Emmett, E. J.; Hayter, B. R.; Willis, M. C. *Angew. Chem. Int. Ed.* **2013**, *52*, 12679-12683.
180. Forgione, P.; Ortgies, D.; Barthelme, A.; Aly, S.; Desharnais, B.; Rioux, S. *Synthesis* **2013**, *45*, 694-702.
181. Forgione, P.; Ortgies, D. *Synlett* **2013**, *24*, 1715-1721.
182. Skillinghaug, B.; Rydfjord, J.; Odell, L. R. *Tetrahedron Lett.* **2016**, *57*, 533-536.
183. Kamiyama, T.; Enomoto, S.; Inoue, M. *Chem. Pharm. Bull.* **1988**, *36*, 2652-2653.
184. Whitmore, F. C.; Hamilton, F. H. *Organic Syntheses, Sodium p-Toluenesulfinate* <http://www.orgsyn.org/demo.aspx?prep=CVIP0492>; Accessed 05.03.2019.
185. Shavnya, A.; Coffey, S. B.; Smith, A. C.; Mascitti, V. *Org. Lett.* **2013**, *15*, 6226-6229.
186. Baskin, J. M.; Wang, Z. *Tetrahedron Lett.* **2002**, *43*, 8479-8483.
187. Shavnya, A.; Coffey, S. B.; Hesp, K. D.; Ross, S. C.; Tsai, A. S. *Org. Lett.* **2016**, *18*, 5848-5851.
188. Kotha, S.; Khedkar, P. *Chem. Rev.* **2012**, *112*, 1650-1680.
189. Gauthier, D. R., Jr.; Yoshikawa, N. *Org. Lett.* **2016**, *18*, 5994-5997.
190. Maloney, K. M.; Kuethe, J. T.; Linn, K. *Org. Lett.* **2011**, *13*, 102-105.
191. Bennett, M. J.; Betancort, J. M.; Bloor, A.; Kaldor, S. W.; Stafford, J. A.; Veal, J. M. 2015; WO 2015/058160 A1.

192. Baskin, J. M.; Wang, Z. *Org. Lett.* **2002**, *4*, 4423-4425.
193. Day, J. J.; Neill, D. L.; Xu, S.; Xian, M. *Org. Lett.* **2017**, *19*, 3819-3822.
194. Markovic, T.; Rocke, B. N.; Blakemore, D. C.; Mascitti, V.; Willis, M. C. *Org. Lett.* **2017**, *19*, 6033-6035.
195. Ely, R.; Richardson, P.; Zlota, A.; Steven, A.; Kargbo, R.; Nawrat, C. C.; Ramirez, A.; Day, D. P.; Knight, J. *Org. Process Res. Dev.* **2017**, *21*, 897-910.
196. Markovic, T.; Rocke, B. N.; Blakemore, D. C.; Mascitti, V.; Willis, M. C. *Org. Lett.* **2018**, *20*, 3148-3149.
197. *Cross-Coupling Reaction Manual: Desk Reference. Sigma Aldrich.*
https://slidelegend.com/cross-coupling-reaction-manual-desk-reference-sigma-aldrich_5a888d751723dd8560ddc7e4.html; Accessed 08.04.2018.
198. Elangovan, A.; Wang, Y. H.; Ho, T. I. *Org. Lett.* **2003**, *5*, 1841-1844.
199. Guram, A. S.; Milne, J. E.; Tedrow, J. S.; Walker, S. D. *Cross Coupling and Heck-Type Reactions Volume 1 C-C Cross Coupling Using Organometallic Partners.*
200. Vitaku, E.; Smith, D. T.; Njardarson, J. T. *J. Med. Chem.* **2014**, *57*, 10257-10274.
201. West, M. J.; Watson, A. J. B. *Org. Biomol. Chem.* **2019**, *17*, 5055-5059.
202. Roughley, S. D.; Jordan, A. M. *J. Med. Chem.* **2011**, *54*, 3451-3479.
203. Baumann, M.; Baxendale, I. R. *Beilstein J. Org. Chem.* **2013**, *9*, 2265-2319.
204. Guchhait, S. K.; Hura, N.; Sinha, K.; Panda, D. *RSC Adv.* **2017**, *7*, 8323-8331.
205. Hibi, S.; Ueno, K.; Nagato, S.; Kawano, K.; Ito, K.; Norimine, Y.; Takenaka, O.; Hanada, T.; Yonaga, M. *J. Med. Chem.* **2012**, *55*, 10584-10600.
206. Friesen, R. W.; Brideau, C.; Chan, C. C.; Charleson, S.; Deschanes, D.; Dube, D.; Ethier, D.; Fortin, R.; Gauthier, Y. J.; Girard, Y.; Gordon, R.; Greig, G. M.; Riendeau, D.; Savoie, C.; Wang, Z.; Wong, E.; Visco, D.; Xu, L. J.; Young, R. N. *Bioorg. Med. Chem. Lett.* **1998**, *8*, 2777-2782.
207. Davies, I. W.; Marcoux, J.-F.; Corley, E. G.; Journet, M.; Cai, D.-W.; Palucki, M.; Wu, J.; Larsen, R. D.; Rossen, K.; Pye, P. J.; DiMichele, L.; Dormer, P.; Reider, P. J. *J. Org. Chem.* **2000**, *65*, 8415-8420.
208. Mao, Z.; Lan, T.; Liu, L.; Yan, L.; Becker, S. 2013; WO 2013/104546 A1.
209. Markovic, T.; Murray, P. R. D.; Rocke, B. N.; Shavnya, A.; Blakemore, D. C.; Willis, M. C. *J. Am. Chem. Soc.* **2018**, *140*, 15916-15923.

210. Sigma Aldrich: Greener Solvent Alternatives.
https://www.sigmaaldrich.com/content/dam/sigma-aldrich/docs/Sigma/Brochure/greener_solvent_alternatives.pdf; Accessed 21.07.2019.
211. Cooper, T. W. J.; Campbell, I. B.; Macdonald, S. J. F. *Angew. Chem. Int. Ed.* **2010**, *49*, 8082-8091.
212. Dufert, M. A.; Billingsley, K. L.; Buchwald, S. L. *J. Am. Chem. Soc.* **2013**, *135*, 12877-12885.
213. Kumbhar, A. *J. Organomet. Chem.* **2017**, *848*, 22-88.
214. Quan, X.; Liu, J.; Rabten, W.; Diomedi, S.; Singh, T.; Andersson, P. G. *Eur. J. Org. Chem.* **2016**, *20*, 3427-3433.
215. Pal, S.; Hwang, W.-S.; Lin, I. J. B.; Lee, C.-S. *J. Mol. Catal. A-Chem.* **2007**, *269*, 197-203.
216. Trivedi, M.; Singh, G.; Nagarajan, R.; Rath, N. P. *Inorganica Chim. Acta* **2013**, *394*, 107-116.
217. Hansen, M. M.; Jolly, R. A.; Linder, R. J. *Org. Process Res. Dev.* **2015**, *19*, 1507-1516.
218. O'Donovan, M. R.; Mee, C. D.; Fenner, S.; Teasdale, A.; Phillips, D. H. *Mutat. Res.* **2011**, *724*, 1-6.
219. Ghorai, A.; Reddy K, S.; Achari, B.; Chattopadhyay, P. *Org. Lett.* **2014**, *16*, 3196-3199.
220. Bharti, S. K.; Roy, R. *Trends Anal. Chem.* **2012**, *35*, 5-26.
221. Gray, A.; Olsson, H.; Batty, I. H.; Priganica, L.; Peter Downes, C. *Anal. Biochem.* **2003**, *313*, 234-245.
222. Liu, H.; Huang, L.; Li, Y.; Fu, T.; Sun, X.; Zhang, Y.-Y.; Gao, R.; Chen, Q.; Zhang, W.; Sahi, J.; Summerfield, S.; Dong, K. *Drug Metab. Dispos.* **2017**, *45*, 449-456.
223. Ballell, L.; Bates, R. H.; Young, R. J.; Alvarez-Gomez, D.; Alvarez-Ruiz, E.; Barroso, V.; Blanco, D.; Crespo, B.; Escribano, J.; Gonzalez, R.; Lozano, S.; Huss, S.; Santos-Villarejo, A.; Martin-Plaza, J. J.; Mendoza, A.; Rebollo-Lopez, M. J.; Remuinan-Blanco, M.; Lavandera, J. L.; Perez-Herran, E.; Gamo-Benito, F. J.; Garcia-

- Bustos, J. F.; Barros, D.; Castro, J. P.; Cammack, N. *ChemMedChem* **2013**, *8*, 313-321.
224. Camurri, G.; Zaramella, A. *Anal. Chem.* **2001**, *73*, 3716-3722.
225. Valko, K.; Bevan, C.; Reynolds, D. *Anal. Chem.* **1997**, *69*, 2022-2029.
226. Valko, K.; Du, C. M.; Bevan, C.; Reynolds, D. P.; Abraham, M. H. *Curr. Med. Chem.* **2001**, *8*, 1137-1146.
227. de Gombert, A.; McKay, A. I.; Davis, C. J.; Wheelhouse, K. M.; Willis, M. C. *Journal of the American Chemical Society* **2020**, *142*, 3564-3576.